BioMed Research International

Biotechnology in Environmental Monitoring and Pollution Abatement

Guest Editors: Kannan Pakshirajan, Eldon R. Rene, and Aiyagari Ramesh

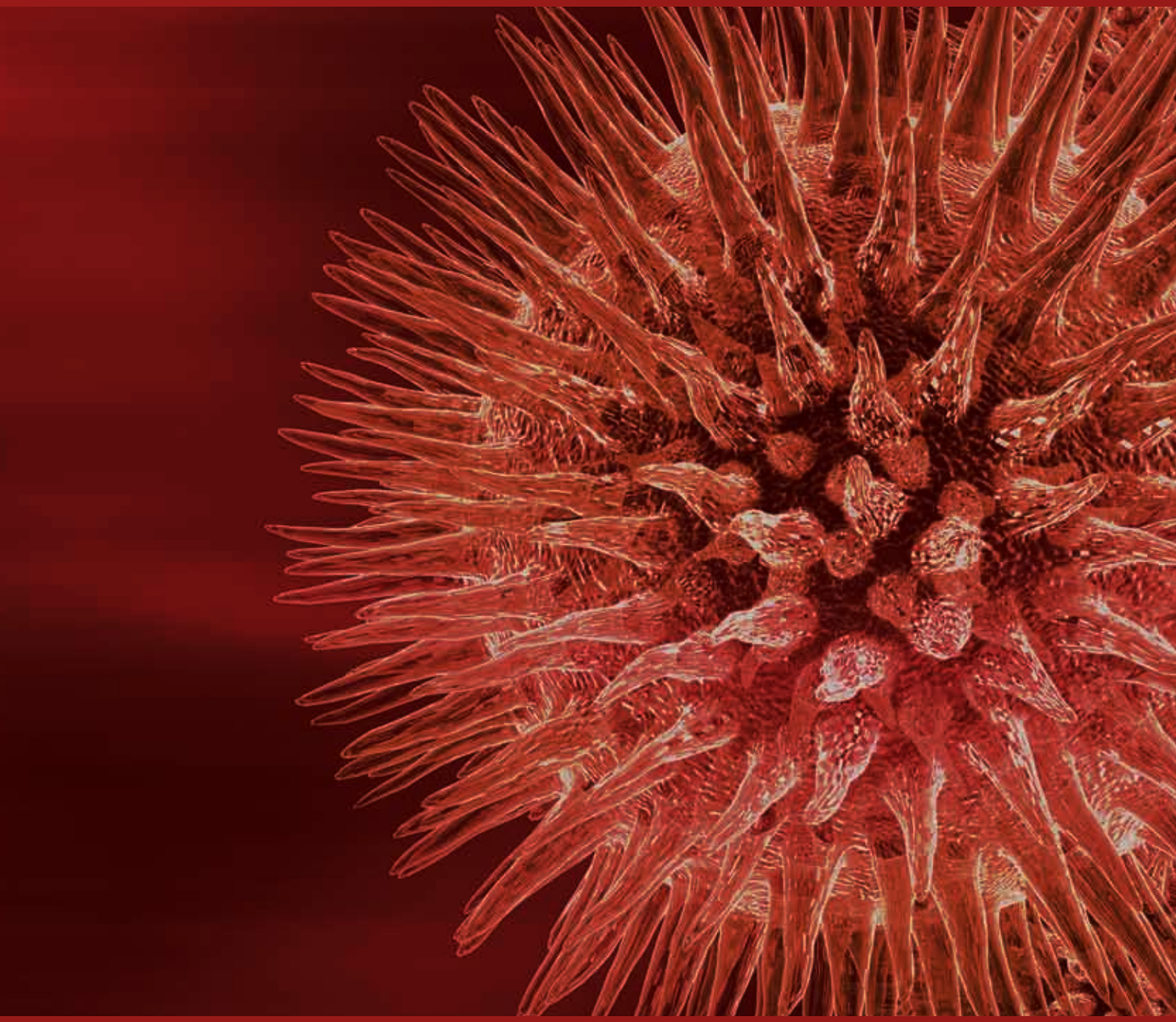

Biotechnology in Environmental Monitoring and Pollution Abatement

BioMed Research International

Biotechnology in Environmental Monitoring and Pollution Abatement

Guest Editors: Kannan Pakshirajan, Eldon R. Rene, and Aiyagari Ramesh

Contents

Hindawi Publishing Corporation
BioMed Research International
Volume 2014, Article ID 235472, 4 pages
http://dx.doi.org/10.1155/2014/235472

Editorial

Biotechnology in Environmental Monitoring and Pollution Abatement

Kannan Pakshirajan,[1] Eldon R. Rene,[2] and Aiyagari Ramesh[1]

[1] *Department of Biotechnology, Indian Institute of Technology Guwahati, Guwahati 781039, Assam, India*
[2] *Pollution Prevention and Resource Recovery Chair Group, Department of Environmental Engineering and Water Technology, UNESCO-IHE Institute for Water Education, Westvest 7, 2611 AX Delft, The Netherlands*

Correspondence should be addressed to Kannan Pakshirajan; pakshi@iitg.ernet.in

Received 9 March 2014; Accepted 9 March 2014; Published 23 April 2014

In recent years, the demand for the use of sustainable and eco-friendly environmental processes is rapidly growing subjected to economic, public, and legislation pressure. Biotechnology provides a plethora of opportunities for effectively addressing issues pertaining to the monitoring, assessment, modeling, and treatment of contaminated water, air, and solid waste streams. In this context, source tracking of environmental pollutants and process modeling using biological based methods are becoming increasingly important, mainly owing to the accuracy and robustness of such techniques. The different biotechniques available nowadays, thus, represent both well-established and novel (bio)technologies, although several aspects of their performance are still to be tested. For instance, the use of novel biocatalysts and reactor designs, the understanding of microbial community dynamics and mechanisms occurring within a (bio)reactor, and the assessment of the performance of (bio)reactors during long-term operation and its modeling. If these mechanisms are understood and the barriers are overcome, novel biotechniques will potentially change the way users rebuild technologies for the sustainable use of different biological processes for wastewater, air, and solid waste treatment.

This special issue received 34 research/review articles over a period of 6 months, of which 21 high-quality papers (62%) were accepted for publication following a double blind peer-review process. These accepted papers focus on the various fundamental and applied engineering aspects of different techniques and processes that have potential practical implications in emerging fields of environmental biotechnology. This special issue highlights certain challenging issues pertaining to environmental monitoring and pollution abatement that can be categorized into five thematic research areas.

Environmental Monitoring and Modeling. In developing countries, water, air, and soil pollution has become a persisting environmental problem due to rapid industrialization and urbanization. Using environmental Kuznets curve (EKC) it was observed that, during early stages of economic development in a particular region, the environment paid a high price for economic growth as the human race used technology to exploit all possible valuable resources. Nevertheless, in agricultural areas, N, P, and K compounds are easily transported by farmland drainage and surface water to valuable water resources resulting in the deterioration of water quality that warrants the use of novel biosensors to monitor water quality. Recently, it has been proposed that cellular-based biosensor technologies, that is, the bioelectric recognition assay (BERA), utilize live, functional cells in a gel matrix coupled with a sensor system that is able to measure changes in the cellular electric properties. Cells that are able to specifically interact with a target analyte produce a unique pattern of electrical potential as a result of their interaction with this analyte.

Concerning modeling, traditionally, the performance of many bioprocesses [1] has been modeled/predicted using

process-based models that are based on mass balance principles, simple reaction kinetics, and a plug flow of water/air stream. An alternate modeling procedure consists of a data driven approach wherein the principles of artificial intelligence (AI) are applied with the help of neural networks [2, 3]. The concept of neural network modeling has widespread applications in the fields of applied biosciences and bioengineering. The following research papers (1–3) were accepted under this category.

(1) *"Environmental Kuznets curve analysis of the economic development and nonpoint source pollution in the Ningxia Yellow River irrigation districts in China"* by C. Mao et al.

(2) *"Back propagation neural network model for predicting the performance of immobilized cell biofilters handling gas-phase hydrogen sulphide and ammonia"* by E. R. Rene et al.

(3) *"Pesticide residue screening using a novel artificial neural network combined with a bioelectric cellular biosensor"* by K. P. Ferentinos et al.

Pollutant Removal and Toxicity. Environmental pollutants such as heavy metals and pesticides are commonly present in water emanating from acid mine drainage or other industries and from agricultural runoffs. These toxic pollutants can accumulate in living organisms and produce adverse effect such as carcinogenicity and acute toxicity. Complete mineralization and/or removal of these pollutants and their toxic byproducts can be achieved using biological process that uses active bacterial/fungal/mixed microbial cultures [4]. Microbial consortia have been shown to be more suitable for bioremediation of recalcitrant compounds such as pesticide residues, as their biodiversity supports environmental survival and increases the number of catabolic pathways available for contaminant biodegradation. In the case of heavy metal contaminated wastewaters, biosorption has emerged as a promising low-cost methodology wherein biological catalysts are employed to remove and recover heavy metals from aqueous solutions [5]. The metal removal mechanism is a complex process that depends on the chemistry of metal ions, cell wall compositions of microorganisms, physiology of the organism, and physicochemical factors like pH, temperature, time, ionic strength, and metal concentration. The following papers (4–8) were selected for publication under this section of the special issue.

(4) *"Dissolution of arsenic minerals mediated by dissimilatory arsenate reducing bacteria: estimation of the physiological potential for arsenic mobilization"* by D. Lukasz et al.

(5) *"Kinetics of molybdenum reduction to molybdenum blue by Bacillus sp. strain A. rzi"* by A. R. Othman et al.

(6) *"The uptake mechanism of Cd(II), Cr(VI), Cu(II), Pb(II), and Zn(II) by mycelia and fruiting bodies of Galerina vittiformis"* by D. Damodaran et al.

(7) *"Toxicity of superparamagnetic iron oxide nanoparticles on green alga Chlorella vulgaris"* by L. Barhoumi and D. Dewez.

(8) *"Enhanced removal of a pesticides mixture by single cultures and consortia of free and immobilized Streptomyces strains"* by M. S. Fuentes et al.

Biofuels Production. Biohydrogen production through anaerobic fermentation is a sustainable alternative for managing the recent (dogging) energy crisis and creating a sustainable green environment. Fermentative hydrogen production processes are technically feasible and economically cost-competitive and have large-scale commercialization implications [6, 7]. Besides some of the pure microbial species, that can be used to produce biofuels, as of late, it was shown that microbes present in the sediments of mangroves have the capability to yield biohydrogen. Mangrove sediments are inherently rich in organic content and offer the following advantages: flexible substrate utilization and the simplicity of handling, no major storage problems, minimal preculturing requirements, and sediments being available at low cost. Alternatively, the development of (bio)energy using marine and freshwater microalgae as a 3rd generation biomass feedstock has also been explored recently because microalgae can grow fast with high specific growth rates and have excellent CO_2 absorption capacity and better regulation of lipid and sugar content under various culture conditions. Microalgae exhibit a high photosynthetic efficiency and a strong capacity to adapt to the environment (e.g., high salinity, heavy metal ion content, presence of toxicants, and high CO_2 concentration). The following papers (9–11) describe the production of biohydrogen and biodiesel.

(9) *"Biohydrogen production and kinetic modeling using sediment microorganisms of Pichavaram mangroves, India"* by P. Mullai et al.

(10) *"Production of biodiesel from Chlorella sp. enriched with oyster shell extracts"* by C. S. Choi et al.

(11) *"Enhancement of biodiesel production from marine alga, Scenedesmus sp. through in situ transesterification process associated with acidic catalyst"* by G. V. Kim et al.

Microbial Products for the Environment. With increasing concern for the natural environment, biosynthetic and biodegradable biopolymers such as poly-β-hydroxybutyrate (PHB) have attracted great interest because of their excellent biodegradability and being environmentally benign and sustainable. The high production cost of PHB can be curtailed by strain development, improving fermentation and separation processes, and using inexpensive carbon source. Due to recent advancements in fermentation technology and allied sciences, alternative purification solutions are under investigation, among which microbiological ways of utilization of byproducts are very interesting and promising. Such a solution could result in better overall process productivity and facilitate the downstream processing. Concerning the use

of enzymes, owing to its lignolytic enzyme system, the white-rot fungus *Phanerochaete chrysosporium* has been applied in many bioremediation studies [8]. Its ability to degrade a variety of pollutants is thus related to the production of lignin peroxidase and manganese peroxidase, two lignin-modifying enzymes generally expressed under nitrogen-limited culture conditions, as well as to the intracellular cytochrome P450 system. Another practical aspect worth highlighting in this section is the use of an enhanced biological phosphorus removal (EBPR) for phosphorus removal from wastewaters. In EBPR, alternative anaerobic and aerobic phases are adopted and polyphosphate accumulating organisms (PAOs) with excess phosphorus accumulation ability can be enriched. During the anaerobic phase, PAOs take up organic carbons such as acetate and propionate and store them as intracellular polymers such as PHBs, with polyphosphate as the energy source and glycogen as the reducing power source. The metabolism of PAOs and dynamics of polymers under different organic carbon concentrations deserves in-depth examination in order to elucidate the function of polymers in EBPR. Investigating the dynamics of polymers under endogenous respiration conditions will also provide solutions for controlling and adjusting the EBPR performance under low organic carbon induced shock conditions. The following papers (12–17) were accepted for publication under the theme of "microbial production for the environment."

(12) *"Degradation of diuron by Phanerochaete chrysosporium: role of ligninolytic enzymes and cytochrome P450"* by J. da Silva Coelho-Moreira et al.

(13) *"Dynamics of intracellular polymers in enhanced biological phosphorus removal processes under different organic carbon concentrations"* by L. Xing et al.

(14) *"Microbial purification of postfermentation medium after 1,3-PD production from raw glycerol"* by D. Szymanowska-Powałowska et al.

(15) *"Rhizobium pongamiae sp. nov. from root nodules of Pongamia pinnata"* by V. Kesari et al.

(16) *"Persistent organic pollutants induced protein expression and immunocrossreactivity by Stenotrophomonas maltophilia PM102: a prospective bioremediating candidate"* by P. Mukherjee and P. Roy.

(17) *"Poly β-hydroxybutyrate production by Bacillus subtilis NG220 using sugar industry wastewater"* by G. Singh et al.

Eco-Efficient Bioprocesses for the Environment. Nutrient-rich wastewater streams when discharged into receiving water bodies often lead to undesirable problems such as algal blooms, eutrophication, and oxygen deficit. For such commonly reported situations in many developing countries, advanced treatment technologies cannot be applied to treat wastewater due to the requirement of high energy and skilled labor force, high operating and maintenance costs. Under such conditions, low-cost natural treatment systems can be effectively used not only for waste treatment, but also for conserving biological communities in poor nations of the world [9]. For the (bio)treatment of slaughterhouse wastewater, sequencing batch reactors (SBRs) were recommended as one of the best options because they are capable of removing organic carbon, nutrients, and suspended solids from wastewater in a single tank and also have low capital and operational costs. In order to maintain the long-term performance of bioreactors (e.g., stirred tank bioreactor), various strategies to improve the oxygen transfer in bioreactors have been proposed, for instance, dispersing a nonaqueous, organic, second liquid-phase that is immiscible to the system. The presence of this organic phase modifies the medium in such a way that it could carry more oxygen and this approach was found successful in the past. The organic phase has strong affinity for oxygen so that it can increase the apparent solubility of oxygen in water, which in turn increases the specific activity of microorganisms, yielding high removal of target pollutant in bioreactors. In this special issue, four papers (18–21) deal with the operational characteristics of natural and conventional bioprocesses and their advantages to treat specific industrial wastewaters.

(18) *"Enhancement of oxygen mass transfer and gas holdup using palm oil in stirred tank bioreactors with xanthan solutions as simulated viscous fermentation broths"* by S. M. Sauid et al.

(19) *"Treatment of slaughter house wastewater in a sequencing batch reactor: performance evaluation and biodegradation kinetics"* by P. Kundu et al.

(20) *"Performance study of chromium (VI) removal in presence of phenol in a continuous packed bed reactor by Escherichia coli isolated from East Calcutta wetlands"* by B. Chakraborty et al.

(21) *"Natural treatment systems as sustainable ecotechnologies for the developing countries"* by Q. Mahmood et al.

It is quite apparent from the discussions and conclusions made by the authors from the papers published in this special issue, as well as other recently published scientific literature related to environmental research, that there is an urgent need to translate most of the lab-based research into field-based research in order to witness sustainable solutions to persisting environmental problems. Future research should focus/address crucial issues pertaining to (i) biomarkers for environmental pollutants, (ii) development of new biosensors for environmental monitoring, (iii) development of new biocatalysts (bacteria, fungi, yeast, and algae) for environmental applications, (iv) development of innovative bioreactors for wastewater and air pollution control, and (v) studies on the socioeconomic implications and technological evaluation of new bioprocesses.

We firmly believe that the collection of papers presented in this special issue will stimulate interest within the global research community and would help peers in their research pursuits.

Acknowledgments

We are grateful to all the authors for their generous support and dedication and for submitting high-quality papers to

this special issue. The final outcome of this special issue would not have been possible without the support of expert reviewers for contributing their knowledge and providing critical insight during the review process. We would also like to thank the respective organizations, IIT Guwahati, India, and UNESCO-IHE, The Netherlands, for supporting our editorial dissemination and outreach activities.

Kannan Pakshirajan
Eldon R. Rene
Aiyagari Ramesh

References

[1] E. R. Rene, M. E. López, M. C. Veiga, and C. Kennes, "Steady- and transient-state operation of a two-stage bioreactor for the treatment of a gaseous mixture of hydrogen sulphide, methanol and α-pinene," *Journal of Chemical Technology & Biotechnology*, vol. 85, pp. 336–348, 2010.

[2] E. R. Rene, S. M. Maliyekkal, L. Philip, and T. Swaminathan, "Back-propagation neural network for performance prediction in trickling bed air biofilter," *International Journal of Environment and Pollution*, vol. 28, no. 3-4, pp. 382–401, 2006.

[3] E. R. Rene, J. H. Kim, and H. S. Park, "An intelligent neural network model for evaluating performance of immobilized cell biofilter treating hydrogen sulphide vapors," *International Journal of Environmental Science and Technology*, vol. 5, no. 3, pp. 287–296, 2008.

[4] N. K. Sahoo, K. Pakshirajan, and P. K. Ghosh, "Biodegradation of 4-bromophenol by *Arthrobacter chlorophenolicus* A6 in a newly designed packed bed reactor," *Journal of Bioscience and Bioengineering*, vol. 115, no. 2, pp. 182–188, 2013.

[5] K. Pakshirajan, M. Izquierdo, and P. N. L. Lens, "Arsenic(III) removal at low concentrations by biosorption using *Phanerochaete chrysosporium* pellets," *Separation Science and Technology*, vol. 48, pp. 1111–1112, 2013.

[6] K. Pakshirajan and J. Mal, "Biohydrogen production using native carbon monoxide converting anaerobic microbial consortium predominantly *Petrobacter* sp.," *International Journal of Hydrogen Energy*, vol. 38, pp. 16020–16028, 2013.

[7] P. Mullai, M. K. Yogeswari, and K. Sridevi, "Optimisation and enhancement of biohydrogen production using nickel nanoparticles—a novel approach," *Bioresource Technology*, vol. 141, pp. 212–219, 2013.

[8] K. Pakshirajan and S. Kheria, "Continuous treatment of coloured industry wastewater using immobilized *Phanerochaete chrysosporium* in a rotating biological contactor reactor," *Journal of Environmental Management*, vol. 101, pp. 118–123, 2012.

[9] Y. T. Tu, P. C. Chiang, J. Yang, S. H. Chen, and C. M. Kao, "Application of a constructed wetland system for polluted stream remediation," *Journal of Hydrology*, vol. 510, pp. 70–78, 2014.

Hindawi Publishing Corporation
BioMed Research International
Volume 2014, Article ID 841892, 12 pages
http://dx.doi.org/10.1155/2014/841892

Research Article

Dissolution of Arsenic Minerals Mediated by Dissimilatory Arsenate Reducing Bacteria: Estimation of the Physiological Potential for Arsenic Mobilization

Drewniak Lukasz, Rajpert Liwia, Mantur Aleksandra, and Sklodowska Aleksandra

Laboratory of Environmental Pollution Analysis, Faculty of Biology, University of Warsaw, Miecznikowa 1, 02-096 Warsaw, Poland

Correspondence should be addressed to Drewniak Lukasz; ldrewniak@biol.uw.edu.pl

Received 11 October 2013; Revised 2 January 2014; Accepted 16 January 2014; Published 2 March 2014

Academic Editor: Aiyagari Ramesh

The aim of this study was characterization of the isolated dissimilatory arsenate reducing bacteria in the context of their potential for arsenic removal from primary arsenic minerals through reductive dissolution. Four strains, *Shewanella* sp. OM1, *Pseudomonas* sp. OM2, *Aeromonas* sp. OM4, and *Serratia* sp. OM17, capable of anaerobic growth with As (V) reduction, were isolated from microbial mats from an ancient gold mine. All of the isolated strains: (i) produced siderophores that promote dissolution of minerals, (ii) were resistant to dissolved arsenic compounds, (iii) were able to use the dissolved arsenates as the terminal electron acceptor, and (iii) were able to use copper minerals containing arsenic minerals (e.g., enargite) as a respiratory substrate. Based on the results obtained in this study, we postulate that arsenic can be released from some As-bearing polymetallic minerals (such as copper ore concentrates or middlings) under reductive conditions by dissimilatory arsenate reducers in indirect processes.

1. Introduction

Arsenic is considered to be one of the most hazardous elements, wherein its toxicity is revealed only when it is present in aqueous or gaseous form. Most of the arsenic-bearing minerals, such as arsenides and sulfarsenides, are considered nontoxic because they are highly insoluble. Problems arise when these primary minerals break down and enter into solution or form more soluble species such as oxides [1]. One of such cases, a common phenomenon in metallurgy industry, is arsenic release from ores and deposits into the environment through mining and smelting operations.

The most abundant and dominant arsenic ore minerals are As-sulfides, including arsenopyrite (FeAsS), realgar (As_4S_4), and orpiment (As_2S_3) [2]. Arsenic minerals are also found as impurities (as minor ores) in the ores of other metals such as gold or copper. Arsenopyrite is very often found in gold ores, while enargite (Cu_3AsS_4) and tennantite ($(Cu,Fe)_{12}As_4S_{13}$) are the most common arsenic-bearing minerals associated with copper sulfide ore bodies [3]. Moreover, the fine fraction of ash produced by smelting of ore concentrates causes the airborne dispersion of arsenic, thus contaminating soil and streams over a wide area. A high arsenic content causes problems in the smelting and further extraction of metals, resulting in a reduction in the quality of the final product [3–5]. Environmental problems are also connected with the arsenic-bearing flotation tailings and mine waters. Arsenic present in these "reservoirs" can be transformed by the microbial activity and this may contribute to the further dissemination of arsenic contamination.

The most common microbial arsenic mobilization processes involve oxidative dissolution of minerals through oxidation of iron, sulfur, or arsenic [6]. Iron oxidizers can promote oxidative dissolution of arsenic minerals through direct or indirect mechanisms, which results in the production of toxic arsenious (H_3AsO_3) and arsenic acids (H_3AsO_4) [7]. In turn, oxidation of arsenic-bearing sulfide minerals causes not only the release of arsenic but also the acidification of waters and their enrichment in sulfate anions and the accompanying heavy metals [8]. Arsenic minerals dissolution can be mediated also at circumneutral pH, but mainly by sulfur- and arsenite-oxidizing microbes. It has been documented that

the release of pyrite-bound arsenic may be caused by (i) oxidation of sulfide in the pyrite lattice [9] or (ii) direct oxidation of arsenic from mineral structure (e.g., arsenopyrite) [10]. The release of arsenic from As-bearing minerals may be also mediated by microbial reductive dissolution. Under reducing conditions, microorganisms can use arsenic compounds as terminal electron acceptors in arsenic respiration [11, 12]. However, this process is thought to be dominant for arsenic displacement from secondary minerals, for example, arsenate adsorbed on scorodite [13] and ferrihydrite [14]. There is no data about dissimilatory reduction of primary arsenic minerals, such as enargite, fangite, or luzonite, in which arsenic occurs as (sulf) arsenates. Thus, the question is whether the microorganisms are capable of removing arsenic from primary arsenic minerals through reductive dissolution. The answer to this question will help to complete the missing knowledge about microbial dissolution of arsenic-bearing minerals and will help to estimate the chance of the potential use of dissimilatory reducers in biomining and bioremediation. The possibility of selective removal of As(III) compounds (whose solubility is higher than As(V) and the level of As(III) sorption on the surface of secondary minerals is much lower and unstable) will be particularly important in industrial processing of As-bearing polymetallic minerals (such as copper ore concentrates or middlings (intermediate during ore processing)), where the presence of arsenic causes many technological and environmental problems.

The aim of this study was characterization of the isolated dissimilatory arsenate reducing bacteria in the context of their potential for arsenic removal from primary arsenic minerals through reductive dissolution. We demonstrated that the isolated strains (i) produce metabolites that promote dissolution of minerals, (ii) are resistant to dissolved arsenic compounds, (iii) are able to use the dissolved arsenates as terminal electron acceptor, and (iv) are able to remove arsenic under anaerobic conditions from As-containing copper ore concentrates and middlings, in which copper minerals were used as the sole terminal electron acceptor.

2. Materials and Methods

2.1. Isolation of Arsenate Dissimilatory Reducing Bacteria, Media and Growth Conditions. Microbial mats samples were collected from an ancient gold mine located in Zloty Stok, Lower Silesia, SW Poland, and were used as the inoculum for isolation of dissimilatory arsenate reducers. Microbial mats and the mine waters are characterized by high arsenic content (~5000–6800 mg/L for mats and ~3000–7000 μg/L for mine waters), slightly alkaline pH (~7, 4–8.0), and stable temperature of 10–12°C throughout the year. 5 mL of microbial mats samples was added to the modified mineral salt medium (MSM) [10] (final volume, 100 mL) containing 2.5 mM sodium arsenate and 5 mM sodium lactate. Cultures were carried out in serum bottles with $CO_2 : N_2$ (in a ratio 20 : 80) injected into the headspace. These bottles were sealed and corked with silicon stoppers secured by aluminium crimp seals. Sampling was performed under $CO_2 : N_2$ (in a ratio 20 : 80) atmosphere in anaerobic glove box (Sigma-Aldrich). Cultures were incubated for 7 days at 22°C and then were subcultured twice for 7 days each. The cultures were then diluted and plated on MSM agar containing 2.5 mM sodium arsenate and 0.004% yeast extract.

All of the isolated strains were routinely grown in lysogeny broth (LB) medium [15] or in MSM medium [NaCl 1.17 (g/L), KCl 0.30 (g/L), NH_4Cl 0.15 (g/L), $MgCl_2 \cdot 6H_2O$ 0.41 (g/L), $CaCl_2$ 0.11 (g/L), KH_2PO_4 0.20 (g/L), Na_2SO_4 0.07 (g/L), and $NaHCO_3$ 2.00 (g/L), pH 8.0] supplemented with yeast extract (0.04% w/v) at 22°C. For siderophores production, bacterial strains were cultivated at 22°C in GASN medium [2 g/L L-asparagine, 7 g/L glucose, 0.96 g/L Na_2HPO_4, 0.44 g/L KH_2PO_4, and 0.2 g/L $MgSO_4 \cdot 7H_2O$, pH 7.0] [16].

2.2. Copper Ore Concentrate and Middlings. Copper ore concentrate and middlings (intermediate during ore processing) were received from KGHM S.A. "Polska Miedź" (Poland). Copper ore concentrate contained 185970 mg Cu/kg, 22169 mg Fe/kg, 2460 mg Pb/kg, 3765 mg As/kg, 533, 1 mg Ni/kg, and 1273 mg Co/kg. Middlings contained 21495 mg Cu/kg, 4290 mg Fe/kg, 291, 5 mg As/kg, 356, 5 mg Ni/kg, and 594 mg Co/kg. The main arsenic minerals are enargite (AsV), tennantite (AsIII), and realgar (AsIII). Arsenopyrite is present as trace mineral. Sandstone, dolomite, and limestone are gangue. Sulphur content is 0.3–0.9% (mainly as sulfides and sulfates).

2.3. Arsenopyrite. Crystals of arsenopyrite were received from ancient gold mine in Zloty Stok.

2.4. Arsenic Respiration Screening Test. The ability of bacterial isolates to reduce As (V) in respiratory processes was tested using MSM agar plate containing 5 mM sodium lactate as the carbon source and 5 mM sodium arsenate as the electron acceptor. Cultures were grown under anaerobic conditions and, after 7 days of cultivation at 22°C, the agar plates were flooded with 0.1 M $AgNO_3$ solution. The reaction between $AgNO_3$ and As (III) or As (V) results in the formation of a coloured precipitate [17]. A brownish precipitate reveals the presence of Ag_3AsO_4 (silver arsenate) in the medium, while a yellow precipitate shows the presence of Ag_3AsO_3 (silver arsenite) (colonies expressing arsenate reductase).

2.5. Chemical Analyses. Solid samples (bacterial biomass, powders of copper ore concentrate, and middlings) were thoroughly dried at 60°C, and then 9 mL 65% HNO_3 and 1 mL 36% H_2O_2 were added to 0.25–0.30 g of the dry mass and digested in a closed system with heating in a microwave oven (Milestone Ethos Plus with Lab Terminal 800 Controller, Italy) [18]. Liquid samples (culture supernatants and siderophores solutions) were placed in 12 mL glass vials (Agillent, USA) and mixed with 65% HNO_3 in a ratio 4 : 1. Quantitative analysis of As, Cu, and Fe was performed by flame atomic absorption spectrometry (FAAS) and graphite furnace atomic absorption spectrometry (GFAAS) (AA Solaar M6 Spectrometer, TJA Solutions, UK) using

standard solution (Merck, Darmstadt, Germany) prepared in 0.5 M HNO_3. Arsenic speciation in culture supernatants was determined as described by Drewniak et al. (2008) [19].

2.6. PCR Amplification and Sequencing: 16S rRNA Gene, arrA and arsC Genes. Amplification of the 16S rRNA genes and the *arsC* genes was performed as described by Drewniak et al. (2008) [20]. For the amplification of the *arrA* genes, primer pair ArrAfwd and ArrArev were used as described by Malasarn et al. (2004) [21]. The PCR products were ligated with the vector pGEM-T-Easy (Promega) and were transformed to chemically competent *Escherichia coli* TG1 cells. Plasmid inserts were sequenced on an ABI3730 DNA analyser (Applied Biosystems) at the Laboratory of DNA Sequencing and Oligonucleotide Synthesis, IBB PAS, using universal M13F and M13R primers. Additional primers 518F and 519R [22] were used for sequencing of the 16S rRNA genes. Partial sequences were assembled using Clone Manager Professional Suite software (version 8) and were verified manually.

2.7. Phylogenetic Analysis. The near full-length 16S rRNA gene sequences (~1.4 kbp) from the isolates and reference sequences from the known arsenic-utilizing bacteria were aligned using ClustalW software (http://www.ebi.ac.uk/clustalw). The obtained alignment was adjusted manually and then used to construct a phylogenetic tree. The unrooted tree was constructed using the distance matrix "Neighbor-Joining Method" with NEIGHBOR from the PHYLIP 3.6 software package [23]. Distance matrices were calculated by DNADIST (PHYLIP) using Jukes-Cantor formula. Bootstrap analysis was carried out 1000 times using SEQBOOT (PHYLIP). A consensus tree was computed with CONSENS (PHYLIP).

2.8. Determination of the Minimum Inhibitory Concentrations of Metals/Metalloids. To examine the minimal inhibitory concentrations (MIC) of heavy metals, 96-well microplates containing LB medium amended with the respective heavy metal compounds were used. Each well of the microplates was inoculated with cells from fresh overnight cultures to a final density of approximately 10^6 cells/mL and then incubated for 48 h at 22°C in aerobic conditions. The following metals and their compounds were used for MIC determination: As (III) 0.0–25.0 mM; As (V) 0.0–500 mM; Cu (II) 0.0–5.0 mM; Cd (II) 0.0–5.0 mM and Co (II) 0.0–5.0 mM; and Fe (III) 0.0–25.0 mM, Ni (II) 0.0–5.0 mM, Pb (II) 0.0–20 mM, and Zn (II) 0.0–5.0 mM. The MIC was defined as the lowest concentration of Me^{n+} that completely inhibited bacterial growth.

2.9. Detection of Siderophores and Their Chemical Nature. The production of siderophores was examined by aerobic growth experiment on GASN medium [16]. The concentration of siderophores present in culture supernatants was measured using the method described by Schwyn and Neilands [24]. A standard curve was prepared with deferoxamine mesylate (DFOB). The quantity of siderophores produced was determined from the standard curve using CAS assay solution [24] and the absorbance value measured at 630 nm after 1 h of incubation [25] and denoted as mM DFOB. Detection of hydroxamate siderophores was performed using $FeCl_3$ test [26] and for catecholates the Arnow test was used [27].

2.10. Test for Dissolution of Arsenic Minerals by Siderophores Produced by the Isolates. Modified method described by Drewniak et al. (2010) [10] was used for determination of bacterial siderophores ability to dissolve arsenopyrite (FeAsS) and arsenic minerals (enargite (Cu_3AsS_4) and tennantite ($(Cu,Ag,Fe,Zn)_{12}As_4S$)) contained in copper ore concentrates and middlings. The following modifications were made: in dissolution reactions, 50 mL of 0.2 mM bacterial siderophores and sterile GASN medium (as a control) were added to 0.5 g of a given, sterile mineral, and the concentrations of As and Fe in the solution were measured after 48 h of incubation in aerobic conditions at 22°C using graphite furnace atomic absorption spectrometry (GFAAS) (AA Solaar M6 Spectrometer, TJA Solutions, UK). The method of siderophores preparation was as follows: (i) strains were grown in GASN medium for 24 h at room temperature in aerobic conditions, (ii) the cultures were then centrifuged (10,000 ×g, 10 min.), and the supernatants were used as siderophore preparations. Siderophores concentration was extrapolated from a standard curve and represented in mM of desferrioxamine B (DFOB).

2.11. Arsenic Minerals Utilization in Respiratory Processes. The ability of the isolates to utilize arsenic containing minerals (copper ore concentrates and middlings obtained from KGHM S.A, Poland) in respiratory processes was examined in the MSM medium supplemented with 5 mM sodium lactate as the electron donor and as the sole carbon source. Sterilized, powdered samples of minerals were added to the MSM medium (100 mL) to a final concentration of 1% (w/v) and were inoculated with cells from fresh overnight cultures to a final density of approximately 10^6 cells/mL. The cultures were incubated at 22°C for 21 days under anaerobic conditions, when the ability to use the investigated minerals as a final electron acceptor was tested. Noninoculated samples were used as controls. The cultures were sampled for chemical analyses (pH, heavy metal concentration, and arsenic speciation) and estimation of colony forming unit (cfu) at the start of the experiment and every 7 days.

2.12. Nucleotide Sequence Accession Number. The 16S rRNA gene sequence of isolated strains has been deposited in GenBank under accession numbers KF986639, KF986640, KF986641, and KF986642.

3. Results and Discussion

3.1. Isolation and Identification of Dissimilatory Arsenate Reducers. Microbial mats form sediments sampled from the ancient Zloty Stok gold mine (SW Poland) were used as the source of arsenic-metabolizing microbes, for several reasons. Our previous studies [20] showed that the physical and chemical conditions prevailing in the Zloty

Stok mine promote the growth and development of arsenic-transforming microbes. Arsenic in the mine is present in soluble form as arsenite and arsenate in mine waters and also occurs as primary (arsenopyrite and lollingite) and secondary minerals (such as scorodite) deposited in the rocks and sediments [28]. The mine waters and sediments also contain high amounts of other heavy metals (e.g., Cu, Co, Mn, and Zn) and therefore the microbial mats seemed to be an ideal source for the isolation of model dissimilatory arsenate reducing bacteria (DARB) that can be capable of dissolution of arsenic-bearing minerals. Regardless of the mechanism of arsenic release from polymetallic ores/minerals, microorganisms that are involved in dissolution processes should be adequately adapted to the surrounding conditions, for example, resistance to arsenic and heavy metals.

Microbial mats were inoculated into the modified MSM medium supplemented with 2.5 mM sodium arsenate and 5 mM sodium lactate. After 7 days of incubation under anaerobic conditions, enrichments were subcultured twice for 7 days each and the cultures were plated on MSM agar. Morphological observations (colony colours and cell shape), physiological test ($AgNO_3$ test), and 16S rRNA gene analysis (ARDRA analysis and sequencing) allowed for the identification of four different strains (OM1, OM2, OM4, and OM17) capable of anaerobic growth with As (V) reduction. BLASTN analysis of partial 16S rDNA sequences (~1.4 kbp) showed that all the isolates belonged to the class γ-Proteobacteria. The nearest known phylogenetic relative of the strain OM1, with a sequence similarity of 99%, is *Shewanella* sp. OTUC2. The strain OM2 showed the highest similarity (99%) to genus *Pseudomonas koreensis* strain JH18. The strain OM4 was closely related (100% of similarity) to genus *Aeromonas hydrophila*, whereas strain OM17 was closely related (99% of similarity) to *Serratia liquefaciens* ATCC 27592. Phylogenetic studies confirmed BLASTN analysis and showed that 16S rRNA gene sequences of all isolates are located in clusters of closely related species within the class γ-Proteobacteria (Figure 1). Interestingly, two strains, *Aeromonas* sp. OM4 and *Serratia* sp. OM17, are the first described representatives of their genera, which are capable of dissimilatory arsenate reduction. So far described *Aeromonas* spp. and *Serratia* spp. strains were able to reduce arsenate, but only using cytoplasmic reductase as a resistance mechanism [20, 29, 30].

All of the tested bacteria showed a broad range of temperature tolerance: 4–37°C, with the optimum at 30°C (OM1, OM2, and OM17) and 37°C (OM4) (Table 1). The pH optimum was found to be slightly acidic or close to neutral (4–7), but growth at alkaline pH (10) was also observed (Table 1). Ability to grow in a broad range of pH and temperature conditions makes the isolated strains potential biotechnological tools for bioremediation of arsenic-contaminated sites. One of the main factors limiting the use of bacteria in bioremediation technologies is a sensitivity of strains to changing physicochemical conditions. The broad spectrum of tolerance to pH and temperature increases the chances of survival in the environment.

3.2. Detoxification Mechanisms. The primary role of microorganisms living under unfavourable environmental conditions is to survive. Detoxification mechanisms that protect against harmful substances are very often connected with processes that require energy supply and sometimes are associated with respiratory processes in which energy is generated. The most common mechanism of detoxification is based on blocking the membrane channels through which toxic substances enter the cell. Another method of protection relies on the active removal out of the cell using specific membrane pumps [31]. Arsenite ions are directly removed by membrane permeases, while arsenates ions require transformation into the arsenites prior to removal. In this study we have verified the level of arsenic resistance and we investigated the presence of cytoplasmic arsenate reductase genes (*arsC*) in the genomes of the isolated strains.

The isolates were hypertolerant to arsenate (250–400 mM) and showed high resistance to arsenite (10–16 mM). *Serratia* sp. OM17 was the most resistant to As (V) isolate, which tolerated concentrations of arsenate up to 400 mM. The highest MIC for As (III) was found for *Aeromonas* sp. OM4, which tolerated concentrations of arsenite up to 16 mM. Such high resistance to arsenic was also found in other arsenic-tolerating microorganisms, but any described arsenic hypertolerant strain was able to use As (V) in dissimilatory arsenate reduction [20, 32]. The presence of *arsC* gene was confirmed in the genomes of all of the tested strains (Table 1). BLASTN results showed that *arsC* genes of *Shewanella* sp. OM1, *Pseudomonas* sp. OM2, and *Serratia* sp. OM17 have a high similarity to cytoplasmic arsenate reductases genes of closely related species. Nucleotide sequence of *arsC* gene of *Shewanella* sp. OM1 is 78% identical to the arsenate reductase gene of *Shewanella putrefaciens* CN-32. The *arsC* sequence of *Pseudomonas* sp. OM2 is 84% identical to the arsenate reductase gene of *Pseudomonas denitrificans* ATCC 13867, while the *arsC* of *Serratia* sp. OM17 is 96% identical to the arsenate reductase gene of *Serratia liquefaciens* ATCC 27592. In turn, the *arsC* gene of *Aeromonas* sp. OM4 is 76% identical to arsenate reductase of *Acidovorax ebreus* TPSY. Phylogenetic analysis showed that the *arsC* genes of the OM isolates are closely related to the arsenate reductase gene sequences of known arsenic resistant strains, but not necessarily from the same species (see Figure S1 available online at http://dx.doi.org/10.1155/2014/841892).

In the context of arsenic minerals dissolution, equally important as arsenic resistance is the tolerance to other heavy metals, such as Cu, Co, Cd, Zn, Fe, Ni, and Pb. The level of resistance to the tested metals was between 0.25 and 4 mM: Cu (II) (for all strains up to 4 mM), Co (II) (OM1 and OM17 0.75 mM, OM2 0.5 mM, and OM4 1 mM), Cd (II) (OM1, OM2, and OM4 0.25 mM and OM17 0.5 mM), Zn (II) (OM1 and OM 17 up to 3.5 mM, OM2 1 mM, and OM4 0.75 mM), Fe (III) (for all the strains up to 2 mM), Ni (III) (OM1 and OM4 up to 3 mM and OM2 and OM17 up to 2.5 mM), and Pb (II) (for all the strains up to 2 mM). Such heavy metal multiresistance enables their active growth in environments rich in heavy metals.

3.3. Description of the Process That Promotes Arsenic Mobilization. The mechanisms of microbial arsenic mobilization depend on many biogeochemical factors, among which

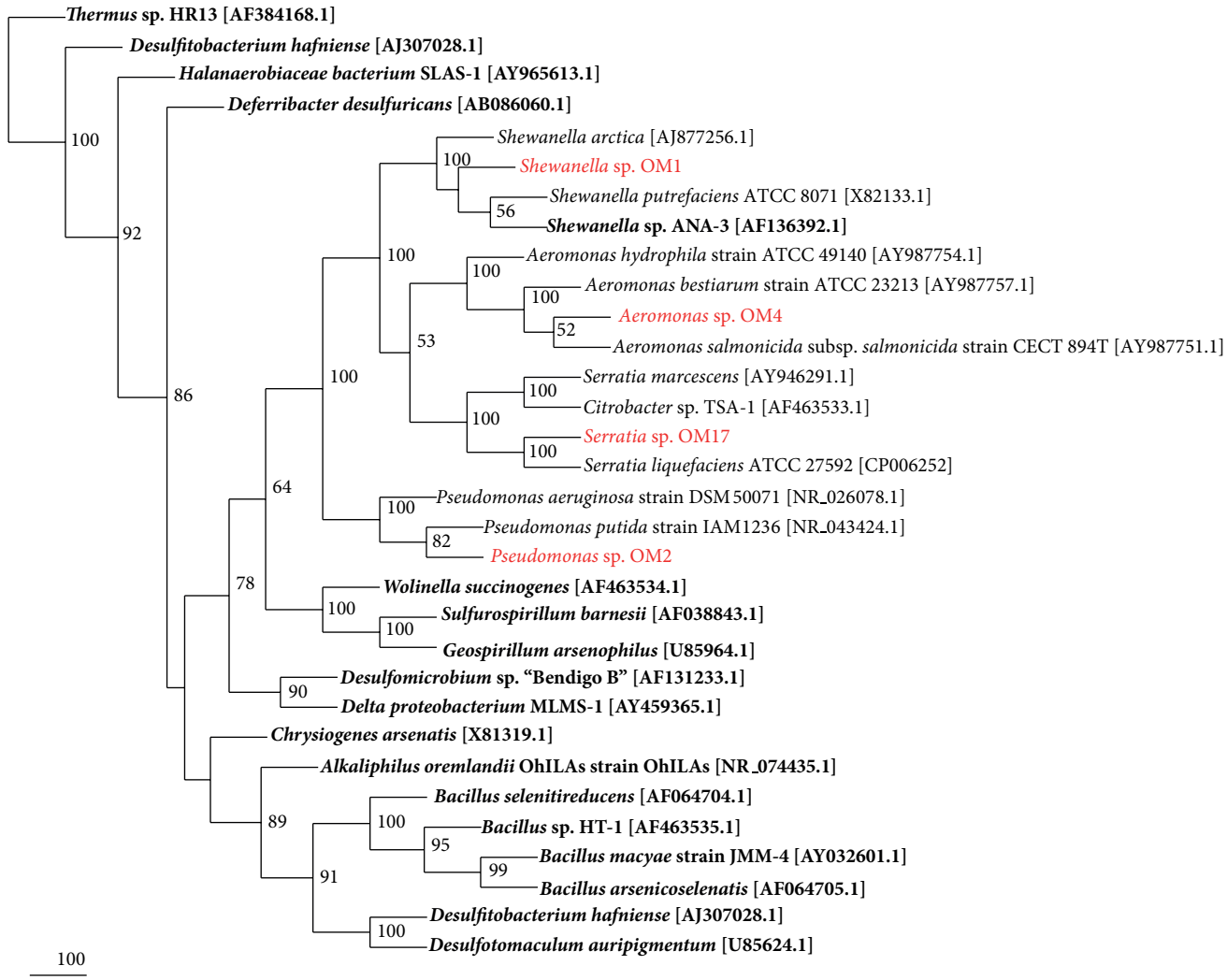

Figure 1: Neighbour-joining tree, computed based on the alignment of 16S rRNA gene sequences, showing the phylogenetic relationship of arsenic-respiring isolates with known arsenic resistant and dissimilatory arsenate reducing bacteria. The analysis included the data from ~1400 nucleotide positions. The tree is a consensus of 100 neighbor-joining trees. Percentage values on each branch represent the corresponding bootstrap probability values obtained in 100 replications and numbers are shown only for values of >50%. Sequences derived from arsenic-respiring isolates (OM1, OM2, OM4, and OM17) are indicated in large bold red type; sequences derived from other dissimilatory arsenate reducing bacteria are indicated in black bold type. The remaining sequences indicated in normal type derived from strains that are only resistant to arsenic.

Table 1: Tolerance to arsenic and arsenate reductase activity and the presence of arsenic metabolism genes.

Strain	Temperature (°C)		pH		MIC for AsV (mM)	MIC for AsIII (mM)	Presence of genes coding for cytoplasmic and respiratory arsenate reductases	
	Range	Optimum	Range	Optimum			*arsC*	*arrA*
Shewanella sp. OM1	4–37	30	5–10	7	350	10	+	+
Pseudomonas sp. OM2	4–37	30	5–9	5	250	14	+	+
Aeromonas sp. OM4	4–37	37	5–8	5	350	16	+	+
Serratia sp. OM17	4–37	30	4–10	4	400	12	+	+

the most important seem to be the following: the presence of the appropriate physiological group of microbes, type of minerals (primary or secondary), pH (acidic or neutral), Eh (reductive or oxidative conditions), and the availability of oxygen or other electron acceptors. Direct mechanisms of arsenic mobilization include oxidative dissolution of primary arsenic minerals and reductive dissolution of secondary arsenic minerals [6].

3.3.1. Arsenate Respiration Process. To test the isolates for the ability to grow by arsenate respiration, anaerobic growth experiments were conducted. All of the isolates grew with 5 mM sodium lactate as the electron donor and 2.5 mM sodium arsenate as the electron acceptor (Figure 2). In almost all of the cultures (except *Aeromonas* sp. OM4) arsenate reduction was observed during the exponential phase, in which the growth rate and the rate of As (V) reduction were proportional. Growth did not occur when medium without arsenate was used or arsenate was completely utilized, indicating that arsenate was required for growth. The *Serratia* sp. OM17 strain was found to be the most efficient isolate, in terms of the highest arsenate reduction rate [7.81 mg As (V) $\cdot L^{-1} \cdot h^{-1}$]. Complete reduction of 2.5 mM (187.5 mg$\cdot L^{-1}$) arsenate into arsenite was observed after 48 h of incubation. Other strains had a slightly lower arsenate reduction rate, and the complete transformation of As (V) into As (III) required at least 72 hours of incubation. *Shewanella* sp. OM1 and *Pseudomonas* sp. OM2 completely reduced 2.5 mM of As (V) to As (III) within 72 hours, while *Aeromonas* sp. OM4 within 96 hours. In addition to the lowest As (V) reduction rate, *Aeromonas* sp. OM4 was not able to completely reduce arsenates.

All of the tested strains were unable to reduce the arsenate at concentrations above 2.5 mM, despite their ability to tolerate high concentrations of As (III) (10–16 mM) and As (V) (250–400 mM). Interestingly, most of dissimilatory arsenate reducers isolated during similar studies were able to reduce arsenate at much higher concentrations, exceeding 10 mM [11, 33] and sometimes reaching up to 40 mM [34], although they come from environments in which the arsenic is present at a similar level as in Zloty Stok gold mine (isolation site of the tested strains).

Similar to other known arsenic respiratory strains, the *arrA* gene (coding for the large subunit of dissimilatory arsenate reductase) was found in the genomes of all of the isolates. BLASTN results showed that all dissimilatory arsenate reductase genes of the isolates (OM1, OM2, OM4, and OM17) are closely related to *arrA* genes detected in metagenomic studies and described as uncultured bacterium clones. In turn, phylogenetic studies with the use of *arrA* sequences of the isolates and known arsenic respiratory bacteria showed that arsenic respiratory genes of the OM (1, 2, 4, and 17) isolates form a common, separate cluster and they are not closely related to the genes of their phylogenetic relatives.

3.3.2. Dissolution of Arsenic Containing Minerals by Metabolites Produced by DARB. Nutrient uptake from minerals may be performed by different mechanisms. Microorganisms may cause disaggregation of minerals through colonization and physical penetration of the mineral surface [35]. Extraction of vital elements from the crystal lattice of minerals may be also supported by organic agents produced by the cells. Among the most common microbial organic agents involved in minerals dissolution are siderophores: high-affinity, metal-binding compounds secreted outside the cell envelope that can chelate metal ions and bind to atoms on the mineral surface. They can effectively bind many metal cations including Fe, Mg, Mn, Cr, Ga, Pl, Pb, Cd, Zn, Cu, Ni, U, Co, Sn, and As [36–40].

Biochemical tests showed that under iron-limiting conditions all the DARB isolates produce siderophores that are classified to the hydroxamate-type. The highest concentration of siderophores in GASN medium after 48 h of incubation at 22°C was noted in the culture of *Aeromonas* sp. OM4 (118 μM) and the lowest in the *Shewanella* sp. OM1 culture (88 μM). *Pseudomonas* sp. OM2 and *Serratia* sp. OM17 produced siderophores at similar levels, 116 μM and 110 μM, respectively.

A further issue that needs clarification is the ability of the siderophores, produced by the selected strains, to dissolve (i) arsenopyrite and (ii) middlings and copper concentrates containing arsenic minerals (enargite, realgar, and tennantite). For this purpose, cell-free metabolites (containing siderophores) obtained from the cultivation of the DARB isolates under iron and arsenic limiting conditions in GASN medium were used.

After 48 h of leaching of arsenic minerals by the DARB siderophores, iron and arsenic were released into the solutions of all of the tested samples. Siderophores produced by most of the tested strains show the capacity to release arsenic from minerals at a level similar to the control. In the case of arsenopyrite dissolution by siderophores, only metabolites produced by *Serratia* sp. OM17 showed significant differences in the release of arsenic in relation to the control sample. The concentration of arsenic in the OM17 siderophores solution was almost eleven times higher than in the control sample (4.07 mg/L of As was noted in *Serratia* sp. OM17 siderophores solution, whereas 0.37 mg/L in sterile GASN medium). Twice as high concentration of arsenic than in the control was observed in the siderophores solution of the *Aeromonas* sp. OM4 strain. The concentration of arsenic mobilized from arsenopyrite by siderophores produced by two other strains (OM1 and OM2) was slightly higher (1.37 and 1.8 times, resp.) than in the control (Figure 3(a)). The release of arsenic from copper concentrate and middlings by siderophores was inefficient and arsenic concentrations were at the level of the control. The highest concentration of arsenic in the middlings dissolution was observed when the siderophores solution of *Shewanella* sp. OM1 was used (1.47 times higher than the control) (Figure 3(b)). In the case of copper ore concentrates, the highest concentration of arsenic was observed when siderophores solution of *Serratia* sp. OM17 was used (1.66 times higher than in the control) (Figure 3(c)).

In contrast to arsenic case, the iron concentration in almost all of the samples was at a much higher level than in the control. The highest iron concentration in arsenopyrite

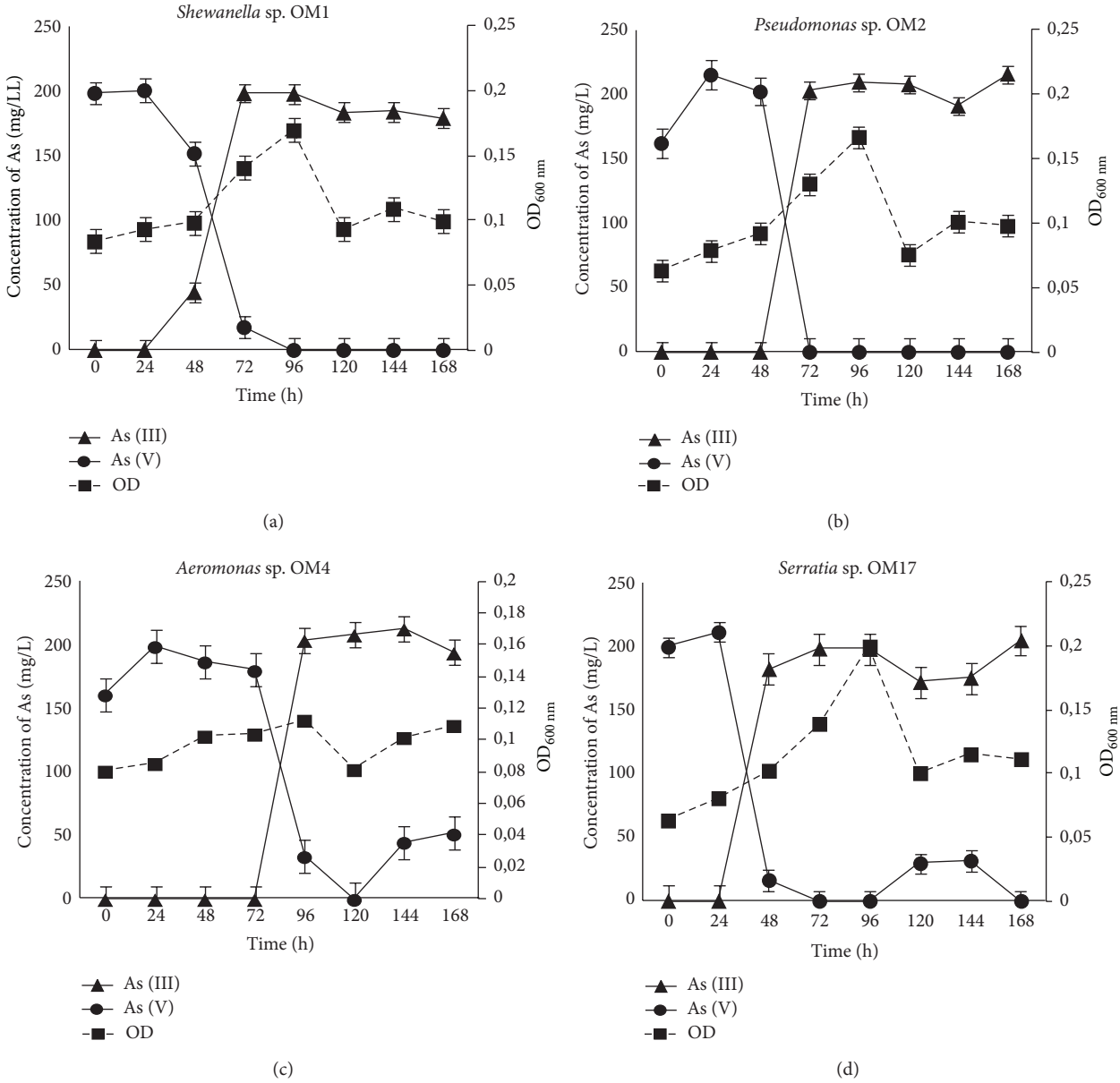

Figure 2: Dissimilatory arsenate reduction mediated by *Shewanella* sp. OM1, *Pseudomonas* sp. OM2, *Aeromonas* sp. OM4, and *Serratia* sp. OM17. Arsenate respiratory processes were tested using cultures grown under anaerobic conditions in the MSM medium, supplemented with 2.5 mM sodium arsenate and 5 mM sodium lactate.

sample was observed in the siderophores solution of *Serratia* sp. OM17 (Figure 3(a)), in which the concentration of Fe exceeded ~72 times the iron content recorded in the control sample. In the middlings and copper ore concentrates samples, the highest iron concentrations were observed when the siderophores solution of *Pseudomonas* sp. OM2 was used (25 times and 12.5 higher than the control in the middlings and copper concentrates, resp.) (Figures 3(b) and 3(c)). Regardless of the copper mineral, the lowest concentration of iron was noted in the case of siderophores produced by *Shewanella* sp. OM1 (only 1.5 times more than in the control with copper concentrates) (Figure 3(c)).

The obtained results demonstrate that siderophores produced by dissimilatory arsenate reducers are involved in dissolution of arsenic containing minerals. Based on the results it can be concluded that the mechanism of arsenic minerals dissolution can be driven by iron uptake through siderophores, while arsenic is released simultaneously as by-product. These results are consistent with the previously described arsenic mobilization mechanisms used by dissimilatory iron reducers [14, 41].

3.4. Removal of Arsenic from As-Containing Minerals. It is commonly known that the release of arsenic from As-bearing

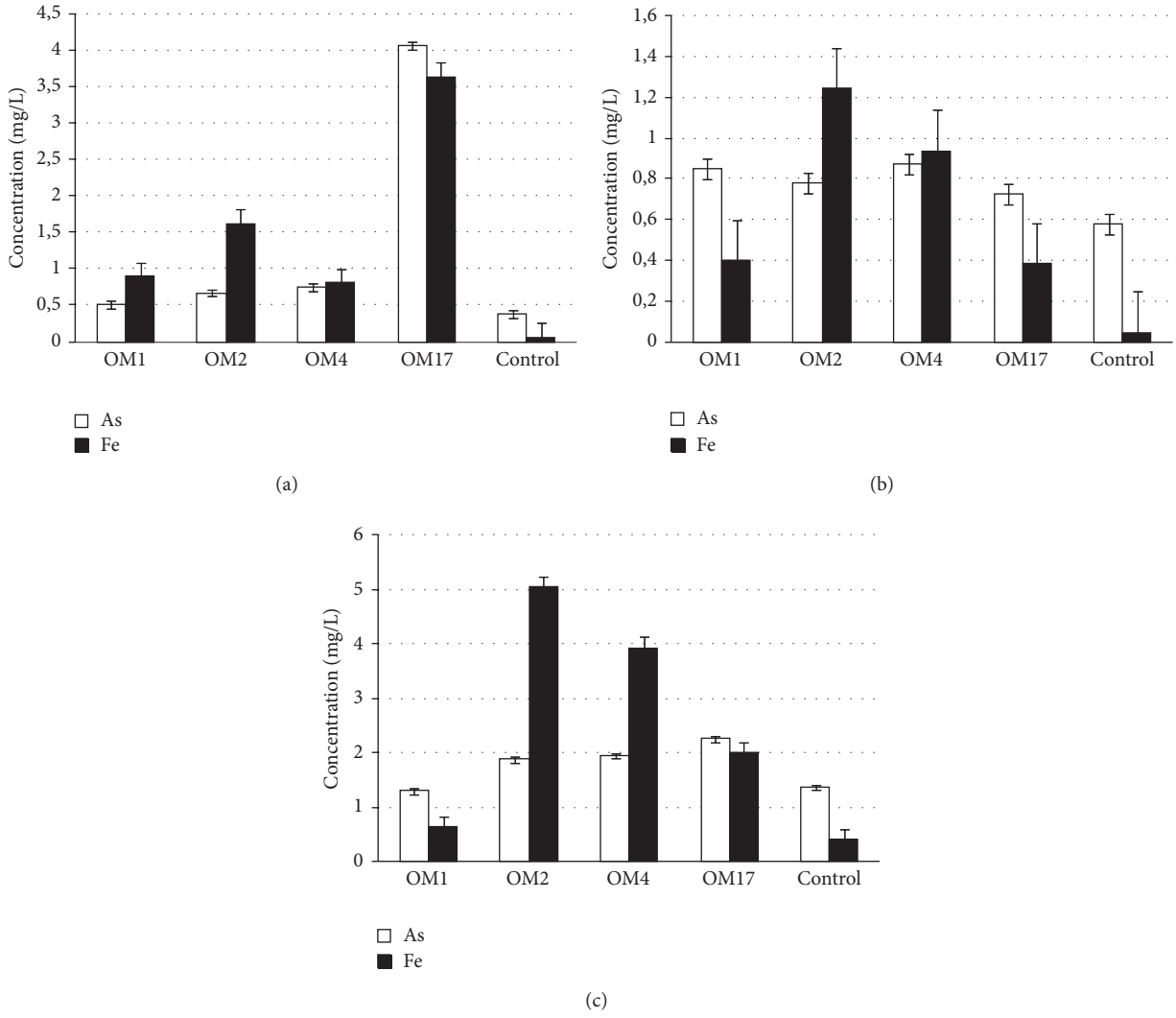

Figure 3: Release of arsenic and iron from arsenopyrite (a), middlings (b), and copper ore concentrates (c), after 48 h of incubation with sterile GASN medium as a control, and siderophores produced by the isolated strains: *Shewanella* sp. OM1, *Pseudomonas* sp. OM2, *Aeromonas* sp. OM4, and *Serratia* sp. OM17.

minerals may take place by two main processes: (i) oxidation of the primary arsenic minerals and (ii) reductive dissolution of the secondary minerals. Primary As-minerals such as arsenopyrite or realgar can be dissolved by direct or indirect mechanisms in the presence of oxygen by chemolithoautotrophic microorganisms [42]. In turn, under reducing conditions, microorganisms can use arsenate adsorbed on the surface of iron minerals (e.g., scorodite or ferrihydrite) as a terminal electron acceptor in arsenic respiration [14, 43].

In the literature, there is not much information concerning the release of arsenic from the primary minerals under reducing conditions. Thus, it is interesting to investigate if under anaerobic conditions bacteria are capable of arsenic mobilization from primary minerals and in particular whether they are able to use such minerals in the process of respiration as an electron donor. In order to verify the above hypothesis we performed respiration experiments using primary arsenic minerals as the final electron acceptors. Arsenopyrite (FeAsS), as one of the most common primary arsenic minerals, containing arsenic in reduced form, was used in this experiment as a control in which bacterial cells have not final electron acceptor. Copper concentrates and middlings were used as a source of primary arsenic mineral (such as enargite), in which arsenic occurs as arsenate. Both Cu-sources are polymetallic and contain arsenic as impurities (0.37% for the concentrates and 0.029% for the middlings). The ability of the isolates to utilize arsenic containing minerals in respiratory processes was examined in the MSM medium supplemented with 5 mM lactate as the electron donor and the sole carbon source and 1% of appropriate mineral as a source of electron donors.

As predicted, none of the isolated strains were capable of using arsenopyrite as a respiratory substrate. Growth was not observed in any culture, but only death phase. Number of

colony forming units decreased from the initial 10^6 cfu/mL to 10^2–10^3 cfu/mL after 21 days of incubation in all cultures. There were no significant changes in pH. After 7 days of incubation pH in all cultures increased to ~8.5 and remained stable until the end of the experiment (in control sample the pH was stable throughout the experiment). The concentrations of arsenic and iron in the supernatants exceeded the levels observed in the control sample (sterile medium), but the amount of mobilized arsenic and iron was low (Figure 4), especially if the total arsenic and iron content in arsenopyrite was taken into account. The mobilization of small amounts of As and Fe from FeAsS by the cells being in decline phase can be explained by an unspecific dissolution of arsenopyrite by metabolites (e.g., ligands and organic acids) released during cell lysis. Thus dissolution in reductive conditions mediated by dissimilatory arsenate reducing bacteria is not the main driving force leading to arsenic mobilization from arsenopyrite, but only a passive process that should be taken into account during long-term environmental risk assessment. These results are in accordance with the current knowledge about the microbiological dissolution of the primary arsenic minerals; that is, the primary arsenic minerals are mainly utilized under aerobic conditions by oxidative dissolution [6].

A quite different effect was observed in the respiration experiments with arsenic containing copper sulfide minerals used as the final electron acceptor. All of the strains were capable of growing under anaeorobic conditions in the MSM medium containing (1%) sterile Cu-minerals as the sole electron acceptor and considerable arsenic concentrations were detected in all of the culture supernatants after 21 days of incubation (Figure 5). In almost all of the cultures, the concentration of arsenic in the culture supernatants increased in time (Figures 5(a1) and 5(b1)) and correlated with the rates of growth (data not shown). The final amount of the removed arsenic oscillated between 19.28 and 81.95 mg/kg (6.6% and 28.1%) for the middlings (Figure 5(a1)) and 7.93 and 76.75 mg/kg (0.21% and 2.03%) for copper ore concentrates (Figure 5(b1)). The most efficient strain, in terms of arsenic release, was *Aeromonas* sp. OM4 strain cultured in middlings and copper ore concentrate (As concentration in culture liquid reached 819.50 and 922.50 μg/L, resp.). The lowest level of arsenic removal was observed for *Shewanella* sp. OM1 culture (As concentration in culture liquid was 192.75 μg/L for middlings and 678.75 μg/L for copper ore concentrates) (Figures 5(a1) and 5(b1)). Irrespective of which strain was used, the effectiveness of arsenic extraction was 10 times higher in the middlings than in the copper ore concentrates leaching experiment. The maximum recovery of arsenic from middlings was 28.11% after 21 days for *Aeromonas* sp. OM4 (Figure 6), while the maximum recovery of arsenic from copper ore concentrates was 2.47% at 21 days for *Pseudomonas* sp. OM2 (Figure 6). For all of the strains, the arsenic recovery process was selective and was not associated with simultaneous removal of copper (Figures 5(a2) and 5(b2)). High concentration of copper was noted in all of the samples at the beginning of cultivation (Figures 5(a2) and 5(b2)), which was probably associated with chemical leaching

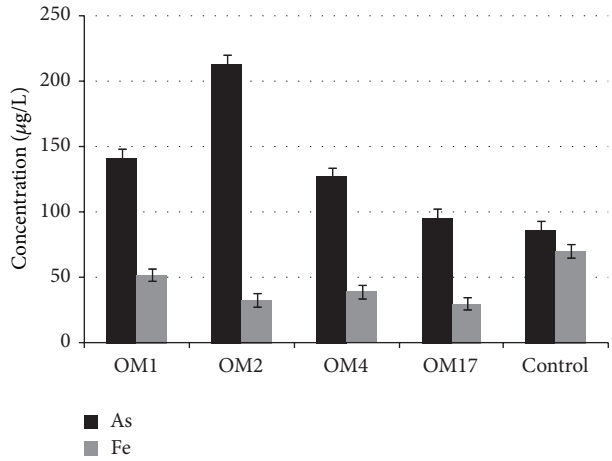

Figure 4: Arsenopyrite dissolution under anaerobic conditions by dissimilatory arsenate reducing bacteria: *Shewanella* sp. OM1, *Pseudomonas* sp. OM2, *Aeromonas* sp. OM4, and *Serratia* sp. OM17. As and Fe concentrations in culture liquid after 21 days of incubation under anaerobic condition in MSM medium supplemented with 1% FeAsS and 5 mM sodium lactate.

of copper (by medium components and residual metabolites from the overnight cultures). Moreover, in all of the cultures and control samples, copper concentration decreased with time. Only in the case of *Serratia* sp. OM17 cultured on middlings, elevated level of copper leaching (767.50 μg/kg) was reported after 21 days of incubation. However, it should be noted that the resulting value represents only 0.04% of the initial copper content. These results may indicate the slow copper precipitation process under neutral conditions (pH fluctuated around 7.5 ± 0.4 during the experiment) and absence of microbial activity connected with the leaching of copper.

On the basis of the above results we can postulate that arsenic can be released from some As-bearing polymetallic minerals (such as copper ore concentrates or middlings) in reductive conditions by dissimilatory arsenate reducers. However, the mechanisms of arsenic release are still unknown. Comparing the data from the arsenopyrite and copper concentrates/middlings respiration experiment, we can only assume that the mechanism of arsenic release from Cu-minerals is indirect. To understand how the DARPs release arsenic from minerals, deep physiological and microbe-mineral interaction (including arsenic speciation) analysis is needed. The ability to use different inorganic electron donors (e.g., Fe^{2+} or S^{2-}), which may be conjugated to electron acceptors other than oxygen (e.g., NO_3^- and $As_3O_5^{3-}$), requires verification. Similarly, the hypothesis that bacteria can utilize polymetallic sulfide as a source of enzyme cofactors such as Mo, Cu, Zn, and Mg [35] must be also verified.

4. Conclusions

In this work, we have shown that dissimilatory arsenate reducing bacteria have a great potential for arsenic

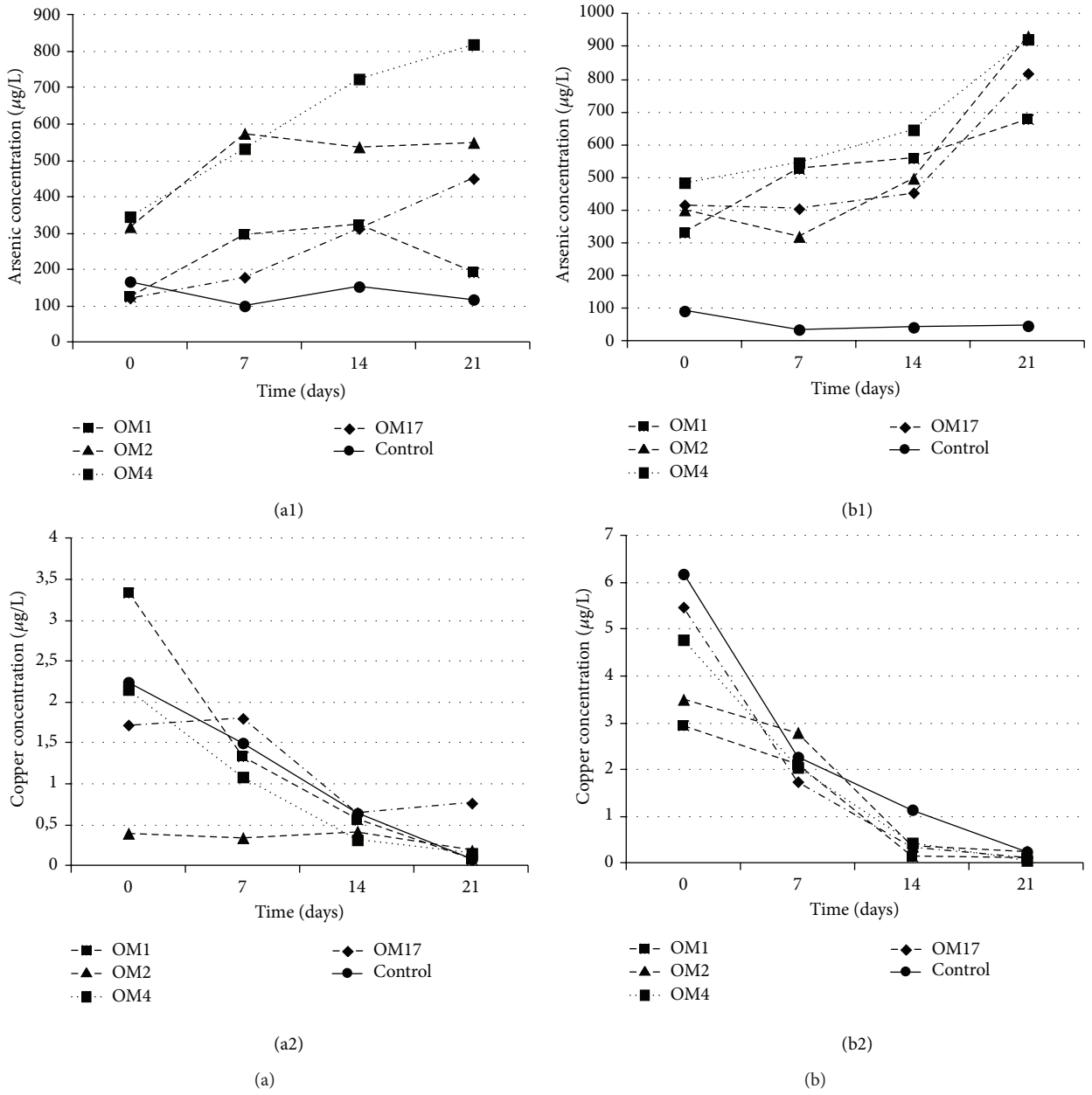

Figure 5: Dissolution of As-bearing copper minerals mediated by dissimilatory arsenate reducing bacteria. Arsenic (1) and copper (2) release during 21 days of incubation in MSM medium supplemented with 5 mM sodium lactate and (a) 1% middlings and (b) 1% copper ore concentrates.

mobilization into the environment, not only from secondary arsenic minerals but also from the primary arsenic minerals deposited in polymetallic ores. All of the isolated strains give positive results in the arsenic respiratory test. They effectively grew with sodium lactate as the electron donor and sodium arsenate as the electron acceptor. Resistance to high concentrations of arsenite and arsenate, as well as a number of other heavy metal compounds, was another common feature of the isolates. Moreover, all of the strains displayed the ability to grow in a broad range of pH values and temperatures and under both aerobic and anaerobic conditions. Under iron-limiting conditions all of the isolated DARBs produced siderophores that were involved in dissolution of arsenic containing minerals. None of the isolated strains were capable of using arsenopyrite as a respiratory substrate, but (low efficient) arsenopyrite dissolution in reductive conditions was observed. We postulate that it was only as a passive process, in which metabolites (e.g., ligands and organic acids) released during cell lysis may play a key role. In turn, utilization of As-bearing copper minerals in respiratory processes was efficiently carried out by most of the isolates. The DARBs strains were capable of growing under anaerobic conditions

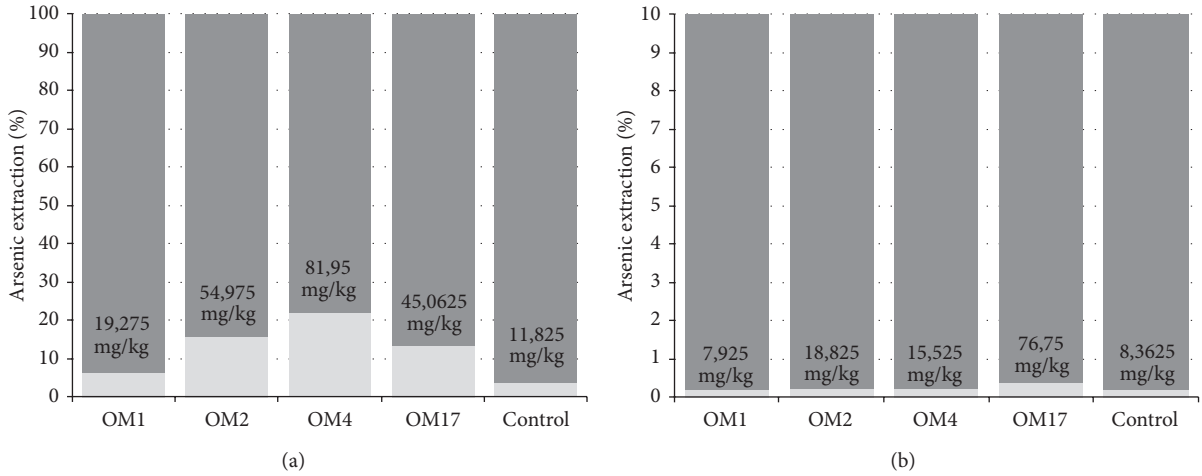

Figure 6: Comparison of effectiveness of arsenic removal from middlings (a) and copper ore concentrates (b) mediated by dissimilatory arsenate reducing bacteria: *Shewanella* sp. OM1, *Pseudomonas* sp. OM2, *Aeromonas* sp. OM4, and *Serratia* sp. OM17.

using As-bearing polymetallic minerals as the sole electron acceptor. Arsenic release from Cu-minerals was selective (not associated with simultaneous removal of copper) and as we concluded the process was indirect. This work clearly showed that the release of arsenic from primary As-minerals included in the polymetallic ores or wastes from their processing (such as copper concentrates and middlings) is possible under reducing conditions, but the mechanism is still unknown and requires further, detailed mineral-microbe interaction studies (to complete understanding).

Conflict of Interests

The authors declare that there is no conflict of interests regarding the publication of this paper.

Acknowledgment

This work was supported by the Polish Ministry of Science and Higher Education in the form of Grant Juventus Plus no. 0079/P01/201070.

References

[1] D. J. Vaughan, "Arsenic," *Elements*, vol. 2, no. 2, pp. 71–75, 2006.

[2] T. H. Hoang, J.-Y. Kim, and S. Bangb, "Source and fate of As in the environment," *Geosystem Engineering*, vol. 13, no. 1, pp. 35–42, 2010.

[3] N. L. Piret, "Removal and safe disposal of arsenic in copper processing," *JOM*, vol. 51, no. 9, pp. 16–17, 1999.

[4] D. Filippou, P. St-Germain, and T. Grammatikopoulos, "Recovery of metal values from copper—arsenic minerals and other related resources," *Mineral Processing and Extractive Metallurgy Review*, vol. 28, no. 4, pp. 247–298, 2007.

[5] J. P. Demaerel, "The behaviour of arsenic in the electrorefining process," in *The Electrorefining and Winning of Copper*, H. J. E, Ed., pp. 195–209, TMS, Warrendale, Pa, USA, 1987.

[6] L. Drewniak and A. Sklodowska, "Arsenic-transforming microbes and their role in biomining processes," *Environmental Science and Pollution Research International*, vol. 20, no. 11, pp. 7728–7739, 2013.

[7] M.-N. Collinet and D. Morin, "Characterization of arsenopyrite oxidizing Thiobacillus. tolerance to arsenite, arsenate, ferrous and ferric iron," *Antonie van Leeuwenhoek, International Journal of General and Molecular Microbiology*, vol. 57, no. 4, pp. 237–244, 1990.

[8] D. B. Johnson and K. B. Hallberg, "The microbiology of acidic mine waters," *Research in Microbiology*, vol. 154, no. 7, pp. 466–473, 2003.

[9] E. D. Rhine, K. M. Onesios, M. E. Serfes, J. R. Reinfelder, and L. Y. Young, "Arsenic transformation and mobilization from minerals by the arsenite oxidizing strain WAO," *Environmental Science and Technology*, vol. 42, no. 5, pp. 1423–1429, 2008.

[10] L. Drewniak, R. Matlakowska, B. Rewerski, and A. Sklodowska, "Arsenic release from gold mine rocks mediated by the activity of indigenous bacteria," *Hydrometallurgy*, vol. 104, no. 3-4, pp. 437–442, 2010.

[11] A. M. Laverman, J. S. Blum, J. K. Schaefer, E. J. P. Phillips, D. R. Lovley, and R. S. Oremland, "Growth of strain SES-3 with arsenate and other diverse electron acceptors," *Applied and Environmental Microbiology*, vol. 61, no. 10, pp. 3556–3561, 1995.

[12] T. Krafft and J. M. Macy, "Purification and characterization of the respiratory arsenate reductase of Chrysiogenes arsenatis," *European Journal of Biochemistry*, vol. 255, no. 3, pp. 647–653, 1998.

[13] D. K. Newman, E. K. Kennedy, J. D. Coates et al., "Dissimilatory arsenate and sulfate reduction in Desulfotomaculum auripigmentum sp. nov," *Archives of Microbiology*, vol. 168, no. 5, pp. 380–388, 1997.

[14] J. Zobrist, P. R. Dowdle, J. A. Davis, and R. S. Oremland, "Mobilization of arsenite by dissimilatory reduction of adsorbed arsenate," *Environmental Science and Technology*, vol. 34, no. 22, pp. 4747–4753, 2000.

[15] J. Sambrook and D. W. Russell, *Molecular Cloning: A Laboratory Manual*, Cold Spring Harbor Laboratory Press, New York, NY, USA, 2001.

[16] A. Bultreys and I. Gheysen, "Production and comparison of peptide siderophores from strains of distantly related pathovars of Pseudomonas syringae and Pseudomonas viridiflava LMG 2352," *Applied and Environmental Microbiology*, vol. 66, no. 1, pp. 325–331, 2000.

[17] D. D. Simeonova, D. Lièvremont, F. Lagarde, D. A. E. Muller, V. I. Groudeva, and M.-C. Lett, "Microplate screening assay for the detection of arsenite-oxidizing and arsenate-reducing bacteria," *FEMS Microbiology Letters*, vol. 237, no. 2, pp. 249–253, 2004.

[18] J. Namieśnik, B. Zygmunt, and A. Jastrzębska, "Application of solid-phase microextraction for determination of organic vapours in gaseous matrices," *Journal of Chromatography A*, vol. 885, no. 1-2, pp. 405–418, 2000.

[19] L. Drewniak, R. Matlakowska, and A. Sklodowska, "Arsenite and arsenate metabolism of sinorhizobium sp. M14 living in the extreme environment of the zloty stok gold mine," *Geomicrobiology Journal*, vol. 25, no. 7-8, pp. 363–370, 2008.

[20] L. Drewniak, A. Styczek, M. Majder-Lopatka, and A. Sklodowska, "Bacteria, hypertolerant to arsenic in the rocks of an ancient gold mine, and their potential role in dissemination of arsenic pollution," *Environmental Pollution*, vol. 156, no. 3, pp. 1069–1074, 2008.

[21] D. Malasarn, C. W. Saltikov, K. M. Campbell, J. M. Santini, J. G. Hering, and D. K. Newman, "*arrA* is a reliable marker for As(V) respiration," *Science*, vol. 306, no. 5695, p. 455, 2004.

[22] D. J. Lane, "16S/23S rRNA sequencing," in *Nucleic Acid Techniques in Bacterial Systematics*, E. Stackebrandt and M. Goodfellow, Eds., pp. 115–175, Wiley, New York, NY, USA, 1991.

[23] J. Felsenstein, *PHYLIP (Phylogeny Inference Package)*, Department of Genome Sciences, University of Washington, Seattle, Wash, USA, 2005.

[24] B. Schwyn and J. B. Neilands, "Universal chemical assay for the detection and determination of siderophores," *Analytical Biochemistry*, vol. 160, no. 1, pp. 47–56, 1987.

[25] F. A. Fekete, V. Chandhoke, and J. Jellison, "Iron-binding compounds produced by wood decaying basidiomycetes," *Applied and Environmental Microbiology*, vol. 55, no. 10, pp. 2720–2722, 1989.

[26] J. B. Neilands, "Microbial iron compounds," *Annual Review of Biochemistry*, vol. 50, pp. 715–731, 1981.

[27] L. E. Arnow, "Colorimetric determination of the components of 3,4-dihydroxyphenylalanine tyrosine mixtures," *The Journal of Biological Chemistry*, vol. 118, p. 531, 1937.

[28] A. Chlebicki, B. Godzik, M. W. Lorenc, and A. Skłodowska, "Fungi and arsenic-tolerant bacteria in the hypogean environment of an ancient gold mine in Lower Silesia, SW Poland," *Polish Botanical Studies*, vol. 19, pp. 81–95, 2005.

[29] C. R. Anderson and G. M. Cook, " Isolation and characterization of arsenate-reducing bacteria from arsenic-contaminated sites in New Zealand," *Current Microbiology*, vol. 48, no. 5, pp. 341–347, 2004.

[30] N. El Aafi, F. Brhadaa, M. Daryb et al., "Rhizostabilization of metals in soils using Lupinus luteus inoculated with the metal resistant rhizobacterium Serratia sp. MSMC541," *International Journal of Phytoremediation*, vol. 14, no. 3, pp. 261–274, 2012.

[31] S. Silver and L. T. Phung, "A bacterial view of the periodic table: genes and proteins for toxic inorganic ions," *Journal of Industrial Microbiology and Biotechnology*, vol. 32, no. 11-12, pp. 587–605, 2005.

[32] D. N. Joshi, S. J. S. Flora, and K. Kalia, "Bacillus sp. strain DJ-1, potent arsenic hypertolerant bacterium isolated from the industrial effluent of India," *Journal of Hazardous Materials*, vol. 166, no. 2-3, pp. 1500–1505, 2009.

[33] S. O. Soda, S. Yamamura, H. Zhou, M. Ike, and M. Fujita, "Reduction kinetics of As (V) to As (III) by a dissimilatory arsenate-reducing bacterium, *Bacillus* sp. SF-1," *Biotechnology and Bioengineering*, vol. 93, no. 4, pp. 812–815, 2006.

[34] D. Y. Sorokin and G. Muyzer, "*Desulfurispira natronophila* gen. nov. sp. nov.: An obligately anaerobic dissimilatory sulfur-reducing bacterium from soda lakes," *Extremophiles*, vol. 14, no. 4, pp. 349–355, 2010.

[35] K. Konhauser, *Introduction To Geomicrobiology*, Blackwell, Oxford, UK, 2007.

[36] A. M. Aiken, B. M. Peyton, W. A. Apel, and J. N. Petersen, "Heavy metal-induced inhibition of *Aspergillus niger* nitrate reductase: applications for rapid contaminant detection in aqueous samples," *Analytica Chimica Acta*, vol. 480, no. 1, pp. 131–142, 2003.

[37] A. Yarnell, "Nature's tiniest geoengineers," *Chemical and Engineering News*, vol. 81, no. 42, pp. 24–25, 2003.

[38] A. Malik, "Metal bioremediation through growing cells," *Environment International*, vol. 30, no. 2, pp. 261–278, 2004.

[39] B. Peyton and W. A. Apel, "Siderophore influence on the mobility of both radionuclides and heavy metals," *INRA Informer*, vol. 5, pp. 2–4, 2005.

[40] A. Nair, A. A. Juwarkar, and S. K. Singh, "Production and characterization of siderophores and its application in arsenic removal from contaminated soil," *Water, Air, and Soil Pollution*, vol. 180, no. 1–4, pp. 199–212, 2007.

[41] D. E. Cummings, F. Caccavo Jr., S. Fendorf, and R. F. Rosenzweig, "Arsenic mobilization by the dissimilatory Fe(III)-reducing bacterium *Shewanella alga* BrY," *Environmental Science and Technology*, vol. 33, no. 5, pp. 723–729, 1999.

[42] C. L. Corkhill and D. J. Vaughan, "Arsenopyrite oxidation—a review," *Applied Geochemistry*, vol. 24, no. 12, pp. 2342–2361, 2009.

[43] K. J. Tufano, C. Reyes, C. W. Saltikov, and S. Fendorf, "Reductive processes controlling arsenic retention: revealing the relative importance of iron and arsenic reduction," *Environmental Science and Technology*, vol. 42, no. 22, pp. 8283–8289, 2008.

Hindawi Publishing Corporation
BioMed Research International
Volume 2014, Article ID 105728, 8 pages
http://dx.doi.org/10.1155/2014/105728

Research Article

Production of Biodiesel from *Chlorella* sp. Enriched with Oyster Shell Extracts

Cheol Soon Choi,[1] Woon Yong Choi,[1] Do Hyung Kang,[2] and Hyeon Yong Lee[3]

[1] *Department of Biomedical Materials Engineering, Kangwon National University, Chuncheon 200-701, Republic of Korea*
[2] *Korea Institute of Ocean Science & Technology (KIOST), P.O. Box 29, Ansan, Seoul 426-744, Republic of Korea*
[3] *Department of Food Science and Engineering, Seowon University, Cheongju 361-742, Republic of Korea*

Correspondence should be addressed to Hyeon Yong Lee; hyeonl@seowon.ac.kr

Received 12 November 2013; Revised 3 January 2014; Accepted 4 January 2014; Published 17 February 2014

Academic Editor: Eldon R. Rene

This study investigated the cultivation of the marine microalga *Chlorella* sp. without supplying an inorganic carbon source, but instead with enriching the media with extracts of oyster shells pretreated by a high-pressure homogenization process. The pretreated oyster shells were extracted by a weak acid, acetic acid, that typically has harmful effects on cell growth and also poses environmental issues. The concentration of the residual dissolved carbon dioxide in the medium was sufficient to maintain cell growth at 32 ppm and pH 6.5 by only adding 5% (v/v) of oyster shell extracts. Under this condition, the maximum cell density observed was 2.74 g dry wt./L after 27 days of cultivation. The total lipid content was also measured as 18.1 (%, w/w), and this value was lower than the 23.6 (%, w/w) observed under nitrogen deficient conditions or autotrophic conditions. The fatty acid compositions of the lipids were also measured as 10.9% of C16:1 and 16.4% of C18:1 for the major fatty acids, which indicates that the biodiesel from this culture process should be a suitable biofuel. These results suggest that oyster shells, environmental waste from the food industry, can be used as a nutrient and carbon source with seawater, and this reused material should be important for easily scaling up the process for an outdoor culture system.

1. Introduction

The increasing consumption of fossil fuels is leading to an energy depletion crisis, and the carbon dioxide arising from the use of fossil fuels is impacting the global environment day by day [1, 2]. In particular, the development of bioenergy using marine and freshwater microalgae as a 3rd generation biomass feedstock has been highlighted [3] because microalgae grow fast and have an excellent CO_2 absorption capacity as well as a relatively easy to control lipid and sugar content under various culture conditions [4–7]. However, in general, the production cost of fuel from microalgae or other marine bioresources is more than two times as high as fossil fuel-derived diesel. To solve this problem, many researchers are trying to lower production costs by screening microalgae that have a high lipid content, performing genetic manipulation on microalgae, minimizing the cost of microalgae culture processes, and so on [8–10]. In other reports, there have been several attempts to develop relatively cheap organic carbon sources, such as acetate for mixed cultures of *Chlorella sorokiniana*, instead of autotrophic cultivation [11–14].

Therefore, in this work, the major portion of the culture production costs has been reduced by using significantly less artificial medium for microalgae growth [15], which is an expensive material. Additionally, we are interested in recycling oyster shells, a waste resource that has caused serious sea pollution, such as the corruption of parasitic organisms and the mass proliferation of pathogenic bacteria [16]. As shown in Table 1, oyster shells contain high amounts of essential minerals and 2.7 g of organic matter per 1 kg and can also serve as an inorganic carbon source by properly treating the calcium carbonates in the oyster shells [17]. This waste material is a potential substitute for expensive essential medium supplements, such as F/2 mixtures in seawater media for microalgal growth [18, 19]. However, $CaCO_3$ dissolves in HCO^{3-}, $CO_3{}^{2-}$, and H_2CO_3 only under acidic conditions and

Table 1: Comparison of the chemical compositions of f/2 medium and 5% oyster shells with seawater.

Chemical composition		Oyster shell (g/L)	f/2 (g/L)
Al_2O_3		0.0042	—
$CaCO_3$		0.959	—
MgO		0.0065	—
NaCl		—	29.23
KCl		—	1.105
MgCl		1.83	—
Na_2O		0.0098	—
$MgSO_4{\cdot}7H_2O$		0.048	11.09
$NaHCO_3$		0.25	0.25
Tris-base		—	1.21
$NaNO_3$		—	0.281
$NaH_2PO_4{\cdot}H_2O$		—	2.12×10^{-2}
Na_2EDTA		—	1.635×10^{-2}
$FeCl_4{\cdot}6H_2O$		—	1.18×10^{-2}
$MnCl_2{\cdot}4H_2O$		—	6.75×10^{-8}
$CoCl_2{\cdot}6H_2O$		—	3.75×10^{-5}
$ZnSO_4{\cdot}7H_2O$		—	3.75×10^{-5}
Na_2MoO_4		—	2.25×10^{-5}
Vitamin B1		—	3.75×10^{-4}
Biotin		—	1.88×10^{-7}
$CaCl_2{\cdot}2H_2O$		—	1.83
Seawater (mol/kg)	Cl^-	0.546	
	Na^+	0.469	
	Mg^{2+}	0.528×10^{-1}	
	SO_4^{2-}	0.282×10^{-1}	
	Ca^{2+}	0.103×10^{-1}	
	K^+	0.102×10^{-1}	
	Br^-	0.844×10^{-3}	
	Sr^{2+}	0.91×10^{-4}	
	F^-	0.68×10^{-4}	
	N_3^-	0.11×10^{-2}	
	P^{3-}	2.84×10^{-6}	

is ultimately converted to CO_2 [20]. For the acidification of oyster shell media, the media need to be made under acid conditions; however, a large amount of acid cannot be added at a given time due to environmental concerns.

Therefore, developing a system to facilitate an increased reaction under mild acid conditions by decomposing the oyster shells is essential. Among the many methods to pulverize oyster shells, a high-pressure homogenization pretreatment process can be applied, which can favorably produce more $CaCO_3$, HCO^{3-}, $CO_3{}^{2-}$, and H_2CO_3 because the oyster shells are broken down to less than 5 μm in size, greatly increasing the surface area of the oyster shells. Oyster shells with a small particle size can easily be decomposed, even by the treatment of a weak acid, such as acetic acid (CHCOOH), and not strong acids, such as sulfuric acid (H_2SO_4) and hydrochloric acid (HCl). Another advantage of using high-pressure homogenization is that small particle sizes are obtained from hard materials through a simple and short process, which is a great benefit in scaling up the pretreatment process. Then, the oyster shells, a marine waste material, can be recycled as they are an excellent resource that supplies both inorganic carbon and essential nutrients. The supply of dissolved carbon dioxide from the culture medium will be the most important consideration in overcoming the limits of scaling up the outdoor culture system because the external supply of carbon dioxide is one of the major bottlenecks for large-scale outdoor culture systems [21, 22].

2. Materials and Methods

2.1. Materials. *Chlorella* sp. was obtained from the Korea Marine Microalgae Culture Center. *Chlorella* sp. was cultured, and then the scaled-up 14 L volume was inoculated at 10% (v/v). 10 w/m^2 of light was applied using a 20 W fluorescent lamp as the light source. The culture conditions were maintained at a stirring speed of 180 rpm and a temperature of 28°C in a 14 L shaking incubator (KF-20 L CONTROL PANEL, KOREA). The cultured cells were filtered through a 0.4 μm filter paper (Whatman, number 1, England) and centrifuged at 3000 rpm for 10 min, and the supernatant of the medium was removed; only the cells in the lower layer were freeze-dried. This sample was sealed and refrigerated at 4°C. The oyster shells supplied as a nutrient source in the culture medium were from Taejon, South Chungcheong Province, South Korea. The collected oyster shells were washed 3 times using DW (distilled water), which removed dirt and impurities. The naturally dried oyster shells were dried again for 24 hours in a dry oven at 105°C and were pulverized using a pestle and a mortar. Using a mesh of 1 mm or less in particle size, pulverized oyster shells were filtered from the sample and used in the experiment. For the basal medium for *Chlorella* sp. growth, f/2 medium was purchased from Sigma (St. Louis, USA) and dissolved in 1 L of seawater. The detailed composition of the f/2 and water mixture was as follows: 29.23 g NaCl, 1.105 g KCl, 11.09 g $MgSO_4{\cdot}\ 7H_2O$, 1.21 g Tris-base, 1.83 g $CaCl_2\ 2H_2O$, 0.25 g $NaHCO_3$, and a 3.0 mL trace metal solution that was composed of 281.3 mg $NaNO_3$, 21.2 mg $NaH_2PO_4{\cdot}H_2O$, 16.35 mg $Na_2{\cdot}EDTA$, 11.8 mg $FeCl_3{\cdot}6H_2O$, 675 μg $MnCl_2{\cdot}4H_2O$, 37.5 μg $CoCl_2{\cdot}6H2O$, 37.5 μg $ZnSO_4{\cdot}7H_2O$, 22.5 μg Na_2MoO_4, 0.375 mg vitamin B1, and 0.188 of μg biotin [23]. In addition, for the nitrogen deficient medium, the amount of $NaNO_3$ in the above basal medium was reduced to 37.5 mg. The remaining composition was prepared and used in the same way as the f/2 medium.

2.2. Pretreatment of Oyster Shells. The pretreatment process for the oyster shells medium using a high-pressure homogenizer (High-pressure Processor; MN400BF; PiCOMAX, Korea) was as follows: oyster shells in the form of dry powder were added to 1 L of distilled water at concentrations of 1, 5, and 10 (%) and were shred for 15–20 minutes at 20,000 rpm by a high-speed grinder. These shells were crushed to a size of approximately 50~70 μm. For the high-pressure homogenization process, the crushed powder was applied at 20,000~25,000 psi of high pressure and recycled two times for 30 min of total operation time, where the oyster

shells were broken down to less than 5 μm in particle size, as observed with DLS (US/90Plus, Brookhaven Instruments Co., USA). Then, the particle powder was dissolved in 1 N acetic acid. After dissolving the powder, 1%, 5%, or 10% (v/v) of the carbonate solution was mixed with the f/2 containing basal culture medium and filtered using a vacuum filtration device to prepare the final culture medium. The pH of final medium was measured to calculate dissolved carbon dioxide concentrations in the medium by (1) and was estimated as 6.8, 6.7, and 6.5 for the cases of adding 1%, 5%, and 10% oyster shell solutions, respectively.

2.3. Experimental Design of Cultivation. A 5 L photobioreactor was illuminated with 10 w/m^2 of light intensity using a 20 W fluorescent lamp at 28°C and 180 rpm of agitation speed. In the photobioreactor, 3 L of basal medium enriched with 1, 5, and 10 (%, v/v) of the dissolved oyster shell solution was added, without additional CO_2. As the control groups, f/2 medium with and without 5% (v/v) carbon dioxide gas that was added to the photoreactor was also used for growing *Chlorella* sp. As a positive control, basal medium enriched with a 5% oyster shell solution was treated by hydrochloric acid, maintaining a pH of 6, and was used to grow *Chlorella* sp. For nitrogen deficient growth, after 15 days of cultivation with the f/2 medium enriched with the 5% oyster shell solution but without supplying carbon dioxide, the medium was drained through two drain pipes at the bottom of the reactor that had a 0.45 um membrane filters installed. Then, nitrogen deficient medium containing 37.5 mg/L $NaNO_3$ in the basal medium was added to the reactor, and the cells were continuously grown for the rest of the cultivation.

2.4. Measurement of the Cell Density and Dissolved CO_2 Concentrations. To measure the cell growth of *Chlorella* sp. in the medium, cells were taken every 3 days from the reactor under the different experimental conditions. Then, the absorbance was measured at a wavelength of 682 nm using a UV/Visible spectrophotometer (Kontron Instruments, Germany), and cell mass was estimated by using calibrated standard curves [24]. For the measurement of dry cell mass, centrifugation was carried out for 15 minutes at 12,000 rpm. The cells were washed 2 times using distilled water and dried at 105°C for 24 hours, and then the dry matter was weighed to determine the dry cell density [25, 26]. The dissolved CO_2 concentration, a carbon source in the medium, was calculated by (1) because, during acid-base equilibrium, pH controls the relative concentrations of each species in the inorganic carbon system [27]:

$$[pCO_2] = \frac{[DIC]}{\left(1 + K_0K_1/[H^+] + K_0K_1K_2/[H^+]^2\right)}, \quad (1)$$

where the equilibrium constants were $K_0 = [H_2CO_3]/[CO_2]$ ($\cong 1.58 \times 10^{-3}$), $K_1 = [H^+][HCO_3^-]$ ($\cong 2.83 \times 10^{-4}$ amol L^{-1}), and $K_2 = /[H_2CO_3]\ [CO_3^{2-}][H^+]$ ($\cong 4.68 \times 10^{-11}$ amol L^{-1}); square brackets indicate molar concentration.

2.5. Measurement of Total Lipid Contents and Fatty Acid Profiles. For the measurement of the lipid content in cells, the Folch method was used. In a 1 g sample of dry cells, a 20 mL solution of $CHCl_3$: methanol (2 : 1, v/v) was added, and the solution was mixed. The mixture was stirred for 30–90 minutes at room temperature and then centrifuged for 15 minutes at 500 rpm. Then, the supernatant was removed, and a 0.9% (w/v) NaCl solution was added to the pelleted cells. After vortexing the mixture for a few seconds, centrifugation was carried out for 15 minutes at 2000 rpm. The supernatant was discarded and the lower fluid layer that contained lipids was dried. The dried fluid was weighed for the determination of the fat content [28, 29].

After the culture was terminated, on the 27th day the fatty acids from the lipids were analyzed by the Folch method. The methyl esterification of the lipids was evaluated by gas chromatography (HP 6890 SERIES, USA) analysis. Methylation was conducted by applying 0.5 N NaOH/MeOH to the obtained lipids. Then, 1.5 mL of BF3-methanol was added, and the solution was reacted at 95°C for 60 minutes. After methyl ester transesterification, 1 mL of hexane was added, and the solution was mixed well. The supernatant (hexane layer) was removed and then analyzed by GC. As a GC detector, a flame ionization detector (FID) was used. Additionally, a SP-2560 GC column (100 m × 0.25 mm × 0.2 μm, number 24056, Supelco, USA) was used. The oven temperature was changed at a rate of 4°C /min from 240°C to 100°C. The injection temperature and detector temperature were set to 250°C and 280°C, respectively. The flow rate was set to 1.0 mL/min and the split ratio to 50 : 1. Lastly, fatty acid analysis was performed by injecting 1 μL for each sample [30].

3. Results and Discussion

3.1. Comparison of Cell Growth in Different Media. Figure 1 shows the comparative results of cell growth and pH for several different culture media. A higher cell density of 2.24 g dry wt/L was obtained for cells growing in f/2 with additional carbon dioxide compared to 2.17 g/L for cells with medium containing 5% oyster shell extracts treated with acetate because of the mild pH of 6.7. On the other hand, for the case of adding 10% or 1% of oyster shells to the media, relatively low cell growth was maintained due to the low pH required for optimal cell growth and the low amounts of essential elements in the medium, respectively, which resulted in a small pH increase during the cultivation. Low amounts of key elements, such as nitrogen and phosphorus, are present in seawater and thus increase the growth of microalgae in combination with the oyster shells [18]. Low concentrations of carbon supply were observed to have little effect on the growth of microalgae. This result was also confirmed by reports that cell mass and productivity decreased because the carbon sources acted as a stressor to the microalgae under conditions where the carbon sources were excessively supplied [31, 32].

In this study, the pH of the medium was varied by adding acetic acid or hydrochloric acid to increase the amount of $CaCO_3$-derived carbon sources (initial pCO_2), an important component in increasing the growth of *Chlorella* sp. The composition of the oyster shell medium affects how much

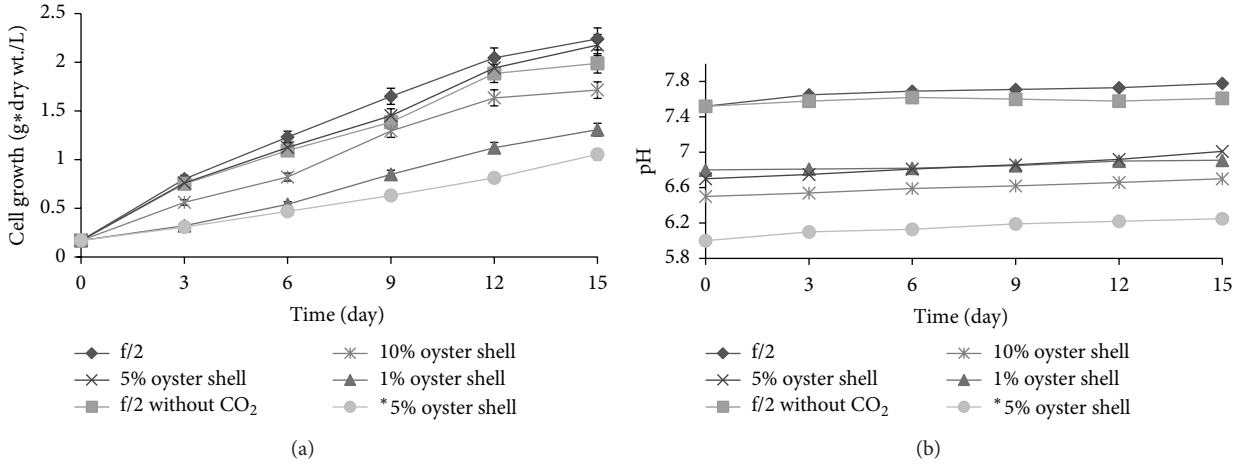

Figure 1: Comparison of cell growth and pH under different culture medium conditions. 1% oyster shells pretreated with a high-pressure homogenization process and acetic acid (pH 6.8); 5% oyster shells pretreated with a high-pressure homogenization process and acetic acid (pH 6.7); 10% oyster shells pretreated with a high-pressure homogenization process and acetic acid (pH 6.5); *5% oyster shells pretreated with a high-pressure homogenization process and hydrochloric acid (pH 6).

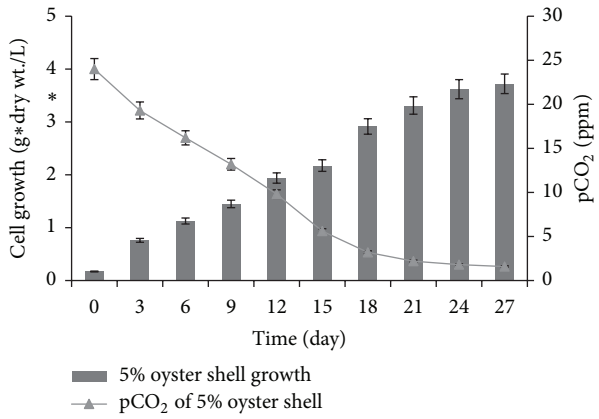

Figure 2: The cell growth and residual dissolved CO_2 concentration in the medium enriched with 5% oyster shells pretreated with a high-pressure homogenization process and acetic acid (pH: 6.7).

Table 2: Comparison of the initial dissolved CO_2 concentrations in several culture media according to the initial pH.

Parameter	Culture medium			
	A	B	C	D
pH value	6.8	6.7	6.5	6
Dissolved CO_2 (ppm)	22	24	32	108

A: 1% oyster shells pretreated with a high-pressure homogenization process and acetic acid; B: 5% oyster shells pretreated with a high-pressure homogenization process and acetic acid; C: 10% oyster shells pretreated with a high-pressure homogenization process and acetic acid; D: 5% oyster shells pretreated with a high-pressure homogenization process and hydrochloric acid.

$CaCO_3$ reacts with CO_2 and H_2O and subsequently exists as dissolved ions, such as HCO^{3-}, CO_3^{2-}, and H_2CO_3. Then, it was converted to CO_2. Therefore, this acid molecule lowers the pH and has an impact on the lipid metabolism and growth of microalgae [23]. Table 2 shows the relationship between the initial pH and dissolved carbon dioxide (pCO_2) that supplies the main carbon source for cell growth. The initial amount of pCO_2 was expected to gradually increase, lowering the pH, which would cause cell growth to increase. However, at a low pH that can maintain a high concentration of dissolved carbon dioxide, cell growth did not increase much, as shown in Figure 1, because the environmental stress due to the lowered pH caused negative consequences for the growth of *Chlorella* sp. [33]. Additionally, the 5 μm sized oyster shells produced by nanogranularization and high-pressure homogenization before treatment and the change in pH were confirmed to increase the initial carbon dioxide content.

As shown in Figure 2, the change in pCO_2 was compared to the growth of *Chlorella* sp. in the 5% oyster shell containing medium. Little change was observed in the carbon dioxide concentration of the medium by the 12th day. However, after 15 days of cultivation, the growth of *Chlorella* sp. rapidly increased because the dissolved carbon dioxide rapidly decreased until the 24th day; thereafter, not much cell growth occurred. These results imply that large amounts of $CaCO_3$ were converted to CO_2, and this molecule was the main carbon source after decreasing the pH during the slow cell growth in the lag phase, which greatly promoted the growth of *Chlorella* sp. Therefore, the growth of *Chlorella* sp. proceeded efficiently by supplying $CaCO_3$ from oyster shells without an external supply of CO_2.

3.2. Cell Growth and Total Lipid Production under Nitrogen Deficiency. In Figure 3, to increase the total amount lipid production and cell growth, *Chlorella* sp. cultured after 15 days was exposed to an insufficient nitrogen source (from 400 mg to 37.5 mg of $NaNO_3$), based on previous experiments [34, 35]. Cell growth was compared between one case where

Table 3: Results of estimating lipid productivity and the fatty acid profiles of cells grown from several culture media under different culture conditions.

Parameter		Culture time					
		21 days (6 days of N depletion)			27 days (12 days of N depletion)		
		A	B	C	A	B	C
Lipid productivity (mg/L/day)		25.5	19.2	20.6	28.8	23.4	25.3
Culture medium	Total lipids (%, w/w)	Fatty acids composition (% of total fatty acids)					
		$C_{14:0}$	$C_{16:0}$	$C_{16:1}$	$C_{18:0}$	$C_{18:1}$	$C_{18:2}$	$C_{18:3}$
A	25.1	12.5	13.8	12.1	11.8	17.5	20.6	13.4
B	21.8	10.8	11.8	11.5	10.7	17.1	19.5	10.8
C	23.6	11.5	12.5	10.9	11.2	16.4	18.5	12.3

A: F/2 medium; B: F/2 medium without CO_2; C: 5% oyster shells pretreated with high-pressure homogenization and acetic acid (pH: 6.7).

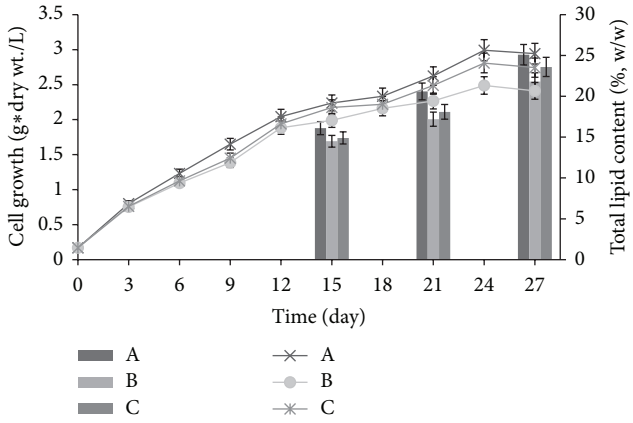

Figure 3: The cell growth (lines) and total lipid production (bars) obtained using different culture media. The arrow was the point where the nitrogen deficient medium was provided after the 15th cultivation day. (A: f/2 medium; B: f/2 medium without CO_2; C: 5% oyster shells pretreated with high-pressure homogenization and acetic acid (pH: 6.7).)

the pH of the 5% oyster shell medium was titrated to 6.7, the most efficient pH for culturing *Chlorella* sp., and another case with the f/2 medium as the control group, where more CO_2 was not added. When cells were grown with f/2 medium and shifted to the nitrogen deficient medium, higher cell density was observed and 2.94 g dry wt/L compared to 2.74 g/L of cell density was observed from the 5% oyster shell enriched medium (pH 6.7). In addition, the maximum cell density, 2.41 g/L, was observed for the f/2 medium without an additional CO_2 supply. The results confirmed that when cells were shifted to the nitrogen deficient medium with the 5% oyster shell enriched medium, relatively good cell growth could be maintained without supplying a carbon source. However, cell growth when cells were initially exposed to nitrogen deficient medium did not increase significantly compared to the cell growth increase observed in previous experiments. These results suggest that insufficient nitrogen sources slow down the growth of *Chlorella* sp. A similar investigation also showed that an adequate supply of nitrogen sources was essential to promote the growth of the microalgae *Chlorella* sp. [34].

In addition to cell growth, when shifting from the normal medium to the nitrogen deficient medium, the lipid contents were greatly increased, comparing the 15th day and the 27th (last) day of culture. For the artificial f/2 medium, the lipid content was 20.6 (%, w/w) on the 21st day and 25.1 (%, w/w) on the 27th day. The 5% oyster shell enriched medium (pH 6.7) was 18.1 (%, w/w) on the 21st day and 23.6 (%, w/w) on the 27th day. Interestingly, in the seawater with f/2 medium where additional CO_2 had not been added, the lipid content was estimated as only 17.2 (%, w/w) on the 21st day and 21.8 (%, w/w) on the 27th day. In general, the total lipid contents exhibited a large increase of 3~5 (%, w/w) after shifting to the nitrogen deficient medium and an especially large increase when grown in the oyster shell enriched medium. This result also implied that low pH acted as an environmental stress on *Chlorella* sp.; therefore, brisk cell lipid metabolism occurred and led to an increase in lipid accumulation [36, 37]. These results indicate that, in culture under stressful conditions, the metabolic changes resulted in an increase in lipid content, rather than the growth of *Chlorella* sp. [34]. Additionally, cells growing in the 5% oyster shell enriched medium exhibited a lipid content under the nitrogen deficient condition that was not much different from the lipid content of cells grown in the artificial seawater f/2 medium. This result also confirmed that oyster shells can be used for the growth of *Chlorella* sp. as well as increasing the total lipid content more efficiently without an additional supply of carbon, although a higher lipid content was observed in the control group.

3.3. Production of Total Lipids and the Fatty Acid Profiles of Algae from the Oyster Shell Enriched Medium. Based on the results in Figure 3, lipid productivity from each medium was estimated in Table 3, and the identities of the fatty acids in the total lipid obtained from each medium are also displayed. For 21 days of cultivation (from the artificial seawater f/2 medium to the nitrogen deficient medium), the lipid productivity was 25.5 mg/L/day, which was lower than the 28.8 mg/L/day productivity from 27 days of cultivation where longer nitrogen depletion was maintained. For the case of adding a 5% oyster shell enriched medium, the lipid productivity was 20.6 mg/L/day after 21 days of cultivation and 25.3 mg/L/day after 27 days of cultivation. Interestingly, in the f/2 medium control group without a CO_2 supply, the lowest

lipid productivities of 19.2 mg/L/day and 23.4 mg/L/day were observed for 21 days and 27 days of cultivation, respectively. A minimal difference in the lipid productivity between the f/2 medium with CO_2 supply and 5% oyster shell enriched medium without CO_2 supply was also confirmed. Thus, the possibility of promoting the continued growth of cells and an adequate lipid content in the absence of an expensive artificial seawater f/2 medium was demonstrated if oyster shells and appropriate nitrogen sources were supplied. Nitrogen induced an increase in the lipid content of the cell and a maximum amount of cell. Several factors contributed to these effects: cells were switched to a nitrogen deficient medium, the pH was increased after the acid treatment of the oyster shells, and the oyster shells underwent a high-pressure homogenization before treatment.

To compare the quality of biodiesel from each lipid, the fatty acid composition of the total lipids obtained from each medium is also shown in Table 3. The fatty acid content of the total lipids from the f/2 medium showed that the C14:0, C16:0, and C18:0 saturated fatty acids were 12.5, 13.8, and 11.8 (%, w/w), respectively, which are the highest observed values. For the case from the 5% oyster shell enriched medium, the results showed 11.5, 12.5, and 11.2 (%, w/w), respectively. In the case of the f/2 medium without a CO_2 supply as the control group, the results showed 10.8, 11.8, and 10.7 (%, w/w), respectively.

For monounsaturated fatty acids, C16:1, the lipid content in the f/2 medium, 5% oyster shell medium, and f/2 medium without CO_2 supply was 12.1, 10.9, and 11.5 (%. w/w), respectively. However, the C18:1 lipid content in the f/2 medium, 5% oyster shell medium, and the f/2 medium without CO_2 supply was 17.5, 16.4, and 17.1 (%. w/w), respectively. In the case of polyunsaturated fatty acids, the C18:2 and C18:3 lipid content in the f/2 medium were 20.6 and 13.4 (%, w/w), respectively. The C18:2 and C18:3 fatty acids were also present in the 5% oyster shell enriched medium, reaching values of 18.5 and 12.3 (%, w/w), respectively. Lastly, the C18:2 and C18:3 fatty acids were 19.5 and 10.8 (%, w/w), respectively, of the fatty acid content for the f/2 medium without CO_2 supply. In general, monounsaturated fatty acids, such as C16 and C18, are known to be suitable as fatty acids for biodiesel [38], and in this work, the total content of C16:1 and C18:1 from the lipids of *Chlorella* sp. was estimated as ca. 30 (%, w/w), showing almost the same results for both the f/2 medium and the 5% oyster shell enriched medium. Therefore, the oyster shell culture medium has several advantages, including representing a cheaper carbon source than the commonly used carbon sources, such as sodium bicarbonate, among others, and does not require an additional supply of CO_2, which will have economic benefits for the scaleup needed for biodiesel production.

4. Conclusion

To overcome economic limitations for producing biodiesel from microalgae, this study cultivated the marine microalga *Chlorella* sp. with simple seawater enriched with 5 (%, v/v) of high-pressure homogenized oyster shells. This medium was observed to continuously provide an inorganic carbon source without adding external inorganic carbon sources, which has represented a bottleneck in scaling up the culture process, especially for outdoor mass cultivation. The high-pressure homogenization helped weak acids to easily dissolve the hard oyster shells, eliminating the need for strong acids due to the increase in the surface areas and mechanical stresses on the surfaces of the hard shells. When this optimal basal medium was changed to a nitrogen deficient medium during cultivation, 2.74 g/L of dry cell density and 23.6 (%, w/w) of total lipid content were obtained. These results were better than a previous investigation using Tris-acetate-phosphorus (TAP) medium, which had 1.76 g/L of dry cell density [39]. Nitrogen deficient conditions were confirmed to dramatically increase the total lipid contents observed, from 18.1 (%, w/w) to 23.6 (%, w/w), but to significantly decrease cell growth. This result implied that better lipid productivity obtained using this medium could be maintained for longer-term cultivation than was possible for the conventional enriched f/2 medium. Fatty acid profiles of the lipids obtained from this oyster containing medium were not much different from the f/2 enriched medium, showing that ca. 25% of the total fatty acids were C16:1 and C18:1 (key fatty acids for biodiesel production) for cells from the f/2 culture medium, while ca. 23% of the fatty acids were these key fatty acids for cells from the 5% oyster shell containing medium. These results confirmed that this unique inexpensive medium has great advantages for reducing environmental issues and for enhancing both cell growth and lipid production under proper culture conditions.

Conflict of Interests

The authors declare that there is no conflict of interests regarding the publication of this paper.

Acknowledgments

This research was supported by a grant from Marine Biotechnology Program funded by Ministry of Oceans and Fisheries, Korea.

References

[1] K. Madhavi, A. Amin, G. V. S. Reddy, and D. V. Redd, "Algal biofuels: a solution to pollution problemas and sustainable development—a review," *Continental Journal of Sustainable Development*, vol. 4, no. 1, pp. 39–44, 2013.

[2] K. Ndimba, R. J. Ndimba, T. S. Johnson et al., "Biofuels as a sustainable energy source: an update of the applications of proteomics in bioenergy crops and algae," *Journal of Proteomics*, vol. 93, no. 20, pp. 234–244, 2013.

[3] J. R. Miranda, P. C. Passarinho, and L. Gouveia, "Pre-treatment optimization of Scenedesmus obliquus microalga for bioethanol production," *Bioresource Technology*, vol. 104, pp. 342–348, 2012.

[4] J. Singh and S. Gu, "Commercialization potential of microalgae for biofuels production," *Renewable and Sustainable Energy Reviews*, vol. 14, no. 9, pp. 2596–2610, 2010.

[5] Z.-Y. Liu, G.-C. Wang, and B.-C. Zhou, "Effect of iron on growth and lipid accumulation in *Chlorella vulgaris*," *Bioresource Technology*, vol. 99, no. 11, pp. 4717–4722, 2008.

[6] G. Huang, F. Chen, D. Wei, X. Zhang, and G. Chen, "Biodiesel production by microalgal biotechnology," *Applied Energy*, vol. 87, no. 1, pp. 38–46, 2010.

[7] H. M. Amaro, A. C. Guedes, and F. X. Malcata, "Advances and perspectives in using microalgae to produce biodiesel," *Applied Energy*, vol. 88, no. 10, pp. 3402–3410, 2011.

[8] M. B. Johnson and Z. Wen, "Development of an attached microalgal growth system for biofuel production," *Applied Microbiology and Biotechnology*, vol. 85, no. 3, pp. 525–534, 2010.

[9] D. H. Lee, "Algal biodiesel economy and competition among bio-fuels," *Bioresource Technology*, vol. 102, no. 1, pp. 43–49, 2011.

[10] J. A. Berges, D. J. Franklin, and P. J. Harrison, "Evolution of an artificial seawater medium: Improvements in enriched seawater, artificial water over the last two decades," *Journal of Phycology*, vol. 37, no. 6, pp. 1138–1145, 2001.

[11] A. R. Mitchell, F. J. Crowe, and M. D. Butler, "Plant performance and water use of peppermint treated with methanol and glycine," *Journal of Plant Nutrition*, vol. 17, no. 11, pp. 1955–1962, 1994.

[12] F.-Y. Feng, W. Yang, G.-Z. Jiang, Y.-N. Xu, and T.-Y. Kuang, "Enhancement of fatty acid production of *Chlorella* sp. (Chlorophyceae) by addition of glucose and sodium thiosulphate to culture medium," *Process Biochemistry*, vol. 40, no. 3-4, pp. 1315–1318, 2005.

[13] J. Choi and S. Y. Lee, "Factors affecting the economics of polyhydroxyalkanoate production by bacterial fermentation," *Applied Microbiology and Biotechnology*, vol. 51, no. 1, pp. 13–21, 1999.

[14] J. Lalucat, J. Imperial, and R. Pares, "Utilization of light for the assimilation of organic matter in *Chlorella* sp. VJ79," *Biotechnology and Bioengineering*, vol. 26, no. 7, pp. 677–681, 1984.

[15] N.-H. Norsker, M. J. Barbosa, M. H. Vermuë, and R. H. Wijffels, "Microalgal production—a close look at the economics," *Biotechnology Advances*, vol. 29, no. 1, pp. 24–27, 2011.

[16] H. W. Kho, S. H. Jang, and N. C. Sung, "Study on the wastewater treatment as a coagulant using the waste oyster shells and loess," *Journal of the Korean Institute of Resources Recycling*, vol. 11, no. 2, pp. 45–51, 2002.

[17] G.-L. Yoon, B.-T. Kim, B.-O. Kim, and S.-H. Han, "Chemical-mechanical characteristics of crushed oyster-shell," *Waste Management*, vol. 23, no. 9, pp. 825–834, 2003.

[18] C. H. Lee, D. K. Lee, M. A. Ali, and P. J. Kim, "Effects of oyster shell on soil chemical and biological properties and cabbage productivity as a liming materials," *Waste Management*, vol. 28, no. 12, pp. 2702–2708, 2008.

[19] W. A. Kratz and J. Myers, "Nutrition and growth of several blue-green algae," *American Journal of Botany*, vol. 42, no. 3, pp. 282–287, 1955.

[20] A. Widjaja, C.-C. Chien, and Y.-H. Ju, "Study of increasing lipid production from fresh water microalgae *Chlorella vulgaris*," *Journal of the Taiwan Institute of Chemical Engineers*, vol. 40, no. 1, pp. 13–20, 2009.

[21] H. Matsumoto, A. Hamasaki, N. Shioji, and Y. Ikuta, "Influence of dissolved oxygen on photosynthetic rate of microalgae," *Journal of Chemical Engineering of Japan*, vol. 29, no. 4, pp. 711–714, 1996.

[22] K. Zhang, N. Kurano, and S. Miyachi, "Optimized aeration by carbon dioxide gas for microalgal production and mass transfer characterization in a vertical flat-plate photobioreactor," *Bioprocess and Biosystems Engineering*, vol. 25, no. 2, pp. 97–101, 2002.

[23] Guillard and R. L. Robert, "Culture of phytoplankton for feeding marine invertebrates," *Culture of Marine Invertebrate Animals*, vol. 1, no. 3, pp. 29–60, 1975.

[24] E. E. Powell, M. L. Mapiour, R. W. Evitts, and G. A. Hill, "Growth kinetics of *Chlorella vulgaris* and its use as a cathodic half cell," *Bioresource Technology*, vol. 100, no. 1, pp. 269–274, 2009.

[25] M. M. Jung and S. Rho, "Comparison of notochord length, dry weight and survival rate of Flat Fish, *Paralichthys olivaceus* (Temminck et Schlegel) larvae on different," *Bull. Marine Res*, vol. 23, pp. 23–28, 1999.

[26] Y. J. Yi, H. Yin, and K. Luo, "Culture conditions effect on the mycelium dry weight activating proteins produce," *Journal of Hunan Agricultural University*, vol. 31, no. 1, pp. 76–78, 2005.

[27] S. T. Summerfelt, B. J. Vinci, and R. H. Piedrahita, "Oxygenation and carbon dioxide control in water reuse systems," *Aquacultural Engineering*, vol. 22, no. 1-2, pp. 87–108, 2000.

[28] W. Tan and G. D. Hogan, "Dry weight and N partitioning in relation to substrate N supply, internal N status and developmental stage in jack pine (Pinus banksiana Lamb.) seedlings: implications for modelling," *Annals of Botany*, vol. 81, no. 2, pp. 195–201, 1998.

[29] S. J. Iverson, S. L. C. Lang, and M. H. Cooper, "Comparison of the bligh and dyer and folch methods for total lipid determination in a broad range of marine tissue," *Lipids*, vol. 36, no. 11, pp. 1283–1287, 2001.

[30] Ö. Tokuşoglu and M. K. Ünal, "Biomass nutrient profiles of three microalgae: *Spirulina platensis*, *Chlorella vulgaris*, and *Isochrisis galbana*," *Journal of Food Science*, vol. 68, no. 4, pp. 1144–1148, 2003.

[31] K. L. Yeh, J. S. Chang, and W.-M. Chen, "Effect of light supply and carbon source on cell growth and cellular composition of a newly isolated microalga *Chlorella vulgaris* ESP-31," *Engineering in Life Sciences*, vol. 10, no. 3, pp. 201–208, 2010.

[32] M. G. de Morais and J. A. V. Costa, "Isolation and selection of microalgae from coal fired thermoelectric power plant for biofixation of carbon dioxide," *Energy Conversion and Management*, vol. 48, no. 7, pp. 2169–2173, 2007.

[33] H. J. Choi and S. M. Lee, "Effect of temperature, light intensity and ph on the growth rate of chlorella vulgaris," *Journal of KSEE*, vol. 33, no. 7, pp. 511–515, 2011.

[34] Q. KaiXian and M. A. Borowitzka, "Light and nitrogen deficiency effects on the growth and composition of Phaeodactylum tricornutum," *Applied Biochemistry and Biotechnology*, vol. 38, no. 1-2, pp. 93–103, 1993.

[35] A. Widjaja, C. C. Chien, and Y. H. Ju, "Study of increasing lipid production from fresh water microalgae *Chlorella vulgaris*," *Journal of the Taiwan Institute of Chemical Engineers*, vol. 40, no. 1, pp. 13–20, 2009.

[36] Q. Hu, C. W. Zhang, and M. Sommerfeld, "Biodiesel from algae: lessons learned over the past 60 years and future perspectivesJournal of Phycology," vol. 42, no. 1, pp. 1–48, 2006.

[37] X. Zhang, Q. Hu, M. Sommerfeld, E. Puruhito, and Y. Chen, "Harvesting algal biomass for biofuels using ultrafiltration membranes," *Bioresource Technology*, vol. 101, no. 14, pp. 5297–5304, 2010.

[38] M. Scarsella, M. P. Parisi, A. D'Urso et al., "Achievements and perspectives in hetero- and mixotrophic culturing of microalgae," *Chemical Engineering Transactions*, vol. 17, pp. 1065–1070, 2009.

[39] L. Wang, Y. Li, P. Chen et al., "Anaerobic digested dairy manure as a nutrient supplement for cultivation of oil-rich green microalgae *Chlorella* sp," *Bioresource Technology*, vol. 101, no. 8, pp. 2623–2628, 2010.

Hindawi Publishing Corporation
BioMed Research International
Volume 2014, Article ID 391542, 11 pages
http://dx.doi.org/10.1155/2014/391542

Research Article

Enhancement of Biodiesel Production from Marine Alga, *Scenedesmus* sp. through *In Situ* Transesterification Process Associated with Acidic Catalyst

Ga Vin Kim,[1] WoonYong Choi,[2] DoHyung Kang,[3] ShinYoung Lee,[1] and HyeonYong Lee[4]

[1] *Department of Bioengineering and Technology, College of Engineering, Kangwon National University, Chuncheon 200-701, Republic of Korea*
[2] *Department of Medical Biomaterial Engineering, Kangwon National University, Chuncheon 200-701, Republic of Korea*
[3] *Korea Institute of Ocean Science & Technology (KIOST), Gyeonggi-do, Ansan-si, P.O. Box 29, Seoul 426-744, Republic of Korea*
[4] *Department of Food Science and Engineering, Seowon University, Cheongju, Chungbuk 361-742, Republic of Korea*

Correspondence should be addressed to ShinYoung Lee; sylee@kangwon.ac.kr and HyeonYong Lee; hyeonl@seowon.ac.kr

Received 8 November 2013; Revised 16 December 2013; Accepted 17 December 2013; Published 13 February 2014

Academic Editor: Kannan Pakshirajan

The aim of this study was to increase the yield of biodiesel produced by *Scenedesmus* sp. through *in situ* transesterification by optimizing various process parameters. Based on the orthogonal matrix analysis for the acidic catalyst, the effects of the factors decreased in the order of reaction temperature (47.5%) > solvent quantity (26.7%) > reaction time (17.5%) > catalyst amount (8.3%). Based on a Taguchi analysis, the effects of the factors decreased in the order of solvent ratio (34.36%) > catalyst (28.62%) > time (19.72%) > temperature (17.32%). The overall biodiesel production appeared to be better using NaOH as an alkaline catalyst rather than using H_2SO_4 in an acidic process, at 55.07 ± 2.18% (based on lipid weight) versus 48.41 ± 0.21%. However, in considering the purified biodiesel, it was found that the acidic catalyst was approximately 2.5 times more efficient than the alkaline catalyst under the following optimal conditions: temperature of 70°C (level 2), reaction time of 10 hrs (level 2), catalyst amount of 5% (level 3), and biomass to solvent ratio of 1 : 15 (level 2), respectively. These results clearly demonstrated that the acidic solvent, which combined oil extraction with *in situ* transesterification, was an effective catalyst for the production of high-quantity, high-quality biodiesel from a *Scenedesmus* sp.

1. Introduction

Biodiesel is an alternative renewable fuel that is derived from vegetable oils, animal fats, spent frying oils, and microbial oils. This fuel can replace petroleum-based fuels and can be used in all types of the currently available diesel engines without them being modified [1, 2].

Extensive investigation of biodiesel manufacturing has been conducted using oil-like materials, such as vegetable oils, animal fats, and used frying oils, which are limited by their availability, and the prices of these materials are more greatly sensitive to the industrial demands for oil. The limited inventories also created a fuel versus food issue that requires consideration of non-food-related feedstock. Therefore, some attempts have been made to produce biodiesel from nonedible resources such as spent frying oils, greases, and *Jatropha*. However, a major criticism of large-scale fuel production from nonedible resources is that vast areas of farmland or native habitats will be consumed, and food prices will increase. Because of these problems, microalgae are currently considered one of the most promising resources for biodiesel production [3–6].

Microalgae exhibit a high photosynthetic efficiency and a strong capacity to adapt to the environment (e.g., high salinity, heavy metal ion content, presence of toxicants, and high CO_2 concentration). Moreover, microalgae can be grown in various climates and on nonarable land, including marginal areas that are unsuitable for agricultural purposes (e.g., desert and seashore lands). The growth of microalgae in liquid medium can be controlled easily, and they can be

cultured in nonpotable water. Moreover, most microalgae (e.g., *Scenedesmus* and *Chlorella*) have very short cell cycles (less than 24 hours) and high oil productivity per hectare. Therefore, microalgae have been predicted to be a new biofuel source that is renewable and is environmentally and economically sustainable [3, 6–9].

Many species of microalgae suitable for producing fuel oil have been identified, that is, *Chlorella*, *Scenedesmus*, *Spirulina*, and *Nostoc* spp. Supplementation of iron to the growth medium under nitrate limitation was found to raise the crude lipid content of *Chlorella* to ~56.6% (dry cell weight). The lipid content of *Scenedesmus obliquus* reached up to ~58.3% (dry cell weight) when lower nitrogen-supplemented medium was utilized [10–13]. In our preliminary studies [14, 15], *Scenedesmus* sp. was shown to be an appropriate source for biodiesel by determining its lipid composition and extraction yield. Therefore, we decided to use this species as a biodiesel feedstock in the present study.

FAMEs (fatty acid methyl esters) are produced via a transesterification process that involves a chemical reaction between triglycerides and an alcohol, generally methanol, in the presence of a catalyst [16, 17]. This process is the one that is most commonly used to produce industrial biodiesel due to the low cost of the catalyst, its utility in mass production, and its high productivity. However, this method often produces a large amount of hazardous solvent waste and is generally cumbersome. This transesterification process requires preextracting the oil from the raw materials. Automated extraction equipment has been successfully developed, but it requires a longer extraction process [6, 18, 19].

Recently, an *in situ* transesterification (or direct transesterification) method that may overcome these limitations has attracted attention. *In situ* transesterification differs from the conventional method because the oil-bearing material directly contacts the acidified or alkalized alcohol instead of preextracted oil reacting with the alcohol. Thus, the extraction and transesterification processes occur in the same step. The alcohol acts as both an extraction solvent and an esterification reagent, which could reduce the production time associated with preextracting the oil and maximize the fatty acid ester yield. By using such reagents, the amount of solvents and the processing period are reduced and the problems of waste disposal are avoided [17, 20, 21].

The most conventional approach to experiment design is to optimize one variable (or one factor) at a time in single-response problems. An increasing number of factors increases the number of design experiments. However, the increasing complexity of product design is such that at least two quality characteristics are frequently simultaneously considered to improve the product quality. Moreover, correlations among multiple responses always exist and may generate conflicts among the optimal parameter settings. Hence, simultaneously optimizing a multiresponse problem is important [22].

The Taguchi method is a powerful experimental design tool that provides a simple, effective, systematic approach to determining the optimal parameters. Furthermore, this approach requires minimum experimental cost and it efficiently reduces the effect of the sources of variation [23]. The design of experiments (DOE) methodology of the Taguchi orthogonal array (OA), a factorial-based approach, has recently become exceeding important due to its application in optimizing biochemical processes [24].

In this biodiesel research study, we investigated using microalgae as the feedstock for biodiesel production. A microalgal *Scenedesmus* sp. was selected for biodiesel production through *in situ* transesterification via acidic catalysis and the synthesis of this biofuel was optimized using the Taguchi method.

2. Materials and Methods

2.1. Materials. Freeze-dried microalgal cells were provided by KORDI (Korea Ocean Research & Development Institute). The microalga was cultured under controlled conditions, and the algal biomass was harvested by centrifugation at 3000 rpm for 10 min. The cells were then freeze-dried, ground (100 mesh), and stored in the freezer. The freeze-dried powder was kept under desiccation of anhydrous sodium sulfate (Daejung Co., Ltd, Shi heung, Korea) overnight, before use.

2.2. In Situ Transesterification via Alkaline or Acidic Catalysis. The *in situ* transesterification process following the method of Ehimen et al. [25] was conducted at the laboratory scale. The alkaline process experiments were conducted under the following conditions: reaction time of 1 to 3 hrs, reaction temperature of 40 to 60°C, quantity of the reacting alcohol (methanol, 99.5%, Daejung Co. Ltd, Shi Heung, Korea) of 20 to 50 mL, and concentrations of sodium hydroxide of 0.5 to 1.5% (w/w of lipid). The reactor had a capacity of 250 mL, and it was immersed in a water bath to maintain the reaction temperature at the desired level. The reaction was conducted under reflux conditions to minimize the solvent loss. The acidic process experiments were conducted under the following conditions: reaction time of 5 to 15 hrs, reaction temperature of 50 to 90°C, biomass to solvent ratio of 5 : 1 to 25 : 1 (v/w), and concentrations of sulfuric acid of 1 to 5% (v/v of solvent). The reactor capacity was 500 mL. A freeze-dried algal biomass (15 g) was mixed with methanol in which sulfuric acid had been dissolved. The scheme of the *in situ* transesterification reaction and product purification steps are shown in Figure 1. Additionally, a freeze-dried algal biomass (5 g) was mixed with methanol in which 0.5% NaOH had been dissolved as an alkaline catalyst. Thus, the acidic catalyst of 5% H_2SO_4 was replaced with sodium hydroxide. The reactor containing the reaction mixture was heated and then maintained at the temperature of interest for the specified periods. After the *in situ* transesterification step, the reaction flask was allowed to stand for 1 hour to allow its contents to settle. The reaction mixture was filtered (Advantec No. 2, Toyo Roshi Inc., Tokyo, Japan) and the residues were washed twice by resuspension in methanol (10 mL) for 10 min to recover any traces of FAME products from the residues. Distilled water (15 mL) was added to the filtrate to facilitate the separation of the hydrophilic components of the extract. This mixture was centrifuged (5000 ×g) for 15 min and then transferred to a separation funnel. Further extraction of the FAME products was achieved by three times for

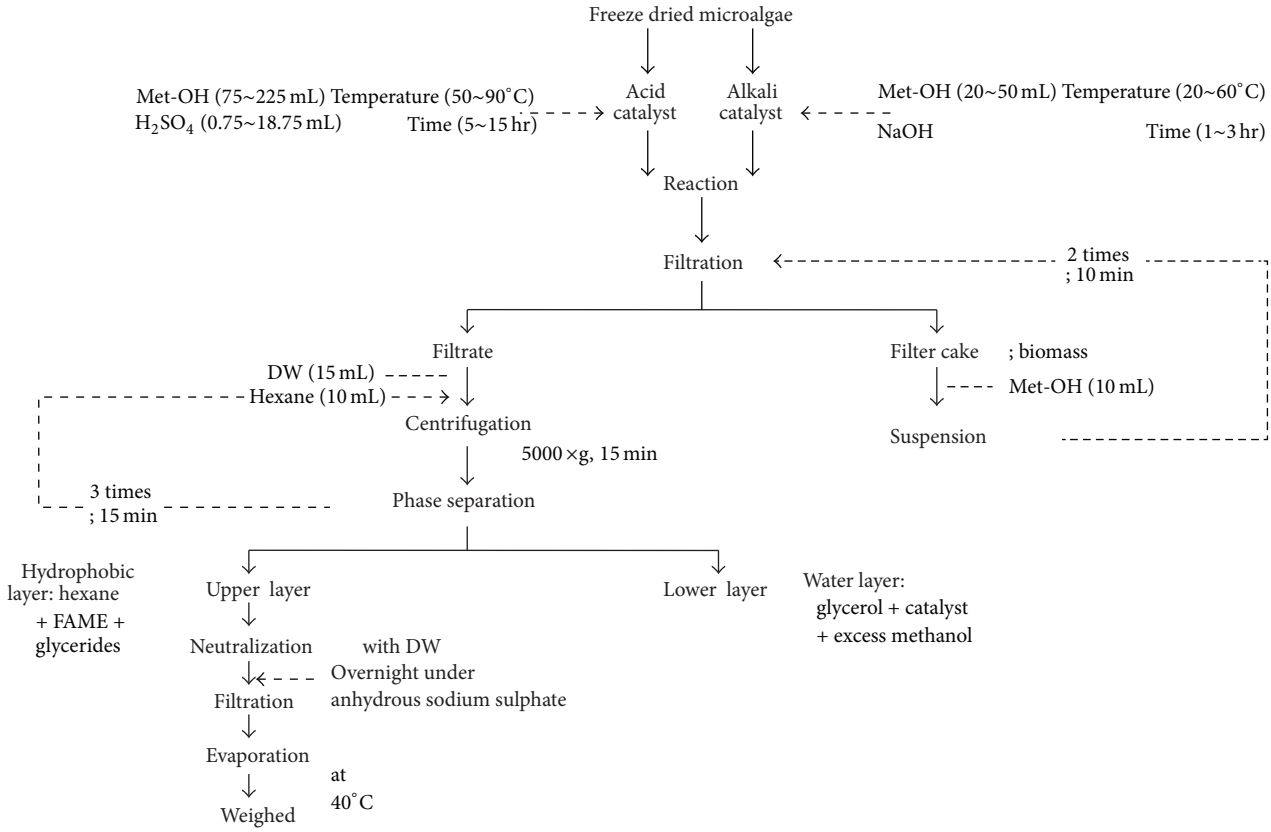

Figure 1: A schematic diagram of the *in situ* acidic and alkaline transesterification reactions.

15 min extractions using 10 mL of hexane. The pooled hexane layer was washed with water (to remove the residual traces of the acidic catalyst and methanol), separated, and then dried over anhydrous sodium sulfate overnight. The extracted solvent layer was filtered (Advantec No. 2, Toyo Roshi Inc., Tokyo, Japan), and its volume was recorded. An aliquot of the extraction solvent (10 mL) containing the FAMEs (crude biodiesel) was transferred to a preweighed glass vial evaporated (40~45°C) for 15 min using a vacuum evaporator (EYELA, Digital Water Bath SB-1000, Japan) and then cooled within a desiccator for 30 min. The mass of the biodiesel was determined gravimetrically, in duplicate. All of the stirred reactions were conducted using a magnetic stirrer system with a constant rotation speed of 500 rpm. The biodiesel yield from the algae oil was calculated using (1) as follows:

$$\text{Biodiesel yield (\%)} = \frac{\text{Algae mass (g)} \times \text{Lipid content (\%)}}{\text{Weight of biodiesel (FAME) (g)}}, \quad (1)$$

in which the amount of FAMEs at each step was determined by collecting them from a TLC plate and weighing them.

2.3. Thin Layer Chromatography (TLC) Analysis. After transesterification, the FAMEs (fatty acid methyl esters (FAME)) and residual triacylglycerides (TAGs) were measured using 0.25 mm thick silica gel G-60 TLC plates (Merck, Darmstadt, Germany). The detailed method was as follows: the elution solvent was n-hexane : diethyl ether (90 : 10, v/v) and after full development to the detection of the FAME spots, the spots were visualized using an iodine vapor and spraying the plates with 10% phosphomolybdic acid (98% purity, Daejung Co., Ltd, Shi Heung, Korea) in ethanol, and then drying them in the oven at 105°C [26]. The mono-, di-, and triglyceride mixture (TAG STD, Supelco, Bellefonte, PA, USA) and commercial biodiesel (FAME, S Company Houston, TX, USA) were used as standards [26]. Additionally, the pigments that remained in the FAME fraction were also separated by TLC, using the same 0.25 mm thick silica gel G-60 plates (Merck, Darmstadt, Germany) that were developed using petroleum ether (99.5%, Daejung Co., Ltd, Shi Heung, Korea) : cyclo hexane (%, Wako, Osaka, Japan) : ethyl acetate (99%, Daejung Co., Ltd, Shi Heung, Korea) : acetone (99.5%, Daejung Co., Ltd, Shi Heung, Korea) : methanol (99.5%, Daejung Co., Ltd, Shi Heung, Korea) (60 : 16 : 10 : 10 : 4, v/v) [27].

2.4. Purification of FAMEs. The FAMEs of the crude biodiesel were purified using silica gel column chromatography. The crude biodiesel was applied to a silica gel chromatography column. The column had been prepared using the previously described slurry of silica gel (18 g) (0.063–0.2 mm, Merck, Darmstadt, Germany) in hexane (300 mL). The n-hexane level was lowered until it was 1 cm above that of the stationary phase. The extracted algal oil was added to the column and eluted using n-hexane : EtOAC (25 : 1, v/v) at a flow rate of

3 mL/min. The FAME fraction had a deep yellow color [28, 29].

2.5. Design of the Experiments: Taguchi Method. Experiments were designed to determine the effects of four factors, the reaction temperature, the reaction period, the amount of catalyst (H_2SO_4), and the biomass to solvent ratio. Nine experiments were designed using the Taguchi method with an L9 three-level-four-factor array [34].

2.6. Analysis of the FAME Fatty Acid Profiles. To determine the fatty acid composition of the FAMEs, gas chromatography (GC, HP 6890 series, Victoria, Australia) was conducted using the following method: 1 μL of FAME that was obtained using *in situ* transesterification via alkaline or acidic catalysis was injected into a GC with a flame ionization detector (FID); an SP-2560 column (100 m × 0.25 mm × 0.2 μm, #24056, Supelco); and an oven temperature that increased at 4°C/min from 100°C to 240°C. The pouring and detector temperatures were set at 250°C and 280°C, respectively, the flow volume was 1.0 mL, and the split ratio was 50 : 1 [30].

2.7. Statistical Analysis. The data are expressed as the mean values ± SDs (standard deviation) and the mean values are the averages of five test results per experiment. The data were analyzed using the Student's *t*-test (SAS 9.1, SAS, Cary, NC, USA). The experiments were repeated at least three times to confirm the results. The data were analyzed using an analysis of variance, and the mean values were considered significantly different at $P < 0.05$. The optimal extraction condition was determined using regression analysis.

3. Results and Discussion

3.1. Optimization of Crude Biodiesel Production Using an Alkaline or Acidic Catalyst. For conventional two-step industrial biodiesel production, methanol is most often used as the reaction solvent with an alkaline catalyst for transesterification because it has several advantages over the simultaneous separation of glycerol, a high product yield, and low price [31], as well as mild processing conditions, short reaction times, and some other economic benefits [32–34]. Rather than this conventional transesterification process, *in situ* transesterification with an alkaline catalyst could be used; however, for the production of biodiesel from microalgae, an alkaline catalyst would not be suitable for the *in situ* transesterification process, due to the characteristically high FFA (free fatty acid) content of the microalgal lipids. *In situ* transesterification of oils containing high concentrations of FFA would result in a partial saponification reaction, leading to soap formation [25]. Soaps can cause the formation of emulsions, which create difficulties in the downstream recovery and purification of the biodiesel [35]. Using inorganic acids, such as hydrochloric acid and sulfuric acid, as reaction catalysts was therefore considered for microalgal lipid transesterification, due to their insensitivity to the FFA content of this lipid feedstock. Consequently, using acidic catalysis facilitates both the biodiesel producing transesterification and esterification reactions [25]. Studies of the catalytic activities of HCl and H_2SO_4 in the transesterification of *Thevetia peruviana* seed oil, cotton seed oil, and vegetable oil, among others, showed that H_2SO_4 exhibited better catalytic activity than HCl [36, 37]. Therefore, for *in situ* transesterification using an alkaline or acidic catalyst, several reaction parameters should be considered such as the reaction temperature, the reaction time, the amount of catalyst, the amount of solvent, the water content, and the agitation speed [36, 37]. To obtain the highest yield of biodiesel, these variables were optimized using the Taguchi methods [38], employing an L9 three-level-four-factor orthogonal array matrix [34]; nine experiments were designed as shown in Tables 1 and 3 for an alkaline or an acidic catalyst, respectively. Using an alkaline catalyst, as shown in Table 1, the biodiesel yield was the lowest and the highest in experiment number 1 and experiment number 8, respectively. Depending on the level of each factor, the yields changed from 11.63 ± 1.06 to 55.07 ± 2.18% and the average yield was 38.45 ± 1.50%. In each factor level (A_i) of the yield (K_i^A) and at each K_i^A value per unit level, the k_i^A (= $K_i^A/3$) were calculated from the difference (R value) between the maximum K_i^A and minimum K_i^A. However, as shown in Table 3, the lowest and highest yields of crude biodiesel were obtained in experiment number 1 and experiment number 7, respectively. Depending on the level of each factor, the yields were changed from 13.03 ± 3.07 to 48.40 ± 0.51% and the average yield was 39.27 ± 0.94%. The factor effects decreased in the order of biomass to solvent ratio (34.36%) > catalyst amount (28.62%) > reaction time (19.72%) > reaction temperature (17.32%). From these factors, the size of the effect of the test parameters could be calculated, as shown in Tables 2 and 4. Table 2 shows the effect of the reaction factors on the mean response using the alkaline catalyst. The effect refers to

Table 1: Experimental factors and levels for the orthogonal array design using the Taguchi method (% w/w, based on the lipid weight).

(a)

Level	Temperature (°C)	Time (hr)	Catalyst amount (% of algal weight, w/w)	Solvent (mL)
	A	*B*	*C*	*D*
1	30	1	0.5	20
2	45	2	1	35
3	60	3	1.5	50

(b)

Run number	*A*	*B*	*C*	*D*	*Y* (%)
1	1	1	1	1	11.63 ± 1.06
2	1	2	2	2	31.33 ± 0.79
3	1	3	3	3	33.29 ± 0.47
4	2	1	2	3	37.08 ± 0.58
5	2	2	3	1	38.13 ± 2.32
6	2	3	1	2	48.54 ± 2.99
7	3	1	3	2	50.07 ± 1.02
8	3	2	1	3	55.07 ± 2.18
9	3	3	2	1	40.89 ± 2.07

Table 2: Analysis of the *in situ* transesterification factors for the yield of crude biodiesel from *Scenedesmus* sp. using the orthogonal array design (% w/w, based on the lipid weight).

	A	B	C	D
K_1	76.25 ± 2.3	98.78 ± 2.7	115.21 ± 6.2	90.65 ± 5.4
K_2	123.75 ± 5.9	124.51 ± 5.3	109.31 ± 3.4	129.94 ± 4.8
K_3	146.01 ± 5.3	122.72 ± 5.5	121.49 ± 3.8	125.42 ± 3.2
k_1	25.42 ± 0.77	32.93 ± 0.88	38.4 ± 2.07	30.22 ± 1.82
k_2	41.25 ± 1.96	41.5 ± 1.76	36.44 ± 1.14	43.31 ± 1.60
k_3	48.67 ± 1.75	40.91 ± 1.84	40.5 ± 1.27	41.81 ± 1.08
R	23.25	8.58	4.06	13.09
Optimal level	3	2	3	2

$K_i^A = \sum$ biodiesel yield at A_i.
$k_i^A = K_i^A/3$.
$R_i^A = \max\{k_i^A\} - \min\{k_i^A\}$.

Table 3: Experimental factors and levels for the orthogonal array design using the Taguchi method (% w/w, based on the lipid weight).

(a)

Level	Temperature (°C)	Time (hr)	Catalyst amount (% of solvent, v/v)	Biomass to solvent ratio (mL, v/w)
	A	B	C	D
1	50	5	1	1 : 5
2	70	10	3	1 : 15
3	90	15	5	1 : 25

(b)

Run number	A	B	C	D	Y (%)
1	1	1	1	1	13.03 ± 3.07
2	1	2	2	2	44.72 ± 0.18
3	1	3	3	3	44.13 ± 0.34
4	2	1	2	3	40.38 ± 0.36
5	2	2	3	1	39.36 ± 0.82
6	2	3	1	2	44.46 ± 1.08
7	3	1	3	2	48.40 ± 0.51
8	3	2	1	3	39.80 ± 1.65
9	3	3	2	1	39.07 ± 0.42

the average value of the crude biodiesel yield for each factor at the different levels. Thus, the average value for each factor at each of the three levels was calculated and plotted (Figure 2). Figure 2 shows the mean effects plot for the crude biodiesel yield of *in situ* transesterification via alkaline catalysis. The dots in the reaction time, amount of catalyst, and solvent quantity show the fluctuations in the biodiesel yield. The lowest biodiesel yield was obtained at the lowest reaction temperature; increasing the reaction temperature resulted in a higher biodiesel yield. The effects of the factors decreased in the order of reaction temperature (47.5%) > solvent quantity (26.7%) > reaction time (17.5%) > catalyst amount (8.3%). The optimal levels of each factor were obtained from the value of k_i^A, and these results lead to the conclusion that the factors that provided the maximal yield were a reaction temperature of 60°C, a solvent quantity of 35 mL, a reaction time of 2 hrs, and an amount of catalyst of 1.5% (based on the lipid weight). However, the effects of the reaction time and the amount of catalyst were weaker than that of the other factors. Therefore, the levels of the recommended factors were as follows: reaction temperature of 60°C (level 3), a solvent quantity of 35 mL (level 2), reaction time of 2 hrs (level 2), and an amount of catalyst of 0.5% (level 1). The theoretical biodiesel yield of 55.07 ± 2.18% ($P < 0.05$) could be obtained using these optimal conditions. Figure 3 shows the mean effects plot for the crude biodiesel yield from *in situ* transesterification via acidic catalysis. The dots in biomass to solvent ratio showed the fluctuations of the biodiesel yield. When the levels of the reaction temperature, reaction time, and amount of catalyst increased, a higher biodiesel yield was obtained. The lowest biodiesel yield was obtained at the lowest biomass to solvent ratio, and the highest biodiesel yield was obtained at the middle level of the biomass to solvent ratio. The optimal levels of each factor were obtained from the value of k_i^A, and these results lead to the conclusion that the factors that provided the maximum yield were a reaction temperature of 90°C, a reaction time of 15 hrs, an amount of catalyst of 5% (base on solvent), and a biomass to solvent ratio of 1 : 15 (w/v). However, the time and temperature effects were lower than that of the other factors, and these conditions were not favorable for biodiesel production. A high reaction temperature increases the cost of biodiesel production [16]. A long reaction time also increases the cost of production [39]. Therefore, a reaction temperature of 70°C (level 2), a reaction time of 10 hrs (level 2), an amount of catalyst of 5% (level 3), and a biomass to solvent ratio of 1 : 15 (level 2) were selected as the optimal conditions. A crude biodiesel yield of 48.41 ± 0.21% ($P < 0.05$) could be obtained under these optimal conditions. The optimal conditions provided almost the same yield of biodiesel as the maximal conditions.

3.2. Identification and Purification of FAMEs. Thin layer chromatography (TLC) is one of the simplest and most widely used methods for separating mixtures for analysis. In this study, it was used to monitor the conversion of the algal lipids to fatty acid methyl esters (FAMEs, namely, biodiesel). The TLC results demonstrated the presence of FAME, TAG, and

Table 4: Analysis of the *in situ* transesterification factors for the yield of crude biodiesel from *Scenedesmus* sp. using the orthogonal array design (% w/w, based on lipid weight).

	A	*B*	*C*	*D*
K_1	102.13 ± 3.61	102.03 ± 4.46	97.26 ± 7.04	91.46 ± 4.71
K_2	124.24 ± 2.00	124.14 ± 2.77	124.50 ± 1.33	137.97 ± 1.13
K_3	127.42 ± 2.61	127.63 ± 0.99	132.04 ± 0.16	124.38 ± 2.38
k_1	34.04 ± 1.20	34.01 ± 1.49	32.42 ± 2.35	30.49 ± 1.57
k_2	41.41 ± 0.67	41.38 ± 0.92	41.50 ± 0.44	45.99 ± 0.38
k_3	42.47 ± 0.87	42.54 ± 0.33	44.01 ± 0.05	41.46 ± 0.79
R	8.43 ± 0.24	8.54 ± 1.16	11.59 ± 2.40	15.50 ± 1.60
Optimal level	3	3	3	2

$K_i^A = \sum$ biodiesel yield at A_i.
$k_i^A = K_i^A/3$.
$R_i^A = \max\{k_i^A\} - \min\{k_i^A\}$.

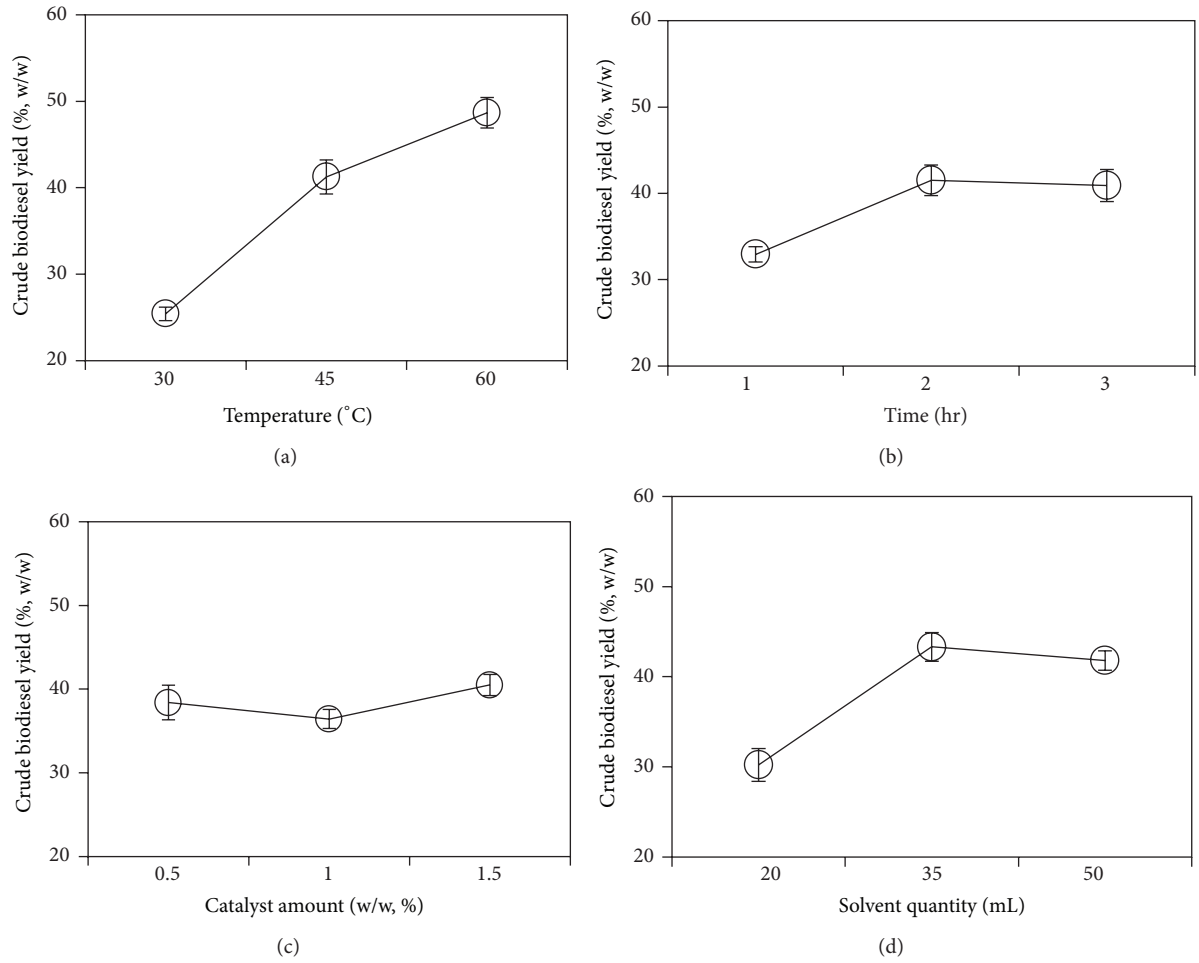

Figure 2: Main effects plot for the reaction factors in *in situ* transesterification via alkali catalysis.

free fatty acids. The TAG standard was a mixture of mono-, di-, and triglycerides, and the FAME standard was a commercial biodiesel (as a comparative standard). Each standard was eluted using n-hexane. The retention factors for methyl ester and triglycerides were calculated as R_f, Me = 0.7–0.73 and R_f, TAG = 0.41–0.45, respectively. The compound with the larger R_f is less polar because it interacts less strongly with the polar adsorbent on the TLC plate. Here, the methyl esters and triglycerides exhibited the characteristics of high nonpolarity. As shown in Figure 4, after the TLC plates had been developed, a dark trace appeared only in the alkaline catalyzed biodiesel, which was green before the visualization reaction was performed. The photosynthetic microalga *Scenedesmus* sp. synthesizes pigments such as chlorophylls

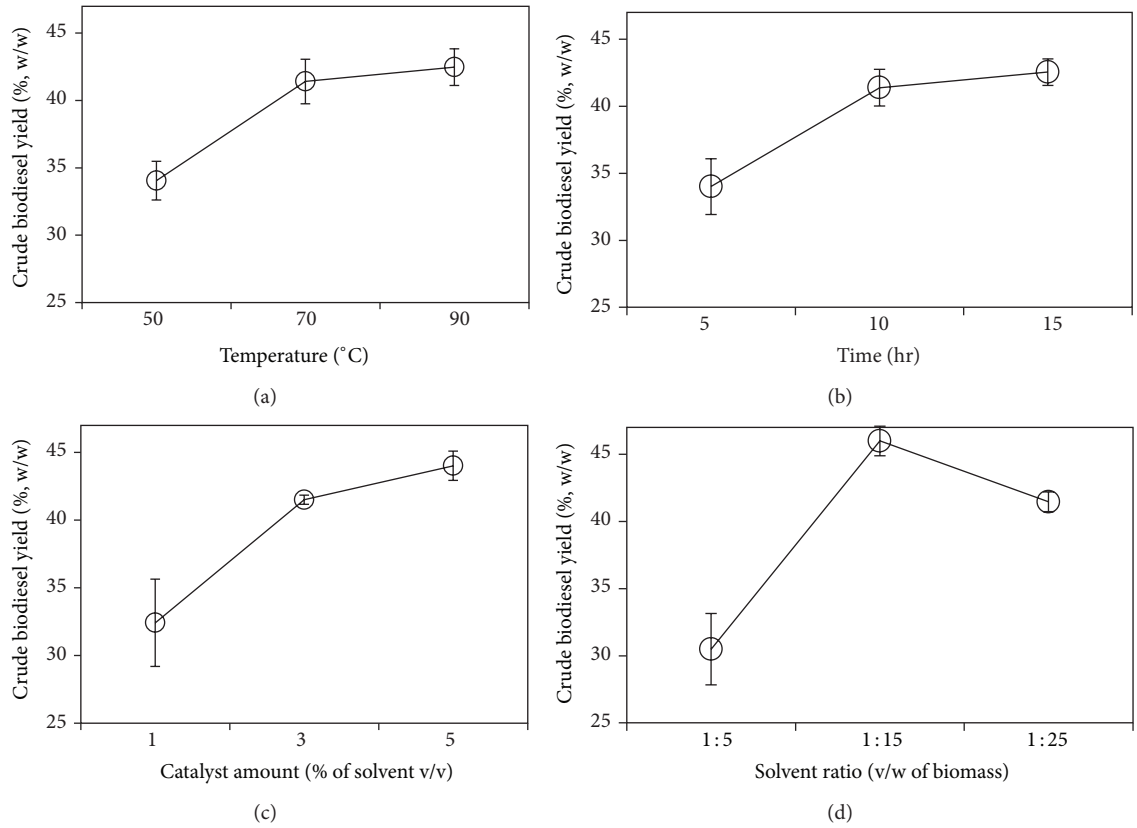

Figure 3: Main effects plot for the reaction factors in *in situ* transesterification via acidic catalysis.

and carotenoids. The dark green trace was considered to contain pigments. TLC was used to identify the pigments, which consisted of chlorophyll a, β-carotene, pheophytin a and b, and other substances (Figure 5) [27]. Silica gel column chromatography of crude alkali-catalyzed biodiesel was used to fractionate the pigments and the FAMEs. The column was eluted with n-hexane : acetone (98.5 : 1.5, v/v). As shown in Figure 6(a), three fractions were obtained from the crude alkali-catalyzed biodiesel. The eluted materials were collected in individual vials and were fractionated depending on the color and weight difference between these vials. Fraction A (tube numbers 1–10) was colorless and transparent, but the colors of fraction B (tube numbers 11–16) and fraction C (tube numbers 17–24) were deep yellow and pale yellow, respectively. The green-pigmented materials adsorbed to the silica gel inside the column. The organic solvent of each vial was evaporated in a dry oven at 40°C for a few days, and then the vials were weighed. The materials inside the vials were redissolved in hexane and were then collected according to fractionation (fractions A, B, and C). Each of the fractions was analyzed using TLC, and the results are shown in Figure 7. TLC on silica gel plate demonstrated the presence of methyl esters, tri-, di-, and monoglycerides and fatty acids in the alkali-catalyzed biodiesel (Figure 7). FAMEs were observed in fractions B and C. Then, we conducted the same experiment using acid-catalyzed biodiesel. The color of fraction A (tube numbers 1–12) was colorless and transparent, but the colors of fraction B (tube numbers 13–23) and fraction C (tube numbers 24–27) were deep yellow and pale yellow (almost colorless), respectively (Figure 6(b)). The materials inside the vials were redissolved in hexane, and then each fraction was collected (fractions A, B, and C). Each fraction was analyzed using TLC, and the results are shown in Figure 8. FAMEs were observed in fraction B. The FAME fraction was purified using silica gel column chromatography, and the purified FAME contents were found to be 29.15% in the crude alkali-catalyzed biodiesel and 83.52% in the acid-catalyzed biodiesel. Approximately 70% of the alkali-catalyzed biodiesel and 16% of the acid-catalyzed biodiesel were found to contain pigments, which consisted of β-carotene, chlorophyll a, pheophytin a and b, and other substances (Figure 5). Therefore, the final purified biodiesel yields obtained from alkali- and acid-catalyzed biodiesel were estimated to be 16.05% and 40.43%, respectively. The yield of the acid-catalyzed biodiesel was approximately 2.5-fold higher than that of the alkali-catalyzed biodiesel. The yield from *in situ* transesterification using an acidic catalyst appeared to be higher than other reported data obtained using the conventional Taguchi method by 27.9~42.6% [40–42]. To evaluate the quality of the biodiesel obtained using these processes, the contents of the major fatty acid in the FAME profiles were estimated, as shown in Table 5. In general, there was not much difference in the fatty compositions of the acidic and alkaline catalyzed analytes; however, higher amounts of $C_{16:0}$ and $C_{18:3}$, the two major fatty acids among the FAMEs, were obtained using acidic

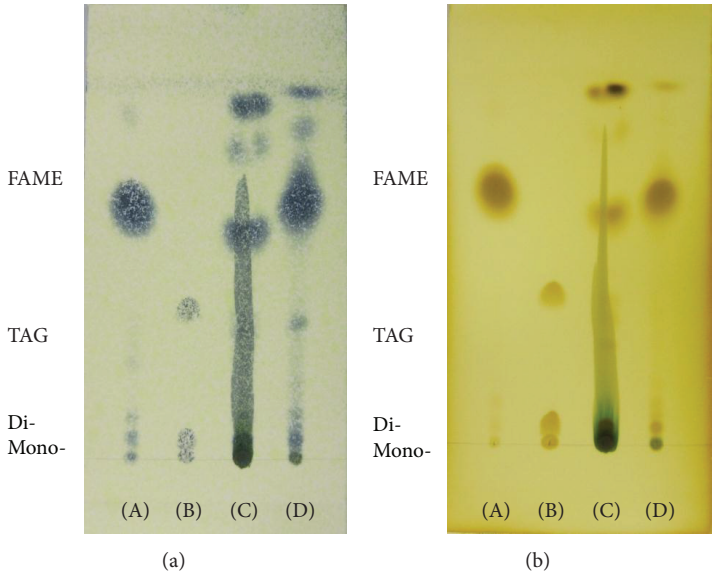

Figure 4: Thin layer chromatograms of crude FAMEs on HPTLC plates that were developed using n-hexane : ether (90 : 10, v/v) and visualized using (a) 10% phosphomolybdic acid in ethanol and (b) iodine vapor. (A) FAMEs (standard); (B) TAGs (standard); (C) *in situ* transesterification via alkaline catalysis; (D) *in situ* transesterification via acidic catalysis.

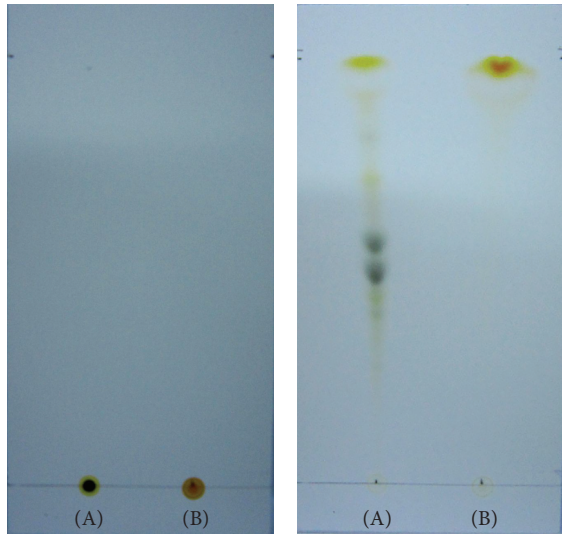

Figure 5: Results of separating the pigment fractions using TLC (20 times dilution with hexane). (a) Before development; (b) after development; (A) crude biodiesel; (B) purified biodiesel.

catalysis, which implies that acidic catalysts can produce better quality biodiesel. These results indicated that the acidic catalyst was a more efficient catalyst than the alkaline catalyst for *in situ* transesterification.

4. Conclusion

To optimize *in situ* transesterification via alkaline or acidic catalysis for the production of biodiesel from *Scenedesmus* sp., several objective variables were analyzed using an L9 orthogonal matrix as follows: the reaction time and temperature and the amounts of catalyst and solvents [34]. In using an acidic catalyst in *in situ* transesterification, the effects of the factors decreased in the order of biomass to solvent ratio (34.36%) > catalyst amount (28.62%) > reaction time (19.72%) > reaction temperature (17.32%). The maximum yield of 48.41 ± 0.21% ($P < 0.05$) (based on lipid weight) was obtained at a biomass to solvent ratio of 1 : 15, H_2SO_4 at 5% (% of solvent, v/v), a reaction time of 10 hrs, and a reaction temperature of 70°C. For the alkaline catalyst, the effects of the factors decreased in the order of the reaction temperature

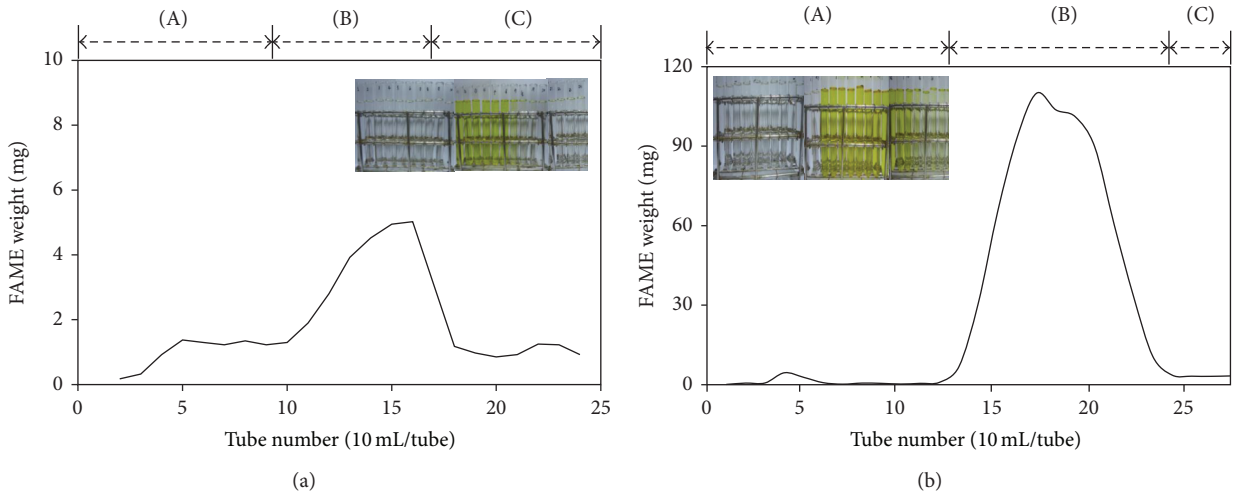

Figure 6: Column chromatographic separation of FAME using an n-hexane : acetone (98.5 : 1.5, v/v) solution from (a) alkali- and (b) acid-catalyzed biodiesels.

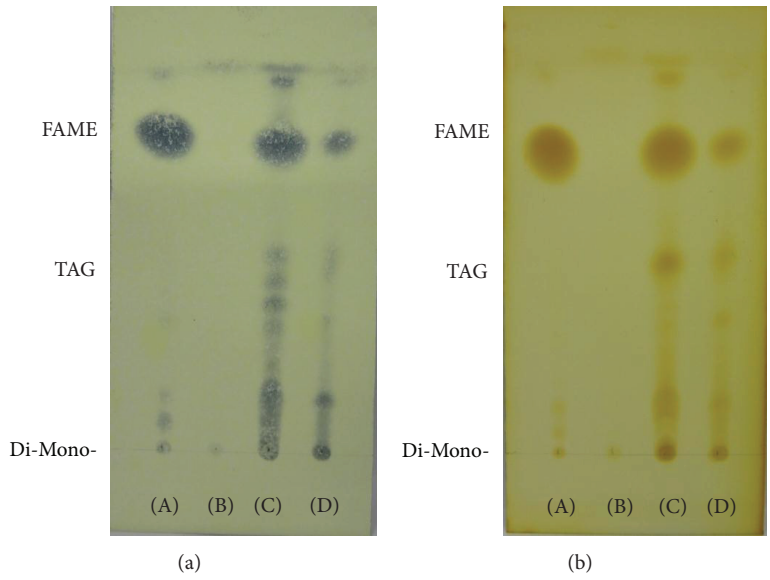

Figure 7: Thin layer chromatograms of the FAME fraction on HPTLC plates that were developed using n-hexane : ether (90 : 10, v/v) and visualized using (a) 10% phosphomolybdic acid in ethanol (b) and iodine vapor. (A) FAME STD; (B) Fraction A (tube numbers: 1–10); (C) Fraction B (tube numbers: 11–16); (D) Fraction C (tube numbers: 17–24).

(47.5%) > solvent quantity (26.7%) > reaction time (17.5%) > amount of catalyst (8.3%). The maximum biodiesel yield of 55.07 ± 2.18% (based on lipid weight) was obtained under the following conditions : solvent quantity of 50 mL, NaOH amount of 0.5% (based on the lipid weight), a reaction time of 2 hrs, and a reaction temperature of 60°C ($P < 0.05$). However, TLC analysis of the FAMEs showed that 48.41% of highly purified FAME was obtained through acidic catalysis, whereas 23.67% was obtained through alkaline catalysis, with less contamination by lipid pigments. It was also found that the quality of the biodiesel produced using the acidic catalyst was better than that produced using the alkaline catalyst by having higher amounts of $C_{16:0}$ and $C_{18:3}$. These results clearly indicated that an *in situ* transesterification process using an acidic catalyst should have an excellent potential for directly producing biodiesel from microalgae [43]. However, the entire process should be further developed to meet the economic feasibility required to scale up to industrial production. Nonetheless, these results could provide information for economically producing biofuels from *Scenedesmus* sp. microalga based on the quantity and quality of the algal biodiesel produced in this study.

Conflict of Interests

The authors declare that there is no conflict of interests regarding the publication of this paper.

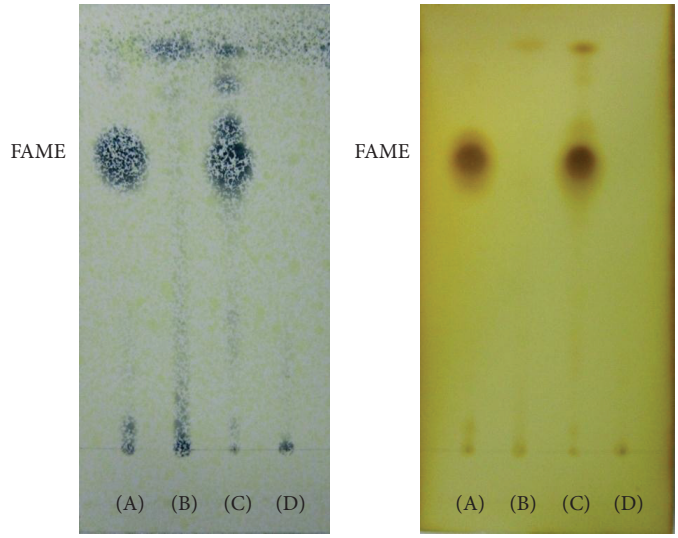

(a) (b)

Figure 8: Thin layer chromatograms of the FAME fractions on HPTLC plates that were developed using n-hexane : ether (90 : 10, v/v) and visualized using (a) 10% phosphomolybdic acid in ethanol and in (b) iodine vapor. (A) FAME STD; (B) fraction A (tube numbers: 1–12); (C) fraction B (tube numbers: 13–23); (D) fraction C (tube numbers: 24–27).

Table 5: Comparison of fatty acids content in *Scenedesmus* sp. by *in situ* transesterification alkali and acid catalysis.

Catalyst	Fatty acids composition (%)						
	$C_{14:0}$	$C_{16:0}$	$C_{16:1}$	$C_{18:0}$	$C_{18:1}$	$C_{18:2}$	$C_{18:3}$
Acid	0.43	33.21	0.69	1.70	0.67	11.59	41.22
Alkali	0.52	30.11	0.99	1.84	0.41	10.51	37.98

Acknowledgment

This research was supported by a grant from Marine Biotechnology Program Funded by Ministry of Oceans and Fisheries, Korea.

References

[1] D. Bajpai and V. K. Tyagi, "Biodiesel: source, production, composition, properties and its benefits," *Journal of Oleo Science*, vol. 55, no. 10, pp. 487–502, 2009.

[2] X. Meng, J. Yang, X. Xu, L. Zhang, Q. Nie, and M. Xian, "Biodiesel production from oleaginous microorganisms," *Renewable Energy*, vol. 34, no. 1, pp. 1–5, 2009.

[3] Y. Chisti, "Biodiesel from microalgae," *Biotechnology Advances*, vol. 25, no. 3, pp. 294–306, 2007.

[4] L. Gouveia and A. C. Oliveira, "Microalgae as a raw material for biofuels production," *Journal of Industrial Microbiology and Biotechnology*, vol. 36, no. 2, pp. 269–274, 2009.

[5] X. Miao, P. Li, R. Li, and J. Zhong, "*In situ* biodiesel production from fast-growing and high oil content chlorella pyrenoidosa in rice straw hydrolysate," *Journal of Biomedicine and Biotechnology*, vol. 2011, Article ID 141207, 8 pages, 2011.

[6] H. P. S. Makkar and K. Becker, "Jatropha curcas, a promising crop for the generation of biodiesel and value-added coproducts," *European Journal of Lipid Science and Technology*, vol. 111, no. 8, pp. 773–787, 2009.

[7] A. Richmond, "Microalgae of economic potential," in *Handbook of Microalgal Mass Culture*, pp. 199–243, Taylor & Francis, New York, NY, USA, 1986.

[8] A. L. Haag, "Algae bloom again," *Nature*, vol. 447, no. 7144, pp. 520–521, 2007.

[9] M. E. Huntley and D. G. Redalje, "CO_2 mitigation and renewable oil from photosynthetic microbes: a new appraisal," *Mitigation and Adaptation Strategies for Global Change*, vol. 12, no. 4, pp. 573–608, 2007.

[10] O. Pulz and W. Gross, "Valuable products from biotechnology of microalgae," *Applied Microbiology and Biotechnology*, vol. 65, no. 6, pp. 635–648, 2004.

[11] R. Raja, S. Hemaiswarya, N. A. Kumar, S. Sridhar, and R. Rengasamy, "A perspective on the biotechnological potential of microalgae," *Critical Reviews in Microbiology*, vol. 34, no. 2, pp. 77–88, 2008.

[12] J. I. Park, H. C. Woo, and J. W. Lee, "Production of bio-energy from microalgae: status and perspectives," *Korean Journal of Chemical Engineering*, vol. 46, no. 5, pp. 833–844, 2008.

[13] T. Matsunaga, M. Matsumoto, Y. Maeda, H. Sugiyama, R. Sato, and T. Tanaka, "Characterization of marine microalga, *Scenedesmus* sp. strain JPCC GA0024 toward biofuel production," *Biotechnology Letters*, vol. 31, no. 9, pp. 1367–1372, 2009.

[14] N. Y. Kim, S. H. Oh, H. Y. Lee, and S. Y. Lee, "Extraction, purification and property of the lipid from *Scenedesmus* sp.," *Korean Society for Biotechnology and Bioengineering Journal*, vol. 25, no. 4, pp. 363–370, 2010.

[15] N. Y. Kim, S. H. Oh, H. Y. Lee, and S. Y. Lee, "Optimization of lipid extraction from *Scenedesmus* sp. using taguchi approach," *Korean Society For Biotechnology and Bioengineering Journal*, vol. 25, no. 4, pp. 371–378, 2010.

[16] A. S. Ramadhas, S. Jayaraj, and C. Muraleedharan, "Biodiesel production from high FFA rubber seed oil," *Fuel*, vol. 84, no. 4, pp. 335–340, 2005.

[17] K. G. Georgogianni, M. G. Kontominas, P. J. Pomonis, D. Avlonitis, and V. Gergis, "Conventional and *in situ* transesterification of sunflower seed oil for the production of biodiesel," *Fuel Processing Technology*, vol. 89, no. 5, pp. 503–509, 2008.

[18] A. I. Carrapiso, L. M. Timón, J. M. Petrón, J. F. Tejeda, and C. García, "*In situ* transesterification of fatty acids from Iberian pig subcutaneous adipose tissue," *Meat Science*, vol. 56, no. 2, pp. 159–164, 2000.

[19] F. Sahena, I. S. M. Zaidul, S. Jinap et al., "Application of supercritical CO_2 in lipid extraction—a review," *Journal of Food Engineering*, vol. 95, no. 2, pp. 240–253, 2009.

[20] J. Qian, F. Wang, S. Liu, and Z. Yun, "*In situ* alkaline transesterification of cottonseed oil for production of biodiesel and nontoxic cottonseed meal," *Bioresource Technology*, vol. 99, no. 18, pp. 9009–9012, 2008.

[21] M. B. Johnson and Z. Wen, "Production of biodiesel fuel from the microalga schizochytrium limacinum by direct transesterification of algal biomass," *Energy and Fuels*, vol. 23, no. 10, pp. 5179–5183, 2009.

[22] M.-Y. Chang, G.-J. Tsai, and J.-Y. Houng, "Optimization of the medium composition for the submerged culture of Ganoderma lucidum by Taguchi array design and steepest ascent method," *Enzyme and Microbial Technology*, vol. 38, no. 3-4, pp. 407–414, 2006.

[23] S. S. Mahapatra and A. Patnaik, "Optimization of wire electrical discharge machining (WEDM) process parameters using Taguchi method," *International Journal of Advanced Manufacturing Technology*, vol. 34, no. 9-10, pp. 911–925, 2007.

[24] S. V. Mohan, N. C. Rao, K. K. Prasad, P. M. Krishna, R. S. Rao, and P. N. Sarma, "Anaerobic treatment of complex chemical wastewater in a sequencing batch biofilm reactor: process optimization and evaluation of factor interactions using the taguchi dynamic DOE methodology," *Biotechnology and Bioengineering*, vol. 90, no. 6, pp. 732–745, 2005.

[25] E. A. Ehimen, Z. F. Sun, and C. G. Carrington, "Variables affecting the *in situ* transesterification of microalgae lipids," *Fuel*, vol. 89, no. 3, pp. 677–684, 2010.

[26] B. Liu and Z. Zhao, "Biodiesel production by direct methanolysis of oleaginous microbial biomass," *Journal of Chemical Technology and Biotechnology*, vol. 82, no. 8, pp. 775–780, 2007.

[27] H. T. Quach, R. L. Steeper, and G. W. Griffin, "An improved method for the extraction and thin-layer chromatography of chlorophyll a and b from spinach," *Journal of Chemical Education*, vol. 81, no. 3, pp. 385–387, 2004.

[28] B. A. McKittrick, S. Dugar, and D. ABurnett, "Sulfur-substituted azetidinone compounds useful as hypocholesterolemic agents," US patent no. 5774467, 1998.

[29] Y. K. Lim, D. K. Kim, and E. S. Yim, "Synthesis of biodiesel from vegetable oil and their characteristics in low temperature," *Journal of the Korean Industrial and Engineering Chemistry*, vol. 20, no. 2, pp. 208–212, 2009.

[30] K. D. Müller, H. Husmann, H. P. Nalik, and G. Schomburg, "Trans-esterification of fatty acids from microorganisms and human blood serum by trimethylsulfonium hydroxide (TMSH) for GC analysis," *Chromatographia*, vol. 30, no. 5-6, pp. 245–248, 1990.

[31] U. Schuchardt, R. Sercheli, and R. M. Vargas, "Transesterification of vegetable oils: a review," *Journal of the Brazilian Chemical Society*, vol. 9, no. 3, pp. 199–210, 1998.

[32] J. M. Encinar, J. F. González, J. J. Rodríguez, and A. Tejedor, "Biodiesel fuels from vegetable oils: transesterification of Cynara cardunculus L. Oils with ethanol," *Energy and Fuels*, vol. 16, no. 2, pp. 443–450, 2002.

[33] U. Rashid and F. Anwar, "Production of biodiesel through optimized alkaline-catalyzed transesterification of rapeseed oil," *Fuel*, vol. 87, no. 3, pp. 265–273, 2008.

[34] M. K. Lam, K. T. Lee, and A. R. Mohamed, "Homogeneous, heterogeneous and enzymatic catalysis for transesterification of high free fatty acid oil (waste cooking oil) to biodiesel: a review," *Biotechnology Advances*, vol. 28, no. 4, pp. 500–518, 2010.

[35] S. Al-Zuhair, "Production of biodiesel: possibilities and challenges," *Biofuels, Bioproducts and Biorefining*, vol. 1, no. 1, pp. 57–66, 2007.

[36] O. O. Oluwaniyi and S. A. Ibiyemi, "Efficacy of catalysts in the batch esterification of the fatty acids of ThevetiaPeruviana seed oil," *Journal of Applied Sciences and Environmental Management*, vol. 7, no. 1, pp. 15–17, 2003.

[37] X. Fan, *Optimization of Biodiesel Production from Crude Cottonseed Oil and Waste Vegetable Oil: Conventional and Ultrasonic Irradiation Methods*, Clemson University, Clemson, SC, USA, 2008.

[38] G. Taguchi, *Introduction to Quality Engineering: Designing Quality into Products and Processes*, 1986.

[39] L. C. Meher, D. Vidya Sagar, and S. N. Naik, "Technical aspects of biodiesel production by transesterification—a review," *Renewable and Sustainable Energy Reviews*, vol. 10, no. 3, pp. 248–268, 2006.

[40] N. Dizge, C. Aydiner, D. Y. Imer, M. Bayramoglu, A. Tanriseven, and B. Keskinler, "Biodiesel production from sunflower, soybean, and waste cooking oils by transesterification using lipase immobilized onto a novel microporous polymer," *Bioresource Technology*, vol. 100, no. 6, pp. 1983–1991, 2009.

[41] R. Xu and Y. Mi, "Simplifying the process of microalgal biodiesel production through *in situ* transesterification technology," *Journal of the American Oil Chemists' Society*, vol. 88, no. 1, pp. 91–99, 2011.

[42] B. D. Wahlen, R. M. Willis, and L. C. Seefeldt, "Biodiesel production by simultaneous extraction and conversion of total lipids from microalgae, cyanobacteria, and wild mixed-cultures," *Bioresource Technology*, vol. 102, no. 3, pp. 2724–2730, 2011.

[43] A. P. Vyas, J. L. Verma, and N. Subrahmanyam, "A review on FAME production processes," *Fuel*, vol. 89, no. 1, pp. 1–9, 2010.

Hindawi Publishing Corporation
BioMed Research International
Volume 2013, Article ID 251354, 9 pages
http://dx.doi.org/10.1155/2013/251354

Research Article

Degradation of Diuron by *Phanerochaete chrysosporium*: Role of Ligninolytic Enzymes and Cytochrome P450

Jaqueline da Silva Coelho-Moreira, Adelar Bracht, Aline Cristine da Silva de Souza, Roselene Ferreira Oliveira, Anacharis Babeto de Sá-Nakanishi, Cristina Giatti Marques de Souza, and Rosane Marina Peralta

Department of Biochemistry, State University of Maringa, 87020-900 Maringá, PR, Brazil

Correspondence should be addressed to Rosane Marina Peralta; rosanemperalta@gmail.com

Received 9 October 2013; Revised 26 November 2013; Accepted 27 November 2013

Academic Editor: Kannan Pakshirajan

The white-rot fungus *Phanerochaete chrysosporium* was investigated for its capacity to degrade the herbicide diuron in liquid stationary cultures. The presence of diuron increased the production of lignin peroxidase in relation to control cultures but only barely affected the production of manganese peroxidase. The herbicide at the concentration of 7 μg/mL did not cause any reduction in the biomass production and it was almost completely removed after 10 days. Concomitantly with the removal of diuron, two metabolites, DCPMU [1-(3,4-dichlorophenyl)-3-methylurea] and DCPU [(3,4-dichlorophenyl)urea], were detected in the culture medium at the concentrations of 0.74 μg/mL and 0.06 μg/mL, respectively. Crude extracellular ligninolytic enzymes were not efficient in the *in vitro* degradation of diuron. In addition, 1-aminobenzotriazole (ABT), a cytochrome P450 inhibitor, significantly inhibited both diuron degradation and metabolites production. Significant reduction in the toxicity evaluated by the *Lactuca sativa* L. bioassay was observed in the cultures after 10 days of cultivation. In conclusion, *P. chrysosporium* can efficiently metabolize diuron without the accumulation of toxic products.

1. Introduction

Agricultural practices are among the main activities responsible for the release of hazardous chemicals into the environment [1]. Among these chemicals, the pesticides (fungicides, herbicides and insecticides) have been used for decades without any control, resulting in a strong contamination of water, air, and foods as well as in the development of pesticide resistant organisms. This problem became more serious during the last years resulting in high risks to human health.

Herbicides are the main class of pesticides used extensively in home gardens and farms all over the world [2]. Diuron is a phenylurea herbicide applied to a wide variety of crops, especially sugar-cane cultures. The compound acts in photosynthetic organisms by blocking electron transport in photosystem II, thus inhibiting photosynthesis. In the environment diuron can be transformed abiotically via hydrolysis and photodegradation reactions, but under natural conditions these reactions occur at very low rates [3]. Due to this, diuron is known as a potential water contaminant being frequently detected at concentrations ranging from 2.7 μg/mL to 2849 μg/mL in surface water and 0.34 to 5.37 μg/mL in groundwater [4]. The dissipation of diuron from the environment is thus mainly due to biotic processes, the aerobic microbial metabolism being the major form of diuron transformation [3, 5]. The main reactions involved are N-demethylation and hydrolysis of the amide bond. In most cases, mono- and didemethylated compounds and 3,4-dichloroaniline appear as the main products of microbial metabolism [3, 6]. These metabolites accumulate in the environment and some of them are more toxic than diuron [7].

The aerobic biodegradation pathway for diuron is well established (Figure 1). It proceeds by successive demethylation steps to form DCPMU [1-(3,4-dichlorophenyl)-3-methylurea], DCPU [1-(3,4-dichlorophenyl)urea], and 3,4 DCA (3,4-dichloroaniline). Several studies describe the capability of soil fungi to degrade diuron with accumulation of

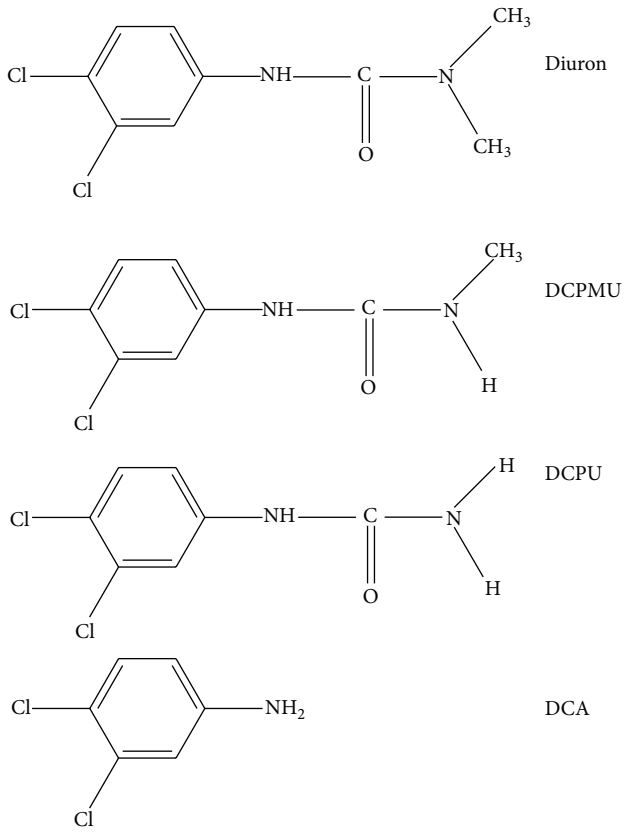

Figure 1: Chemical structure of diuron and its main metabolites DCPMU, DCPU, and DCA.

these N-demethylated metabolites [7–9]. Among white-rot fungi, the degradation of diuron is generally attributed to the action of extracellular enzymes, the lignin-modifying enzymes typically produced by these fungi [10–13]. However, the products generated in the degradation have not yet been characterized and no efforts have been done to evaluate their toxicity.

The model of white-rot fungus for many bioremediation studies is *Phanerochaete chrysosporium* [14]. Its ability to degrade pollutants appears to be related especially to the production of lignin peroxidase and manganese peroxidase, two lignin-modifying enzymes generally expressed under nitrogen-limited culture conditions [15], as well as to the intracellular cytochrome P450 system [16]. The transformation of diuron by *P. chrysosporium* in liquid cultures has already been documented in both stationary and shaken conditions [11, 12]. Stationary cultures are advantageous over shaken cultures because they work without mechanical energy requirements, thus increasing the feasibility of the technique for application in large scale treatment of wastewater. The metabolic processing of diuron by *P. chrysosporium* is still not completely clarified specially with respect to the metabolites that are produced and the role of cytochrome P450 in the degradation. Taking this into consideration, the objectives of this work were to study the removal of diuron from liquid cultures of *P. chrysosporium* with special interest in the role of cytochrome P450 and identification of demethylated metabolites. Attempts were also done to compare the toxicity of diuron metabolites with the parent molecule.

2. Materials and Methods

2.1. Chemicals. The enzymatic substrates, diuron (≥98%), DCPMU, DCPU 3,4-DCA (3,4-dichloroaniline), and ABT (1-aminobenzotriazole) were obtained from Sigma Chemical Corp. (St Louis, MO). Stock solutions of diuron, DCPMU, DCPU, 3,4-DCA, and ABT were prepared by dissolving standards in dimethyl sulfoxide (DMSO), filtering through a millipore membrane (0.45 mm), and storing at 4°C. PDA was obtained from Difco Laboratories (Detroit, MI). The solvents used in the HPLC analyses were of chromatographic grade and all other reagents were of analytical grade.

2.2. Microorganism and Inoculum. *Phanerochaete chrysosporium* was obtained from the André Tosello Foundation (ATCC 24725) and cultured on potato dextrose agar (PDA) for 7 days at 28°C. Mycelial plugs measuring 15 mm in diameter were made and used as inoculum for liquid cultures.

2.3. Culture Conditions. The experiments were performed in liquid medium under stationary conditions at 28°C in the dark. *P. chrysosporium* was cultivated in 125 mL Erlenmeyer flasks using three mycelial disks on PDA plates (approximately 15 mm in diameter) for up to 12 days. Each flask contained 25 mL of a medium prepared with a mineral solution without nitrogen source [17] containing 1.2 mmol/L ammonium tartrate in order to obtain a nitrogen-limited medium, that is favorable to ligninolytic enzyme production. Additionally, to induce the ligninolytic enzymes, a corn cob extract rich in phenolic compounds was used. For preparation of the extract, an aqueous suspension containing 3% corn cob powder (w/v) was boiled for 5 minutes and filtered through Whatman filter paper number 1 to retain the residues and to avoid diuron adsorption on the insoluble corn cob. Afterwards, the mineral solution was prepared using the corn cob extract enriched with 1% glucose as carbon source. The medium was previously sterilized by autoclaving at 121°C for 15 min.

2.4. Effect of Diuron in the Biomass Production of P. chrysosporium. Increasing amounts of diuron dissolved in DMSO (30 to 100 μmol/L) were added to the liquid medium at the beginning of the cultivation. The DMSO volume added was not superior to 30 μL in order to not affect the fungal metabolism. After 10 days the cultures were interrupted by filtration and the mycelia were washed three times with distilled water and dried to constant weight at 50°C.

2.5. Time Course of Enzyme Production and Diuron Degradation. To evaluate the capability of *P. chrysosporium* liquid cultures to degrade diuron, each culture flask received a volume of a diuron stock solution in DMSO (10 mg/mL) to give a final concentration of 30 μmol/L (7 μg/mL). The flasks were then

agitated to mix the herbicide solution and inoculated with the fungus. Two types of controls were conducted in parallel. In the first, the fungus was inoculated in liquid medium without herbicide. The second control consisted of sterile medium containing the same amount of diuron (abiotic control). All flasks were incubated for up to 12 days. At periodic intervals, the cultures were interrupted by filtration, and the culture extracts were used to evaluate the lignin-modifying enzymes, lignin peroxidase and manganese peroxidase, as well as the residual diuron and its metabolites by high-performance liquid chromatography (HPLC).

2.6. Lignin-Modifying Enzyme Assays. Manganese peroxidase (Mn peroxidase) activity was assayed by the oxidation of 1 mmol/L $MnSO_4$ in 50 mmol/L sodium malonate buffer pH 4.5, in the presence of 0.1 mmol/L H_2O_2. Manganic ions (Mn^{3+}) form a complex with malonate, which absorbs at 270 nm (ε_{270} = 11,590 M^{-1} cm^{-1}) [18]. Lignin peroxidase activity was determined by spectrophotometric measurement at 310 nm of the H_2O_2-dependent veratraldehyde formation from 0.4 mmol/L veratryl alcohol in 0.1 mol/L tartrate buffer of pH 3.0 [19]. Laccase activity was assayed by measuring the oxidation of 2,7′-azinobis [3-ethylbenzothiazolone-6-sulfonic acid] diammonium salt (ABTS) [20]. The enzymatic activities were expressed as International Units (U), defined as the amount of enzyme required to produce 1 μmol product per min at 40°C.

2.7. Analysis of Residual Diuron and Identification of Diuron Metabolites. For extraction of diuron and its metabolites from the mycelia, a volume of 6 mL of acetonitrile was added to the cells and the mixture was maintained for 2 h under agitation at 130 rpm. The mycelial extracts were obtained after centrifugation at 5,000 rpm for 15 min at 4°C. The concentrations of diuron and its metabolites in the culture media and in the mycelial extracts were determined using an HPLC system (Shimadzu, Tokyo) with an LC-20AT Shimadzu system controller, Shimadzu SPD-20 A UV-VIS detector, equipped with a reversed Shimpack C18 column (4.6 × 250 mm), maintained at 40°C. The mobile phase consisted of water (solvent A) and acetonitrile (solvent B) at a flow rate of 0.8 mL/min. The gradient program started with 25% acetonitrile increasing to 85% in 15 minutes. The column was equilibrated for 10 minutes before the next injection. The UV detection was made at 245 nm and the injection volume was 20 μL. All samples in triplicate were filtered through a membrane filter (0.45 μm) before injection. The concentrations of diuron and its metabolites were determined using calibration curves constructed with peak areas of authentic standards (diuron, DCPMU, DCPU, and DCA). The identification of the compounds was based on their respective retention times and on the fortification of the samples with standards. Under the conditions employed, diuron was eluted at 11.6 min, DCPMU at 10.6 min, DCPU at 9.5 min, and 3,4-DCA at 12.1 min.

2.8. Cytochrome P450 Inhibition Studies. The cytochrome P450 inhibitor, 1-aminobenzotriazole (ABT), was added to *P. chrysosporium* cultures at the start of the cultivation to obtain a final concentration of 1 mmol/L. A diuron stock solution was added to a final concentration of 30 μmol/L (7 μg/mL). Control cultures without cytochrome P450 inhibitor were incubated in parallel. The cultures were inoculated and incubated as described above. The diuron degradation in the presence and absence of ABT was measured after 5 and 10 days of cultivation.

2.9. In Vitro Degradation of Diuron by Extracellular P. chrysosporium Crude Enzymes. The capability of extracellular *P. chrysosporium* crude enzymes to degrade diuron was evaluated using 7-day culture filtrates according to the protocol described previously [21]. The reaction mixture (1 mL) contained (final concentration) 7 μg/mL diuron, 40 U/L crude lignin peroxidase, 50 U/L manganese peroxidase, and 0.1 mmol/L H_2O_2 in tartrate buffer 0.1 mol/L, pH 3.0. The effects of adding 0.5 mmol/L $MnSO_4$ and 0.5 mmol/L veratryl alcohol were tested separately or in combination. All reactions were conducted in sterile tubes at room temperature. After 24 h, the reaction mixtures were filtrated with a membrane filter (0.45 μm) before the HPLC analyses.

2.10. Toxicological Test. The toxicity assessment of crude culture filtrates and abiotic control samples was conducted using lettuce seeds (*Lactuca sativa*). The crude filtrates were obtained from 10-day cultures using an initial concentration of diuron of 7 μg/mL. The bioassay was conducted with five dilutions of each sample in water (v/v) (100, 80, 50, 20, and 10%). Twenty seeds were placed in 90 mm diameter Petri dishes containing filter paper saturated with 3 mL of different dilutions of samples or water (control) [22]. After 5 days, the number of germinated seeds was counted and the lengths of the radicles and hypocotyls were measured. The data were represented as absolute germination percentage and relative growth compared to the control as follows:

$$\text{Absolute germination (\%)} = \frac{\text{GS}}{\text{TS}} \times 100,$$

$$\text{Relative growth of the radicle/hypocotyl (\%)} = \frac{\text{LS}}{\text{LC}} \times 100, \quad (1)$$

where GS = number of germinated seeds, TS = number of total seeds, LS = average length of the sample, and LC = average length of the control.

To calculate the dose that produced 50% inhibition of germination or growth (LD_{50}), the coefficient of inhibition I (%) for each parameter was calculated as follows:

$$I\,(\%)_{\text{germination}} = \frac{\text{GSC} - \text{GSS}}{\text{GSC}} \times 100,$$

$$I\,(\%)_{\text{radicle/hypocotyl growth}} = \frac{\text{LC} - \text{LS}}{\text{LC}} \times 100, \quad (2)$$

where GSC = number of germinated seeds in control and GSS = number of germinated seeds in sample.

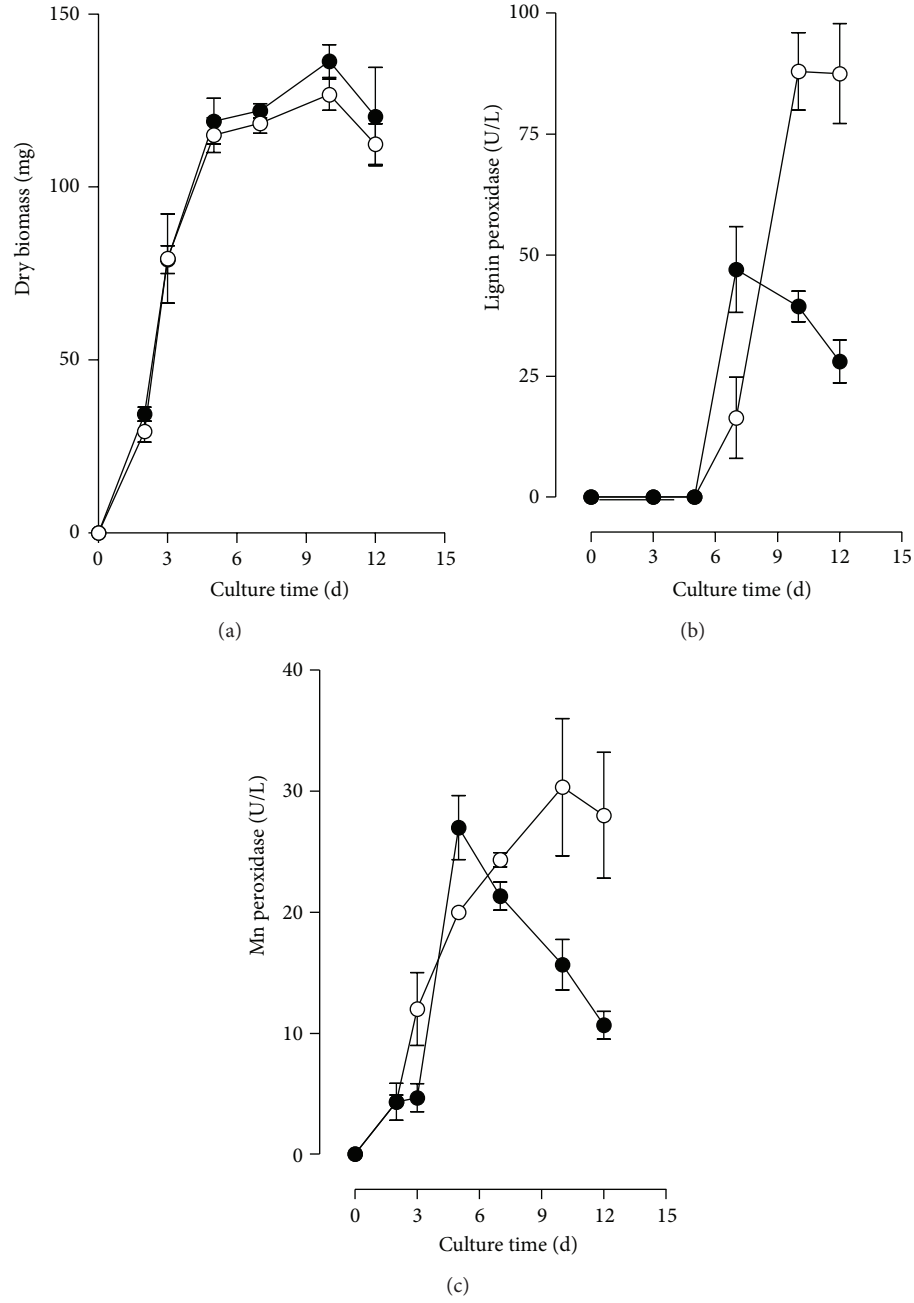

Figure 2: Effect of diuron in the biomass production (a), production of lignin peroxidase (b), and production of manganese peroxidase (c). Absence of diuron (Control cultures) (●); with 7 μg/mL diuron (○).

3. Results

3.1. Effects of Diuron on Biomass Production and Production of Ligninolytic Enzymes. Concentrations of diuron up to 80 μmol/L (18.6 μg/mL) only barely affected the fungal biomass produced after 10 days of cultivation when compared with the fungal biomass obtained in the absence of herbicide. An increase to 100 μmol/L (23.2 μg/mL) in the concentration of diuron resulted in high inhibition of the biomass production. At 7 μg/mL of diuron, the growth curve was very similar to the growth curve in the absence of herbicide (Figure 2(a)). The addition of diuron increased the LiP activities from 47 U/L (at day 7) to 88 U/L (at day 10) (Figure 2(b)). The maximal Mn peroxidase activity was barely affected by the presence of diuron. After 5 days of cultivation, the levels of Mn peroxidase were 22.4 and 20.0 U/L in the presence and absence of diuron (Figure 2(c)). After 10 days of cultivation, the levels of Mn peroxidase found in the culture filtrates in the presence and absence of diuron were 29.4 and 15.4, respectively. Laccase activity was not detected under any condition with or without diuron.

3.2. Diuron Degradation Experiments. P. chrysosporium showed high rates of diuron removal in the corn cob liquid

Table 1: Effects of 1-aminobenzotriazole on diuron transformation and metabolites production by *P. chrysosporium*.

P. chrysosporium culture	Recupered diuron and produced metabolites (μg/mL)					
	5 days			10 days		
	Diuron	DCPMU	DCPU	Diuron	DCPMU	DCPU
Inhibitor free-control	1.72 ± 0.41	0.54 ± 0.20	0.06 ± 0.01	0.26 ± 0.03	0.16 ± 0.06	0.06 ± 0.01
ABT (1 mmol/L)	5.25 ± 0.50	0.22 ± 0.01	0.04 ± 0.01	4.07 ± 0.12	0.32 ± 0.01	0.04 ± 0.02

medium under the nitrogen-limited condition used in this work (Figure 3) and this fact seems to be associated with the mycelium growing phase. After 5 days of cultivation, the fungus was able to remove approximately 52% of diuron and at the end of the experiment the removal reached 94%. Concomitantly with the removal of diuron, the formation of diuron metabolites was detected, namely, DCPMU and DCPU. Identification of the metabolites was carried out by comparison of their retention times with those obtained by injecting standards under the same conditions as well as by spiking the samples with stock standard solutions. The concentration of DCPMU reached 0.74 μg/mL at day 5 and decreased to 0.08 μg/mL at the end of the experiment. Only traces of the metabolite DCPU were observed (less than 0.06 μg/mL) during the whole cultivation. An unidentified peak (retention time of 15.2 min) was detected with a maximal area at day 7 and decreased until the end of the experiment. No 3,4-DCA production was detected in the *P. chrysosporium* cultures. All these compounds were not observed in cultures without diuron.

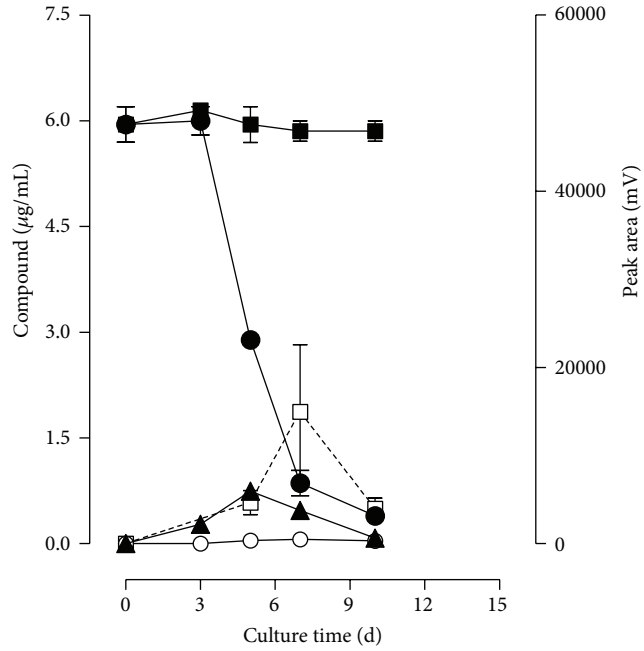

Figure 3: Time course of diuron degradation (●) and formation of DCPMU (▲), DCPU (○), and an unknown product (□) eluted at 15.2 min. Recovery of diuron (■) from the uninoculated control culture is also shown.

3.3. Effect of Cytochrome P450 Inhibitor on Fungal Metabolism. The involvement of the cytochrome P450 in the diuron degradation was examined by adding the cytochrome P450 inhibitor (ABT) to the cultures containing the herbicide at the beginning of the cultivation. The diuron degradation was clearly inhibited by the addition of 1 mmol/L ABT. As shown in Figure 4, in cultures where ABT was added, higher concentrations of diuron were observed, whereas in inhibitor-free cultures diuron was almost completely removed when compared to the uninoculated controls. The addition of ABT did not affect the fungal biomass production (not shown).

The production of N-demethylated metabolites was clearly affected by the presence of the cytochrome P450 inhibitor. The formation of the metabolite DCPMU was the most strongly inhibited. As shown in Table 1, in control cultures the levels of DCPMU decreased until the end of the experiments, suggesting that this compound was metabolized by the fungus. In contrast, in the presence of ABT this metabolite accumulated in the medium, as can be observed by the slight increase of its concentration at day 10, which indicates that the metabolization of DCPMU was also inhibited by ABT. The effect of ABT on the formation of the metabolite DCPU was less pronounced causing a slight decrease of its level when compared with the control.

The amounts of diuron and its metabolites in the culture filtrate and mycelial extract after 5 days of cultivation are shown in Table 2. It is noteworthy to mention that, in fractional terms, the amounts of DCPMU and DCPU in the mycelial extract exceeded those of the parent compound diuron by factors of 1.73 and 1.99, respectively. Furthermore, the total amount of diuron and its metabolites inside and outside of the cells corresponds to 61.6% of the amount of diuron added to the cultures. This indicates that a substantial fraction was removed. Unfortunately, chromatographic analyses of 10 d-mycelial extracts could not be evaluated considering the presence of interfering molecules, also present in the cell extracts obtained in the absence of diuron.

3.4. Degradation of Diuron by Crude Enzymatic Extract. The capability of crude enzymatic extracts to degrade diuron *in vitro* was tested under different conditions (Table 3). No significant differences ($P < 0.05$) were observed between the control and the treatments containing enzymes and mediators.

3.5. Toxicity Tests. The samples showed moderate toxic effects without dilution (100%) or when the samples were diluted by a factor of 1.25 (80%) (Table 4). Toxic effects of the samples were observed on the radicles and hypocotyl, such as

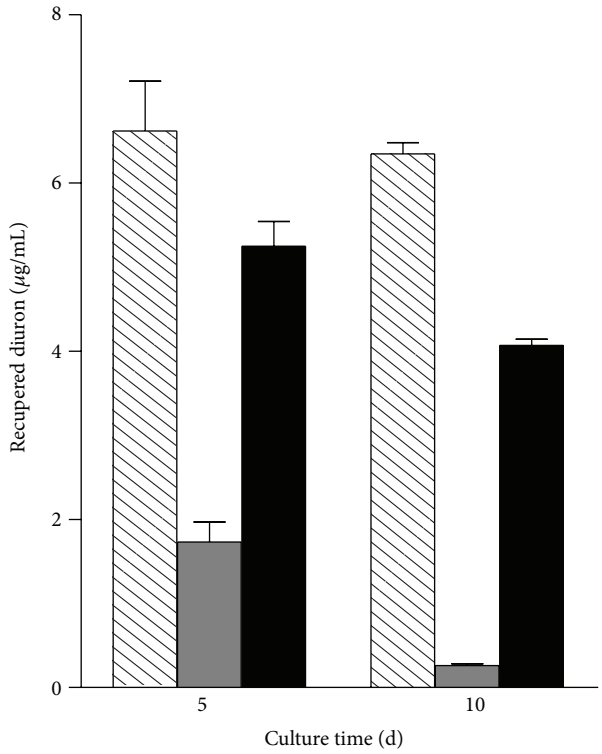

Figure 4: Effect of the cytochrome P450 inhibitor (ABT) on diuron degradation. Treatments: abiotic controls (striped bars), inhibitor-free control (grey bars), and cultures with ABT (black bars).

Table 2: Distribution of residual diuron and its metabolites between culture filtrates and mycelial extracts of *P. chrysosporium* after 5 days of cultivation.

Compound	Residual diuron and metabolites after 5 days (μg)		
	Culture filtrate	Mycelial extract	Total
Diuron	71.3 ± 3.3	11.0 ± 0.8	82.3
DCPMU	18.5 ± 0.5	5.6 ± 0.1	24.1
DCPU	1.1 ± 0.1	0.37 ± 0.1	1.5

An amount of 175 μg of diuron was added at zero time in each culture.

reduction in size, necrosis, and fragility. In relation to the radicle growth, no reduction in the toxicity between treated and nontreated samples (abiotic control) was observed. In relation to the hypocotyl development, it was possible to observe a reduction in the toxicity after transformation of diuron by *P. chrysosporium*: while nontreated samples promoted an effective inhibition of the hypocotyl growth, treated samples allowed a better development of this structure, what demonstrates a detoxification of the medium by the fungal treatment. In these analyses, the inhibition coefficient allowed to calculate the LD_{50}. In this case, the LD_{50} indicates the acute toxicity of the samples and its value represents the sample dilution (v/v) that produced 50% inhibition of germination or growth. The lower the LD_{50} value, the more toxic the sample. Therefore, it is possible to compare the toxicities of different samples. For radicle growth, the LD_{50} values were 15.4% and 58.7% for nontreated and treated samples, respectively. For hypocotyl growth, the LD_{50} was of 51.6% for nontreated and of 95.1% for treated samples. The highest LD_{50} values were achieved with treated samples, indicating that there is a smaller toxicity for 10-day-treated samples. Therefore, a detoxification process seems to have occurred in presence of the fungus.

4. Discussion

It is well known that *P. chrysosporium* possesses a great ability to degrade herbicides, for example, isoproturon [23], atrazine [24], propanil [11], bentazon [25], and also diuron [10]. Most studies have obtained the greatest degradation levels in solid state cultures, whereas in liquid medium the degradation efficiency seems to be smaller. In this study, the stationary liquid culture was used because it is specially suitable for wastewater treatment due to its simplicity and low cost, providing conditions for high removal of diuron and identification of the main metabolites.

The expression of ligninolytic enzymes by *P. chrysosporium* in the liquid system used in this work was favored by the limitation of nitrogen and by the presence of soluble corn cob phenolics. Different studies where the capability of *P. chrysosporium* to degrade herbicides was evaluated have suggested the participation of ligninolytic enzymes in the process based on a temporal coincidence between herbicide degradation and maximal enzyme activities [10, 23]. The participation of extracellular enzymes in the transformation of several herbicides by some white-rot fungi, including *P. chrysosporium,* was conclusively demonstrated by studies performed with purified enzymes and compiled in a recent review [2]. In the present work a temporal correlation between production of ligninolytic enzymes and initial diuron degradation was evidenced. However, no transformation of the herbicide was observed when the crude culture filtrates were incubated *in vitro* with diuron. These results indicate that the first steps of diuron transformation seem to be more associated with the mycelial components than with the extracellular enzymes. In relation to the increase in the activity of lignin peroxidase, this phenomenon is not necessarily related to the herbicide transformation, since this effect can be due to several alterations in cell physiology or in plasmatic membrane structure, which reflect the adaptation of the fungus to the polluted environment [26]. These considerations support the hypothesis that diuron degradation involves an intracellular enzymatic system and weaken the hypothesis of extracellular LiP and MnP participations in the initial reactions. Two other observations of the present work reinforce the hypothesis that the degradation of diuron started intracellularly: the considerable amounts of diuron, DCPMU, and DCPU found in fresh mycelia and the inhibition of degradation caused by ABT, a cytochrome P450 inhibitor.

The participation of an intracellular enzymatic mechanism, represented mainly by cytochrome P450, in the degradation of different xenobiotics has been extensively considered in the last years. Purification of fungal cytochrome P450, in order to obtain conclusive data, has been accomplished in only a few studies, due to the difficulties in keeping

Table 3: Degradation of diuron by enzymatic crude filtrate from *P. chrysosporium* cultures after 24 h.

Treatment	Veratryl alcohol (0.5 mM)	H_2O_2 (0.1 mM)	$MnSO_4$ (0.5 mM)	Crude filtrate*	Recupered diuron (μg/mL)
Control	–	–	–	–	6.47 ± 0.43
1	+	+	+	+	7.40 ± 0.46
2	–	+	–	+	6.34 ± 0.72
3	+	+	–	+	5.98 ± 0.35
4	–	+	+	+	6.27 ± 0.31
5	+	–	–	+	5.66 ± 0.48
6#	+	+	+	+	7.39 ± 0.39

*40.0 U/L of lignin peroxidase activity and 50 U/L of manganese peroxidase activity. All the treatment contained diuron (7 μg/mL) and sodium malonate buffer 50 mM, pH 4.5. Control was run only with diuron and buffer. #Treatment 6 was performed using boiled crude enzyme. Degradation values are means ± SD ($n = 3$).

Table 4: Parameters measured for *L. sativa* bioassay.

Sample dilution (v/v)	Absolute germination (%)		Relative growth averages (%)			
			Radicle		Hypocotyl	
	Abiotic control	10-day treatment	Abiotic control	10-day treatment	Abiotic control	10-day treatment
10%	84.1 ± 2.0	95.0 ± 3.1	42.2 ± 3.7	77.0 ± 4.1*	113.1 ± 7.0	116.2 ± 4.2
20%	80.3 ± 3.6	88.3 ± 2.8*	36.3 ± 8.6	102.6 ± 8.5*	49.8 ± 5.8	122.3 ± 7.3*
50%	78.3 ± 5.7	90.3 ± 5.7*	27.6 ± 2.2	42.8 ± 6.9*	52.2 ± 4.3	88.7 ± 10.5*
80%	58.3 ± 7.6	78.3 ± 2.8*	21.0 ± 1.0	28.4 ± 2.5*	33.4 ± 2.9	65.5 ± 10.4*
100%	31.6 ± 5.7	60.0 ± 7.0*	9.2 ± 1.7	26.8 ± 2.4*	20.8 ± 3.8	44.2 ± 7.2*

The percentage of the absolute germination and the growth averages for lettuce seed bioassays were calculated at five dilutions of nontreated (abiotic control) and 10-day-treated samples, in triplicates. *Significant differences between samples for the same parameter analyzed ($P < 0.05$) by t-test.

the activation of the enzymes during microsome preparation. Hence, most conclusions were drawn from the results of indirect experiments consisting in the addition of specific cytochrome P450 inhibitors to the culture medium, such as piperonyl butoxide and 1-aminobenzotriazole, the same strategy used in the present work. Two recent studies reinforced the importance of this system in the *P. chrysosporium* degradation of pentachlorophenol [27] and phenanthrene [28]. In the latter study strong evidence has been presented for the participation of cytochrome P450 monooxygenases in anthracene metabolism by *P. chrysosporium*.

The chromatographic analysis demonstrated that diuron was effectively transformed by the fungus. DCPMU was the major N-demethylated metabolite identified and did not accumulate in the medium, suggesting that this compound was further degraded by the fungus. Another metabolite appeared in the medium but, unfortunately, it could not be identified by the methods employed in the present work.

Besides *P. chrysosporium* [10–12], other white-rot species, such as *Bjerkandera adusta* and *Trametes versicolor* [12, 13] and *Pleurotus ostreatus* [11, 12], have also been reported to degrade diuron in liquid cultures. In these studies no efforts were made to identify the transformation products. Our results show that diuron transformation by *P. chrysosporium* appears to be similar to that described for some soil fungi, that is, by successive N-demethylation, but with no formation and accumulation of 3,4-DCA, considered to be the most toxic and persistent metabolite of diuron [3].

Although diuron has been efficiently degraded in fungal cultures, conclusions drawn from this kind of experiments should not be extrapolated straightforwardly to nature because the biological degradation is frequently incomplete and may produce metabolites that are more toxic than the initial compound. The toxicological tests using lettuce seeds as bioindicators represent an effort to compare the toxicity of treated and nontreated diuron samples and thus to assess the effectiveness of *P. chrysosporium* in reducing environmental contamination [22]. Previous studies showed that diuron is transformed by fungal cultures producing N-demethylated metabolites with a higher toxicity than diuron [7, 29]. In such works, the toxicity was evaluated according to the Microtox test after isolation and concentration of the metabolites. The present work was conducted to evaluate the general toxicity of the culture extracts after just a single centrifugation step, used in order to clean the samples. The results showed a significant decrease in the toxicity of culture extracts at the end of the fungal treatment, which coincided with the decrease of the medium concentrations of both diuron and its metabolites due to the degradation processes and also to the uptake of these compounds into the cells.

5. Conclusion

The present study emphasizes the capability of *P. chrysosporium* to degrade the herbicide diuron. The fungus was able to remove 94% of the herbicide after 10 days of cultivation

with no apparent accumulation of toxic products. This work complements the results obtained by other authors which demonstrate that demethylation at the terminal nitrogen of the diuron molecule is the initial degradation reaction in fungal metabolism. To our knowledge, this is the first study that demonstrates the involvement of cytochrome P450 in the transformation of diuron and its metabolites by *P. chrysosporium*.

Conflict of Interests

The authors declare that there is no conflict of interests regarding the publication of this paper.

Acknowledgments

This work was supported by the Conselho Nacional de Pesquisa e Desenvolvimento (CNPq) and Coordenação de Aperfeiçoamento de Pessoal de Nivel Superior (CAPES). Rosane Marina Peralta and Adelar Bracht are Research Fellows of CNPq.

References

[1] H. Harms, D. Schlosser, and L. Y. Wick, "Untapped potential: exploiting fungi in bioremediation of hazardous chemicals," *Nature Reviews Microbiology*, vol. 9, no. 3, pp. 177–192, 2011.

[2] J. S. Coelho-Moreira, G. M. Maciel, R. Castoldi et al., "Involvement of lignin-modifying enzymes in the degradation of herbicides," in *Herbicides—Advances in Research*, pp. 165–187, 2013.

[3] S. Giacomazzi and N. Cochet, "Environmental impact of diuron transformation: a review," *Chemosphere*, vol. 56, no. 11, pp. 1021–1032, 2004.

[4] United States Environmental Protection Agency, "EPA," 2013, http://www.epa.gov/espp/litstatus/effects/diuron_efed_chapter.pdf.

[5] J. A. Field, R. L. Reed, T. E. Sawyer, S. M. Griffith, and P. J. Wigington Jr., "Diuron occurrence and distribution in soil and surface and ground water associated with grass seed production," *Journal of Environmental Quality*, vol. 32, no. 1, pp. 171–179, 2003.

[6] J. E. Cullington and A. Walker, "Rapid biodegradation of diuron and other phenylurea herbicides by a soil bacterium," *Soil Biology and Biochemistry*, vol. 31, no. 5, pp. 677–686, 1999.

[7] C. Tixier, M. Sancelme, F. Bonnemoy, A. Cuer, and H. Veschambre, "Degradation products of a phenylurea herbicide, diuron: synthesis, ecotoxicity, and biotransformation," *Environmental Toxicology and Chemistry*, vol. 20, no. 7, pp. 1381–1389, 2001.

[8] N. Badawi, S. Rønhede, S. Olsson et al., "Metabolites of the phenylurea herbicides chlorotoluron, diuron, isoproturon and linuron produced by the soil fungus *Mortierella* sp," *Environmental Pollution*, vol. 157, no. 10, pp. 2806–2812, 2009.

[9] L. Ellegaard-Jensen, J. Aamand, B. B. Kragelund, A. H. Johsen, and S. Rosendahl, "Strains of the soil fungus *Mortierella* show different degradation potentials for the phenylurea herbicide diuron," *Biodegradation*, vol. 24, no. 6, pp. 765–774, 2013.

[10] L. E. Fratila-Apachitei, J. A. Hirst, M. A. Siebel, and H. J. Gijzen, "Diuron degradation by *Phanerochaete chrysosporium* BKM-F-1767 in synthetic and natural media," *Biotechnology Letters*, vol. 21, no. 2, pp. 147–154, 1999.

[11] C. Torres-Duarte, R. Roman, R. Tinoco, and R. Vazquez-Duhalt, "Halogenated pesticide transformation by a laccase-mediator system," *Chemosphere*, vol. 77, no. 5, pp. 687–692, 2009.

[12] A. Khadrani, F. Seigle-Murandi, R. Steiman, and T. Vroumsia, "Degradation of three phenylurea herbicides (chlortoluron, isoproturon and diuron) by micromycetes isolated from soil," *Chemosphere*, vol. 38, no. 13, pp. 3041–3050, 1999.

[13] G. D. Bending, M. Friloux, and A. Walker, "Degradation of contrasting pesticides by white rot fungi and its relationship with ligninolytic potential," *FEMS Microbiology Letters*, vol. 212, no. 1, pp. 59–63, 2002.

[14] C. O. Adenipekun and R. Lawal, "Uses of mushrooms in bioremediation: a review," *Biotechnology Molecular Biology Review*, vol. 7, no. 3, pp. 62–68, 2012.

[15] S. W. Kullman and F. Matsumura, "Metabolic pathways utilized by *Phanerochaete chrysosporium* for degradation of the cyclodiene pesticide endosulfan," *Applied and Environmental Microbiology*, vol. 62, no. 2, pp. 593–600, 1996.

[16] D. Ning, H. Wang, and Y. Zhuang, "Induction of functional cytochrome P450 and its involvement in degradation of benzoic acid by *Phanerochaete chrysosporium*," *Biodegradation*, vol. 21, no. 2, pp. 297–308, 2010.

[17] H. A. Vogel, "A convenient growth medium for Neurospora crassa," *Microbial Genetic Bulletin*, vol. 13, pp. 42–43, 1956.

[18] H. Wariishi, K. Valli, and M. H. Gold, "Manganese(II) oxidation by manganese peroxidase from the basidiomycete *Phanerochaete chrysosporium*. Kinetic mechanism and role of chelators," *Journal of Biological Chemistry*, vol. 267, no. 33, pp. 23688–23695, 1992.

[19] M. Tien and T. K. Kirk, "Lignin-degrading enzyme from *Phanerochaete chrysosporium*: purification, characterization and catalytic properties of a unique H_2O_2-requiring oxygenase," *Proceedings of the National Academy of Sciences of the United States of America*, vol. 81, pp. 2280–2284, 1984.

[20] H. Hou, J. Zhou, J. Wang, C. Du, and B. Yan, "Enhancement of laccase production by *Pleurotus ostreatus* and its use for the decolorization of anthraquinone dye," *Process Biochemistry*, vol. 39, no. 11, pp. 1415–1419, 2004.

[21] N. Hiratsuka, M. Oyadomari, H. Shinohara, H. Tanaka, and H. Wariishi, "Metabolic mechanisms involved in hydroxylation reactions of diphenyl compounds by the lignin-degrading basidiomycete *Phanerochaete chrysosporium*," *Biochemical Engineering Journal*, vol. 23, no. 3, pp. 241–246, 2005.

[22] M. C. Sobrero and A. Ronco, "Ensayo de toxicidad aguda con semillas de lechuga (*Lactuca sativa* L.)," in *Ensayos Toxicológicos y Métodos de Evaluación de Calidad de Aguas*, pp. 71–79, 2004.

[23] M. Del Pilar Castillo, S. Von Wirén-Lehr, I. Scheunert, and L. Torstensson, "Degradation of isoproturon by the white rot fungus *Phanerochaete chrysosporium*," *Biology and Fertility of Soils*, vol. 33, no. 6, pp. 521–528, 2001.

[24] C. Mougin, C. Laugero, M. Asther, and V. Chaplain, "Biotransformation of s-triazine herbicides and related degradation products in liquid culture by the white rot fungus *Phanerochaete chrysosporium*," *Pesticide Science*, vol. 49, pp. 169–177, 1997.

[25] M. D. P. Castillo, P. Ander, J. Stenström, and L. Torstensson, "Degradation of the herbicide bentazon as related to enzyme production by *Phanerochaete chrysosporium* in two solid substrate fermentation systems," *World Journal of Microbiology and Biotechnology*, vol. 16, no. 3, pp. 289–295, 2000.

[26] G. M. Zeng, A. W. Chen, G. Q. Chen et al., "Responses of *Phanerochaete chrysosporium* to toxic pollutants: physiological

flux, oxidative stress, and detoxification," *Environmental Science and Technology*, vol. 46, pp. 7818–7825, 2012.

[27] D. Ning and H. Wang, "Involvement of cytochrome P450 in pentachlorophenol transformation in a white rot fungus," *Phanerochaete Chrysosporium*, vol. 7, no. 9, Article ID e45887, 2012.

[28] N. L. Chigu, S. Hirosue, C. Nakamura, H. Teramoto, H. Ichinose, and H. Wariishi, "Cytochrome P450 monooxygenases involved in anthracene metabolism by the white-rot basidiomycete *Phanerochaete chrysosporium*," *Applied Microbiology and Biotechnology*, vol. 87, no. 5, pp. 1907–1916, 2010.

[29] C. Tixier, P. Bogaerts, M. Sancelme et al., "Fungal biodegradation of a phenylurea herbicide, diuron: structure and toxicity of metabolites," *Pesticide Management Science*, vol. 56, pp. 455–462, 2000.

Hindawi Publishing Corporation
BioMed Research International
Volume 2013, Article ID 149120, 11 pages
http://dx.doi.org/10.1155/2013/149120

Research Article

The Uptake Mechanism of Cd(II), Cr(VI), Cu(II), Pb(II), and Zn(II) by Mycelia and Fruiting Bodies of *Galerina vittiformis*

Dilna Damodaran, Raj Mohan Balakrishnan, and Vidya K. Shetty

Department of Chemical Engineering, National Institute of Technology Karnataka, Surathkal, Srinivasnagar 575 025, India

Correspondence should be addressed to Raj Mohan Balakrishnan; rajmohanbala@gmail.com

Received 15 August 2013; Revised 21 October 2013; Accepted 22 October 2013

Academic Editor: Kannan Pakshirajan

Optimum concentrations of heavy metals like copper, cadmium, lead, chromium, and zinc in soil are essential in carrying out various cellular activities in minimum concentrations and hence help in sustaining all life forms, although higher concentration of these metals is lethal to most of the life forms. *Galerina vittiformis*, a macrofungus, was found to accumulate these heavy metals into its fleshy fruiting body in the order Pb(II) > Cd(II) > Cu(II) > Zn(II) > Cr(VI) from 50 mg/kg soil. It possesses various ranges of potential cellular mechanisms that may be involved in detoxification of heavy metals and thus increases its tolerance to heavy metal stress, mainly by producing organic acids and phytochelatins (PCs). These components help in repairing stress damaged proteins and compartmentalisation of metals to vacuoles. The stress tolerance mechanism can be deduced by various analytical tools like SEM-EDX, FTIR, and LC-MS. Production of two kinds of phytochelatins was observed in the organism in response to metal stress.

1. Introduction

Metal pollutants are released into the environment in many ways at potentially harmful levels [1]. In some areas, origin of heavy metals and metalloids in food chain is geological rather than anthropogenic; hence microorganisms in such areas develop effective strategy to cope with the harmful consequence of metal and metalloid exposures. Generally the heavy metal ions like Cd(II), Cr(VI), Cu(II), Pb(II), and Zn(II) are very reactive. Many of them possess high affinity especially for sulfhydryl groups in proteins and small biological molecules. As a consequence, the metal can critically affect function in many biological systems, as enzyme inhibitors or in other ways disturbing the pathways causing various lethal disorders.

Over the last decades, biosorption has emerged as a promising low cost methodology for the removal of metals from the environment, where biological components are employed to remove and recover heavy metals from aqueous solutions [2–4]. The metal removal mechanism is a complex process that depends on the chemistry of metal ions, cell wall compositions of microorganisms, physiology of the organism, and physicochemical factors like pH, temperature, time, ionic strength, and metal concentration [5]. The biosorption of heavy metals from soil process through phytoremediation is widely discussed. Researchers have studied phytoremediation thoroughly within last few decades and have understood that phytoremediation solely cannot solve all issues regarding heavy metal pollution because of its limitations like selectivity of plant, climatic inhibitions, tolerance to heavy metals, and back contamination by depuration or from ashes of fire woods; hence there is a need of a robust methodology which can go hand in hand with other techniques to remediate heavy metal contaminated areas more quickly, effectively, and economically.

Mushrooms or macrofungi can act as effective biosorbent alternative to plants in removing toxic metals from soil and the process is referred to as mycoremediation. Mushroom mycelia can serve as biological filters since their aerial structures consist of large biomass and have a tough texture which makes them potential sorbents [6]. Mushrooms are known to have high metal/metalloid tolerance which helps them to thrive and accumulate metals from the contaminated environment. They also have shorter life cycle (30 days) and better adaptability compared to plants; hence mycoremediation can be regarded as an evolved remediation technique.

To understand and to engineer the bioaccumulation efficiency a thorough study on the mechanism of metal removal is essential.

Mushrooms response to metal stress in the environment by producing stress compounds of proteinous and nonproteinous origin. The cap of the mushrooms has been found to produce stress related factors which govern in metal ion uptake, that is, metallothionein glutothionine, and plastocyanin. Fungi have evolved metal tolerance and accumulation mechanism. Compared to microfungi, the mushrooms play a major role in accumulating heavy metals. Fruiting bodies of the mushrooms are considered to be advantageous to plants as they have shorter life cycle (30 days) and better adaptability compared to plants; hence mycoremediation can be regarded as an evolved remediation technique. The major factors governing the metal uptake are bioavailability and nature of soil. The bioavailability of metals is affected by numerous soil factors, such as cation exchange capacity [7], pH [8–10], and organic matter content [11, 12]. Understanding the mechanism of metal uptake from the soil to the fruiting bodies helps us to improvise the process by biotechnological tools; hence the study on the uptake mechanism plays a significant role in developing better remediation technique.

2. Materials and Methods

2.1. Bioaccumulation Studies. *Galerina vittiformis* spawns were used as the inoculums for *in vitro* fruiting body production. The spawns were mixed with soil mixture and were incubated at 23 ± 3°C in dark conditions. Casing of spawns was carried out in trays of 25 × 20 × 5 cm dimensions, sterilized with 70% alcohol. Soils used for the study were mixed with heavy metal (as $PbNO_3$, $CdSO_4$, $CuSO_4$, $K_2Cr_2O_7$, and $ZnNO_3$) solutions to attain 50 mg kg^{-1} concentration and were dried in an oven. The dried soil was mixed with sawdust in the ratio of 3 : 1 (w/w). Sawdust increases the porosity and helps in better mushroom production. These soil mixtures were used for all bioaccumulation studies. Spawns were cased with the soil mixture and soil layer of about 3 to 4 cm thick was prepared. Cased trays were incubated in the dark conditions at 22 ± 2°C and 85 ± 5% relative humidity for a period of 25 days with periodical monitoring. At the end of the 25th day, the fruiting bodies formed were harvested using sterile forceps and allowed to dry at room temperature. 1 g of the dried biomass samples was mixed with 2 mL of 65% HNO_3 and 6 mL of HCl and then digested in a microwave digester (CEM-MARS, USA) at 600 W for 20 min. The digested mixtures were cooled and were made up to 50 mL using deionized water. The cooled mixture is then filtered using Whatman No. 1 filter paper. These samples were analyzed for metal contents using atomic absorbtion spectrometer (AAS) [13, 14].

2.2. Mechanism of Bioaccumulation. To determine the tolerance and accumulation mechanism employed by mushrooms the fruiting bodies were analysed for primary and secondary stress components produced by them. The dried fruiting bodies and their extracts were analysed by various modern techniques, namely, scanning electron microscopy with energy dispersive X-ray analysis, fourier transforms infrared spectroscopy analysis, and liquid chromatography coupled with mass spectrometry to understand their metal uptake mechanisms.

2.2.1. Scanning Electron Microscopy (SEM) with Energy Dispersive X-Ray Analysis (EDX). In order to understand the role of surface activity on metal accumulation the toughs of fungal mycelia were subjected to SEM and EDX. The fungal mat obtained was harvested and dried in oven at 60°C. Theses dried biomasses were treated with 10% glutaraldehyde and then incubated for about 10–12 hours at 4°C. Further the biomass was treated with alcohol gradations (10%, 30%, 50%, 80%, and 100%) for 2 min to remove the water content [15, 28–30]. The pretreated specimens were then sputtered with gold particles using a sputter coater under vacuum and then observed under a scanning electron microscope (JSM-6380; JEOL, Tokyo) at an accelerating voltage of 12 or 15 kV to capture the images. EDX of these images was performed at 20 kV.

2.2.2. Fourier Transforms Infrared Spectroscopy Analysis (FTIR). The fruiting bodies and mycelia of *G. vittiformis* after the bioaccumulation studies were isolated and washed with distilled water and oven-dried at 60°C (Rotek, India). The dried biomass was then powdered and analyzed by Thermo Nicolet 6700, FTIR spectrometer to identify the functional groups and bonds present in them in response to heavy metal uptake which were responsible for the metal accumulation in cytosol.

To characterise the stress components produced in these biomass, FTIR was performed on fruiting body extracts. The stress components were extracted using Tris buffer system; 3 g of dried fruiting body was grounded using liquid nitrogen in a mortor and pestle; the homogenised extract was mixed with 3X Tris buffer (30 mM Tris, 250 mM NaCl, pH 7.6) in ice bath; centrifuged at 12,000 g for 15 min at 4°C; the supernatant was collected and stored at −20°C. The extract was then subjected to both FTIR and liquid chromatography coupled with mass spectra (LC-MS).

2.2.3. Analysis of Stress Factors Using LC-MS. Fruiting body extracts were characterised using a liquid chromatographic column equipped with Accela pump and an Accela autosampler (Thermo Fisher Scientific, San Jose, CA, USA). Separation of analytes was conducted on a Luna PFP (2) analytical column (100 mm × 2.0 mm, 3 μm). The LC mobile phases were (a) ammonium formate 0.75 mM adjusted to pH 3.5 with formic acid and (b) methanol. Separation was performed under isocratic conditions with 99% mobile phase A at flow rate of 200 μL/min and a column temperature of 35°C. Total run time per sample was 10 min and all injection volumes were 10 μL. Mass spectrometric analysis was performed using a TSQ Quantum Access (Thermo Fisher Scientific, San Jose, CA, USA) triple quadrupole mass spectrometer coupled with electrospray ionization (ESI) operated in multiple reactions

Figure 1: Fruiting body initials of organism *Galerina vittiformis* after 25 days of incubation in tray systems.

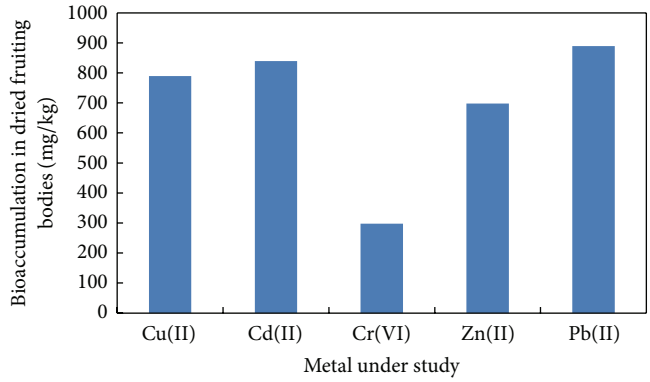

Figure 2: Bioaccumulation of metals by fruiting bodies of *Galerina vittiformis*.

monitoring (MRM) in positive mode. The MRM for GSH (m/z 308.1 → m/z 76.2 + 84.2 + 161.9) and GSSG (m/z 613.2 → m/z 230.5 + 234.6 + 354.8) were performed with collision energy optimized for each transition. The operating conditions for MS analysis were as follows: spray voltage, 2500 V; capillary temperature and voltage, 280°C and 35 V, respectively; Sheath gas and auxiliary gas flow, 30 and 5 arbitrary units, respectively; tube lens offset, 84 V for GSH and 115 V for GSSG. The mass spectrometer was employed in MS/MS mode using argon as collision gas. Data acquisition and analysis were performed with Xcalibur software, version 2.0 (Thermo Fisher Scientific, San Jose, CA, USA).

3. Result and Discussions

3.1. Bioaccumulatation in Fruiting Bodies of Mushrooms. Fruiting bodies of *Galerina vittiformis* produced after 25 days of incubation are shown in Figure 1. The results of bioaccumulation study are presented in Figure 2. The fruiting bodies act as the site of heavy metal accumulation and they can be easily separated from soil. This is considered to be advantageous over phytoremediation. In phytoremediation heavy metals are accumulated in plant parts like roots, twigs, and leaves and improper disposal methods increase the risk of back contamination. The levels of heavy metals accumulated in the fruiting bodies are shown in Figure 2 and are as follows: Cu(II) (800 mg kg^{-1}), Cd(II) (852 mg kg^{-1}), Cr(VI) (30 mg kg^{-1}), Pb(II) (900 mg kg^{-1}), and Zn(II) (700 mg kg^{-1}). Thus the bioaccumulation potential of fruiting bodies of *G. vittiformis* was found to be in the following order: Pb(II) > Cd(II) > Cu(II) > Zn(II) > Cr(VI). Various researchers have found that organism's ability to accumulate heavy metals varies from species to species, at different stages of life cycle, amount of metal ion concentrations in the soil, nature of soil, and so forth [16, 21, 31–34].

The bioaccumulation potential of *G. vittiformis* was found to be higher than that of those mushroom species reported in the literature (summarized in Table 1). From Table 1 it is observed that nonedible mushroom species accumulate higher amounts of metal ions than the edible species. However, the bioaccumulation profile indicates that metal accumulation capability is species specific and mainly depends on its accumulation mechanism [20, 35–39].

3.2. Mechanism of Bioaccumulation. Heavy metals are known to act as a general protoplasmic poison, inducing the denaturation of proteins and nucleic acids [22, 40]. They can also break apart biological molecules into even more reactive species (such as reactive oxygen species) which will also disrupt biological processes. Hence only those species which can successfully tolerate these physiological stresses can successfully survive in heavy metal laden environment. Mushrooms respond to metal stress in the environment by producing stress compounds of proteinous and nonproteinous origin. The pileus (cap) of the mushrooms has been found to produce stress factors which help in sequestering the accumulated metal ions into their vacuoles. The most common stress components produced by plants and fungi are metallothionein (MT), glutothionine (GSH), phytochelatins (PCs), and plastocyanin [41]. From the studies of Inouhe et al. [42], Mehra et al. [43], Münger and Lerch [44], and Lerch [45], it is observed that macrofungi have evolved metal tolerance and accumulation mechanism compared to microfungi. Understanding the mechanism of the metal uptake from the soil to the fruiting bodies helps us to improvise the process by advanced molecular biology tools. Hence study on the uptake mechanism plays a significant role in developing better remediation technique.

3.2.1. Morphological Studies by Scanning Electron Microscopy (SEM) with Energy Dispersive X-Ray Analysis (EDX). The effect of heavy metal on the morphology of *Galerina vittiformis* during the bioaccumulation process was studied through SEM image analysis. Figure 3(a) revealed that the hyphae of *G. vittiformis* were cylindrical, septate, and branched before exposure to heavy metal. As shown in Figure 3(b) characteristic change in the morphology, curling, and formation of hyphal coils in response to Cd(II) stress is observed. Similar observations were made when exposed to other heavy metals. Cánovas et al. [46] reported that the surface of *Aspergillus* sp. also had rough texture due to protrusions on the hyphae on exposure to 50 mM of arsenate solution. Such modifications on the surface of fungi indicate the production of intracellular compounds due to heavy metals stress and result in increase in pressure within the mycelia

Table 1: Heavy metal content in fruiting body (sporocarp) of various mushrooms.

Sl. number	Mushroom species	Metal content in sporocarp, mg kg^{-1} of dry wt.	References
1	*Agaricus bisporus*[1]	Pb (4), Cd (3.48), Cu (5.)	[15]
	Boletus edulis[1]	Cu (66.4), Cd (6.58), Pb (3.03)	
	Lepiota rhacodes[2]	Pb (66), Cd (3.7)	
	Paxillus rubicondulus[1]	Pb (0.69), Cd (0.78), Cu (51.0) Zn (16.8)	
2	*Agaricus bisporus*[1]	Cu (107), Pb (1), Zn (57.)	[16]
3	*Helvella leucomelaena*[2]	Pb (4.8), Cd (.0)	[17]
	Pleurotus sp.[1]	Pb (3.4), Cd (1.18), Cu (13.6), Zn (9.8)	
4	*Tricholoma terreum*[1]	Cu (5), Zn (179), Cd (0.56), Pb (4.4)	[18]
	Helvella leucomelaena[2]	Pb (3.1), Cd (1.1)	
5	*Paxillus involutus*[2]	Cu (57.0), Pb (1.6.0), Fe (991), Cd (0.84), Pb (3)	[19]
	Rhizopogonaceae *luteolus*[1]	Cu (13), Zn (30), Mn (13), Fe (620), Cd (0.26), Pb (2.8).	
	Omphalotus olearius[2]	Cu (21), Zn (27), Mn (36), Fe (95), Cd (1.3), Pb (5.2).	
	Hygrophorus hedyricii[2]	Cu (37), Zn (97),Mn (11), Fe (395), Cd (1.2), Pb (2.7)	
	Ciocybe dealbata[2]	Cu (41), Zn (115), Mn (30), Fe (386), Cd (0.86), Pb (3.2)	
	Lepiota alba[2]	Cu (29), Zn (86), Mn (22), Fe (779), Cd (0.8), Pb (5.8)	
6	*Tricholoma terreum*[2]	Pb (4), Cd (1.6), Cu (35.8), Zn (48.0)	[20]
	Agaricus bisporus[1]	Pb (0.8), Cd (0.78)	
7	*Pseudevernia furfuracea*[2]	Al (12.51), As (0.23), Cd (0.19), Cu (2.5), Cr (0.11), Pb (5.1), Zn (17.9), Mn (12.9)	[21]
	Scorpiurus circinatum[2]	Al (17.51), As (0.32), Cd (0.35), Cu (3.2), Cr (1.1), Pb (6.3), Zn (46.1), Mn (46.7)	
8	*Aspergillus foetidus*[2]	Al (32.5), Co (5.95), Cr (6.23), Mg (44.9), Zn (2.4), Ni (189.5)	[22]
9	*Poria* sp.[2]	Zn (90.3), Cu (30.8), Pb (1.0), Mn (31.3), Cd (0.1)	[23]
	Nectria cinnabarina[1]	Zn (30.1), Cu (29.3), Pb (1.9), Cd (0.2), Mn (19.3)	
	Ganoderma lucidum[1]	Zn (60.1), Cu (43.8), Pb (0.7), Mn (30.4), Cd (0.31)	
	Paragyrodous sphaerosporous[1]	Zn (115), Cu (34.4), Pb (0.4), Mn (37.3), Cd (0.2)	
	Polyporus frondosus[1]	Zn (120.1), Cu (34.4), Pb (0.4), Mn (37.3), Cd (0.2)	
10	*Phellinus badius*[2]	Cd (110), Cu (60), Hg (61), Ni (56)	[3]
	Phellinus sanguineus[2]	Cd (80), Cu (42), Hg (35), Ni (66)	
11	*Tricholoma terreum*[2]	Pb (3.64), Cu (34.86), Cd (0.67), Zn (54.13), Cr (2.54)	[24]
	Boletus badius[1]	Cu (44.54), Pb (4.48), Cd (0.91), Zn (34.17), Fe (264.62), Cr (2.86)	
	Russula delica[1]	Cu (19.55), Pb (2.02), Cd (1.22), Zn (38.5), Cr (6.95)	
13	Pleurotus platypus[1]	Cd (34.9), Pb (27.10)	[25]
	Agaricus bisporus[1]	Cd (33.7), Pb (29.67)	
14	*Lactarius deliciosus*[1]	Cd (0.26), Cr (0.12), Cu (6.15), Pb (0.73), Zn (76.7)	[26]
	Rhizopogon roseolus[1]	Cd (0.18), Cr (0.10), Cu (21.2), Pb (2.03), Zn (36.7)	
	Russula delica[1]	Cd (0.42), Cr (0.27), Cu (52.2), Pb (0.77), Zn (58.2)	
15	*Sarcosphaera crassa*[1]	Ag (0.044), As (8.03), Cd (0.016), Cr (0.98), Pb (0.02)	[27]
	Cantharellus cibarius[1]	Ag (0.022), As (0.03), Cd (0.036), Cr (0.69), Pb (0.04)	
	Suillus luteus[1]	Ag (0.015), As (0.15), Cd (0.034), Cr (0.15), Pb (0.06)	
	Morchella rigida[1]	Ag (0.087), As (0.24), Cd (0.007), Cr (0.44), Pb (0.02)	
	Agrocybe aegerita[1]	Ag (0.074), As (0.44), Cd (0.010), Cr (0.25), Pb (0.018)	
15	***Galerina* sp.**[2]	**Cd** (**85**), **Pb** (**900**), **Cu** (**800**), **Zn** (**700**), **Cr** (**30**)	

[1]Edible, [2]Nonedible.

leading to the outward growth of the cell wall structures [47]. Courbot et al. [48] have also observed that the impact of metal stresses had led to production of thiol compounds, especially GSH and MT due to intracellular detoxification of cadmium in the fungi, *Paxillus involutus*. According to them, the cell wall protrusions indicate increased formation of intracellular vacuoles that serve as storage compartments for thiol containing compounds. These compounds are responsible for the binding of metal ions into the intracellular regions and accumulate them in the vacuoles, thereby reducing their toxicity in the cytoplasm and improving tolerance levels. The energy dispersive spectroscopy (EDS) analysis was done to analyze the metal ionic concentrations in the mycelial surface indicating mycofilteration. The results of EDS analysis for the control mycelia and mycelium treated with Cd(II) are shown in Figure 4 and Table 2 and Figure 5 and Table 3,

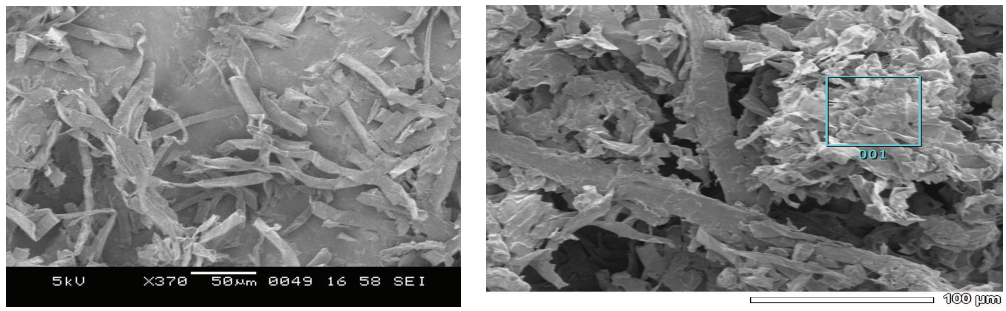

(a) (b)

Figure 3: SEM images of organism *G. vittiformis* (a) untreated (b) Cd(II) treated (500–700X magnification).

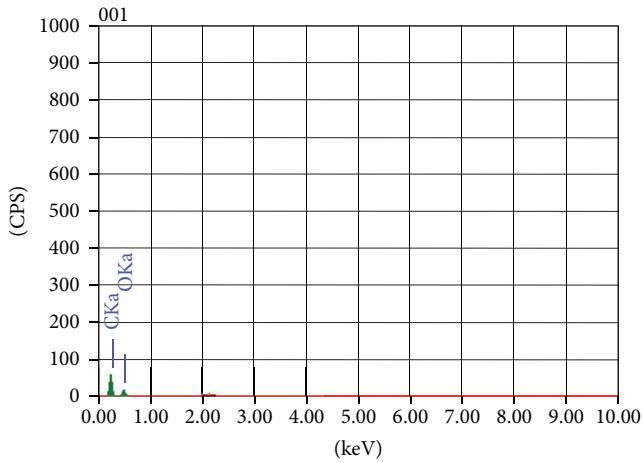

Figure 4: EDS analysis showing the metal content in *G. vittiformis* (control).

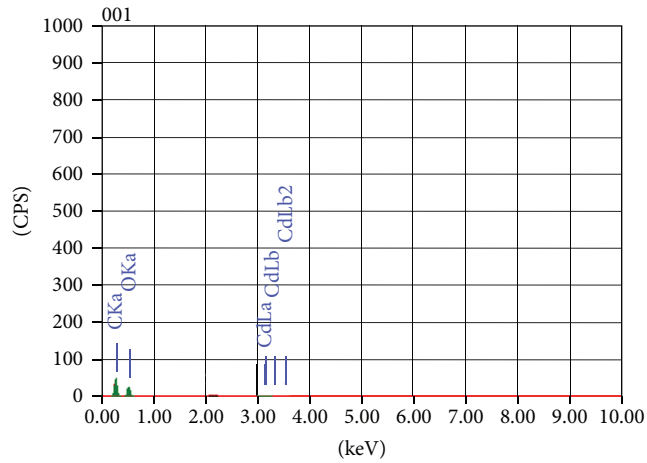

Figure 5: EDS analysis of organism *G. vittiformis* treated with Cd(II).

Table 2: EDS quantitative analysis of organism *G. vittiformis* (control).

Element	KeV	Mass%	Error%	At%	K
C K	0.277	59.75	0.17	66.41	68.8722
O K	0.525	40.25	1.08	33.59	31.1278
Total		100		100	

Table 3: EDS quantitative analysis of organism *G. vittiformis* treated with Cd(II).

Element	keV	Mass%	Error%	At%	K
C K	0.277	50.25	0.15	57.62	53.19
O K	0.525	49.15	0.72	42.30	45.850
Cd L	3.132	0.60	0.72	0.07	0.9590
Total		100		100	

respectively. Only traces of Cd(II) were observed in EDS spectra whereas EDS of the mycelia exposed to other metals such as Cu(II), Pb(II), and Zn(II) showed no visible peaks for the metals (EDS spectra not shown), indicating the nondetectable levels of metals on the surface of the mycelia by SEM-EDS. Presence of traces or absence of metal peaks in the EDS spectra indicates that the metal removal by the mycelia of *Galerina vittiformis* may be attributed to vigorous intracellular bioaccumulation mechanism, rather than adsorption on the surface.

3.2.2. Fourier Transform Infrared Spectroscopy (FTIR). FTIR spectra of fruiting bodies extracts of *Galerina vittiformis* after bioaccumulation studies were analyzed to determine the presence and disappearance of any functional groups involved in metal accumulation mechanism. The FTIR spectrum was assessed by comparing the absorption bands of *G. vittiformis* grown on metal (Cu(II), Cd(II), Cr(VI), Pb(II), and Zn(II)) (50 mg/kg) contaminated soil to that of its spectrum obtained from control. Any changes in the finger print region, that is, 1000–1500 (amide-II and II regions) and 1500–1000 cm^{-1} (amide-III regions) which indicates the presence of higher amounts of acids, protenitous, and nonproteious compounds by *G. vittiformis* upon exposure to Cd(II), Cu(II), Pb(II), Cr(VI), and Zn(II). Each FTIR spectrum was studied thoroughly by comparing the peak values to their standard FTIR charts to determine the represented functional groups [32, 49–52]. The FTIR graphs obtained for all the studied metal ions are compared with control FTIR graphs to analyze

the presence of stress factors produced during metal stress (Figure 6). The FTIR graphs of fruiting body obtained from Cr(VI) laden soil system showed the presence of stress related components like oxalic acid, that is, 1658 ± 5 and 1253 ± 5 and thiol group, that is, 2550 ± 5 (Figure 7) [53]. Similar peaks are also observed in the FTIR graphs of Pb(II) and Cd(II). Only thiol groups (2550 ± 5) are observed in Figure 8 for Cu(II) and Zn(II). Researchers like Qian and Krimm [54], Yang et al. [55], and Shi et al. [56] have used FTIR to detect the presence of both primary and secondary stress factors. FTIR gives only a preliminary identification of stress factors; hence the extracts are further subjected for LC-MS analysis to determine the components. Stress components present in the cellular extracts are further characterized by LC-MS analysis.

3.2.3. Liquid Chromatography-Mass Spectrometry Analysis (LC-MS). Metal homeostasis requires intracellular complexation of metals when there is a cellular surplus and later release of metals to metal requiring apoproteins. The excess metal ions are stored in the storage sites within the cell, for example, vacuoles [41]. LC-MS helps to identify those proteinous and nonproteinous metal ion trafficking components of *G. vittiformis* cells.

The LC-MS chromatograms for Pb(II) are shown in Figures 9(a) and 9(b). The data are obtained from Luna PFP (2) analytical column using ammonium formate and methanol as eluting buffers. Figure 9(a) shows the retention time in minutes and Figure 9(b) shows the *m/z* ratio of each components present in fruiting body extracts. The peaks obtained in chromatograms were analyzed with the database to determine the components. On comparison with the literature it is observed that Figure 9(a) showed 2 peaks at 6–10 min retention, that is, 7.4 and 8.6 indicating the presence of cysteine (Cys) and glutamine (Glu) residues which are the subunits of phytochelatins (γ-glutamylcysteine). Figure 9(a) also indicated 2 major peaks at 14–25 min retention time, that is, 14.9 and 22.3 indicated the presence of 2 types of phytochelatins (PC_2 and PC_3, resp.) while Figure 9(b) showed *m/z* peaks of glutathione (GSH), PC_2, and PC_3 at 307, 538 and 679, respectively. Similar kinds of chromatograms obtained for both Cd(II) and Cr(II) indicate the presence of phytochelatins (PCs). Figures 10(a) and 10(b) show the chromatogram of Cu(II) indicating the presence of both PC_2 and PC_3 (539 and 679 *m/z* peaks) [56–59].

From the studies of Grill et al. [60], Gekeler et al. [61], Liedschulte et al. [62], and Gill and Tuteja [63], it was revealed that the Phytochelatin of the general formula $(\gamma\text{-Glu-Cys})_n$ is the principal heavy metal detoxifying component in both plant and fungal kingdom. The phytochelatins can be viewed as linear polymers of the γ-glutamylcysteine (γ-Glu-Cys) portion of glutathione. These peptides could be enzymatically produced by stepwise condensation of γ-Glu-Cys moieties to growing phytochelatin chain (PC). The PC plays a key role in maintaining cell homeostasis under heavy metal stress by binding to heavy metals like Cd, Zn, Cr, and so forth and trafficking them to vacuoles or periplasmic space for storage [63]. Hence from the result of the present study, the mechanism of metal accumulation can be summarised in

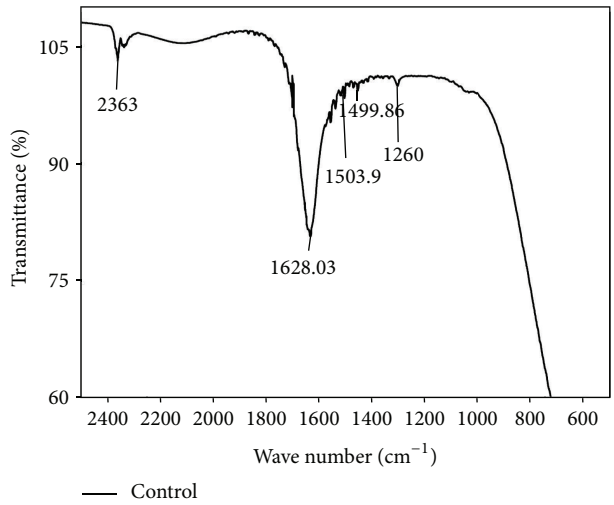

Figure 6: 2D-FTIR results of *G. vittiformis* at metal free environment (control).

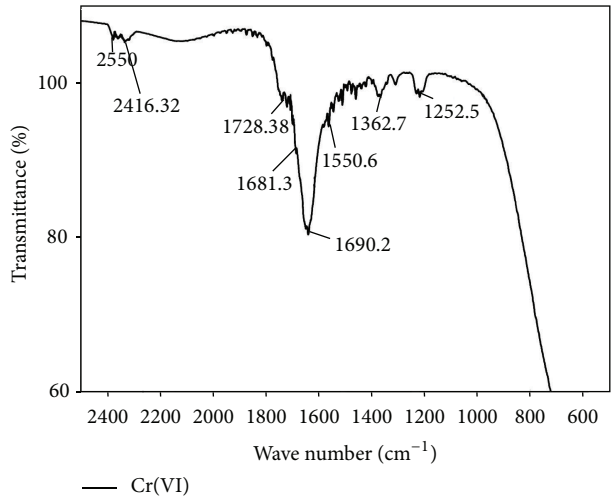

Figure 7: 2D-FTIR results of *G. vittiformis* at Cr(VI) laden soil system.

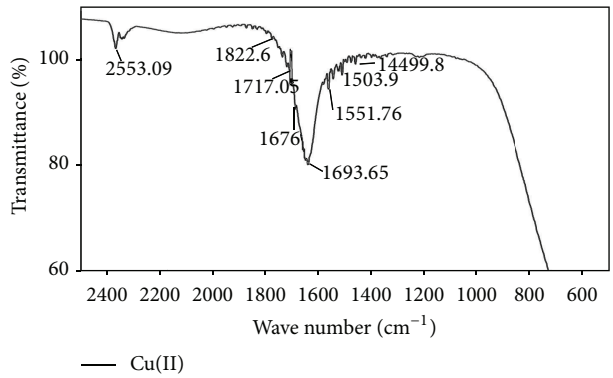

Figure 8: 2D-FTIR results of *G. vittiformis* at Cu(II) laden soil system.

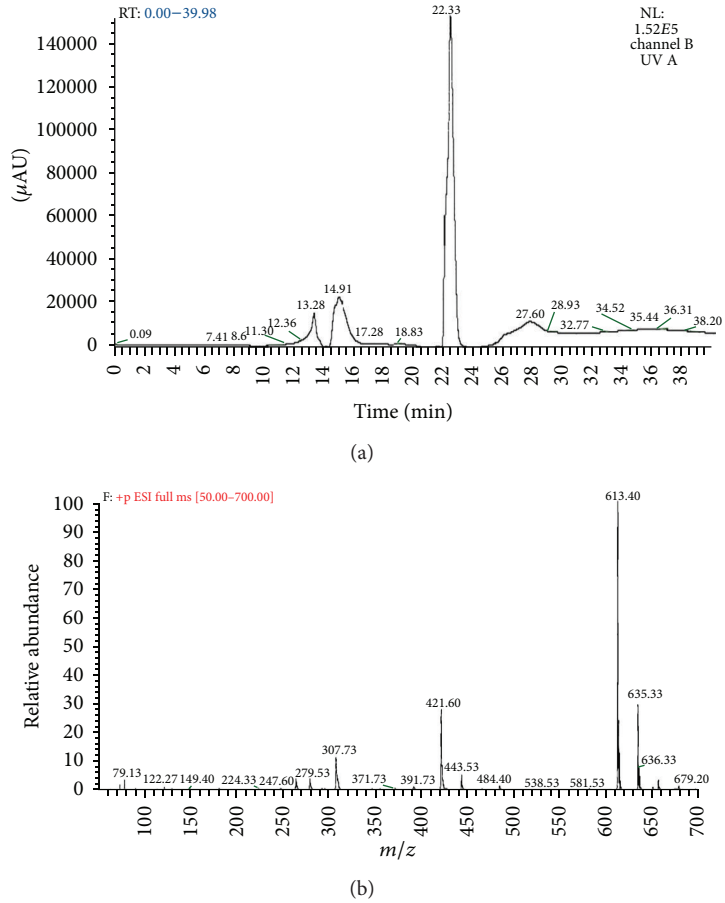

Figure 9: (a) Chromatogram produced by LC-MS analysis for Pb(II) at various retention times (min). (b) Chromatogram produced by LC-MS analysis for Pb(II) at various m/z ratios.

Figure 11. Similar heavy metal accumulation mechanism of PC was reported in various metal resistant plants and algal species [41, 57, 60, 64–70].

4. Conclusion

Removal mechanism of Cu(II), Cd(II), Cr(VI), Pb(II), and Zn(II) metals from contaminated soil using a macrofungus, *Galerina vittiformis,* was investigated in *in vitro* system.

(i) *G. vittiformis* shows efficient bioaccumulation potential in removing most potent heavy metals unlike other known organisms.

(ii) Trace amounts of metal ions are observed in SEM-EDX in the surface indicating primary adsorption step in accumulation.

(iii) FTIR spectral analysis indicates the presence of secondary stress components like organic acids, phytochelatins, and so forth.

(iv) The subunits of phytochelatin chain (PC); that is, Glu-Cys moieties are observed in LC-MS analysis.

(v) *G.vittiformis* produced two types of Phytochelatins, namely, PC_2 and PC_3 in response to Cu(II), Cd(II), Cr(VI), Pb(II), and Zn(II) metal stress.

(vi) Phytochelatins are known to transfer the excess metal ions to the vacuole of the cell, thereby reducing the cellular toxicity.

Hence from analysis reports of SEM-EDX, FTIR, and LC-MS, phytochelatin plays a major role in removing heavy metal from soil by *G. vittiformis*. The study of mechanism is significant as any modifications in the gene regulating phytochelatin production can be modified to increase the metal accumulation ability. Mycoremediation can be considered as an alternative to other known methods in heavy metal removal from the soil owing to its short action period and better accumulation efficiency. Integration of this technology with advanced agronomical and engineering skills can transform mycoremediation as a competitive remediation tool.

Conflict of Interests

The authors (Ms. Dilna Damodaran, Dr. Vidya Shetty k, and Dr. RajMohan) declare that there is no conflict of interests regarding the publication of this paper.

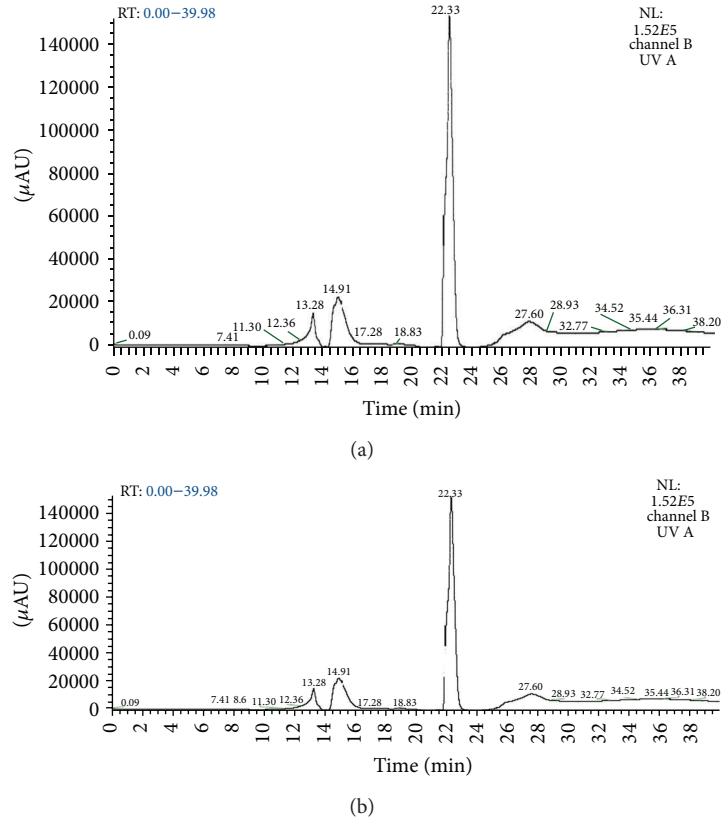

Figure 10: (a) Chromatogram produced by LC-MS analysis for Cu(II) at various retention times (min). (b) Chromatogram produced by LC-MS analysis for Cu(II) at various *m/z* ratios.

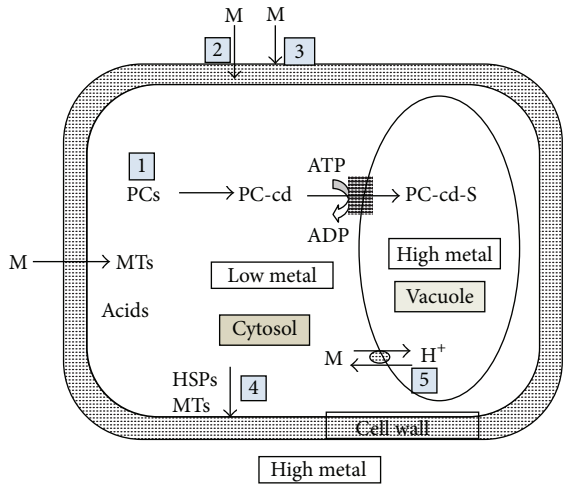

Figure 11: Schematic representation of the proposed mechanism of metal uptake by *Galerina vittiformis*. (1) Metal adsorption on fungal mycelial surface which acts as roots of fruiting bodies. (2) Uptake and storing in periplasmic space passive absorption. (3) PC and acid production in response to metal stress. (4) Acids act as HSPs (heat shock proteins) that bind to metal and store them to periplasmic space. (5) Transport and accumulation of metals in vacuole.

References

[1] S. V. Avery, "Metal toxicity in yeasts and the role of oxidative stress," *Advances in Applied Microbiology*, vol. 49, pp. 111–142, 2001.

[2] J. L. Schnoor, "Phytoremediation: ground-water remediation technologies," Analysis Centre Technology Evaluation Report TE 98-1, William Pitt Way, Pittsburgh, PA, USA, 1997.

[3] J. S. Bardan, O. Radziah, S. A. Wahid, A. Husin, and F. S. Zadeh, "Column bioleaching of arsenic and heavy metals from gold

mine tailings by *Aspergillus fumigates*," *Clean—Soil, Air, Water*, vol. 40, no. 6, pp. 607–614, 2012.

[4] F. M. Morsy, S. H. A. Hassan, and M. Koutb, "Biosorption of Cd(II) and Zn(II) by *Nostoc commune* isotherm and kinetics studies," *Clean—Soil, Air, Water*, vol. 39, no. 7, pp. 680–687, 2011.

[5] V. Mishra, C. Balomajumder, and V. K. Agarwal, "Zn(II) ion biosorption onto surface of eucalyptus leaf biomass: isotherm, kinetic, and mechanistic modeling," *Clean—Soil, Air, Water*, vol. 38, no. 11, pp. 1062–1073, 2010.

[6] Z. Volesky and S. Holan, "Biosorption of heavy metals," *Biotechnology Progress*, vol. 11, pp. 235–250, 1995.

[7] R. Moore, W. D. Clark, and D. Vodopich, *Botany*, WCB/McGraw-Hill, Dubuque, Iowa, USA, 3rd edition, 1998.

[8] V. Hornburg, G. Welp, and G. Brummer, "Verhalten von schwermetallen in boden," in *Extraktion Mobiler Schwermetalle Mittels $CaCl_2$ und NH_4NO_3. Z. Pflanzenernaehr*, vol. 158, pp. 137–145, Bodenk, Springer, Berlin,Germany, 2nd edition, 1995.

[9] K. J. Reddy, L. Wang, and S. P. Gloss, "Solubility and mobility of copper, zinc and lead in acidic environments," *Plant and Soil*, vol. 171, no. 1, pp. 53–58, 1995.

[10] U. Schmidt, "Enhancing phytoextraction: the effect of chemical soil manipulation on mobility, plant accumulation, and leaching of heavy metals," *Journal of Environmental Quality*, vol. 32, no. 6, pp. 1939–1954, 2003.

[11] C. Bliefert, *Umweltchemie*, Wiley-VCH, Weinheim, Germany, 1994.

[12] Z. Li and L. M. Shuman, "Heavy metal movement in metal-contaminated soil profiles," *Journal of Soil Science*, vol. 161, no. 10, pp. 656–666, 1996.

[13] K. Pakshirajan, A. N. Worku, M. A. Acheampong, H. J. Lubberding, and P. N. Lens, "Cr(III) and Cr(VI) removal from aqueous solutions by cheaply available fruit waste and algal biomass," *Applied Biochemistry and Biotechnology*, vol. 170, no. 3, pp. 498–513, 2013.

[14] P. Oei, *Mushroom Cultivation with Special Emphasis on Appropriate Techniques for Developing Countries*, Tool, Amsterdam, The Netherlands, 1st edition, 1996.

[15] S. Srivastava and I. S. Thakur, "Biosorption potency of *Aspergillus niger* for removal of chromium (VI)," *Journal of Current Microbiology*, vol. 53, no. 3, pp. 232–237, 2006.

[16] I. Turkekul, M. Elmastas, and M. Tuzen, "Determination of iron, copper, manganese, zinc, lead, and cadmium in mushroom samples from Tokat, Turkey," *Food Chemistry*, vol. 84, no. 3, pp. 389–392, 2004.

[17] K. Mitra, *Studies on the uptake of heavy metal pollutants by edible mushrooms and its effects on their growth productivity and mammalian system [Ph.D. thesis]*, University of Calcutta, Kolkata, India, 1994.

[18] A. Demirbaş, "Concentrations of 21 metals in 18 species of mushrooms growing in the East Black Sea region," *Food Chemistry*, vol. 75, no. 4, pp. 453–457, 2001.

[19] F. Yilmaz, I. Mustafa, and M. Melek, "Heavy metal levels in some macro fungi," *Turkish Journal of Botany*, vol. 27, no. 1, pp. 45–56, 2003.

[20] F. Zhu, L. Qu, W. Fan, M. Qiao, H. Hao, and X. Wang, "Assessment of heavy metals in some wild edible mushrooms collected from Yunnan Province, China," *Environmental Monitoring and Assessment*, vol. 179, no. 1–4, pp. 191–199, 2011.

[21] A. Basile, S. Sorbo, G. Aprile, B. Conte, and C. R. Castaldo, "Comparison of the heavy metal bioaccumulation capacity of an epiphytic moss and an epiphytic lichen," *Environmental Pollution*, vol. 151, no. 2, pp. 401–407, 2008.

[22] W. Ge, D. Zamri, H. Mineyama, and M. Valix, "Bioaccumulation of heavy metals on adapted *Aspergillus foetidus*," *Adsorption*, vol. 17, no. 5, pp. 901–910, 2011.

[23] B. N. Ita, J. P. Essien, and G. A. Ebong, "Heavy metal levels in fruiting bodies of edible and non-edible mushrooms from the Niger Delta region of Nigeria," *Enzyme and Microbial Technology*, vol. 32, pp. 78–89, 2006.

[24] O. Isildak, I. Turkekul, M. Elmastas, and H. Y. Aboul-Enein, "Bioaccumulation of heavy metals in some wild-grown edible mushrooms," *Analytical Letters*, vol. 40, no. 6, pp. 1099–1116, 2007.

[25] R. Vimala and N. Das, "Biosorption of cadmium (II) and lead (II) from aqueous solutions using mushrooms: a comparative study," *Journal of Hazardous Materials*, vol. 168, no. 1, pp. 376–382, 2009.

[26] A. Çayir, M. Coşkun, and M. Coşkun, "The heavy metal content of wild edible mushroom samples collected in Canakkale Province, Turkey," *Biological Trace Element Research*, vol. 134, no. 2, pp. 212–219, 2010.

[27] M. Konuk, A. Afyon, and D. Yağiz, "Minor element and heavy metal contents of wild growing and edible mushrooms from Western Black Sea region of Turkey," *Fresenius Environmental Bulletin*, vol. 16, pp. 1359–1362, 2007.

[28] S. J. Haswell, *Atomic Absorption Spectrometry: Theory, Design and Applications*, Elsevier, Amsterdam, The Netherlands, 1991.

[29] G. W. Susan, A. E. Kaminsky, and S. Tanya, "High spatial resolution surface imaging and analysis of fungal cells using SEM and AFM," *Micron*, vol. 39, no. 4, pp. 349–366, 2008.

[30] K. Pakshirajan and T. Swaminathan, "Biosorption of lead, copper, and cadmium by *Phanerochaete chrysosporium* in ternary metal mixtures: statistical analysis of individual and interaction effects," *Applied Biochemistry and Biotechnology*, vol. 158, no. 2, pp. 457–469, 2009.

[31] M. C. González, R. C. Gonzalez, S. F. Wright, and K. A. Nichols, "The role of glomalin, a protein produced by arbuscular mycorrhizal fungi, in sequestering potentially toxic elements," *Environmental Pollution*, vol. 130, no. 3, pp. 317–323, 2004.

[32] M. Thomet, E. Vogel, and U. Krahenbuhl, "The uptake of cadmium and zinc by mycelia and their accumulation in mycelia and fruiting bodies of edible mushrooms," *European Food Research and Technology*, vol. 209, no. 5, pp. 317–324, 1999.

[33] X.-H. Chen, H.-B. Zhou, and G.-Z. Qiu, "Analysis of several heavy metals in wild edible mushrooms from regions of China," *Bulletin of Environmental Contamination and Toxicology*, vol. 83, no. 2, pp. 280–285, 2009.

[34] L. Chen, S. L. Luo, X. Xiao et al., "Application of plant growth-promoting endophytes (PGPE) isolated from *Solanum nigrum* L. for phytoextraction of Cd-polluted soils," *Applied Soil Ecology*, vol. 46, no. 3, pp. 383–389, 2010.

[35] D.-L. Huang, G.-M. Zeng, X.-Y. Jiang et al., "Bioremediation of Pb-contaminated soil by incubating with *Phanerochaete chrysosporium* and straw," *Journal of Hazardous Materials*, vol. 134, no. 1–3, pp. 268–276, 2006.

[36] D.-L. Huang, G.-M. Zeng, C.-L. Feng et al., "Degradation of lead-contaminated lignocellulosic waste by *Phanerochaete chrysosporium* and the reduction of lead toxicity," *Environmental Science & Technology*, vol. 42, no. 13, pp. 4946–4951, 2008.

[37] P. A. Wuyep, A. G. Chuma, S. Awodi, and A. J. Nok, "Biosorption of Cr, Mn, Fe, Ni, Cu and Pb metals from petroleum refinery effluent by calcium alginate immobilized mycelia of *Polyporus squamosus*," *Scientific Research and Essay*, vol. 2, pp. 217–221, 2007.

[38] Z.-X. Niu, L.-N. Sun, T.-H. Sun, Y.-S. Li, and H. Wang, "Evaluation of phytoextracting cadmium and lead by sunflower, ricinus, alfalfa and mustard in hydroponic culture," *Journal of Environmental Sciences A*, vol. 19, no. 8, pp. 961–967, 2007.

[39] A. Demirbaş, "Metal ion uptake by mushrooms from natural and artificially enriched soils," *Food Chemistry*, vol. 78, no. 1, pp. 89–93, 2002.

[40] M. Joho, M. Inouhe, H. Tohoyama, and T. Murayama, "Nickel resistance mechanisms in yeasts and other fungi," *Journal of Industrial Microbiology*, vol. 14, no. 2, pp. 164–168, 1995.

[41] J. L. Hall, "Cellular mechanism of heavy metal detoxification and tolerance: a review article," *Journal of Experimental Botany*, vol. 53, pp. 1–11, 2002.

[42] M. Inouhe, M. Sumiyoshi, H. Tohoyama, and M. Joho, "Resistance to cadmium ions and formation of a cadmium-binding complex in various wild-type yeasts," *Plant and Cell Physiology*, vol. 37, no. 3, pp. 341–346, 1996.

[43] R. K. Mehra, E. B. Tarbet, W. R. Gray, and D. R. Winge, "Metalspecic synthesis of 2 metallthioneins and g-glutamyltransferase peptides in Candida *glabrata*," *Proceedings of the National Academy of Sciences of the United States of America*, vol. 85, pp. 8815–8819, 1988.

[44] K. Münger and K. Lerch, "Copper metallothionein from the fungus *Agaricus bisporus* chemical and spectroscopic properties," *Biochemistry*, vol. 24, no. 24, pp. 6751–6756, 1985.

[45] K. Lerch, "Copper metallothionein, a copper-binding protein from *Neurospora crassa*," *Nature*, vol. 284, pp. 368–370, 1980.

[46] D. Cánovas, R. Vooijs, H. Schat, and V. de Lorenzo, "The role of thiol species in the hypertolerance of *Aspergillus* sp. P37 to arsenic," *The Journal of Biological Chemistry*, vol. 279, no. 49, pp. 51234–51240, 2004.

[47] K. Paraszkiewicz, P. Bernat, M. Naliwajski, and J. Długoński, "Lipid peroxidation in the fungus *Curvularia lunata* exposed to nickel," *Archives of Microbiology*, vol. 192, no. 2, pp. 135–141, 2010.

[48] M. Courbot, L. Diez, R. Ruotolo, M. Chalot, and P. Leroy, "Cadmium-responsive thiols in the ectomycorrhizal fungus *Paxillus involutus*," *Applied and Environmental Microbiology*, vol. 70, no. 12, pp. 7413–7417, 2004.

[49] J. Ivanova, T. Toncheva-Panova, G. Chernev, and B. Samuneva, "Effect of Ag^{2+}, Cu^{2+} and Zn^{2+} containing hybrid nano matrixes on the green algae *Chlorella keissleri*," *Journal of Applied Plant Physiolology*, vol. 34, pp. 339–348, 2008.

[50] K. Paraszkiewicz, P. Bernat, M. Naliwajski, and J. Długoński, "Lipid peroxidation in the fungus *Curvularia lunata* exposed to nickel," *Archives of Microbiology*, vol. 192, no. 2, pp. 135–141, 2010.

[51] W. K. Surewicz, H. H. Mantsch, and D. Chapman, "Determination of protein secondary structure by Fourier transform infrared spectroscopy," *Biochemistry*, vol. 32, no. 2, pp. 389–394, 1993.

[52] P. Kalač and L. Svoboda, "A review of trace element concentrations in edible mushrooms," *Food Chemistry*, vol. 69, no. 3, pp. 273–281, 2000.

[53] M. Caliskan, "Germin, an oxalate oxidase, has a function in many aspects of plant life," *Turkish Journal of Biology*, vol. 24, pp. 717–724, 2000.

[54] W. Qian and S. Krimm, "Vibrational analysis of glutathione," *Biopolymers*, vol. 34, no. 10, pp. 1377–1394, 1994.

[55] T.-H. Yang, A. Dong, J. Meyer, O. L. Johnson, J. L. Cleland, and J. F. Carpenter, "Use of infrared spectroscopy to assess secondary structure of human growth hormone within biodegrable microspheres," *Journal of Pharmaceutical Sciences*, vol. 88, no. 2, pp. 161–165, 1999.

[56] Y.-B. Shi, J.-L. Fang, X.-Y. Liu, L. Du, and W.-X. Tang, "Fourier transform IR and fourier transform raman spectroscopy studies of metallothionein-III: amide I band assignments and secondary structural comparison with metallothioneins-I and -II," *Biopolymers*, vol. 65, no. 2, pp. 81–88, 2002.

[57] E. Camera, M. Rinaldi, S. Briganti, M. Picardo, and S. Fanali, "Simultaneous determination of reduced and oxidized glutathione in peripheral blood mononuclear cells by liquid chromatography-electrospray mass spectrometry," *Journal of Chromatography B*, vol. 757, no. 1, pp. 69–78, 2001.

[58] S. A. Odoemelam, C. U. Iroh, and J. C. Igwe, "Copper (II), cadmium (II) and lead (II) adsorption kinetics from aqueous metal solutions using chemically modified and unmodified cocoa pod husk (*Theobroma cacao*) waste biomass," *Research Journal of Applied Sciences*, vol. 6, no. 1, pp. 44–52, 2011.

[59] S. Robina, N. Levequeb, C. C. Masuyera, and P. Humbertc, "LC-MS determination of oxidized and reduced glutathione in human dermis: a micro dialysis study," *Journal of Chromatography B*, vol. 879, no. 30, pp. 3599–3606, 2011.

[60] E. Grill, E. L. Winnacker, and M. H. Zenk, "Phytochelatins, a class of heavy metal complexing peptidesof higher plants," *Science*, vol. 230, pp. 674–676, 1985.

[61] W. Gekeler, E. Grill, E.-L. Winnacker, and M. H. Zenk, "Algae sequester heavy metals via synthesis of phytochelatin complexes," *Archives of Microbiology*, vol. 150, no. 2, pp. 197–202, 1988.

[62] V. Liedschulte, A. Wachter, A. Zhigang, and T. Rausch, "Exploiting plants for glutathione (GSH) production: uncoupling GSH synthesis from cellular controls results in unprecedented GSH accumulation," *Plant Biotechnology Journal*, vol. 8, no. 7, pp. 807–820, 2010.

[63] S. S. Gill and N. Tuteja, "Cadmium stress tolerance in crop plants: probing the role of sulfur," *Plant Signaling and Behavior*, vol. 6, no. 2, pp. 215–222, 2011.

[64] F. F. Nocito, C. Lancilli, B. Crema, P. Fourcroy, J.-C. Davidian, and G. A. Sacchi, "Heavy metal stress and sulfate uptake in Maize roots," *Plant Physiology*, vol. 141, no. 3, pp. 1138–1148, 2006.

[65] W. B. Ammar, C. Mediouni, B. Tray, M. H. Ghorbel, and F. Jemal, "Glutathione and phytochelatin contents in tomato plants exposed to cadmium," *Biologia Plantarum*, vol. 52, no. 2, pp. 314–320, 2008.

[66] S. K. Yadav, "Heavy metals toxicity in plants: an overview on the role of glutathione and phytochelatins in heavy metal stress tolerance of plants," *South African Journal of Botany*, vol. 76, no. 2, pp. 167–179, 2010.

[67] B. V. Tangahu, S. R. Sheikh Abdullah, H. Basri, M. Idris, N. Anuar, and M. Mukhlisin, "A review on heavy metals (As, Pb, and Hg) uptake by plants through phytoremediation," *International Journal of Chemical Engineering*, vol. 2011, Article ID 939161, 31 pages, 2011.

[68] R. England and K. J. Wilkinson, "Determination of phytochelatins in algal samples using LC-MS," *International Journal of Environmental Analytical Chemistry*, vol. 91, no. 2, pp. 185–196, 2011.

[69] C. Scheidegger, M. J. F. Suter, R. Behra, and L. Sigg, "Characterization of lead-phytochelatins complexes by nano electro spray ionization mass spectrometry," *Frontiers in Micorbiology*, vol. 3, no. 41, pp. 1–7, 2012.

[70] S. Volland, D. Schaumloffel, D. Dobritzsch, G. J. Krauss, and U. L. Meind, "Identification of phytochelatins in the cadmium-stressed conjugating green alga *Micrasterias denticulate*," *Chemosphere*, vol. 91, pp. 448–454, 2013.

Hindawi Publishing Corporation
BioMed Research International
Volume 2013, Article ID 647974, 11 pages
http://dx.doi.org/10.1155/2013/647974

Research Article

Toxicity of Superparamagnetic Iron Oxide Nanoparticles on Green Alga *Chlorella vulgaris*

Lotfi Barhoumi[1,2] and David Dewez[1]

[1] *Département de Chimie, Université du Québec à Montréal, CP 8888, Succursale Centre-Ville, Montréal, QC, Canada H3C 3P8*
[2] *Laboratoire de Physiologie Intégrée, Faculté des Sciences de Bizerte, Université de Carthage, Zarzouna 7021, Tunisia*

Correspondence should be addressed to David Dewez; dewez.david@uqam.ca

Received 31 July 2013; Revised 29 October 2013; Accepted 4 November 2013

Academic Editor: Aiyagari Ramesh

Toxicity of superparamagnetic iron oxide nanoparticles (SPION) was investigated on *Chlorella vulgaris* cells exposed during 72 hours to Fe_3O_4 (SPION-1), $Co_{0.2}Zn_{0.8}Fe_2O_4$ (SPION-2), or $Co_{0.5}Zn_{0.5}Fe_2O_4$ (SPION-3) to a range of concentrations from 12.5 to 400 $\mu g\,mL^{-1}$. Under these treatments, toxicity impact was indicated by the deterioration of photochemical activities of photosynthesis, the induction of oxidative stress, and the inhibition of cell division rate. In comparison to SPION-2 and -3, exposure to SPION-1 caused the highest toxic effects on cellular division due to a stronger production of reactive oxygen species and deterioration of photochemical activity of Photosystem II. This study showed the potential source of toxicity for three SPION suspensions, having different chemical compositions, estimated by the change of different biomarkers. In this toxicological investigation, algal model *C. vulgaris* demonstrated to be a valuable bioindicator of SPION toxicity.

1. Introduction

Due to their physicochemical features, superparamagnetic iron oxide nanoparticles (SPION) are widely used in medical applications such as contrast agents for magnetic resonance imaging and heating mediators for cancer therapy [1, 2]. A recent review of SPION-induced toxicity studies at cellular level in animal and human cells indicated that SPION can penetrate the cellular system by both passive diffusion and endocytosis, causing several toxic effects through the alteration of genes expressions and the generation of oxidative radicals [3]. However, their production and extensive use may contaminate aquatic environments via wastewater input, representing a risk of toxicity for different freshwater organisms. Besides endocrine disruptor and pharmaceuticals, metallic engineered nanoparticles represent one of the most important hazardous materials altering freshwater qualities. Many studies showed that the toxicity of metallic engineered nanoparticles was directly related to their surface chemistry, hydrodynamic size, chemical composition, and solubility in aqueous solution [4, 5]. A recent study demonstrated that SPION have antibacterial properties with the ability to alter metabolic functions at a higher efficiency than antibiotics or metals salts [6]. Therefore, it is of high importance to determine the toxicity potential at cellular level of hazardous metallic nanomaterials in relation to their uptake by aquatic microorganisms. In aquatic environments, green algae represent the main source of biomass production essential for animals of higher ecological trophic levels. As being able to bioaccumulate metallic contaminants, algae can be used as a bioindicator of aquatic ecosystem health. However, bioaccumulation effects of SPION on algae have been poorly examined, and such toxicological studies were mostly done on terrestrial plant species grown hydroponically [7, 8]. Currently, there is only one study concerning the toxic effects of Fe_3O_4 nanoparticles (35 nm) on the green alga *Chlorella vulgaris* treated 72 h to a nominal concentration range from 200 to 1600 $\mu g\,mL^{-1}$. In this study, authors showed an induction of oxidative stress and an alteration of photosynthetic activity based on absorbed CO_2 fixation [9]. Therefore, a more in-depth toxicological investigation needs to be performed to better characterise the toxicity of SPION on the cell physiology of green algae.

In the present study, the green alga *Chlorella vulgaris* was used as a unicellular plant model organism for the toxicity characterisation of Fe_3O_4 (SPION-1), $Co_{0.2}Zn_{0.8}Fe_2O_4$ (SPION-2), and $Co_{0.5}Zn_{0.5}Fe_2O_4$ (SPION-3). Algal cells were exposed during 24, 48, and 72 hours in order to evaluate the evolution of SPION toxicity impact on the entire cellular system by evaluating the change in photochemical reactions of photosynthesis, cell division, and the induction of oxidative stress. This work permitted determining the risk of SPION toxicity on the viability of green algae and therefore the potential use of this algal species in a bioassay of SPION toxicity.

2. Material and Methods

2.1. Biological Material. The freshwater green alga *Chlorella vulgaris* was obtained from the *Canadian Phycological Culture Centre* (CPCC, University of Waterloo, ON, Canada). Algal culture was prepared in sterile BG-11 liquid growth medium (pH = 7; ionic strength = 0.0201) having the following final concentrations of salts composition [10]: 1.5 g L^{-1} of $NaNO_3$, 0.04 g L^{-1} of $K_2HPO_4{\cdot}3H_2O$, 0.075 g L^{-1} of $MgSO_4{\cdot}7H_2O$, 0.036 g L^{-1} of $CaCl_2{\cdot}2H_2O$, 6×10^{-3} g L^{-1} of $C_6H_8O_7$ (citric acid), 6×10^{-3} g L^{-1} of $C_6H_5FeO_7$ (ferric citrate), 10^{-3} g L^{-1} of $Na_2EDTA{\cdot}2H_2O$, 0.02 g L^{-1} of Na_2CO_3, 2.86 mg L^{-1} of H_3BO_3, 1.81 mg L^{-1} of $MnCl_2{\cdot}4H_2O$, 0.222 mg L^{-1} of $ZnSO_4{\cdot}7H_2O$, 0.390 mg L^{-1} of $Na_2MoO_4{\cdot}2H_2O$, 0.079 mg L^{-1} of $CuSO_4{\cdot}5H_2O$, and 0.0494 mg L^{-1} of $Co(NO_3)_2{\cdot}6H_2O$. Algal cells were grown under continuous light intensity of 100 μmol m^{-2} s^{-1} (SYLVANIA GRO-LUX Wide Spectrum light F40/GRQ/AQ/WS) at 24°C ± 1. Aliquots of algal samples were used for experiments when algal culture reached the exponential growth phase. The change of cell density was determined by monitoring the optical density at 750 nm, and the calculation was based on a standard correlation with the cell density measured using a multisizer Z3 (Beckman Coulter Inc., USA).

2.2. Synthesis of SPION. Superparamagnetic iron oxide nanoparticles (SPION) as Fe_3O_4 (SPION-1), $Co_{0.2}Zn_{0.8}Fe_2O_4$ (SPION-2), and $Co_{0.5}Zn_{0.5}Fe_2O_4$ (SPION-3) were produced according to the procedure reported in [11], by using the polyol process starting from $Co(CH_3CO_2)_2{\bullet}4H_2O$, $Zn(CH_3CO_2)_2{\bullet}2H_2O$ and $Fe(CH_3CO_2)_2$ as precursor salts and diethylene glycol as a solvent.

2.3. Stock Solution and SPION Characterization. In the preparation of stock solutions, SPION were suspended in culture medium at a concentration of 1 g L^{-1} and homogenized by ultrasonication during 30 min at 4°C to break up agglomerates. After sonication, stock solutions were mix with a vortex for 1 min, and various concentrations of SPION were prepared in culture medium for experiments. Size distribution was determined by dynamic light scattering (DLS) with a ZetaPlus particle sizer (Brookhaven Instrument Corporation, USA) using 90Plus Particles Sizing Software (Ver. 4.20). Zeta potential of SPION suspensions in culture medium was evaluated by the electrophoretic mobility method with the ZetaPlus system.

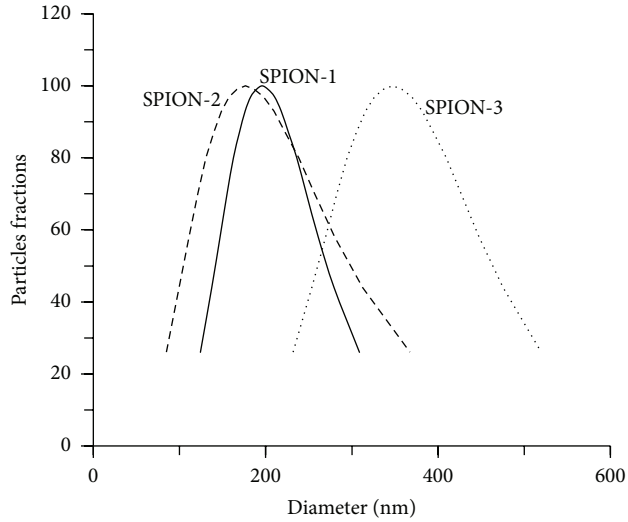

Figure 1: Particle size distribution of SPION-1 (Fe_3O_4), SPION-2 ($Co_{0.2}Zn_{0.8}Fe_2O_4$), and SPION-3 ($Co_{0.5}Zn_{0.5}Fe_2O_4$) suspensions in the culture medium.

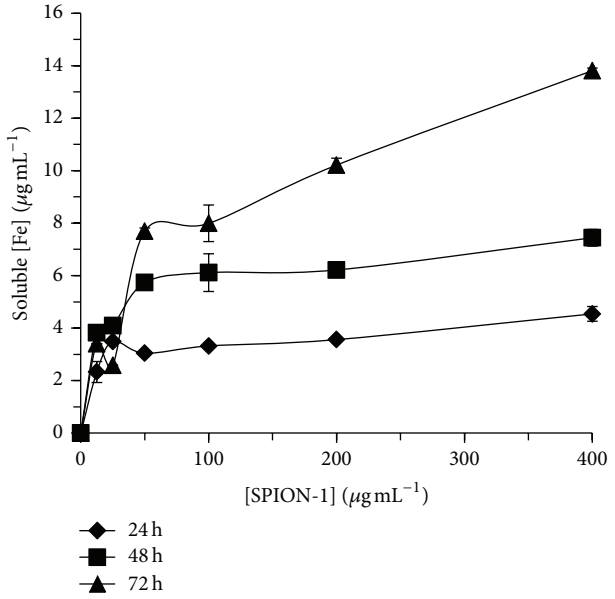

Figure 2: Soluble fraction of free Fe released from SPION-1 (Fe_3O_4) suspension in culture medium at 24, 48, and 72 h of exposure.

2.4. Experimental Treatments. In each treatment condition, the initial density of algal cells was of 10^6 cells mL^{-1} in a final volume of 50 mL. Algal samples were exposed during 24, 48, and 72 h to 12.5, 25, 50, 100, 200, and 400 mg L^{-1} of SPION-1, SPION-2, or SPION-3, under the same illumination and temperature condition used for growing stock cultures. For the control sample, the same media composition was used but without any trace of SPION.

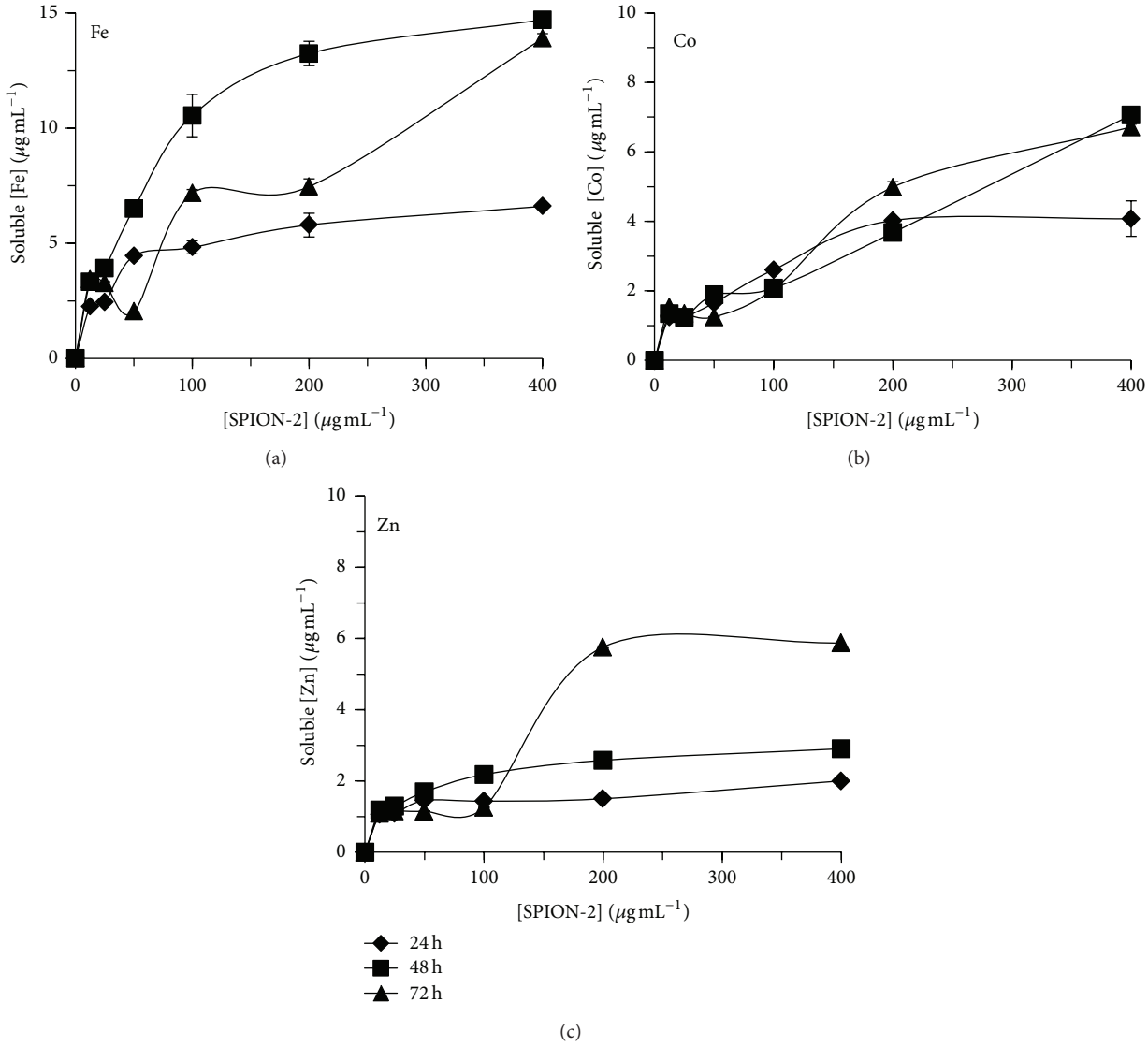

Figure 3: Soluble fraction of free Fe, Co, and Zn released from SPION-2 ($Co_{0.2}Zn_{0.8}Fe_2O_4$) suspension in culture medium at 24, 48, and 72 h of exposure.

2.5. Growth Inhibition Test. The relative cell division rate (RCDR) was evaluated for 72 h according to [12], as RCDR = $(\ln W_{72\,h} - \ln W_0)/72$ h, where $W_{72\,h}$ represents cell density at 72 h and W_0 the initial cell density.

2.6. Bioaccumulation of Fe, Co, and Zn. To separate SPION from cells, a sucrose gradient prepared in BG-11 media was done directly in a Beckman centrifuge tube inclined at a 30° angle in order to get 6 layers of different sucrose densities (5 mL of each sucrose solution 120, 100, 80, 60, 40, and 20%). Algal cells of control and SPION-treated samples were collected by centrifugation. Their pellets were slowly placed on top of sucrose gradient tubes which were centrifuged at 1,000 rpm during 30 min in a swinging-bucket 5810R centrifuge (Eppendorf, Germany). It resulted in the formation of a pellet of SPION at the bottom of the tube. The algal cells layer was recuperated with a glass Pasteur pipette and filtered on a 0.45 μm filter previously dried and weighted. To remove SPION weakly bound to the cell surface or the filter, 3 × 10 mL of 10 mM ethylenediaminetetraacetic acid in BG-11 medium was slowly passed through the filter. Filters were dried at 95°C for 24 h and weighted to calculate algal dry weight. Filters were then placed in acid-washed glass tubes in which 4 mL of HNO_3 and 500 μL H_2O_2 were added. Samples were digested during 48 h at room temperature before being diluted to 20% HNO_3 in Milli-Q purified water for the quantification of Fe, Co, and Zn using atomic absorption spectrometry analysis (Varian SpectrAA 220 FS, USA). Obtained Fe, Co, and Zn concentrations were normalized to the dry weight.

2.7. Soluble Fraction of Fe, Co, and Zn. Solubility of free Fe, Co, and Zn released from SPION suspensions were determined in culture medium. SPION suspensions was incubated during 24, 48, and 72 h in the same condition as described

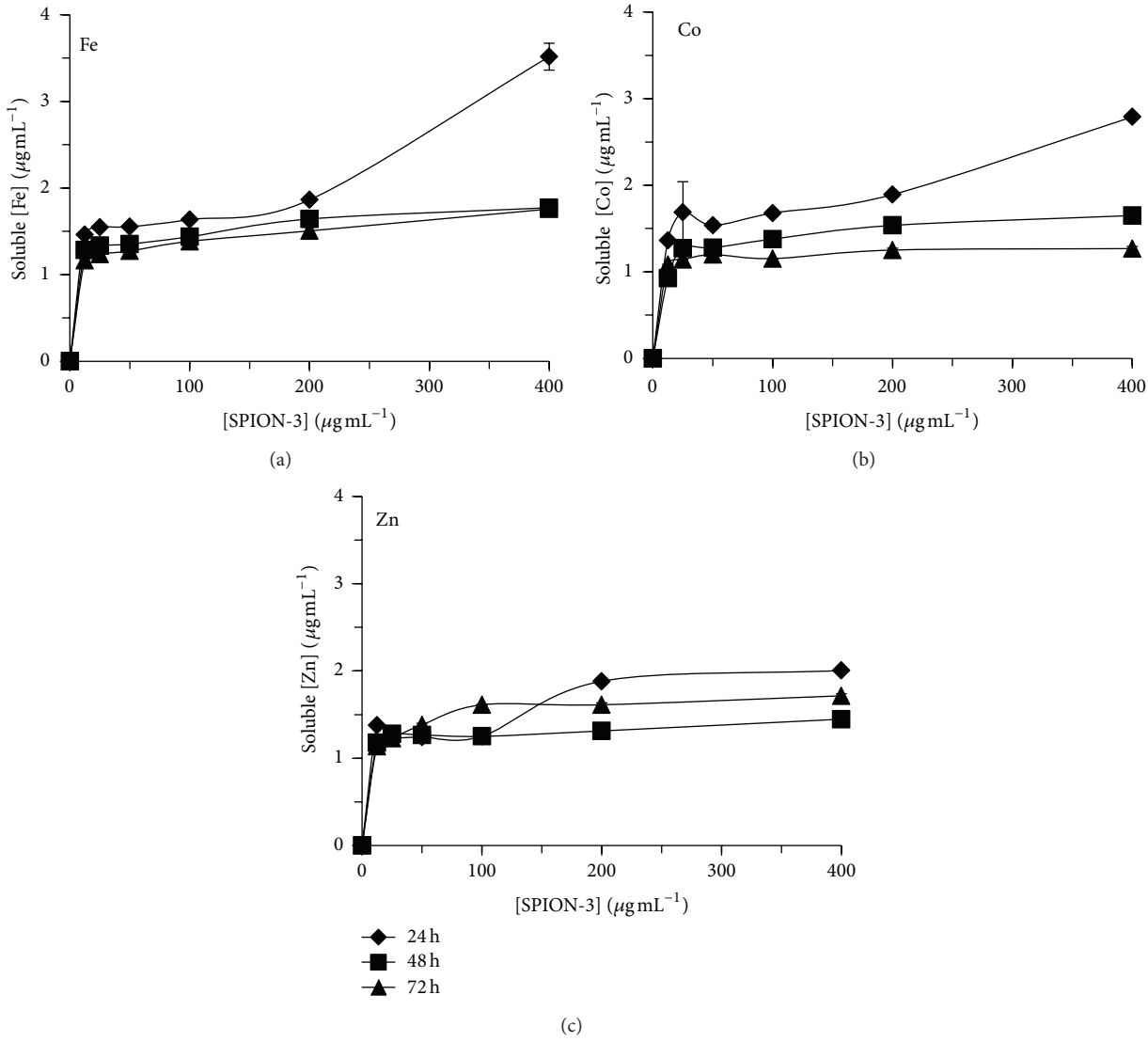

Figure 4: Soluble fraction of Fe, Co, and Zn released from SPION-3 ($Co_{0.5}Zn_{0.5}Fe_2O_4$) suspension in culture medium at 24, 48, and 72 h of exposure.

above for treatment. After incubation, NPs were removed by centrifugation at 12,000 g for 30 min and the supernatant was collected for analysis. Quantification of free Fe, Co, and Zn in solution was measured by atomic absorption spectrometry (Varian SpectrAA 220 FS, USA).

2.8. Production of ROS. The fluorescent dye 2′,7′-dichlorodihydrofluorescein diacetate ((H_2DCFDA) Invitrogen Molecular Probe, USA) was used as an indicator of ROS according to [13]. Cellular esterases hydrolyze this probe into the nonfluorescent compound 2′,7′-dichlorodihydrofluorescein (H_2DCF), which is better retained within cells. In the presence of ROS and cellular esterases, H_2DCF is transformed into the highly fluorescent compound 2′,7′-dichlorofluorescein (DCF). H_2DCFDA stock solution (10 mM) was prepared in ethanol in the dark. After 72 h of treatment, 1 mL of algal samples was exposed during 15 min to 0.2 mM of H_2DCFDA in the dark. The ROS level was determined by measuring the fluorescence emission at 530 nm with a flow cytometer (FACScan system, Becton Dickinson Instruments, USA). Cytometry results were analysed using the WinMDI 2.8 software. Algal cells were separated from noncellular particles by using a relationship between particle size and red fluorescence level, originating from chlorophyll fluorescence emission. A positive control sample using methyl viologen was done to verify the assay (data not shown).

2.9. Cellular Viability. Viability of algal cells was estimated using the fluorescein diacetate ((FDA) Invitrogen Molecular Probe, USA) method according to [14]. FDA is a nonpolar ester compound which passes through cell membranes. Once inside the cell, FDA is hydrolyzed by esterases (enzymes present in viable cells) to produce fluorescein, accumulating in cell wall and emitting fluorescence under UV illumination.

After 72 h of treatment, 1 mL of algal samples was exposed during 15 min to 0.2 mM of FDA in the dark. Cell viability was determined by measuring the fluorescence emission at 530 nm with a flow cytometer (FACScan System, Becton Dickinson Instruments, USA). Cytometry results were analysed using the WinMDI 2.8 software. Algal cells were separated from noncellular particles by using a relationship between particle size and red fluorescence level, originating from chlorophyll fluorescence emission. A positive control sample using methyl viologen was done to verify the assay (data not shown).

2.10. Chl a Fluorescence Emission. Photosynthetic electron transport was monitored from the change in the rapid rise of Chl *a* fluorescence emission using a "Plant Efficiency Analyser" fluorometer (Handy-PEA, Hansatech Ltd., UK). Total chlorophyll (Chl) content ($a + b$) was extracted in 100% methanol at 65°C and quantified with a spectrophotometer (Lambda 40, Perkin-Elmer, USA) according to the formula indicated in [15]: Total Chl (μg mL^{-1}) = (24.93 × $A_{652.4}$ + 1.44 × $A_{665.2}$).

Prior to fluorescence measurements, algal samples were transferred into clean sterile 2 mL glass vials and dark-adapted for 30 min. An aliquot of 5 μg of total chlorophyll was gently filtered using low pressure filtration and algal cells were uniformly placed on a 13 mm glass fibre filter (Millipore, USA). The fluorescence induction was triggered using a 1 s saturating flash of 3500 μmol m^{-2} s^{-1}. The fluorescence intensity at 20 μs was considered as the *O* value (F_O); fluorescence intensities for *K*, *J*, and *I* transients were determined at 300 μs (F_K), 2 ms (F_J), and 30 ms (F_I), respectively. the maximum fluorescence yield reached maximal value of fluorescence intensity (F_M) under saturating illumination. Different photosynthetic-based fluorescence parameters related to the functional state of Photosystem II were calculated [16, 17]: the maximum efficiency of PSII electron transport, $F_V/F_M = (F_M - F_O)/F_M$; the absorption of photons by light harvesting antenna complexes (ABS) per active reaction center (RC), ABS/RC = $((F_K - F_O)/0.25) \times (1/(F_J - F_O)) \times (F_M/(F_M - F_O))$; the relative variable fluorescence yield at *J* transient, estimating the fraction of Q_A in its reduced state, $V_J = (F_J - F_O)/(F_M - F_O)$; and the performance index of PSII photosynthetic activity, P.I. = RC/ABS × $((F_M - F_O)/F_O) \times ((1 - V_J)/V_J)$.

2.11. Statistical Analysis. All treatments were performed in triplicate. Means and standard deviations were calculated for each treatment. Significant differences between control and treated plants were determined by one-way analysis of variance (ANOVA) followed by a Dunnett's multiple comparison (DMC) test where *P* value less than 0.05 was considered significant.

3. Results

3.1. Characterisation of SPION. When SPION were suspended in the media, nanoparticles formed agglomerates during the first minutes, as indicated by the distribution of hydrodynamic particles size diameter, which was caused by the content of salts in the media. Analysis by dynamic light scattering showed SPION-1, SPION-2, and SPION-3 suspensions in culture media to have an average diameter of particle size distribution of 195.9, 176.5, and 347.2 nm, respectively (Figure 1). These distributions of hydrodynamic size of SPION were found to be stable in the culture medium during the entire experimental exposure. Furthermore, measurements of zeta potential (mV) indicated that SPION were negatively charged in the media with values of −25.68 (±1.38), −29.14 (±3.85), and −28.06 (±1.19), respectively, for SPION-1, SPION-2, and SPION-3.

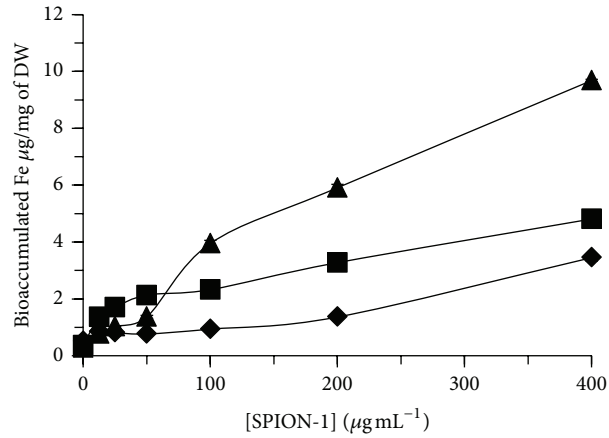

Figure 5: Bioaccumulated content of Fe in algal cells of *Chlorella vulgaris* exposed during 24 h (♦, diamond), 48 h (■, square), and 72 h (▲, triangle) to different concentrations of SPION-1 (Fe_3O_4).

3.2. Solubility and Bioaccumulation of SPION. The soluble fraction of free Fe, Co, and Zn released from SPION-1, SPION-2, and SPION-3 suspensions in culture medium was determined at 24, 48, and 72 hours (Figures 2, 3, and 4). The quantity of soluble Fe, Co, and Zn in the medium was dependent on the time of exposure, the SPION composition, and their concentration. When *C. vulgaris* was exposed to 12.5 μg mL^{-1} of SPION-1 (Fe_3O_4) during 72 h, the proportion of the soluble fraction of free Fe was of 27% compared to the nominal concentration of SPION-1, and it decreased to 3% for 400 μg mL^{-1} of SPION-1 (Figure 2). However, the solubility of SPION-2 ($Co_{0.2}Zn_{0.8}Fe_2O_4$) was dependent on the metal species. When algal cells were exposed during 72 h to 12.5 μg mL^{-1} of SPION-2, proportions of free Fe, Co, and Zn in the soluble fraction were, respectively, of 27, 12, and 9% compared to the nominal concentration of SPION-2 (Figure 3). For the exposure concentration of 400 μg mL^{-1}, the quantity of soluble Fe, Co, and Zn decreased to 3, 2, and 1%, respectively. Concerning the solubility of SPION-3 ($Co_{0.5}Zn_{0.5}Fe_2O_4$), concentrations of Fe, Co, and Zn in the soluble fraction at 72 h were of 9% each when compared to the nominal concentration of 12.5 μg mL^{-1}. For the exposure concentration of 400 μg mL^{-1}, concentrations of Fe, Co, and Zn in the soluble fraction were less than

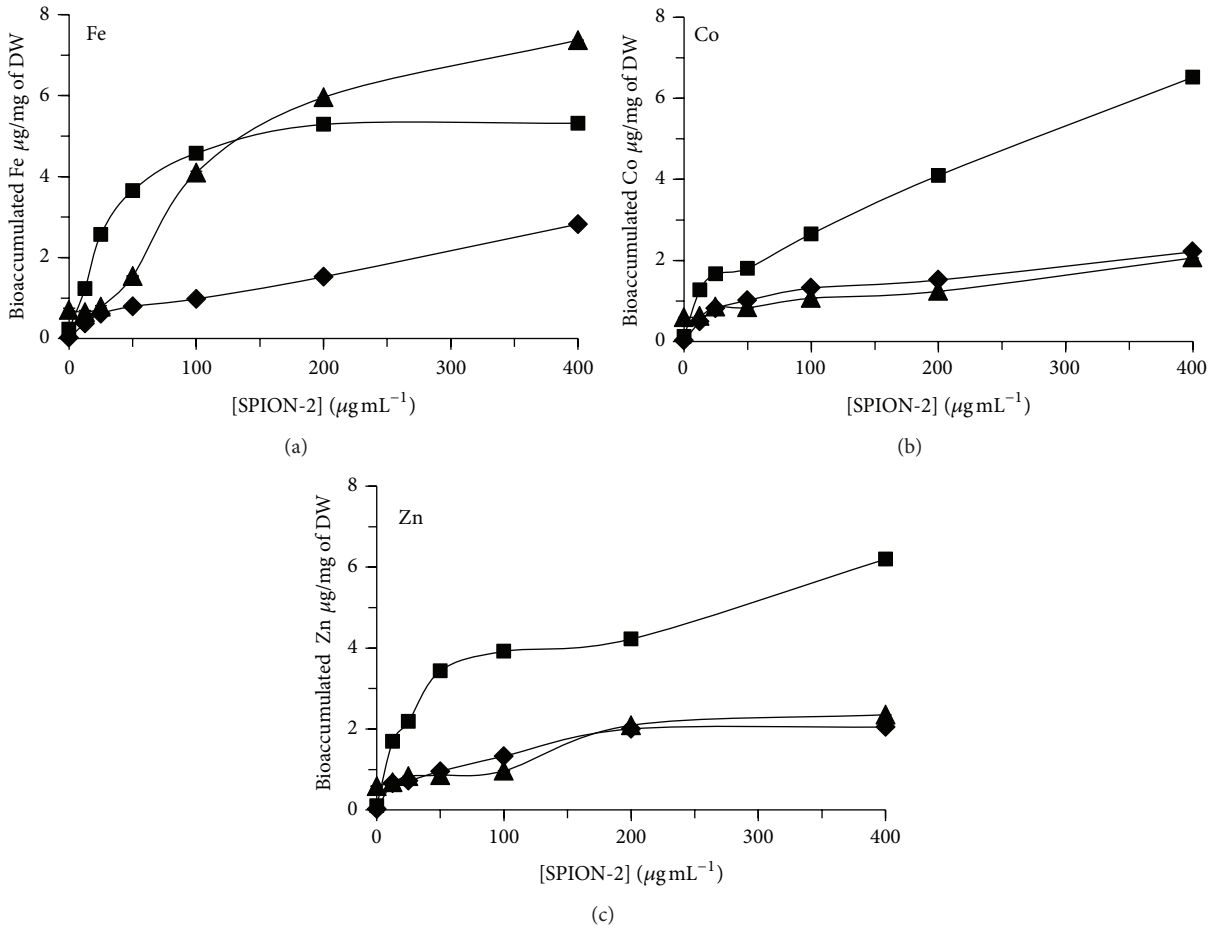

Figure 6: Bioaccumulated content of Fe, Co, and Zn in algal cells of *Chlorella vulgaris* exposed during 24 h (♦, diamond), 48 h (■, square), and 72 h (▲, triangle) to different concentrations of SPION-2 ($Co_{0.2}Zn_{0.8}Fe_2O_4$).

0.5% in comparison to the nominal concentration of SPION-3. Indeed, we observed that the agglomeration of SPION increased their precipitation/sedimentation at the bottom of the experimental flask, which was directly related to the increasing concentration tested and time of exposure. This effect may cause the reduction of the surface contact of nanoparticles with the medium explaining the decrease in SPION solubilisation related to their concentration and time of exposure.

The bioaccumulation of total Fe, Co, and Zn was also quantified in algal biomass of *C. vulgaris* exposed during 24, 48, and 72 h to SPION (Figures 5, 6, and 7). For SPION-1, the accumulated contents of Fe in algal biomass increased in dependence on the concentration of SPION and the time of exposure (Figure 5). The bioaccumulated content of Fe increased by 35-fold for algal cells treated during 72 h to 400 μg mL^{-1} of SPION-1 compared to control. Under this treatment condition, Fe bioaccumulation increased by 2.81-fold from 24 to 72 h. Concerning SPION-2, the accumulated contents of Fe, Co, and Zn increased in algal biomass in relation to the concentration of SPION (Figure 6). The content of Fe reached its maximum value at 72 h which increased by 10.4-fold for 400 μg mL^{-1} of SPION compared to control. On the other hand, the contents of Co and Zn attained their maximal values at 48 h which increased, respectively, by 53.7-and 62.8-fold for 400 μg mL^{-1} of SPION compared to control. When *C. vulgaris* was exposed to SPION-3, the bioaccumulation of Fe, Co, and Zn increased in relation to the concentration of SPION (Figure 7). At 72 h of exposure, values of Fe, Co, and Zn contents increased, respectively, by 4.42-, 3.29-, and 5.47-fold for 400 μg mL^{-1} of SPION compared to control.

3.3. Inhibition of the Relative Cell Division Rate. When algal cells of *C. vulgaris* were exposed during 72 h to SPION at concentrations varying from 12.5 to 400 μg mL^{-1}, the inhibition of the relative cell division rate based on the change of cell density was dependent on the tested SPION concentration (Table 1). Under concentration exposure of 400 μg mL^{-1}, the relative cell division rate decreased significantly compared to the control by 47.8, 21.8, and 15.8% for SPION-1, SPION-2, and SPION-3, respectively.

3.4. Inhibition of Photosynthetic Electron Transport. The change of Chl *a* fluorescence emission was used to monitor the photosynthetic electron transport when algal cells of

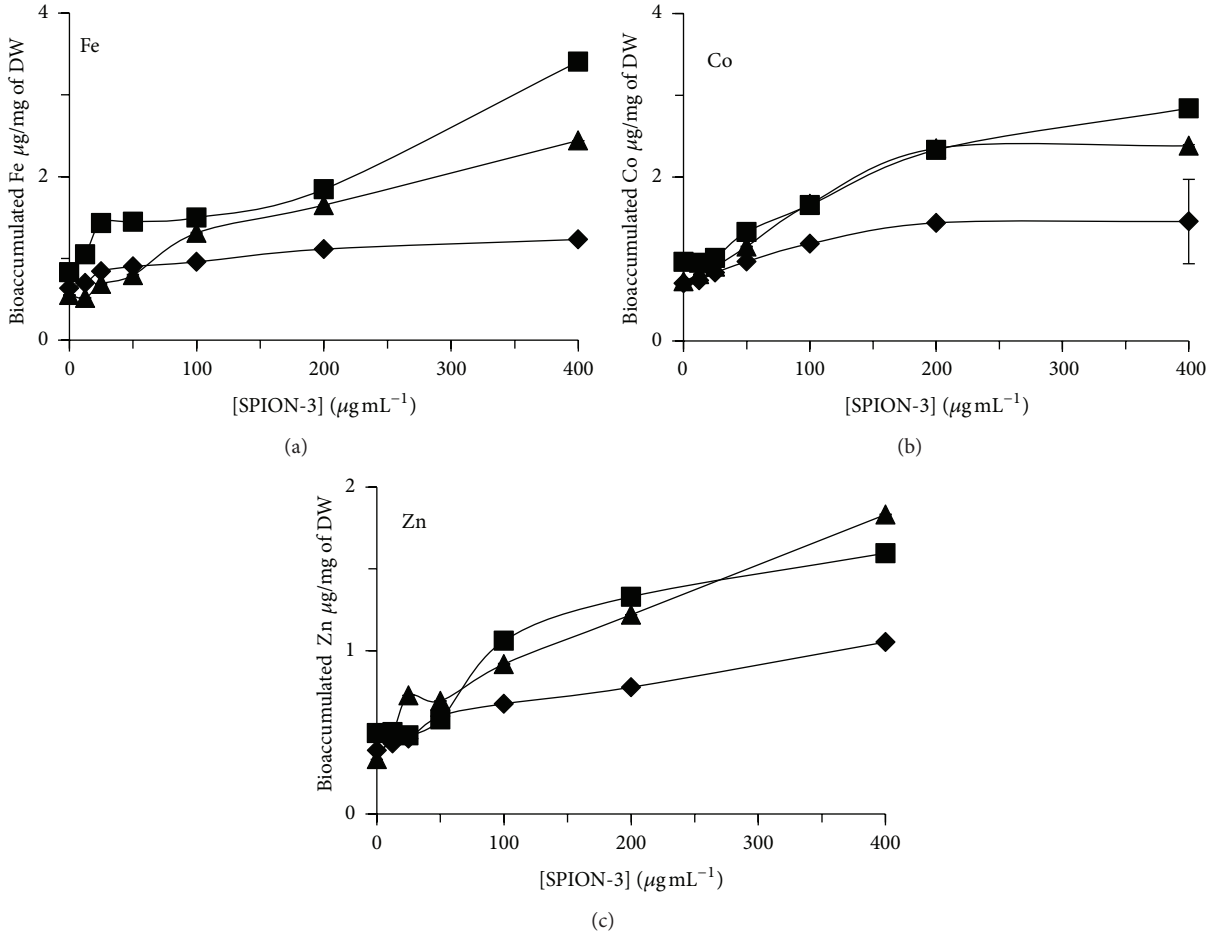

Figure 7: Bioaccumulated content of Fe, Co, and Zn in algal cells of *Chlorella vulgaris* exposed during 24 h (♦, diamond), 48 h (■, square), and 72 h (▲, triangle) to different concentrations of SPION-3 ($Co_{0.5}Zn_{0.5}Fe_2O_4$).

Table 1: Change in the relative cell division rate (RCDR) when *C. vulgaris* was exposed to SPION during 72 h.

[SPION] μg/mL	RCDR (10^{-6})		
	SPION-1	SPION-2	SPION-3
0	0.335 ± 0.01	0.335 ± 0.01	0.335 ± 0.01
12.5	0.305 ± 0.05	0.307 ± 0.05	0.317 ± 0.004
25	0.308 ± 0.008	0.298 ± 0.006	0.318 ± 0.007
50	0.307 ± 0.02	0.297 ± 0.018	0.309 ± 0.004
100	0.266 ± 0.05	0.291 ± 0.007	0.306 ± 0.025
200	0.220 ± 0.008	0.264 ± 0.002	0.286 ± 0.005
400	0.175 ± 0.123	0.262 ± 0.0033	0.282 ± 0.004

C. vulgaris were exposed during 72 h to SPION toxicity. The kinetics of Chl *a* fluorescence indicated a decrease of fluorescence yields at *J*, *I*, and *M* levels without any change in their time of appearance, which was related to SPION concentration (See Supplementary Figures available online at http://dx.doi.org/10.1155/2013/647974). Furthermore, the change of photosynthetic-fluorescence parameters estimated from the fluorescence kinetic was used as biomarkers of SPION effect on PSII photochemistry (Figure 8). The strongest effect on photosynthetic electron transport was observed under 400 $\mu g\,mL^{-1}$ of SPION treatment. Under this condition, the value of ABS/RC parameter increased significantly compared to the control by 43, 29, and 81% for SPION-1, SPION-2, and SPION-3, respectively. This change indicated a decrease of functional PSII reaction centers able to perform photochemical reactions. Also, V_J values, indicating the level of $Q_A^-/Q_{A(total)}$, increased significantly compared to the control by 32, 23, and 12%, respectively, for SPION-1, SPION-2, and SPION-3, due to the inhibition of PSII electron transport flow toward to plastoquinone pool. However, the maximal quantum yield of PSII (F_V/F_M) decreased by 14, 12, and 35%, respectively, for SPION-1, SPION-2, and SPION-3. Moreover, the PSII performance index, P.I., was used as a global parameter integrating all PSII photochemical reactions from light harvesting energy transfer to electron transport. When algal cells of *C. vulgaris* were exposed during 72 h to 400 $\mu g\,mL^{-1}$ of SPION, P.I. values decreased significantly compared to the control by 78, 65, and 85% for SPION-1, SPION-2, and SPION-3, respectively.

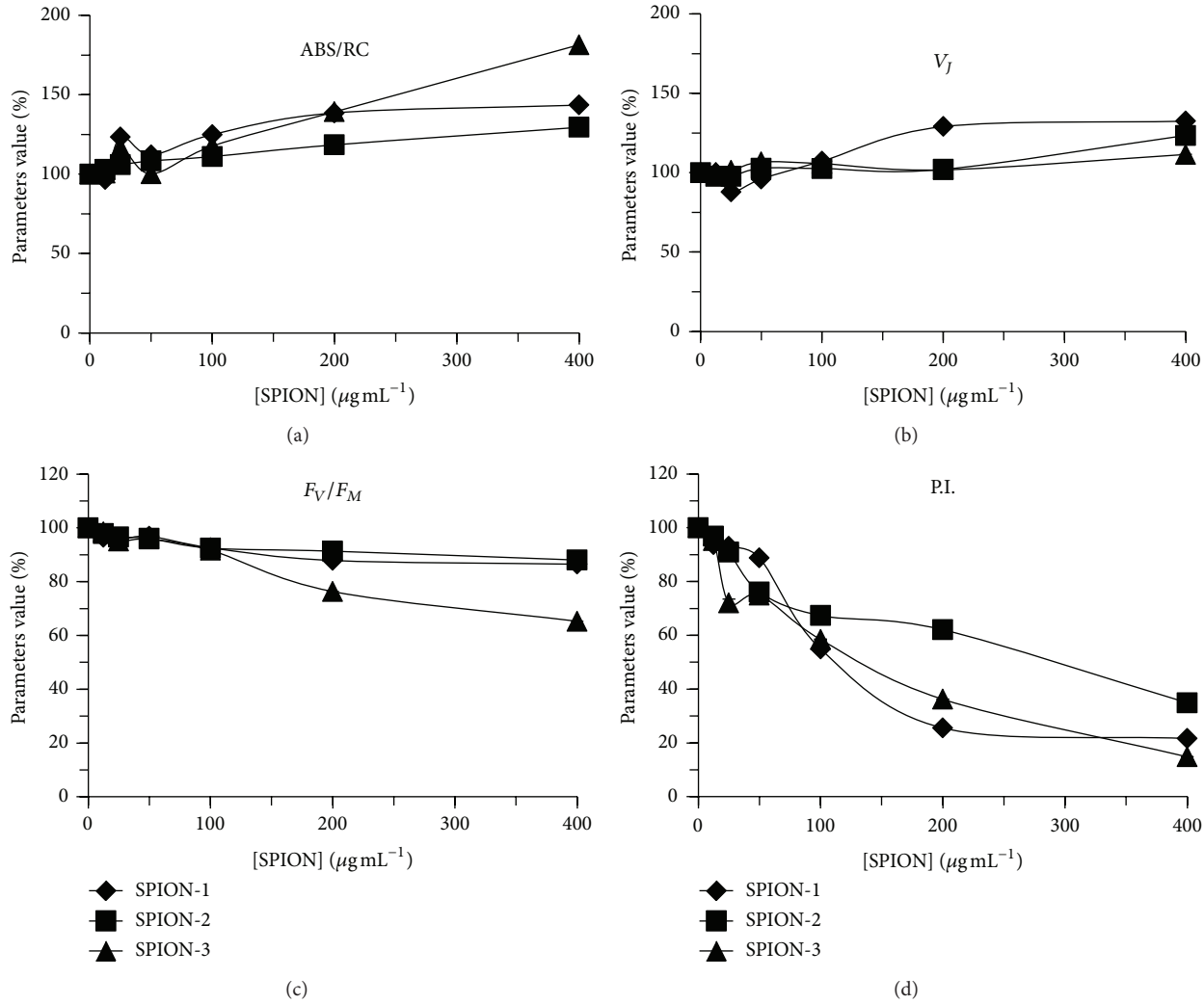

Figure 8: Change of different photosynthetic-based fluorescence parameters for algal cells of *Chlorella vulgaris* exposed during 72 h to different concentrations of SPION-1 (Fe_3O_4), SPION-2 ($Co_{0.2}Zn_{0.8}Fe_2O_4$), and SPION-3 ($Co_{0.5}Zn_{0.5}Fe_2O_4$). Maximal PSII quantum yield: F_V/F_M; ratio between the number of active PSII reaction centers and light harvesting Chl antenna size: ABS/RC; relative variable fluorescence yield at J transient: V_J; performance index of PSII photochemical activity: P.I.

3.5. Production of Reactive Oxygen Species Related to Cell Viability. The formation of ROS per viable cells was determined for *C. vulgaris* exposed during 72 h to SPION (Figure 9). Under these conditions, cell viability decreased significantly compared to control from 50 μg mL^{-1} of SPION, indicating an induction of cellular oxidative stress. The production of ROS per viable cells increased significantly compared to control which was dependent on SPION species and concentration.

4. Discussion

4.1. Toxicity of SPION-1, SPION-2, and SPION-3. In this study, toxic effects of SPION-1, -2, and -3 were investigated on algal cells of *C. vulgaris*, which were caused by the deterioration of photochemical activities of photosynthesis, the induction of oxidative stress, and the inhibition of cell division rate. This complex cellular alteration was dependent on SPION chemical composition and its concentration in solution. Based on our results, it is evident that the bioaccumulation of free Fe, Co, and Zn from the soluble fraction was contributing to the toxicity impact in algal cells. It was previously proposed that the release of free metal ions from metallic nanoparticle suspensions represented a major source of toxicity for the growth rate of aquatic microorganisms [18, 19]. However, it is difficult to determine if the release of free metal ions from nanoparticles is the only contribution to the toxicity impact in the algal cellular system. Indeed, solubilisation of nanoparticles can take place either in the media or inside the cell, which possess an acidic pH environment favorable for particle solubility [20]. Therefore, another hypothesis is that SPION may also contribute directly to the toxicity impact. Recently, it was suggested for direct toxicity mechanisms of nanoparticles to induce a direct alteration of

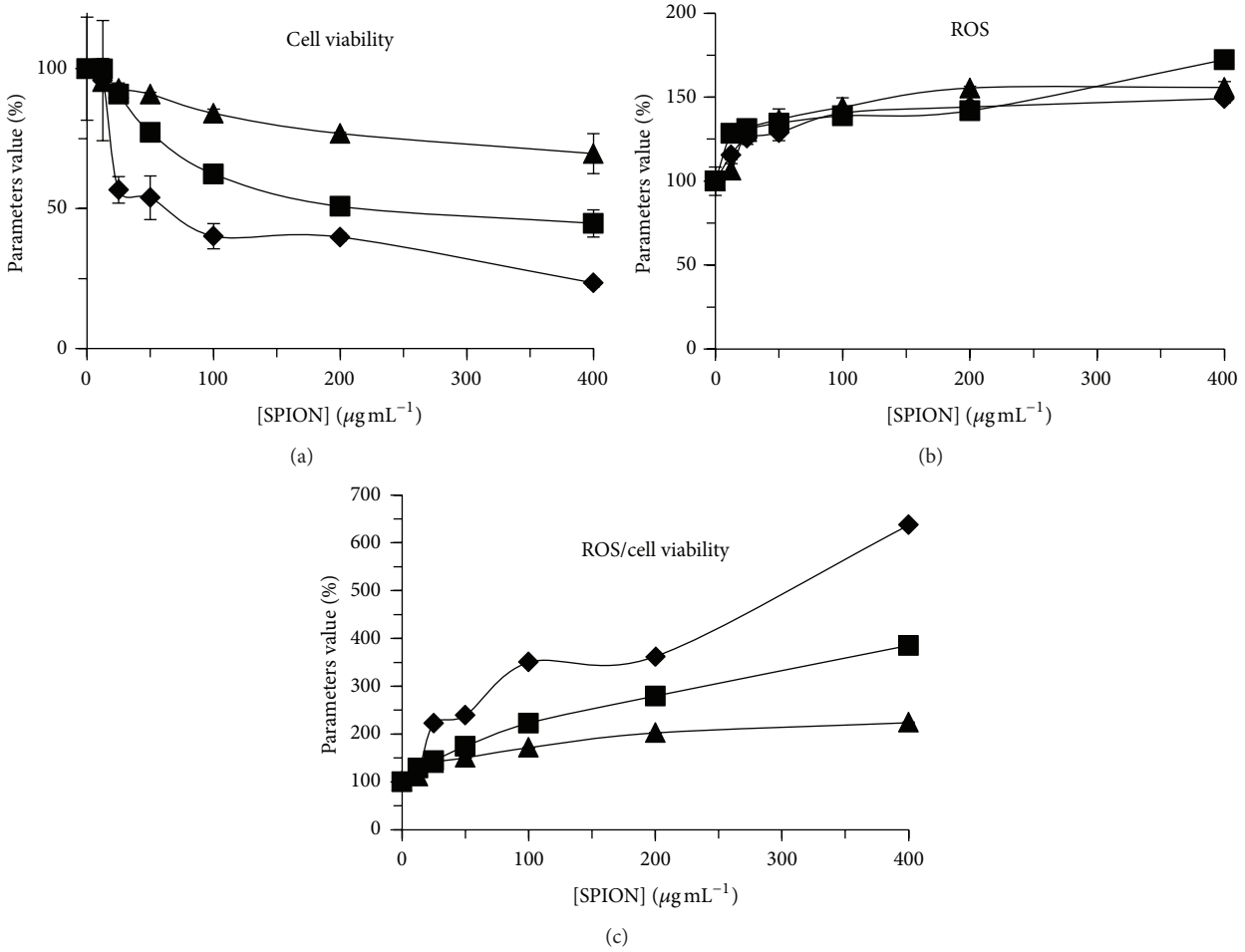

Figure 9: Change in the production of reactive oxygen species (ROS), cellular viability, and the ratio ROS/viable cells for *Chlorella vulgaris* exposed during 72 h to different concentrations of SPION-1 (⧫, diamond), SPION-2 (■, square), and SPION-3 (▲, triangle).

cellular exchanges with the media due to particles binding on cell membrane [21]. It was also shown for bioaccumulated Fe_3O_4 nanoparticles to cause direct toxic effects inside plant cells [8].

Moreover, the increase of production of reactive oxygen species per cell viability was related to the increasing exposure concentration of SPION, indicating that the induction of cellular oxidative stress was caused by the bioaccumulation of Fe, Co, and Zn. Indeed, it was shown in previous studies that metallic nanoparticles can cause the formation of ROS *via* the Fenton reaction or the disruption of major physiological processes [22, 23]. Also, the charged metallic surface of nanoparticles can trigger the formation of ROS by catalytic reduction of oxygen into superoxide anion, leading to oxidative damage into proteins, lipids, nucleic acids, and pigments [24].

When algal cells of *C. vulgaris* were exposed during 72 h to different concentrations of SPION suspensions, the relative cellular division rate was strongly inhibited for SPION-1 compared to SPION-2 and SPION-3. Under these treatment conditions, the production of ROS per viable cells was the highest for SPION-1. Indeed, Fe is well known to generate in cell free radical oxidations causing lipid peroxidation [25]. Furthermore, the change of fluorescence parameter P.I. indicated a stronger inhibition of photosynthesis for SPION-1. Therefore, according to the change of these biomarkers, the toxicity impact in algal cells of *C. vulgaris* was the strongest for SPION-1 suspensions.

4.2. Significance of Biochemical Biomarkers. In this study, two different biochemical biomarkers were used to characterize the toxicity of SPION: the production of ROS per viable cells and the photosynthetic-based fluorescence parameters. The change of parameter ROS/cell viability permitted determining the potential source of cellular toxicity causing the inhibition of cell division rate. On the other hand, fluorescence parameters related to PSII photochemical reactions have been shown to be sensitive biomarkers of SPION toxicity to *C. vulgaris* cells. Indeed, the Chl *a* fluorescence emission is demonstrated to be related to water-splitting system functions at PSII reaction center and to oxidoreduction states of electron transport carriers [26, 27]. Therefore, our results showed evidence for SPION to cause inhibitory effects on the PSII water-splitting system and the photoactivation of PSII

reaction centers. In comparison to other fluorescence indicators, the performance index of PSII activity, representing an integrative indicator of all PSII photochemical reactions [17], was the most sensitive biomarker of the deterioration of PSII functions caused by SPION toxicity.

5. Conclusion

Nowadays, a large quantity of metallic nanoparticles is produced and their toxic potential as hazardous contaminants in aquatic environment needs to be investigated in order to develop specific bioassays for nanoparticles toxicity assessment. In this regard, microalgae represent sensitive organisms to be used in bioassay toxicity testing for the assessment of hazardous materials. In this toxicological investigation, we clearly showed the potential source of toxicity of three SPION suspensions, having different chemical compositions. The algal model *C. vulgaris* demonstrated to be a valuable bioindicator of SPION cellular toxicity which was indicated by the deterioration of photochemical activities of photosynthesis, the induction of oxidative stress, and the inhibition of cell division rate. Therefore, this work permitted characterising the cellular toxicity impact of these SPION with different biomarkers. A good understanding of these toxicological interactions will permit better understanding the risk of SPION toxicity for aquatic organisms.

Abbreviations

Chl: Chlorophyll
NP: Nanoparticles
PEA: Plant Efficiency Analyzer
PSII: Photosystem II
ROS: Reactive oxygen species
SPION: Superparamagnetic iron oxide nanoparticles
TEM: Transmission electron microscope.

Conflict of Interests

The authors declare that they have no conflict of interests.

Acknowledgments

This work was performed at the Department of Chemistry (UQAM). The authors acknowledge the financial support provided by both the Faculty of Sciences and the Department of Chemistry (UQAM). The authors wish to thank L. Ben Taherc, L. Samia Smiric, and H. Abdelmelekb for providing nanopowder of Fe_3O_4, $Co_{0.2}Zn_{0.8}Fe_2O_4$, and $Co_{0.5}Zn_{0.5}Fe_2O_4$.

References

[1] A. Ito, M. Shinkai, H. Honda, and T. Kobayashi, "Medical application of functionalized magnetic nanoparticles," *Journal of Bioscience and Bioengineering*, vol. 100, no. 1, pp. 1–11, 2005.

[2] D. L. Huber, "Synthesis, properties, and applications of iron nanoparticles," *Small*, vol. 1, no. 5, pp. 482–501, 2005.

[3] N. Singh, G. J. S. Jenkins, R. Asadi, and S. H. Doak, "Potential toxicity of superparamagnetic iron oxide nanoparticles (SPION)," *Nano Reviews*, vol. 1, Article ID 5358, 2010.

[4] I. Bhatt and B. N. Tripathi, "Interaction of engineered nanoparticles with various components of the environment and possible strategies for their risk assessment," *Chemosphere*, vol. 82, no. 3, pp. 308–317, 2011.

[5] M. Delay and F. H. Frimmel, "Nanoparticles in aquatic systems," *Analytical and Bioanalytical Chemistry*, vol. 402, no. 2, pp. 583–592, 2012.

[6] E. N. Taylor, K. M. Kummer, N. G. Durmus, K. Leuba, K. M. Tarquinio, and T. J. Webster, "Superparamagnetic iron oxide nanoparticles (SPION) for the treatment of antibiotic-resistant biofilms," *Small*, vol. 8, pp. 3016–3027, 2012.

[7] H. Zhu, J. Han, J. Q. Xiao, and Y. Jin, "Uptake, translocation, and accumulation of manufactured iron oxide nanoparticles by pumpkin plants," *Journal of Environmental Monitoring*, vol. 10, no. 6, pp. 713–717, 2008.

[8] Y. K. Mushtaq, "Effect of nanoscale Fe_3O_4, TiO_2 and carbon particles on cucumber seed germination," *Journal of Environmental Science and Health A*, vol. 46, no. 14, pp. 1732–1735, 2011.

[9] X. Chen, X. Zhu, R. Li, H. Yao, Z. Lu, and X. Yang, "Photosynthetic toxicity and oxidative damage induced by nano-Fe_3O_4 on *Chlorella vulgaris* in aquatic environment," *Open Journal of Ecology*, vol. 2, pp. 21–28, 2012.

[10] R. Rippka, J. Deruelles, and J. B. Waterbury, "Generic assignments, strain histories and properties of pure cultures of cyanobacteria," *Journal of General Microbiology*, vol. 111, no. 1, pp. 1–61, 1979.

[11] H. Basti, L. Ben Tahar, L. S. Smiri et al., "Catechol derivatives-coated Fe_3O_4 and γ-Fe_2O_3 nanoparticles as potential MRI contrast agents," *Journal of Colloid and Interface Science*, vol. 341, no. 2, pp. 248–254, 2010.

[12] W. A. Hoffmann and H. Poorter, "Avoiding bias in calculations of relative growth rate," *Annals of Botany*, vol. 90, no. 1, pp. 37–42, 2002.

[13] I. B. Gerber and I. A. Dubery, "Fluorescence microplate assay for the detection of oxidative burst products in tobacco cell suspensions using 2′,7′-dichlorofluorescein," *Methods in Cell Science*, vol. 25, no. 3-4, pp. 115–122, 2004.

[14] P. Mayer, R. Cuhel, and N. Nyholm, "A simple *in vitro* fluorescence method for biomass measurements in algal growth inhibition tests," *Water Research*, vol. 31, no. 10, pp. 2525–2531, 1997.

[15] A. R. Wellburn, "The spectral determination of chlorophylls *a* and *b*, as well as total carotenoids, using various solvents with spectrophotometers of different resolution," *Journal of Plant Physiology*, vol. 144, no. 3, pp. 307–313, 1994.

[16] L. Force, C. Critchley, and J. J. S. Van Rensen, "New fluorescence parameters for monitoring photosynthesis in plants 1: the effect of illumination on the fluorescence parameters of the JIP-test," *Photosynthesis Research*, vol. 78, no. 1, pp. 17–33, 2003.

[17] R. J. Strasser, A. Srivastava, and M. Tsimilli-Michael, "Analysis of the chlorophyll a fluorescence transient," in *Chlorophyll fluorescence A signature of Photosynthesis, Advances in Photosynthesis and respiration*, G. G. Papageorgiou, Ed., pp. 321–362, Kluwer Academic, Dodrecht, The Netherlands, 2004.

[18] N. M. Franklin, N. J. Rogers, S. C. Apte, G. E. Batley, G. E. Gadd, and P. S. Casey, "Comparative toxicity of nanoparticulate ZnO, bulk ZnO, and $ZnCl_2$ to a freshwater microalga (*Pseudokirchneriella subcapitata*): the importance of particle

solubility," *Environmental Science and Technology*, vol. 41, no. 24, pp. 8484–8490, 2007.

[19] V. Aruoja, H.-C. Dubourguier, K. Kasemets, and A. Kahru, "Toxicity of nanoparticles of CuO, ZnO and TiO_2 to microalgae *Pseudokirchneriella subcapitata*," *Science of the Total Environment*, vol. 407, no. 4, pp. 1461–1468, 2009.

[20] A. M. Studer, L. K. Limbach, L. Van Duc et al., "Nanoparticle cytotoxicity depends on intracellular solubility: comparison of stabilized copper metal and degradable copper oxide nanoparticles," *Toxicology Letters*, vol. 197, no. 3, pp. 169–174, 2010.

[21] S. Lin, P. Bhattacharya, N. C. Rajapakse, D. E. Brune, and P. C. Ke, "Effects of quantum dots adsorption on algal photosynthesis," *Journal of Physical Chemistry C*, vol. 113, no. 25, pp. 10962–10966, 2009.

[22] T. Xia, M. Kovochich, J. Brant et al., "Comparison of the abilities of ambient and manufactured nanoparticles to induce cellular toxicity according to an oxidative stress paradigm," *Nano Letters*, vol. 6, no. 8, pp. 1794–1807, 2006.

[23] X. Hu, S. Cook, P. Wang, and H.-M. Hwang, "*In vitro* evaluation of cytotoxicity of engineered metal oxide nanoparticles," *Science of the Total Environment*, vol. 407, no. 8, pp. 3070–3072, 2009.

[24] W. J. Stark, "Nanoparticles in biological systems," *Angewandte Chemie—International Edition*, vol. 50, no. 6, pp. 1242–1258, 2011.

[25] F. Q. Schafer, S. Y. Qian, and G. R. Buettner, "Iron and free radical oxidations in cell membranes," *Cellular and Molecular Biology*, vol. 46, no. 3, pp. 657–662, 2000.

[26] D. Dewez, N. A. Ali, F. Perreault, and R. Popovic, "Rapid chlorophyll a fluorescence transient of Lemna gibba leaf as an indication of light and hydroxylamine effect on photosystem II activity," *Photochemical and Photobiological Sciences*, vol. 6, no. 5, pp. 532–538, 2007.

[27] D. Dewez, N. Boucher, F. Bellemare, and R. Popovic, "Use of different fluorometric systems in the determination of fluorescence parameters from spinach thylakoid membranes being exposed to atrazine and copper," *Toxicological and Environmental Chemistry*, vol. 89, no. 4, pp. 655–664, 2007.

Hindawi Publishing Corporation
BioMed Research International
Volume 2013, Article ID 761082, 8 pages
http://dx.doi.org/10.1155/2013/761082

Research Article

Dynamics of Intracellular Polymers in Enhanced Biological Phosphorus Removal Processes under Different Organic Carbon Concentrations

Lizhen Xing,[1] Li Ren,[1] Bo Tang,[2] Guangxue Wu,[2] and Yuntao Guan[2]

[1] *School of Municipal and Environmental Engineering, Shandong Jianzhu University, Jinan, Shandong, 250101, China*
[2] *Key Laboratory of Microorganism Application and Risk Control (MARC) of Shenzhen, Graduate School at Shenzhen, Tsinghua University, Shenzhen, Guangdong, 518055, China*

Correspondence should be addressed to Guangxue Wu; wu.guangxue@sz.tsinghua.edu.cn

Received 7 October 2013; Accepted 16 November 2013

Academic Editor: Kannan Pakshirajan

Enhanced biological phosphorus removal (EBPR) may deteriorate or fail during low organic carbon loading periods. Polyphosphate accumulating organisms (PAOs) in EBPR were acclimated under both high and low organic carbon conditions, and then dynamics of polymers in typical cycles, anaerobic conditions with excess organic carbons, and endogenous respiration conditions were examined. After long-term acclimation, it was found that organic loading rates did not affect the yield of PAOs and the applied low organic carbon concentrations were advantageous for the enrichment of PAOs. A low influent organic carbon concentration induced a high production of extracellular carbohydrate. During both anaerobic and aerobic endogenous respirations, when glycogen decreased to around 80 ± 10 mg C per gram of volatile suspended solids, PAOs began to utilize polyphosphate significantly. Regressed by the first-order reaction model, glycogen possessed the highest degradation rate and then was followed by polyphosphate, while biomass decay had the lowest degradation rate.

1. Introduction

Eutrophication means the overgrowth of algae and cyanobacteria, and, after their death, it causes water pollution by the depletion of oxygen and the release of toxins. Phosphorus in discharged wastewater is one of the main elements contributing to eutrophication and the worsening water quality. In order to reduce or control eutrophication of water bodies, enhanced biological phosphorus removal (EBPR) has been applied widely for phosphorus removal from wastewaters [1]. In EBPR, alternative anaerobic and aerobic phases are adopted and polyphosphate accumulating organisms (PAOs) with excess phosphorus accumulation ability will be enriched [1]. During the anaerobic phase, PAOs take up organic carbons such as acetate and propionate and store them as intracellular polymers such as poly-β-hydroxybutyrate (PHB), with polyphosphate as the energy source and glycogen as the reducing power source [1]. In the liquid, the concentration of organic carbon decreases while the concentration of phosphate increases. During the aerobic phase, PAOs synthesize new organisms, restore polyphosphate, and replenish glycogen with stored PHB as the energy and organic carbon sources [1]. In the liquid, phosphorus concentration decreases. PAOs can accumulate polyphosphate with proportions to the total dry biomass weight in the range of 4–15%, which is much higher than that of 2% of general microorganisms [2]. Phosphorus will be removed from wastewater by removing residue activated sludge with high phosphorus content from the wastewater treatment system.

Polyphosphate, PHB, and glycogen are three important polymers of PAOs in EBPR, and the accurate analysis of these components plays an important role in elucidating their dynamics in EBPR. For polyphosphate and PHB, there are some well-recognized analytical methods, while for glycogen, usually, the carbohydrate in activated sludge is converted to glucose under acidic conditions by heating and then analyzed by high-pressure liquid chromatography (HPLC) or spectrophotometer [3]. By this method, the concentration of

glycogen inside the biomass will be overestimated by around 40% [3], because carbohydrate in the biomass includes not only intracellular glycogen but also extracellular carbohydrate in extracellular polymeric substances (EPS). Therefore, so as to accurately describe dynamics of intracellular polymers of PAOs, intracellular and extracellular polymers should be differentiated.

During weekend and wet seasons, EBPR may experience deterioration or even failure due to the overflow or the low organic carbon concentration, and this phenomenon is named as the "monday peak" [4, 5]. Ahn et al. [6] found that, after being shocked from the low organic carbon, 20 days were required for PAOs to recover to the normal condition. How to ensure the stable operation of EBPR during low organic carbon conditions is one of the important tasks for wastewater treatment. Performance of EBPR depends on not only the amount of PAOs acclimated but also on the polymers of PAOs due to their important function during biochemical metabolism of PAOs. Most of previous studies have focused on the dynamics of PHB [7] while less focused on glycogen or polyphosphate. As mentioned above, glycogen and polyphosphate also play very important roles in EBPR. Therefore, for further studies, it is necessary to examine dynamics of all these polymers of PAOs in EBPR studies. Under adequate organic carbon conditions, microorganisms will experience excess biomass production and endogenous respiration is not obvious. However, under endogenous conditions, biomass production will be affected and endogenous respiration of PAOs may be dominated. For polymer dynamics under endogenous respiration conditions, there are some contrary conclusions. Lopez et al. [8] obtained that PAOs degraded polyphosphate during the initial several days, while Yilmaz et al. [9] obtained that polyphosphate was released within one day. Therefore, examining dynamics of polymers of PAOs is an important aspect to maintain activities of PAOs [10, 11], and this should be further investigated.

In this study, metabolism of PAOs and dynamics of polymers under different organic carbon concentrations were examined so as to elucidate the function of polymers in EBPR. In addition, dynamics of polymers under endogenous respiration conditions was also investigated to provide some clues for controlling and adjusting the EBPR during low organic carbon shocking conditions.

2. Materials and Methods

2.1. PAOs Acclimation. PAOs were acclimated in two sequencing batch reactors (SBRs) with different influent organic carbon concentrations at 25°C. One SBR (SBR-L) was supplied with a low sodium acetate (NaAc) concentration (chemical oxygen concentration, named as COD, of around 200 mg/L) and the other SBR (SBR-H) with a high NaAc concentration (COD of around 400 mg/L). The effective SBR working volume was 6 L and the SBR phases of fill, mixing, aeration, settlement, and withdrawal were controlled by timers. The SBRs were operated 4 cycles per day and each cycle included 120 min of anaerobic phase with 10 min of fill phase, 180 min of aerobic phase, 40 min of settlement phase, and idle/withdrawal of 20 min. During the fill phase, influent wastewater of 3 L was pumped by peristaltic pumps into the reactor. Each day, at the same time before the settlement phase, 600 mL of mixed liquor was withdrawn from the reactor to maintain the sludge retention time of around 10 days. The SBRs were seeded with activated sludge taken from Nanshan wastewater treatment plants in Shenzhen, China.

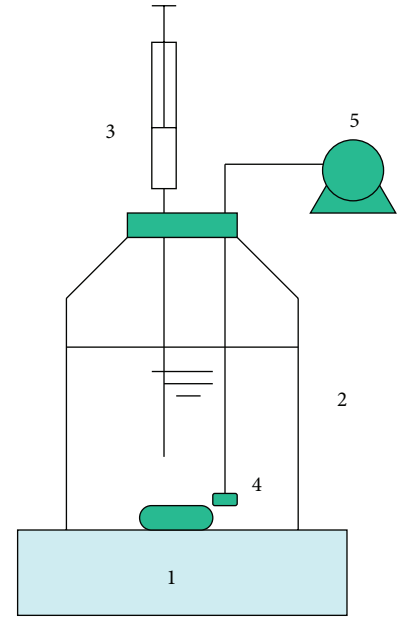

Figure 1: Diagram of the batch experiment reactor. (1) Magnetic stirrer; (2) reactor; (3) liquid sampler; (4) aeration stone; (5) air pump. 4 and 5 only worked during the aerobic condition.

Synthetic wastewater was treated in both reactors. The synthetic wastewater for SBR-L was comprised of NaAc of 255 mg/L, Na_2HPO_4 of 91.6 mg/L, NH_4Cl of 76.5 mg/L, $CaCl_2{\cdot}2H_2O$ of 14 mg/L, $MgSO_4{\cdot}5H_2O$ of 90 mg/L, trace elements of 0.12 mL/L, and yeast extract of 10 mg/L. For the SBR-H, only the NaAc concentration was changed to 510 mg/L, while other components were the same as those of the SBR-L. The components of trace elements were made according to those of Smolders et al. [12].

2.2. Batch Experiments. Batch experiments were carried out at 25°C with activated sludge taken from the parent SBRs at steady state. Each batch experiment included activated sludge taken from SBR-H and SBR-L, respectively. For each batch experiment, 400 mL of mixed liquor was withdrawn from the parent SBRs and then filled in a 600 mL capped glass flask (Figure 1). On the cap, several ports were made for sampling, aeration, and so forth. The ports were sealed with tubes for taking samples and so forth. Each batch experiment was replicated and only average results were presented.

In order to examine dynamics of polymers of PAOs under anaerobic conditions, excess organic carbon was supplied and dynamics of different parameters were examined including glycogen, PHB, acetate, and orthophosphate (PO_4^{3-}-P). At the beginning of the experiment, acetate was supplied to the two batch reactors with the initial concentration of 1000 mg/L

and then capped to start the experiment. Samples were taken at intervals of 10 min or 15 min.

Endogenous experiments were carried out under both anaerobic and aerobic conditions to examine dynamics of polymers of PAOs. For the anaerobic endogenous experiment, activated sludge mixed liquor taken from the parent reactor was placed in glass flasks directly with an initial nitrogen gas purging for 5 minutes. For the aerobic endogenous experiments, activated sludge mixed liquor taken from the parent SBRs was aerated constantly. Samples were taken at intervals of 12 or 24 hours and each endogenous experiment lasted for 168 hours.

2.3. Analytical Methods. Volatile suspended solids (VSS), suspended solids (SS), ammonium nitrogen (NH_4^+-N), and PO_4^{3-}-P were measured according to standard methods for the examination of water and wastewater [13].

PHB was measured with the methods of Karr et al. [14] and Rodgers and Wu [15]. Total carbohydrate of biomass was measured according to Lanham et al. [16]: (a) 2 mL of mixed liquor sample was added into a glass tube with 1 mL of deionized water and 0.3 mL of 6 M HCl and then mixed; (b) the mixer was digested at 100°C for 2 h; (c) after cooling down to room temperature, the digested liquor was centrifuged at 12000 rpm for 2 min, and the supernatant was taken for the measurement of glucose by HPLC. Extracellular carbohydrate was extracted according to the method of Li and Yang [17] and Sponza [18]: (a) 2 mL of mixed liquor was heated at 60°C for 30 min; (b) the heated samples were then centrifuged at 12000 rpm for 2 min, and EPS was released from the biomass to the supernatant. The extracellular carbohydrate inside the supernatant was then pretreated as that of the total carbohydrate and then analyzed by HPLC.

PHB, NaAc, and glucose were measured with the HPLC equipment (Shimadzu LC-20A, Japan). PHB and acetate were measured with the UV detector at 210 nm, while glucose was measured with the RID 10-A detector. All these parameters were measured using the Aminex column (HPX-87H, Bio-Rad, USA). The testing conditions used during the HPLC testing were (a) the mobile phase of 0.1% sulfuric acid at the flow rate of 0.6 mL/min; (b) the column temperature of 40°C; (c) the detector cell temperature of 40°C; (d) the injection volume of 20 μL for PHB and the testing duration of 35 min; while those for glucose of 50 μL and 15 min and for acetate of 20 μL and 20 min, respectively.

3. Results and Discussion

3.1. Acclimation of PAOs and Dynamics of Polymers in Typical Cycles. By using two different influent acetate concentrations, one with a high influent acetate concentration of SBR-H and the other of SBR-L, after 60 days of acclimation, the two SBRs reached steady state. Under steady state, for SBR-H, the SS was 2345 ± 60 mg/L, VSS was 1725 ± 68 mg/L, and the effluent PO_4^{3-}-P was 5.42 ± 0.4 mg/L, while for SBR-L, the SS was 1320 ± 50 mg/L, VSS was 930 ± 56 mg/L, and the effluent PO_4^{3-}-P was 8.28 ± 0.5 mg/L. In spite of the relatively high effluent PO_4^{3-}-P concentrations in both reactors, which could be due to the high influent PO_4^{3-}-P concentration applied, a high phosphorus content in the biomass was obtained for both reactors. The phosphorus content inside the dry biomass was 9.2% in SBR-H and 13.2% in SBR-L. The sludge yield coefficient was 23.6 mg SS/g COD or 17.5 mg VSS/g COD in SBR-H and was 26.5 mg SS/g COD or 18.6 mg VSS/g COD in SBR-L.

Dynamics of parameters in typical cycles in both reactors are shown in Figure 2. Typical EBPR characteristics were observed in both reactors. In SBR-H, during the anaerobic phase, PHB reached the peak in the initial 30 min with the value of 54.1 mg PHB-C/g VSS; the released PO_4^{3-}-P was 59.6 mg P/g VSS and the concentration of glycogen decreased to 53.5 mg C/g VSS. In SBR-L, in the anaerobic phase, PHB reached the peak value of 34.1 mg PHB-C/g VSS at minute 45; the released PO_4^{3-}-P was 64.26 mg P/g VSS and the concentration of glycogen decreased to 49.8 mg C/g VSS.

In spite of different influent acetate concentrations applied in both reactors, similar sludge yield coefficients were obtained in SBR-H and SBR-L, indicating that sludge production was not significantly affected by the influent organic carbon concentrations. However, a slightly higher phosphorus content was obtained of 13.2% in SBR-L than that of 9.2% in SBR-H. In addition, anaerobic phosphorus release potential was similar in both reactors, with values of 54.6 mg P/g VSS in SBR-H and of 58.9 mg P/g VSS in SBR-L. These results showed that, in the anaerobic and aerobic alternating system, a low influent organic carbon concentration favoured the acclimation of PAOs, which could be due to the high competition ability of PAOs compared with their competitors of glycogen accumulating organisms under low organic carbon conditions. Similar results were also obtained by Tu and Schuler [19].

3.2. Anaerobic Dynamics of Polymers of PAOs with Excess Supply of Organic Carbons. Anaerobic dynamics of polymers of PAOs with excess supply of organic carbons is shown in Figure 3. From Figure 3, it is shown that, from minute 50, a high variation in the concentration of various parameters occurred and the regressed biokinetics of polymers is given in Table 1 with durations from minutes 0 to 50 (Phase A) and from minutes 50 to 115 (Phase B).

After supply with excess acetate, PAOs degraded glycogen for supplying reducing power and partial energy. In SBR-H, the total carbohydrate decreased from 189.8 mg C/g VSS to 122.8 mg C/g VSS and the intracellular carbohydrate decreased from 108.3 mg C/g VSS at minute 0 to 38.9 mg C/g VSS at minute 50, while the extracellular carbohydrate kept relatively stable at 82.8 ± 2.2 mg C/g VSS; the decreased intracellular carbohydrate concentration was 69.5 mg C/g VSS during the whole reaction phase. In SBR-L, the total carbohydrate decreased from 238.0 mg C/g VSS to 198.5 mg C/g VSS and the intracellular carbohydrate decreased from 145.5 mg C/g VSS to 56.0 mg C/g VSS, while the extracellular carbohydrate slightly increased with the average concentration of 128.1 ± 29.8 mg C/g VSS; the decreased intracellular carbohydrate concentration was 89.7 mg C/g VSS during the whole reaction phase. These results showed that the intracellular carbohydrate was mainly used for biochemical metabolism during the

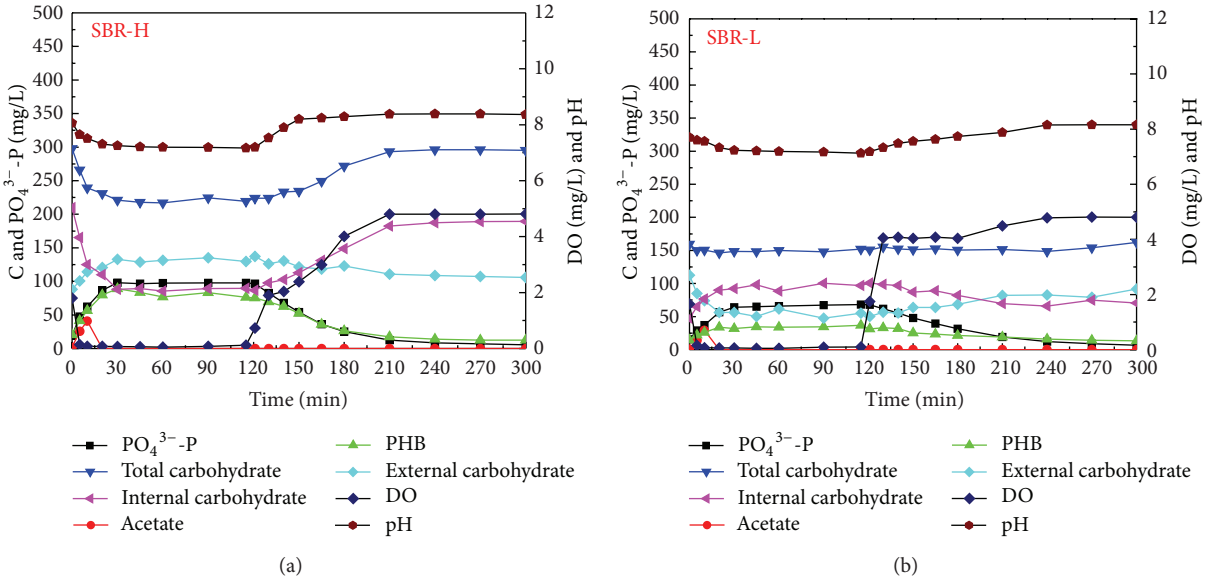

Figure 2: Dynamics of different parameters in typical cycles of SBR-H and SBR-L.

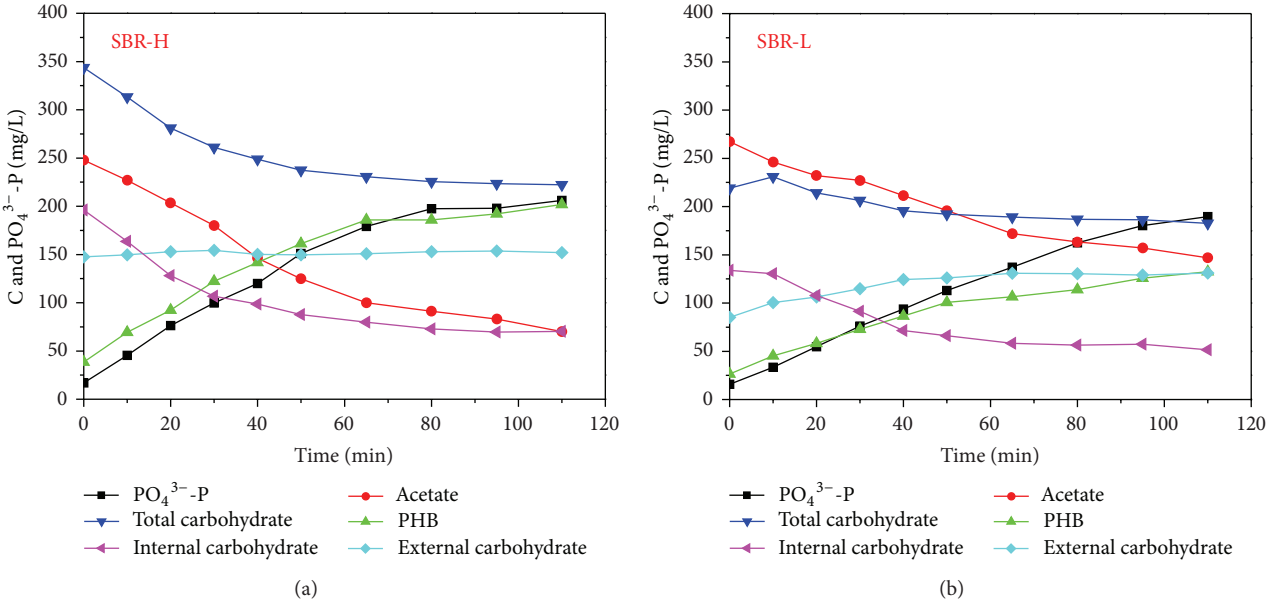

Figure 3: Anaerobic dynamics of polymers of PAOs with excess supply of organic carbons.

anaerobic phase, consistent with previous studies, such as that of Wu and Rodgers [20]. This also shows that it is necessary to differentiate the intracellular and extracellular carbohydrate for investigating dynamics of polymer in EBPR. For the extracellular carbohydrate, a slightly higher concentration of 128.3 mg C/g VSS existed in SBR-L than that of 82.8 mg C/g VSS in SBR-H. Extracellular carbohydrate is one main component of EPS [17, 18], and the above results showed that a low influent organic carbon condition induced a high extracellular carbohydrate production, which might be due to the fact that EPS production was a response to low nutrient condition as a protective mechanism for experiencing unfavourable low organic carbon conditions.

By comparing the regressed data in Table 1, during Phase A, $r_{\text{PHB-C/NaAc-C}}$ was similar in both reactors, indicating that the acetate could be taken up and stored as PHB efficiently, while, during Phase B, a slightly high $r_{\text{PHB-C/NaAc-C}}$ value was obtained in SBR-H. In spite of a slight variation of $r_{\text{Glycogen-C/NaAc-C}}$, there was no significant difference in both reactors during both phases. During the whole reaction phase, $r_{\text{PO4-P/NaAc-C}}$ in SBR-L was higher than that in SBR-H, indicating a high energy requirement from polyphosphate degradation in SBR-L, which showed that there might be high PAO activities or a higher number of PAOs in SBR-L than that in SBR-H. The calculated mole ratios between the released phosphorus and the utilized acetate were 0.40 mol P/mol C in

Table 1: Regressed biokinetic coefficients of polymers of PAOs under anaerobic conditions with the supply of excess organic carbon.

	Phase A: 0–50 min		Phase B: 50–110 min	
	SBR-H	SBR-L	SBR-H	SBR-L
$r_{\text{PHB-C/NaAc-C}}$ (mg/mg)	0.97 (0.98)	1.08 (0.99)	0.72 (0.97)	0.66 (0.87)
$r_{\text{PO4-P/NaAc-C}}$ (mg/mg)	1.03 (0.98)	1.44 (0.97)	1.05 (0.95)	1.66 (0.95)
$r_{\text{Glycogen-C/NaAc-C}}$ (mg/mg)	0.85 (0.90)	1.10 (0.92)	0.35 (0.90)	0.28 (0.94)

Table 2: Regressed biokinetics of biomass or polymers by the first-order equation under both anaerobic and aerobic endogenous respirations (1/d).

	SBR-H		SBR-L	
	Anaerobic	Aerobic	Anaerobic	Aerobic
SS	0.074 (0.98)	0.070 (0.98)	0.074 (0.94)	0.082 (0.95)
VSS	0.041 (0.86)	0.048 (0.89)	0.038 (0.82)	0.058 (0.90)
Total carbohydrate	0.034 (0.65)	0.074 (0.92)	0.029 (0.56)	0.034 (0.67)
Internal carbohydrate	0.137 (0.96)	0.226 (0.96)	0.209 (0.93)	0.194 (0.98)
Polyphosphate	0.098 (0.94)	0.084 (0.97)	0.089 (0.99)	0.091 (0.99)

SBR-L and 0.28 mol P/mol C in SBR-H during Phase A and were 0.14 mol P/mol C and 0.16 mol P/mol C during Phase B. During Phase A, a high reaction rate existed due to the existence of high external organic carbons, and the calculated polyphosphate requirement was in the theoretical range of 0.25–0.75 mol P/mol C [12], while during Phase B, due to the limitation of intracellular carbohydrate and the slow activity of PAOs, the biokinetics were relatively slow and were different from those of Phase A.

3.3. Dynamics of Polymers of PAOs during Anaerobic and Aerobic Endogenous Respirations. Under anaerobic and aerobic endogenous respiration conditions, dynamics of polymers of PAOs and sludge concentrations are shown in Figure 4.

Under starve conditions, microorganisms will experience endogenous respiration [8, 21], and except the reduction in the biomass concentration, consumption of polymers (for PAOs, glycogen, PHB, etc.) also occurs to provide the required maintenance energy. In SBR-H, during the anaerobic endogenous respiration, different utilization modes of polyphosphate and glycogen occurred, with the main utilization of glycogen initially and after 48 hours, with a quick utilization of polyphosphate. During the 168 hours of anaerobic endogenous respiration, glycogen decreased from 99.1 mg C/g VSS to 34.3 mg C/g VSS in SBR-H and the phosphorus released was 60.2 mg P/g VSS, while in SBR-L, glycogen decreased from 115.5 mg C/g VSS to 21.2 mg C/g VSS and the phosphorus released was 91.8 mg P/g VSS. During the 168 hours of aerobic endogenous respiration, glycogen decreased from 99.6 mg C/g VSS to 23.7 mg C/g VSS in SBR-H and the phosphorus released was 52.7 mg P/g VSS, while in SBR-L, glycogen decreased from 115.0 mg C/g VSS to 38.7 mg C/g VSS in SBR-H and the phosphorus released was 89.3 mg P/g VSS. These results showed that, during endogenous respiration, PAOs acclimated under the low influent organic carbon conditions utilized a higher amount of polymers than those of PAOs acclimated under a high influent acetate concentration.

During the anaerobic endogenous respiration, when the glycogen concentration decreased to 67.1 mg C/g VSS in SBR-H and 85.4 mg C/g VSS in SBR-L, degradation of polyphosphate occurred rapidly while this process was inhibited therebefore. During the aerobic endogenous respiration, when the glycogen concentration decreased to 81.8 mg C/g VSS in SBR-H and 87.2 mg C/g VSS in SBR-L, degradation of polyphosphate also occurred significantly with a high increase in the liquid phosphate concentration. These results showed that degradation of polyphosphate during endogenous respiration was controlled by the glycogen concentration and glycogen was firstly utilized as the energy source. When the glycogen concentration reached around 80 ± 10 mg C/g VSS, degradation of polyphosphate occurred. These showed that PAOs might prefer to utilize glycogen during the endogenous respiration for maintenance purposes [8, 20, 22, 23] and then utilize polyphosphate when the glycogen decreased to a certain level. Lopez et al. [8] also found that during the aerobic endogenous respiration, PAOs utilized PHA, glycogen, and polyphosphate sequentially, and phosphate release occurred after 16 hours of aerobic endogenous respiration.

For dynamics of all parameters during endogenous respiration, they were regressed by the first-order degradation equation and the results are shown in Table 2. There was no significant difference for biomass decay under anaerobic and aerobic conditions, which were close to those of 0.015–0.032 1/d obtained by Lu et al. [23], while they were lower than those of 0.14-0.15 1/d obtained in other studies [8, 20]. It should be noticed that, in most studies, biomass during decay was represented by the decrease in the concentration of VSS, while different environmental conditions might induce different intracellular or extracellular polymer concentrations, which might affect the description of biomass decay by using the parameter of VSS. Compared with the decay of biomass, decay coefficients of intracellular polymers were much higher. In addition, the degradation coefficient of glycogen was higher than that of polyphosphate. These results showed that during endogenous respiration, microorganisms

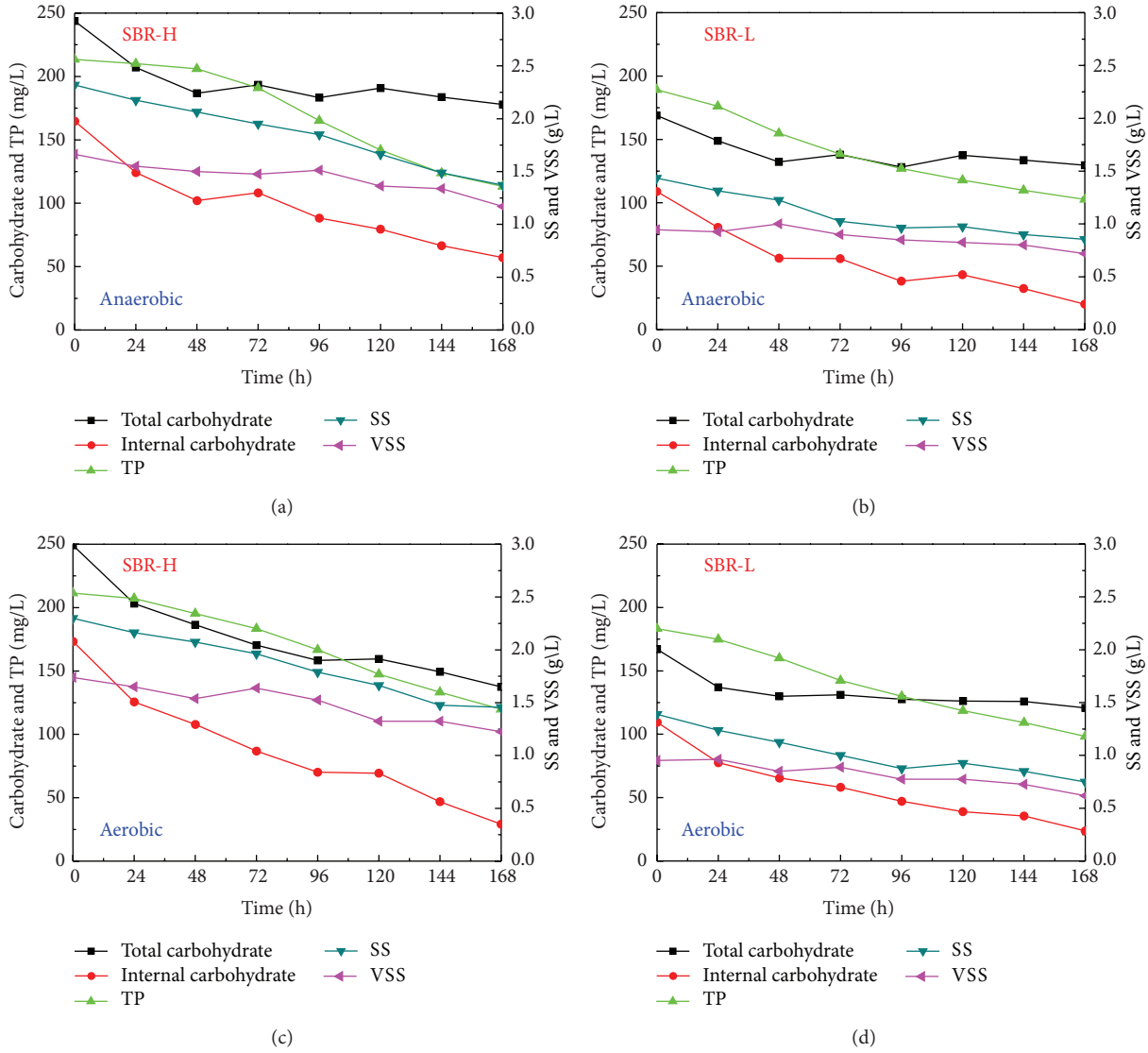

Figure 4: Dynamics of polymers of PAOs and sludge concentrations during anaerobic and aerobic endogenous respirations.

would prefer to utilize stored polymers to maintain their activities. Comparing between degradation coefficients during both anaerobic and aerobic endogenous respirations, it was surprising to see there was not much difference for both decay of biomass and polymers.

During the anaerobic endogenous respiration, the degradation of intracellular carbohydrate in SBR-L was higher than that in SBR-H, which could be due to a slightly earlier utilization of polyphosphate in SBR-H and this might retard the utilization of glycogen, while under the aerobic endogenous respiration, the degradation of intracellular carbohydrate was slightly lower in SBR-L than that in SBR-H, which could be due to the fact that PAOs in SBR-L experienced starve conditions longer than those in SBR-H during acclimation, and they might had been used to the starve conditions better. For carbohydrate, there was a significant difference in biokinetics by using the total carbohydrate or the intracellular carbohydrate, confirming results from the previous study of Wu and Rodgers [20]. The anaerobic intracellular carbohydrate degradation rate was lower than that obtained by Wu and Rodgers [20], while similar results were obtained during the aerobic endogenous respiration. In the present study, PAOs were acclimated and all experiments were carried out at 25°C, while PAOs are psychrophile [24, 25]. The high temperature used in the present study might cause the decreased biokinetic activities, including a low anaerobic intracellular degradation coefficient.

4. Conclusions

Dynamics of polymers of PAOs under different organic carbon concentrations, including typical cycles, anaerobic metabolism with supply of excess organic carbon, and both anaerobic and aerobic endogenous respiration, were examined. Influent organic carbon concentrations had little influence on the yield of PAOs and the anaerobic polyphosphate release,

while a low influent organic carbon concentration favoured the acclimation of PAOs and induced a high production of extracellular carbohydrate. During both anaerobic and aerobic endogenous respirations, when glycogen decreased to below around 80 ± 10 mg C/g VSS, PAOs began to utilize polyphosphate significantly. Regressed by the first-order reaction model, the degradation of glycogen possessed the highest reaction rate and was then followed by polyphosphate, while biomass decay had the lowest reaction rate.

Conflict of Interests

The authors declare that there is no conflict of interests regarding the publication of this paper.

Acknowledgments

This study was supported by the National Natural Science Foundation of China (51108242) and the Scientific Research Foundation for the Returned Overseas Chinese Scholars, State Education Ministry, China.

References

[1] T. Mino, M. C. M. Van Loosdrecht, and J. J. Heijnen, "Microbiology and biochemistry of the enhanced biological phosphate removal process," *Water Research*, vol. 32, no. 11, pp. 3193–3207, 1998.

[2] H. G. Schlegel, *General Microbiology*, Cambridge University Press, Cambridge, UK, 1993.

[3] L. S. Serafim, P. C. Lemos, C. Levantesi, V. Tandoi, H. Santos, and M. A. M. Reis, "Methods for detection and visualization of intracellular polymers stored by polyphosphate-accumulating microorganisms," *Journal of Microbiological Methods*, vol. 51, no. 1, pp. 1–18, 2002.

[4] A. R. Pitman, S. L. V. Venter, and H. A. Nicholls, "Practical experience with biological phosphorus removal plants in Johannesburg," *Water Science and Technology*, vol. 15, no. 3-4, pp. 233–259, 1983.

[5] H. Miyake and E. Morgenroth, "Optimization of enhanced biological phosphorus removal after periods of low loading," *Water Environment Research*, vol. 77, no. 2, pp. 117–127, 2005.

[6] C. H. Ahn, H.-D. Park, and J. K. Park, "Enhanced biological phosphorus removal performance and microbial population changes at high organic loading rates," *Journal of Environmental Engineering*, vol. 133, no. 10, pp. 962–969, 2007.

[7] C. H. Ahn, J. K. Park, and K. S. Kim, "Microbial adaptability to organic loading changes in an enhanced biological phosphorus removal process," *Journal of Environmental Engineering*, vol. 132, no. 8, pp. 909–917, 2006.

[8] C. Lopez, M. N. Pons, and E. Morgenroth, "Endogenous processes during long-term starvation in activated sludge performing enhanced biological phosphorus removal," *Water Research*, vol. 40, no. 8, pp. 1519–1530, 2006.

[9] G. Yilmaz, R. Lemaire, J. Keller, and Z. Yuan, "Effectiveness of an alternating aerobic, anoxic/anaerobic strategy for maintaining biomass activity of BNR sludge during long-term starvation," *Water Research*, vol. 41, no. 12, pp. 2590–2598, 2007.

[10] R. Brun, M. Kühni, H. Siegrist, W. Gujer, and P. Reichert, "Practical identifiability of ASM2d parameters—systematic selection and tuning of parameter subsets," *Water Research*, vol. 36, no. 16, pp. 4113–4127, 2002.

[11] L. Tijhuis, M. C. M. Van Loosdrecht, and J. J. Heijnen, "A thermodynamically based correlation for maintenance Gibbs energy requirements in aerobic and anaerobic chemotrophic growth," *Biotechnology and Bioengineering*, vol. 42, no. 4, pp. 509–519, 1993.

[12] G. J. F. Smolders, J. Van der Meij, M. C. M. Van Loosdrecht, and J. J. Heijnen, "Model of the anaerobic metabolism of the biological phosphorus removal process: stoichiometry and pH influence," *Biotechnology and Bioengineering*, vol. 43, no. 6, pp. 461–470, 1994.

[13] APHA, AWWA, and WPCF, *Standard Methods for the Examination of Water and Wastewater*, American Public Health Association, Washington, DC, USA, 19th edition, 1995.

[14] D. B. Karr, J. K. Waters, and D. W. Emerich, "Analysis of poly-β-hydroxybutyrate in Rhizobium japonicum bacteroids by ion-exclusion high-pressure liquid chromatography and UV detection," *Applied and Environmental Microbiology*, vol. 46, no. 6, pp. 1339–1344, 1983.

[15] M. Rodgers and G. Wu, "Production of polyhydroxybutyrate by activated sludge performing enhanced biological phosphorus removal," *Bioresource Technology*, vol. 101, no. 3, pp. 1049–1053, 2010.

[16] A. Lanham, A. Ricardo, M. Coma et al., "Optimisation of glycogen quantification in mixed microbial cultures," *Bioresource Technology*, vol. 118, pp. 518–525, 2012.

[17] X. Y. Li and S. F. Yang, "Influence of loosely bound extracellular polymeric substances (EPS) on the flocculation, sedimentation and dewaterability of activated sludge," *Water Research*, vol. 41, no. 5, pp. 1022–1030, 2007.

[18] D. T. Sponza, "Extracellular polymer substances and physicochemical properties of flocs in steady- and unsteady-state activated sludge systems," *Process Biochemistry*, vol. 37, no. 9, pp. 983–998, 2002.

[19] Y. Tu and A. J. Schuler, "Low acetate concentrations favor polyphosphate-accumulating organisms over glycogen-accumulating organisms in enhanced biological phosphorus removal from wastewater," *Environmental Science and Technology*, vol. 47, pp. 3816–3824, 2013.

[20] G. Wu and M. Rodgers, "Dynamics and function of intracellular carbohydrate in activated sludge performing enhanced biological phosphorus removal," *Biochemical Engineering Journal*, vol. 49, no. 2, pp. 271–276, 2010.

[21] X.-D. Hao, Q.-L. Wang, J.-Y. Zhu, and M. C. M. Van Loosdrecht, "Microbiological endogenous processes in biological wastewater treatment systems," *Critical Reviews in Environmental Science and Technology*, vol. 40, no. 3, pp. 239–265, 2010.

[22] H. Satoh, T. Mino, and T. Matsuo, "Uptake of organic substrates and accumulation of polyhydroxyalkanoates linked with glycolysis of intracellular carbohydrates under anaerobic conditions in the biological excess phosphate removal processes," *Water Science and Technology*, vol. 26, no. 5-6, pp. 933–942, 1992.

[23] H. Lu, J. Keller, and Z. Yuan, "Endogenous metabolism of Candidatus Accumulibacter phosphatis under various starvation conditions," *Water Research*, vol. 41, no. 20, pp. 4646–4656, 2007.

[24] U. G. Erdal, Z. K. Erdal, and C. W. Randall, "The competition between PAOs (phosphorus accumulating organisms) and GAOs (glycogen accumulating organisms) in EBPR (enhanced

biological phosphorus removal) systems at different temperatures and the effects on system performance," *Water Science and Technology*, vol. 47, no. 11, pp. 1–8, 2003.

[25] C. M. López-Vázquez, C. M. Hooijmans, D. Brdjanovic, H. J. Gijzen, and M. C. M. van Loosdrecht, "Factors affecting the microbial populations at full-scale enhanced biological phosphorus removal (EBPR) wastewater treatment plants in The Netherlands," *Water Research*, vol. 42, no. 10-11, pp. 2349–2360, 2008.

Hindawi Publishing Corporation
BioMed Research International
Volume 2013, Article ID 371058, 9 pages
http://dx.doi.org/10.1155/2013/371058

Research Article

Kinetics of Molybdenum Reduction to Molybdenum Blue by *Bacillus* sp. Strain A.rzi

A. R. Othman,[1] N. A. Bakar,[1] M. I. E. Halmi,[1] W. L. W. Johari,[2] S. A. Ahmad,[1] H. Jirangon,[3] M. A. Syed,[1] and M. Y. Shukor[1]

[1] *Department of Biochemistry, Faculty of Biotechnology and Biomolecular Sciences, University Putra Malaysia, 43400 Serdang, Selangor, Malaysia*
[2] *Department of Environmental Science, Faculty of Environmental Studies, Universiti Putra Malaysia, 43400 Serdang, Selangor, Malaysia*
[3] *Department of Microbiology, Faculty of Biotechnology and Biomolecular Sciences, University Putra Malaysia, 43400 Serdang, Selangor, Malaysia*

Correspondence should be addressed to M. Y. Shukor; mohdyunus@upm.edu.my

Received 14 September 2013; Accepted 28 October 2013

Academic Editor: Kannan Pakshirajan

Molybdenum is very toxic to agricultural animals. Mo-reducing bacterium can be used to immobilize soluble molybdenum to insoluble forms, reducing its toxicity in the process. In this work the isolation of a novel molybdate-reducing Gram positive bacterium tentatively identified as *Bacillus* sp. strain A.rzi from a metal-contaminated soil is reported. The cellular reduction of molybdate to molybdenum blue occurred optimally at 4 mM phosphate, using 1% (w/v) glucose, 50 mM molybdate, between 28 and 30°C and at pH 7.3. The spectrum of the Mo-blue product showed a maximum peak at 865 nm and a shoulder at 700 nm. Inhibitors of bacterial electron transport system (ETS) such as rotenone, sodium azide, antimycin A, and potassium cyanide could not inhibit the molybdenum-reducing activity. At 0.1 mM, mercury, copper, cadmium, arsenic, lead, chromium, cobalt, and zinc showed strong inhibition on molybdate reduction by crude enzyme. The best model that fitted the experimental data well was Luong followed by Haldane and Monod. The calculated value for Luong's constants p_{max}, K_s, S_m, and n was 5.88 μmole Mo-blue hr^{-1}, 70.36 mM, 108.22 mM, and 0.74, respectively. The characteristics of this bacterium make it an ideal tool for bioremediation of molybdenum pollution.

1. Introduction

Heavy metals are ubiquitously applied in numerous industrial processes. This has resulted in heavy metals contamination of many environmental systems in Malaysia [1–3]. Molybdenum is an example of a heavy metal with numerous applications in industries. It is a significant pollutant with levels as high as thousands of ppm found in aquatic bodies and soils [4, 5]. The toxicity of molybdenum compounds has been studied intensively in animals [6, 7]. Cows are the most affected with dramatic scouring occurring at 20–50 mg Mo/kg body weight, followed by sheep and pigs [8]. In Malaysia, molybdenum is produced as a byproduct of copper from a mine in Sabah [9].

Like other heavy metals pollution, scientists have turned towards bioremediation, a cheaper alternative using the ability of microbe to remove and resist heavy metals via mechanisms such as sequestration, bioreduction, biosorption, transport mechanisms, bioprecipitation, and/or chelation [10]. Microbial reduction of molybdate (Mo^{6+}) to Mo-blue was first reported in 1896 [11]. Since the last thirteen years, almost all of the reported bacteria capable of microbiological reduction of molybdate to molybdenum blue [12–25] came from our work. Screening for novel molybdenum reducers is required in order to develop a cost-effective bioremediation work for cleaning up molybdenum pollutants in the environment [26]. Numerous commercial bioremediating bacteria use *Bacillus* spp. as this genus offers several advantage such as

extreme environmental tolerance due to its capability to form endospore and a fast doubling time [27]. In this work, we report on the isolation of a novel molybdenum-reducing *Bacillus* sp. strain A.rzi and its kinetics of molybdenum reduction to molybdenum blue (Mo-blue).

2. Experimental

2.1. Molybdenum-Reducing Bacterium Isolation. Soil samples were taken from a metal recycling plant in Kajang, Selangor, in December 2007. Soil sample (five gram) was suspended in 50 mL of phosphate buffered saline (1x). Suitable serial dilutions (aliquot 0.1 mL) were spread onto molybdenum selective agar of low phosphate (2.9 mM phosphate) media (pH 7.5) supplemented with glucose (10 gL^{-1}) as the carbon source, NaCl (5 gL^{-1}), $(NH_4)_2SO_4$ (3 gL^{-1}), $Na_2MoO_4{\cdot}2H_2O$ (2.42 gL^{-1}), $MgSO_4{\cdot}7H_2O$ (0.5 gL^{-1}), yeast extract (0.5 gL^{-1}), and $Na_2HPO_4{\cdot}2H_2O$ (0.51 gL^{-1}) [17]. The strongest blue colony on the plate was transferred into 50 mL of liquid low phosphate media. Molybdenum-reducing bacterial strains such as *Serratia* sp. strain Dr.Y8, *Serratia* sp. strain Dr.Y5, *S. marcescens* strain Dr.Y9, *Enterobacter* sp. strain Dr.Y13, *Pseudomonas* sp. strain DRY2, *Serratia marcescens* strain DRY6, *Acinetobacter calcoaceticus* strain Dr.Y12, and *Enterobacter cloacae* strain 48 were obtained from our culture collection and *E. coli* K12 was obtained from American Type Culture Collection, Rockville, USA. The bacteria were grown and maintained on the above low phosphate liquid and solid media, respectively.

2.2. Molyvbdenum-Reducing Bacterium Identification. Identification of the bacterium was performed by using Biolog GP microplate (Biolog, Hayward, CA, USA) according to the manufacturer's instructions and molecular phylogenetic studies. Genomic DNA was prepared through alkaline lysis method. PCR amplification was carried out using a Biometra T Gradient PCR (Montreal Biotech Inc., Kirkland, QC). The PCR mixture comprises 0.5 pM of the following primers: 5′-AGAGTTTGATCCTGGCTCAG-3′ and 5′-AAGGAGGTGATCCAGCCGCA-3′ corresponding to the forward and reverse primers of 16S rDNA, respectively [28], 2.5 U of Taq DNA polymerase (Promega), 200 μM of each deoxynucleotide triphosphate, and 1x reaction buffer. The reaction mixture had a final volume of 50 μL. The 16S rDNA gene from the genomic DNA was amplified by PCR using the following conditions: an initial denaturation at 94°C for 3 min; 25 cycles at 94°C for 1 min, 50°C for 1 min, and 72°C for 2 min; and a final extension at 72°C for 10 min. The Big Dye terminator kit (Perkin-Elmer Applied Biosystems) was used for cycle sequencing. The resultant 1306 bases were compared to similar sequence in the GenBank database using the NCBI Blast server (http://blast.ncbi.nlm.nih.gov/Blast.cgi). The 16s rRNA ribosomal gene sequence was deposited in GenBank under the accession number EU835195.

2.3. Phylogenetic Analysis. Alignment of 20 16S rRNA gene sequences closely matching strain A.rzi retrieved from GenBank was carried out using clustal_W [29]. The construction of the phylogenetic tree was carried out using PHYLIP, version 3.573 (J. Q. Felsenstein, PHYLIP—phylogeny inference package, version 3.573, Department of Genetics, University of Washington, Seattle, WA (http://evolution.genetics.washington.edu/phylip.html)). *S. marcescens* was the outgroup in the cladogram. The neighbour-joining/UPGMA method was used to construct the evolutionary distance matrices the DNADIST algorithm program. A distance matrix was used instead of the laborious maximum likelihood or parsimony approaches. The model used in the nucleotide substitution is from Jukes and Cantor [30]. Phylogenetic tree was constructed based on the neighbour-joining method adopted from Saitou and Nei [31]. Confidence levels for individual branches within the tree were checked for each algorithm by repeating the PHYLIP analysis with 1000 bootstraps [32] using the SEQBOOT program in the PHYLIP package. The jackknife approach can also be used. Majority rule (50%) consensus trees were constructed using the Ml methods [33]. The tree was viewed using the TreeView program [34].

2.4. Crude Enzyme Preparation. The preparation of crude enzyme was based on the modified method of Shukor et al. [35]. Experiments were carried out at 4°C unless stated otherwise. A 2 L culture was grown overnight on high phosphate media (HPM) containing $MgSO_4{\cdot}7H_2O$ (0.5 gL^{-1}), NaCl (5 gL^{-1}), $(NH_4)_2SO_4$ (3 gL^{-1}), $NaMoO_4{\cdot}2H_2O$ (12.1 gL^{-1} or 50 mM), yeast extract (1 gL^{-1}), glucose (10 gL^{-1}) as an electron donor source, and Na_2HPO_4 (100 mM) at pH 7.3. The bacterial cells were first harvested at 10000 ×g for 20 min at 4°C. The pellet was washed several times and reconstituted with 10 mL of 50 mM Tris buffer (pH 7.0) containing 1 mM phenylmethanesulphonyl sfluoride (PMSF) as a protease inhibitor and 2 mM of DTT as a reducing agent for protecting the thiol group in the enzyme. The cells were then subjected to sonication on a Biosonik 111 sonicator for a total sonication time of 2 hours with intermittent cooling on an ice bath and then ultracentrifuged at 105000 ×g for 90 min at 4°C. The supernatant is the crude enzyme and was used for further studies. Enzyme was assayed according to the method of Shukor et al. [35] by adding 100 μL of NADH (80 mM stock) 1 mL of a reaction mixture consisting of laboratory-prepared phosphomolybdate (LPP) electron acceptor substrates prepared in 50 mM citrate-phosphate buffer pH 5.0 at room temperature. The final concentration of LPP was 8 mM. To start the reaction, fifty microlitres of crude Mo-reducing enzyme were added. The absorbance increase in a one minute incubation period was read at 865 nm. The definition of one unit of Mo-reducing activity is the amount of enzyme that produces 1 nmole of Mo-blue per minute at room temperature. The specific extinction coefficient for the product Mo-blue at 865 nm is 16.7 $mM^{-1}{\cdot}cm^{-1}$ [36].

2.5. Studies on the Effects of Metal Ions and Respiratory Inhibitors. Inhibitors such as sodium azide, antimycin A, rotenone, and potassium cyanide were dissolved in deionised water and/or in acetone [37]. Metal ions were dissolved in 20 mM Tris·Cl buffer (pH 7.0). A preincubation of the inhibitors or metal ions with one hundred microlitres of enzyme in

Table 1: Various kinetic models for effect of substrate on Mo-blue production.

Author	Model	Author
Monod	$p = p_{\max}\dfrac{S}{K_S + S}$	Monod [38]
Haldane	$p = p_{\max}\dfrac{S}{S + K_S + (S^2/K_i)}$	Haldane [39]
Luong	$p = p_{\max}\dfrac{S}{K_s + S}\left(\dfrac{1 - S}{S_m}\right)^n$	Mulchandani et al. [40]

the reaction mixture was carried out at 4°C for 10 minutes. The incubation mixture was warmed to room temperature before NADH was added to start the reaction. The total reaction mixture was 1.0 mL. As a control for inhibitors that was dissolved in acetone such as rotenone and antimycin A, 50 μL of acetone was added in the reaction mixture without inhibitors. The linear increase in absorbance at 865 nm was measured after an incubation period of 5 minutes.

2.6. Characterization of the Molybdate Reduction Reaction Using the Dialysis Tubing Method. The dialysis tubing method is a modification of the method applied by Hem [41] to identify whether the reduction of heavy metals seen physiologically was due to biotic chemicals produced by the cells or catalyzed through an enzymatic route. The dialysis tubing method of Shukor et al. [23] was used in this work.

2.7. Determination of Kinetic Parameters for Molybdate Reduction to Molybdenum Blue. Determination of intrinsic growth kinetic parameters for strain A.rzi was not possible due to the property of the molybdenum blue that form a precipitate together with the bacterial mass [18–25]. Hence, only the reduction kinetics was studied. Several substrate inhibition kinetic models available such as Haldane and Luong were compared to the commonly used Monod. In this work molybdenum reduction kinetics is represented as Mo-blue production rate. The formula for the above model is shown in Table 1, where p, $p_{\max}$, K_s, K_i, S, S_m, and n are specific Mo-blue production rate (hr^{-1}), maximum Mo-blue production rate (hr^{-1}), half-saturation constant (mM), inhibition constant (mM), substrate concentration (mM), critical substrate concentration above which production of Mo-blue completely stops (mM), and the exponent representing the impact of the substrate to $p_{\max}$, respectively. The Mo-blue production rate is calculated based on the linear portion of the Mo-blue production against time.

2.8. Statistical Analysis. Comparison between groups was performed using a Student's t-test or a one-way analysis of variance (ANOVA) with post hoc analysis by Tukey's test. $P < 0.05$ was considered statistically significant.

3. Results

3.1. Identification of Mo-Reducing Bacterium. A Gram-positive spore-forming bacterium capable of molybdenum reduction to molybdenum blue was isolated from a metal-contaminated soil. The bacterium was identified through phylogenetic analyses of the 16S rRNA ribosomal gene sequence of the bacterium. A high bootstrap value (>75%) of 79.8% was obtained when strain A.rzi is genetically linked to *Bacillus* sp. (Figure 1). This is a novel molybdenum-reducing Gram positive bacterium (Figure 1). The identifications performed using GP2 plate with the BIOLOG system gave 98% probability, 0.747 similarity, and 3.56 distance value to *Bacillus pumilus* B. At this juncture, we tentatively assigned this bacterium as *Bacillus* sp. strain A.rzi.

3.2. Comparison of Mo-Blue Production among Mo-Reducing Isolates. When grown in 10 mM molybdate as the benchmark molybdate concentration, strain A.rzi ranked as the second best together with *Serratia* sp. strain Dr.Y5 in producing Mo-blue (Table 2). The optimal carbon sources of either sucrose or glucose supporting molybdate reduction for each bacterium [18–25] were used in this comparison work. Mo-blue production increases dramatically after 18 hours of static growth, reaching maximal production after 23 hours of incubation (Figure 2).

3.3. The Effects of Phosphate and Molybdate Concentrations. The effect of molybdate concentration on molybdate reduction (Figure 3) showed that the optimum concentration of molybdate was between 50 and 60 mM. Concentrations higher than 80 mM molybdate were strongly inhibitory. At 50 mM molybdate, molybdate reduction was strongly critical of phosphate concentration with a sharp optimum at 4 mM and a near complete inhibition of Mo-reduction at higher phosphate concentrations (Figure 4).

3.4. The Effect of pH and Temperature on Molybdate Reduction. The optimum temperature supporting molybdate reduction was in the range from 28 to 30°C (Figure 5). The effect of pH was carried out using 50 mM of Tris and 10 mM of phosphate buffers spanning the pH from 7.0 to 9.0. The optimum pH for molybdenum reduction is pH 7.3 (data not shown).

3.5. The Effect of Electron Donor Sources on Molybdate Reduction. Glucose was the most effective supplement as an electron donor for supporting molybdate reduction. This was followed by sucrose, maltose, mannose, mannitol, lactose, and starch (Figure 6). Glucose was optimum at 1% (w/v).

3.6. Mo-Blue Absorbance Spectrum. The spectrum of Mo-blue obtained from the growth medium shows a maximum peak near the far red region between 860 and 870 nm and a shoulder approximately at 710 nm (Figure 7).

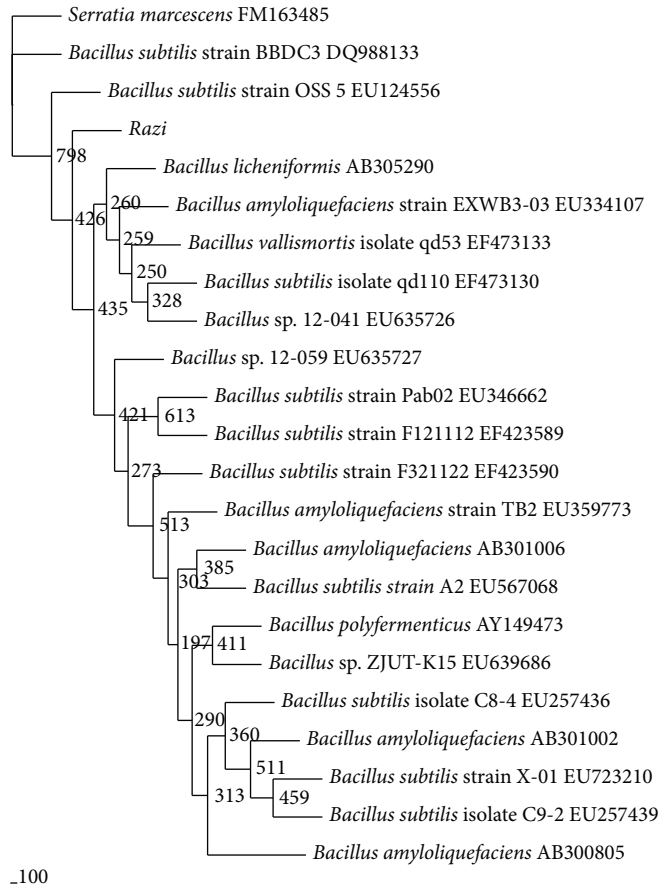

Figure 1: Phylogram (neighbour-joining method) indicating the 16s rRNA genetic relationship between 20 other related references microorganisms from the GenBank database and strain A.rzi. *S. marcescens* is the outgroup. Species names of bacteria were followed by the accession numbers of 16s rRNA. The internal labels at the branching points are the bootstrap value. *Scale bar* represents 100 nucleotides substitution.

Table 2: Amount of Mo-blue produced by a 24-hour static culture of strain A.rzi. Values are mean ± standard error ($n = 3$).

Bacteria	Micromole Mo-blue
Bacillus sp. strain A.rzi	7.82 ± 0.24^{a}
Serratia sp. strain Dr.Y8	10.41 ± 0.13^{b}
S. marcescens strain Dr.Y9	9.86 ± 0.44^{b}
Serratia sp. strain Dr.Y5	7.87 ± 0.15^{a}
Pseudomonas sp. strain DRY2	6.94 ± 0.65^{c}
Enterobacter sp. strain Dr.Y13	6.91 ± 0.15^{c}
Acinetobacter calcoaceticus strain Dr.Y12	5.86 ± 0.14^{d}
Serratia marcescens strain DRY6	2.84 ± 0.23^{e}
Enterobacter cloacae strain 48	2.17 ± 0.56^{e}
Escherichia coli K12	0.96 ± 0.04^{f}

Value with the same letter is not significantly different ($P > 0.05$).

3.7. Studies on the Effects of Metal Ions and Respiratory Inhibitors. Preliminary results indicated that stannous and ferrous ions resulted in a chemical reduction of phosphomolybdate to Mo-blue in the reaction mixture. Hence these metal ions were omitted from this study. At 0.1 mM, mercury, copper, cadmium, arsenic, lead, chromium, cobalt, and zinc showed strong inhibition on molybdate reduction by crude enzyme (Figure 8).

It was found that the inhibitors antimycin A, potassium cyanide, sodium azide, and rotenone did not inhibit more than 10% of the Mo-reducing activity in strain A.rzi (data not shown).

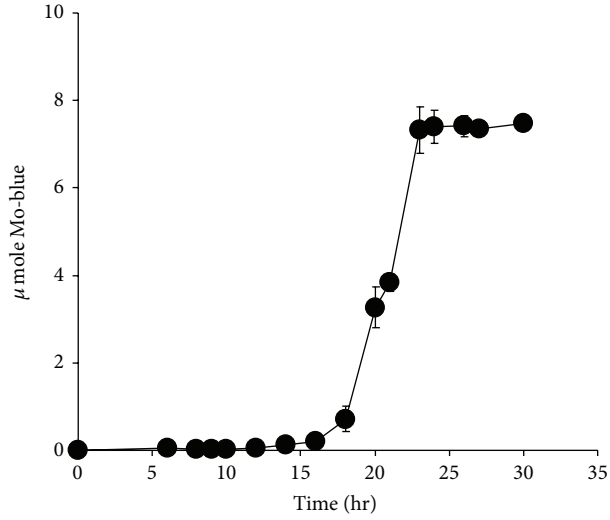

Figure 2: Time course profile of Mo-blue production from strain A.rzi.

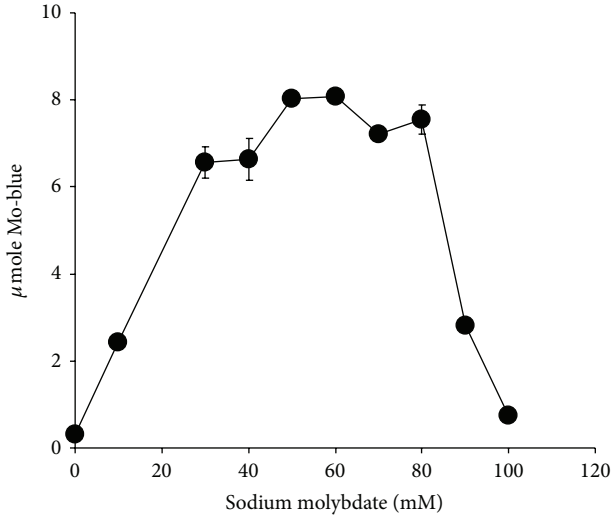

Figure 3: The effect of molybdate on molybdate reduction by strain A.rzi. Error bars represent mean ± standard error ($n = 3$).

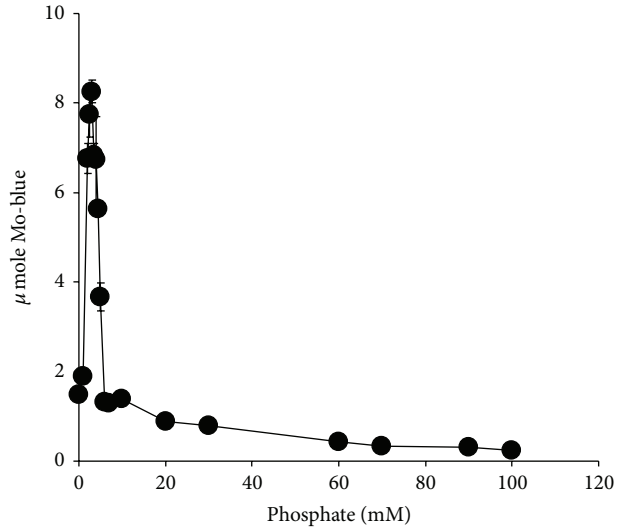

Figure 4: The effect of phosphate on molybdate reduction by strain A.rzi. Error bars represent mean ± standard error ($n = 3$).

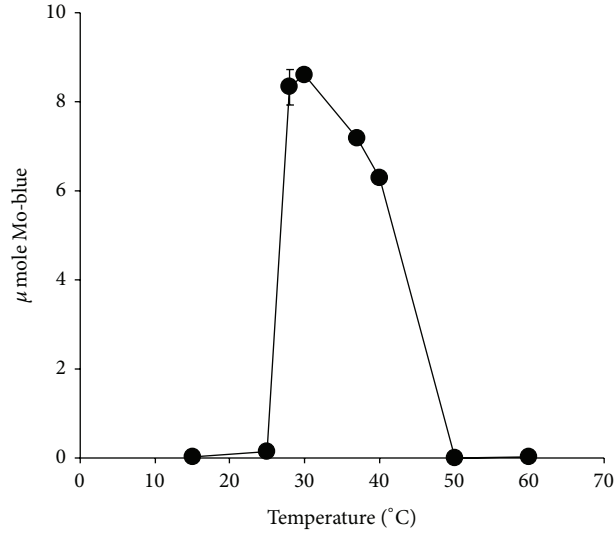

Figure 5: The effect of temperature on molybdate reduction by strain A.rzi. Error bars represent mean ± standard error ($n = 3$).

3.8. Characterization of the Molybdate Reduction Reaction Using the Dialysis Tubing Method. The results showed that 95% of the amount of Mo-blue formed (13.775 μmole) was found in the dialysis tube, while only 5% (1.225 μmole) was found at the outside of the tube.

3.9. Kinetics of Molybdenum Blue Production. Data from the experimental value in batch studies was fitted to several kinetic models of growth or product formation, that is, Monod, Luong, and Haldane. CurveExpert Professional software (Version 1.6) with custom equation algorithm that leads to the minimization of the sums of square of residuals was used to find the constants. The best model that fitted the experimental data well was Luong followed by Haldane and Monod with correlation coefficient values of 0.99, 0.83, and 0.36, respectively (Figure 9). The calculated value for p_{max}, K_s, S_m, and n was 5.88 μmole Mo-blue hr^{-1}, 70.36 mM, 108.22 mM, and 0.74, respectively.

4. Discussions

In the last decade, works on microbial molybdenum reduction to Mo-blue have been restricted to our isolates [18–25, 35, 36, 42]. The enzyme responsible for the reduction has never been purified. Despite this, novel enzyme assay for this enzyme has been developed [35] and purification of this enzyme is being intensely pursued. Our quest for more variety of Mo-reducing bacteria to suit a plethora of environmental conditions has led us to the discovery of this

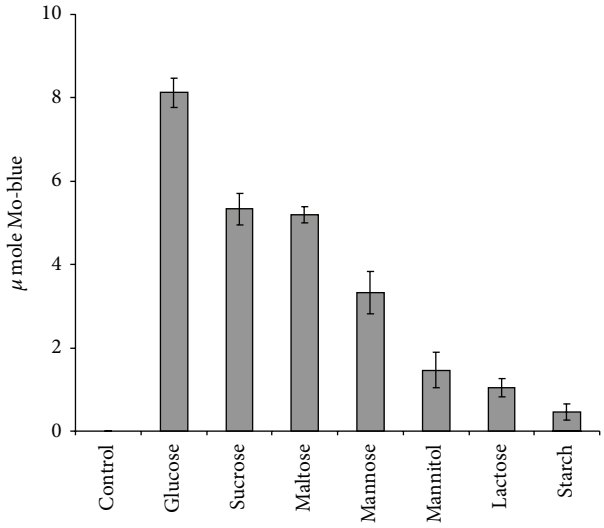

Figure 6: Molybdate reduction using various electron donor sources. Error bars represent mean ± standard error ($n = 3$).

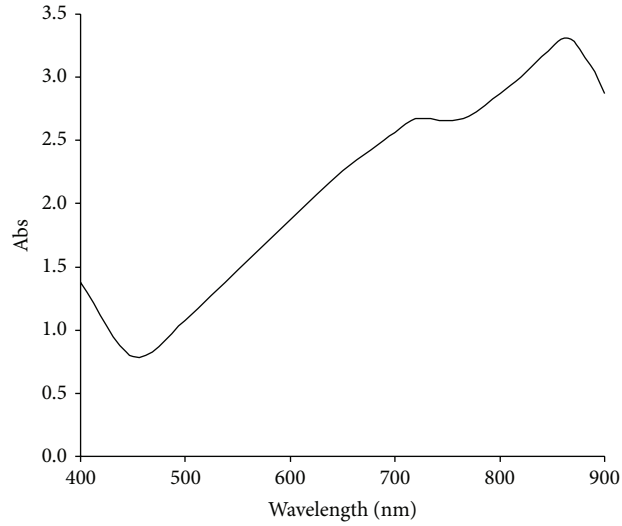

Figure 7: Scanning spectrum of Mo-blue from *Bacillus* sp. strain A.rzi after 24 hours of static incubation.

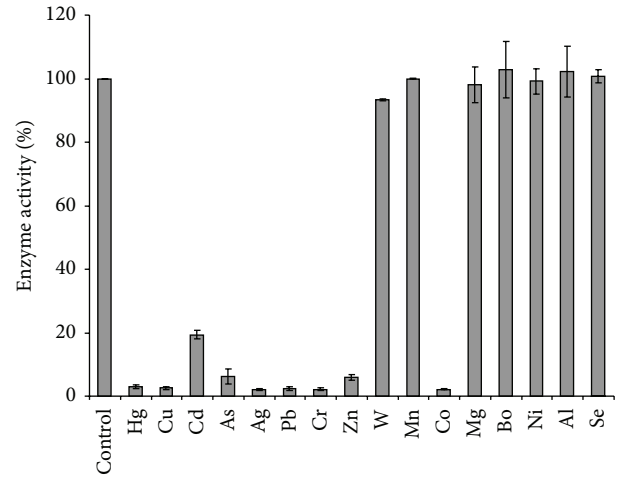

Figure 8: The effect of heavy metals (0.1 mM) on molybdate reduction by strain A.rzi. Error bars represent mean ± standard error ($n = 3$).

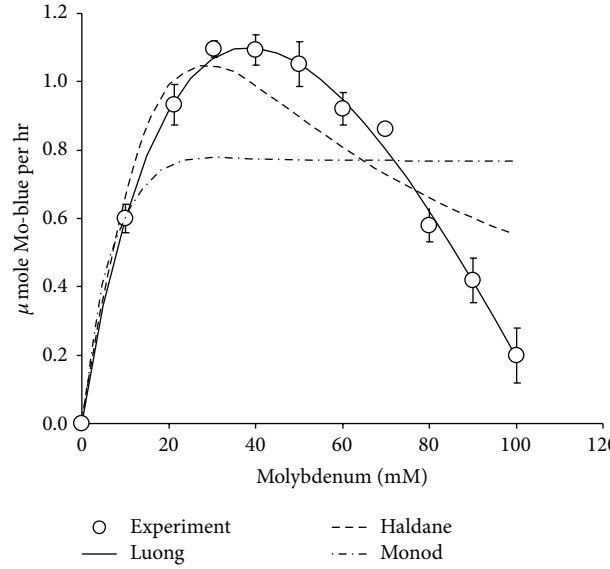

Figure 9: Kinetics of molybdenum blue production by strain A.rzi. Data represents mean ± standard error ($n = 3$).

bacterium. Molybdenum bioremediation can take advantage of this genus ability to produce spores that can be stored for long period and highly resistant to environmental stresses including heavy metals [43].

This bacterium was able to produce comparable molybdenum to other previously isolated strains. Furthermore it is able to reduce a high initial concentration of sodium molybdate of 80 mM. Average reduction at moderate starting molybdate concentrations from previous studies ranges from 25 to 55 mM [17–25]. Tolerance and reduction at concentrations higher than 20 mM are an advantage to a microbe as molybdenum pollution could reach as high as 2000 ppm (20.8 mM molybdate) [44], a concentration lethal to ruminant [45].

The optimum ratio of phosphate to molybdate concentrations is important for overall molybdenum reduction to molybdenum blue. The results obtained in this work show some similarity to the results obtained from *Serratia* sp. strain Dr.Y8 [19] and *S. marcescens* strain Dr.Y9 [21]. Other strains show a lower requirement for molybdenum of between 15 and 50 mM but with a similar optimal phosphate at 5 mM [18, 20, 22–25]. The inhibitory effect shown by high phosphate concentrations is probably due to physical interaction with the phosphomolybdate substrate and not through inhibiting the enzymatic action. This has been discussed in detail in other similar publications [18–25]. The Mo-blue spectrum obtained in this strain is similar to all of the other Mo-reducing strains

[18–25, 42] indicating that a common phosphomolybdate species is involved.

Optimal pH and temperature supporting molybdenum reduction for this bacterium were found to be within the range of optimum pH and temperature of nearly all Mo-reducing bacteria isolated to date which varies from pH 6 to 8 and from 30 to 40°C, respectively [18–25]. The temperature range suits tropical climate bioremediation environment [46].

The discovery that glucose was the best electron donor to molybdenum reduction is similar to results obtained from several other Mo-reducing bacteria [20, 22, 24]. Support of Mo-reduction using starch is unique to this strain as this genus is known for its production of amylases [47]. Other Mo-reducing bacteria require sucrose [19, 21] or fructose [25]. Since molybdenum reduction is growth associated [18–25], the use of glucose and all of the other readily assimilable carbon sources reflect a growth-associated process of molybdenum reduction. This process is ubiquitous in this and other Mo-reducing bacteria.

Toxic metal ions such as mercury, copper, cadmium, lead, chromium, and ions showed a similar trend of inhibition to other Mo-reducing bacteria [18–25]. The inhibition by arsenic, cobalt, and zinc is only reported for this strain. In a related area, the bioremediation of chromium is also affected by heavy metals ions [48–51].

The results obtained indicate that the electron transport chain (ETC) or system of this bacterium is not the site of molybdate reduction. The result is in agreement with many of the more recent isolated Mo-reducing bacteria [18–25]. In contrast, the electron transport chain has been suggested as the site of molybdate reduction in EC 48 [17]. The inhibitors inhibit at specific sites of the electron transport chain. Antimycin A is an inhibitor to cytochrome b. Rotenone inhibits NADH dehydrogenase. Sodium azide and cyanide are inhibitors to cytochrome d oxidase [37]. The same respiratory inhibitors have been used to find the location or identity of many metal-reducing enzymes with mixed results. It was discovered that rotenone, cyanide, and azide failed to inhibit chromate reduction in *E. coli* [50] and in *Pseudomonas mendocina* [51]. In contrast, both azide and cyanide were found to inhibit the reduction of chromate in *Bacillus subtilis* indicating the involvement of the ETC [52].

The dialysis tubing is the standard technique first developed by Hem [41] to distinguish between chemical and enzymatic reduction of metal ions by bacteria and has been modified to accommodate molybdenum reduction in bacteria [53]. The dialysis tubing experiment suggests that Mo-reduction is exclusively enzymatic in origin as the 5% of Mo-blue found at the outside of the tubing is almost all due to slow leakage of the Mo-blue formed.

Most studies on the reduction kinetics of heavy metals such as mercury [54], arsenate [55], and chromate [56] reported a Haldane-type inhibition by the substrate metal ions. However, molybdenum reduction to Mo-blue showed a clear strong inhibition of Mo-blue production rate at high concentration of molybdenum with a calculated critical concentration of molybdenum that completely inhibited Mo-blue production at 108.22 mM. Unlike the more commonly reported Haldane model [39], the Luong model allows for the determination of the critical concentration of substrate that could completely inhibit production of product [40] as evident from this work. This is the first time existing models of kinetic studies being applied to model Mo-blue production in bacterium.

To conclude, we reported on the isolation of a novel molybdenum reducing bacterium from the *Bacillus* genus. Features of this bacterium, such as temperature, pH, and concentration of phosphate that supported the optimal reduction of molybdenum blue, were similar to other reported molybdenum-reducing bacterial species. The absorption spectrum of the Mo-blue product was very similar to other Mo-reducing bacteria isolated to date indicating probably the same phosphomolybdate species involved in bacterial reduction process. The reduction of molybdenum to Mo-blue is predominantly enzymatic as evident from the dialysis tubing experiment. This bacterium is sensitive towards heavy metals as was similarly discovered in previously isolated molybdenum-reducing bacteria and could pose a problem if the bioremediation site is cocontaminated with other toxic heavy metals. We also showed for the first time that the Luong model of substrate (molybdate) inhibition kinetics of Mo-blue production was better than the Haldane model. We are currently focusing on the isolation of metal-resistant Mo-reducing bacteria and the purification of the Mo-reducing enzyme.

Conflict of Interests

The authors declare that there is no conflict of interests regarding the publication of this paper.

Acknowledgment

This project was supported by funds from the Research University Grant Scheme (RUGS), Project no. 05-01-09-0750RU/F1.

References

[1] J. K. Katnoria, S. Arora, R. Bhardwaj, and A. Nagpal, "Evaluation of genotoxic potential of industrial waste contaminated soil extracts of Amritsar, India," *Journal of Environmental Biology*, vol. 32, no. 3, pp. 363–367, 2011.

[2] M. Y. Shukor, N. A. Bakar, A. R. Othman, I. Yunus, N. A. Shamaan, and M. A. Syed, "Development of an inhibitive enzyme assay for copper," *Journal of Environmental Biology*, vol. 30, no. 1, pp. 39–44, 2009.

[3] M. Alina, A. Azrina, A. S. M. Yunus, S. M. Zakiuddin, H. M. I. Effendi, and R. M. Rizal, "Heavy metals (mercury, arsenic, cadmium, plumbum) in selected marine fish and shellfish along the straits of Malacca," *International Food Research Journal*, vol. 19, no. 1, pp. 135–140, 2012.

[4] G. K. Davis, "Molybdenum," in *Metals and Their Compounds in the Environment: Occurrence, Analysis and Biological Relevance*, E. Merian, Ed., pp. 1089–1100, VCH Weinheim, New York, NY, USA, 1991.

[5] R. B. King, M. Long, and J. bK. Sheldon, *Practical Environmental Bioremediation: The Field Guide*, Lewis Publisher, Boca Raton, Fla, USA, 1992.

[6] DOE, *Malaysia Environmental Quality Report 2006*, Department of Environment, Ministry of Natural Resources and Environment, Putrajaya, Malaysia, 2007.

[7] L. T. Fairhall, R. C. Dunn, N. E. Sharpless, and E. A. Pritchard, *The Toxicity of Molybdenum*, United States Public Health Service, Public Health Bulletin, 1945.

[8] E. J. Underwood, "Environmental sources of heavy metals and their toxicity to man and animals," *Progress in Water Technology*, vol. 11, no. 4-5, pp. 33–45, 1979.

[9] F. S. Yong, "Mamut copper mine—the untold story. The national seminar on the Malaysian minerals industry," in *Minerals: Underpinning Yesterday's Needs, Today's Development and Tomorrow's Growth*, Venue, Sabah, Malaysia, 2000.

[10] R. Z. Sayyed and S. B. Chincholkar, "Growth and siderophores production in *Alcaligenes faecalis* is regulated by metal ions," *Indian Journal of Microbiology*, vol. 50, no. 2, pp. 179–182, 2010.

[11] A. Capaldi and B. Proskauer, "Beiträge zur Kenntnis der Säurebildung bei Typhusbacillen und Bacterium coli," *Zeitschrift für Hygiene und Infectionskrankheiten*, vol. 23, no. 3, pp. 452–474, 1896.

[12] A. Jan, "La reduction biologique du molybdate d'ammonium par les bactéries du genre Serratia," *Bulletin des Sciences Pharmacologiques*, vol. 46, pp. 336–339, 1939.

[13] C. A. Woolfolk and H. R. Whiteley, "Reduction of inorganic compounds with molecular hydrogen by *Micrococcus lactilyticus*. I. Stoichiometry with compounds of arsenic, selenium, tellurium, transition and other elements," *Journal of Bacteriology*, vol. 84, pp. 647–658, 1962.

[14] E. M. Bautista and M. Alexander, "Reduction of inorganic compounds by soil microorganisms," *Soil Science Society of America Journal*, vol. 36, pp. 918–920, 1972.

[15] A. M. Campbell, A. D. Campillo-Campbell, and D. B. Villaret, "Molybdate reduction by *Escherichia coli* K-12 and its chl mutants," *Proceedings of the National Academy of Sciences of the United States of America*, vol. 82, no. 1, pp. 227–231, 1985.

[16] T. Sugio, Y. Tsujita, T. Katagiri, K. Inagaki, and T. Tano, "Reduction of Mo^{6+} with elemental sulfur by *Thiobacillus ferrooxidans*," *Journal of Bacteriology*, vol. 170, no. 12, pp. 5956–5959, 1988.

[17] B. Ghani, M. Takai, N. Z. Hisham et al., "Isolation and characterization of a Mo^{6+}-reducing bacterium," *Applied and Environmental Microbiology*, vol. 59, no. 4, pp. 1176–1180, 1993.

[18] M. Y. Shukor, S. H. M. Habib, M. F. A. Rahman et al., "Hexavalent molybdenum reduction to molybdenum blue by *S. Marcescens* strain Dr. Y6," *Applied Biochemistry and Biotechnology*, vol. 149, no. 1, pp. 33–43, 2008.

[19] M. Y. Shukor, M. F. Rahman, Z. Suhaili, N. A. Shamaan, and M. A. Syed, "Bacterial reduction of hexavalent molybdenum to molybdenum blue," *World Journal of Microbiology and Biotechnology*, vol. 25, no. 7, pp. 1225–1234, 2009.

[20] M. Y. Shukor, M. F. Rahman, N. A. Shamaan, and M. S. Syed, "Reduction of molybdate to molybdenum blue by *Enterobacter* sp. strain Dr.Y13," *Journal of Basic Microbiology*, vol. 49, supplement 1, pp. S43–S54, 2009.

[21] S. M. Yunus, H. M. Hamim, O. M. Anas, S. N. Aripin, and S. M. Arif, "Mo (VI) reduction to molybdenum blue by *Serratia marcescens* strain Dr. Y9," *Polish Journal of Microbiology*, vol. 58, no. 2, pp. 141–147, 2009.

[22] M. F. A. Rahman, M. Y. Shukor, Z. Suhaili, S. Mustafa, N. A. Shamaan, and M. A. Syed, "Reduction of Mo(VI) by the bacterium *Serratia* sp. strain DRY5," *Journal of Environmental Biology*, vol. 30, no. 1, pp. 65–72, 2009.

[23] M. Y. Shukor, M. F. Rahman, Z. Suhaili, N. A. Shamaan, and M. A. Syed, "Hexavalent molybdenum reduction to Mo-blue by *Acinetobacter calcoaceticus*," *Folia Microbiologica*, vol. 55, no. 2, pp. 137–143, 2010.

[24] M. Y. Shukor, S. A. Ahmad, M. M. M. Nadzir, M. P. Abdullah, N. A. Shamaan, and M. A. Syed, "Molybdate reduction by *Pseudomonas* sp. strain DRY2," *Journal of Applied Microbiology*, vol. 108, no. 6, pp. 2050–2058, 2010.

[25] H. K. Lim, M. A. Syed, and M. Y. Shukor, "Reduction of molybdate to molybdenum blue by *Klebsiella* sp. strain hkeem," *Journal of Basic Microbiology*, vol. 52, no. 3, pp. 296–305, 2012.

[26] C. Neunhäuserer, M. Berreck, and H. Insam, "Remediation of soils contaminated with molybdenum using soil amendments and phytoremediation," *Water, Air, and Soil Pollution*, vol. 128, no. 1-2, pp. 85–96, 2001.

[27] R. Mohandass, P. Rout, S. Jiwal, and C. Sasikala, "Biodegradation of benzo[a]pyrene by the mixed culture of *Bacillus cereus* and *Bacillus vireti* isolated from the petrochemical industry," *Journal of Environmental Biology*, vol. 33, no. 6, pp. 985–989, 2012.

[28] R. Devereux and S. S. Wilkinson, "Amplification of ribosomal RNA sequences," in *Molecular Microbial Ecology Manual*, A. D. L. Akkermans, J. D. van Elsas, and F. J. de Bruijn, Eds., pp. 1–17, Kluwer Academic, Dodrecht, The Netherlands, 2nd edition, 2004.

[29] J. D. Thompson, D. G. Higgins, and T. J. Gibson, "CLUSTAL W: improving the sensitivity of progressive multiple sequence alignment through sequence weighting, position-specific gap penalties and weight matrix choice," *Nucleic Acids Research*, vol. 22, no. 22, pp. 4673–4680, 1994.

[30] T. H. Jukes and C. R. Cantor, "Evolution of protein molecules," in *Mammalian Protein Metabolism*, H. N. Munro, Ed., pp. 21–132, Academic Press, New York, NY, USA, 1969.

[31] N. Saitou and M. Nei, "The neighbor-joining method: a new method for reconstructing phylogenetic trees," *Molecular Biology and Evolution*, vol. 4, no. 4, pp. 406–425, 1987.

[32] J. Felsenstein, "Confidence limits on phylogenies: an approach using the bootstrap," *Evolution*, vol. 39, no. 4, pp. 783–791, 1985.

[33] T. Margush and F. R. McMorris, "Consensus n-trees," *Bulletin of Mathematical Biology*, vol. 43, no. 2, pp. 239–244, 1981.

[34] R. D. M. Page, "TreeView: an application to display phylogenetic trees on personal computers," *Computer Applications in the Biosciences*, vol. 12, no. 4, pp. 357–358, 1996.

[35] M. Y. Shukor, M. F. Rahman, N. A. Shamaan, C. H. Lee, M. I. A. Karim, and M. A. Syed, "An improved enzyme assay for molybdenum-reducing activity in bacteria," *Applied Biochemistry and Biotechnology*, vol. 144, no. 3, pp. 293–300, 2008.

[36] M. Y. Shukor, N. A. Shamaan, M. A. Syed, C. H. Lee, and M. I. A. Karim, "Characterization and quantification of molybdenum blue production in *Enterobacter cloacae* strain 48 using 12-molybdophosphate as the reference compound," *Asia Pacific Journal of Molecular Biology and Biotechnology*, vol. 8, pp. 166–172, 2000.

[37] R. M. C. Dawson, D. C. Elliot, and W. H. Elliot, Eds., *Data for Biochemical Research*, Clarendon Press, Oxford, UK, 1969.

[38] J. Monod, "The growth of bacterial cultures," *Annual Review of Microbiology*, vol. 3, pp. 371–394, 1949.

[39] J. B. S. Haldane, *Enzymes*, Longman Green, London, UK, 1930.

[40] A. Mulchandani, J. H. T. Luong, and C. Groom, "Substrate inhibition kinetics for microbial growth and synthesis of poly-β-hydroxybutyric acid by *Alcaligenes eutrophus* ATCC 17697," *Applied Microbiology and Biotechnology*, vol. 30, no. 1, pp. 11–17, 1989.

[41] J. D. Hem, "Chemical factors that influence the availability of iron and manganese in aqueous solution," *Geological Society of America Bulletin*, vol. 83, pp. 443–450, 1972.

[42] M. Y. Shukor, H. Adam, K. Ithnin, I. Yunus, N. A. Shamaan, and A. Syed, "Molybdate reduction to molybdenum blue in microbe proceeds via a phosphomolybdate intermediate," *Journal of Biological Sciences*, vol. 7, no. 8, pp. 1448–1452, 2007.

[43] D. D. Runnells, D. S. Kaback, and E. M. Thurman, "Geochemistry and sampling of molybdenum in sediments, soils, and plants in Colorado," in *Molybdenum in the Environment*, W. R. Chappel and K. K. Peterson, Eds., Marcel Dekker, New York, NY, USA, 1976.

[44] S. Sinnakkannu, A. R. Abdullah, N. M. Tahir, and M. R. Abas, "Degradation of metsulfuron methyl in selected malaysian agricultural soils," *Fresenius Environmental Bulletin*, vol. 13, no. 3, pp. 258–261, 2004.

[45] A. M. Hassan, B. M. Haroun, A. A. Amara, and A. Ehab, "Serour production and characterization of keratinolytic protease from new wool-degrading *Bacillus* species isolated from Egyptian ecosystem," *BioMed Research International*, vol. 2013, Article ID 175012, 14 pages, 2013.

[46] R. Elangovan, L. Philip, and K. Chandraraj, "Hexavalent chromium reduction by free and immobilized cell-free extract of arthrobacter rhombi-RE," *Applied Biochemistry and Biotechnology*, vol. 160, no. 1, pp. 81–97, 2010.

[47] G. B. Sau, S. Chatterjee, and S. K. Mukherjee, "Chromate reduction by cell-free extract of *Bacillus firmus* KUCr1," *Polish Journal of Microbiology*, vol. 59, no. 3, pp. 185–190, 2010.

[48] A. C. Poopal and R. S. Laxman, "Studies on biological reduction of chromate by *Streptomyces griseus*," *Journal of Hazardous Materials*, vol. 169, no. 1–3, pp. 539–545, 2009.

[49] U. Thacker and D. Madamwar, "Reduction of toxic chromium and partial localization of chromium reductase activity in bacterial isolate DM1," *World Journal of Microbiology and Biotechnology*, vol. 21, no. 6-7, pp. 891–899, 2005.

[50] H. Shen and Y. Wang, "Characterization of enzymatic reduction of hexavalent chromium by *Escherichia coli* ATCC 33456," *Applied and Environmental Microbiology*, vol. 59, no. 11, pp. 3771–3777, 1993.

[51] J. M. Rajwade, P. B. Salunke, and K. M. Pknikar, "Biochemical basis of chromate reduction by *Pseudomonas mendocina*," in *Proceedings of the International Biohydrometallurgy Symposium*, R. Amils and A. Ballester, Eds., pp. 105–114, Elsevier, New York, NY, USA, 1999.

[52] C. Garbisu, I. Alkorta, M. J. Llama, and J. L. Serra, "Aerobic chromate reduction by *Bacillus subtilis*," *Biodegradation*, vol. 9, no. 2, pp. 133–141, 1998.

[53] M. Y. Shukor, M. A. Syed, C. H. Lee, M. I. A. Karim, and N. A. Shamaan, "A method to distinguish between chemical and enzymatic reduction of molybdenum in *Enterobacter cloacae* strain 48," *Malaysian Journal of Biochemistry*, vol. 7, pp. 71–72, 2002.

[54] P. Głuszcz, J. Petera, and S. Ledakowicz, "Mathematical modeling of the integrated process of mercury bioremediation in the industrial bioreactor," *Bioprocess and Biosystems Engineering*, vol. 34, no. 3, pp. 275–285, 2011.

[55] M. Sukumar, "Reduction of hexavalent chromium by *Rhizopus oryzae*," *African Journal of Environmental Science and Technology*, vol. 4, no. 7, pp. 412–418, 2010.

[56] S. O. Soda, S. Yamamura, H. Zhou, M. Ike, and M. Fujita, "Reduction kinetics of As (V) to As (III) by a dissimilatory arsenate-reducing bacterium, *Bacillus* sp. SF-1," *Biotechnology and Bioengineering*, vol. 93, no. 4, pp. 812–815, 2006.

Hindawi Publishing Corporation
BioMed Research International
Volume 2013, Article ID 409675, 9 pages
http://dx.doi.org/10.1155/2013/409675

Research Article

Enhancement of Oxygen Mass Transfer and Gas Holdup Using Palm Oil in Stirred Tank Bioreactors with Xanthan Solutions as Simulated Viscous Fermentation Broths

Suhaila Mohd Sauid,[1] Jagannathan Krishnan,[1] Tan Huey Ling,[1] and Murthy V. P. S. Veluri[2]

[1] *Faculty of Chemical Engineering, Universiti Teknologi MARA (UiTM), 40450 Shah Alam, Selangor, Malaysia*
[2] *Faculty of Chemical Engineering, Manipal International University, 71800 Nilai, Negeri Sembilan Darul Khusus, Malaysia*

Correspondence should be addressed to Jagannathan Krishnan; jagannathan@salam.uitm.edu.my

Received 13 August 2013; Accepted 1 October 2013

Academic Editor: Eldon R. Rene

Volumetric mass transfer coefficient (k_La) is an important parameter in bioreactors handling viscous fermentations such as xanthan gum production, as it affects the reactor performance and productivity. Published literatures showed that adding an organic phase such as hydrocarbons or vegetable oil could increase the k_La. The present study opted for palm oil as the organic phase as it is plentiful in Malaysia. Experiments were carried out to study the effect of viscosity, gas holdup, and k_La on the xanthan solution with different palm oil fractions by varying the agitation rate and aeration rate in a 5 L bench-top bioreactor fitted with twin Rushton turbines. Results showed that 10% (v/v) of palm oil raised the k_La of xanthan solution by 1.5 to 3 folds with the highest k_La value of 84.44 h^{-1}. It was also found that palm oil increased the gas holdup and viscosity of the xanthan solution. The k_La values obtained as a function of power input, superficial gas velocity, and palm oil fraction were validated by two different empirical equations. Similarly, the gas holdup obtained as a function of power input and superficial gas velocity was validated by another empirical equation. All correlations were found to fit well with higher determination coefficients.

1. Introduction

In aerobic fermentations, the bioreactor performance greatly depends on its oxygen transfer capacities. Oxygen is a soluble substrate, but its solubility in aqueous media at ambient conditions is very low [1]. Thus, actively growing cells can consume all the dissolved oxygen quickly and, hence, oxygen has to be supplied continuously by mass transfer from air to the growth medium [2]. If the oxygen transfer rate to the aqueous phase exceeds the rate of oxygen consumed by the cells, cell growth continues at an exponential rate when other nutrients are not limited. However, when oxygen is not enough, the microorganisms' metabolic rate decreases drastically leading to reduced growth and productivity.

Xanthan gum is a natural polysaccharide produced by *Xanthomonas campestris* and is an important industrial biopolymer. It is widely used in industries such as foods and cosmetics, pharmaceutical and petroleum industry as emulsion stabilizer, thickener, dispersing agent and drilling fluid, and for many more applications [3]. Xanthan gum is soluble in cold or hot water and its solution can be highly viscous even at low concentration. Xanthan gum solutions show non-Newtonian behavior, that is, pseudoplastic or shear thinning, and the viscosity decreases with increasing shear rate. Besides, the viscosity also depends on its concentration, temperature, concentration of salts, and pH [4]. The fermentations of xanthan gum production are often associated with a significant decrease in oxygen transfer rate because of the increase in viscosity from accumulation of xanthan. As *X. campestris* is a strictly aerobic microorganism, oxygen is an essential nutrient both for growth and for xanthan production. Therefore, oxygen limitation turns into the controlling step in the whole process of xanthan production [5].

There have been various strategies to improve the oxygen transfer in bioreactors. Some of the previous researchers [6–10] adopted an approach of dispersing a nonaqueous, organic, second liquid phase that is immiscible to the system, referred to later as organic phase(s). The presence of organic phase

modifies the medium in such a way that it could carry more oxygen and this approach was found successful in the past. The organic phase has strong affinity for oxygen so that it can increase the apparent solubility of oxygen in water [7]. The organic compounds used were hydrocarbons, perfluorocarbons, and vegetable oils.

This method also was applied in xanthan gum fermentation by Ju and Zhao [11] and Kuttuva et al. [12]. They postulated that this method has the ability to solve the viscosity problem and indirectly enhance the oxygen transfer. This was proven by Lo et al. [8] who found that in 3.5% of xanthan solution, the k_La values in the xanthan solution-hexadecane emulsion (0.50 v/v) system were higher than the k_La values obtained in a centrifugal packed bed reactor and stirred tank reactor. While those researchers opted for higher organic phase concentration, this study has focused on the effect of palm oil on the viscosity and the oxygen transfer characteristics in xanthan solution at lower oil concentrations.

In this work, palm oil was chosen as the organic phase to study the oxygen transfer characteristics such as effect of viscosity, gas holdup, and mass transfer coefficient on the xanthan gum solution by varying the agitation rate and aeration rate in a stirred tank bioreactor.

2. Materials and Methods

2.1. Bioreactor. Experiments were carried out in an automated 5 L bench-top bioreactor (Biostat B, Sartorius BBI Systems, Germany) with a working volume of 4 L. The height/diameter ratio of glass vessel was 2 : 1. It was equipped with pH electrode (Mettler Toledo, Switzerland), dissolved oxygen (DO) probe (Mettler Toledo, Switzerland), temperature, and antifoam sensor. An overhead stirrer (Heidolph RZR 2102 Control, Germany) with agitation controller and torque reading was mounted on the stirrer shaft on top of the bioreactor for mixing. The bioreactor mixing system was equipped with four baffles and two impellers. Twin Rushton turbine blades spaced 80 mm apart having 64 mm diameter and 13 mm width were used. There was a ring sparger underneath the bottom turbine having of 14 holes 1 mm size each. Standard operating procedure was carried out on each experiment and the DO and pH probes were calibrated before starting bioreactor. For all experiments, the bioreactor was aerated at three different rates, namely, 0.25, 0.75, and 1.25 vvm and agitated at three different speeds, namely, 400, 600, and 800 rpm. The bioreactor used in this study is shown in Figure 1. All the experiments were carried out at atmospheric pressure and the temperature was maintained at 30°C.

2.2. Model Media. The investigation of the effect of palm oil on k_La was conducted in a model media, xanthan gum solutions to represent aqueous solutions of different viscosities as a fermentation broth. In this research, commercial food grade xanthan gum obtained from Bagus Bakery, Malaysia, was used and the xanthan gum solution was prepared at 0.25% (w/v). Xanthan gum was selected as it showed a good non-Newtonian (pseudoplastic) behavior as required besides being inexpensive.

Figure 1: Experimental setup.

2.3. Palm Oil. Palm oil used in this research was RBD (refined, bleached, and deodorized) palm olein obtained from Alami Technological Services Sdn Bhd, Malaysia. Its viscosity and density were measured as 67.85 cP and 818 kg/m^3 at the ambient temperature, respectively. The oxygen solubility of palm oil is 47.7 mg/L at 30°C [13] and it has low solubility in water, around 100 mg/L at 28°C [14].

2.4. Rheology Measurements. The viscosity measurement of xanthan gum solution was conducted using a viscometer (Brookfield LVDV-II+Pro, USA) at 30°C with a SC4-25 spindle. The shear stress versus shear rate data were analyzed as per the Ostwald de Waele or power law model given in (1). In order to study the effect of palm oil dosage, experiments were carried out at different volumetric fractions (0, 5, 10, 15, 20, and 50%) of palm oil in the xanthan solution:

$$\tau = K\gamma^n. \tag{1}$$

2.5. Power Input. The power input was measured by using an overhead stirrer with torquemeter (Heidolph RZR 2102 Control, Germany). The power input was obtained by applying the following:

$$P = 2\pi N\left(T - T_o\right). \tag{2}$$

2.6. Probe Response Time of DO Meter. In determining k_La values, it is important to find out the probe response time. Response time, τ_r, is defined as the time needed to record 63% of the final value measured when exposed to a stepwise change of concentration [15]. The probe response time was determined by transferring the dissolved oxygen probe (InPro 6820 Series, Mettler Toledo, Switzerland) from oxygen-free solution (0% saturation value) to an oxygen saturated solution (100% saturation value). The abrupt rise in the DO reading from 0% to 100% was monitored and recorded every five seconds. Then, the probe response was modeled as first-order dynamic as described by García-Ochoa et al. [5] in the following:

$$\frac{dC_{\text{me}}}{dt} = \frac{C_L - C_{\text{me}}}{\tau_r}. \tag{3}$$

Upon linearization, (3) became

$$\ln \frac{C_L - C_{\text{me}}}{C_L - C_{\text{me}_o}} = -\frac{t}{\tau_r}. \quad (4)$$

A plot of $\ln(C_L - C_{\text{me}}/C_L - C_{\text{me}_o})$ against t yielded a straight line with inverse slope value of $1/\tau_r$. From that the probe response time obtained was found to be 24.16 s.

2.7. Volumetric Mass Transfer Coefficient. For the k_La value determination the static gassing out method was employed throughout the experiments. This was performed by firstly purging the system (xanthan solution with palm oil) with nitrogen gas until the dissolved oxygen fell to zero. When DO was stabilized at 0% value, the nitrogen valve was switched off and, simultaneously, the aeration was started and time was marked as zero ($t = 0$). The gradual increase of DO concentration was monitored and recorded until it reached a steady value at 100%. In order to calculate the k_La value, (5) was used:

$$\frac{dC_L}{dt} = k_La\left(C_L^* - C_L\right) \quad (5)$$

which on integration yielded

$$\ln\left(1 - \frac{C}{C^*}\right) = -k_La \cdot t. \quad (6)$$

The k_La value was determined from the slope of plot $\ln(1 - C_L/C_L^*)$ versus t where C_L^* is the equilibrium dissolved oxygen concentration. The effect of the probe response was neglected as the time required for the oxygen transfer $1/k_La$ was high compared to the dynamic response of the probe ($1/k_La \gg 10\tau_r$) [12]. However, in case of the slower response, the dynamic response of the probe must be taken into account for the calculation of k_La [15–17]. Considering the effect of response time of the DO probe used, the k_La value obtained from (6) served only as the initial guess value to compute the actual k_La value. Combining (3) and (5) yielded a nonlinear regression (7) for the experimental DO data which was later solved numerically to find the actual k_La value. Consider

$$C_{\text{me}} = C^* + \frac{C^* - C_{\text{me}_o}}{1 - \tau_r k_La}\left[\tau_r k_La \exp\left(-\frac{t}{\tau_r}\right) - \exp\left(-k_La \cdot t\right)\right]. \quad (7)$$

2.8. Gas Holdup. The gas holdup of the system was measured by the difference between the average liquid level with and without aeration using (8) given below. Consider

$$\varepsilon_G = \frac{H_{G+L} - H_L}{H_{G+L}}. \quad (8)$$

2.9. Empirical Correlations. There are several empirical correlations found in the published literature to predict k_La values; however, the one developed by Cooper et al. [18] is widely used. It relates k_La to the specific power input and the superficial gas velocity as given in the following:

$$k_La = \delta\left(\frac{P_g}{V_L}\right)^{\beta} v_s^{\alpha}. \quad (9)$$

The power input term in the correlation includes all the effects of flow and turbulence on bubble dispersion and the mass transfer boundary layer according to Doran [1]. The values of the constants may vary depending on the system's geometry, the range of variables investigated, and the experimental technique applied. The range of values of β and α for Newtonian fluids varied between 0.4 to 0.95 and 0.2 to 0.75, respectively [19].

However, Nielsen et al. [20] modified (9) to include the organic phase term as in (10), where (P_g/V_L) represents the power input term, v_s represents the superficial gas velocity term, and ϕ_{ORG} represents the palm oil fraction term. The symbols of δ, β, α, and γ represent the empirical constants to be determined. Consider

$$k_La = \delta\left(\frac{P_g}{V_L}\right)^{\beta} v_s^{\alpha}(1 - \phi_{\text{ORG}})^{\gamma}. \quad (10)$$

Gas holdup, ε_G, generally depends on superficial gas velocity, power consumption, surface tension and viscosity of liquids and solid concentration [15]. For an agitated reactor, the most common gas holdup correlation used is as shown by (11) [21–23]. The symbols χ, λ, and ω represent empirical constants specific to the system under investigation. Consider

$$\varepsilon_G = \chi\left(\frac{P_g}{V_L}\right)^{\lambda} v_s^{\omega}. \quad (11)$$

3. Results and Discussion

The presence of palm oil in xanthan solution resulted in significant changes in the viscosity and rheological behavior, volumetric mass transfer coefficient, and gas holdup with respect to the different values of palm oil volume fraction, agitation rate, and aeration rate. The results obtained are discussed as follows.

3.1. Effect of Palm Oil on the Viscosity and Rheology of Xanthan Gum Solution. Xanthan solution (0.25%, w/v) exhibited a non-Newtonian pseudoplastic behavior. As palm oil was added into the xanthan solution at different oil fractions as presented in the Table 1, the rheological characteristics were changed. It was observed that the addition of palm oil slightly reduced the value of n and increased the value of K gradually in the power law (1). As the n value reduced with increase in the palm oil fractions, the degree of the pseudoplasticity of the xanthan solution increased with the increase in palm oil fraction than the pure xanthan solution.

The viscosities of the xanthan solution with different palm oil fractions were measured as a function of the shear rate and the trend showed that, for all palm oil fractions, the viscosity decreased with the increase in shear rate and reached almost plateau at the higher shear rates. This trend showed that the solutions were in good agreement with the pseudoplastic nature of the xanthan solution. The apparent viscosity of the solutions at different palm oil fractions at a shear rate of 12.56 s^{-1} was illustrated in Figure 2. It showed that the viscosity of xanthan solution increased gradually as the palm oil fraction was increased. Similar trend was obtained by Ma

Table 1: Rheological characteristics of xanthan solution at different palm oil fractions.

Palm oil volume fraction (%)	Flow index, n	Consistency index, K (cP^n)
0	0.4243	1108
5	0.4228	1191
10	0.4217	1280
15	0.4214	1334
20	0.4009	1399
50	0.344	2526

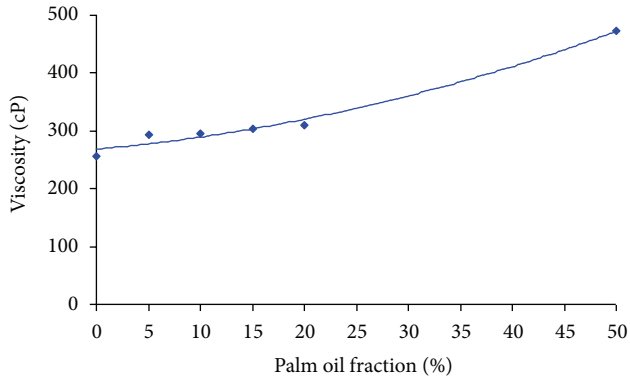

Figure 2: Variation of apparent viscosity of xanthan solution with palm oil fraction at a shear rate of 12.56 s^{-1}.

and Babosa-Cánovas [24] and they explained that, since the mean distance between the droplets was smaller, it facilitated compacting of oil, thereby leading to increase in the viscosity.

3.2. Effect of Palm Oil on k_La in Xanthan Gum Solution. Figure 3 showed the effect of palm oil on k_La as a function of agitation and aeration rate at different palm oil fraction. Comparing the values of k_La at the agitation rates of 400, 600, and 800 rpm, respectively, it was observed that the k_La values increased with the increase in agitation rate. Similar trends were also observed when the aeration rate was increased. The increase in aeration and agitation rate increased the degree of the liquid turbulence in the bioreactor. The liquid turbulence created was favorable to increase the k_La as it reduced the liquid film thickness at the gas-liquid interface [25]. Furthermore, the agitation was responsible for producing smaller bubbles, thus increasing the interfacial area, a, and it also increased the residence time of air bubbles [15, 25]. As a consequence, higher k_La with the increasing aeration and agitation rate was observed.

From the Figure 2, it is clearly showed that k_La was enhanced in the presence of palm oil. It was found that k_La was higher at 10% of oil fraction than that of pure xanthan solution for all the aeration and agitation rates. The highest k_La, 84.44 h^{-1}, was obtained at 1.25 vvm and 800 rpm. Most importantly, k_La values obtained for 10% oil fraction at 600 rpm were almost similar to that of 800 rpm. This observation proved that with the presence of 10% of palm

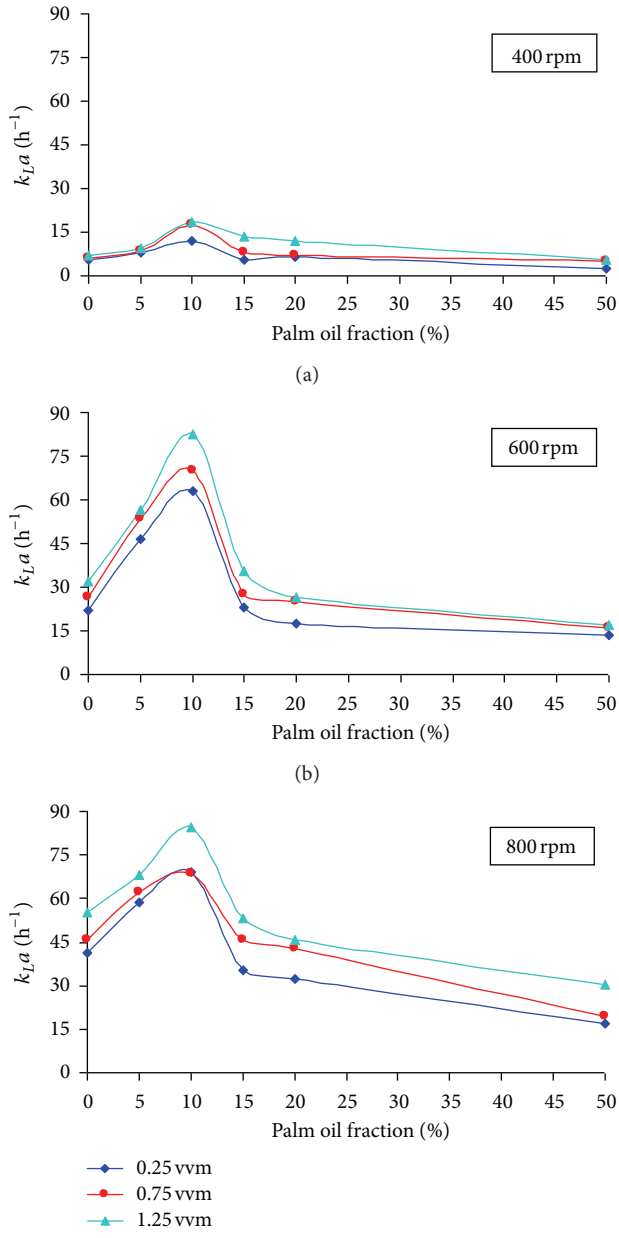

Figure 3: Influence of palm oil on k_La at varying agitation and aeration rate.

oil in the xanthan solution, high oxygen transfer could be obtained without supplying any additional energy.

Rols et al. [26] suggested a few possible reasons for the increments in k_La with the addition of organic phases to the fermentation broth. The increments in k_La was resulted from the increase in the liquid turbulence contributed from the rigid organic phase droplets. In addition to that the organic phase formed a thin layer at the gas-liquid interface acting as intermediary for transport of oxygen to the aqueous phase.

Further, as suggested by Yoshida et al., [6] the spreading coefficient value, S, also plays a major role in altering the oxygen transfer capability of the system. For an organic phase having a negative value of spreading coefficient would

Table 2: The enhancement factor of k_La at 10% palm oil fraction.

Agitation rate	Aeration rate		
	0.25 vvm	0.75 vvm	1.25 vvm
	$(k_La)_{po}/(k_La)_o$	$(k_La)_{po}/(k_La)_o$	$(k_La)_{po}/(k_La)_o$
400 rpm	2.23	2.95	2.71
600 rpm	2.85	2.65	2.59
800 rpm	1.68	1.49	1.52

form into floating lens like droplets in the system, while the coefficient being positive, the organic phase would spread on the water surface like a surface active agent to lower the surface tension and thereby increase the interfacial area, a, ultimately increasing k_La. Since the palm oil used in the present work also has a positive value of spreading coefficient (S = 38.3 mN/m), it is evident that the surface tension of the xanthan solution was reduced by the palm oil and hence decreased the air bubble size leading to increased interfacial area and k_La. Similar results were reported by Yoshida et al. [6] for toluene in water and oleic acid in water system with toluene and oleic acid having positive values of spreading coefficient.

The enhancements of k_La at 10% of oil fraction were more evident at 400 rpm and 600 rpm than the enhancements at 800 rpm. This could be seen in the form of enhancement factor as shown in Table 2. Enhancement factor can be defined as the ratio of k_La value in xanthan solution with palm oil, $(k_La)_{po}$ to that of pure xanthan solution, $(k_La)_o$ both measured at the same aeration and agitation rate. In this table, it could be observed that k_La was enhanced by almost three times at 400 rpm and 600 rpm compared to that of 800 rpm as the enhancement factor was only 1.57 in average.

The enhancement factor decreased with increase in the aeration and agitation rate. Similar trend was also observed by Galaction et al. [9] for the dodecane as the organic phase in the fermentation broth. They justified that reduction in the enhancement factor was due to the disruption of the dodecane superficial film or the removal of dodecane droplets from the bubble surface caused by the intensification of the mixing and turbulence at higher aeration and agitation rate. However, in this study, when the agitation rate was increased to 800 rpm, the mixing was intense and with further addition of the palm oil yielded tiny bubbles, thereby lowering the value of k_L [1] which contributed to the lower enhancement factor at 800 rpm compared to that of 400 and 600 rpm.

However, further increase in the oil fractions was found to decrease the k_La values. With the increase in palm oil fraction, the viscosity as well as the degree of the pseudoplasticity was found to increase as shown in Table 1. Small bubbles that produced in such solution remained in the solutions due to reduced rising velocity. They became rigid spheres having lower k_L value due to surface immobility and no gas circulation [17, 28]. Therefore, it is concluded that the effect of the increase in viscosity and the change in rheology of the solution with the increase in palm oil fraction outweighed the effect of decreased surface tension, which resulted in the decrease of k_La.

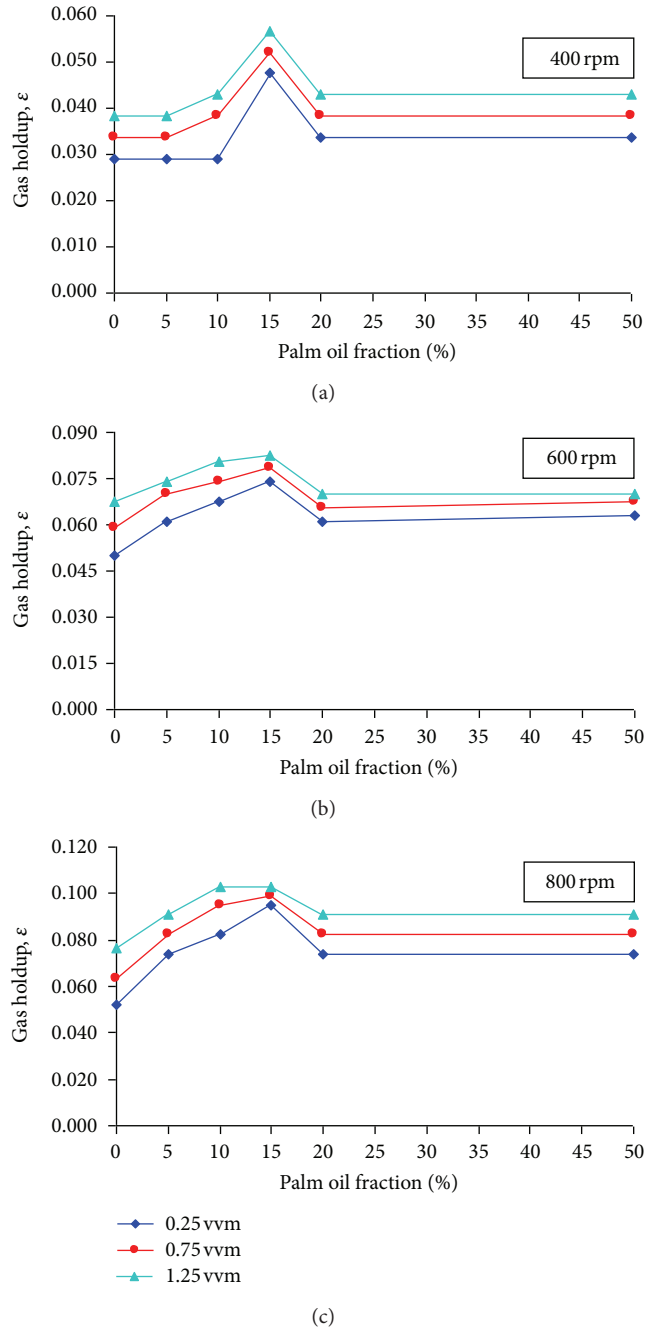

Figure 4: Influence of palm oil on gas holdup at varying agitation and aeration rate.

3.3. Effect of Palm Oil on Gas Holdup in Xanthan Gum Solution. As seen in Figure 4, the effect of palm oil on gas holdup in the xanthan solution showed similar trend for all the ranges of agitation and aeration rate studied. The gas holdup increased with the increase in palm oil fraction up to 15%. The increase in the gas holdup with the palm oil addition could be due to the dispersion of small bubbles in the system. As discussed earlier in Section 3.2, palm oil might have spread on the bubble surface, thus reducing the surface tension and decreasing the bubble size. The smaller bubbles had induced the gas holdup due to their low rise velocity and

Table 3: The empirical constants for k_La reported in the literature and in the current study.

Reference	Liquid system	Type of impeller	Constant β	Constant α	Constant γ	Valid for P_g/V_L (kW/m^3)	R^2	Average error, %	Correlation
[10]	Perfluorocarbon (PFC) in YPD medium with inactive cells	Rushton turbine	0.302	0.699	−1.378	NA	NA	15.7	Nielsen et al. [20] (10)
[20]	n-Hexadecane in broth medium	Rushton turbine	0.31	0.70	1.70	NA	NA	NA	
[27]	Methyl ricinoleate in *Yarrowia lipolytica* broth	Rushton turbine	0.6	0.8	−22	NA	NA	NA	
[27]	Tween 80 in *Yarrowia lipolytica* broth	Rushton turbine	0.4	0.7	−449	NA	NA	NA	
Current study	Xanthan gum solution with 0 to 10% palm oil fraction	Rushton turbine	0.4773	0.1620	−6.6029	0.079 to 1.11	0.77	58.75	Nielsen et al. [20] (10)
	Xanthan gum solution with 0% palm oil fraction	Rushton turbine	0.6674	0.2076	−6.6029	0.141 to 1.11	0.89	46.55	
Current study	Xanthan gum solution with 5% palm oil fraction	Rushton turbine	0.5361	0.1225	−6.1622	0.094 to 0.89	0.78	58.74	Nielsen et al. [20] (10)
	Xanthan gum solution with 10% palm oil fraction	Rushton turbine	0.4078	0.1702	−8.2896	0.079 to 0.89	0.68	46.47	
	Xanthan gum solution with 15% palm oil fraction	Rushton turbine	0.4401	0.4253	−2.7865	0.058 to 0.83	0.74	40.93	
	Xanthan gum solution with 20% palm oil fraction	Rushton turbine	0.4885	0.2777	−1.6270	0.039 to 0.72	0.98	15.59	
	Xanthan gum solution with 50% palm oil fraction	Rushton turbine	0.4334	0.1605	−0.0697	0.031 to 0.64	0.86	34.40	
Current study	Xanthan gum solution with 0% palm oil fraction	Rushton turbine	0.6674	0.2076	—	0.141 to 1.11	0.89	46.55	Cooper et al. [18] (9)
	Xanthan gum solution with 5% palm oil fraction	Rushton turbine	0.5361	0.1225	—	0.094 to 0.89	0.78	58.73	
	Xanthan gum solution with 10% palm oil fraction	Rushton turbine	0.4078	0.1702	—	0.079 to 0.89	0.68	46.47	
	Xanthan gum solution with 15% palm oil fraction	Rushton turbine	0.5343	0.3054	—	0.058 to 0.83	0.96	18.80	
	Xanthan gum solution with 20% palm oil fraction	Rushton turbine	0.4994	0.2740	—	0.039 to 0.72	0.98	14.00	
	Xanthan gum solution with 50% palm oil fraction	Rushton turbine	0.4458	0.3391	—	0.031 to 0.64	0.91	27.67	

longer residence time in the system than the bigger bubbles [1, 29]. This result is in agreement with Kawase and Moo-Young [30] who also found increments in gas holdup in their CMC solution with antifoam addition. They postulated that antifoam promoted the bubble breakup rather than bubble coalescence.

However, when the palm oil fraction reached beyond 20%, the gas holdup decreased and maintained the same until 50%. As mentioned in Section 3.1, palm oil addition into the xanthan solution changed the viscosity and the degree of pseudoplasticity of the solution. According to Machon et al. [31], the increase in the degree of pseudoplasticity had affected the stirrer's ability to dissipate power to the system to create smaller bubbles when the sparged air passed through and into the stirrer region. In addition, when the viscosity of the system increased, the degree of the liquid turbulence decreased which induced the bubble coalescence and these occurrences increased the proportion of larger bubbles in the liquid [32, 33] which had high rise velocities raced to the surface and ultimately reduced the gas holdup. Furthermore, even though the gas holdups at these fractions (20% and 50%) were lower than at the rest of the oil fraction, they were still higher than the holdup in pure xanthan solution. Hence, some of the tiny bubbles tend to remain lodged in the solution which contributed to the higher gas holdup. Similar occurrences were also observed by Doran [1].

3.4. Correlations for Volumetric Mass Transfer Coefficient in Xanthan Gum Solution. This experimental study is the first of its kind to report the correlations for k_La obtained for palm oil in xanthan solution. Other organic phases were used in various fermentation broths and for a few bioreactor systems. Equation (10) was used to fit the correlations for k_La in the literature which are listed in Table 3. whereas in this study, the experimental data was fitted into both correlations (9) and (10) to find k_La for palm oil in xanthan solution.

Table 4: The empirical constants for ε_G by (11) reported in the literature and in the current study.

Reference	Liquid system	Constant χ	Constant λ	Constant ω	Type of impeller	R^2	Average relative error (%)	Valid for P_g/V_L (kW/m^3)
[21]	Water	—	0.25	0.75	Flat blade turbine	NA	NA	NA
[22]	Na_2SO_4	—	0.4903	0.5788	Rushton turbine	NA	9.3	NA
[23]	Tap water	—	0.478	0.4910	Disc turbine-pitched blade	0.98	NA	NA
[23]	Tap water	—	0.4244	0.6904	Rushton turbine	0.98	NA	NA
Current study	Xanthan gum solution with 0% palm oil fraction	0.0080	0.2385	0.2180	Rushton turbine	0.74	14.47	0.141–1.11
	Xanthan gum solution with 5% palm oil fraction	0.0061	0.3501	0.1435	Rushton turbine	0.90	12.15	0.094–0.89
	Xanthan gum solution with 10% palm oil fraction	0.0065	0.3528	0.1626	Rushton turbine	0.93	10.87	0.079–0.89
	Xanthan gum solution with 15% palm oil fraction	0.0161	0.2507	0.0773	Rushton turbine	0.98	3.27	0.058–0.83
	Xanthan gum solution with 20% palm oil fraction	0.0119	0.2558	0.1395	Rushton turbine	0.96	5.99	0.039–0.72
	Xanthan gum solution with 50% palm oil fraction	0.0178	0.1890	0.1690	Rushton turbine	0.84	12.06	0.031–0.64

Equation (9) considered the effect of superficial gas velocity and power input on k_La while (10) took into account the effect of palm oil fraction in addition. The experimental data was fitted well into both equations with high correlation coefficients. The values of the empirical constants obtained are listed in Table 3.

While using (9), the k_La values obtained were highly dependent on the specific power input supplied and the empirical constants obtained were within the range suggested by Winkler [19]. This indicated that a change in specific power input would change the k_La significantly than the change in the superficial gas velocity. However, while using (10), the exponent of palm oil fraction dominated the correlation. This meant that the oil fraction had the highest influence on k_La. The negative sign at the exponent value showed that adding palm oil up to 10% volume fraction would increase the k_La.

According to Kawase and Moo-Young [34], for a non-Newtonian system, the suggested values of β are between 0.37 and 0.80, while, for α, the values are between 0.20 and 0.84. Comparing the values in Table 3, it was found that β values obtained in this study were within the range specified by Kawase and Moo-Young [34]. However, for α, the values were found lower at 5% and 10% oil fractions, respectively. As this constant is a measure of aeration rate, it corresponds to lower k_La values compared to that of other oil fractions. It might be due to insufficient aeration compared to the other oil fraction. However, the constant γ was not comparable. This could be due to the difference in the bioreactor geometry, type of organic phase used in the study, and different rheological behavior of the bioreactor systems.

3.5. Correlations for Gas Holdup in Xanthan Gum Solution. Again this study is the first of its kind to report the correlation for ε_G obtained for palm oil in xanthan solution. Few researchers used (11) for their agitated vessels handling different solution, to fit the correlation for ε_G which are listed in Table 4.

The correlations found in the literature considered only the empirical constants λ and ω in (11), whereas in this study all the three terms were considered and the results are listed in Table 4. For xanthan solution, the empirical constants ranged within $0.0061 < \chi < 0.0178$, $0.1890 < \lambda < 0.3528$, and $0.0773 < \omega < 0.2180$. As the value of λ was more than the other two constants for all palm oil fractions, it could be concluded that the change in specific power input had more impact on gas holdup than the change in superficial gas velocity for xanthan solution.

As shown in Table 4, it can be seen that the λ values obtained in this study are comparable with the value obtained by de Figueiredo and Calderbank [21]. However, due to the significant difference in the type and properties such as viscosity and rheological behavior of the organic phase used, a slight variation in the values of λ and ω is observed when compared to the literature.

4. Conclusions

The volumetric mass transfer coefficient, k_La, of xanthan solution was measured at varying operating variables and palm oil fraction in a stirred tank bioreactor. It was evident that the addition of palm oil up to 10% volume fraction enhanced k_La by 1.5 to 3 folds with the highest k_La value of 84.44 h^{-1}. It was also found that increase in palm oil fraction

increased the viscosity and rheology of the xanthan solution. This favorable effect was contributed from the properties of palm oil that promoted the production of small bubbles. This ultimately outweighed the positive effect on bubble size and therefore affected both k_La and gas holdup. The k_La values obtained were also correlated with the power input, superficial gas velocity, and palm oil fraction in two different forms of equations which were found to fit well with very high correlation coefficients.

Abbreviations

a: Gas liquid interfacial area per unit volume (m^2/m^3)
C_L^*: Oxygen concentration in the equilibrium with the gas phase (mg/L), also known as the solubility (at the phase boundary)
C_L: Actual dissolved oxygen concentration in the liquid (mg/L)
CMC: Carboxymethyl cellulose
DO: Dissolved oxygen
C_{me}: DO concentration in the liquid measured by the probe (mg/L)
H_{G+L}: Level of aerated liquid (cm)
H_L: Level of unaerated liquid (cm)
K: Consistency index ($Pa{\cdot}s^n$)
k_L: Liquid phase oxygen transfer coefficient (m/s)
k_La: Volumetric mass transfer coefficient (h^{-1})
n: Flow behavior index (dimensionless)
N: Impeller speed, s^{-1}
P: Power input, W
(P_g/V_L): Specific power input in an aerated condition, W/m^3
T: Working torque, N·m
T_o Blank torque, N·m
S: Spreading coefficient, mN/m
ε_G: Gas holdup
τ : Shear stress (N/m^2)
γ : Shear rate (s^{-1})
τ_r: Response time (s)
v_s: Superficial gas velocity, m/s
vvm: Gas volume flow per liquid volume per minute (volume per volume per minute)
ϕ_{ORG}: Oil fraction in the bioreactor
δ, β, α, γ: Empirical constants for k_La, specific to the system under investigation
χ, λ, ω: Empirical constants for ε_g, specific to the system under investigation.

Conflict of Interests

The authors declare that they have no conflict of interests.

Authors' Contribution

All of the authors contributed to a similar extent, overall, and all authors have seen and agreed to the submission of this paper.

Acknowledgment

This work was financially supported by the Ministry of Science, Technology and Innovation (MOSTI), Malaysia, through the research Grant no. 100-IRDC/SF 16/6/2(50/2007).

References

[1] P. M. Doran, *Bioprocess Engineering Principles*, Academic Press, London, UK, 1996.

[2] S. M. Sauid and V. V. P. S. Murthy, "Effect of palm oil on oxygen transfer in a stirred tank bioreactor," *Journal of Applied Sciences*, vol. 10, no. 21, pp. 2745–2747, 2010.

[3] B. Katzbauer, "Properties and applications of xanthan gum," *Polymer Degradation and Stability*, vol. 59, no. 1–3, pp. 81–84, 1998.

[4] F. García-Ochoa, V. E. Santos, J. A. Casas, and E. Gómez, "Xanthan gum: production, recovery, and properties," *Biotechnology Advances*, vol. 18, no. 7, pp. 549–579, 2000.

[5] F. García-Ochoa, E. G. Castro, and V. E. Santos, "Oxygen transfer and uptake rates during xanthan gum production," *Enzyme and Microbial Technology*, vol. 27, no. 9, pp. 680–690, 2000.

[6] F. Yoshida, T. Yamane, and Y. Miyamoto, "Oxygen absorption into oil-in-water emulsions: a study on hydrocarbon fermentors," *Industrial and Engineering Chemistry*, vol. 9, no. 4, pp. 570–577, 1970.

[7] J. L. Rols and G. Goma, "Enhanced oxygen transfer rates in fermentation using soybean oil-in-water dispersions," *Biotechnology Letters*, vol. 13, no. 1, pp. 7–12, 1991.

[8] Y. M. Lo, C. H. Hsu, S. T. Yang, and D. B. Min, "Oxygen transfer characteristics of a centrifugal, packed-bed reactor during viscous xanthan fermentation," *Bioprocess and Biosystems Engineering*, vol. 24, no. 3, pp. 187–193, 2001.

[9] A.-I. Galaction, D. Cascaval, C. Oniscu, and M. Turnea, "Enhancement of oxygen mass transfer in stirred bioreactors using oxygen-vectors. 1. Simulated fermentation broths," *Bioprocess and Biosystems Engineering*, vol. 26, no. 4, pp. 231–238, 2004.

[10] P. F. F. Amaral, M. G. Freire, M. H. M. Rocha-Leão, I. M. Marrucho, J. A. P. Coutinho, and M. A. Z. Coelho, "Optimization of oxygen mass transfer in a multiphase bioreactor with perfluorodecalin as a second liquid phase," *Biotechnology and Bioengineering*, vol. 99, no. 3, pp. 588–598, 2008.

[11] L.-K. Ju and S. Zhao, "Xanthan fermentations in water/oil dispersions," *Biotechnology Techniques*, vol. 7, no. 7, pp. 463–468, 1993.

[12] S. G. Kuttuva, A. S. Restrepo, and L.-K. Ju, "Evaluation of different organic phases for water-in-oil xanthan fermentation," *Applied Microbiology and Biotechnology*, vol. 64, no. 3, pp. 340–345, 2004.

[13] J. C. Allen and R. J. Hamilton, *Rancidity in Foods*, Chapman & Hall, New York, NY, USA, 1994.

[14] K. Ahmad, C. C. Ho, W. K. Fong, and D. Toji, "Properties of palm oil-in-water emulsions stabilized by nonionic emulsifiers," *Journal of Colloid and Interface Science*, vol. 181, no. 2, pp. 595–604, 1996.

[15] P. F. Stanbury and A. Whitaker, *Principles of Fermentation Technology*, Butterworth-Heinemann, Great Britain, UK, 2nd edition, 1995.

[16] W. A. Brown, "Developing the best correlation for estimating the transfer of oxygen from air to water," *Chemical Engineering Education*, vol. 35, no. 2, pp. 134–147, 2001.

[17] F. Garcia-Ochoa and E. Gomez, "Bioreactor scale-up and oxygen transfer rate in microbial processes: an overview," *Biotechnology Advances*, vol. 27, no. 2, pp. 153–176, 2009.

[18] C. M. Cooper, G. A. Fernstrom, and S. A. Miller, "Performance of agitated gas-liquid contactors," *Industrial & Engineering Chemistry*, vol. 36, pp. 504–509, 1944.

[19] M. A. Winkler, Ed., *Chemical Engineering Problems in Biotechnology*, Elsevier Science, England, UK, 1990.

[20] D. R. Nielsen, A. J. Daugulis, and P. J. McLellan, "A novel method of simulating oxygen mass transfer in two-phase partitioning bioreactors," *Biotechnology and Bioengineering*, vol. 83, no. 6, pp. 735–742, 2003.

[21] M. M. L. de Figueiredo and P. H. Calderbank, "The scale-up of aerated mixing vessels for specified oxygen dissolution rates," *Chemical Engineering Science*, vol. 34, no. 11, pp. 1333–1338, 1979.

[22] T. Moucha, V. Linek, and E. Prokopová, "Gas hold-up, mixing time and gas-liquid volumetric mass transfer coefficient of various multiple-impeller configurations: rushton turbine, pitched blade and techmix impeller and their combinations," *Chemical Engineering Science*, vol. 58, no. 9, pp. 1839–1846, 2003.

[23] K. Saravanan, V. Ramamurthy, and K. Chandramohan, "Gas holdup in multiple impeller agitated vessels," *Modern Applied Science*, vol. 3, no. 2, pp. 49–59, 2009.

[24] L. Ma and G. V. Barbosa-Cánovas, "Rheological characterization of mayonnaise. Part II: flow and viscoelastic properties at different oil and xanthan gum concentrations," *Journal of Food Engineering*, vol. 25, no. 3, pp. 409–425, 1995.

[25] R. K. Finn, "Agitation-aeration in the laboratory and in industry," *Microbiology and Molecular Biology Reviews*, vol. 18, pp. 254–274, 1954.

[26] J. L. Rols, J. S. Condoret, C. Fonade, and G. Goma, "Mechanism of enhanced oxygen transfer in fermentation using emulsified oxygen-vectors," *Biotechnology and Bioengineering*, vol. 35, no. 4, pp. 427–435, 1990.

[27] N. Gomes, M. Aguedo, J. Teixeira, and I. Belo, "Oxygen mass transfer in a biphasic medium: influence on the biotransformation of methyl ricinoleate into γ-decalactone by the yeast Yarrowia lipolytica," *Biochemical Engineering Journal*, vol. 35, no. 3, pp. 380–386, 2007.

[28] K. G. Clarke and L. D. C. Correia, "Oxygen transfer in hydrocarbon-aqueous dispersions and its applicability to alkane bioprocesses: a review," *Biochemical Engineering Journal*, vol. 39, no. 3, pp. 405–429, 2008.

[29] G. D. Najafpour, *Biochemical Engineering and Biotechnology*, Elsevier, Amsterdam, The Netherlands, 2007.

[30] Y. Kawase and M. Moo-Young, "Influence of antifoam agents on gas hold-up and mass transfer in bubble columns with non-newtonian fluids," *Applied Microbiology and Biotechnology*, vol. 27, no. 2, pp. 159–167, 1987.

[31] V. Machon, J. Vlcek, A. W. Nienow, and J. Solomon, "Some effects of pseudoplasticity on hold-up in aerated, agitated vessels," *The Chemical Engineering Journal*, vol. 19, no. 1, pp. 67–74, 1980.

[32] S. J. Arjunwadkar, K. Sarvanan, P. R. Kulkarni, and A. B. Pandit, "Gas-liquid mass transfer in dual impeller bioreactor," *Biochemical Engineering Journal*, vol. 1, no. 2, pp. 99–106, 1998.

[33] F. García-Ochoa and E. Gómez, "Mass transfer coefficient in stirred tank reactors for xanthan gum solutions," *Biochemical Engineering Journal*, vol. 1, no. 1, pp. 1–10, 1998.

[34] Y. Kawase and M. Moo-Young, "Volumetric mass transfer coefficients in aerated stirred tank reactors with Newtonian and non-Newtonian media," *Chemical Engineering Research and Design*, vol. 66, no. 3, pp. 284–288, 1988.

Hindawi Publishing Corporation
BioMed Research International
Volume 2013, Article ID 265618, 9 pages
http://dx.doi.org/10.1155/2013/265618

Research Article

Biohydrogen Production and Kinetic Modeling Using Sediment Microorganisms of Pichavaram Mangroves, India

P. Mullai,[1] Eldon R. Rene,[2] and K. Sridevi[1]

[1] *Pollution Control Research Laboratory, Department of Chemical Engineering, Annamalai University, Annamalai Nagar, Tamil Nadu 608 002, India*
[2] *Core Group Pollution Prevention and Resource Recovery, Department of Environmental Engineering and Water Technology, UNESCO-IHE, P.O. Box 3015, 2601 DA, Delft, The Netherlands*

Correspondence should be addressed to P. Mullai; pmullai@yahoo.in

Received 11 September 2013; Accepted 11 October 2013

Academic Editor: Kannan Pakshirajan

Mangrove sediments host rich assemblages of microorganisms, predominantly mixed bacterial cultures, which can be efficiently used for biohydrogen production through anaerobic dark fermentation. The influence of process parameters such as effect of initial glucose concentration, initial medium pH, and trace metal (Fe^{2+}) concentration was investigated in this study. A maximum hydrogen yield of 2.34, 2.3, and 2.6 mol H_2 mol^{-1} glucose, respectively, was obtained under the following set of optimal conditions: initial substrate concentration—10,000 mg L^{-1}, initial pH—6.0, and ferrous sulphate concentration—100 mg L^{-1}, respectively. The addition of trace metal to the medium (100 mg L^{-1} $FeSO_4 \cdot 7H_2O$) enhanced the biohydrogen yield from 2.3 mol H_2 mol^{-1} glucose to 2.6 mol H_2 mol^{-1} glucose. Furthermore, the experimental data was subjected to kinetic analysis and the kinetic constants were estimated with the help of well-known kinetic models available in the literature, namely, Monod model, logistic model and Luedeking-Piret model. The model fitting was found to be in good agreement with the experimental observations, for all the models, with regression coefficient values >0.92.

1. Introduction

Fossil Fuels are the primary energy source for the world's increasing energy consumption. According to a recent survey, total world energy use rises from 524 quadrillion British thermal units (Btu) in 2010 to 630 quadrillion Btu in 2020 and to 820 quadrillion Btu in 2040 [1]. This fossil fuel eventually leads to foreseeable depletion due to limited energy resources; however, in the last few years, research and development activities pertaining to large-scale production of alternate resources of energy such as biodiesel, biohydrogen and bioethanol have risen [2–8]. In the days of fast depleting fossil fuel, biohydrogen has become a promising and viable energy source owing to its inherent advantages: zero-pollution, carbon-free, inexhaustible, recyclable, and highest energy density. However, most of hydrogen is currently produced from non-renewable sources using natural gas (50%), petroleum-derived naphthenes and distillates (30%), coal (18%), and electricity produced from variety of fuels (2%). Since this strategy leads to the depletion of non-renewable energy sources and is considered as a less ecofriendly alternative, it becomes crucial to go in for the production of sustainable energy source.

Biohydrogen production through anaerobic fermentation is a sustainable alternate for the energy crisis and green environment [9–12]. Fermentative hydrogen production processes are technically feasible and economically competitive and have large-scale commercialization possibilities [8, 13–16]. The present work focuses on biohydrogen production by dark fermentative approach using mangrove sediments of Pichavaram (located in Tamil Nadu, India). It is known that no research has been made using the sediments of mangroves, new mixed consortia to produce biohydrogen. Mangrove sediments are inherently rich in organic content [17–19]. The advantages of this sediment can be summarized as follows: flexible substrate utilization and the simplicity

of handling, no major storage problems, no problems with strain degradation, no preculturing required, and sediments are available at low cost.

A kinetic model can adequately describe the relationship among the different state variables and explain the behavior of fermentation quantitatively by providing useful information that can be subsequently used for analysis, design, and operation of any fermentation process [20–22]. The unstructured kinetic models are frequently employed for modeling microbial systems because they are simple, yet can provide useful information about the process [11, 23, 24]. In this study, three unstructured kinetic models, namely, Monod, logistic, and Luedeking-Piret models [25, 26] were used to determine the kinetic parameters.

2. Materials and Methods

2.1. Selective Enrichment on Biohydrogen Producing Mangrove Sediments. The sediments were collected from the mangrove rhizosphere of Pichavaram, Tamil Nadu, India, at a depth of 100 cm, and later stored in sterile polythene bags. Heat-shock treatment was done on this sediment sample, by constant heating at 110°C for 2 h, in order to stimulate spore germination and eliminate all vegetative cells, particularly methanogens. The coarse particles were removed using a stainless steel mesh, while the finer fractions were stored at 4°C [27].

2.2. Nutrient Medium. The nutrient medium (non-sterilized) used in this study had the following chemical composition (per litre): NH_4Cl—0.5 mg, K_2HPO_4—0.25 mg, $MgCl_2{\cdot}6H_2O$—0.3 mg, $NiSO_4$—0.016 mg, $CoCl_2$—0.025 mg, $ZnCl_2$—0.0115 mg, $CuCl_2$—0.0105 mg, $CaCl_2$—0.005 mg, and $MnCl_2$—0.015 mg.

2.3. Batch Experiments. Batch tests were conducted in duplicate, in 1 L Erlenmeyer flasks (working volume: 0.7 L), fitted air-tightly with rubber septum, and adequately sealed using commercially available fix gels. The effect of process parameters on biohydrogen yield, namely, the influence of initial substrate concentration (glucose), initial pH, and trace metal, Fe^{2+} concentration, was evaluated by carrying out experiments at different low to high levels of these parameters, and the average values of biohydrogen yield were presented. The pH of the growth medium was adjusted using 1N HCl or 1N NaOH during the start of the experiments. The growth medium was inoculated with 100 g of pretreated sediment under aseptic conditions, and the flasks were incubated at 35°C for fermentation.

2.4. Analytical Methods. The biohydrogen gas was measured using wet gas flow meter (Toshniwal, India). The gas content was analyzed using a gas chromatograph (Shimadzu, 221-70026-34, Japan) equipped with a thermal conductivity detector (TCD), and the column was packed with dual packed column. The operating temperatures of the column, detector and injector, were 40°C, 80°C, and 50°C, respectively. Biomass concentration was measured as volatile suspended solid (VSS) and analyzed according to Standard Methods [28]. Glucose concentration was measured by DNS method using spectrophotometer (Elico, India) at a λ_{max} of 550 nm [29]. The sludge granules were characterized using scanning electron microscope (SEM) (JEOL-JSM, 5300, Japan) at a resolution of 4.5 nm at 15 kVA with a working distance of 8 mm.

3. Results and Discussion

Biohydrogen fermentation reached nearly constant values at the end of 120 h for each batch tests, including their duplicates. Glucose degradation efficiencies, cumulative biohydrogen gas, and hydrogen yields were calculated for each set of experimental condition.

3.1. Effect of Initial Glucose Concentration. For initial glucose concentrations of 4,000, 7,000, 10,000, 13,000, and 16,000 mg L^{-1}, the values of cumulative biohydrogen production and glucose degrading efficiencies were 430, 1190, 2600, 2200, and 2099 mL and 75, 83, 90, 80, and 72%, respectively (Figure 1). The effect of initial glucose concentration was observed when the initial medium pH was kept constant at 6.0 for all the test vials. It was observed that biohydrogen production increased with an increase in glucose concentration from 4,000 to 10,000 mg L^{-1}, and after that the biohydrogen production decreased with further increase in glucose concentration. A maximum biohydrogen yield of 2.34 mol H_2 mol^{-1} glucose was obtained when initial glucose concentration was 10,000 mg L^{-1}. Furthermore, when initial glucose concentration was increased to 13,000 mg L^{-1} and 16,000 mg L^{-1}, the hydrogen yield obtained was 2.02 and 1.46 mol H_2 mol^{-1} glucose, respectively (Figure 1). The decrease in biohydrogen production at higher substrate concentrations might be due to the formation of more volatile fatty acids (data not shown here) which resulted in over-acidification of bacterial cultures, thereby reducing the medium pH, and thus inhibited fermentation. Several reports have shown that although high substrate concentrations showed high biohydrogen production initially, they tend to drop to low levels due to simultaneous acid inhibition, and increased partial pressure of hydrogen in the flask [30, 31]. Maintaining the carbon source levels at an optimum, in bioreactors, is an important parameter during pilot-scale trials and during the continuous production of biohydrogen. Failure to do so could affect the growth rate of the microorganism, its specific substrate utilization rate, enzyme activity, and overall yield of the process itself. Hence, to avoid the formation of volatile fatty acids and the phenomena of substrate inhibitions, the concentration of the substrate (glucose) in the liquid-phase must be maintained at optimal levels.

3.2. Effect of Medium pH. The profile of cumulative biohydrogen gas production at various initial medium pH conditions is shown in Figure 2. The optimum initial glucose concentration of 10,000 mg L^{-1} was constantly maintained

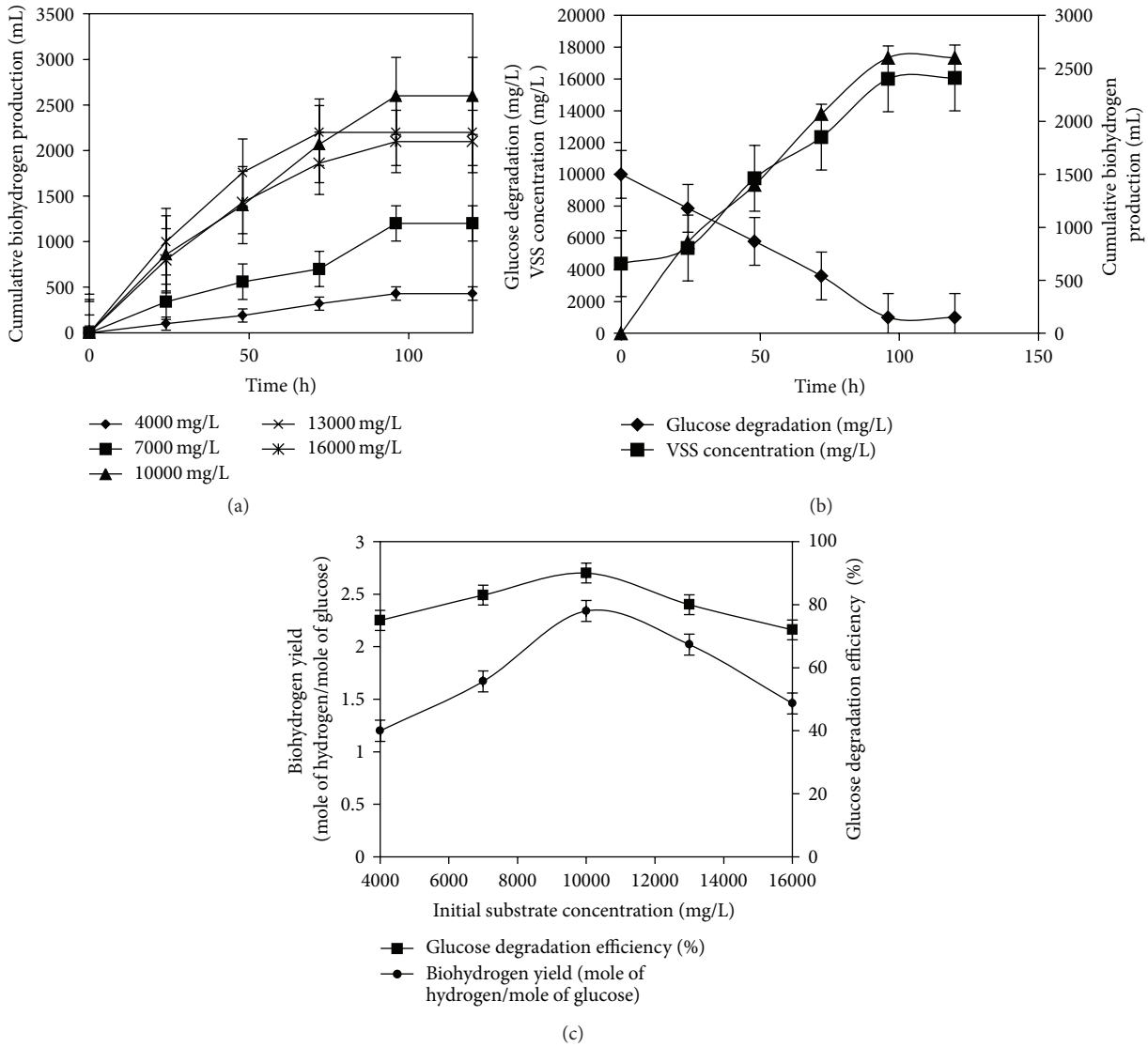

Figure 1: (a) Profile of cumulative biohydrogen production at various initial glucose concentrations. (b) Dynamic profile of glucose degradation, biomass concentration, and cumulative biohydrogen production. (c) Biohydrogen yield and glucose degradation efficiency for various initial glucose concentrations.

for these experiments. The substrate degradation efficiencies obtained were 83, 75, 80, 90, and 83%, respectively, at initial pH values of 4.5, 5.0, 5.5, 6.0, and 6.5. The final pH of these test vials at the end of the test period ranged from 1.9 to 3.4. The medium pH is an important operational parameter for hydrogen production, since it affects anaerobic pathways and the activities of hydrogenase enzymes [32]. When the initial medium pH was varied by keeping initial substrate concentration constant at 10,000 mg L^{-1}, the maximum hydrogen yield of 2.3 mol H_2 mol^{-1} glucose was obtained at an initial pH of 6.0 (Figure 2). Initially, when the medium pH was at 4.5, the lowest hydrogen yield of 0.9 mol H_2 mol^{-1} glucose obtained indicated that the higher acidic condition inhibited the fermentation. The hydrogen yield substantially increased to 2.3 mol H_2 mol^{-1} glucose at the pH of 6.0. The hydrogen yield decreased to 2.0 mol H_2 mol^{-1} glucose at a higher pH value (6.5). It was found that, under near neutral pH condition, a significant amount of substrates was consumed by bacterial growth other than hydrogen production which was verified by the higher biomass concentration at higher pH. Thus, it could be stated that the favourable pH for this mixed bacterial culture was 6.0. Similar results of maximum hydrogen production at the pH of 6.0 were reported [33].

3.3. Effect of Fe^{2+} Concentration. Figure 3 illustrates the effect of fermentation time on the cumulative hydrogen production in batch tests under different Fe^{2+} concentrations. The values of cumulative biohydrogen production for five different Fe^{2+} concentrations: 100, 200, 300, 400, and 500 mg L^{-1} were 3040, 2800, 2610, 2300, and 1180 mL, respectively, and the corresponding substrate degradation efficiencies were 94, 92, 91, 90, and 80%. Hydrogen yields of 2.6, 2.3, 2.1, 1.8, and 0.9 mol

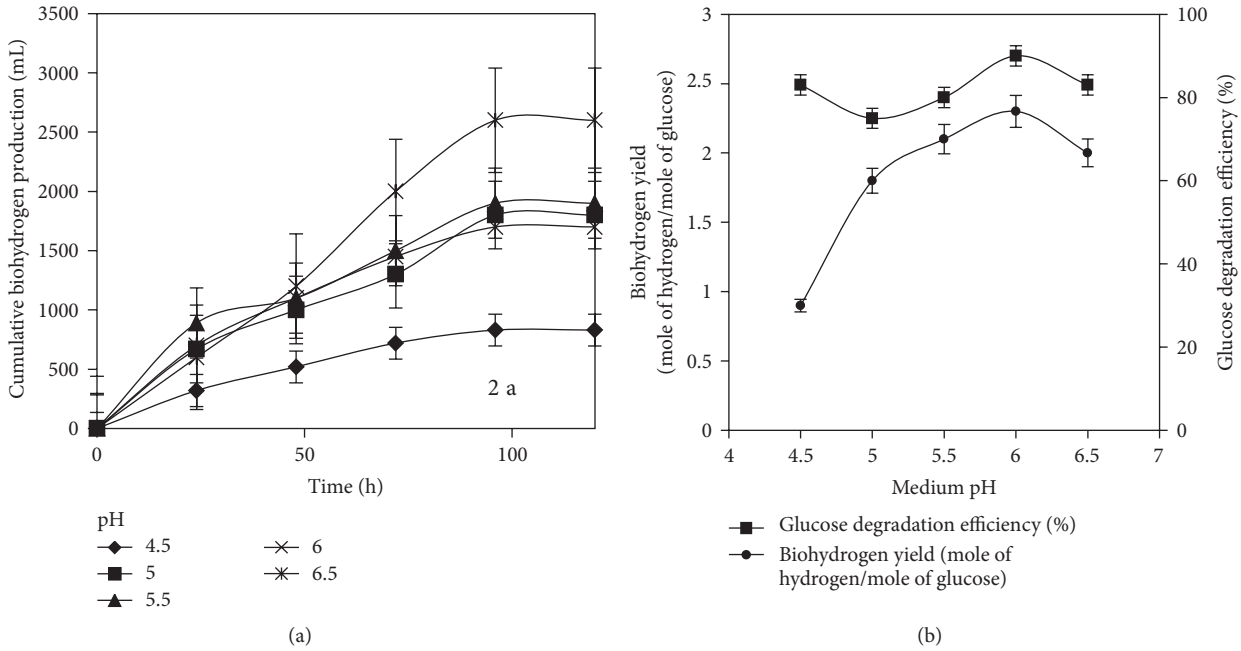

Figure 2: (a) Profile of cumulative biohydrogen production at various medium pH. (b) Biohydrogen yield and glucose degradation efficiency for various medium pH.

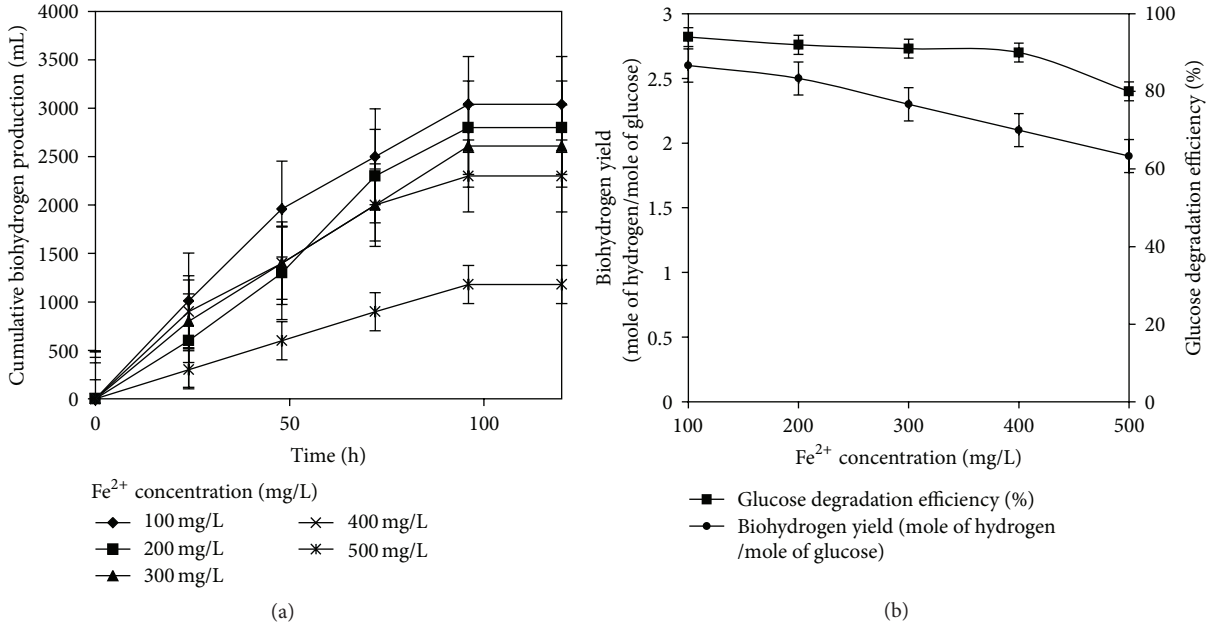

Figure 3: (a) Profile of cumulative biohydrogen production at different Fe^{2+} concentrations. (b) Biohydrogen yield and glucose degradation efficiency for various Fe^{2+} concentrations.

H_2 mol^{-1} glucose were obtained for various concentrations of iron as illustrated in Figure 3. At 100 mg L^{-1} of Fe^{2+} concentration, the biohydrogen production was at its maximum (2.6 mol H_2 mol^{-1} glucose), and it was found to decrease when the Fe^{2+} concentration was increased (Figure 3). Similar trend was obtained by previous researchers [34–36]. The addition/presence of Fe^{2+} concentration in the fermentation medium could influence the fermentative hydrogen production by influencing the activity of hydrogenase enzyme. The literature reports have shown that metal ions affect the microrganisms involved in hydrogen fermentation, beyond a threshold concentration range, and these effects include the

Table 1: Comparison of kinetic parameters for Monod model.

Process	Type of culture	Substrate	μ_{max}	K_s	R^2	Author
Batch	Mixed anaerobic culture	Sucrose	0.078 h^{-1}	—	—	[26]
Batch	*Clostridium pasteurianum* CH4	Sucrose	0.31 h^{-1}	4.39 g COD L^{-1}	0.935	[37]
Batch	Mixed sludge	Glucose	0.03 g biomass/g biomass/day	—	—	[38]
Batch	Mixed culture	Xylose	0.17 h^{-1}	0.75 g/L	—	[39]
Sequential batch	Activated sludge	Glucose	0.125 h^{-1}	—	—	[40]
Batch	Acidogenic mixed culture	Glucose	0.163 h^{-1}	—	—	[41]
Batch	Acidogenic mixed culture	Fructose	0.108 h^{-1}	—	—	[41]
Batch	Anaerobic acclimatized banana stem sludge	Banana stem waste	0.111 h^{-1}	0.330 g/L	0.902	[42]
Batch	Sediments of Pichavaram mangroves	Glucose	0.166 h^{-1}	0.112 g/L	0.971	Present study

Table 2: Comparison of kinetic parameters of logistic model.

Process	Type of culture	Substrate	k (h^{-1})	R^2	Author
Batch	*Rhodobacter sphaeroides*	Malic acid	0.098	0.98	[25]
Batch	Sludge	Glucose	—	0.99	[26]
Batch	Sediments of Pichavaram mangroves	Glucose	0.034	0.943	Present study

following: decreased hydrogen production rate, an increase in lag-phase time, and formation of soluble microbial products [34].

3.4. Kinetics of Biohydrogen Production in Batch Culture

3.4.1. Cell Growth Kinetics as a Function of Substrate. Monod kinetics was applied to study the cell growth kinetics during biohydrogen production. Monod kinetics is given by the following equation:

$$\mu = \frac{1}{x}\frac{dx}{dt} = \frac{\mu_{max} S}{K_s + S}, \tag{1}$$

where μ is the specific growth rate (h^{-1}), μ_{max} is the maximum specific growth rate (h^{-1}), x is the cell concentration ($g\,L^{-1}$), and K_s is the substrate consumption rate constant ($g\,L^{-1}$). Equation (1) may be linearized, as shown in (2) to estimate the kinetic parameters, and regression analysis is used to find the best fit for a straight line on a plot of $1/\mu$ versus $1/S$ to determine the values of μ_{max} and K_s (Figure 4):

$$\frac{1}{\mu} = \frac{K_s}{\mu_{max}} \cdot \frac{1}{S} + \frac{1}{\mu_{max}}. \tag{2}$$

Table 1 shows the different values of kinetic parameters obtained from Monod model, while Figure 4 shows the correlation between the model fitted and experimental values. The μ_{max} and K_s were calculated as 0.166 h^{-1} and 0.112 $g\,L^{-1}$ respectively.

3.4.2. Cell Growth Rate as a Function of Cell Concentration. The specific growth rate for the logistic curve relates the change of specific growth rate with respect to change in cell concentration (x). The Riccatti equation is given by the following equation:

$$\frac{dx}{dt} = kx\left(1 - \beta x\right), \tag{3}$$

where $\beta = 1/x_{max}$.

On integrating and applying the limits,

$$\int_{x_0}^{x} \frac{dx}{x\left(1 - \beta x\right)} = k\int_0^t dt,$$
$$e^{kt} = \frac{x\left(1 - \beta x_0\right)}{x_0\left(1 - \beta x\right)}. \tag{4}$$

Rearranging the above equation, cell concentration x is given by

$$x = \frac{x_0 e^{kt}}{1 - \beta x_0\left(1 - e^{kt}\right)}. \tag{5}$$

x_{max} and k kinetic parameters are calculated using logistic curve.

However, for the purposes of batch hydrogen production experiments, where the initial substrate concentrations and the inoculation volume are kept constant, the logistic model is only a fair approximation of the growth curve. From Figure 5, kinetic parameters were estimated and their values were as follows: k = 0.061 h^{-1}; x_{max} = 30.74 gVSS L^{-1}. Table 2 shows the comparison of different kinetic parameters for the logistic model. The experimental and model fitted specific growth rates were significant with high regression coefficient values. From Figure 5, it could be inferred that the model performed well during the simulation of batch reactors performance, with respect to the glucose and biomass concentration.

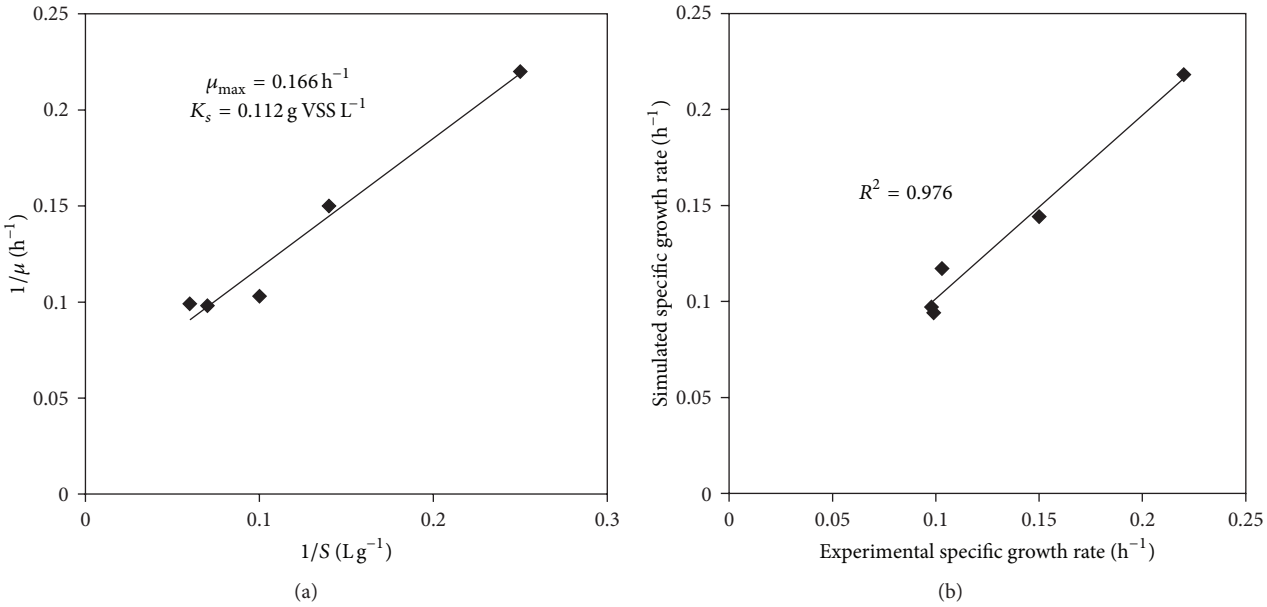

Figure 4: Monod model for substrate utilization kinetics.

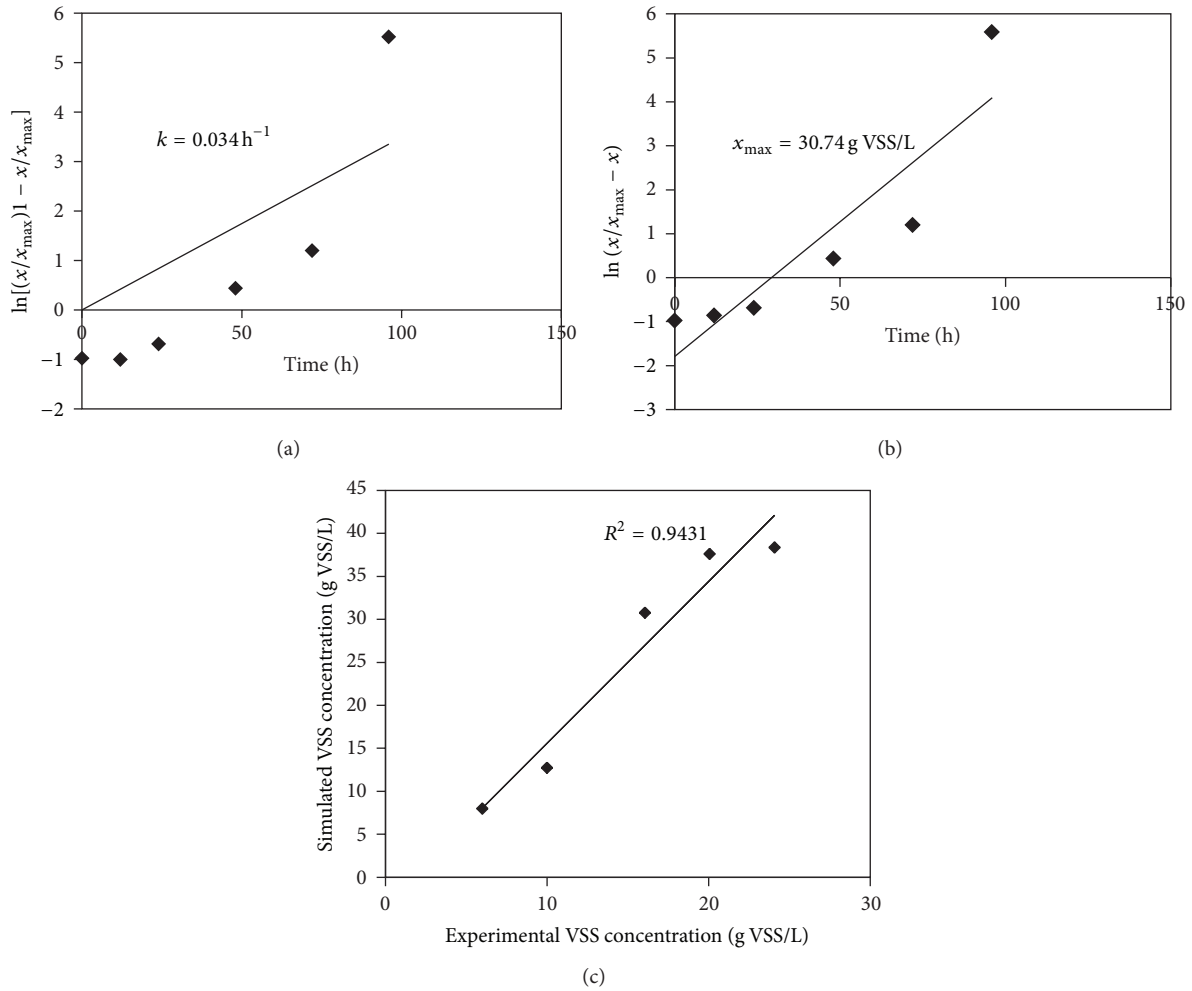

Figure 5: Logistic model for cell growth kinetics.

Table 3: Comparison of kinetic parameters of Luedeking-Piret model.

Process	Type of culture	Substrate	$Y_{P/x}$	R^2	Author
Batch	*Clostridium butrycum* CGS5	Xylose	0.041	0.910	[37]
Batch	Mixed microflora	Wheat stalk	—	>0.855	[43]
Batch	Sediments of Pichavaram mangroves	Glucose	11.04	0.999	Present study

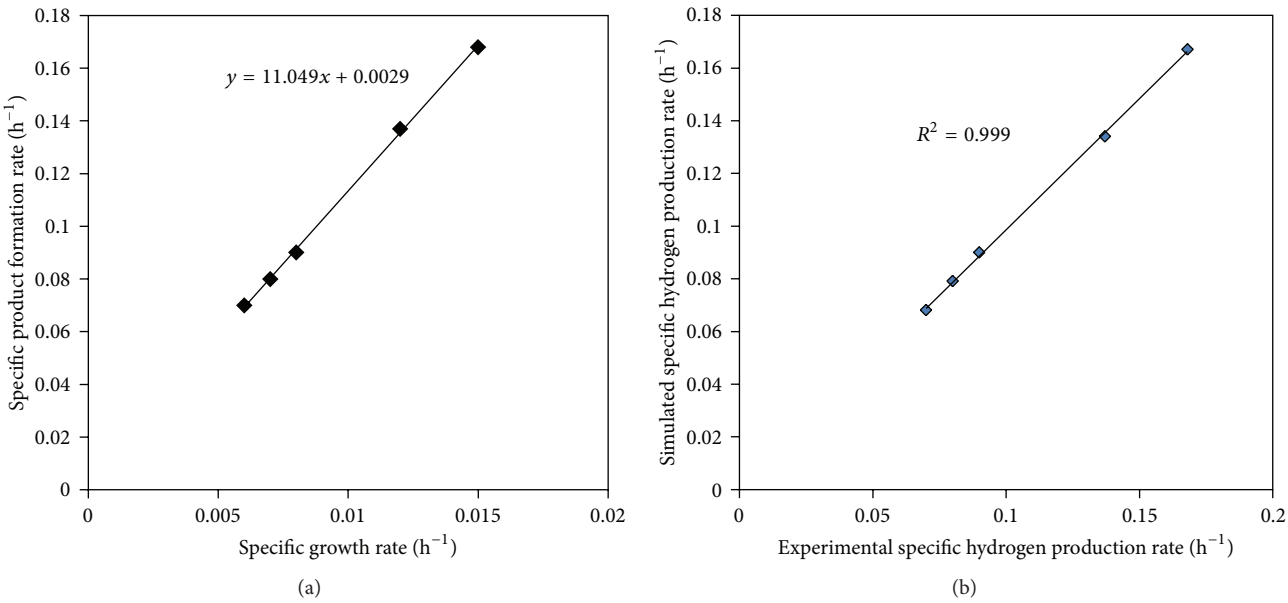

Figure 6: Luedeking-Piret model for product formation kinetics.

3.4.3. Cell Growth Rate as a Function of Product Formation. The Luedeking-Piret model shown in (6) has been widely used to describe the relationship between hydrogen producing bacterial growth rate and product formation rate:

$$\frac{dp}{dt} = Y_{P/x}\frac{dx}{dt} + \beta x, \tag{6}$$

where dp/dt is the product formation rate (h^{-1}), dx/dt is the specific growth rate (h^{-1}), P is the product (biohydrogen production), x is the cell concentration ($g\,L^{-1}$), $Y_{P/x}$ is the growth associate product yield coefficient, and β is the non-growth associated product yield coefficient.

Table 3 shows the values of different kinetic parameters estimated for this model. A plot of specific growth rate versus product formation rate, as shown in Figure 6, indicates that hydrogen is purely a growth associated product. The growth associate product yield coefficient ($Y_{P/x}$) was calculated by plotting specific hydrogen production rate versus specific growth rate, and the value was found to be 11.04. From Figure 6, it could be inferred that the model performed well with R^2 value of 0.999.

3.4.4. Microscopic Examination of Hydrogen Producing Granule. Scanning electron micrographs showed that the granules had multiple cracks with cavities on the surface (Figure 7). These cavities were likely to facilitate the passage of nutrients and substrate as well as the release of hydrogen. Bacterial cells were distributed all over the granules.

Furthermore, considering the practicality of this research work, microbiological analyses are warranted at this stage to characterize the dominant anaerobic consortium responsible for biohydrogen production. In general, kinetic models are applied in order to study and assess the metabolic features of defined cultures. Further studies in this field should be aimed at the following aspects: optimization studies with different innocula, substrates and process parameters, evaluation of the performance, and economics of a continuous biohydrogen production processes (bioreactors).

4. Conclusions

The results from batch tests showed that initial substrate (glucose) concentration, medium pH, and Fe^{2+} concentration had influence on the biohydrogen yield. Maximum biohydrogen yields were found to be 2.34, 2.3, and 2.5 mol H_2 mol^{-1} glucose at the following conditions: initial substrate concentration—10,000 mg L^{-1}, medium pH—6.0, and Fe^{2+} concentration—100 mg L^{-1}, respectively. The addition of trace metal to the medium at a concentration of 100 mg L^{-1} was found to enhance biohydrogen production although higher metal ion concentrations reduced biohydrogen production. The kinetics of batch anaerobic hydrogen production was estimated by fitting the experimental data

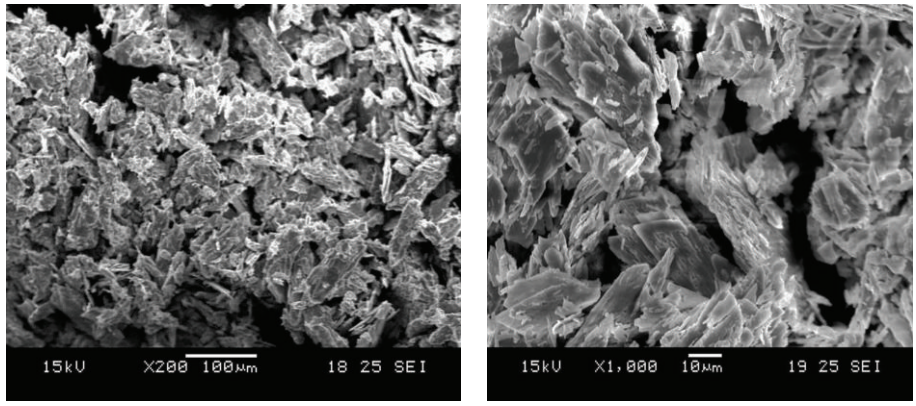

(a) (b)

Figure 7: SEM image of typical hydrogen-producing granule.

to the well-known unstructured kinetic models. The Monod model, logistic model, and Luedeking-Piret model were used to describe the kinetics of cell growth rate as a function of substrate, cell concentration, and product formation, respectively, in the hydrogen production process, and the corresponding kinetic constants were estimated. The results showed that high regression co-efficient values (R^2) were obtained between the model fitted and the experimental observations for the different models, namely, as 0.976, 0.943, and 0.999, respectively.

Nomenclature

μ: Specific growth rate (h^{-1})
μ_{max}: Maximum specific growth rate (h^{-1})
x: Microbial concentration (g VSS L^{-1})
x_0: Initial microbial concentrations (g VSS L^{-1})
K_s: Substrate consumption rate (g L^{-1})

k: Apparent specific growth rate (h^{-1})
x_{max}: Maximum microbial concentration (g VSS L^{-1})
P: Cumulative biohydrogen production (mL)
$Y_{P/x}$: Growth associate product yield coefficient
β: Non-growth associated product yield coefficient.

Conflict of Interests

The authors declare that there is no conflict of interests.

Authors' Contribution

The authors of this research article contributed to a similar extent overall and agreed to submit the paper.

Acknowledgments

The authors thank the Ministry of Earth Sciences, Government of India, New Delhi, for funding this research project (No: MOES/MRDF-11/1/25/P/09-PC-III) and Pollution Control Research Laboratory, Department of Chemical Engineering, Annamalai University, India, for laboratory and analytical facilities.

References

[1] International energy outlook, "U.S. Energy Information Administration," pp. 300, 2013.

[2] D. B. Levin, L. Pitt, and M. Love, "Biohydrogen production: prospects and limitations to practical application," *International Journal of Hydrogen Energy*, vol. 29, no. 2, pp. 173–185, 2004.

[3] S. Venkata Mohan, Y. Vijaya Bhaskar, and P. N. Sarma, "Biohydrogen production from chemical wastewater treatment in biofilm configured reactor operated in periodic discontinuous batch mode by selectively enriched anaerobic mixed consortia," *Water Research*, vol. 41, no. 12, pp. 2652–2664, 2007.

[4] M. T. Skonieczny, *Biological hydrogen production from industrial wastewater with Clostridium beijerinckii [M.S. dissertation]*, McGill University, 2008.

[5] G. E. Diwani, N. K. Attia, and S. I. Hawash, "Development and evaluation of biodiesel fuel and by-products from jatropha oil," *International Journal of Environmental Science and Technology*, vol. 6, no. 2, pp. 219–224, 2009.

[6] H. Le Man, S. K. Behera, and H. S. Park, "Optimization of operational parameters for ethanol production from korean food waste leachate," *International Journal of Environmental Science and Technology*, vol. 7, no. 1, pp. 157–164, 2010.

[7] H. N. Abubackar, M. C. Veiga, and C. Kennes, "Biological conversion of carbon monoxide: rich syngas or waste gases to bioethanol," *Biofuels, Bioproducts and Biorefining*, vol. 5, no. 1, pp. 93–114, 2011.

[8] P. Mullai, M. K. Yogeswari, and K. Sridevi, "Optimisation and enhancement of biohydrogen production using nickel nanoparticles—a novel approach," *Bioresource Technology*, vol. 141, pp. 212–219, 2013.

[9] P. Mullai, K. Sampath, and P. L. Sabarathinam, "Kinetic models anaerobic digestion of penicillin-G wastewater," *Chemical Engineering World*, vol. 38, no. 12, pp. 161–164, 2003.

[10] P. Mullai, S. Arulselvi, H.-H. Ngo, and P. L. Sabarathinam, "Experiments and ANFIS modelling for the biodegradation

of penicillin-G wastewater using anaerobic hybrid reactor," *Bioresource Technology*, vol. 102, no. 9, pp. 5492–5497, 2011.

[11] P. Mullai, H. H. Ngo, and P. L. Sabarathinam, "Substrate removal kinetics of an anaerobic hybrid reactor treating pharmaceutical wastewater," *Journal of Water Sustainability*, vol. 1, no. 3, pp. 301–312, 2011.

[12] R. Kothari, D. P. Singh, V. V. Tyagi, and S. K. Tyagi, "Fermentative hydrogen production—an alternative clean energy source," *Renewable and Sustainable Energy Reviews*, vol. 16, no. 4, pp. 2337–2346, 2012.

[13] F. R. Hawkes, R. Dinsdale, D. L. Hawkes, and I. Hussy, "Sustainable fermentative hydrogen production: challenges for process optimisation," *International Journal of Hydrogen Energy*, vol. 27, no. 11-12, pp. 1339–1347, 2002.

[14] N. Ren, J. Li, B. Li, Y. Wang, and S. Liu, "Biohydrogen production from molasses by anaerobic fermentation with a pilot-scale bioreactor system," *International Journal of Hydrogen Energy*, vol. 31, no. 15, pp. 2147–2157, 2006.

[15] S. Robaire, *Biological hydrogen production using Citrobacter amalonaticus Y19 to catalyze the water-gas shift reaction [M.S. dissertation]*, McGill University, 2006.

[16] K. Vijayaraghavan and M. A. M. Soom, "Trends in biohydrogen generation—a review," *Environmental Sciences*, vol. 3, pp. 255–271, 2006.

[17] K. Kathiresan, "A review of studies on Pichavaram mangrove, Southeast India," *Hydrobiologia*, vol. 430, no. 1–3, pp. 185–205, 2000.

[18] K. Kathiresan, "Why are mangroves degrading?" *Current Science*, vol. 83, no. 10, pp. 10–25, 2002.

[19] D. Zhu, G. Wang, H. Qiao, and J. Cai, "Fermentative hydrogen production by the new marine Pantoea agglomerans isolated from the mangrove sludge," *International Journal of Hydrogen Energy*, vol. 33, no. 21, pp. 6116–6123, 2008.

[20] J. Wang and W. Wan, "Kinetic models for fermentative hydrogen production: a review," *International Journal of Hydrogen Energy*, vol. 34, no. 8, pp. 3313–3323, 2009.

[21] R. Zhao, H. Liu, H. Hu et al., "A fundamental research on combustion chemical kinetic model's precision property," *Science China Technological Sciences*, vol. 53, no. 8, pp. 2222–2227, 2010.

[22] P. Mullai, E. R. Rene, H. S. Park, and P. L. Sabarathinam, "Adaptive network based fuzzy interference system (ANFIS) modeling of an anaerobic wastewater treatment process," in *Handbook of Research on Industrial Informatics and Manufacturing Intelligence: Innovations and Solutions*, M. A. Khan and A. Q. Ansari, Eds., pp. 252–270, IGI, New York, NY, USA, 2012.

[23] J. E. Bailey and D. F. Ollis, *Biochemical Engineering Fundamentals*, Tata MaGraw-Hill, New Delhi, India, 1986.

[24] K. Nath and D. Das, "Modeling and optimization of fermentative hydrogen production," *Bioresource Technology*, vol. 102, no. 18, pp. 8569–8581, 2011.

[25] H. Koku, I. Eroğlu, U. Gündüz, M. Yücel, and L. Türker, "Kinetics of biological hydrogen production by the photosynthetic bacterium Rhodobacter sphaeroides O.U. 001," *International Journal of Hydrogen Energy*, vol. 28, no. 4, pp. 381–388, 2003.

[26] Y. Mu, G. Wang, and H.-Q. Yu, "Kinetic modeling of batch hydrogen production process by mixed anaerobic cultures," *Bioresource Technology*, vol. 97, no. 11, pp. 1302–1307, 2006.

[27] J. Niessen, F. Harnisch, M. Rosenbaum, U. Schröder, and F. Scholz, "Heat treated soil as convenient and versatile source of bacterial communities for microbial electricity generation," *Electrochemistry Communications*, vol. 8, no. 5, pp. 869–873, 2006.

[28] APHA, *Standard Methods for the Examination of Waste and Wastewater*, American Public Health Associations, New York, NY, USA, 1995.

[29] G. L. Miller, "Use of dinitrosalicylic acid reagent for determination of reducing sugar," *Analytical Chemistry*, vol. 31, no. 3, pp. 426–428, 1959.

[30] J. Wang and W. Wan, "The effect of substrate concentration on biohydrogen production by using kinetic models," *Science in China B*, vol. 51, no. 11, pp. 1110–1117, 2008.

[31] W. M. Alalayah, M. S. Kalil, A. A. H. Kadhum, J. M. Jahim, and N. M. Alauj, "Effect of environmental parameters on hydrogen production using *Clostridium saccharoperbutylacetonicum* N1-4(ATCC 13564)," *American Journal of Environmental Sciences*, vol. 5, no. 1, pp. 80–86, 2009.

[32] S. K. Khanal, W.-H. Chen, L. Li, and S. Sung, "Biological hydrogen production: effects of pH and intermediate products," *International Journal of Hydrogen Energy*, vol. 29, no. 11, pp. 1123–1131, 2004.

[33] M. Ferchichi, E. Crabbe, G.-H. Gil, W. Hintz, and A. Almadidy, "Influence of initial pH on hydrogen production from cheese whey," *Journal of Biotechnology*, vol. 120, no. 4, pp. 402–409, 2005.

[34] Y. J. L. Young Joon Lee, T. Miyahara, and T. Noike, "Effect of iron concentration on hydrogen fermentation," *Bioresource Technology*, vol. 80, no. 3, pp. 227–231, 2001.

[35] H. Yang and J. Shen, "Effect of ferrous iron concentration on anaerobic bio-hydrogen production from soluble starch," *International Journal of Hydrogen Energy*, vol. 31, no. 15, pp. 2137–2146, 2006.

[36] J. Wang and W. Wan, "Effect of Fe^{2+} concentration on fermentative hydrogen production by mixed cultures," *International Journal of Hydrogen Energy*, vol. 33, no. 4, pp. 1215–1220, 2008.

[37] Y.-C. Lo, W.-M. Chen, C.-H. Hung, S.-D. Chen, and J.-S. Chang, "Dark H_2 fermentation from sucrose and xylose using H_2-producing indigenous bacteria: feasibility and kinetic studies," *Water Research*, vol. 42, no. 4-5, pp. 827–842, 2008.

[38] Y. Sharma and B. Li, "Optimizing hydrogen production from organic wastewater treatment in batch reactors through experimental and kinetic analysis," *International Journal of Hydrogen Energy*, vol. 34, no. 15, pp. 6171–6180, 2009.

[39] P. Kongjan, B. Min, and I. Angelidaki, "Biohydrogen production from xylose at extreme thermophilic temperatures (70°C) by mixed culture fermentation," *Water Research*, vol. 43, no. 5, pp. 1414–1424, 2009.

[40] F. J. Fernández-Morales, J. Villaseñor, and D. Infantes, "Modeling and monitoring of the acclimatization of conventional activated sludge to a biohydrogen producing culture by biokinetic control," *International Journal of Hydrogen Energy*, vol. 35, no. 20, pp. 10927–10933, 2010.

[41] F. J. Fernández, J. Villaseñor, and D. Infantes, "Kinetic and stoichiometric modelling of acidogenic fermentation of glucose and fructose," *Biomass and Bioenergy*, vol. 35, no. 9, pp. 3877–3883, 2011.

[42] N. Zainol, "Kinetics of biogas production from banana stem waste," in *Biogas*, S. Kumar, Ed., p. 408, InTech, Europe, 2012.

[43] X. Yuan, X. Shi, P. Zhang, Y. Wei, R. Guo, and L. Wang, "Anaerobic biohydrogen production from wheat stalk by mixed microflora: kinetic model and particle size influence," *Bioresource Technology*, vol. 102, no. 19, pp. 9007–9012, 2011.

Hindawi Publishing Corporation
BioMed Research International
Volume 2013, Article ID 463401, 9 pages
http://dx.doi.org/10.1155/2013/463401

Research Article

Back Propagation Neural Network Model for Predicting the Performance of Immobilized Cell Biofilters Handling Gas-Phase Hydrogen Sulphide and Ammonia

Eldon R. Rene,[1] M. Estefanía López,[2] Jung Hoon Kim,[3] and Hung Suck Park[3]

[1] *Core Group Pollution Prevention and Resource Recovery, Department of Environmental Engineering and Water Technology, UNESCO-IHE Institute for Water Education, P.O. Box 3015, 2601 DA Delft, The Netherlands*
[2] *Chemical Engineering Laboratory, Faculty of Sciences, University of La Coruña, Rúa da Fraga 10, 15008 La Coruña, Spain*
[3] *Department of Civil and Environmental Engineering, University of Ulsan, P.O. Box 18, Ulsan 680-749, Republic of Korea*

Correspondence should be addressed to Hung Suck Park; parkhs@ulsan.ac.kr

Received 7 August 2013; Accepted 9 September 2013

Academic Editor: Kannan Pakshirajan

Lab scale studies were conducted to evaluate the performance of two simultaneously operated immobilized cell biofilters (ICBs) for removing hydrogen sulphide (H_2S) and ammonia (NH_3) from gas phase. The removal efficiencies (REs) of the biofilter treating H_2S varied from 50 to 100% at inlet loading rates (ILRs) varying up to 13 g H_2S/m^3·h, while the NH_3 biofilter showed REs ranging from 60 to 100% at ILRs varying between 0.5 and 5.5 g NH_3/m^3·h. An application of the back propagation neural network (BPNN) to predict the performance parameter, namely, RE (%) using this experimental data is presented in this paper. The input parameters to the network were unit flow (per min) and inlet concentrations (ppmv), respectively. The accuracy of BPNN-based model predictions were evaluated by providing the trained network topology with a test dataset and also by calculating the regression coefficient (R^2) values. The results from this predictive modeling work showed that BPNNs were able to predict the RE of both the ICBs efficiently.

1. Introduction

A typical landfill gas consists of methane (45–60% v/v), carbon dioxide (40–60% v/v), and other compounds that include nitrogen, oxygen, sulphides, ammonia, carbon monoxides, and trace constituents. The amount of landfill gas generated is proportional to the amount of organic waste present and is produced by the bacteria during decomposition. These gases can easily move through the landfill surface to the ambient air and then to the community with the wind. The sulphur compounds (mercaptans and hydrogen sulphide) are the main contributors to the persisting odor problem from landfills, which are also considered toxic [1]. On the other hand, ammonia is both a potentially toxic product of refuse degradation and an essential nutrient for the bacteria responsible for this. The presence of these pollutants in the atmosphere has shown to cause significant damage to both human health and natural environment [2, 3]. In South Korea, there are a large number of landfills that do not incorporate suitable strategies to prevent these emissions from reaching the nearby community. Hence, there arises potential necessity to adapt worthy control techniques for effectively removing these emissions from landfills.

Biological treatment systems such as biofilters, and biotrickling filters have been demonstrated for several decades to be a cost effective technology for the treatment of waste gases containing low concentrations of contaminants at large flow rates [4–6]. The high removal efficiencies (REs) achieved along with its uncomplicated and flexible design, low operational, and maintenance costs edges biofilters over other biological treatment techniques such as biotrickling filters and bioscrubbers [7–11]. Biofilters can effectively remove H_2S and NH_3 emissions from waste-gas streams using a bed of biologically active material such as compost, peat, and wood bark. Belatedly, immobilization of microbes in suitable support matrix such as alginate beads or suitable polymeric materials has gained popularity in the research domain of biofiltration. The principal advantages of adopting

immobilization techniques in biofiltration is to provide high cell concentrations, improve genetic stability, protecting the microbes from shear damage, and to enhance favorable microenvironment for microbes (nutrient gradients and pH). *Pseudomonas putida* CH11 was tested for the removal of H_2S in both batch and continuous systems (pH: 6.0–8.0), yielding maximum removal rate and saturation constant values of $V_m = 1.36$ g S/day·kg dry bead and $K_s = 45.9$ ppm, respectively [12]. A biofilter inoculated with *Nitrosomonas europaea* was used to remove gaseous ammonia, in the concentration range of 10 or 20 ppm showed 99% RE after 4 days of operation [13]. The effects of operational factors such as retention time, temperature, and inlet concentration on the performance of a biofilter packed with *Thiobacillus thioparus* immobilized with Ca-alginate pellets were evaluated and found to have an optimal S-loading of 25 g/m^3·h, in order to achieve high removal of that compound [14]. For the treatment of landfill gas containing H_2S and NH_3, they can be easily treated by two immobilized cell biofilters (ICB) with different microorganisms in series or single ICB column with mixed microorganisms, as shown in our previous studies [2, 3].

Traditionally, the performance of biofilters has been modeled/predicted using process-based models that are based on mass balance principles, simple reaction kinetics, and a plug flow of air stream [15–18]. The main advantages of these process models are that, they are anchored on the underlying physical process and the results obtained from these process models generally provide a good understanding and interpretation of the system. However, this depends on numerous model parameters and obligates selective information on specific growth rate of microbes, biofilm thickness and density, values of diffusivity, partition, yield and distribution coefficients, intrinsic adsorption, and so forth [19–21]. The accurate estimation of some of these parameters requires elaborated technical facilities and expertise, the absence of which hinders the preciseness of the model and limits the application and reliability of the model.

An alternate modeling procedure consists of a data driven approach wherein the principles of artificial intelligence (AI) is applied with the help of neural networks [22]. The concept of neural network modeling has widespread applications in the field of applied science and engineering. An ANN-based model was developed to simulate different types of biomass for a gasification process and it was demonstrated that the model predicted profiles matched closely to the experimental values [23]. ANN model based on wavelet packet decomposition, entropy, and neural networks was formulated to predict the long-term performance of a wastewater treatment plant [24]. A 3-layered neural network with the standard back propagation algorithm was used in their study and the authors reported that the model was able to predict plant performance better. Recently, an ANN-based software was developed to predict thermal power plant effluent temperature that could help in optimizing load generation among different power generation units and this software demonstrated its ability to predict the canal temperature over the normal operating range with high accuracy [25]. With respect to the application of ANN for optimization purposes, ANN and genetic algorithm-based techniques were combined together to optimize media constituents, in order to enhance lipase production by soil microbes [26]. The results from their study showed that ANN-based model was able to predict the system behavior clearly showing lipolytic activity of 7.69 U/mL. It has been shown quite recently that the performance of biofilters and/-or biotrickling filters can be predicted from prior estimation of easily measurable operational parameters using ANNs [27–30]. In our previous studies, ANN-based predictive approach was proposed to model the performance of individually operated ICBs for H_2S and NH_3 removal, respectively [31, 32]. The outputs of the model were RE and EC, respectively, while the input parameters to the model were inlet concentration, loading rate, flow rate, and filter-bed pressure drop, respectively. The results for the H_2S operated ICB showed that a multilayer network (4-4-2) with back propagation algorithm was able to predict the ICB performance effectively with a R^2 values of 0.9157 and 0.9965 for removal efficiency and elimination capacity, respectively [31]. Similarly, for the ICB treating NH_3, multilayer network (4-4-2) with error back propagation predicted the RE and EC with R^2 values of 0.9825 and 0.9982, respectively [32].

The objectives of this research work were to experimentally evaluate the collective performance of two biofilters treating H_2S and NH_3 and to predict the ICBs performance parameter, namely RE, using one back propagation neural network (BPNN). Experiment data collected from our previous studies [2, 3] were thus integrated for predicting the RE profiles of H_2S and NH_3 using the BPNN. The input parameters to the model were unit flow (gas-flow rate/volume) and inlet concentrations, while the output parameter was the RE of the ICBs. After model development, the input parameters were subjected to sensitivity analysis in order to understand their effects on the RE profiles.

2. The Simple Back Propagation Neural Network Approach

Multilayer perceptron (MLP) using the back propagation algorithm [26, 33] is the most widely used neural network for forecasting/prediction purposes [34–36]. Neural networks acquire their name from the simple processing units in the brain called neurons which are interconnected by a network that transmits signals between them. These can be thought of as a black box device that accepts inputs and produces a desired output. MLP generally consists of three layers; an input layer, a hidden layer, and an output layer [36]. Each layer consists of neurons which are connected to the neurons in the previous and flowing layers by connection weights (W_{ij}). These weights are adjusted according to the mapping capability of the trained network. An additional bias term (θ_j) is provided to introduce a threshold for the activation of neurons. The input data (X_i) is presented to the network through the input layer, which is then passed to the hidden layer along with the weights. The weighted output (X_iW_{ij}) is

then summed and added to a threshold to produce the neuron input (I_j) in the output layer that can be represented by

$$I_j = \sum_{i,j=1}^{i,j=8} W_{ij} X_i + \theta_j. \quad (1)$$

This neuron input passes through an activation function $f(I_j)$ to produce the desired output Y_j. The most commonly used activation function is the logistic sigmoid function which takes the form;

$$f\left(I_j\right) = \frac{1}{1 + e^{-I_j}}. \quad (2)$$

3. Modeling Methodology

3.1. Model Input-Outputs and Data Division. A combined neural network-based predictive model was developed for the two biofilters using unit flow (X_1) and inlet concentration (X_2) as the model inputs and removal efficiency (Y_1) as the output. The experimental data was divided into training (N_{Tr}, 75%) and test data (N_{Te}, 25%). The test data was set aside during network training and was only used for evaluating the predictive potentiality of the trained network. The basic statistics of the variables for the training and test matrix is shown in Tables 1 and 2, respectively.

3.2. Error Evaluation. The closeness of prediction between the experimental and model predicted outputs were evaluated by computing the determination coefficient values as shown below [27];

$$R^2 = \left[\frac{\sum_{i=1}^{N} \left(Y_{\mathrm{model}_i} - \overline{Y_{\mathrm{model}}}\right)\left(Y_{\mathrm{observed}_i} - \overline{Y_{\mathrm{observed}}}\right)}{(N-1)\, S_{Y_{\mathrm{model}}} S_{Y_{\mathrm{observed}}}} \right]^2, \quad (3)$$

where Y_{model_i}—predictions made by the model, Y_{observed_i}—observed true values from experiments, N—number of cases analyzed, $\overline{Y}$—average value, and S_Y—standard deviations.

3.3. Data Preprocessing and Randomization. Experimental data collected from the biofilters during the 67 × 2 days (2 denotes the two biofilters) of continuous operation was randomized to obtain a spatial distribution of the data, which accounts for both steady state and transient (or) quasi-steady-state operations. The data was also normalized and scaled to the range of 0 to 1 using (4), so as to suit the transfer function in the hidden (sigmoid) and output layer (linear)

$$\widehat{X} = \frac{X - X_{\min}}{X_{\max} - X_{\min}}, \quad (4)$$

where $\widehat{X}$ is the normalized value and $X_{\min}$ and $X_{\max}$ are the minimum and maximum values of X respectively.

3.4. Network Parameters. The internal parameters of the back propagation network, namely, epoch size, error function, learning rate (η), momentum term (α), training cycle (T_c), and transfer function are to be appropriately selected to obtain the best network architecture that gives high predictions for the performance variables. In this study, the number of neurons in the input layer ($N_I = 2$) and output layer ($N_O = 1$) were chosen based on the number of input and output variables to the network. A detailed study on the effect of internal network parameters on the performance of back propagation networks [37] and the procedure involved in selecting the best network topology has been described elsewhere [34, 35]. However, in most instances, literature suggests the use of a trial and error approach where the performance goal is set by the user. In this study, the best values of the network parameters were chosen by carrying out simulations using a trial and error approach. The best network was chosen based on the maximum predictability of the network for the test data by analyzing the determination coefficient values.

3.5. Software Used. BPNN-based predictive modeling was carried out using the shareware version of the neural network and multivariable statistical modeling software, NNMODEL (Version 1.4, Neural Fusion, NY, USA).

3.6. Experimental Materials and Methods. The details of the experimental strategy adopted, inoculum, media composition, preparation of immobilized packing media, experimental setup, ICB operation, and analytical techniques for data collection have been detailed in our previously published work [2, 3].

4. Results and Discussions

4.1. Experimental. The initial inlet loading rates (ILRs) to both the biofilters were sufficiently low (<1 gH_2S (or) NH_3/m^3·h), that allowed the immobilized microbes to acclimatize themselves to the vapor phase pollutant. Once acclimatized (high removal, RE > 95%), the ICBs were subjected to a step-wise increase in ILRs by gradually varying the inlet concentration of either H_2S or NH_3 to the ICBs. During every step increase in the ILR, it was observed that the biofilter took about 2 to 4 d to adapt to the new concentration and reached a new steady state value shortly. Initially, when the loading rates were <1 g/m^3·h, the RE increased gradually from 45 to ~100%, which indicated good activity of the immobilized cells to treat these pollutants. The removal profiles and EC achieved for both the biofilters during the entire operational steps are shown in Figures 1 and 2, as a function of the ILRs. For the ICB treating H_2S vapors, the input was changed in 7 steps up to a ILR of 8 gH_2S/m^3·h, during which the RE remained constant at 82%. It has been shown that H_2S metabolism by heterotrophic sulphur oxidizing bacteria is a detoxification process and high inlet concentrations have often been reported to decrease the H_2S removal efficiency [15]. The EC profiles were almost linear till an ILR of 8 gH_2S/m^3·h, which indicates that the biofilter performed with 100% efficiency till this critical load [9]. For the ICB treating NH_3, it is evident that the RE was nearly >95%

Table 1: Basic statistics of the training data set.

Variable	Basic statistics					
	N	Mean	Std deviation	Minimum	Maximum	Sum square
Inputs						
Unit flow, per min	102	1.46	0.36	0.93	2.46	148.92
Concentration, ppmv	102	57.92	27.84	10	150	5908
Outputs						
RE, %	102	94.33	9.69	52.5	100	9621.8

Table 2: Basic statistics of the test data set.

Variable	Basic statistics					
	N	Mean	Std deviation	Minimum	Maximum	Sum square
Inputs						
Unit flow, per min	32	1.44	0.33	0.92	2.46	46.15
Concentration, ppmv	32	61	27.01	12	150	1952
Outputs						
RE, %	32	94.32	7.31	66.8	100	3018.1

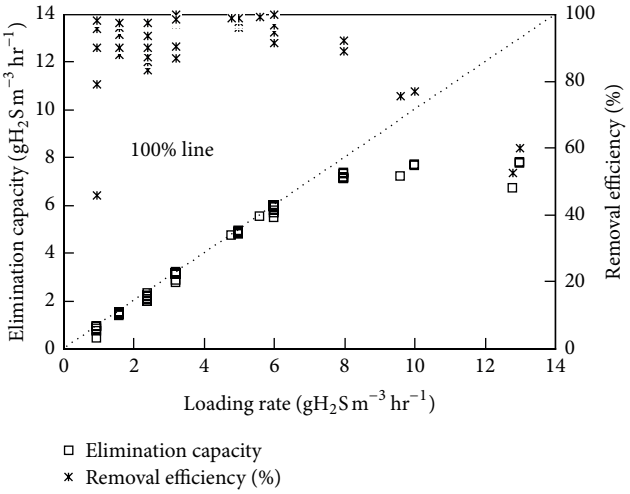

Figure 1: Effect of inlet loading rate on the elimination capacity and removal efficiency profiles of the immobilized cell biofilter handling H_2S vapors (More details can be seen in [3]).

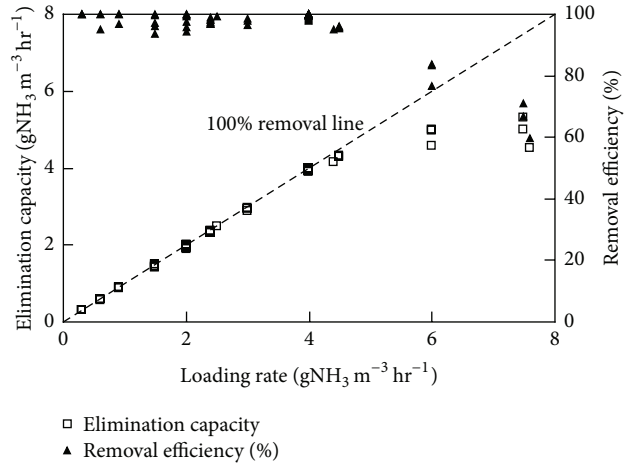

Figure 2: Effect of inlet loading rate on the elimination capacity and removal efficiency profiles of the immobilized cell biofilter handling NH_3 vapors (More details can be seen in [2]).

up to a ILR of 4.5 gNH_3/m^3·h. However, when the ILR was increased significantly by varying both the concentration and flow rate to values as high as 7.5 gNH_3/m^3·h, a noticeable decrease in the RE values from 100% to ~60% was observed. The critical NH_3 loading rate to the biofilter was considered as 4.5 gNH_3/m^3·h. Pressure drop values were sufficiently low during the operational time for both of the ICBs (0.1–1.7 cm of H_2O) and did not cause any significant operational problem. These values of pressure drop are within the safe operational range suggested for full-scale biofilter operation [2, 4, 9].

4.2. BPNN Modeling

4.2.1. Network Architecture. Artificial neural network-based models requires the best combinations of network parameters such as training cycle (T_c), neurons in the input (N_I), hidden (N_H) and output layer (N_O), learning rate (η), momentum term (α), and a good algorithm for the predictions to be accurate [2, 3, 36]. In this study, the models for predicting the RE of ICBs were trained and tested adequately with the experimental data and evaluated by the determination coefficient values between the measured and predicted outputs from the network. Table 3 shows the different network parameters used for training the network. The algorithm used for training in this study was the standard back error propagation (BEP) algorithm, which has potentially shown to exhibit high capability in predicting process variables [38, 39]. The model was trained using different combinations of these parameters so as to achieve maximum determination coefficient values (target value = 1, i.e., 100% correlation between measured and predicted variables). This was achieved by a vigorous

Table 3: Network training parameters for choosing the best network architecture.

Training parameters	Range of values	Best value
Training cycle	1000–40000	40000
Number of neurons in input layer	2	2
Number of neurons in hidden layer	2–8	2
Number of neurons in output layer	1	1
Learning rate	0.1–0.9	0.9
Momentum term	0.1–0.9	0.3
Fixed parameters during training		
Error tolerance	0.0001	
Epoch size	25	
Training algorithm	Standard BEP	
Number of training data set	102	
Number of test data set	32	
R^2 training	0.8716	
R^2 testing	0.8484	

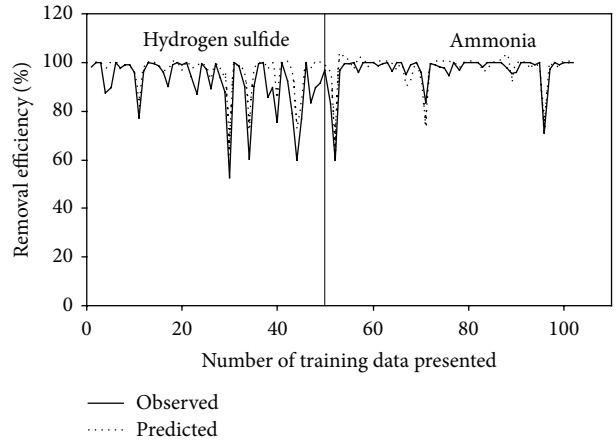

Figure 3: Observed and BPNN predicted values of removal efficiency profiles during training.

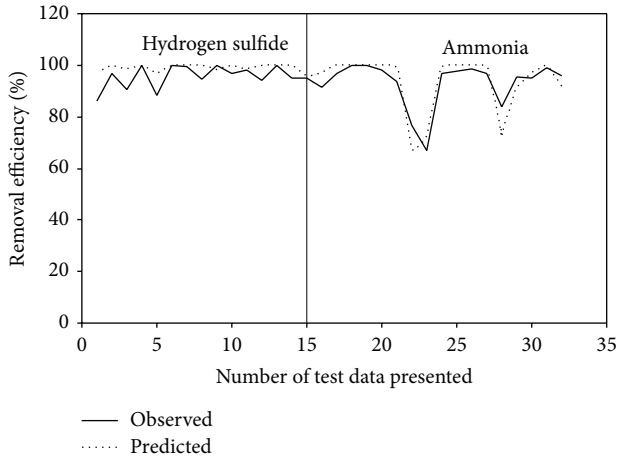

Figure 4: Observed and BPNN predicted values of removal efficiency profiles during testing.

trial and error approach by keeping some training parameters constant and by slowly moving the other parameters over a wide range of values, as suggested in some previous works [26, 34, 35]. A trial and error approach was followed in this study to determine the best network topology and the effect of internal network parameters due to the following reasons: (i) there were several parameters whose values had to be varied from low to high values (example: learning rate from 0.1–1; momentum term from 0.1–1), by keeping other parameters constant, and (ii) although several literatures have suggested different heuristic rules for selecting the (best) parameters, adequate training of the network always remains a key issue during ANN modeling, as this largely depends on the complexity of the process, the quality of data obtained, and the nature of interpretation done by the user. In this study, the following observations were made during training: (i) increasing the number of neurons in the hidden layer from 2 to 8 did not significantly increase the R^2 values, and the value of 2 was finally chosen, (ii) the training cycle appears to have a tremendous influence in increasing the R^2 values and it was observed that the model predictions were high and significant when the training cycle was set to 40,000, (iii) similarly, high learning rates seem to invariably increase the prediction efficiency, and (iv) low values of momentum term showed R^2 values greater than 0.84 in the test data during the predictions of RE. The R^2 values during training and testing were 0.8716 and 0.8484, respectively. Thus, only about 13–16% of the total deviations could not be explained by the model for predicting the combined removal efficiency profiles in the ICBs. The best network architecture for this combined model is 2-2-1. The results from this study indicate high learning rate (η-0.9), low momentum term (α-0.3), and a training cycle of 40,000 with 2 neurons in the hidden layer (N_H) are favorable values of the internal network parameters.

4.2.2. Predictive Potentiality of the Model. The performance parameter of the ICB treating H_2S and NH_3, namely RE, for the training and test data is shown in Figures 3 and 4, respectively. It can be observed that some of the data points for both H_2S and NH_3 were not predicted properly by the BPNN model, thus leading to large errors, ~13%. This could be due to the quasi-steady-state attained in the two ICBs, when the loading rate was step increased from one level to another. During this stage, the biofilter took some time (3 to 4 d) to adjust itself to the new concentration, thereby achieving steady state removals [2, 3]. Moreover, corroborating these deviations is the less critical load in the NH_3 biofilter (4.5 g/m^3·h) in comparison to the H_2S biofilter (8 g/m^3·h). This decrease in critical loads and corresponding removal profiles would have caused an impact in the networks generalization pattern while predicting the performance parameters, a pattern that has been often reported in biofilter and biotrickling filter operations [7, 9, 12]. However, the BPNN-based model showed good predictive ability for performance variables as seen from the closeness of the fit between the experimental and predicted observations.

Anew, the predictive capacity of the network was also evaluated in terms of its relative deviation, that is, (RE_{exp}–

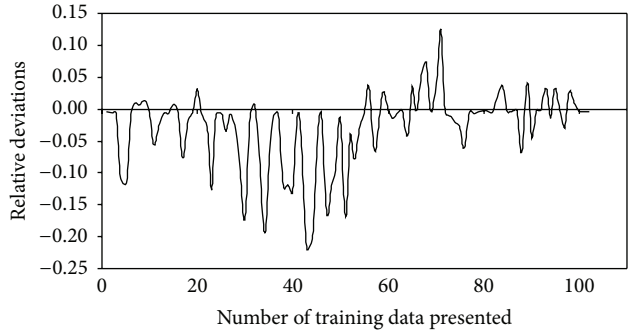

Figure 5: Relative deviations observed during model predictions for removal efficiency in the training data set.

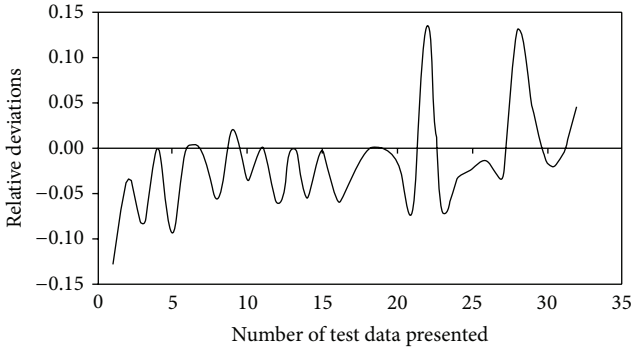

Figure 6: Relative deviations observed during model predictions for removal efficiency in the test data set.

$RE_{pred})/RE_{exp}$. These deviations for removal efficiency predicted by model during network training and testing are shown in Figures 5 and 6, respectively. The relative deviations are more significant, that is, >15% in some cases, which can be attributed to the change in load to the ICBs. This could be further explained by the EC profiles showed in Figures 1 and 2, respectively. For higher initial concentration and higher flow rate (high loading rates), the EC of the filter bed increased at a slower rate, becoming nearly constant at inlet loads beyond 8 g H_2S/m^3·h and 4.5 g NH_3/m^3·h, respectively. This phenomenon could be possibly due to the reaction and diffusion limitation steps as explained by Ottengraf [38], or by any one of the following mechanism; (i) smaller pore sizes in the media could restrict the accessibility of nutrients on the pore surface by the microorganisms, while at large pore size the specific surface area may be the limiting factor, (ii) at high cell densities, intra particle pore diffusion limitations have shown to play a significant role in reducing the elimination capacities, and (iii) microenvironmental conditions inside the encapsulated media could also vary with position and affect the physiology of the cells. The decline in RE at high loading rates could also be attributed to some complex mechanisms associated with the removal profiles in the immobilized media, where the waste air is first scrubbed and/-or absorbed in the liquid biofilm and then oxidized by the microorganisms.

Table 4: Weights and bias terms obtained after network training.

(a) Input to hidden layer weights

	W_{11}	W_{12}
Unit flow, per min	−6.61	−8.00
Concentration, ppmv	2.49	−26.6
Bias term	−8.19	1.95

W_{11}, W_{12}: Weights between neurons in input layer and hidden layer.

(b) Hidden to output layer weights

	RE, %
W_{21}	1.56
W_{22}	2.28
Bias term	−1.03

W_{21}, W_{22}: Weights between neurons in hidden layer and output layer.

Table 5: Sensitivity analysis of inputs for the trained network.

Parameters	Absolute average sensitivity, AAS
	RE, %
Unit flow, per min	0.5628
Concentration, ppmv	0.4371

The weights and bias terms between the hidden layer connections [39] obtained after network training is given in Table 4. In order to evaluate the significant effect of the input parameters on the developed model, a sensitivity analysis was carried out by estimating the Absolute Average Sensitivity (AAS). The sensitivity is calculated by summing the changes in the output variables caused by moving the input variables by a small amount over the entire training set. The AAS is the absolute values of the change in the input [40]. The computed AAS value on different input parameters for model is shown in Table 5. Unit flow (0.5628) appears to have a more significant effect in predicting RE profiles in the ICBs than the concentration term. The results from this analysis reveal the degree of relevance of the input parameters to the outputs. Figure 7 shows the contour plot of RE, as a function of the concentration and unit flow for the ICB. This contour plot can be interpreted as follows: RE > 93.7% can be consistently maintained in the ICB, if the following condition is met: inlet H_2S or NH_3 concentration is constantly maintained at less than 120 ppmv, at a unit flow of 2 per min.

The predictive ability of the proposed model using the concepts of artificial intelligence and the back propagation algorithm was high and significant, as ascertained from the R^2 value between the measured and predicted outputs in the training and test data for predicting RE of the ICB. This work could enable researches to extend and intensify research in BPNNs for evaluating pilot scale ICBs, besides helping in optimizing their state variables. For practical applications, ANNs can be used for real-time identification of state variables from the biofilter by continuously monitoring several important (easily measurable) parameters such as, inlet pollutant concentrations (using a gas chromatograph), gas flow rate (using a mass flow controller), humidity (using relative humidity sensors), filter bed pH, and temperature

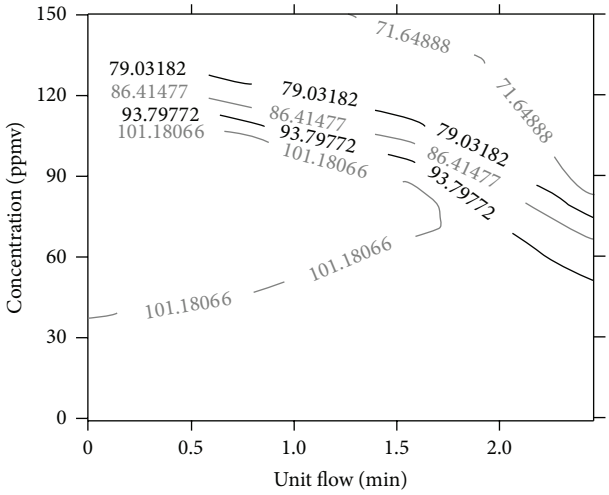

Figure 7: Contour plot showing the operating regime to achieve greater than 93.7% removal efficiency.

(using appropriate sensors). Real-time prediction of pollutant RE is then possible, wherein the acquired data (after proper noise filtering) is continuously integrated to an existing database of information (model inputs and outputs) and the ANN model can then be trained in either online or offline mode. Although, ANNs have found widespread application in real-time control of different industrial (chemical) processes and wastewater treatment systems, this research area still remains unexplored for the monitoring and real-time control of waste-gas treatment systems.

5. Conclusions

The RE of two individually operated immobilized cell biofilters (ICBs) was modeled using unit flow and inlet concentration as the input parameters. The best network architecture (2-2-1), determined by a trial and error approach showed that, high learning rates (η-0.9), low momentum term (α-0.3), with a training cycle of 40,000, are favorable conditions for high performance predictions. The developed BPNN model was able to identify all the peaks and plains of the data under different operating conditions with much less error (<15%). High REs (>93.7%) can be consistently maintained in the ICB, if the inlet H_2S or NH_3 concentration is maintained at <120 ppmv, at a unit flow of 2 per min, irrespective of the ICB operating volume. Furthermore, the results from this study evoke that neural networks can capture and extract complex relations among the easily measurable parameters, like unit flow and concentration, in an ICB process and forebode the performance in a meaningful manner.

Abbreviations, Symbols, and Nomenclature

AAS: Absolute average sensitivity
AI: Artificial intelligence
ANN: Artificial neural network
BPNN: Back propagation neural network
BEP: Back error propagation
EC: Elimination capacity, $g/m^3 \cdot h$
ICBs: Immobilized cell biofilters
MLP: Multi layered perceptron
RE: Removal efficiency, %
C/N: Carbon to nitrogen ratio
R^2: Regression coefficient
W_{ij}: Connection weights between layers
θ_{ij}: Bias terms
X_1, X_2: Inputs to the neural network model
Y_1: Output from the neural network model
N_{Tr}: Number of data points in the training data set
N_{Te}: Number of data points in the test data set
N: Number of cases analyzed
η: Learning rate
α: Momentum term
T_c: Training cycle
N_I: Number of neurons in the input layer
N_O: Number of neurons in the output layer
N_H: Number of neurons in the hidden layer
RE_{exp}: Experimental removal efficiency, %
RE_{pred}: Predicted removal efficiency, %.

Disclosure

There are no disclosures for this paper.

Conflict of Interests

The authores declare there is no conflict of interests.

Author Contribution

All authors of this paper contributed to a similar extent, and all authors have seen and agreed to the submission of this paper. M. Estefanía López contributed in analyzing the data and elucidating the effect of network parameters.

Acknowledgments

The authors would like to acknowledge the Ulsan Regional Environmental Technology Research Centre in Ulsan, South Korea, for their continual financial support in this field of experimental and modeling research.

References

[1] F.-K. Huang, G. S. Wang, and Y. L. Tsai, "Rainfall reliability evaluation for stability of municipal solid waste landfills on slope," *Mathematical Problems in Engineering*, vol. 2013, Article ID 653282, 10 pages, 2013.

[2] J. H. Kim, E. R. Rene, and H. S. Park, "Performance of an immobilized cell biofilter for ammonia removal from contaminated air stream," *Chemosphere*, vol. 68, no. 2, pp. 274–280, 2007.

[3] J. H. Kim, E. R. Rene, and H. S. Park, "Biological oxidation of hydrogen sulfide under steady and transient state conditions in

an immobilized cell biofilter," *Bioresource Technology*, vol. 99, no. 3, pp. 583–588, 2008.

[4] C. Kennes and M. C. Veiga, "Fungal biocatalysts in the biofiltration of VOC-polluted air," *Journal of Biotechnology*, vol. 113, no. 1-3, pp. 305–319, 2004.

[5] Ó. J. Prado, M. C. Veiga, and C. Kennes, "Treatment of gas-phase methanol in conventional biofilters packed with lava rock," *Water Research*, vol. 39, no. 11, pp. 2385–2393, 2005.

[6] E. R. Rene, D. V. S. Murthy, and T. Swaminathan, "Performance evaluation of a compost biofilter treating toluene vapours," *Process Biochemistry*, vol. 40, no. 8, pp. 2771–2779, 2005.

[7] E. R. Rene, M. Montes, M. C. Veiga, and C. Kennes, "Styrene removal from polluted air in one and two-liquid phase biotrickling filter: steady and transient-state performance and pressure drop control," *Bioresource Technology*, vol. 102, no. 13, pp. 6791–6800, 2011.

[8] F. J. Álvarez-Hornos, C. Gabaldón, V. Martínez-Soria, M. Martín, P. Marzal, and J. M. Penya-roja, "Biofiltration of ethylbenzene vapours: influence of the packing material," *Bioresource Technology*, vol. 99, no. 2, pp. 269–276, 2008.

[9] C. Kennes and M. C. Veiga, "Conventional Biofilters," in *Bioreactors for Waste Gas Treatment*, C. Kennes and M. C. Veiga, Eds., pp. 47–98, Kluwer Academic, Dodrecht, The Netherlands, 2001.

[10] B. M. Langolf and G. T. Kleinheinz, "A lava rock-based biofilter for the treatment of alpha-pinene," *Bioresource Technology*, vol. 97, no. 15, pp. 1951–1958, 2006.

[11] R. A. Pandey, K. V. Padoley, S. S. Mukherji et al., "Biotreatment of waste gas containing pyridine in a biofilter," *Bioresource Technology*, vol. 98, no. 12, pp. 2258–2267, 2007.

[12] Y.-C. Chung, C. Huang, and C.-P. Tseng, "Biodegradation of hydrogen sulfide by a laboratory-scale immobilized *Pseudomonas putida* CH11 biofilter," *Biotechnology Progress*, vol. 12, no. 6, pp. 773–778, 1996.

[13] Y.-C. Chung and C. Huang, "Biotreatment of ammonia in air by an immobilized *Nitrosomonas europaea* biofilter," *Environmental Progress*, vol. 17, no. 2, pp. 70–76, 1998.

[14] Y.-C. Chung, C. Huang, and C.-P. Tseng, "Operation optimization of *Thiobacillus thioparus* CH11 biofilter for hydrogen sulfide removal," *Journal of Biotechnology*, vol. 52, no. 1, pp. 31–38, 1996.

[15] M. A. Deshusses, G. Hamer, and I. J. Dunn, "Behavior of biofilters for waste air biotreatment. 1. Dynamic model development," *Environmental Science and Technology*, vol. 29, no. 4, pp. 1048–1058, 1995.

[16] Y. Jin, M. C. Veiga, and C. Kennes, "Performance optimization of the fungal biodegradation of α-pinene in gas-phase biofilter," *Process Biochemistry*, vol. 41, no. 8, pp. 1722–1728, 2006.

[17] S. P. P. Ottengraf and A. H. C. Van Den Oever, "Kinetics of organic compound removal from waste gases with a biological filter," *Biotechnology and Bioengineering*, vol. 25, no. 12, pp. 3089–3102, 1983.

[18] Z. Shareefdeen, B. C. Baltzis, Y.-S. Oh, and R. Bartha, "Biofiltration of methanol vapor," *Biotechnology and Bioengineering*, vol. 41, no. 5, pp. 512–524, 1993.

[19] P. Saravanan, K. Pakshirajan, and P. Saha, "Batch growth kinetics of an indigenous mixed microbial culture utilizing m-cresol as the sole carbon source," *Journal of Hazardous Materials*, vol. 162, no. 1, pp. 476–481, 2009.

[20] J.-H. Kim, X. Guo, S. K. Behera, and H.-S. Park, "A unified model of ammonium oxidation rate at various initial ammonium strength and active ammonium oxidizer concentrations," *Bioresource Technology*, vol. 100, no. 7, pp. 2118–2123, 2009.

[21] S. K. Behera, J.-H. Kim, X. Guo, and H.-S. Park, "Adsorption equilibrium and kinetics of polyvinyl alcohol from aqueous solution on powdered activated carbon," *Journal of Hazardous Materials*, vol. 153, no. 3, pp. 1207–1214, 2008.

[22] E. R. Rene and M. B. Saidutta, "Prediction of water quality indices by regression analysis and artificial neural networks," *International Journal of Environmental Research*, vol. 2, no. 2, pp. 183–188, 2008.

[23] B. Guo, D. Li, C. Cheng, Z.-A. Lü, and Y. Shen, "Simulation of biomass gasification with a hybrid neural network model," *Bioresource Technology*, vol. 76, no. 2, pp. 77–83, 2001.

[24] D. Hanbay, I. Turkoglu, and Y. Demir, "Prediction of wastewater treatment plant performance based on wavelet packet decomposition and neural networks," *Expert Systems with Applications*, vol. 34, no. 2, pp. 1038–1043, 2008.

[25] C. E. Romero and J. Shan, "Development of an artificial neural network-based software for prediction of power plant canal water discharge temperature," *Expert Systems with Applications*, vol. 29, no. 4, pp. 831–838, 2005.

[26] M. A. Haider, K. Pakshirajan, A. Singh, and S. Chaudhry, "Artificial neural network-genetic algorithm approach to optimize media constituents for enhancing lipase production by a soil microorganism," *Applied Biochemistry and Biotechnology*, vol. 144, no. 3, pp. 225–235, 2008.

[27] A. Elías, G. Ibarra-Berastegi, R. Arias, and A. Barona, "Neural networks as a tool for control and management of a biological reactor for treating hydrogen sulphide," *Bioprocess and Biosystems Engineering*, vol. 29, no. 2, pp. 129–136, 2006.

[28] E. R. Rene, S. M. Maliyekkal, L. Philip, and T. Swaminathan, "Back-propagation neural network for performance prediction in trickling bed air biofilter," *International Journal of Environment and Pollution*, vol. 28, no. 3-4, pp. 382–401, 2006.

[29] E. R. Rene, M. Estefanía López, M. C. Veiga, and C. Kennes, "Neural network models for biological waste-gas treatment systems," *New Biotechnology*, vol. 29, no. 1, pp. 56–73, 2011.

[30] I. Chairez, I. García-Peña, and A. Cabrera, "Dynamic numerical reconstruction of a fungal biofiltration system using differential neural network," *Journal of Process Control*, vol. 19, no. 7, pp. 1103–1110, 2009.

[31] E. R. Rene, J. H. Kim, and H. S. Park, "An intelligent neural network model for evaluating performance of immobilized cell biofilter treating hydrogen sulphide vapors," *International Journal of Environmental Science and Technology*, vol. 5, no. 3, pp. 287–296, 2008.

[32] E. R. Rene, J. H. Kim, and H. S. Park, "Immobilized cell biofilter: results of performance and neural modeling strategies for NH_3 vapor removal from waste gases," *Aerosol and Air Quality Research*, vol. 9, no. 3, pp. 379–384, 2009.

[33] S. C. Chukwu and A. N. Nwachukwu, "Analysis of some meteorological parameters using artificial neural network method for Makurdi, Nigeria," *African Journal of Environmental Science and Technology*, vol. 6, pp. 182–188, 2012.

[34] D. E. Rumelhart, G. E. Hinton, and R. J. Williams, "Learning representations by back-propagating errors," *Nature*, vol. 323, no. 6088, pp. 533–536, 1986.

[35] H. R. Maier and G. C. Dandy, "The effect of internal parameters and geometry on the performance of back-propagation neural networks: an empirical study," *Environmental Modelling and Software*, vol. 13, no. 2, pp. 193–209, 1998.

[36] H. R. Maier and G. C. Dandy, "Neural network based modelling of environmental variables: a systematic approach," *Mathematical and Computer Modelling*, vol. 33, no. 6-7, pp. 669–682, 2001.

[37] K. Hornik, M. Stinchcombe, and H. White, "Multilayer feedforward networks are universal approximators," *Neural Networks*, vol. 2, no. 5, pp. 359–366, 1989.

[38] S. P. P. Ottengraf, "Exhaust gas purification," in *Biotechnology: A Comprehensive Treatise*, H. J. Rhem and G. Reed, Eds., vol. 8, pp. 425–452, VCH, Weinheim, Germany, 1986.

[39] G. R. Chegini, J. Khazaei, B. Ghobadian, and A. M. Goudarzi, "Prediction of process and product parameters in an orange juice spray dryer using artificial neural networks," *Journal of Food Engineering*, vol. 84, no. 4, pp. 534–543, 2008.

[40] J. M. Zurada, A. Malinowski, and I. Cloete, "Sensitivity analysis for minimization of input data dimension for feedforward neural network," in *Proceedings of the IEEE International Symposium on Circuits and Systems*, pp. 447–450, June 1994.

Hindawi Publishing Corporation
BioMed Research International
Volume 2013, Article ID 949107, 7 pages
http://dx.doi.org/10.1155/2013/949107

Research Article

Microbial Purification of Postfermentation Medium after 1,3-PD Production from Raw Glycerol

Daria Szymanowska-Powałowska, Joanna Piątkowska, and Katarzyna Leja

Department of Biotechnology and Food Microbiology, Poznań University of Life Sciences, ul. Wojska Polskiego 48, 60-527 Poznan, Poland

Correspondence should be addressed to Daria Szymanowska-Powałowska; darszy@up.poznan.pl

Received 15 July 2013; Revised 28 August 2013; Accepted 30 August 2013

Academic Editor: Kannan Pakshirajan

1,3-Propanediol (1,3-PD) is an important chemical product which can be used to produce polyesters, polyether, and polyurethanes. In the process of conversion of glycerol to 1,3-PD by *Clostridium* large number of byproducts (butyric, acetic and lactic acid) are generated in the fermentation medium. The aim of this work was to isolate bacteria strains capable of the utilization of these byproducts. Screening of 30 bacterial strains was performed using organic acids as carbon source. Selected isolates were taxonomically characterized and identified as *Alcaligenes faecalis* and *Bacillus licheniformis*. The most active strains, *Alcaligenes faecalis* JP1 and *Bacillus licheniformis* JP19, were able to utilize organic acids almost totally. Finally, it was find out that by the use of coculture (*C. butyricum* DSP1 and *A. faecalis* JP1) increased volumetric productivity of 1,3-PD production (1.07 g/L/h) and the yield equal to 0.53 g/g were obtained in bioreactor fermentation. Moreover, the only by-product present was butyric acid in a concentration below 1 g/L.

1. Introduction

As the production of biofuels from raw materials continuously increases, optimization of production processes is necessary. A very important issue is the development of wasteless methods of biodiesel production. One way of utilization of glycerol generated in biodiesel production is its microbial conversion to 1,3-PD [1]. However, during this process different accompanying metabolites, such as organic acids and ethanol, are also synthesized from which the main product, 1,3-PD, must be separated [2, 3]. Difficulties in its separation arise from its high boiling point and the presence of two hydroxyl groups which make it strongly hydrophilic, and therefore complicate its extraction. There are many methods of purification of 1,3-PD [4, 5]; however, physical and mechanical methods of purification are very expensive. An effective method of 1,3-PD separation is an evaporation process coupled to vacuum distillation. However, the main disadvantages of that method are high demand for energy, and, moreover, the need to remove proteins and salts before this process. Other methods of purification also have limitations. Electrodialysis, used for desalination before evaporation, causes low product yield due to losses. Liquid-liquid extraction requires large amounts of solvent. Cyclic sorption and desorption on zeolite also poses problems, such as the requirement of dewatering step and high chance of contamination (due to uninterrupted link between the bioreactor and the separation equipment). Reactive extraction is a relatively complicated process. The removal of proteins, ethanol, and salts is necessary before the reaction. Additionally, trace amounts of aldehyde in 1,3-PD interferes with the polymerization of PTT. Aqueous two-phase extraction requires large amounts of methanol and difficulty in separation of the two alcohols occur. Chromatography consumes more energy than the simple evaporation and distillation, and while high overall purity and yield of 1,3-PD can be obtained, the resulting 1,3-PD solution is not concentrated but diluted because of the low selectivity and capacity of resin or absorbent. Additionally, the efficiency of

chromatographic matrices is susceptible to deterioration if feeds are not desalinated and deproteinized [4].

Alternative purification solutions are under investigation, among which microbiological ways of utilization of by-products are very interesting and promising [6–8]. Many reports exist concerning the use of coculture in 1,3-PD production [9–11]. There is, however, a lack of information on cocultures formed by a 1,3-PD producer and a microorganism capable of utilization of 1,3-PD by-products. Such a solution could result in better overall process productivity and facilitate the downstream processing.

The aim of this work was the isolation of new strains able to utilize organic acids, as sole carbon sources, which are generated during the production of 1,3-PD from glycerol. Furthermore, the possibility of enhancing the kinetic parameters of microbial 1,3-PD productions by the use of coculture were investigated.

2. Materials and Methods

2.1. Pure Culture Inoculum. In the conversion process of raw glycerol to 1,3-PD a bacteria strain, *C. butyricum* DSP1, was used. *C. butyricum* DSP1 was previously isolated from ruminal fluid and collected in the Department of Biotechnology and Food Microbiology, Poznan University of Life Sciences Poland, and deposited at the Polish Collection of Microorganisms PCM.

The strain was maintained in Reinforced Clostridial Medium (RCM, Oxoid, UK) in serum bottles at 4°C. Precultures of pure culture inoculum were cultivated in Hungate test tubes in appropriate cultivation media (37°C, 18 h). Bacteria from the genus *Clostridium* were cultured in a chamber for cultivation of anaerobic microorganisms (the Whitley MG500, Don Whitley Scientific, Shipley, UK), without pH regulation and stirring.

The enrichment of isolated bacteria *A. faecalis* biomass was carried out in medium (CM) consisting of (per liter deionized water): 2.0 g $C_2H_7NO_2$, 2.0 g K_2HPO_4, 0.2 g $MgSO_4$ and 50 μL solution of $CaCl_2$. Precultures of pure culture inoculum were incubated under relative anaerobic conditions in an incubation chamber (32°C, 20 h).

2.2. Isolation and Screening Medium. The isolation medium for new strains was Nutrient Broth Agar and glucose (2%). The composition of the screening medium was (per liter deionized water): 33.5 g $C_3H_8O_2$, 4.65 g C_3H_7COOH, 1.69 g CH_3COOH, 2.76 g $C_2H_4OHCOOH$, 3.0 g $C_3H_5(OH)_3$, and 0.34 g C_2H_5OH.

2.3. Isolation Process. Bacteria strains able to organic acids utilization were isolated from typical sources of methanogenic fermentations (fermented chocolate, ensilages, and slurry). The first stage in the isolation of the desired strains was based on the pour-plate method. After the incubation period (48 h, 32°C), single colonies that had different morphological traits and the characteristics of a given bacterium genus were collected using disposable loops. Cells were maintained at −80°C in the culture broth supplemented with 20% glycerol.

2.4. Screening. Obtained isolates were cultivated on post-fermentation broth. After the production of 1,3-PD from glycerol and biomass separation, permeate was inoculated by *A. faecalis* and *B. licheniformis* bacteria isolates (10% v/v). The process was carried out for 7 days, in 32°C, without pH regulation (pH at the beginning of the process adjusted to 7.15), and in strictly anaerobic conditions. Samples were taken in 24 hours intervals—the changes of glycerol, 1,3-PD, and organic acids were analyzed by HPLC.

2.5. Bacterial Identification. Total DNA from bacteria was extracted with Genomic Mini AX Bacteria Kit (A & A Biotechnology, Gdansk, Poland) after an initial 1 h incubation in 50.0 mg/mL lysozyme (Sigma, Poland) at 37°C. Sequences encoding small subunits of 16S rRNA were amplified by PCR using SDBact0008aS20 and SUniv1492bA21 primers [12]. The PCR products were purified using the Clean-up Kit (A & A Biotechnology, Gdansk, Poland) and sequenced at Genomed (Warsaw, Poland) using the primers used for PCR and a primer for an inner sequence (GTGCCAGCMGCCGCCGTAA). The sequences obtained were arranged into contigs and identified using the BLAST service of the GenBank database [13].

2.6. Phylogenetic Analyses. The sequences encoding the 16S rRNA of *C. butyricum* DSP1 and *A. faecalis* strains were compared with the randomly selected sequences of *Clostridium* sp. and *Alcaligenes* sp. in GenBank. The sequences were aligned using the ClustalW program as implemented in BioEdit (version 7.0.9). The phylogenetic analyses were conducted using the MEGA 4.0 software [12]. The neighbour-joining method was used for phylogenetic reconstruction, and the p-distance was used for distance analysis. The best phylogenetic distance tree is shown.

2.7. Fermentation Medium. The composition of the fermentation medium was (per liter deionized water): 0.26 g K_2HPO_4; 0.02 g KH_2PO_4; 1.23 g $(NH_4)_2SO_4$; 0.1 g $MgSO_4 \times 7H_2O$; 0.01 g $CaCl_2 \times 2H_2O$; 0.01 g $FeCl_2 \times 7H_2O$, and 2.0 g yeast extract. The fermentation medium was supplemented with crude glycerol (Wratislavia-Bio, Wroclaw, Poland) at a concentration of 80.0 ± 1.0 g/L in batch fermentation. The crude glycerol composition was (w/w) 85.6% glycerol, 6% NaCl, 11.2% moisture, and pH 6.5. The media were autoclaved (121°C, 20 min.).

2.8. Fermentation Experiments. Fermentations were carried out in bioreactor (2L) (Sartorius Stedim, Germany). The temperature of the process was 37°C, stirring rate was 60 rpm, pH was automatically regulated with 5 M NaOH at 7.0 ± 0.1. The process was carried out using two bacteria strains. At the beginning of the process, bacteria were grown separately in two vessels (200 mL) connected to the bioreactor. In the first vessel *C. butyricum* DSP1 was cultivated on RCM medium, and in the second, *A. faecalis* JP1 was cultivated on CM

medium. This preliminary stage was continued for 18–20 hours. After this time, the medium in the bioreactor was inoculated with *C. butyricum* DSP1 (using peristaltic pump) and the synthesis of 1,3-PD started. When the concentration of metabolites (both 1,3-PD and organic acids) increased, the second bacteria culture—*A. feacalis* JP1—was fed into the bioreactor. Samples from the bioreactor were taken at intervals every 2–5 hours. All data presented are means of two independent experiments performed under the same culture conditions.

2.9. Analytical Methods. 1,3-PD, glycerol, and organic acids were assayed by high performance liquid chromatography.

Samples for chemical analysis were first centrifuged at 10,000 g for 10 min at 4°C (Multifuge 3SR, Germany), filtered through a 0.22 μm membrane filter (Millex-GS, Millipore, USA), and then analyzed on an HPLC system (Agilent Technologies 1200 series).

Agilent Technolgies 1200 series system equipped with a refractive index detector was used. Analyses were performed isocratically at a flow rate of 0.6 mL/min. on an Aminex HPX-87H 300 × 7.8 column (Bio-Rad, CA, USA) at a constant temperature of 65°C. H_2SO_4 (0.5 mN) was the mobile phase. External standards were applied for identification and quantification of peaks area. Retention times (Rt) determined for the targeted compounds for were as follows: 1,3-PD—17.17 min; glycerol—13.03 min; butyric acid—20.57 min; acetic acid—14.4 min; lactic acid—11.19 min; ethanol—21.34 min.

2.9.1. Determination of Interactions between of A. feacalis Jp1, B. licheniformis Jp19 and C. butyricum Dsp1. In order to verify if any antagonisms exist between the tested *A. feacalis* JP1 and *B. licheniformis* JP19 strains in relation to *C. butyricum* DSP1 analyses were conducted, including preparation of culture media for *A. feacalis* JP1 and *B. licheniformis* JP19 strains, separation of culture media into fractions (the supernatant and precipitate), preparation of *C. butyricum* DSP1 and analyses of activity of the obtained liquid culture and the supernatant by the well method.

2.9.2. Preparation of Culture Liquid Media. Antibacterial activity was determined using 24 h cultures of *A. feacalis* JP1 (media CA) and *B. licheniformis* JP19 (media with 2% glucose). Cultures were run at a temperature of 32°C.

2.9.3. Separation of the Culture Liquid Media into Fractions. In order to obtain supernatants (S), the cultures of analyzed strains were centrifuged (5000 ×g; 10 min). Analyses of the supernatant were aimed at the determination of antagonistic activity of bacterial exocellular metabolites.

2.9.4. Preparation of Indicator Microorganisms. Indicator microorganism (*C. butyricum* DSP1) was transferred to test tubes containing 10 mL RCM medium (to proliferate biomass). Cultures were run at 37°C for 24 h. Then, in order to obtain a distinct confluent layer, the liquefied agar medium was inoculated with 10% (v/v) 24 h culture of the indicator culture and poured onto Petri dishes.

2.9.5. Analyses of Antibacterial Activity of Liquid Culture Medium and the Supernatant Fraction. After solidification of the Tryptose Sulfite Cycloserine Agar (TSC, Oxoid, UK) inoculated with indicator microorganism, wells were made using a cork borer. Each well was supplemented with 150 μL liquid culture medium or 150 μL supernatant fraction of the analyzed strain. After incubation (24 h, 32°C, anaerobic), the diameters of the zones of growth inhibition were measured. Bacteriostatic properties were determined by measuring the growth inhibition zone diameter (growth limitation of the indicator strain).

3. Results

3.1. Isolation and Characterization of Microorganisms Able to Organic Acids Utilizations. There is only little literature data about purification of postfermentation broths in the microbial 1,3-PD synthesis [10]. Chemical purification processes are expensive [4]. Thus, in this work, the perspectives of utilization of microorganisms to remove the by-products, synthesized during the production of 1,3-PD from glycerol was considered. As an isolation source probes from methanogenic fermentation were chosen. Finally, 30 bacteria isolates were obtained. These were cultured on postfermentation broth of typical composition for propanediol fermentation carried out by *C. butyricum*. The aim was to screen for microorganisms able to decrease the concentrations of organic acids and ethanol without changing the amount of 1,3-PD. Changes in concentrations of compounds in the postfermentation broth after 7 days of cultivation are presented in Table 1.

Fifteen strains exerting the most significant influence on the broth composition (Table 1) were selected for further study. Unfortunately, some strains utilized both—organic acids and 1,3-PD. It disqualified these strains for the purpose of postfermentation broth purification. Also strains utilizing glycerol were omitted.

Nine of the obtained strains had significant influence of the amount of organic acids and had no influence on 1,3-PD level. Strains number 1, 12, 15, and 19 were able to partially or completely utilize organic acids. The best isolates were selected for identification. Five of them belonged to the *Alcaligenes faecalis* species and four to *Bacillus licheniformis* (Table 2). Some strains (of the 15 selected isolates) were able to utilize organic acids very slowly. For example, strain no 1 metabolized it in 24 hours, while strain no 15 in 120 hours. For this reason, *A. faecalis* JP1 (isolate no 1) was chosen for further experiments.

To determine the relationship between the *C. butyricum* DSP1 strain and the *A. faecalis* strains, a phylogenetic tree was built based on the nucleotide sequences of the genes encoding 16S rRNA (Figure 1).

The antibacterial activity test indicated that strain *A. faecalis* JP1 has no antagonistic activity towards *C. butyricum*

Table 1: Compounds of postfermentative broth after 7 days of cultivation of the isolates.

Strain number	Utilization level						Time*
	Butyric acid	Acetic acid	Lactic acid	Ethanol	1,3-PD	Glycerol	
1	++	+++	+++	−	−	−	24 h
2	+	+++	+	−	−	+	NA
3	+	+++	+	−	−	+	NA
5	++	+++	+	−	−	−	NA
6	+	+	−	−	+	+	NA
7	−	+	−	−	−	+	NA
9	+	+++	++	−	−	+	NA
11	+	+++	+	−	−	−	NA
12	++	+++	++	−	−	−	96 h
15	++	+++	+++	−	−	−	120 h
17	−	+++	+	−	−	−	NA
19	+	+++	+++	−	−	−	96 h
21	+		++	−	−	−	NA
25	+	−	+	−	+	+	NA
29	−	−	++	−	+	+	NA

+++: complete utilization.
++: utilization of more than 50%.
+: insignificant utilization (<10%).
−: lack of utilization.
*Time until 90% organic acids utilization.
NA: not applicable.

Table 2: Identification on new isolates by amplification of 16S rRNA.

Strains number	Isolation source	Species	Homology to geneare
1	Fermented silage with manure	*Alcaligenes faecalis*	99%
5	Fermented silage with manure	*Alcaligenes faecalis*	98%
12	Fermented silage with manure	*Alcaligenes faecalis*	97%
15	Fermented silage with manure	*Alcaligenes faecalis*	98%
21	Fermented silage with manure	*Alcaligenes faecalis*	96%
3	Fermented chocolate	*Bacillus licheniformis*	98%
9	Fermented silage with manure	*Bacillus licheniformis*	97%
11	Fermented silage with manure	*Bacillus licheniformis*	96%
12	Fermented chocolate	*Bacillus licheniformis*	97%

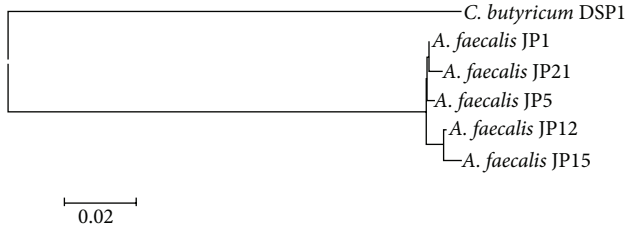

Figure 1: 16S rRNA-based phylogenetic tree showing the position *C. butyricum* DSP1 among related *A. faecalis* strains.

DSP1 used in 1,3-PD production. However, strains *B. licheniformis* inhibits growth of *C. butyricum* strain (data not shown).

3.2. Cultivation of Coculture Consisting of C. butyricum Dsp1 and A. faecalis Jp1. Fermentation by-products cause toxic stress which can damage bacteria cells, presence of these products also inhibits polymerization reactions in polyurethane production [14, 15]. Thus, efforts were taken to remove the by-products of the glycerol conversion to 1,3-PD in a microbiological way. Two bacteria strains were used *C. butyricum* DSP1 and *A. faecalis* JP1. In the first step of the experiment the fermentation medium was inoculated with *C. butyricum*. The synthesis of 1,3-PD started ca. 13 hour after inoculation. Glycerol was utilized and 1,3-PD was synthesized. During the fermentation, as the amount of 1,3-PD reached 25 g/L, butyric acid level was at 1.68 g/L, lactic acid—1.34 g/L, and acetic acid—1.21 g/L, an inoculum culture of *A. faecalis* was added to the fermentation tank. During the first 3 h after inoculation with the second strain, the level of 1,3-PD was still increasing. In 32 h of fermentation, a significant decrease (up to 20%) of lactic and acetic acid concentration was observed. Simultaneously, the productivity of 1,3-PD increased (between 31 and 35

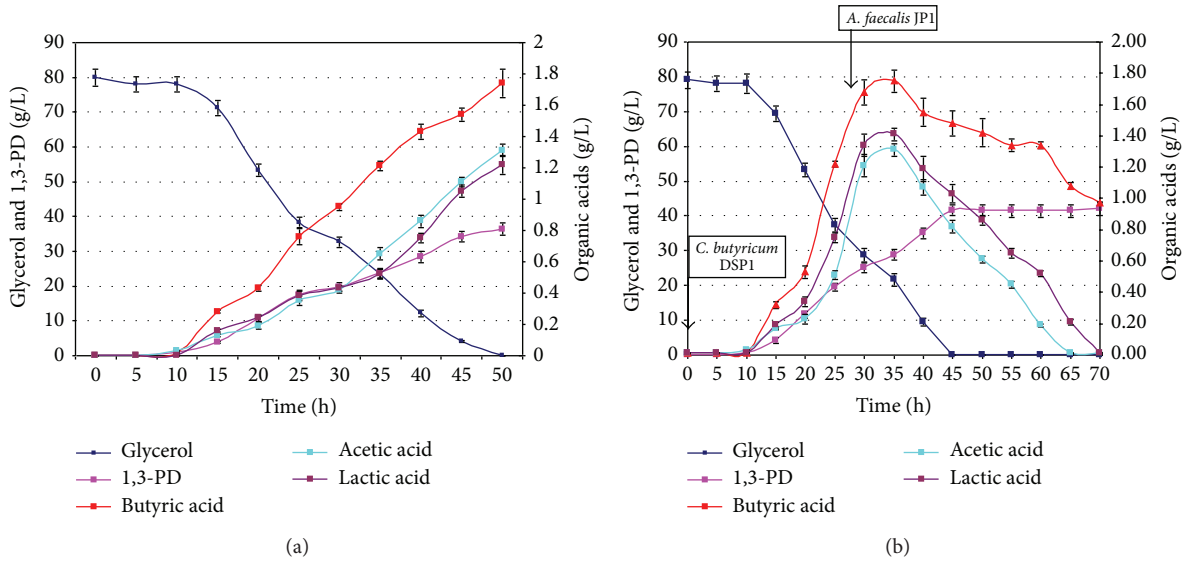

FIGURE 2: Changes in substrate and metabolites concentration during the conversion of glycerol to 1,3-PD by (a) monoculture of *C. butyricum* DSP1 and (b) coculture of *C. butyricum* DSP1 and *A. faecalis* JP1.

hour of fermentation it was equal 1.55 g/L/h). Complete glycerol utilization was observed in 39 h, the yield of 1,3-PD production was 0.53 g/g crude glycerol. The process was carried until complete lactic and acetic acids utilization (Figure 2(b)).

4. Discussion

Methanogenic fermentation is a very interesting source of microorganism which can be applied in industrial processes of glycerol utilization [10, 11, 16]. The reason for this situation is probably the fact that glycerol is often added into methanogenic fermentation as an additional carbon source [17]. Thus, microorganisms obtained from this source tolerate high osmotic pressures. In this work, strains from silage fermented with manure and fermented chocolate were obtained. During methane production (in the acido- and acetogenesis steps) some organic acids are produced. Next, these acids are converted to gases. Thus, the authors selected such isolation sources to obtain strains resistant to high concentration of organic acids and able to utilize it. Finally, 30 isolates were obtained and their metabolic activity was tested. The best strains were *A. faecalis* JP1 and *B. licheniformis* JP19. Organic acids such as acetic acid and butyric acid are formed as by-products in the fermentation of glycerol to 1,3-PD. These compounds inhibit the growth of *C. butyricum* and deteriorate its ability to biotransform glycerol to 1,3-PD. The acids formed increase the hydrogen ion concentration in the fermentation broth, diffuse into the cell, and can lead to its death. In order to prevent it, the activity of proton pumping proteins increases resulting in higher ATP consumption. The activation of this defense mechanism leads to decreased cell metabolic activity, lower production of biomass, and metabolites. Biebl [18] described the influence of butyric and acetic acids (apart from 1,3-PD, the main primary metabolites of propanediol fermentation) on *C. butyricum*. The author determined the concentrations that inhibited the growth of the bacterium: butyric acid—19 g/L and acetic acid—27 g/L. Thus, the limitation by organic acid concentration during 1,3-PD synthesis is a very important issue, especially in fed-batch fermentations and at the end of the process. Removal of these by-products can increase the metabolic activity of bacteria producing 1,3-PD. Colin et al. [19] examined the influence of the addition of butyrate and acetate on *C. butyricum* CNCM 1211 strain during conversion of glycerol into 1,3-PD. The addition of these metabolites in concentrations of 2.5–15.0 g/L distinctly affected the bacterium viability and its metabolism. Significant observations were made during the research. The addition of acetate triggered an increase in biomass concentration and butyrate production, and at the same time reduced the yield of 1,3-PD, whereas the addition of butyrate resulted in increased diol synthesis, reduction in biomass, and butyrate production. The presented results enable to propose a thesis that reduction in butyrate synthesis in the cell ensures the appropriate amount of NADH, which is vital for the synthesis of 1,3-propanediol. In the present study, partial removal of butyric acid did not influence the number of microorganisms because the biomass already reached the plateau before inoculation with *A. faecalis* JP1. The decreased amounts of acetic and lactic acids obtained in cocultures were accompanied by better fermentation parameters then the control. The obtained yield and volumetric productivities were 15% and 30% higher, respectively. Other reports exist that concern the use of cocultures for enhanced 1,3-PD production [8, 9]. Selembo et al. [8] performed a model experiment with *C. butyricum* and *Methanosarcina mazei,* a microorganism capable of utilization of the 1,3-PD fermentation by-products. Bizukojc et al. [9] used an unidentified coculture to convert glicerol to 1,3-PD and

hydrogen. Hereby, selected strain of the *Alcaligenes* genera possesses some very beneficial properties that make it fit for cocultures with *C. butyricum*. The optimal temperature for the *Alcaligenes* is in the range of 30–37°C, which complies with optimal temperature for the *Clostridium*. Bacteria form the *Alcaligenes* genera shows the ability to consume oxygen and generate anaerobic conditions necessary for *C. butyricum* strain. It seems that both bacteria can live in syntrophy. On the other hand, because of the determined antagonism, the isolated *B. licheniformis* JP19 strain may be used for the purification of 1,3-PD but not in direct coculture with *C. butyricum*. The antagonistic effects result probably from the production of proteolytic and bacteriolytic enzymes (such as n-acetylmuramoyl-l-alanine amidase, EC 3.5.1.2.8) [20]. As *B. licheniformis* has tolerance to high concentration of organic acids and solvents it could still be utilized after a separate fermentation process for the purpose of purification [21].

5. Conclusions

The application of isolates from the *Alcaligenes* and *Bacillus* genera as means of purification of postfermentation broth is a promising method of removing organic acids.

However imperfect the procedures described in this work are and further investigation is necessary, such approach gives hope that the production of biodiesel may become soon a completely wasteless process. Furthermore, the removal of toxic by-products can lead to increased efficiency of the microbial synthesis of 1,3-PD and, in result, make the process more economically viable.

Conflict of Interests

The authors declare that there is no conflict of interests regarding the publication of this paper.

Acknowledgments

The paper was prepared within the framework of project PO IG 01.01.02-00-074/09 cofunded by The European Union from The European Regional Development Fund within the framework of the Innovative Economy Operational Programme 2007–2013.

References

[1] A.-P. Zeng and W. Sabra, "Microbial production of diols as platform chemicals: recent progresses," *Current Opinion in Biotechnology*, vol. 22, no. 6, pp. 749–757, 2011.

[2] A.-P. Zeng, "Pathway and kinetic analysis of 1,3-propanediol production from glycerol fermentation by *Clostridium butyricum*," *Bioprocess Engineering*, vol. 14, no. 4, pp. 169–175, 1996.

[3] G. Kaur, A. K. Srivastava, and S. Chand, "Advances in biotechnological production of 1,3-propanediol," *Biochemical Engineering Journal*, vol. 64, pp. 106–118, 2012.

[4] Z.-L. Xiu and A.-P. Zeng, "Present state and perspective of downstream processing of biologically produced 1,3-propanediol and 2,3-butanediol," *Applied Microbiology and Biotechnology*, vol. 78, no. 6, pp. 917–926, 2008.

[5] A.-I. Qatibi, A. Bories, and J.-L. Garcia, "Sulfate reduction and anaerobic glycerol degradation by a mixed microbial culture," *Current Microbiology*, vol. 22, no. 1, pp. 47–52, 1991.

[6] M. F. Temudo, G. Muyzer, R. Kleerebezem, and M. C. M. van Loosdrecht, "Diversity of microbial communities in open mixed culture fermentations: impact of the pH and carbon source," *Applied Microbiology and Biotechnology*, vol. 80, no. 6, pp. 1121–1130, 2008.

[7] W. Sabra, D. Dietz, D. Tjahjasari, and A.-P. Zeng, "Biosystems analysis and engineering of microbial consortia for industrial biotechnology," *Engineering in Life Sciences*, vol. 10, no. 5, pp. 407–421, 2010.

[8] P. A. Selembo, J. M. Perez, W. A. Lloyd, and B. E. Logan, "Enhanced hydrogen and 1,3-propanediol production from glycerol by fermentation using mixed cultures," *Biotechnology and Bioengineering*, vol. 104, no. 6, pp. 1098–1106, 2009.

[9] M. Bizukojc, D. Dietz, J. Sun, and A.-P. Zeng, "Metabolic modelling of syntrophic-like growth of a 1,3-propanediol producer, *Clostridium butyricum*, and a methanogenic archeon, *Methanosarcina mazei*, under anaerobic conditions," *Bioprocess and Biosystems Engineering*, vol. 33, no. 4, pp. 507–523, 2010.

[10] D. Dietz and A. P. Zeng, "Efficient production of 1, 3-propanediol from fermentation of crude glycerol with mixed cultures in a simple medium," *Bioprocess and Biosystems Engineering*, 2013.

[11] A. Suau, R. Bonnet, M. Sutren et al., "Direct analysis of genes encoding 16S rRNA from complex communities reveals many novel molecular species within the human gut," *Applied and Environmental Microbiology*, vol. 65, no. 11, pp. 4799–4807, 1999.

[12] K. Tamura, J. Dudley, M. Nei, and S. Kumar, "MEGA4: molecular Evolutionary Genetics Analysis (MEGA) software version 4.0," *Molecular Biology and Evolution*, vol. 24, no. 8, pp. 1596–1599, 2007.

[13] A.-P. Zeng, A. Ross, H. Biebl, C. Tag, B. Gunzel, and W. D. Deckwer, "Multiple product inhibition and growth modeling of *Clostridium butyricum* and *Klebsiella pneumoniae* in glycerol fermentation," *Biotechnology and Bioengineering*, vol. 44, no. 8, pp. 902–911, 1994.

[14] P. Kubiak, K. Leja, K. Myszka et al., "Physiological predisposition of various *Clostridium* species to synthetize 1, 3-propanediol from glycerol," *Process Biochemistry*, vol. 47, pp. 308–1319, 2012.

[15] D. Szymanowska-Powałowska, P. Kubiak, and A. Lewicki, "The methane fermentation medium as an attractive source of bacteria from genus *Clostridium* capable of converting glycerol into 1, 3-propylene glycol," *Journal of Biotechnology, Computational Biology and Bionanotechnology*, vol. 93, no. 1, pp. 68–77, 2012.

[16] M. S. Fountoulakis and T. Manios, "Enhanced methane and hydrogen production from municipal solid waste and agro-industrial by-products co-digested with crude glycerol," *Bioresource Technology*, vol. 100, no. 12, pp. 3043–3047, 2009.

[17] D. R. Boone, R. W. Castenholz, G. M. Garrity, D. J. Brenner, N. R. Krieg, and J. T. Staley, *Bergey's Manual of Systematic Bacteriology*, The Williams & Wilkins Company, Baltimore, Md, USA, 2005.

[18] H. Biebl, "Glycerol fermentation of 1,3-propanediol by *Clostridium butyricum*. Measurement of product inhibition by use of a pH-auxostat," *Applied Microbiology and Biotechnology*, vol. 35, no. 6, pp. 701–705, 1991.

[19] T. Colin, A. Bories, C. Lavigne, and G. Moulin, "Effects of acetate and butyrate during glycerol fermentation by *Clostridium butyricum*," *Current Microbiology*, vol. 43, no. 4, pp. 238–243, 2001.

[20] A. Kuroda, Y. Sugimoto, T. Funahashi, and J. Sekiguchi, "Genetic structure, isolation and characterization of a *Bacillus licheniformis* cell wall hydrolase," *Molecular and General Genetics*, vol. 234, no. 1, pp. 129–137, 1992.

[21] S. Torres, A. Pandey, and G. R. Castro, "Organic solvent adaptation of Gram positive bacteria: applications and biotechnological potentials," *Biotechnology Advances*, vol. 29, no. 4, pp. 442–452, 2011.

Hindawi Publishing Corporation
BioMed Research International
Volume 2013, Article ID 267968, 7 pages
http://dx.doi.org/10.1155/2013/267968

Research Article

Environmental Kuznets Curve Analysis of the Economic Development and Nonpoint Source Pollution in the Ningxia Yellow River Irrigation Districts in China

Chunlan Mao,[1,2] Ningning Zhai,[2,3] Jingchao Yang,[1,2] Yongzhong Feng,[2,3] Yanchun Cao,[1,2] Xinhui Han,[2,3] Guangxin Ren,[2,3] Gaihe Yang,[2,3] and Qing-xiang Meng[4]

[1] *College of Forestry, Northwest A&F University, Yangling, Shaanxi 712100, China*
[2] *The Research Center of Recycle Agricultural Engineering and Technology of Shaanxi Province, Yangling, Shaanxi 712100, China*
[3] *College of Agronomy, Northwest A&F University, Yangling, Shaanxi 712100, China*
[4] *College of Resources and Environment, Henan Agricultural University, Zhengzhou, Henan 450002, China*

Correspondence should be addressed to Yongzhong Feng; fengyz@nwsuaf.edu.cn

Received 22 May 2013; Revised 26 July 2013; Accepted 19 August 2013

Academic Editor: Eldon R. Rene

This study applies the environmental Kuznets curve to test the relationship between the regional economic growth and the different types of agricultural nonpoint source pollution loads in the Ningxia Yellow River irrigation area by using the Johnes export coefficient method. Results show that the pollution load generated by crop cultivation and livestock-breeding industries in the Ningxia Yellow River irrigation area shows an inverted U-shaped feature; however, this feature is absent in living-sewage pollution load. Crop pollution has shown a decreasing trend since 1997 because of the increased per capita income of farmers. Livestock-breeding pollution load reached its turning point when the per capita income of farmers reached 8386.74 RMB. Therefore, an increase in the per capita income of farmers corresponds to an increase in the livestock-breeding pollution load in the Ningxia Yellow River irrigation area.

1. Introduction

Agricultural nonpoint source pollution has become a growing environment problem, contributing so much to water eutrophication in the world [1] and influencing 30% to 50% of the total land area of the world. In addition, 12% of 1200 million ha of degraded land is caused by agricultural nonpoint source pollution [2, 3]. According to the Environmental Protection Agency, agricultural nonpoint source pollution accounts for 52% of the total nitrogen (TN) in surface waters and covers 60% to 87% of the basin total input in Sweden, 60% of environment load in the Netherlands, and 94% of 270 rivers in Denmark [4]. Also, nonpoint source pollution represents more than 94% of nutrient loads except for mineral phosphorus (50%) [5]. Overall, the loss of nitrogen and phosphorus can be transported by farmland drainage and surface water to water which results in deterioration of water quality and accelerates agricultural nonpoint source pollution. According to the survey, 80% of 532 rivers all suffered from nitrogen pollution [6]. Every year, approximately 92% and 88% of the TN in the Yangtze River and Yellow River, respectively, came from agriculture sources, in which half of these values were caused by fertilizers [7].

Environmental pollution has become a serious concern because of rapid industrialization and resource depletion [8]. In 1955, Kuznets found that the relationship between income inequality and economic growth has an inverted U-shaped feature [9]. This relationship is denoted as the environmental Kuznets curve (EKC). EKC implies that in the early stages of economic development, the environment paid a high price for economic growth because people used technology to exploit resources [10–12]. In other words, environmental quality degradation increases in early stage of economic growth and slows down in later stage as economy develops.

Thus, the EKC reveals a dynamic changeable process of environmental quality as the fortunes [13]. One reason an EKC might emerge is, namely, the absence of corresponding willingness for reducing environmental damages with initial income growth [14]. Many literatures have reviewed theoretical developments, empirical studies and contributions of EKC, and challenges, analyzed indicators of environmental degradation favoring the EKC hypothesis, and proposed that developing countries could benefit from developed countries standards [13, 15, 16]. Copeland and Taylor [17] noted that the EKC literature demonstrated the important potential for an income effect on environment quality focusing on the relation between economic growth and environmental degradation.

Economic growth as well as science and technology advancements has fostered public awareness regarding environment protection; the application of advanced environmental management techniques results in the gradual reduction of harmful emissions, thereby substantially improving environmental condition [18–20]. Since its proposal, the EKC hypothesis has been widely used in developed countries. However, not all studies fit the EKC hypothesis. In 1991, Grossman and Krueger analyzed urban air quality by using the global environmental monitoring system and found that the relationship between SO_2 and smoke fits the inverted EKC hypothesis; that is, the content of suspended particles in the atmosphere increases when the per capita GDP has vertex ranging from \$4000 to \$5000 [21]. Currently, several investigations on EKC have already been performed in China. Li and Bao [22] analyzed the trend changes in the "three wastes" (gas waste, water waste, and residues waste) in eastern, western, and central China. Their results showed that these areas have not reached the EKC turning point for pollutants. The indices in Beijing [23] and Shanghai [24] have exceeded this turning point and showed decreasing trends. In Anhui province, the EKC showed U-shaped and inverted U-shaped features [25]. EKC is mostly associated with industrial pollution and is rarely applied in analyzing the relationship between agricultural pollution and economics.

The Ningxia Yellow River irrigation area not only supports the social economic development of Ningxia but also halts the Tengger and Mu Us Deserts from spreading. The Ningxia Yellow River irrigation area is more affected by ecological factors than by economic factors. However, large amounts of returned water considerably influence the water environment in the Yellow River downstream. Currently, limited research is available on the relationship between agricultural economic growth and ecological environment changes. The statistical data of 11 counties in the Ningxia Yellow River irrigation area were collected, arranged, and analyzed. The characteristics of animal manure and rural domestic pollution (i.e., human feces and rural domestic sewage) were estimated and evaluated according to national standards and relevant literature. The EKC hypothesis was applied to find a curve that fits the data on animal manure and rural domestic pollution. This study has a theoretical and realistic significance in the control of agricultural nonpoint source pollution and in the environmental maintenance in the Yellow River irrigation area.

2. Materials and Methods

2.1. Experimental Area. The Ningxia Yellow River irrigation area is divided into Qingtong Xia and Weining irrigation districts, involving Yinchuan City, Zhongwei City (except HaiRMB county), Wuzhong City (except Yanchi and Tongxin counties), and Shizuishan City (see Figure 1). A total of 11 counties and 20 state-owned farms and animal farms were included. The agricultural population is 1678 thousand, covering 48.4% of the total population (i.e., 3468 thousand). The Ningxia Yellow River irrigation area is a typical area of rice and corn crop rotation in the northwest arid and semiarid area in China and receives annually an average of 7 billion m^3 of water from the Yellow River, approximately 93% to 95% of which is used as agricultural water and only 25 billion m^3 of water returns to the Yellow River. On the basis of the monitoring reports, the water quality of the main ditches of the Yellow River irrigation districts is of inferior class V and has high NO^{3-}–N and NH^{4+}–N contents [26]. Approximately 61% to 66% TN and 76% to 81% NH^{4+}–N came from farming. The NH^{4+}–N concentration in drainage was generally 20 mg/L to 30 mg/L and even reaches 70 mg/L, thus inducing substantial influence on the water quality along the Lower Yellow River [27]. From 2002 to 2007, the average amount of N fertilizer applied was 301 kg/hm^2, which is 1.6 times the national average amount [28].

2.2. Experimental Methods

2.2.1. Estimation Method of Nonpoint Source Pollution Load. Nonpoint source pollution load must first be estimated before estimating the losses of nonpoint source pollution in these districts. This study adopted the Jones export coefficient method [29], which directly establishes the relationship between land use and agricultural nonpoint pollution load of receiving water using easily accessible information such as land utilization conditions. The Jones export coefficient method is expressed as follows:

$$L = \sum_{i=1}^{n} E_i \left[A_i \left(I_i\right)\right] + P, \tag{1}$$

where L is the total pollution (pollutant load) in kg; E is the output coefficient of type i pollutants in kg·$km^{-2\cdot a-1}$, which is the year output of unit area per capita or pollution of each head of livestock; A_i is the land use area of type i livestock, which is in km^2; type i pollutant is in kg; P is the amount of pollutant with rainfall, which is ignored in this study as the EKC relationships are more likely to hold for pollutants of more short-term and local impacts with, rather than those with more global, indirect, and long-term impacts.

2.2.2. Selection of the EKC Model. The general model of EKC is as follows (see [30]):

$$E = \alpha + \beta_1 Y + \beta_2 Y_2 + \beta_3 Y_3 + u, \tag{2}$$

where E is the pollution index of a certain county or area; Y is the economic growth indicator usually replaced by per

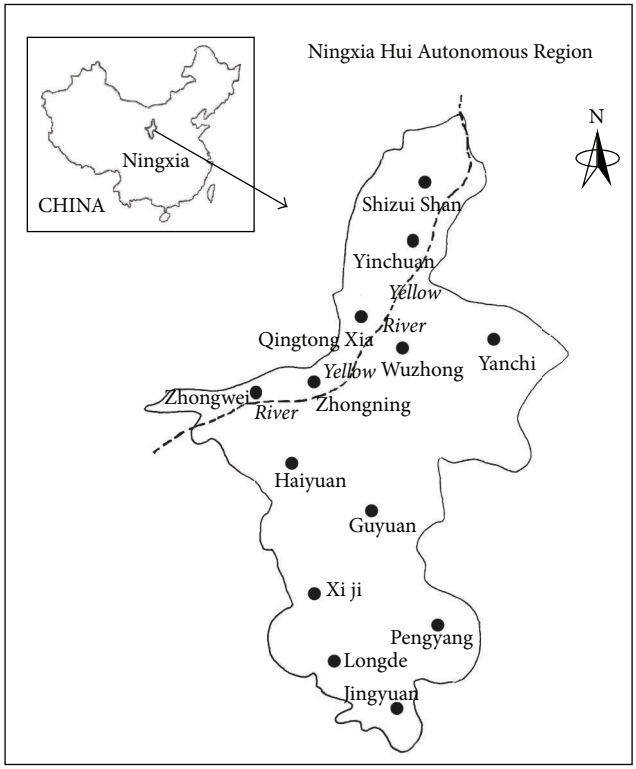

Figure 1: Location of the study area at the Yellow River irrigation area in the northern part of Ningxia along the Yellow River, China.

capita GDP (this study utilized the per capita net income of farmers); α is the intercept; β_1, β_2, and β_3 are unknown parameters; u is a random error. The turning point of the model can be obtained through first curvature vector. The "turning point" is the point beyond which increases in economic development result in reduction in environmental pollution, as expressed in the following equation:

$$X_t = \frac{\partial Y}{\partial X}. \quad (3)$$

The following relationships were observed between agricultural nonpoint source pollution and economic development levels which can be categorized into 7 types including: (1) monotonic increasing, (2) monotonic decreasing, (3) inverted U-shaped (EKC type, where $\beta_1 > 0$, $\beta_2 < 0$, $\beta_3 = 0$, and the "turning point" is calculated at $X_t = -\beta_1/2\beta_2$ for models), (4) U-shaped, (5) N-shaped, (6) insignificance (INSIG), and (7) none [31].

2.3. Data Analysis. This study used Eviews.6.0 in analyzing the crop planting area, number of livestock breeds, agriculture population, and per capita income of farmers in Ningxia from 1990 to 2008 and Origin 7.5 in making graphics. Data were obtained from Ningxia Statistical Yearbook by Ningxia Bureau of Statistics.

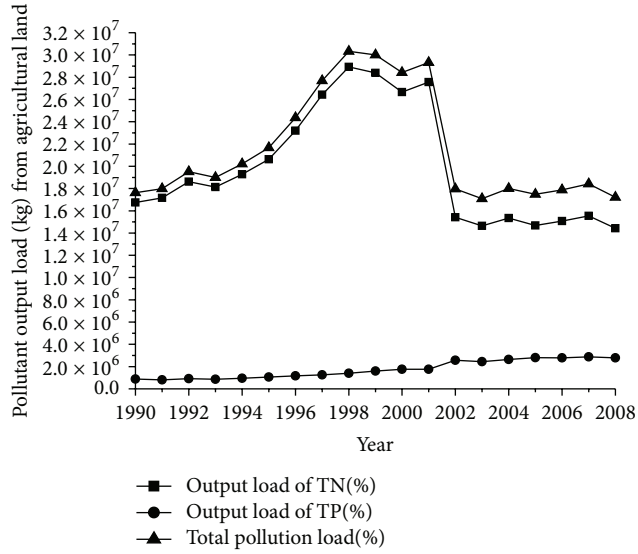

Figure 2: Pollutant output load (kg) from agricultural land in 1990–2008.

3. Results

3.1. Evaluation of the Nonpoint Source Pollution Load of the Ningxia Yellow River Irrigation Districts

3.1.1. Pollutant Loads from Agricultural Lands. The main food crops in the Ningxia Yellow River irrigation region are rice, corn, and wheat. Hence, the study adopted an area-weighted average of these three crops as the pollutant output coefficient of agricultural lands [32]. Different pollutant output coefficients of agricultural land were calculated according to fertilizer usage and fertilizer churn rate from 1990 to 2008. Calculation results are presented in Figure 2.

3.1.2. Pollutant Output Load of Livestock Discharge. The pollutant output coefficient of livestock discharge represents the total discharge from livestock industries each year (i.e., 365 days). Most of the TN and total phosphorus (TP) pollution came from livestock discharge. Given that the amount of discharge depends on numerous factors, such as livestock species, growth period, forage, and weather, this study adopted reference amount of related livestock to determine the amount of discharge [33, 34]. A pig produces 3.5 kg of feces and 3.5 kg of urine daily; a cow produces 25 kg of feces and 10 kg of urine daily; a sheep produces 2.6 kg of feces and 0.4 kg of urine daily. Normally, the growth period of cattle and sheep is 365 days, whereas that of a pig is 150 days. The nitrogen and phosphorus annual emissions in livestock pollutants are calculated using feces production, output coefficient of nitrogen and phosphorus, and number of livestock by using the following formula: TN and TP annual emissions = individual feces production × feeding period × number of livestock × output coefficient of nitrogen and phosphorus $\times 10^{-3}$. Figure 3 shows the average pollutant content in livestock feces.

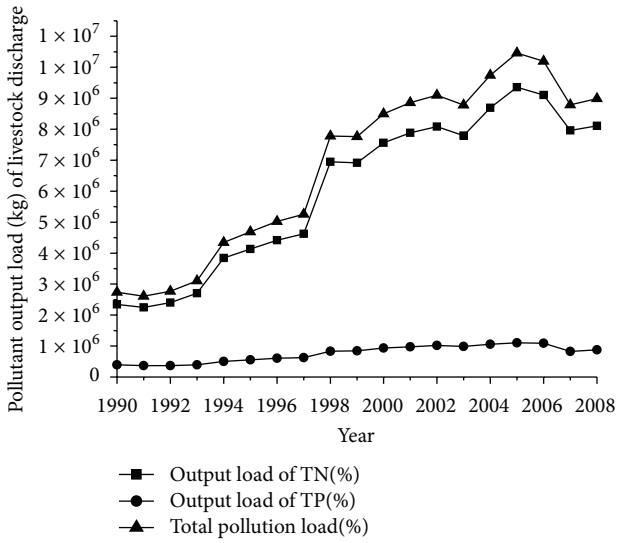

Figure 3: Pollutant output load (kg) of livestock discharge in 1990–2008.

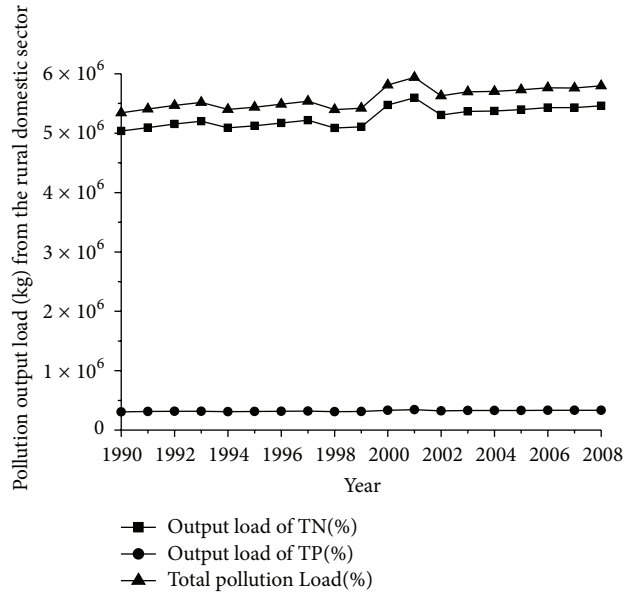

Figure 4: Pollution output load (kg) from the rural domestic sector in 1990–2008.

3.1.3. Pollution Output Load from the Rural Domestic Sector. The distribution of population in rural areas is generally sparse. Rural areas have been polluted to a certain degree because of pollutant discharge. However, current pollutant treatment equipment is still inadequate to remove pollution in these areas. The average nitrogen and phosphorus contents in the per capita domestic sewage per day are 5 and 0.44 g, respectively [35]. Wastage rate is estimated at 100%, given that no unified sewage treatment equipment is available in rural areas. The pollution output load from the rural domestic sector (see Figure 4) can be calculated by using the following formula: amount of annual pollutant discharge = per capita average discharge per day × agricultural population × 365 × levels of pollutants (i.e., TN and TP) × wastage rate.

3.2. Empirical Analysis of Pollution Load in the EKC Equation

3.2.1. Testing the Relationship between the Agricultural Pollution Load and the Per Capita Income Growth. Table 1 shows that the result of the quadratic regression is perfect, but the determination coefficient (0.47) is not ideal. Thus, the relationship did not fit the EKC hypothesis. The relationship between the agricultural pollution load and the per capita income has a typical inverted-U EKC feature because the second-order coefficient is negative. The regression equation is as follows:

$$E_{\text{plant}} = -18.4389 + 7.6465y - 0.5115y^2. \quad (4)$$

First, the derivative of the regression equation was obtained, where the inflection point reflects the per capita income of farmers. The calculation results denote that a per capita income of 1762.49 RMB results in the occurrence of the inflection point of the agricultural industry. In an economic perspective, this result implies that a per capita income below 1762.49 RMB corresponds to gains in the agricultural industry. Consequently, a per capita income equal to or higher than 1762.49 RMB corresponds to losses in the agricultural industry. The per capita income of farmers in the Ningxia Yellow River irrigation districts was nearly 1762.49 RMB in 1997; thus, the planting industry in this region currently experiences a downward trend (see Table 1).

3.2.2. Testing the Relationship between Livestock-Breeding Pollution Load and Per Capita Income Growth. As shown in Table 2, the effects of the quadratic and cubic regressions are perfect; the t-test results show that the effect of the quadratic regression is relatively good. The regression equation is expressed as follows:

$$E_{\text{animal}} = -11.2718 + 4.5599y - 0.2524y^2. \quad (5)$$

The relationship between livestock-breeding pollution load and per capita income presents a typical inverted U-shaped EKC feature because the second-order coefficient is negative. The results of the regression equation were derived, and the turning point of the per capita income was obtained. The results show that the per capita income of farmers was approximately 8386.74 RMB when pollution load reaches its turning point. In terms of economics, this finding indicates that the livestock-breeding pollution load increases with increasing the per capita income of farmers when the latter is below 8386.74 RMB; otherwise, an opposite trend is shown when the income reaches or exceeds 8386.74 RMB. The per capita income of farmers has constantly increased in the Ningxia Yellow River irrigation districts from 1990 to 2008 and has reached 4559.8 RMB in 2008. Thus, pollution load will continue to increase until the income of farmers reaches 8386.76 RMB.

3.2.3. Testing the Relationship between Living-Sewage Pollution Load and Per Capita Income Growth. Table 3 shows the

Table 1: Relationship between agricultural pollution load and per capita income.

Curve type	Constant term	First-order coefficient	Second-order coefficient	Third-order coefficient	R^2	F
Quadratic coefficient	−18.4389 (−2.43)**	7.6465 (3.74)***	−0.5115 (−3.74)***	—	0.47	6.99
Three coefficients	35.0630 (0.26)	−13.8673 (−0.26)	2.3615 (0.33)	−0.1274 (−0.40)	0.47	4.48

Note. ***, **, and *, respectively, represent significance levels in 1%, 5%, and 10%. The t-test results are written in brackets.

Table 2: Relationship between breeding industry pollution load and per capita income.

Curve type	Constant term	First-order coefficient	Second-order coefficient	Third-order coefficient	R^2	F
Quadratic coefficient	−11.2718 (−1.86)*	4.5599 (2.79)**	−0.2524 (−2.31)**	—	0.93	114.48
Three coefficients	172.8145 (1.80)*	−69.4635 (−1.80)*	9.6328 (1.87)*	−0.4385 (−1.92)*	0.95	90.34

Note. ***, **, and *, respectively, represent significance levels in 1%, 5%, and 10%. The t-test results are written in brackets.

Table 3: Relationship between living-sewage pollution load and per capita income.

Curve type	Constant term	First-order coefficient	Second-order coefficient	Third-order coefficient	R^2	F
Quadratic coefficient	9.5409 (10.48)***	−0.2893 (−1.18)	0.0221 (1.35)	—	0.64	14.40
Three coefficients	22.6854 (1.44)	−5.5748 (−0.88)	0.7280 (0.86)	−0.0313 (−0.84)	0.66	9.65

Note. ***, **, and *, respectively, represent significance levels in 1%, 5%, and 10%. The t-test results are written in brackets.

regression analysis of living-sewage pollution load and per capita income growth. As shown in the table, the fitting effects of the quadratic and cubic regressions are imperfect, and the t-test of the coefficients is insignificant. Therefore, the relationship between living-sewage pollution load and per capita income growth does not fit the EKC model.

4. Discussion

The EKC hypothesis implies that a low total population and slow economic growth rate have been observed before economic growth; thus, the development and utilization of resources have been limited, and the negative influence of technology on the environment has been negligible. During the initial phase of economic growth, the development-resource intensive industry and the polluting technology, combined with population growth, have significantly hastened economic growth, thereby resulting in increased environmental pollution. As the EKC reflected that technological, political, economic conditions and environmental awareness existed at the same time [36], after economic development reached a certain level, the human capital and clean technology intensive industries have played an important role in decreasing environmental degradation. In addition, with the increased awareness of environmental hazards, greater public demands for a healthier and cleaner environment have become popular [13]. People prefer to see the low-income countries turn their attention to protect the environment at earlier stages of development than creating pressure for environmental protection, and they pay more attention to sustainable development. Furthermore, environmental regulations also have played a significant role in environmental protection and the more sustainable policies can create higher levels of development at a lower environmental cost to seek "win-win" policies that yield both economic and environmental gains, such as environmental legislation and market-based incentives, import instead of exploitation of resources to reduce environmental degradation. In a word, at higher levels of development, combining structural change about information-intensive industries and services with increased environmental awareness, adoption of environmental regulations, better technology, and higher environmental expenditures, results in gradual decline of environmental degradation [37].

The EKC hypothesis, which is solely based on the perspective of economics, analyzes the relationship between environment pollution load and economic development. The inverted-U hypothesis summarizes economic growth practices. Economic growth mode and economic formation are different in each region. Therefore, the two factors are not guaranteed to have the same patterns in environmental pollution [38]. Aside from income, many factors such as natural and social factors, environmental policy of a county or region, investment environment, and public consciousness of environmental protection influence the environment [39]. The irreversible ecological threshold is characterized by an inverted U-shaped feature. When this instance occurs, the possibility of solving environmental problems will drop to zero. If the environment pollution reaches a level that is higher than the ecological irreversible threshold, then the destruction of the ecological environment cannot be restored.

The Ningxia Yellow River irrigation area benefits from western development; thus, economic development induces negligible influence to the environment. The environmental awareness of farmers during farming operations constantly improves with increased investments in education. Improving the national economy and the income of farmers results in improved farm facilities and increased utilization of agricultural technology. Moreover, precision fertilization and controlled pesticide use effectively help in the prevention of agricultural pollution. Currently, the demand for meat products is still high, and the breeding industry has become

the main source of income in these areas. Therefore, pollution load will increase because of breeding expansion and increased per capita income.

5. Conclusions

This study shows that crop cultivation and livestock-breeding pollution load in the Ningxia Yellow River irrigation area fit the EKC hypothesis. Agricultural pollution load and per capita income reached their turning point in 1997. Thus, pollution load gradually decreases as the income increases. However, this finding is not a good indicator for the decrease in total pollution because the above result utilizes an environmental economics point of view. The regression relation of the per capita income of farmers and the livestock-breeding pollutants in the last 19 years shows typical characteristics of EKC; however, livestock-breeding emission is consistently increasing. Much time is needed before the per capita income of farmers reaches 8386.74 RMB, which is the turning point for this factor, because the per capita income of farmers is only 4559.8 RMB in 2008. In addition, with the population growth, demands for resources, such as drinking water, energy use, and traffic volumes, are still increasing with the waste generation increasing in quantity and toxicity which can produce nonpoint resource pollution. Thus, pollution load will continue to increase with increasing income, and this phenomenon will increase in severity after ten years. Thus, it is the priority to ascertain the relationship between the economic growth and environmental quality of Ningxia Yellow River irrigation area for developing environmental management programs and management policy. This study helps us understand the relationship between human activities and pollutant loads to protect environment, especially the aquatic ecosystems. In addition, it is also helpful for identifying the main factors that lead to the agricultural nonpoint source pollution in Ningxia Yellow River irrigation area. Furthermore, our work is important to determine the appropriate mode of economic development of Ningxia Yellow River irrigation area which can be valuable for other researchers. However, further study is needed on the reduction of agricultural pollution and maximization of livestock waste to determine the dispersion of livestock and poultry farms as well as aquaculture farming areas in the Ningxia Yellow River irrigation area. The control of nonpoint source pollution has become an important task of agricultural soil and water environment field, hence, the river basin pollution control should also be paid more attention in the following work, and more work should be done to investigate the comprehensive control measures of agricultural nonpoint source pollution.

Conflict of Interests

The authors affirm that they have no financial affiliation or involvement with any commercial organization with direct financial interest in the subject or materials discussed in this paper and deny any conflict of interests related to this study.

Acknowledgments

Financial support for this work was provided by China's Technology Support Project for the 12th Five-year Plan: High-yielded Biogas Technology Integrated Demonstration on Mixing Materials (Grant no.: 2011BAD15B03), the National Water Pollution Control and Management Technology Major Projects (2009ZX07212-004-01-3).

References

[1] J. Ma, X. Chen, and Y. Shi, "Distinguishing the main pollution source an efficient way in agricultural non-point source pollution control," *Advanced Materials Research*, vol. 347–353, pp. 2195–2199, 2012.

[2] Y. Zheng and X. J. Wang, "Advances and prospects for nonpoint source pollution studies," *Advance in Water Science*, vol. 13, pp. 105–110, 2002.

[3] L. P. Cao, X. Y. Wang, and X. J. Guang, "The policies for control and management of nonpoint source pollution and its research progress," *Geography and Geo-Information Science*, vol. 20, pp. 90–94, 2004.

[4] A. L. Yang and Y. M. Zhu, "The study of nonpoint source pollution of surface water environment," *Techniques and Equipment for Environmental Pollution Control*, vol. 7, pp. 60–67, 1999.

[5] Y. Wu and J. Chen, "Investigating the effects of point source and nonpoint source pollution on the water quality of the East River (Dongjiang) in South China," *Ecological Indicators*, vol. 32, pp. 294–304, 2013.

[6] P. Chang, P. Zhu, and H. Niu, "Nitrogen and phosphorus loss of farmland agriculral non-point source pollution and its prevention," *Chinese Journal of Soil Science*, vol. 41, pp. 509–512, 2010.

[7] A. P. Zhang, S. Q. Yang, J. Yi, and Z. L. Yang, "Analysis on current situation of water pollution and pollutant sources in Ningxia Yellow River irrigation region," *Chinese Journal of Eco-Agriculture*, vol. 18, no. 6, pp. 1295–1301, 2010.

[8] M. Galeotti and A. Lanza, "Desperately seeking environmental Kuznets," *Environmental Modelling and Software*, vol. 20, no. 11, pp. 1379–1388, 2005.

[9] S. Kuznets, "Economic growth and income equality," *American Economic Review*, vol. 45, pp. 1–28, 1955.

[10] M. Pasche, "Technical progress, structural change, and the environmental Kuznets curve," *Ecological Economics*, vol. 42, no. 3, pp. 381–389, 2002.

[11] N. Khanna and F. Plassmann, "The demand for environmental quality and the environmental Kuznets Curve hypothesis," *Ecological Economics*, vol. 51, no. 3-4, pp. 225–236, 2004.

[12] S. Dietz and W. N. Adger, "Economic growth, biodiversity loss and conservation effort," *Journal of Environmental Management*, vol. 68, no. 1, pp. 23–35, 2003.

[13] S. Dinda, "Environmental Kuznets curve hypothesis: a survey," *Ecological Economics*, vol. 49, no. 4, pp. 431–455, 2004.

[14] M. Munasinghe, "Is environmental degradation an inevitable consequence of economic growth: tunneling through the environmental Kuznets curve," *Ecological Economics*, vol. 29, no. 1, pp. 89–109, 1999.

[15] D. I. Stern, "The rise and fall of the environmental Kuznets curve," *World Development*, vol. 32, no. 8, pp. 1419–1439, 2004.

[16] R. Roy Chowdhury and E. F. Moran, "Turning the curve: a critical review of Kuznets approaches," *Applied Geography*, vol. 32, no. 1, pp. 3–11, 2012.

[17] B. R. Copeland and M. S. Taylor, "Trade and environment: a partial synthesis," *American Journal of Agricultural EcoNomics*, vol. 77, no. 3, pp. 765–771, 1995.

[18] S. Dinda, "A theoretical basis for the environmental Kuznets curve," *Ecological Economics*, vol. 53, no. 3, pp. 403–413, 2005.

[19] J. Fan and H. H. Hu, "Research and application of EKC," *Mathematics in Pract Ice and Theory*, vol. 32, pp. 944–951, 2002.

[20] Y. W. Li, Z. M. Xu, Y. Wang, and W. X. Jiao, "Study on the environmental Kuznets curve CHINA population," *Resources and Environment*, vol. 15, pp. 7–14, 2005.

[21] Y. Y. Yang, *Economics of Population, Resources and Environment*, China Economic Publishing House, Beijing, China, 2004.

[22] Z. Li and X. B. Bao, "Estimate china's environmental Kuznets curve," *Science & Technology Review*, vol. 25, pp. 57–58, 2002.

[23] Y. P. Wu, S. C. Dong, and J. F. Song, "Modeling economic growth and environmental degradation of Beijing," *Geographical Research*, vol. 21, pp. 239–246, 2002.

[24] K. Yang, M. Ye, and X. Q. Xu, "Environmental Kuznets characteristics of municipal solid waste growth in Shanghai city," *Geographical Research*, vol. 22, pp. 60–66, 2003.

[25] K. Y. Wu and X. J. Chen, "Study on the relationship between economic growth and environmental degradation of Anhui province," *Chongqing Environmental Science*, vol. 25, pp. 9–11, 2003.

[26] A. P. Zhang, S. Q. Yang, Q. Z. Zhang, S. J. Yang, and Z. L. Yang, "Influence factor and countermeasures of irrigation return flow pollution in Ningxia Yellow River water irrigation district," *Chinese Journal of Eco-Agricultural*, vol. 16, pp. 1037–1042, 2008.

[27] S. J. Yang, A. P. Zhang, Z. L. Yang, and S. Q. Yang, "Agricultural nonpoint source pollution in Ningxia irrigation district and preliminary study of load estimation methods," *Scientia Agricultura Sinica*, vol. 42, pp. 3947–3955, 2009.

[28] G. Q. Liu and S. Q. Yang, "Analyzed on present situation of subsiding water from cropland in Ningxia irrigation area from the Huanghe river," *Journal of Irrigation and Drainage*, vol. 29, pp. 104–108, 2010.

[29] P. J. Johnes, "Evaluation and management of the impact of land use change on the nitrogen and phosphorus load delivered to surface waters: the export coefficient modelling approach," *Journal of Hydrology*, vol. 183, no. 3-4, pp. 323–349, 1996.

[30] R. Jha and K. V. B. Murthy, "An inverse global environmental Kuznets curve," *Journal of Comparative Economics*, vol. 31, no. 2, pp. 352–368, 2003.

[31] H. Li, T. Grijalva, and R. P. Berrens, "Economic growth and environmental quality: a meta-analysis of environmental Kuznets curve studies," *Economics Bulletin*, vol. 17, no. 5, pp. 1–11, 2007.

[32] C. Peng, P. Zhu, H. H. Niu, Q. Li, and Y. L. Hang, "Nitrogen and phosphorus loss of farmland agriculral nonpoint source pollution and its prevention," *Chinese Journal of Soil Science*, vol. 41, pp. 509–511, 2010.

[33] M. K. Zhang, J. G. Li, and Z. P. Bian, "Best management practices for controlling agricultural nonpoint pollution," *Acta Agriculturae Zhejiangensis*, vol. 17, pp. 244–250, 2005.

[34] X. D. Han, "Application of optimal management practice to NPSP control," *Shanghai Environmental Sciences*, vol. 19, pp. 102–104, 2000.

[35] L. H. Xue and L. Z. Yang, "Research advances of export coefficient model for non-point source pollution," *Chinese Journal of Ecology*, vol. 28, no. 4, pp. 755–761, 2009.

[36] G. M. Grossman and A. B. Krueger, "Economic growth and the environment," *Quarterly Journal of Economics*, vol. 110, no. 2, pp. 353–377, 1995.

[37] D. I. Stern, M. S. Common, and E. B. Barbier, "Economic growth and environmental degradation: the environmental Kuznets curve and sustainable development," *World Development*, vol. 24, no. 7, pp. 1151–1160, 1996.

[38] C. H. Zhang and H. Y. Liu, "Adaptive evaluation on existence of EKC hypothesis," *Journal of Beihua University*, vol. 10, pp. 29–31, 2009.

[39] B. B. Chu, "Study on the relationship between economic development and environment quality of Taihu," *Environmental Science and Management*, vol. 33, pp. 51–54, 2008.

Hindawi Publishing Corporation
BioMed Research International
Volume 2013, Article ID 373412, 8 pages
http://dx.doi.org/10.1155/2013/373412

Research Article

Performance Study of Chromium (VI) Removal in Presence of Phenol in a Continuous Packed Bed Reactor by *Escherichia coli* Isolated from East Calcutta Wetlands

Bhaswati Chakraborty,[1] Suvendu Indra,[1] Ditipriya Hazra,[1] Rupal Betai,[1] Lalitagauri Ray,[2] and Srabanti Basu[1]

[1] *Department of Biotechnology, Heritage Institute of Technology, Chowbaga Road, Anandapur, Kolkata 700107, India*
[2] *Department of Food Technology and Biochemical Engineering, Jadavpur University, S. C. Mallik Road, Kolkata 700032, India*

Correspondence should be addressed to Srabanti Basu; srabanti_b@yahoo.co.uk

Received 26 April 2013; Revised 22 July 2013; Accepted 23 July 2013

Academic Editor: Kannan Pakshirajan

Organic pollutants, like phenol, along with heavy metals, like chromium, are present in various industrial effluents that pose serious health hazard to humans. The present study looked at removal of chromium (VI) in presence of phenol in a counter-current continuous packed bed reactor packed with *E. coli* cells immobilized on clay chips. The cells removed 85% of 500 mg/L of chromium (VI) from MS media containing glucose. Glucose was then replaced by 500 mg/L phenol. Temperature and pH of the MS media prior to addition of phenol were 30°C and 7, respectively. Hydraulic retention times of phenol- and chromium (VI)-containing synthetic media and air flow rates were varied to study the removal efficiency of the reactor system. Then temperature conditions of the reactor system were varied from 10°C to 50°C, the optimum being 30°C. The pH of the media was varied from pH 1 to pH 12, and the optimum pH was found to be 7. The maximum removal efficiency of 77.7% was achieved for synthetic media containing phenol and chromium (VI) in the continuous reactor system at optimized conditions, namely, hydraulic retention time at 4.44 hr, air flow rate at 2.5 lpm, temperature at 30°C, and pH at 7.

1. Introduction

Environmental pollution due to structured and unstructured industrial growth and inadequate effluent treatment due to lack of awareness and insufficient treatment facility has become a serious health hazard in the world [1, 2]. Fresh water bodies are contaminated with different types of pollutants both organic and inorganic. One of the leading organic pollutants in water bodies is the phenolic compounds and the untreated metals, like chromium, which were another source of prolific water pollution.

Chromium is a multivalent ion, among which Chromium (III) and Chromium (VI) form stable compounds. Chromium (VI) compounds (as in chromates, CrO_4^{-}, and dichromates, $Cr_2O_7^{-2}$) [3] are mostly water soluble and are extremely toxic to human. It causes severe health hazards like allergic reactions, respiratory disorder, diarrhea, stomach and intestinal bleedings, cramps, and liver and kidney damage. Chromium (VI) is mutagenic in nature and leads to cancer [3–11]. Chromium (VI) is placed in the 16th position of the priority list prepared by the Agency for Toxic Substances and Diseases Registry (ATSDR) [12]. Thus Environmental Protection Agency (EPA), USA, has recommended the safety limit of chromium (VI) in potable water to be less than 50 μg/L [2, 13], and for industrial discharge it is 5 mgL^{-1} [2]. The main source of chromium (VI) pollution of surface water is effluent from tanning, plastic, pigment, and paint manufacturing industries [5]. Industrial effluents like tannery effluent have been found to contain 80–250 mgL^{-1} chromium (VI) [2, 14]. Chromium (VI) can be removed both by chemical as well as biological processes. Chemical methods like precipitation, ion exchange, and electrochemical treatments have several disadvantages like incomplete conversion of chromium (VI) and ineffective removal of the metal from dilute metal solutions [15, 16] whereas biological detoxification of chromium

(VI) can be done by cellular adsorption, conversion to nontoxic trivalent chromium, and bioaccumulation [15–20].

Several studies have been carried out for removal of chromium (VI) using microorganisms under laboratory condition [15–20]. In all cases, chromium (VI) had been used as the only stress factor in the growth media. Numerous tanneries are located in and around Kolkata whose effluents contain both chromium (VI) and phenol [21]. In the present study, attempt has been made to use microorganisms for removal of chromium (VI) in presence of an organic pollutant phenol which acted as the sole source of carbon. The bacterial strain used in the study was isolated from the East Calcutta Wetlands, the major waste degradation site for the metropolitan city Kolkata (previously known as Calcutta). The site received domestic waste of the city as well as industrial wastes, predominantly from the tanneries situated at the outskirts of the city. The performance of the reactor system under various hydraulic retention times, air flow rates, temperature, and pH conditions was studied, and reaction conditions were optimized.

2. Materials and Methods

2.1. Bacterial Strain Selection. A mixed bacterial consortium was isolated from soil of East Calcutta Wetlands, a Ramsar site in India. The mixed culture was then acclimatized in phenol using it as the sole source of carbon over a period of three months.

Three pure strains were isolated from the mixed bacterial culture and identified by 16s rRNA method. Phylogenetic tree was constructed using Phylogenetic Tree Builder, and percentage homology was determined using ClustalW. Biochemical characterization was done following standard procedures.

A comparative batch kinetic study of phenol degradation by individual bacterial species was carried out in presence of phenol as the sole source of carbon. The strain showing maximum phenol degradation rate was *Escherichia coli*. The strain, initially found to degrade phenol and remove chromium (VI) from medium separately, has been introduced to a continuous packed bed reactor. Media contained both phenol and chromium (VI). This study is engaged in checking the efficacy of this bacterial species for removal of chromium (VI) singularly as well as simultaneously with phenol to increase the efficiency of effluent treatment.

2.2. Media Composition. The hexavalent chromium containing synthetic mineral salt (MS) media used in the experimental study is prepared from analytical grade chemicals procured from Merck, India. Either Phenol or glucose was used as source of carbon for growing the organisms. Composition of MS media (g/L) was potassium dihydrogen phosphate: 0.68; dipotassium hydrogen phosphate: 1.73; ferrous sulfate: 0.03; ammonium nitrite: 0.1; magnesium sulfate: 0.1; calcium chloride: 0.02; manganese sulfate: 0.03; glucose: 2.0. For using phenol as the source of carbon, 500 mg of phenol was added instead of 2 g glucose. Chromium (VI) was added to the media in form of potassium dichromate.

2.3. Packed Bed Reactor System. The packed bed reactor was a bench scale reactor of volume 1000 mL. The clay chips used as packing material were derived from earthen tea cups used in West Bengal, a state in Eastern India. These tea cups were disposable and nonbiodegradable. They thus produced a huge bulk of solid waste. The bulk of solid waste could be reduced by recycling the clay chips. The used tea cups were collected from the vendors, washed, and dried under the sun. Then they were broken into smaller pieces. The broken pieces were sifted, and similar sized pieces were selected for packing the column reactor. The void volume (ε) was 0.81707, and the equivalent diameter ($D_p = \sqrt[3]{(6V_p/\pi)}$, where V_p was mean volume of a chip in cubic centimetre) was 1.08 cm. The column reactor made of Borosil glass had an aspect ratio 10 : 1. The bed volume was 80% of the total reactor volume.

The *E. coli* cells (24 h old) suspended in MS media containing 500 mgL^{-1} of phenol as the sole source of carbon were circulated through the reactor bed with the help of a peristaltic pump at the rate of 3 mL/min for 12 h through the inlet port located at 110 mm from the base of the reactor. 5 mL cell samples were collected before and after immobilization process, and their cell optical densities were measured at 600 nm by a UV-VIS spectrophotometer (Shimadzu). The difference of the two values was the cell loading factor. It was found that the *E. coli* cells were immobilized on the clay chips to 70% of its initial cell mass. The cells were allowed to grow on the clay chips for 5 days in the reactor by passing 500 mgL^{-1} of phenol through the reactor semicontinuously. The supernatant was drained out each morning for 5 days till sufficient cell growth occurs on the clay chips.

First the chromium (VI) removal capability of the cells was studied using glucose as the sole source of carbon, such that only one toxic material, that is, chromium (VI), was present in the media. The purpose of the study was to check whether the organism can tolerate chromium (VI) in presence of a common source of carbon. The concentration of chromium (VI) in the MS media containing 2% glucose as the sole source of carbon was 500 mgL^{-1}. The synthetic media was introduced into the reactor with the help of a peristaltic pump at different hydraulic retention times and air flow rates at 30°C and pH 7. The air was introduced into the reactor by a sparger in countercurrent direction, and the air flow rates were measured by a rotameter made of perspex. The system attained steady state when the input flow rate was equal to output flow rate of media. The two output sample collection ports were at 25 mm and 50 mm from the base of the reactor. At steady state the samples were collected from the lower port as well as the upper port, and the output concentrations of chromium (VI) were the same for both the ports for a single trial. For each hydraulic retention time and air flow rate, experimental trials were conducted in triplicate at a time interval of 15 mins. The hydraulic retention times were varied from 3.33 h to 8.88 h and air flow rates were varied from 1 lpm to 3 lpm.

Glucose was replaced by phenol as the only source of carbon, and the cells thus had to biodegrade both phenol and chromium (VI). The synthetic media containing 500 mgL^{-1} of phenol and 500 mgL^{-1} chromium (VI) was introduced

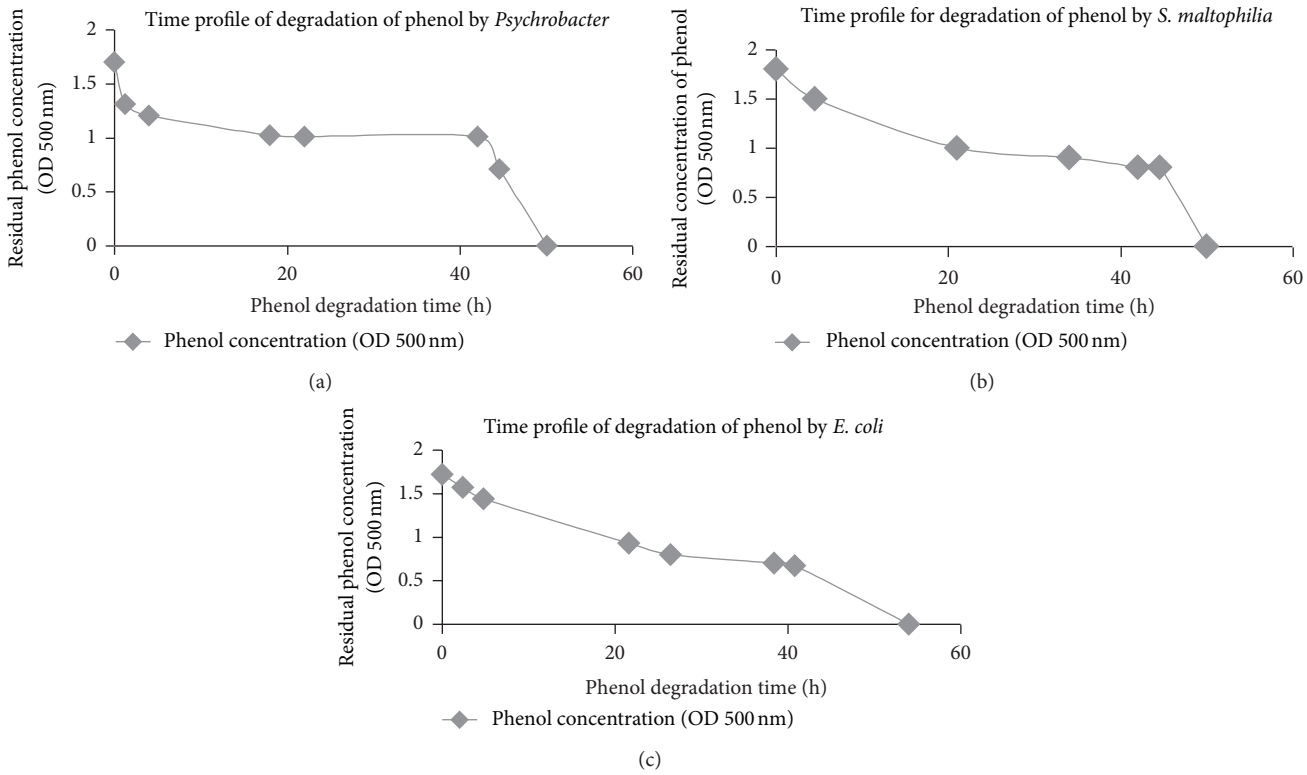

Figure 1: (a) Time profile of degradation of phenol by *Psychrobacter sp.* (b) Time profile of degradation of phenol by *S. maltophilia*. (c) Time profile of degradation of phenol by *E. coli*.

into the reactor with the help of a peristaltic pump. Air was sparged into the reactor in countercurrent direction to the substrate. The steady state system was studied at various substrate flow rates and air flow rates at room temperature simultaneously. The rate of removal of chromium (VI) from the synthetic media was measured spectrophometrically. Then further studies were done on the performance of the continuous reactor system in removal of Cr(VI) in presence of phenol. The reaction conditions were optimized based on removal efficiency of chromium (VI) at room temperature. Then the removal efficiency of the packed bed reactor was studied under the optimized substrate and air flow rates at different temperature and pH conditions.

2.4. Scanning Electron Microscopy (SEM) and Energy Dispersive X-Ray Spectrometry (EDS) Study. SEM and EDS were done with clay chips, bacteria immobilized clay chips, and bacteria immobilized on clay chips after treatment with chromium (VI) to obtain their topographical characterization and mineral composition. SEM photographs were taken after coating the samples with palladium by JFC-1600 Auto fine Coater with a scanning electron microscope (JSM 6360) using 17 kV. EDS was done to ascertain the presence of chromium using instrument INCA-MICS, 01736-03-04.

2.5. Analytical Study. Phenol in the output sample was quantified spectrophotometrically at 490 nm using UV-VIS spectrophotometer (Shimadzu) by potassium ferricyanide and aminoantipyrine assay following the standard protocol (APHA) [22]. Chromium quantification was done spectrophotometrically at 540 nm using UV-VIS spectrophotometer (Shimadzu) with diphenylcarbazide following the standard procedure [22].

3. Results and Discussion

3.1. Selection of Strain from the Mixed Bacterial Consortium. The three bacterial strains constituting the mixed bacterial consortium identified by 16rRNA analysis were found to be *Psychrobacter sp.*, *Stenotrophomonas maltophilia*, and *Escherichia coli*.

The rate of phenol degradation by each bacterial species was studied individually in batch process (from Figure 1) and compared as shown in Figure 2. *Escherichia coli* exhibited highest rate of phenol degradation (Figure 2) and was selected for further studies to measure its potential as a multiple toxic substance remover, in this case chromium (VI), in presence of phenol.

The 16s rRNA sequence of *E. coli* strain isolated from the soil sample of ECW was analyzed for strain identification, and the phylogenetic tree thus constructed to establish its homologous bacterial strains was shown in Figure 3. The microbe was found to be most similar to *Escherichia coli* (GenBank entry: AF233451). The next closest homologue was found to be *Escherichia coli*; K-12 (Genbank entry: M87049). In both cases the homology with the *E. coli* of present work

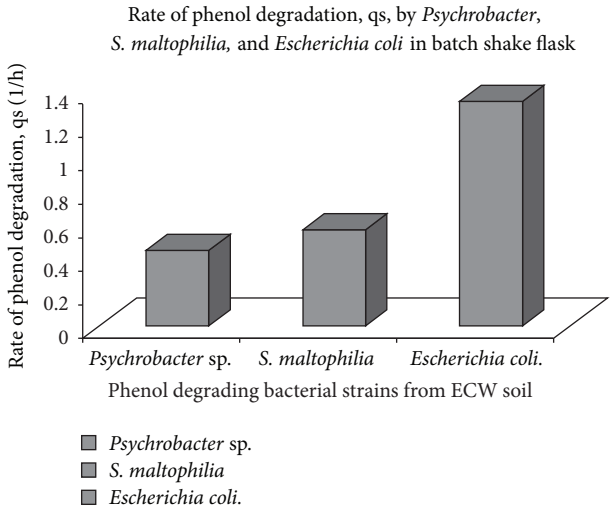

Figure 2: Comparative rate of phenol degradation by *Psychrobacter*, *Stenotrophomonas,* and *Escherichia coli*.

Table 1: Biochemical characterization of *E. coli*.

Biochemical tests	Response of *E. coli* isolated from ECW soil
Gram staining	−
Lactose	+
Mannitol	+
Methyl Red	+
Voges-Proskauer	−
Citrate	−
Gelatin	−
Acid-fast	+
Oxidase	−
Catalase	+

isolated from ECW soil was found to be 100%. Results of the biochemical tests are given in Table 1.

3.2. SEM and EDS Results. SEM photographs of clay chips and clay chips containing immobilized *E. coli* cells are given in Figures 4(a) and 4(b). A polishing effect on the surface of clay chips was observed after immobilizing the *E. coli* cells. Figure 4(c) represents the SEM photograph of clay chips containing *E. coli* cells after removal of chromium (VI). EDS profiles are given in Figures 4(d), 4(e), and 4(f). It was observed that carbon content increased with immobilization. Percentage of carbon content was 5.78 and 26.53% before and after immobilization, respectively. Chromium was absent in clay chips both with and without immobilized cells before treatment with chromium. Presence of chromium was reported (0.49% of the total elements) on the clay chips after treatment with chromium (VI). The result indicated that adsorption and bioaccumulation of chromium took place, and these mechanisms were responsible, at least partly, for removal of chromium.

3.3. Removal Efficiency of Chromium (VI) Using Glucose as the Sole Source of Carbon. MS media supplemented with 2% glucose as the sole source of carbon and 500 mgL^{-1} chromium (VI) was passed through the PBR immobilized with *E. coli* cells for determination of removal efficiency of chromium. The observations made on the runs conducted at different media-flow rates in a countercurrent packed bed reactor immobilized with *E. coli* were analyzed. The result showed increase in removal efficiency with increase in media flow rate till a threshold value. The removal efficiency of chromium (VI) was calculated for each substrate flow rate. It was observed from Figure 5 that the removal efficiency increased as hydraulic retention time (HRT = V/Q, where V = effective volume of reactor in mL and Q = substrate flow rate in mL/min) increased for relatively lower HRT of substrate, but at higher HRT values the removal efficiency decreased. This could be because of an existence of an external diffusion layer and also saturation of cellular metabolism. The rate of transfer of substrate through the diffusion was inversely proportional to the thickness of this layer. On the other hand, the thickness of this layer was inversely proportional to the substrate flow rate through the reactor [23, 24]. The hydraulic retention time of the substrate in the reactor was inversely proportional to substrate flow rate. Thus the rate of diffusion of substrate to the *E. coli* cells decreased at higher hydraulic retention time [24]. As a result the removal efficiency of chromium (VI) effectively decreased at higher HRT. The maximum removal efficiency was 85% with hydraulic retention time of 4.44 h (Figure 5).

3.4. Effect of Air Flow Rates in Presence of Glucose on Chromium (VI) Removal Efficiency. The effect of rate of aeration on removal efficiency of chromium (VI) was studied as *E. coli* is an aerobic organism. For aerobes, the rate of metabolic activities depends on rate of oxygenation. Thus the air flow rate was varied from 0 lpm to 3 lpm for each glucose substrate flow rate. The rate of Chromium removal increased with air flow rates till 2–2.5 lpm. But beyond that the rate of removal of chromium (VI) decreased due to profuse foaming. Foaming caused changes in both the size and composition of the air bubble. It altered the dissolved oxygen profile due to heterogeneous dispersion in the reactor volume. Due to increased residence time of the air bubble in the reactor the air bubble became oxygen depleted; CO_2 accumulated in the air bubble replacing the oxygen. CO_2 is toxic to cells and inhibits their metabolic activities. Thus accumulation of CO_2 in the reactor space due to foaming decreased the removal efficiency of chromium (VI) by *E. coli* cells. The maximum removal efficiency (Figure 5) was at the hydraulic retention time of glucose 4.44 h with an air flow rate of 2 lpm. The maximum chromium (VI) removal efficiency was found to be 85% in glucose medium.

3.5. Removal Efficiency of Chromium (VI) Using Phenol as the Sole Source of Carbon. The synthetic media used for the study was prepared by dissolving phenol (500 mgL^{-1}) and chromium (VI) (500 mgL^{-1}) in MS media. Phenol was the sole source of carbon present in the media for the

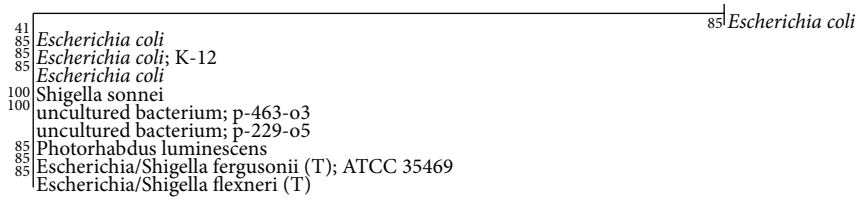

Figure 3: Phylogenetic tree of *E. coli* isolated from ECW soil with related genera of bacteria.

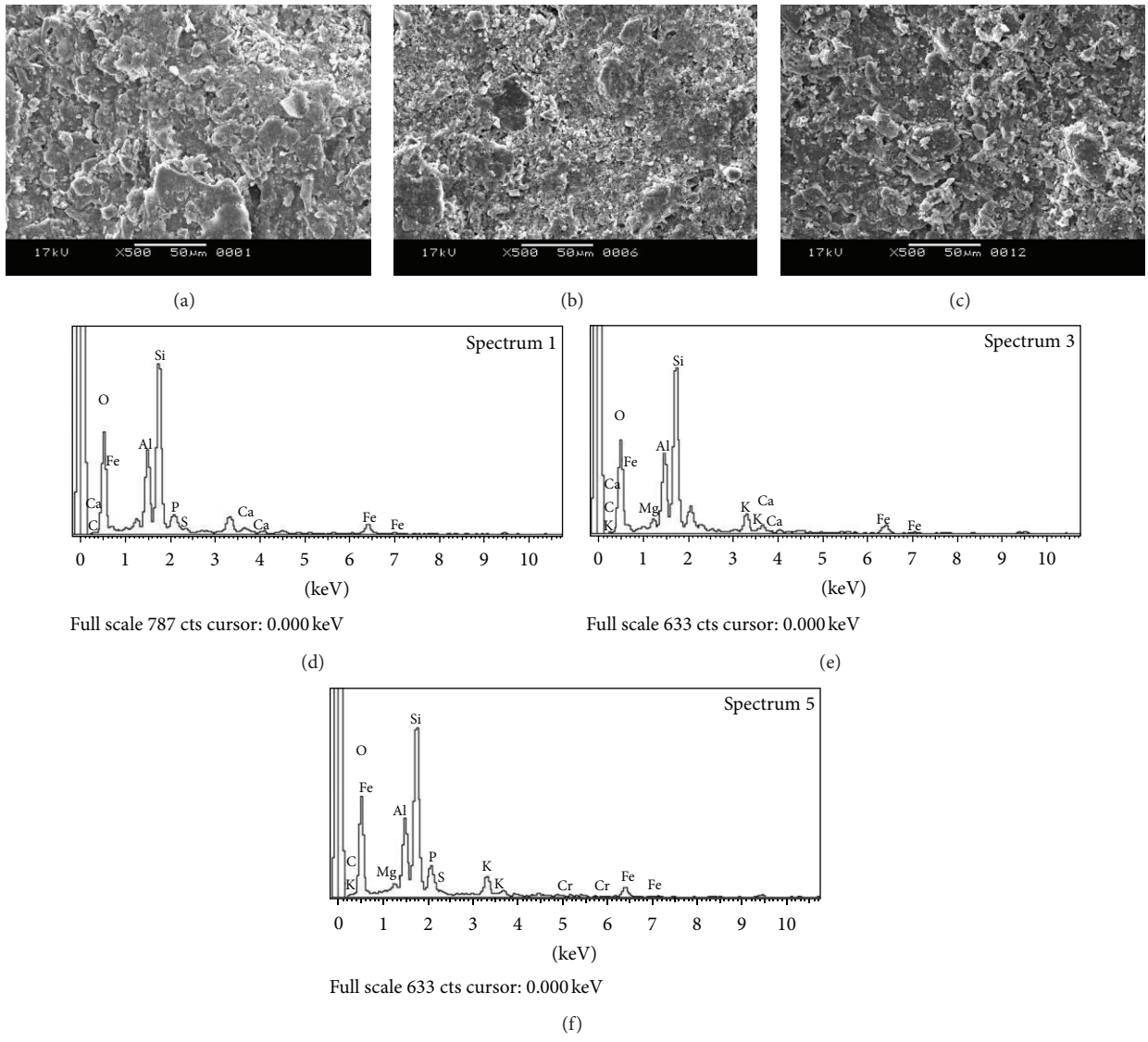

Figure 4: (a) SEM image of clay chip before immobilizing with *E. coli* cells. (b) SEM image of clay chip after immobilizing *E. coli* cells on to it. (c) SEM image of immobilized clay chip after treatment with phenol and chromium (VI). (d) EDS image of clay chip before immobilizing with *E. coli* cells. (e) EDS image of clay chip after immobilizing *E. coli* cells on to it. (f) EDS image of immobilized clay chip after treatment with phenol and chromium (VI).

immobilized *E. coli* cells. The substrate flow rate was varied from 1.5 mL/min to 4 mL/min; that is, the hydraulic retention time (HRT = V/Q, where V = effective volume of reactor in mL and Q = substrate flow rate in mL/min) was varied from 3.33 h to 8.88 h. The effect of phenol flow rate on chromium (VI) removal efficiency was similar to the effect of glucose flow rate. The best removal of chromium (VI) occurred at HRT value of 4.44 h as was observed from Figure 6.

3.6. Effect of Air Flow Rates in Presence of Phenol on Chromium (VI) Removal Efficiency. The *E. coli* cells are aerobic in nature;

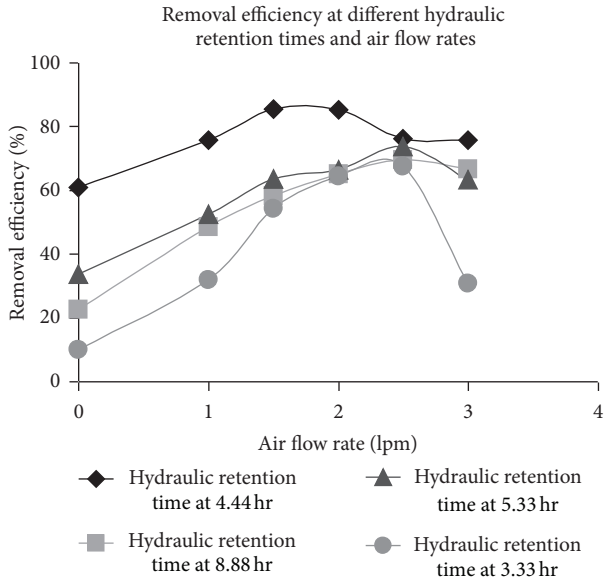

Figure 5: Removal efficiency of chromium (VI) by *E. coli* at different hydraulic retention times of glucose-containing medium and air flow rates.

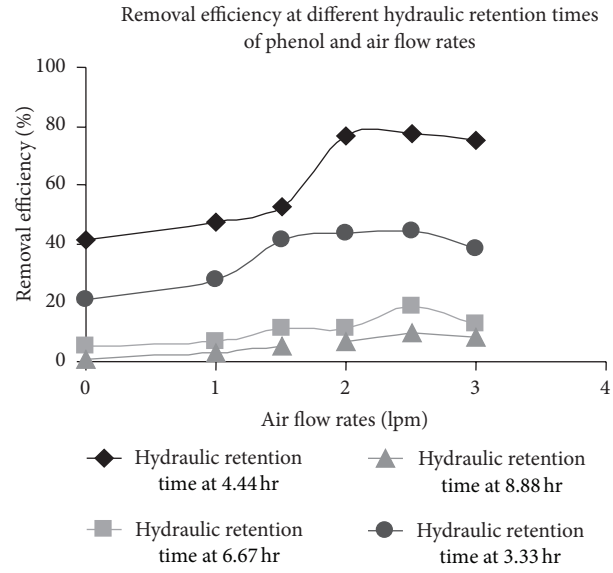

Figure 6: Removal efficiency of chromium (VI) by *E. coli* at different hydraulic retention times of phenol and air flow rates.

thus aeration of the reactor is a primary necessity to sustain the culture. To note the effect of rate of aeration on the removal efficiency of chromium (VI), the air flow rates were varied as 0 lpm, 1 lpm, 1.5 lpm, 2 lpm, and 2.5 lpm for each substrate flow rate. The removal efficiency profile with respect to air flow rates was studied as shown in Figure 6, and it was observed that removal of chromium (VI) increased with increasing air flow rates till the process became independent of rate of oxygenation. With further increase in aeration rate it was found that removal efficiency reduced due to excessive foaming in the reactor leading to insufficient gas-liquid interfacial diffusion [25].

The maximum chromium (VI) removal efficiency of 77.7% was observed at a phenol-chromium (VI) hydraulic retention time of 4.44 hr with an air flow rate of 2.5 lpm in the countercurrent continuous packed bed reactor. Requirement of higher air flow rate for removal of chromium in presence of phenol could be explained in the following manner. Glucose is the most easily metabolized source of carbon. On the other hand, phenol has inhibitory action on cells. Moreover, conversion of phenol to TCA cycle intermediates requires action of oxidase which utilizes molecular oxygen. Thus metabolism of phenol consumes more oxygen than glucose. As a result, higher flow rate of oxygen is required to have the same chromium removal in presence of phenol than glucose.

3.7. Effect of Temperature on the Performance of the Continuous Packed Bed Reactor. The performance efficiency of the reactor system containing both phenol and chromium (VI) as pollutants was studied at different temperatures from 10°C to 50°C. The immobilized cells were fed with MS media containing 500 mgL^{-1} chromium (VI) and 500 mgL^{-1} phenol at a hydraulic retention time of 4.44 h. The air flow rates were varied from 0 lpm to 2.5 lpm. The temperature of the media was maintained at 10°C, 15°C, 30°C, 40°C, and 50°C, respectively and removal efficiency of chromium (VI) was measured for each temperature. The system proved to be in working condition and was able to remove chromium (VI) at both the limiting temperature conditions. *E. coli* is a mesophilic organism, but there are reports on survival/adaptation of *E. coli* in extreme temperatures [26–28]. It has been reported that protein profile of an *E. coli* cell changes with change in temperature (tested between 13.5°C and 46°C) which makes the cell adapt to different temperatures [28]. The rate of removal was significantly less as compared to the rate of removal at 30°C under similar air flow rates as evident from Figure 7. The rate of degradation of *E. coli* proteins increased at temperatures above 37°C [28], and it was observed that the rate of removal of chromium (VI) was lowest at 50°C for all air flow rates.

3.8. Effect of pH on the Performance of the Continuous Packed Bed Reactor. For the hydraulic retention time of phenol and chromium(VI) at 4.4 h, pH of the synthetic media containing phenol and chromium (VI) was varied from pH 1 to pH 12. The effect of pH was studied under different aeration rates from 1 lpm to 2.5 lpm, as shown in Figure 8. *E. coli* was seen to remove chromium even at pH 1 and pH 3. Maximum chromium (VI) removal efficiency of 77.7% was observed at 2.5 lpm air flow rate at pH 7. Reports corroborative of our observation of survival of *E. coli* at extreme pH conditions were available [29–31].

The optimum pH for growth of *E. coli* is pH 7.0. The strain could survive at extreme pH conditions under lower air flow rate. At higher air flow rate, foaming started, and removal of chromium (VI) was reduced even with the minimum foam formation under extreme pH conditions. This may be due to the fact that the growth of organisms was reduced under the

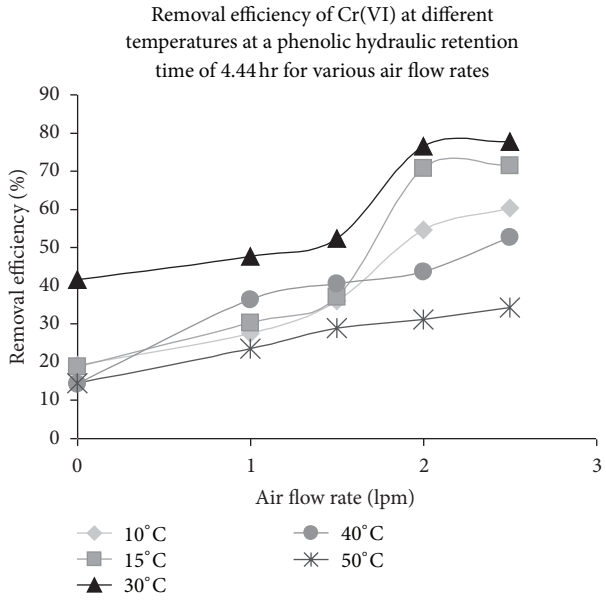

Figure 7: Removal efficiency of chromium (VI) by *E. coli* at different temperatures and air flow rates at phenolic chromium (VI) media and HRT of 4.44 h.

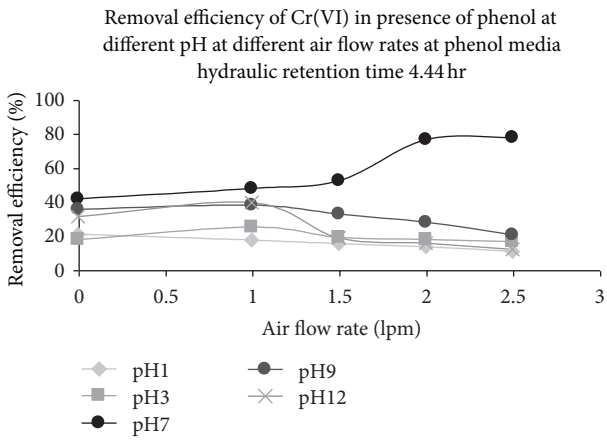

Figure 8: Removal efficiency of chromium (VI) by *E. coli* at different pH and air flow rates at phenolic chromium (VI) media and hydraulic retention time of 4.44 h.

dual stress caused by extreme pH as well as carbon dioxide accumulation in the system due to foam formation.

Previous studies conducted by other researchers on removal of chromium (VI) by different bacterial species have shown removal efficiencies to vary from 24.2% to 74.9% [32–35], in batch culture and without presence of a second stress element in media. Previous works showed 48% removal of 500 mgL^{-1} chromium (VI) over a period of four days and 40% removal in biofilter mode for the same initial chromium (VI) concentration in batch culture [32]. Some other researchers removed up to 74.9% of the influent chromium concentration of 100 mgL^{-1} [34]. Rengifo-Gallego et al. attained a removal efficiency of 62.85% using bacterial consortium for an initial chromium (VI) concentration of 5 mgL^{-1} in a bioreactor [35]. Most of the work done on removal of chromium was done using glucose as the sole source of carbon. On the other hand, the present study reported chromium removal of 85% in presence of glucose in the media, which is much higher than the other studies reported and 77.7% in presence of phenol, the second stress factor, in the media in a continuous countercurrent packed bed reactor.

4. Conclusion

The *E. coli* strain isolated from a mixed bacterial consortium from soil of East Calcutta Wetlands could remove chromium utilizing phenol as the sole source of carbon continuously in a packed bed reactor using clay chips as the immobilizing matrix. The optimum conditions for operating the reactor were HRT: 4.44 h; air flow rate: 2.5 lpm; temperature: 30°C, and pH: 7. The maximum removal efficiency of chromium (VI) under the above optimized condition was 77.7%. The system has potential for treatment of mixed waste containing both organic pollutants and heavy metals present in tannery effluent.

References

[1] A. Pandey, D. Bera, A. Shukla, and L. Ray, "Studies on Cr(VI), Pb(II) and Cu(II) adsorption-desorption using calcium alginate as biopolymer," *Chemical Speciation and Bioavailability*, vol. 19, no. 1, pp. 17–24, 2007.

[2] D. Bera, P. Chattopadhyay, and L. Ray, "Continuous removal of chromium from tannery wastewater using activated sludge process-Determination of kinetic parameters," *Indian Journal of Chemical Technology*, vol. 19, no. 1, pp. 32–36, 2012.

[3] S. R. Popuri, S. Kalyani, S. R. Kachireddy, and A. Krishnaiah, "Biosorption of hexavalent chromium from aqueous solution by using prawn pond algae (Sphaeroplea)," *Indian Journal of Chemistry*, vol. 46, no. 2, pp. 284–289, 2007.

[4] J. W. Moore and S. Ramamurthy, *Organic Chemicals in Natural Water, Applied Monitoring and Impact Assessment*, Springer, New York, NY, USA, 1984.

[5] NAS, *Medical and Biologic Effects of Environmental Pollutants*, National Academy of Sciences, Washington, DC, USA, 1974.

[6] S. Sharma and A. Adholeya, "Detoxification and accumulation of chromium from tannery effluent and spent chrome effluent by Paecilomyces lilacinus fungi," *International Biodeterioration and Biodegradation*, vol. 65, no. 2, pp. 309–317, 2011.

[7] P. E. Enterline, "Respiratory cancer among chromate workers," *Journal of Occupational Medicine*, vol. 16, no. 8, pp. 523–526, 1974.

[8] F. J. Roe and R. L. Carter, "Chromium carcinogenesis: calcium chromate as a potent carcinogen for the subcutaneous tissues of the rat," *British Journal of Cancer*, vol. 23, no. 1, pp. 172–176, 1969.

[9] H. Nishioka, "Mutagenic activities of metal compounds in bacteria," *Mutation Research*, vol. 31, no. 3, pp. 185–189, 1975.

[10] A. J. Mearns, P. S. Oshida, and M. J. Sherwood, "Chromium effects on coastal organisms," *Journal of the Water Pollution Control Federation*, vol. 48, no. 8, pp. 1929–1939, 1976.

[11] A. I. Zouboulis, M. X. Loukidou, and K. A. Matis, "Biosorption of toxic metals from aqueous solutions by bacteria strains

isolated from metal-polluted soils," *Process Biochemistry*, vol. 39, no. 8, pp. 909–916, 2004.

[12] Y. Chen and G. Gu, "Preliminary studies on continuous chromium (VI) biological removal from wastewater by anaerobic-aerobic activated sludge process," *Bioresource Technology*, vol. 96, no. 15, pp. 1713–1721, 2005.

[13] S. Sultan and S. Hasnain, "Reduction of toxic hexavalent chromium by Ochrobactrum intermedium strain SDCr-5 stimulated by heavy metals," *Bioresource Technology*, vol. 98, no. 2, pp. 340–344, 2007.

[14] A. Baral and R. D. Engelken, "Chromium-based regulations and greening in metal finishing industries in the USA," *Environmental Science and Policy*, vol. 5, no. 2, pp. 121–133, 2002.

[15] S. S. Ahluwalia and D. Goyal, "Microbial and plant derived biomass for removal of heavy metals from wastewater," *Bioresource Technology*, vol. 98, no. 12, pp. 2243–2257, 2007.

[16] C. Quintelas, B. Fernandes, J. Castro, H. Figueiredo, and T. Tavares, "Biosorption of Cr(VI) by three different bacterial species supported on granular activated carbon—a comparative study," *Journal of Hazardous Materials*, vol. 153, no. 1-2, pp. 799–809, 2008.

[17] L. Fude, B. Harris, M. M. Urrutia, and T. J. Beveridge, "Reduction of Cr(VI) by a consortium of sulfate-reducing bacteria (SRB III)," *Applied and Environmental Microbiology*, vol. 60, no. 5, pp. 1525–1531, 1994.

[18] D. C. Sharma and C. F. Forster, "Removal of hexavalent chromium using sphagnum moss peat," *Water Research*, vol. 27, no. 7, pp. 1201–1208, 1993.

[19] H. Shen and Y. T. Wang, "Biological reduction of chromium by *E. coli*," *Journal of Environmental Engineering*, vol. 120, no. 3, pp. 560–572, 1994.

[20] H. Shen and Y. T. Wang, "Characterization of enzymatic reduction of hexavalent chromium by *Escherichia coli* ATCC 33456," *Applied and Environmental Microbiology*, vol. 59, no. 11, pp. 3771–3777, 1993.

[21] "Pollutants in tannery effluents," UNIDO/US/RAS/92/120, 2000.

[22] *Standard Methods for the Examination of Water and wasteWaters*, APHA (American Public Health Association), AWWA (American water Works Association) and AEF (American Environment Federation), Washington, DC, USA, 20th edition, 1998.

[23] M. D. Lilly, W. E. Hornby, and E. M. Crook, "The kinetics of carboxymethylcellulose—ficin in packed beds," *Biochemical Journal*, vol. 100, no. 3, pp. 718–723, 1966.

[24] F. N. Kök, M. Y. Arica, C. Halıcıgil, G. Alaeddinoğlu, and V. Hasırcı, "Biodegradation of aldicarb in a packed-bed reactor by immobilized Methylosinus," *Enzyme and Microbial Technology*, vol. 24, no. 5-6, pp. 291–296, 1999.

[25] P. F. Stanbury, A. Whitaker, and S. J. Hall, *Principle of Fermentation Technology*, Butterworth-Heinemann, 2nd edition, 2008.

[26] M. T. Nguyen, "The effect of temperature on the growth of the bacteria *Escherichia coli* DH5a," *Saint Martin's University Biology Journal*, vol. 1, pp. 87–94, 2006.

[27] K. Kovářová, A. J. B. Zehnder, and T. Egli, "Temperature-dependent growth kinetics of *Escherichia coli* ML 30 in glucose-limited continuous culture," *Journal of Bacteriology*, vol. 178, no. 15, pp. 4530–4539, 1996.

[28] S. L. Herendeen, R. A. VanBogelen, and F. C. Neidhardt, "Levels of major proteins of *Escherichia coli* during growth at different temperatures," *Journal of Bacteriology*, vol. 139, no. 1, pp. 185–194, 1979.

[29] Y. Sun, T. Fukamachi, H. Saito, and H. Kobayashi, "Respiration and the F1Fo-ATPase enhance survival under acidic conditions in *Escherichia coli*," *PLoS ONE*, vol. 7, no. 12, Article ID e52577, 2012.

[30] K. N. Jordan, L. Oxford, and C. P. O'Byrne, "Survival of low-pH stress by *Escherichia coli* O157:H7: correlation between alterations in the cell envelope and increased acid tolerance," *Applied and Environmental Microbiology*, vol. 65, no. 7, pp. 3048–3055, 1999.

[31] Y. Sun, T. Fukamachi, H. Saito, and H. Kobayashi, "Atp requirement for acidic resistance in *Escherichia coli*," *Journal of Bacteriology*, vol. 193, no. 12, pp. 3072–3077, 2011.

[32] S. Ilhan, M. N. Nourbakhsh, S. Kilicharslan, and H. Ozdag, "Removal of chromium, lead and copper ions from industrial wastewaters by Staphylococcus saprophyticus," *Turkish Electronic Journal of Biotechnology*, vol. 2, pp. 50–57, 2004.

[33] A. Kumar, B. S. Bisht, and B. D. Joshi, "Bioremediation potential of three acclimated bacteria with reference to heavy metal removal from waste," *International Journal of Environmental Sciences*, vol. 2, no. 2, pp. 896–908, 2011.

[34] A. Smrithi and K. Usha, "Isolation and characterization of chromium removing bacteria from tannery effluent disposal site," *International Journal of Advanced Biotechnology and Research*, vol. 3, no. 3, pp. 644–652, 2012.

[35] A. L. Rengifo-Gallego, E. Pena-Salamanca, and N. Benitez-Campo, "The effect of chromium removal by algae-bacteria Bostrychia calliptera (Rhodomelaceae) consortia under laboratory conditions," *Revista de Biologia Tropica*, vol. 60, no. 3, pp. 1055–1064, 2012.

Hindawi Publishing Corporation
BioMed Research International
Volume 2013, Article ID 952641, 10 pages
http://dx.doi.org/10.1155/2013/952641

Research Article

Poly β-Hydroxybutyrate Production by *Bacillus subtilis* NG220 Using Sugar Industry Waste Water

Gulab Singh,[1] Anish Kumari,[1] Arpana Mittal,[1] Anita Yadav,[2] and Neeraj K. Aggarwal[1]

[1] *Department of Microbiology, Kurukshetra University, Kurukshetra 136119, India*
[2] *Department of Biotechnology, Kurukshetra University, Kurukshetra 136119, India*

Correspondence should be addressed to Neeraj K. Aggarwal; neerajkuk26@rediffmail.com

Received 4 April 2013; Revised 16 June 2013; Accepted 17 June 2013

Academic Editor: Kannan Pakshirajan

The production of poly β-hydroxybutyrate (PHB) by *Bacillus subtilis* NG220 was observed utilizing the sugar industry waste water supplemented with various carbon and nitrogen sources. At a growth rate of 0.14 g h^{-1} L^{-1}, using sugar industry waste water was supplemented with maltose (1% w/v) and ammonium sulphate (1% w/v); the isolate produced 5.297 g/L of poly β-hydroxybutyrate accumulating 51.8% (w/w) of biomass. The chemical nature of the polymer was confirmed with nuclear magnetic resonance, Fourier transform infrared, and GC-MS spectroscopy whereas thermal properties were monitored with differential scanning calorimetry. In biodegradability study, when PHB film of the polymer (made by traditional solvent casting technique) was subjected to degradation in various natural habitats like soil, compost, and industrial sludge, it was completely degraded after 30 days in the compost having 25% (w/w) moisture. So, the present study gives insight into dual benefits of conversion of a waste material into value added product, PHB, and waste management.

1. Introduction

The diverse group of chemicals used in making of plastic is highly known to be highly toxic and poses a serious threat to biosphere. These substances besides hitting hard to ecosystem can also cause an array of problems like birth defects, cancer, damage of nervous, and immune systems. Polypropylene—the key ingredient for plastic—is a petroleum product and becomes increasingly expensive. With increasing concern for the environment, biosynthetic and biodegradable biopolymers have attracted great interest because of their excellent biodegradability and being environmentally benign and sustainable.

The PHAs (hydroxyalkanoic acid) are synthesised by wide range of microorganisms as intracellular carbon and energy reserve material under nutrient limiting conditions [1]. The first identified PHA, poly-β-hydroxybutyrate (PHB) from *Bacillus megaterium*, is drawing much attention due to having physical properties similar to petroplastic polypropylene [2] with advantage of being completely biodegradable (into water, carbon dioxide, and methane under anaerobic conditions) by microorganisms in natural environments. The high production cost of PHB can be curtailed by strain development, improving fermentation and separation processes, and using inexpensive carbon source. In PHB production, about 40% of the total production cost is accounted for raw material, and thus, the use of inexpensive carbon source or even waste organic materials could be highly significant.

Annually, the million tons of organic wastes are produced from the wide array of industries and in this context, contribution from sugar industries is worst in terms of effluent production—out of all the major sugar manufacturing units, that is, mill house, process house, boiler house, alcohol producing unit, and distilleries [3]. The quantity of waste water generated ever increasing with sugar production—where a typical sugar mills consume around 2000 litres of water and generate about 1000 litres of waste water per ton of cane—crushed. The waste water contains floor washing waste water and condensate water, sugarcane juice, syrup and molasses, and so forth. The sugar mill effluent has a

high biochemical oxygen demand (BOD) and if discharged untreated, increased BOD effects aquatic ecosystem and has ultimate impact on human health.

The sugar industries need spending lots of money on the treatment of waste water treatment to adhere to regulatory standards.

Thus the two different problems, namely, the pollution due to synthetic plastic and generation of organic rich waste from sugar industries could uniquely addressed by producing the bioplastic using the organic waste as nutrient source.

However, this carbohydrate waste lacks certain mineral nutrient, particularly nitrogen in relation to the amount of oxidizable carbon present and still may require nutrient supplementation.

Here, an attempt was made to use the sugar industry waste water after nutritive adjustment for the production of PHB using an isolate *Bacillus subtilis NG220*.

2. Materials and Methods

2.1. Bacterial Isolation and Culturing. *Bacillus subtilis* NG220 was isolated on carbon rich nutrient agar medium [(w/v) glucose 1%, beef extract 0.3%, peptone 0.5%, and sodium chloride 0.8%, agar 1.5%] from the soil sample collected from sugarcane field area. The presence of intracellular PHB granules was confirmed with the help of staining with Sudan black B and Nile blue A [4]. The culture was maintained on the nutrient agar medium (w/v) (beef extract 0.3%, peptone 0.5%, sodium chloride 0.8%, and agar 1.5%) and stored at 4°C.

2.2. Morphological, Biochemical and Molecular Characterisation. The isolate was morphologically characterized by observing the standard microbiological methods. The biochemical characterization of the isolate was done by series of biochemical tests including carbohydrate fermentation, H_2S production, MR-VP test, and Catalase test. Further, for molecular characterization, the PCR amplification of 16S rDNA was done at 95°C for 5 min, 95°C for 30 sec. 52°C for 30 sec. 72°C for 1 min, and 72°C for 10 min. The universal primer 16sF-5′ AGA GTT TGA TCC TGG CTC AG 3′ and 16sR-5′ ACG GCT ACC TTG TTA CGA CTT 3′ were used. PCR product was purified by column (Merck bioscience, India) and was sequenced with AB instrument 3730XL. The obtained sequence was subjected to search for closest possible species using distance matrix based on nucleotide sequence homology (using Kimura-2 parameter) and BLAST tools available at National Centre for Biotechnology Information (NCBI). Phylogenetic analysis was done by using the Phylip package and ClustalW.

2.3. Preparation of Seed Inoculum. One loop full of the culture from slant was inoculated in 5 mL of sterile nutrient broth (beef extract 0.3%, peptone 0.5%, sodium chloride 0.8%). After incubation for 24 h at 30°C, 1% (v/v) of culture having 10^8 cells/mL was aseptically transferred into 50 mL, sterile nutrient broth and incubated at 30°C for 18 h.

Table 1: Physiochemical characteristics of sugar industry waste water.

Parameter	Concentration (mg/L)
pH	4.2–6.9
Total solids	1,076 ± 414
Suspended solid	631 ± 227.4
COD	1,395 ± 317
BOD	1,300 ± 238
COD/BOD	1.6 ± 0.49
BOD/N/P	100 : 1.69 : 0.69
Nitrogen	11.48 ± 6.54
Phosphorous	4.36 ± 2.47

2.4. Substrate Preprocessing. Untreated sugar industry effluent was collected from the Saraswati Sugar Mills, Yamunanagar, Haryana, India, and was stored at 4°C until used. The effluent was filtered through the muslin cloth to remove the undesired solid materials. Appropriately diluted, filtered waste water was used as PHB production medium (Table 1).

2.5. Production, Detection, Extraction, and Purification of PHB. The PHB production was followed in 250 mL Erlenmeyer flask containing 50 mL sugar industry waste water as production medium under stationary condition of growth. After 72 h of incubation at 30°C, culture broth was centrifuged at 8000 rpm for 15 min. The portion of the palette was resuspended in 1 mL of sterile distilled water sonicated (Hielscher, Germany) in 0.2% aq. sol. of Nile blue A, air-dried the smear and observed under phase contrast microscope [4]. Remaining amount of the pellet obtained was used for extraction and recovery of PHB according to Law and Slepecky [5] with minor modifications. Briefly, the harvested cells were lyophilized and the dry cell mass weight was noted. The dry cell mass was subsequently incubated with 10 mL sodium hypochlorite at 50°C for 1 h for cells lysis. The cell extract obtained was centrifuged at 12000 rpm for 30 min, then washed sequentially with distilled water, acetone, and absolute ethanol, and dissolved in 10 mL boiling chloroform (Sigma Aldrich). After evaporation 10 mL of conc. sulphuric acid was added and placed in water bath for 10 min at 100°C to convert the PHB into crotonic acid. On cooling, absorbance was taken at 235 nm [6] using PHB (Sigma Aldrich) as standard.

2.6. Polymer Analysis

2.6.1. NMR Analysis: ^1H Nuclear Magnetic Resonance. The identity of individual monomer unit was confirmed by proton nuclear magnetic resonance (^{1}H-NMR) spectroscopy. ^{1}H-NMR spectra of PHB sample were recorded in CDCl3 on Bruker ACF 300 spectrophotometer at 300 MHz by using "Tetramethylsilane" as internal standard [7].

2.6.2. FT-IR Analyses. FT-IR analysis of the polymer sample was carried out on MB-3000, ABB FTIR spectrophotometer in the range 4000–600 cm^{-1}.

Table 2: Experimental culture conditions for optimization of various parameters under stationary condition of growth*.

Rigid parameter	Name of the parameter			
	Incubation period (h)	pH	Inoculum age (h)	Temperature (°C)
Incubation period (h)	Observed	7	18	30
pH	72	Observed	18	30
Inoculum age (h)	72	7	Observed	30
Temperature (°C)	72	7	18	Observed

*Production medium containing treated undiluted sugar industry waste water.

2.6.3. DSC Analysis. TA Q10 series instrument was used to carry out thermal analysis of PHB sample under flowing nitrogen atmosphere at a heating rate of 10°C min^{-1}; α-alumina powder was used as reference material using aluminium sample holder for taking thermogram [8]. In order to ensure the uniformity of temperature and good reproducibility, small amount (2–5 mg) of sample was taken. To verify the reproducibility duplicate runs were adopted under the same experimental conditions.

2.6.4. GC-MS Analysis. Purified polymer, prepared as described before, was dissolved in chloroform (5 mg PHB mL^{-1}), and 3 μL was injected into a GC-MS instrument (Model 6890; Hewlett Packard). The column and temperature profile used for GC analysis were as described by Schubert et al. [9].

2.7. Optimization of PHB Production. The optimization for maximum PHB production by *Bacillus subtilis* NG220 was carried out under stationary conditions of growth using sugar industry waste water as production medium. The sugar industry waste water was filtered through muslin cloth and then rough filter paper before any study to remove any type of debris or solid waste. Several cultural parameters were evaluated to determine their effect on biomass and PHB production using sugar industry waste water. The optimized value for each parameter was selected and kept constant for further experiments. The fermentation was carried out in 250 mL Erlenmeyer flask containing 50 mL sugar industry waste water as production medium, under stationary as well as shaking condition of growth. Several cultural parameters like time of incubation (24–120 h), temperature of incubation (20–50°C), supplementation of various carbon and nitrogen sources, inoculum age and size (12–42 h, 1–3%), effect of pH (4–8), and so forth, were evaluated to determine their effect on biomass accumulation and PHB production.

2.7.1. Effect of Carbon and Nitrogen Source on PHB Production. Production of PHB was followed using the optimized values of various parameters obtained from different experiments as per Table 2. PHB production was carried out using production medium supplemented with different carbon sources at 1% (w/v), namely, dextrose, xylose, sucrose, rhamnose, mannitol, maltose, lactose monohydrate, mannose, galactose, starch, and raffinose pentahydrate. PHB production was also studied using production medium supplemented with various inorganic (ammonium chloride, ammonium sulphate, di-ammonium hydrogen phosphate, and ammonium di-hydrogen phosphate, ammonium per sulphate) and organic (peptone, urea, and tryptone) nitrogen sources at 1% (w/v). Further, effect of the selected carbon and nitrogen source on PHB production was investigated at their different concentrations.

2.8. Preparation of Polymer Blend Sheet. Conventional solvent cast technique [10] was used for preparation of polymer blend sheet. The PHB powder extracted from *Bacillus subtilis* NG220 was mixed with soluble starch in ratio of 4 : 1 (w/w) and then dissloved in 20 mL of chloroform. The solution was poured into an open flat Petri plate and allowed to evaporate slowly at room temperature. The sheet was then cut into small pieces and used for degradation studies.

2.9. Degradation of Polymer Sheet. Biodegradability testing was performed by soil burial method [11]. A preweighted, 30 mm pieces were buried either into 200 g of freshly collected soil sample, compost, or sludge in wide mouth glass beakers. The beakers were filled with 200 g of soil, sludge or, compost. The mouths of the beakers were kept open and incubated at room temperature up to 40 days. Different moisture content (15%, 20%, 25%, and 30%) in the samples was maintained by adding sterile water to study the effect of the moisture on degradation of PHB films. Degradation of PHB was recorded as the loss of the weight after definite period of incubation.

3. Results and Discussion

3.1. Isolation of PHB Producing Bacteria. More than 300 isolates from different ecological niches were obtained on nutrient agar medium. The simplest first line screening program for PHB producing bacteria is the use of Sudan black B staining. The isolates which were found positive for PHB granules after Staining with Sudan black B (i.e., showing dark spot inside the pink coloured cells) were further confirmed for their PHB producing potential with Nile Blue A, a more specific dye for PHB granules, in which bright orange colour fluorescence was observed under the phase contrast microscopy.

3.2. Identification of Isolate. The isolate NG220 used in the present study was morphologically and biochemically characterised as per given in Table 3.

The isolate on the basis of their morphological and biochemical characteristics identified as *Bacillus sp.* (Bergey's

Table 3: Morphological and biochemical characteristics of isolate NG220.

	Observation
Morphological characters	
Elevation	Umbonate
Edge	Entire with undulate
Internal character	Rough
Colour	Creamy off-white
Biochemical characters	
Gram reaction	Gram +ve rod
Glucose fermentation	+ve
Sucrose fermentation	+ve
Lactose fermentation	−ve
H_2S production	−ve (no gas observed)
MR test	+ve
VP test	−ve
Catalase test	+ve

Manual 9th ed.) when further characterized with 16S r-RNA genes for sequence homology (using BLAST and distance matrix based nucleotide sequence homology (Table 4)) isolate NG220 had the closest matching with the *Bacillus subtilis* (Figure 1) and was reffered to as *Bacillus subtilis* NG220. The 16S r-RNA sequence of the isolate has been submitted to the NCBI gene bank (Accession no. JQ797306).

3.3. Physiochemical Characterization of Sugar Industry Waste Water. The waste water had a high COD (1395 ± 317 mg/L) and BOD (1300 ± 238 mg/L). The nitrogen and phosphorous concentration in the sugar industry waste water were recorded as 11.48 ± 6.54 mg/L and 4.36 mg/L, respectively. The waste water has acidic to neutral pH and have high load of suspended solid. This waste water was used for PHB accumulation studies by the isolate with or without supplementation of different carbon and nitrogen sources.

3.4. Microbial Growth and PHB Production in Sugar Industry Waste Water. As such there is no report for PHB accumulation by microbial cells using sugar industry waste water. In different concentration of sugar industry waste water, growth of *Bacillus subtilis* NG220 was observed (Table 5) and the maximum growth was noted in undiluted (100% v/v) sugar industry waste water after 72 h of incubation at 30°C. Dilution of waste water not only affected the microbial growth but also PHB accumulation. This may be due to the fact that with increasing dilution of waste water the carbon and other nutrient got diluted and was not able to support microbial growth. Under unoptimized conditions *Bacillus subtilis* NG220 was observed to accumulate about 4.928 g/L of PHB after 72 h.

3.5. Characterisation of Extracted Polymer

3.5.1. ^{1}H-NMR Spectroscopy. The chemical nature of extracted polymers from *Bacillus subtilis* NG220 was confirmed by ^{1}H-NMR spectroscopy. The ^{1}H-NMR spectra (Figure 2(a)) showed the presence of three signals, characteristic of the polymer of HB. The ^{1}H-NMR spectra of polymer extracted from isolate showed a doublets at 0.85 ppm, corresponding to the methyl group (–CH3), and two multiplets at 1.23 and 1.56 ppm corresponding to methylene group (–CH2–) and methyne (–CH–) group, respectively [12]. In this study with reference PHB standard, the nature of polymer produced by the isolate was confirmed.

3.5.2. Fourier Transforms Infrared Spectroscopy (FTIR). Polymer extracted from *Bacillus subtilis* NG220 was used for recording IR spectra in the range 4000–600 cm^{-1}. IR spectra (Figure 2(b)) showed two intense absorption band at 1705 and 1034 cm^{-1}, specific for C=O and C–O stretching vibrations, respectively. The absorption bands at 2916 and 2955 cm^{-1} are due to C–H stretching vibrations of methyl, methylene groups. These prominent absorption bands confirm the structure of poly-β-hydroxybutyrate.

3.5.3. DSC Analysis of PHB Polymer. The melting temperature of the extracted PHB sample obtained was determined using DSC. The thermal properties of the polymer such as the melting temperature (T_m) are crucial for polymer processing. The melting temperature of extracted PHB (132.54°C) (Figure 2(c)) was lower as compared to that was reported in the literature (173–180°C). The melting point near to 130°C showed that the extracted PHB contained the nearly 15 mol% HV in the PHB polymer [13].

3.5.4. GC-MS Analysis of Extracted PHB. In this study, the PHB was methanolysed in the presence of sulphuric acid and methanol, and the methanolysed 3HB was then analyzed by GC-MS. Figure 2(d) showed that a common molecular fragment of the 3HB methyl ester ion chromatogram of the PHB produced. A predominant peak corresponding to the 3HB methyl ester was noted at 2.1 min, while four other small peaks were observed at 2.7, 3.3, 3.5, and 3.8 min. Of these, the peak at 3.3 min was speculated to be an impurity based on its ion fragment pattern. The retention times and ion fragment patterns of the peaks at 2.7 and 3.8 min were identical to those of the methyl esters of 3HV and 3HHx, respectively. Nevertheless, the 3HHx content was negligible in this copolymer (less than 0.1 mol%). The peak at 3.5 min also had an ion fragment pattern similar to that of the 3HHx methyl ester; however, its retention time was not identical to that of 3HHx.

3.6. Optimization of PHB Production

3.6.1. PHB Production versus Incubation Time. The PHB production in sugar industry waste water was followed for 96 h under stationary growth conditions. The production of PHB increased up to 72 h (5.191 g/L), and thereafter, got reduced (5.125 g/L after 96 h) (Figure 3(a)). The decrease of PHB production after 72 h might indicate that the bacteria used PHB as nutrient source. Matavulj and Molitoris [14] reported that the highest PHB level in *Agrobacterium radiobacter* was achieved during stationary growth phase after 96 h. The observation was supported by Yüksekdağ et al. [15].

Table 4: Distance matrix analysis for homology (Kitmura-parameter-2) for isolate NG220.

B. lichnif	0									
B. sp. BTB_C	0	0								
B. subtilis	0.01	0.01	0							
Query_NG220	0.01	0.01	0	0						
B. amyloliq	0.01	0.01	0	0	0					
B. atropae	0.02	0.02	0.01	0.01	0.01	0				
B. pumilus A	0.03	0.03	0.03	0.03	0.03	0.02	0			
B. cereus AT	0.06	0.06	0.06	0.06	0.06	0.06	0.06	0		
B. thuringi	0.06	0.06	0.06	0.06	0.06	0.06	0.06	0	0	
B. Anthraci	0.06	0.06	0.06	0.06	0.06	0.06	0.06	0	0	0
B. coahuile	0.06	0.06	0.06	0.06	0.06	0.06	0.06	0.04	0.04	0.04

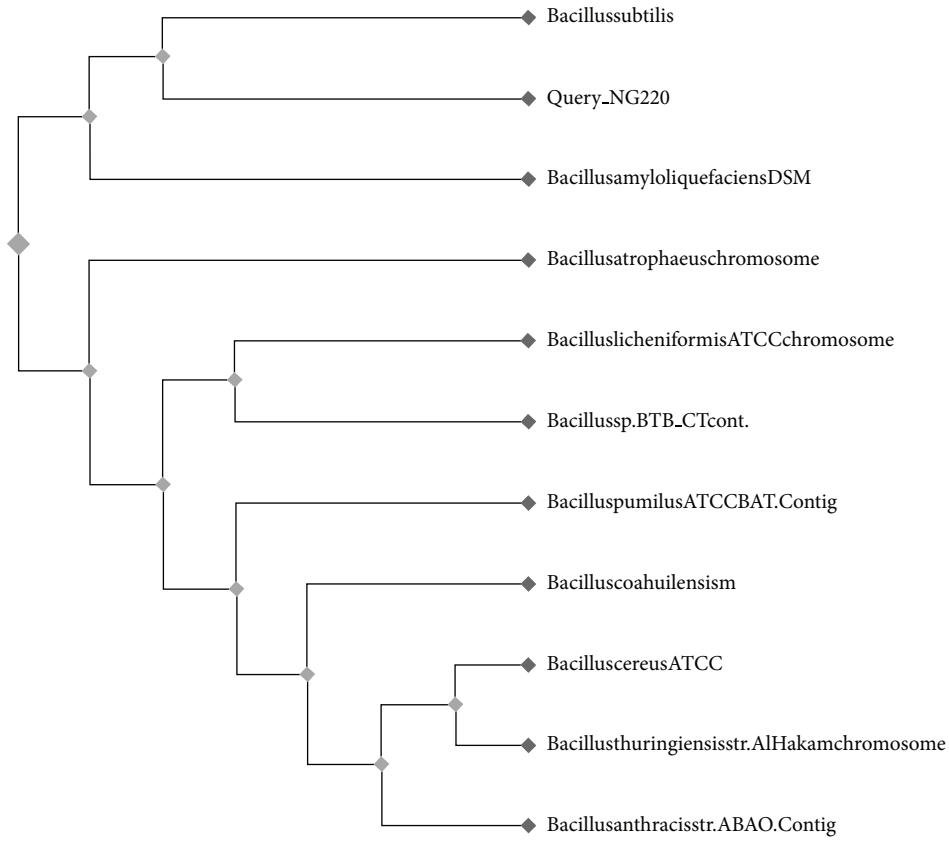

Figure 1: Phylogenetic tree of isolate NG220.

Table 5: Growth and PHB production with sugar industry waste water.

% sugar industry waste water (v/v)	Biomass* (g/L)	PHB* (g/L)
20	0.48	—
40	0.66	—
60	0.82	—
80	4.42	0.012
100	10.211	4.928

*Biomass and PHB production after 72 h of incubation at 30°C with preprocessed sugar industry waste water.

3.6.2. Effect of Incubation Temperature and pH on PHB Production. The maximum PHB production of 5.201 g/L was recorded at 40°C after 72 h. The increase of temperature beyond 40°C has negative impact on PHB production (Figure 3(b)). The decrease in PHB production at high temperature could be due to low PHB polymerase enzyme activity [15].

The effect of pH variations on PHB production is shown in Figure 3(c). From analysis it is clear that pH 7 was favourable for PHB production by *Bacillus subtilis* NG220 in sugar industry waste water. The current observation was in

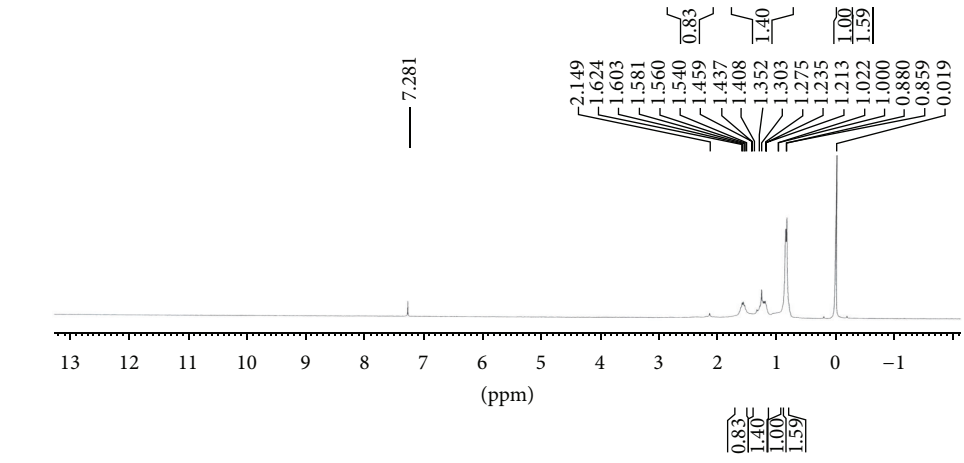

(a)

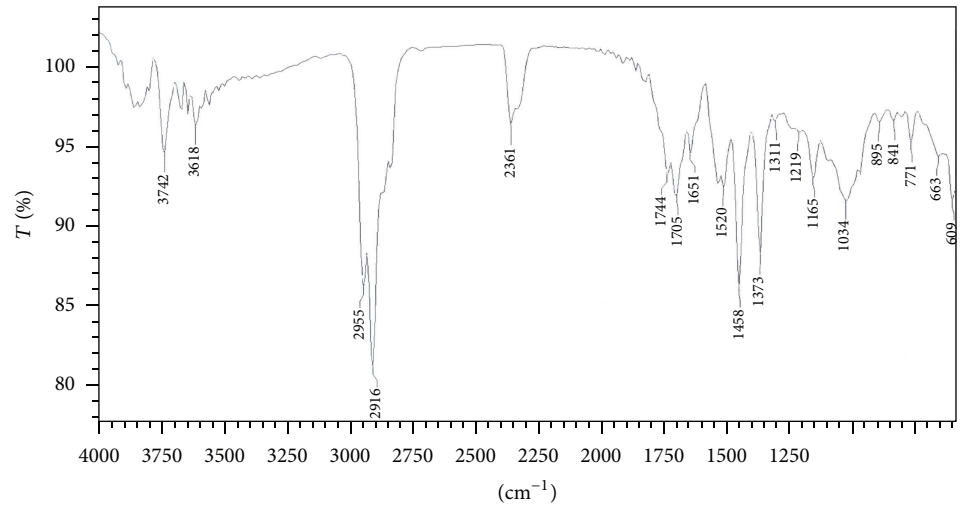

(b)

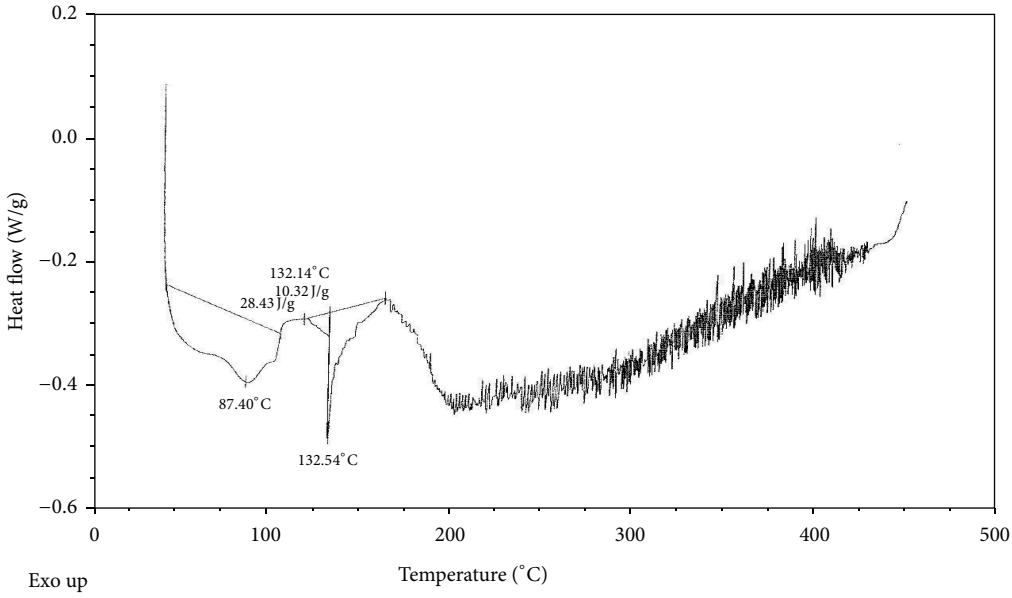

(c)

Figure 2: Continued.

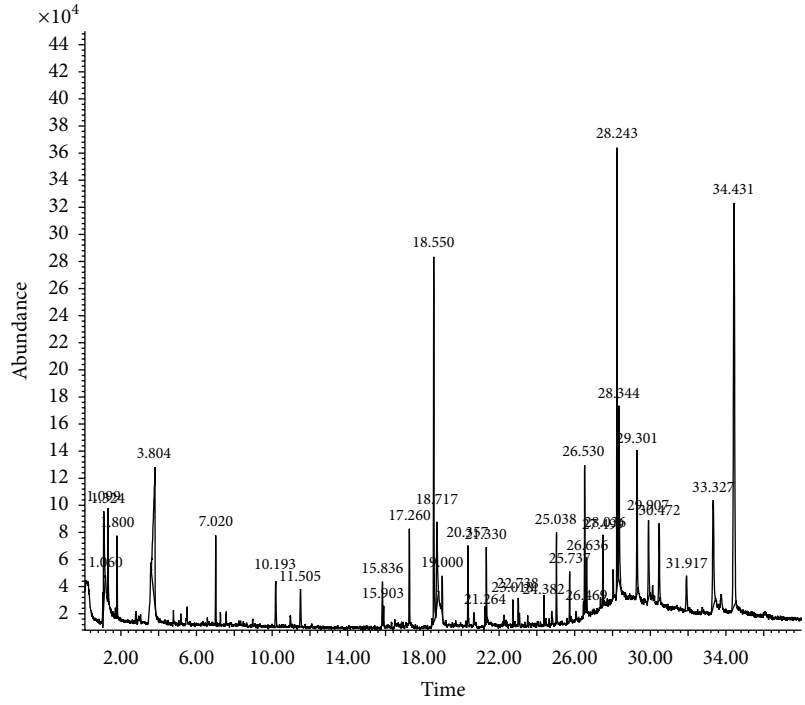

(d)

Figure 2: (a) NMR spectra, (b) FTIR spectra, (c) thermogram by DSC analysis, and (d) GC-MS spectra of extracted PHB polymer.

agreement with Aslim et al. [16] where the authers observed that the maximum PHB was produced (0.01 to 0.5 g/L) at pH 7 by *Rhizobium* strain grown on yeast extract mannitol broth while studying the effect of different pH on exopolysaccharide and PHB production in two strains of *Rhizobium meliloti*. Tavernier et al. [17] reported that these two strains showed higher PHB content at pH 7.0. Shivakumar [18] reported optimum pH between 6.8 and 8.0 for PHB production by *Alcaligenes eutrophus*.

3.6.3. Age of Inoculum. The maximum PHB production has been achieved after 72 h when the sugar industry waste water was inoculated with 18 h old inoculum (1% v/v), at 40°C (Figure 3(d)). Kumbhakar et al. [19] also reported that root nodule bacteria have produced maximum PHB with 12 h and 16 h old inoculum. Ramadas et al. [20] achieved the maximum PHB production by *Bacillus sphaericus* when production medium was inoculated with 16 h old inoculum.

3.6.4. Effect of Different Carbon and Nitrogen Source Supplementation on PHB Production. To find the best available carbon source and its optimum concentration for maximum PHB production, commercial carbohydrates dextrose, xylose, sucrose, rhamnose, mannitol, maltose, lactose monohydrate, mannose, galactose, starch, and raffinose were tried as a sole carbon source supplement to sugar industry waste water under stationary culture conditions. From Figure 3(e) analysis it is clear that maltose supplementation to production media gave PHB yield of 5.254 g/L. Hori et al. [21] reported that PHB content in *B. megaterium* reached maximum level in a medium containing glucose as carbon source. The study conducted by Wu et al. [22] reported that *Bacillus sp.* JMa5 accumulated 25%–35%, (w/w) PHB during sucrose fermentation [23]. Working with different carbon sources in MSM broth, Khanna and Srivastava [24] observed higher PHB yield on fructose by *A. Eutrophus* [24]. Out of various organic and inorganic nitrogen sources ammonium sulphate (1% w/v) supported the maximum (5.297 g/L) PHB production followed by peptone and tryptone (Figure 3(f)). In the literature, ammonium sulphate is reported to be the best nitrogen source for PHB production in different microorganism such as *Alcaligenes eutrophus* [25], *Methylobacterium sp.* [26], and *Sinorhizobium fredii* [27]. The highest PHB was obtained in ammonium sulphate by halotolerant photosynthetic bacteria *Rhodobacter Sphaeroides* when cultivated under aerobic and dark conditions [28]. The highest level of PHB accumulation was observed in the media with protease peptone as nitrogen sources by Aslim et al. [16] in *B. subtilis 25* and in *B. megaterium 12*.

3.7. Evaluation of Kinetics Parameters. The evaluation of kinetic parameter for batch fermentation was studied with respect to PHB and biomass production using sugar industry waste water as production media. The *Bacillus subtilis* NG220 grew at the rate $0.141\,\mathrm{g\,L^{-1}\,h^{-1}}$ of production media and accumulated 51.8% of PHB at the rate of $0.0072\,\mathrm{g\,g^{-1}}$ (biomass) $\mathrm{h^{-1}}$. Coats et al. have reported that in some mixed cultures or activated sludge, PHA production could be as high as over 50% of the cell dry weight (CDW) [29].

3.8. Degradation of PHB Sheet. Polymers in natural environment are degraded through hydrolysis, mechanical, thermal,

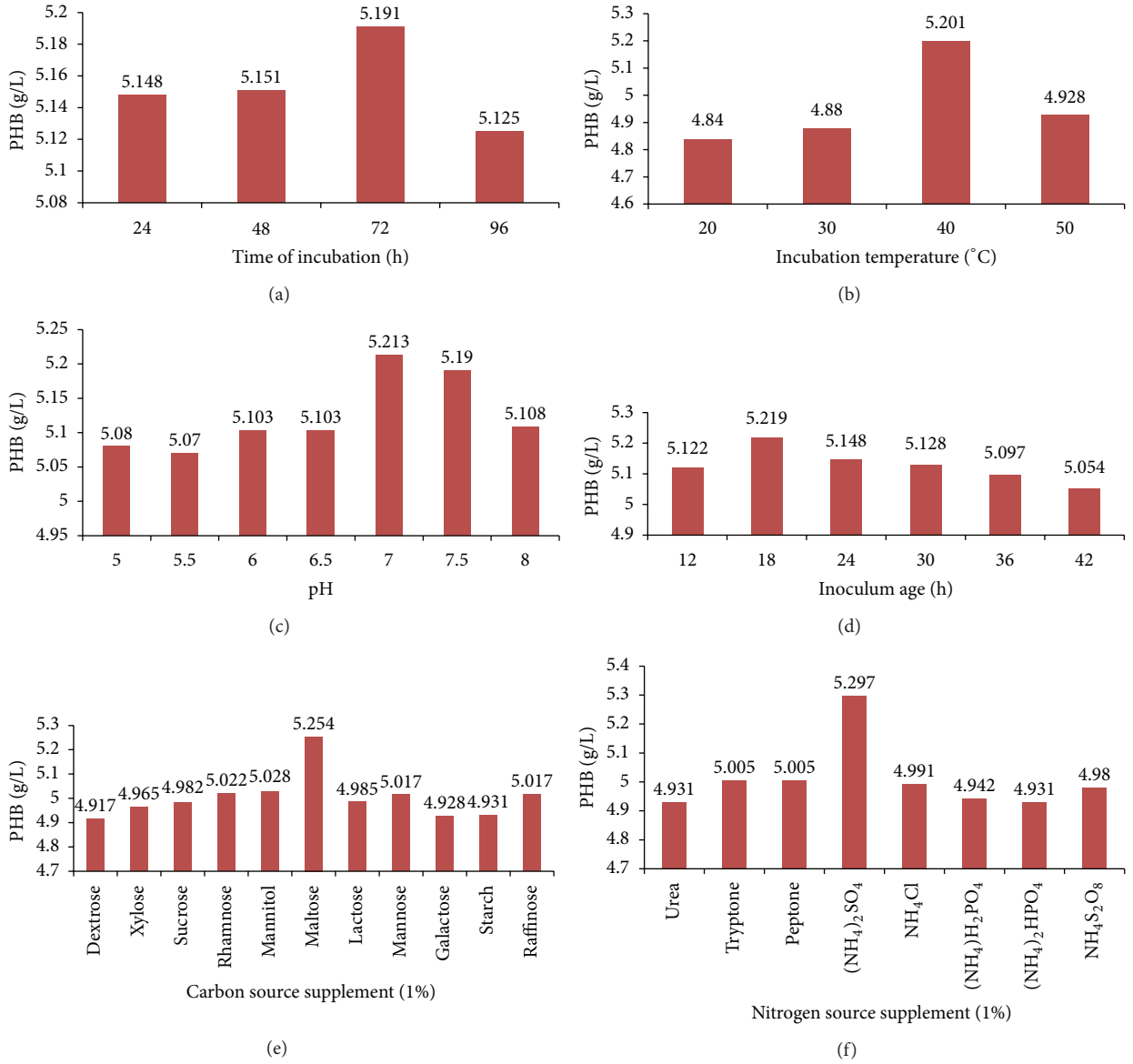

FIGURE 3: Optimization of cultural conditions for *Bacillus subtilis* NG220.

oxidative, and photochemical destruction, and biodegradation. One of the valuable properties of PHB is its biodegradability, and it was studied in simulated natural environment (in soil, compost, and industrial sludge) in laboratory. All test pieces of PHB starch blend sheet lost weight during incubation, but the degree of weight loss varied widely with environment in which the polymer sheets were incubated. The compost was found to be the better for degradation of PHB films compared to soil and industrial sludge. It is further supported by increase microbial load (5.0×10^6 cfu/mL^{-1} to more than 3.0×10^9 cfu mL^{-1}/g) (Table 6) in compost after 30 days, where PHB could serve as nutrient source by microflora. The microbial population was increased in compost after 30 days. The bacteria detected on the degraded PHB films were dominated by the genera *Pseudomonas*, *Bacillus*, *Azospirillum*, *Mycobacterium*, *Streptomyces*, *Aspergillus*, and Penicillium [30]. The rate of degradation of the PHB films was 25.3% and 50.2% within 30 days in compost containing 10% and 15% moisture, respectively, while in the compost containing the 20% and 25% moisture the PHB films were found to be degraded into fine pieces in 30 days resulting into 80.2% and 100% loss in wt of PHB films (Figure 4) indicating the importantance of moisture content of the compost. Similar observation was noted by Wang et al. [11], Woolnough et al. [31], and Kulkarni et al. [10].

4. Conclusion

The isolate *Bacillus subtilis* NG220 from sugarcane field area was able to efficiently utilize the sugar industry waste water as nutrient source for PHB production. The first line of impression of this study concludes that the sugar industry waste

Table 6: Degradation of polymer sheet in natural samples.

Natural sample	Incubation (days)	% weight loss of polymer sheet	Microbial population
Soil	0	0	3.0×10^6
	10	30.2 ± 0.5	4.0×10^7
	20	43.5 ± 1.2	4.9×10^7
	30	70.6 ± 2.6	5.2×10^8
	40	98.3 ± 2.1	5.4×10^8
Compost	0	0	5×10^6
	10	50.2 ± 0.5	2×10^7
	20	80.2 ± 0.5	1.2×10^8
	30	100%	3.0×10^9
Industrial sludge	0	0	2.5×10^5
	10	26.3 ± 1.2	3.2×10^6
	20	57.6 ± 1.5	4.9×10^6
	30	73.6 ± 1.5	5.6×10^6
	40	97.2 ± 22	6.0×10^6

*Degradation study was followed in lab conditions at room temperature.

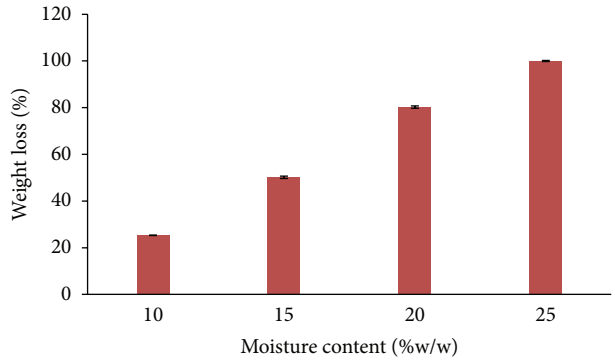

Figure 4: Effect of moisture content on PHB degradation in compost.

water could directly serve as an inexpensive nutrient source for production of biodegradable plastic. Thus, this study may solve the problem of costly treatment of sugar industry waste water as well as high production cost of biodegradable bioplastic and help in conservation of petroleum products which were used in the commercial production of plastic production.

Acknowledgments

The authors express their sincere gratitude to the Department of Science and Technology, Government of India, for providing the financial aid for this research work. The authors also acknowledge the Saraswati Sugar Mills (SSM), Ltd., Yamuna Nagar, for providing the untreated waste water. The authors are very thankful to the Department of Chemistry, Kurukshetra University, Kurukshetra, for providing the necessary facilities for NMR, FTIR, and DSC analysis of the polymer.

References

[1] A. J. Anderson and E. A. Dawes, "Occurrence, metabolism, metabolic role, and industrial uses of bacterial polyhydroxyalkanoates," *Microbiological Reviews*, vol. 54, no. 4, pp. 450–472, 1990.

[2] E. R. Howells, "Opportunities in biotechnology for the chemical industry," *Chemistry & Industry*, vol. 8, pp. 508–511, 1982.

[3] C. Wood, *Environment Impact Asseesment: A Comparative Review*, Longman, Harlow, UK, 1995.

[4] S. Banziger, P. D. N. Tobler, and H. Brandl H, *The Formation of Reserve Polymers in Bacillus megaterium*, Microbial Ecology Course, University of Zurich, Zurich, Switzerland, 2001.

[5] J. H. Law and R. A. Slepecky, "Assay of poly-beta-hydroxybutyric acid," *Journal of Bacteriology*, vol. 82, pp. 33–36, 1961.

[6] I. Y. Lee, H. N. Chang, and Y. H. Park, "A simple method for recovery of microbial poly β-hydroxybutrate by alkaline solution treatment," *Journal of Microbiology and Biotechnology*, vol. 5, pp. 238–240, 1995.

[7] H. Yoshie, S. Ozasa, K. Adachi, H. Nagai, M. Shiga, and Y. Nakamura, "Nuclear magnetic resonance of ^{59}Co in Gd_2Co_7," *Journal of Magnetism and Magnetic Materials*, vol. 104–107, no. 2, pp. 1449–1450, 1992.

[8] L. M. W. K. Gunaratne, R. A. Shanks, and G. Amarasinghe, "Thermal history effects on crystallisation and melting of poly(3-hydroxybutyrate)," *Thermochimica Acta*, vol. 423, no. 1-2, pp. 127–135, 2004.

[9] P. Schubert, N. Kruger, and A. Steinbuchel, "Molecular analysis of the Alcaligenes eutrophus poly(3-hydroxybutyrate) biosynthetic operon: identication of the N terminus of poly(3-hydroxybutyrate) synthase and identification of the promoter," *Journal of Bacteriology*, vol. 173, no. 1, pp. 168–175, 1991.

[10] S. O. Kulkarni, P. P. Kanekar, J. P. Jog et al., "Characterisation of copolymer, poly (hydroxybutyrate-co-hydroxyvalerate) (PHB-co-PHV) produced by Halomonas campisalis (MCM B-1027), its biodegradability and potential application," *Bioresource Technology*, vol. 102, no. 11, pp. 6625–6628, 2011.

[11] S. Wang, C. Song, W. Mizuno et al., "Estimation on biodegradability of poly(3-hydroxybutyrate-co-3-hydroxyvalerate) (PHB/V) and numbers of aerobic PHB/V degrading microorganisms in different natural environments," *Journal of Polymers and the Environment*, vol. 13, no. 1, pp. 39–45, 2005.

[12] M. Thirumala, S. V. Reddy, and S. K. Mahmood, "Production and characterization of PHB from two novel strains of Bacillus spp. isolated from soil and activated sludge," *Journal of Industrial Microbiology and Biotechnology*, vol. 37, no. 3, pp. 271–278, 2010.

[13] H. Mitomo, P. J. Barham, and A. Keller, "Crystallization and morphology of poly(β-hydroxybutyrate) and its copolymer," *Polymer Journal*, vol. 19, no. 11, pp. 1241–1253, 1987.

[14] M. Matavulj and H. P. Molitoris, "Fungal degradation of polyhydroxyalkanoates and a semiquantitative assay for screening their degradation by terrestrial fungi," *FEMS Microbiology Reviews*, vol. 103, no. 2-4, pp. 323–331, 1992.

[15] Z. N. Yüksekdağ, B. Aslim, Y. Beyatli, and N. Mercan, "Effect of carbon and nitrogen sources and incubation times on poly-beta-hydroxybutyrate (PHB) synthesis by Bacillus subtilis 25 and *Bacillus megaterium* 12," *African Journal of Biotechnology*, vol. 3, no. 1, pp. 63–66, 2004.

[16] B. Aslim, Z. N. Yuksekdag, and Y. Beyatli, "Determination of growth quantities of certain *Bacillus* species isolated from soil," *Turkish Electronic Journal of Biotechnology*, pp. 24–30, 2002.

[17] P. Tavernier, J.-C. Portais, J. E. Nava Saucedo, J. Courtois, B. Courtois, and J.-N. Barbotin, "Exopolysaccharide and poly-β-hydroxybutyrate coproduction in two Rhizobium meliloti strains," *Applied and Environmental Microbiology*, vol. 63, no. 1, pp. 21–26, 1997.

[18] S. Shivakumar, "Polyhydroxybutyrate (PHB) production using agro-industrial residue as substrate by Bacillus thuringiensis IAM 12077," *International Journal of ChemTech Research*, vol. 4, no. 3, pp. 1158–1162, 2012.

[19] S. Kumbhakar, P. K. Singh, and A. S. Vidyarthi, "Screening of root nodule bacteria for the production of polyhydroxyalkanoate (PHA) and the study of parameters influencing the PHA accumulation," *African Journal of Biotechnology*, vol. 11, no. 31, pp. 7934–7946, 2012.

[20] N. V. Ramadas, S. K. Singh, C. R. Soccol, and A. Pandey, "Polyhydroxybutyrate production using agro-industrial residue as substrate by *Bacillus sphaericus* NCIM 5149," *Brazilian Archives of Biology and Technology*, vol. 52, no. 1, pp. 17–23, 2009.

[21] K. Hori, M. Kaneko, Y. Tanji, X.-H. Xing, and H. Unno, "Construction of self-disruptive *Bacillus megaterium* in response to substrate exhaustion for polyhydroxybutyrate production," *Applied Microbiology and Biotechnology*, vol. 59, no. 2-3, pp. 211–216, 2002.

[22] Q. Wu, H. Huang, G. Hu, J. Chen, K. P. Ho, and G.-Q. Chen, "Production of poly-3-hydroxybutrate by Bacillus sp. JMa5 cultivated in molasses media," *Antonie van Leeuwenhoek, International Journal of General and Molecular Microbiology*, vol. 80, no. 2, pp. 111–118, 2001.

[23] M. Singh, "Cane sugar industry in India," in *Proceedings of the XXIII ISSCT Congress*, New Delhi, India, 1999.

[24] S. Khanna and A. K. Srivastava, "Statistical media optimization studies for growth and PHB production by *Ralstonia eutropha*," *Process Biochemistry*, vol. 40, no. 6, pp. 2173–2182, 2005.

[25] A. A. Koutinas, Y. Xu, R. Wang, and C. Webb, "Polyhydroxybutyrate production from a novel feedstock derived from a wheat-based biorefinery," *Enzyme and Microbial Technology*, vol. 40, no. 5, pp. 1035–1044, 2007.

[26] M.-S. Kim, J.-S. Baek, and J. K. Lee, "Comparison of H2 accumulation by *Rhodobacter sphaeroides* KD131 and its uptake hydrogenase and PHB synthase deficient mutant," *International Journal of Hydrogen Energy*, vol. 31, no. 1, pp. 121–127, 2006.

[27] Z. Liangqi, X. Jingfan, F. Tao, and W. Haibin, "Synthesis of poly (3-hydroxybutyrate-co-3-hydroxyoctanoate) by a Sinorhizobium fredii strain," *Letters in Applied Microbiology*, vol. 42, no. 4, pp. 344–349, 2006.

[28] K. Sangkharak and P. Prasertsan, "Nutrient optimization for production of polyhydroxybutyrate from halotolerant photosynthetic bacteria cultivated under aerobic-dark condition," *Electronic Journal of Biotechnology*, vol. 11, no. 3, 2008.

[29] E. R. Coats, F. J. Loge, M. P. Wolcott, K. Englund, and A. G. McDonald, "Synthesis of polyhydroxyalkanoates in municipal wastewater treatment," *Water Environment Research*, vol. 79, no. 12, pp. 2396–2403, 2007.

[30] A. P. Bonartsev, V. L. Myshkina, D. A. Nikolaeva et al., "Biosynthesis, biodegradation, and application of poly(3-hydroxybutyrate) and its copolymers: natural polyesters produced by diazotrophic bacteria," in *Communicating Current Research and Educational Topics and Trends in Applied Microbiology*, A. Méndez-Vilas, Ed., pp. 295–307, Formatex, Badajoz, Spain, 2007.

[31] C. A. Woolnough, L. H. Yee, T. Charlton, and L. J. R. Foster, "Environmental degradation and biofouling of 'green' plastics including short and medium chain length polyhydroxyalkanoates," *Polymer International*, vol. 59, no. 5, pp. 658–667, 2010.

Hindawi Publishing Corporation
BioMed Research International
Volume 2013, Article ID 134872, 11 pages
http://dx.doi.org/10.1155/2013/134872

Research Article

Treatment of Slaughter House Wastewater in a Sequencing Batch Reactor: Performance Evaluation and Biodegradation Kinetics

Pradyut Kundu, Anupam Debsarkar, and Somnath Mukherjee

Environmental Engineering Division, Civil Engineering Department, Jadavpur University, Kolkata 32, India

Correspondence should be addressed to Somnath Mukherjee; snm_ju@yahoo.co.in

Received 27 April 2013; Revised 9 July 2013; Accepted 9 July 2013

Academic Editor: Eldon R. Rene

Slaughterhouse wastewater contains diluted blood, protein, fat, and suspended solids, as a result the organic and nutrient concentration in this wastewater is vary high and the residues are partially solubilized, leading to a highly contaminating effect in riverbeds and other water bodies if the same is let off untreated. The performance of a laboratory-scale Sequencing Batch Reactor (SBR) has been investigated in aerobic-anoxic sequential mode for simultaneous removal of organic carbon and nitrogen from slaughterhouse wastewater. The reactor was operated under three different variations of aerobic-anoxic sequence, namely, (4+4), (5+3), and (3+5) hr. of total react period with two different sets of influent soluble COD (SCOD) and ammonia nitrogen (NH_4^+-N) level 1000 ± 50 mg/L, and 90 ± 10 mg/L, 1000 ± 50 mg/L and 180 ± 10 mg/L, respectively. It was observed that from 86 to 95% of SCOD removal is accomplished at the end of 8.0 hr of total react period. In case of (4+4) aerobic-anoxic operating cycle, a reasonable degree of nitrification 90.12 and 74.75% corresponding to initial NH_4^+-N value of 96.58 and 176.85 mg/L, respectively, were achieved. The biokinetic coefficients (k, K_s, Y, k_d) were also determined for performance evaluation of SBR for scaling full-scale reactor in future operation.

1. Introduction

The continuous drive to increase meat production for the protein needs of the ever increasing world population has some pollution problems attached. Pollution arises from activities in meat production as a result of failure in adhering to Good Manufacturing Practices (GMP) and Good Hygiene Practices (GHP) [1]. Consideration is hardly given to safety practices during animal transport to the abattoir, during slaughter and dressing of hides and flesh [2]. For hygienic reasons abattoirs, use large amount of water in processing operations (slaughtering and cleaning), which produces large amount of wastewater. The major environmental problem associated with this abattoir wastewater is the large amount of suspended solids and liquid waste as well as odor generation [3]. Effluent from slaughterhouses has also been recognized to contaminate both surface and groundwater because during abattoir processing, blood, fat, manure, urine, and meat tissues are lost to the wastewater streams [4]. Leaching into groundwater is a major part of the concern, especially due to the recalcitrant nature of some contaminants [5]. Blood, one of the major dissolved pollutants in abattoir wastewater, has the highest COD of any effluent from abattoir operations. If the blood from a single cow carcass is allowed to discharge directly into a sewer line, the effluent load would be equivalent to the total sewage produced by 50 people on average day [6]. The major characteristics of abattoir wastes are high organic strength, sufficient organic biological nutrients, adequate alkalinity, relatively high temperature (20 to 30°C) and free of toxic material. Abattoir wastewaters with the previous characteristics are well suited to anaerobic treatment and the efficiency in reducing the BOD_5 ranged between 60 and 90% [7]. The high concentration of nitrates in the abattoir wastewater also exhibits that the wastewater could be treated by biological processes. Nitrogenous wastewater when discharged to receiving water bodies leads to undesirable problems such as algal blooms and eutrophication in addition to oxygen deficit. The dissolved oxygen level further depleted if organic carbon along

Table 1: Different available technologies used to treat slaughterhouse wastewater.

Sl no.	Technology adopted	Input characteristics of slaughterhouse wastewater	Observations	References
(1)	Anaerobic treatment of slaughterhouse wastewaters in a UASB (Upflow Anaerobic Sludge Blanket) reactor and in an anaerobic filter (AF).	Slaughterhouse wastewater showed the highest organic content with an average COD of 8000 mg/L, of which 70% was proteins. The suspended solids content represented between 15 and 30% of the COD.	The UASB reactor was run at OLR (Organic Loading Rates) of 1–6.5 kg COD/m^3/day. The COD removal was 90% for OLR up to 5 kg COD/m^3/day and 60% for an OLR of 6.5 kg COD/m^3/day. For similar organic loading rates, the AF showed lower removal efficiencies and lower percentages of methanization.	Ruiz et al. [9]
(2)	Anaerobic sequencing batch reactors.	Influent total chemical oxygen demand (TCOD) ranged from 6908 to 11 500 mg/L, of which approximately 50% were in the form of suspended solids (SS).	Total COD was reduced by 90% to 96% at organic loading rates (OLRs) ranging from 2.07 to 4.93 kg m^{-3} d^{-1} and a hydraulic retention time of 2 days. Soluble COD was reduced by over 95% in most samples.	Massé and Masse [10]
(3)	Moving bed sequencing batch reactor for piggery wastewater treatment.	COD, BOD, and suspended solids in the range of 4700–5900 mg/L, 1500–2300 mg/L, and 4000–8000 mg/L, respectively.	COD and BOD removal efficiency was greater than 80% and 90%, respectively at high organic loads of 1.18–2.36 kg COD/m^3·d. The moving-bed SBR gave TKN removal efficiency of 86–93%.	Sombatsompop et al. [11]
(4)	Fixed bed sequencing batch reactor (FBSBR).	The wastewater has COD loadings in the range of 0.5–1.5 Kg COD/m^3 per day.	COD, TN, and phosphorus removal efficiencies were at range of 90–96%, 60–88%, and 76–90%, respectively.	Rahimi et al. [12]
(5)	Chemical coagulation and electrocoagulation techniques.	COD and BOD_5 of raw wastewater in the range of 5817 ± 473 and 2543 ± 362 mg/L.	Removal of COD and BOD_5 more than 99% was obtained by adding 100 mg/L PACl and applied voltage 40 V.	Bazrafshan et al. [13]
(6)	Hybrid upflow anaerobic sludge blanket (HUASB) reactor for treating poultry slaughterhouse wastewater.	Slaughterhouse wastewater showed total COD 3000–4800 mg/L, soluble COD 1030–3000 mg/L, BOD5 750–1890 mg/L, suspended solids 300–950 mg/L, alkalinity (as $CaCO_3$) 600–1340 mg/L, VFA (as acetate) 250–540 mg/L, and pH 7–7.6.	The HUSB reactor was run at OLD of 19 kg COD/m^3/day and achieved TCOD and SCOD removal efficiencies of 70–86% and 80–92%, respectively. The biogas was varied between 1.1 and 5.2 m^3/m^3 d with the maximum methane content of 72%.	Rajakumar et al. [14]
(7)	Anaerobic hybrid reactor was packed with light weight floating media.	COD, BOD and Suspended Solids in the range of 22000–27500 mg/L, 10800–14600 mg/L, and 1280–1500 mg/L, respectively.	COD and BOD reduction was found in the range of 86.0–93.58% and 88.9–95.71%, respectively.	Sunder and Satyanarayan [15]

with nutrient sinks into the water environment. Hence, it is very much necessary to control the discharge of combined organic carbon and nitrogen laden wastewater by means of appropriate treatment. Biological treatment has been proved to be comparatively innocuous and more energy efficient of treating wastewater if good process control could be ensured [8]. Several researchers successfully used different technologies for treatment of slaughterhouse wastewater containing organic carbon and nitrogen (COD and TKN) in laboratory and pilot scale experiment. Table 1 had shown the previous research findings about slaughterhouse wastewater treatment by the different investigators.

Among the various biological treatment processes, sequencing batch reactor (SBR) is considered to be an improved version of activated sludge process, which operates in fill and draw mode for biological treatment of wastewater. An SBR operates in a pseudobatch mode with aeration and sludge settlement both occurring in the same tank. SBRs are operated in fill-react-settle-draw-idle period sequences. The major differences between SBR and conventional continuous-flow, activated sludge system is that the SBR tank carries out the functions of equalization, aeration, and sedimentation in a time sequence rather than in the conventional space sequence of continuous-flow systems. Sequencing batch reactors (SBRs) are advocated as one of the best available techniques (BATs) for slaughterhouse wastewater treatment [16, 17] because they are capable of removing organic carbon, nutrients, and suspended solids from wastewater in a single tank and also have low capital and operational costs.

Biological treatment of wastewater containing organic carbon and nitrogen (COD and TKN) is also carried out in laboratory and pilot scale experiment by several researchers

successfully [18–26]. Nutrients in piggery wastewater with high organic matter, nitrogen, and phosphorous content were biological removed by Obaja et al. [27] in a sequencing batch reactor (SBR) with anaerobic, aerobic, and anoxic stages. The SBR was operated with wastewater containing 1500 mg/L ammonium and 144 mg/L phosphate, a removal efficiency of 99.7% for nitrogen and 97.3% for phosphate was obtained. A full-scale SBR system was evaluated by Lo and Liao [28] to remove 82% of BOD and more than 75% of nitrogen after a cycle period of 4.6 hour from swine wastewater. Mahvi et al. [29] carried out a pilot-scale study on removal of nitrogen both from synthetic and domestic wastewater in a continuous flow SBR and obtained a total nitrogen and TKN removal of 70–80% and 85–95%, respectively. An SBR system demonstrated by Lemaire et al. [30] to high degree of biological remove of nitrogen, phosphorus, and COD to very low levels from slaughterhouse wastewater. A high degree removal of total phosphorus (98%), total nitrogen (97%), and total COD (95%) was achieved after a 6-hour cycle period. Moreover, SBRs have been successfully used to treat landfill leachate, tannery wastewater, phenolic wastewater, and various other industrial wastewaters [31–34].

In the present investigation, an attempt has been made to explore the performance efficacy of SBR technology for simultaneous removal of soluble carbonaceous organic matter and ammonia nitrogen from slaughterhouse wastewater and also to determine the biokinetic constants for carbon oxidation, nitrification, and denitrification under different combination of react periods (aerobic/anoxic).

2. Material and Methods

2.1. Seed Acclimatization for Combined Carbon Oxidation and Nitrification. The active microbial seed was cultured under ambient condition in the laboratory by inoculating 200 mL sludge as collected from an aeration pond of M/S Mokami small-scale slaughterhouse located in the village Nazira, South 24 Parganas district (West Bengal), India, to a growth propagating media composed of 500 mL dextrose solution having concentrations of 1000 mg/L, 250 mL ammonium chloride (NH_4Cl) solution having concentration of 200 mg/L and 250 mL of nutrient solution in 3000 mL capacity cylindrical vessel. The composition of the nutrient solution in 250 mL distilled water was comprised of 60.0 mg K_2HPO_4, 40.0 mg KH_2PO_4, 500.0 mg $MgSO_4{\cdot}7H_2O$, 710.0 mg $FeCl_3{\cdot}6H_2O$, 0.1 mg $ZnSO_4{\cdot}7H_2O$, 0.1 mg $CuSO_4{\cdot}5H_2O$, 8.0 mg $MnCl_2{\cdot}2H_2O$, 0.11 mg $(NH_4)_6Mo_7O_{24}$, 100.0 mg $CaCl_2{\cdot}2H_2O$, 200.0 mg $CoCl_2{\cdot}6H_2O$, 55.0 mg $Al_2(SO_4)_3{\cdot}16H_2O$, 150.0 mg H_3BO_3. Finally 800 mL volume of distilled water was added to liquid mixture to make a volume of 2 L and the mixture was continuously aerated with intermittent feeding with dextrose solution having concentrations of 1000 mg/L and ammonium chloride (NH_4Cl) having concentration of 200 mg/L as a carbon and nitrogen source, respectively. The acclimatization process was continued for an overall period of 90 days. The biomass growth was monitored by the magnitude of sludge volume index (SVI) and mixed liquor suspended solid (MLVSS) concentration in the reactor. pH in the reactor was maintained in the range 6.8–7.5 by adding required amount of sodium carbonate (Na_2CO_3) and phosphate buffer. The seed acclimatization phase was considered to be over when a steady-state condition was observed in terms of equilibrium COD and NH_4^+-N reduction with respect to a steady level of MLVSS concentration and SVI in the reactor.

Denitrifying seed was cultured separately in 2.0 L capacity aspirator bottle under anoxic condition. 500 gm of digested sludge obtained from the digester of a nearby sewage treatment plant (STP) was added to 1.0 L of distilled water. The solution was filtered and 250 mL of nutrient solution along with 250 mL dextrose solution as carbon source and 100 mL potassium nitrate solution (KNO_3) as the source of nitrate nitrogen (NO_3^--N) was added to it. The resulting solution was acclimatized for denitrification purpose under anoxic condition. Magnetic stirrer was provided for proper mixing of the solution. Denitrifying seed was acclimatized against a nitrate-nitrogen concentration varying from 10–90 mg/L as N, over a period of three months.

2.2. Experimental Procedure. The experimental work was carried out in a laboratory scale SBR, made of Perspex sheet of 6 mm thickness, having 20.0 L of effective volume. In order to assess the treatability of slaughterhouse wastewater in an SBR, the real-life wastewater samples were collected from two different locations (i) the raw (untreated) wastewater from the main collection pit and (ii) the primary treated effluent from the inlet box of aeration basin. The wastewater samples were collected 4 (four) times over the entire course of the study in 25.0 L plastic containers and stored in a refrigerator at approximately 4.0°C. The effluent quality was examined as per the methods described in "Standard Methods" [35] for determining its initial characteristics which are exhibited in Table 2.

The settled effluent was poured in the reactor of 20.0 L capacity to perform necessary experiments. 2.5 L of preacclimatized mixed seed containing carbonaceous bacteria, nitrifier, and denitrifier was added in the reactor containing 20.0 L of pretreated slaughterhouse wastewater to carry out the necessary experiments. Oxygen was supplied through belt-driven small air compressor. A stirrer of 0.3 KW capacity was installed at the center of the vessel for mixing the content of the reactor. Air was supplied to the reactor during aerobic phase of react period with the help of diffused aeration system. However, during the anoxic phase the stirrer was allowed only to operate for mixing purpose and air supply was cut off. A timer was also connected to compressor for controlling the sequence of different react period (aerobic and anoxic). A schematic diagram of the experimental setup is shown in Figure 1.

The cycle period for the operation of SBR was taken as 10 hour, with a fill period of 0.5 hour, overall react period of 8.0 hours, settle period of 1.0 hour, and idle/decant period of 0.5 hour. The overall react period was divided into aerobic and anoxic react period in the following sequences:

Combination-1: 4-hour aerobic react period and 4-hour anoxic react period.

Table 2: Characteristics and composition of slaughterhouse wastewater.

Parameters	Raw wastewater					Pretreated wastewater				
	Set-1	Set-2	Set-3	Set-4	Range	Set-1	Set-2	Set-3	Set-4	Range
pH	8.0	8.2	8.5	8.4	8.0–8.5	7.5	7.2	8.5	7.8	7.5–8.5
TSS (mg/L)	10120	12565	14225	13355	10120–14225	2055	2280	2540	2386	2055–2540
TDS (mg/L)	6345	7056	7840	6865	6345–7840	2800	3065	3230	3185	2800–3230
DO (mg/L)	0.8	1.1	0.9	1.3	0.8–1.3	1.2	1.4	1.5	1.6	1.2–1.6
SCOD (mg/L)	6185	6525	6840	6455	6185–6840	830	945	1045	925	830–1045
BOD_5 at 20°C (mg/L)	3000	3200	3500	3350	3000–3500	210	240	265	252	210–265
TKN (mg/L as N)	1050	1130	1200	1165	1050–1200	305	420	525	485	305–525
NH_4^+ N (mg/L as N)	650	695	735	710	650–735	95	155	191	125	95–191

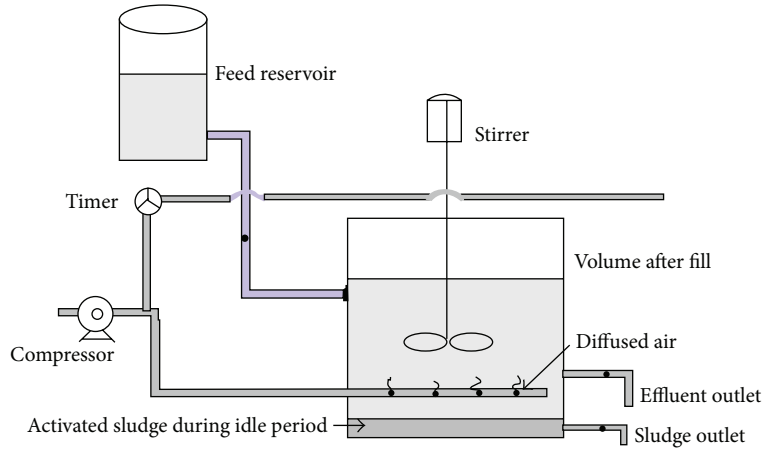

Figure 1: A schematic diagram of the experimental setup.

Combination-2: 5-hour aerobic react period and 3-hour anoxic react period.

Combination-3: 3-hour aerobic react period and 5-hour anoxic react period.

The performance study was carried out with pretreated slaughterhouse wastewater with same initial soluble chemical oxygen demand (SCOD) and two different ammonia nitrogen (NH_4^+-N) concentration of 1000 ± 50 mg/L and 90 ± 10 mg/L, 1000±50 mg/L and 180±10 mg/L, respectively. During the fill period of 30 min duration, 16.0 L of slaughterhouse wastewater was transferred under gravity from a feeding tank into the reactor. The mechanical mixer was operated continuously with a speed of 400 rpm from the beginning of the fill phase till the end of the total react phase for proper mixing of liquid in the reactor. During the draw phase, the supernatant wastewater was decanted until the liquid volume in the reactor was decreased to 4.0 L. sludge retention time (SRT) was manually controlled by withdrawal of volume of the mixed liquor from the reactor every day at the onset of the commencement of settle phase. The reactor was continuously run for 120 days. The initial pH values in the reactor were kept in between 7.1 and 7.7, whereas the sludge volume index (SVI) has been kept within the range of 75–85 mL/gm, for obtaining good settling property of the biomass. It has been reported that SRT should be longer than 10 days to achieve efficient nitrogen removal [36]. The SRT of 20–25 days as maintained for carbon oxidation and nitrification in the present SBR system for treatment of wastewater as suggested by Tremblay et al. [37].

During the time course of the study, 100 mL of sample was collected from the outlet of the reactor at every 1.0 hour interval, till completion of the fill period. The samples were analyzed for the following parameters: pH, DO, MLSS, MLVSS, COD, NH_4^+-N, NO_2^--N, and NO_3^--N as per the methods described in "Standard Methods" [35]. The pH of the solution was measured by a digital pH meter. NH_4^+-N, NO_2^--N, and NO_3^--N were estimated by respective ion selective electrodes in ISE meter. COD was analyzed by closed reflux method using dichromate digestion principle in digester. Dissolved oxygen (DO) was measured electrometrically by digital DO meter. Mixed liquor suspended solids (MLSS) and Mixed liquor volatile suspended solids (MLVSS) were measured by gravimetric method at temperature of 103–105°C and 550 ± 50°C in muffle furnace, respectively.

2.3. Carbon Oxidation and Nitrification Kinetics in SBR. Biokinetic parameters play an important role in designing and optimizing an activated sludge process. The biokinetic constants describe the metabolic performance of the microorganisms when subjected to the substrate and other components of the specific wastewater. These biokinetic coefficients yield a set of realistic design parameters, which can be used in rationalizing the design of the activated sludge process for a specific substrate.

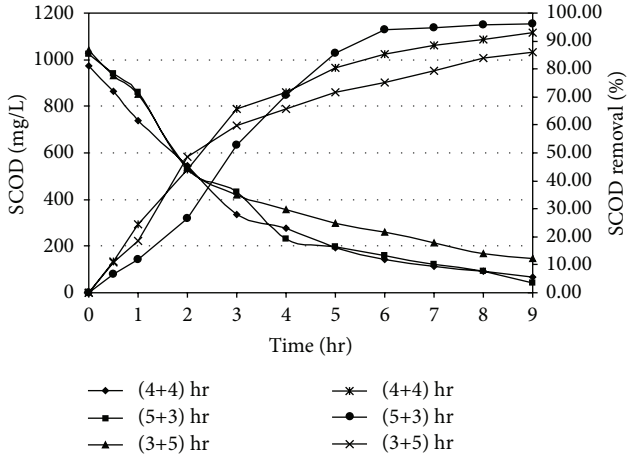

Figure 2: Carbon oxidation profile under different react period combination [Initial SCOD = 1000 ± 50 mg/L; Initial NH_4^+-N = 90 ± 10 mg/L as N].

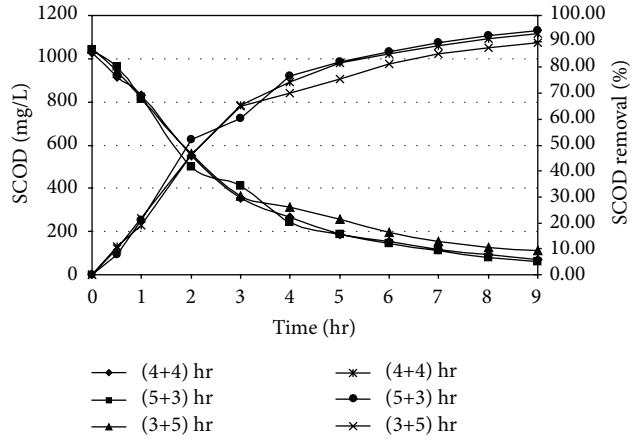

Figure 3: Carbon oxidation profile in SBR under different react period combination [Initial SCOD = 1000±50 mg/L; Initial NH_4^+-N = 180 ± 10 mg/L as N].

2.3.1. Substrate Removal Kinetics. The substrate removal constants, namely, half saturation concentration (K_s) and the maximum rate of substrate utilization (k) were determined from the Lawrence and McCarty's modified Monod equation [38] given below:

$$\frac{1}{U} = \left(\frac{K_s}{k}\right)\left(\frac{1}{S}\right) + \frac{1}{k} \quad (1)$$

S = Substrate (SCOD and NH_4^+-N) concentration at any time in reactor (mg/L), U = Specific substrate utilization rate = $(S_0 - S)/\theta X$ (mg of SCOD or mg of NH_4^+-N/day/mg of MLVSS), θ = Contact time (day), X = MLVSS at any time in the reactor (mg/L), S_0 = Substrate (SCOD and NH_4^+-N) concentration of the influent (mg/L).

The plots made between $1/U$ and $1/S$ develops into a straight line with K_s/k as its slope and $1/k$ as its intercept.

2.3.2. Sludge Growth Kinetics. The sludge growth kinetic constants namely the yield coefficient (Y) and the endogenous decay coefficient (K_d), were determined from the Lawrence and McCarty's modified Monod equation [38] given below:

$$\frac{1}{\theta} = YU - K_d, \quad (2)$$

where U = Specific substrate utilization rate (mg of SCOD or mg of NH_4^+-N/day/mg of MLVSS), θ = Contact time (day), k_d = Endogenous decay coefficient (day^{-1}), and Y = Yield coefficient (mg of MLVSS produced/mg of SCOD or NH_4^+-N).

A graph drawn between $1/\theta$ and U gives a straight line, with Y as its slope and k_d as its intercept.

2.4. Denitrification Kinetics in SBR. In almost all cases denitrification started occurring at the onset of anoxic period and specific denitrification rate (q_{DN}) was calculated under different initial organic carbon and NH_4^+-N concentrations for different react period combinations, namely, (4+4), (5+3), (3+5) hrs over the respective anoxic environment.

3. Results and Discussion

3.1. Carbon Oxidation Performance. Organic carbon, which is the source of energy for heterogenic and denitrifying microorganism, was estimated as chemical oxygen demand (COD). In the present experiment, in correspondance to an initial SCOD of 975.25 mg/L and initial NH_4^+-N concentration of 87.52 mg/L as N, it has been observed that the major fraction of SCOD removal took place within 4 or 5 hrs of aerobic react period. In anoxic phase, further SCOD removal has been noticed as shown in Figure 2. Li et al. [39] obtained that the maximum removal efficiency of COD (96%) for treatment of slaughterhouse wastewater which was marginally higher than the result of this present study. COD removal profile was also observed in similar pattern in the presence of higher initial NH_4^+-N concentration of 185.24 mg/L as N and initial SCOD of 1028.55 mg/L in a separate set of experiment. The results are plotted in Figure 3. It is revealed from Figures 2 and 3 that the rate of organics utilization by the dominant heterotrophs during initial aerobic react period was more as compared to its rate of removal during anoxic period. The carbon utilization bacteria used up bulk amount COD for energy requirement and growth. The removal efficiency of COD in the suspended growth reactor system depends on COD : TKN ratio. The mean COD : TKN ratio recommended for adequate carbon oxidation and nutrient removal as 10–12 [40]. In the present investigation, COD : TKN ratio was approximately 11.14 which was in agreement in their recommendation. The removal efficiency also depends on react time. The carbon utilizing bacteria obviously and is able to degrade more COD and produce CO_2 with production of new cells due to enhancement of aeration time. A marked improvement has been noticed for higher percentage removal of COD during increase of aeration time. A similar observation was noticed by Kanimozhi and Vasudevan [41]. Due to the increase of time and COD load more cells to be produced eventually higher degree of organic removal. When the react period was changed into 5-hour aerobic followed by a reduced 3.0 hour anoxic, a marginal improvement of SCOD

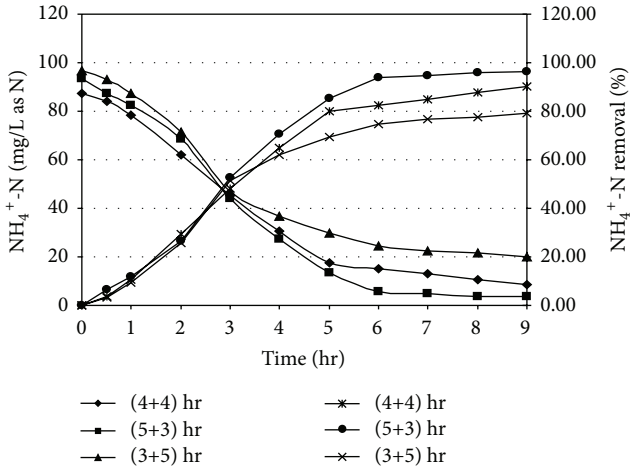

Figure 4: Ammonia oxidation profile in SBR under different react period combination [Initial SCOD = 1000±50 mg/L; Initial NH_4^+-N = 90 ± 10 mg/L as N].

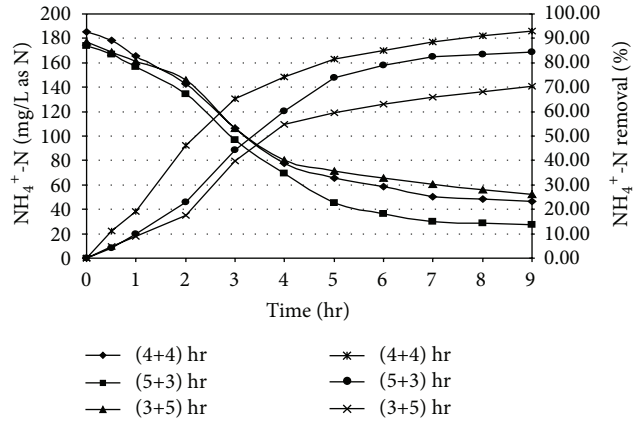

Figure 5: Ammonia oxidation profile in SBR under different react period combination [Initial SCOD = 1000±50 mg/L; Initial NH_4^+-N = 180 ± 10 mg/L as N].

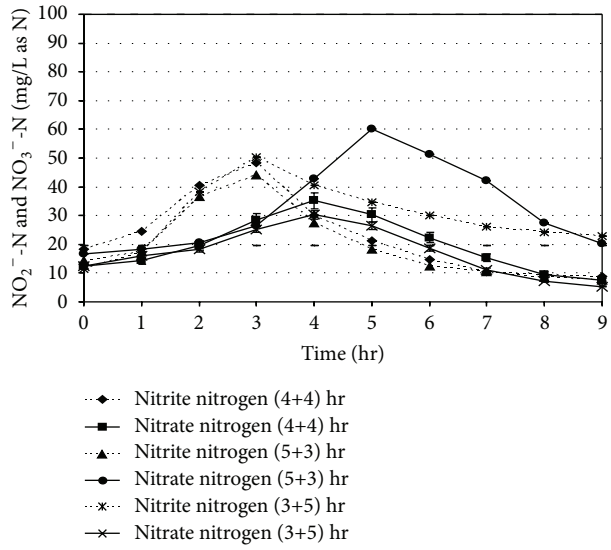

Figure 6: Nitrite and nitrate concentration profiles in SBR under different react period combination [initial SCOD = 1000 ± 50 mg/L and initial NH_4^+-N = 90 ± 10 mg/L as N].

removal in aerobic phase (77.27%) and anoxic phase (96.07%) with an initial SCOD of 1023.22 mg/L was observed due to enhanced aeration time. On the other hand, when the react period was subsequently changed to 3.0 hour, aerobic period followed by 5.0-hour anoxic period, a marginal decrease of SCOD removal in aerobic phase (65.64%) and anoxic phase (86.07%) with an initial SCOD of 1042.52 mg/L was obtained due to lag of aeration time.

3.2. Nitrification Performance. Ammonia oxidation took place due to the presence of previously acclimatized nitrifying organisms within the reactor as mixed culture. The nitrification results are shown in Figures 4 and 5. In case of specific cycle period of 4 hr (aerobic) and 4 hr (anoxic), it was observed that at the end of 8 hr react period of reaction, 90.12% nitrification could achieved for an initial NH_4^+-N was approximately 87.52 mg/L as Fongsatitkul et al. [40] obtained maximum 93% removal efficiency of soluble nitrogen for treatment of abattoir wastewater which was slightly higher than our result. The ammonia oxidation occurred in two phases; a fraction of ammonia was assimilated by cell-mass for synthesis of new cell during carbon oxidation and, in the subsequent phase, dissimilatory ammonia removal took place for converting NH_4^+-N into NO_2^--N and NO_3^--N under aerobic period. The dissimilatory removal of ammonia depends on the population of nitrifiers and oxidation time. The descending trend of ammonia removal for higher level of initial concentration of NH_4^+-N was attributed due to limitation of enzymatic metabolism of nitrifiers. When the reactor system was operated in 5 hr (aerobic) and 3 hr (anoxic) mode of react cycle, an overall performance of ammonia oxidation was improved from 90.12 to 96.20% and 84.41% for initial NH_4^+-N of 93.54 mg/L and 173.88 mg/L as N, respectively. Higher oxidation period was also recommended by earlier investigators [42, 43] for describing similar kind of experiment on landfill leachate treatment in SBR. The results reveal the fact that the extension of aeration period helped to enhance the oxidation efficiency for the present system. It was also observed that when aerobic period was reduced to 3.0 hr, ammonia oxidation reduced to 79.18% and 70.53% corresponding to initial NH_4^+-N value of 96.58 mg/L and 176.85 mg/L, respectively, at the end of 8 hr react period.

3.3. Denitrification Performance. The nitrite and nitrate nitrogen (NO_2^--N and NO_3^--N) level in the reactor during the total reaction period is shown in Figure 6. The maximum nitrite level was observed in between 2.5 and 3.0 hr of react period. The peak nitrate (NO_3^-) level was found to be formed close to 4.0 hr of aeration period for (4+4) and (3+5) hr combinations of react period. A time lag of one hour for maximum nitrate formation was also noticed after the attainment of the maximum NO_2^--N level in the reactor. For (5+3) hr react period combination, the formation of NO_3^- showed

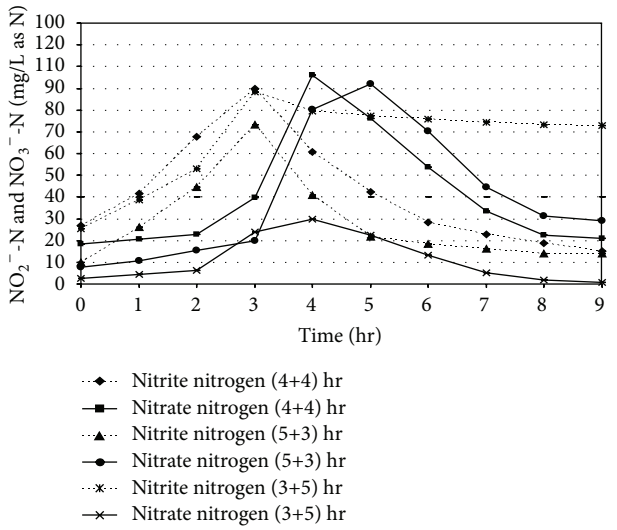

Figure 7: Nitrite and nitrate concentration profiles in SBR under different react period combination [initial SCOD = 1000 ± 50 mg/L and initial NH_4^+-N = 180 ± 10 mg/L as N].

a time-dependent factor as the peak was found at the end of 5.0 hrs. In the Figure 6, after 4.0 hr of aeration period, the NO_3^- level was found to be 35.21 mg/L as N corresponding to initial NH_4^+-N level of 87.52 mg/L as N and NO_3^- concentration of 12.35 mg/L as N, respectively. On the other hand, after 5.0 hour of aerated react period, NO_3^--N concentration in the reactor was found to be 60.24 mg/L as N for an initial NH_4^+-N and NO_3^--N concentration of 93.54 and 16.52 mg/L as N, respectively. The maximum NO_3^--N concentration for (3+5) hour react period combination was found to be 25.31 mg/L as N for the initial NH_4^+-N concentration of 96.58 mg/L as N and NO_3^--N level of 12.35 mg/L as N. The experimental results clearly indicate the necessity of longer aeration period for achieving maximum utilization of ammonia by the nitrifiers.

In Figure 7, after 4.0 hour of anoxic react period, nitrate (NO_3^-) was reduced to 22.29 mg/L as N from its peak concentration of 96.22 mg/L as N, which achieved a 76.83% removal of nitrate for initial NH_4^+-N concentration 185.24 mg/L as N. During denitrification phase, the residual soluble COD concentration as available was found to be more than the stoichiometric organic carbon requirement for effective denitrification. When the anoxic react period was reduced to 3.0 hr, it was observed that, nitrate concentration after 5 hr of aerobic period was found to be maximum (92.11 mg/L as N), per cent removal of nitrate descended from 76.83 to 66.16% for initial NH_4^+-N concentration 173.88 mg/L as N, due to insufficient of anoxic period.

3.4. MLVSS, pH, Alkalinity, and DO Profiles in the SBR during Experiment. The pH and alkalinity values of a biological system are vital parameters for microbial denitrification. The value of pH increases for ammonification and denitrification, decreases for organic carbon oxidation and nitrification. Alkalinity is not only important for nitrification and denitrification, but to also be used for indicating the system stability.

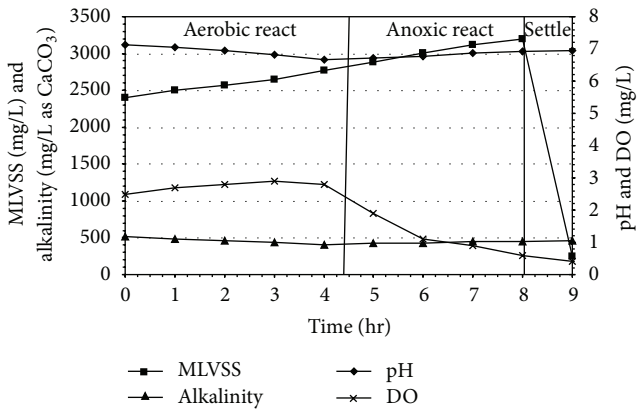

Figure 8: MLVSS, pH, alkalinity, and DO profiles for slaughterhouse wastewater treatment in SBR under (4+4) hr react period combination.

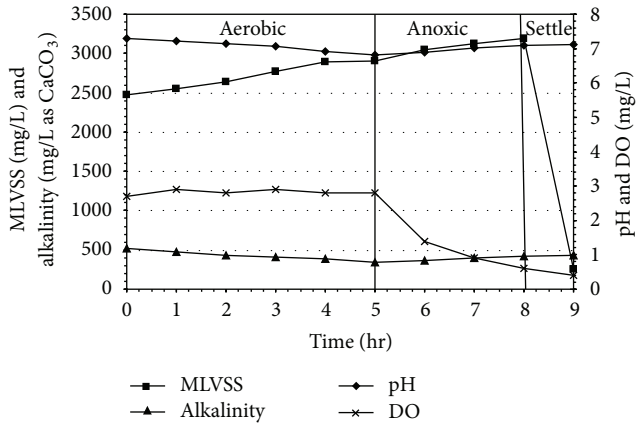

Figure 9: MLVSS, pH, alkalinity, and DO profiles for slaughterhouse wastewater treatment in SBR under (5+3) hr react period combination.

Alkalinity was found to have a close correlation with SBR operating conditions, since different extents of nitrification (alkalinity consumption) and denitrification (alkalinity production) contribute to the variation of alkalinity in the system. During the aerobic phase, the minimal value of the pH curve was characterized the end of nitrification (Figures 8, 9, and 10). At the beginning of anoxic react phase, when ammonia nitrogen concentration was reduced considerably, pH starts to increase. This has occurred between 4.0 and 5.0 hr after the starting of aerobic react period in all experimental sets. The DO profile exhibited a sharp fall after which DO concentration decreased markedly at anoxic phase and reached minimum value. In the present, study the DO level remained almost steady during the entire aerobic react period with a marginal increase in DO level, but a marked descending trend was observed during the anoxic period in all the reaction sets irrespective of initial SCOD and ammonia concentrations. Under strict anaerobic condition the DO should be equal to zero, but anoxic environment starts from DO level less than 1.5 mg/L. At the start of anoxic react period most of the cases, DO was found to be less than 1.5 mg/L and at the end of anoxic react period the value becomes less than 1.0 mg/L.

Table 3: Evaluation of biokinetic coefficients for carbon oxidation from slaughterhouse wastewater in SBR.

Initial SCOD (mg/L)	(4+4) hr react period combination	(5+3) hr react period combination	(3+5) hr react period combination	Standard values for kinetic constants [44]
1000 ± 50	(i) Substrate utilization- $y = 70.32x + 0.215$ (ii) Microbial growth- $y = 0.522x - 0.051$ *Kinetic constants*: k (day^{-1}) = 4.65 K_s (mg/L SCOD) = 327.06 Y (mg VSS/mg SCOD) = 0.522 k_d (day^{-1}) = 0.051	(i) Substrate utilization- $y = 68.22x + 0.187$ (ii) Microbial growth- $y = 0.622x - 0.057$ *Kinetic constants*: k (day^{-1}) = 5.34 K_s (mg/L SCOD) = 364.81 Y (mg VSS/mg SCOD) = 0.622 k_d (day^{-1}) = 0.057	(i) Substrate utilization- $y = 42.65x + 0.285$ (ii) Microbial growth- $y = 0.485x - 0.047$ *Kinetic constants*: k (day^{-1}) = 3.50 K_s (mg/L SCOD) = 149.64 Y (mg VSS/mg SCOD) = 0.485 k_d (day^{-1}) = 0.047	K (day^{-1}) = (2–10) K_s (mg/L SCOD) = (15–70) Y (mg VSS/mg SCOD) = (0.4–0.8) k_d (day^{-1}) = (0.025–0.075)

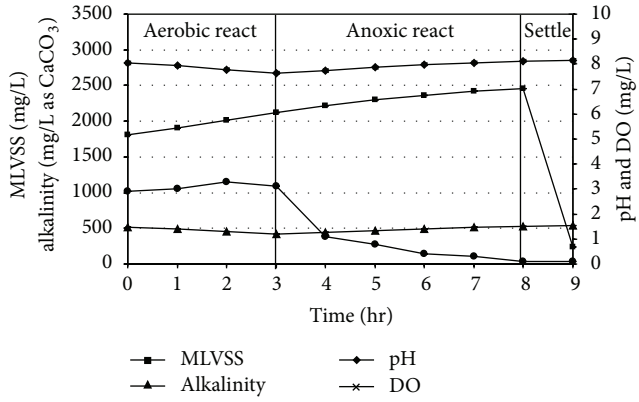

Figure 10: MLVSS, pH, alkalinity, and DO profiles for slaughterhouse wastewater treatment in SBR under (3+5) hr react period combination.

3.5. Kinetic Study for Organic Carbon Removal from Slaughterhouse Wastewater in SBR. In the present study, the performance evaluation of the SBR system was also carried out from the view point of reaction kinetics determination for treating slaughterhouse wastewater. The values for the reciprocal of specific substrate utilization rate ($1/U$) were plotted against the reciprocal of effluent SCOD ($1/S$) and substrate removal kinetics was evaluated using (1) as stated earlier. The slope of the straight line is (K_s/k) and intercept is ($1/k$). The reciprocal of the contact time ($1/\theta$) were plotted against the specific substrate utilization rate (U) and microbial growth kinetics was evaluated using (2). The yield coefficient (Y) was determined from the slope of the line and the endogenous decay coefficient (k_d) was obtained from intercept, $k_d = -C$. The values of biokinetic coefficients (k, K_s, Y, k_d) for combined carbon-oxidation and nitrification are listed in Table 3.

From Table 3, it has been estimated that the value of yield coefficient (Y) for the heterotrophs is in the range from 0.485 to 0.622. The yield coefficient was found to be improved with the increase in aeration period. The half velocity constant (K_s) values were found in the range of 149.64 to 364.81 for different combinations of react period. In the case of (5+3) combination of react cycle, the k and Y values are marginally higher than (4+4) and (3+5) combination. It was attributed to the fact that, after the initial acclimatization; the heterotrophs converted the carbon content at 5.0 hrs period of time more efficiently. After 5.0 hrs of aerobic react period, the available carbon content was reduced considerably and a fraction of heterotrophs attained endogenous state of condition while the nitrifiers are rejuvenated and started nitrification activity. This metabolism is also supported by the value of endogenous decay rate constant (k_d). In the case of (5+3) combination of react cycle k_d value is found to be 0.057 which is between 0.051 and 0.047 for the cases of (4+4) and (3+5) react period combinations, respectively. The values of biokinetic coefficients, other than K_s, such as k, Y, k_d as obtained from the test results for carbon-oxidation and nitrification are also in congruence with their respective typical values [44].

3.6. Kinetic Study for Ammonium Nitrogen Removal from Slaughterhouse Wastewater in SBR. The nitrification removal kinetics for mixed population (heterotrophs and nitrifiers) followed an identical pattern to organic carbon removal kinetics. A fraction of biological oxidation was attributed to the fact that a mixed population performed in the reactor along with nitrifiers. The linear graphs are plotted between ($1/S$) and ($1/U$) for substrate utilization kinetics under three different combinations of react period, namely, (4+4), (5+3), and (3+5), respectively, using (1). Microbial growth kinetics was evaluated using (2), which were determined by plotting straight lines between ($1/\theta$) and (U) under three different combinations of react period, namely, (4+4), (5+3) and (3+5) hrs, respectively. The kinetic coefficient values for nitrification from the previous plots are given in Table 4. It has been clearly shown earlier that an increasing trend of higher removal efficiency for ammonia oxidation could be observed for extension of the aerobic react period beyond 4 hrs. This previous phenomenon also reflected the magnitudes of biokinetic constants under all experimental combinations of react period. The kinetic coefficients Y, k_d, and K_s were found to be in the range of 0.205 to 0.284, 0.037 to 0.051, and 21.83 to 70.93, respectively. The ammonia concentration found in the slaughterhouse wastewater was very high 180 ± 10 mg/L as N for an inlet SCOD concentration of 1000 ± 50 mg/L, which are not usually present in any municipal wastewater stream. For this reason, the K_s value was found to be higher than the standard values (0.2–5.0 mg/L) considered for nitrification of municipal wastewater stream [44].

Table 4: Evaluation of biokinetic coefficients for nitrification from slaughterhouse wastewater in SBR.

Initial NH_4^+-N (mg/L as N)	(4+4) hr react period combination	(5+3) hr react period combination	(3+5) hr react period combination	Standard values for kinetic constants [44]
180 ± 10	(i) Substrate utilization- $y = 2.371x + 0.047$ (ii) Microbial growth- $y = 0.234x - 0.047$ k (day^{-1}) = 21.27 K_s (mg/L NH_4^+-N) = 50.44 Y (mg VSS/mg NH_4^+-N) = 0.234 k_d (day^{-1}) = 0.047	(i) Substrate utilization- $y = 2.412x + 0.034$ (ii) Microbial growth- $y = 0.284x - 0.051$ k (day^{-1}) = 29.41 K_s (mg/L NH_4^+-N) = 70.93 Y (mg VSS/mg NH_4^+-N) = 0.284 k_d (day^{-1}) = 0.051	(i) Substrate utilization- $y = 1.223x + 0.056$ (ii) Microbial growth- $y = 0.205x - 0.037$ k (day^{-1}) = 17.85 K_s (mg/L NH_4^+-N) = 21.83 Y (mg VSS/mg NH_4^+-N) = 0.205 k_d (day^{-1}) = 0.037	k (day^{-1}) = (1–30) K_s (mg/L NH_4^+-N) = (0.2–5.0) Y (mg VSS/mg NH_4^+-N) = (0.1–0.3) k_d (day^{-1}) = (0.03–0.06)

Table 5: Denitrification rates during anoxic react phase for treatment of slaughterhouse wastewater in SBR.

Initial NH_4^+-N (mg/L as N)	Initial SCOD (mg/L)	React period combination (Aerobic/Anoxic)	Avg. anoxic SCOD utilization rate (q_{SCOD}) (mg SCOD/gm MLVSS. hr)	Specific denitrification rate (q_{DN}) (mg N/gm MLVSS. hr)							
				1.0 hr	2.0 hr	3.0 hr	4.0 hr	5.0 hr	Avg. (3.0 hrly)	Avg. (4.0 hrly)	Avg. (5.0 hrly)
185.24	1028.55	(4+4)	26.25	4.49	5.57	5.85	3.89	—	5.30	4.95	—
173.88	1023.22	(5+3)	34.87	4.27	5.51	4.16	—	—	4.64	—	—
176.85	1042.52	(3+5)	38.15	4.57	5.55	6.16	7.24	6.23	5.42	5.88	5.95

3.7. Denitrification Rates for Treatment of Slaughterhouse Wastewater in SBR. Specific denitrification rate (q_{DN}) was measured in terms of the rate of NO_3^--N removed per unit mass of denitrifying microorganisms, for three different react period combinations, namely, (4+4), (5+3), and (3+5) under the respective anoxic environment and the results are listed in Table 5. The specific denitrification rate (q_{DN}) is expressed on average basis spanningover respective anoxic periods of 3.0, 4.0, and 5.0 hours. The average specific denitrification rate (q_{DN}), in (5+3), (4+4), and (3+5) cases was found to increase considerably with the increase in average anoxic SCOD utilization rate (q_{SCOD}) when primary treated effluent was considered for treatment in present SBR system. Average specific denitrification rate (q_{DN}) varied from 4.64 to 5.42 mg of N/gm MLVSS. hr for primary treated slaughterhouse wastewater for 3 hr anoxic period. The average 4.0 hourly specific denitrification rate (q_{DN}) varied from 4.95 to 5.88 mg of N/gm MLVSS. hr. The previous rate of specific denitrification rate (q_{DN}) was found to be followed in similar results as reported by Barnes and Bliss [45].

4. Conclusions

The present experimental investigation demonstrated that sequential batch reactor (SBR) is a variable and efficient biological method to treat slaughterhouse wastewater in a single unit. The total react period of 8 hr (4 hr aerobic and 4 hr anoxic) yielded optimum carbon oxidation, nitrification, and denitrification for treatment of carbonaceous and nitrogenous wastewater. The increase in MLVSS level in the reactor exhibited the growth favoring environment of the microorganism. The pH level in the SBR descended initially during aerobic period due to nitrification and carbon oxidation followed by an increasing trend indicating the existence of denitrifiers. This phenomenon has also been established by the variation of alkalinity level during aerobic and anoxic react period. The estimated values of biokinetic coefficients (k, K_s, Y, k_d) showed reasonable agreement with the literature values. The kinetic data and rate reaction constants could be used for the design of a field scale SBR for treating slaughterhouse wastewater. A design rationale can be evaluated on the basis of present experimental data for the purpose of application of this technology in similar plants. The outcome of the present investigation results would be helpful for making a design rationale for SBR treatment of slaughterhouse wastewater and a pilot plant study can be conducted with real-life wastewater sample by application of derived data of present study. In the future scope of the study, microbial genomics study including phosphate removal aspects would be also considered. The influence of solid retention time (SRT) should be explored also. A real-time kinetics profile with automatic data plotting could be derived for explaining the process in more rational way. It is also suggested that optimization of the process and operation variable may be examined with soft computing tools using various statistical approach.

Acknowledgment

This study was supported by the Research Funds of Jadavpur University, Jadavpur, Kolkata, India.

References

[1] A. O. Akinro, I. B. Ologunagba, and O. Yahaya, "Environmental implications of unhygienic operation of a city abattoir in Akure, Western Nigeria," *ARPN Journal of Engineering and Applied Sciences*, vol. 4, no. 9, pp. 311–315, 2009.

[2] V. P. Singh and S. Neelam, "A survey report on impact of abattoir activities management on environments," *Indian Journal of Veterinarians*, vol. 6, pp. 973–978, 2011.

[3] S. M. Gauri, "Treatment of wastewater from abattoirs before land application: a review," *Bioresource Technology*, vol. 97, no. 9, pp. 1119–1135, 2006.

[4] Y. O. Bello and D. T. A. Oyedemi, "Impact of abattoir activities and management in residential neighbourhoods: a case study of Ogbomoso, Nigeria," *Journal of Social Science*, vol. 19, pp. 121–127, 2009.

[5] D. Muhirwa, I. Nhapi, U. Wali, N. Banadda, J. Kashaigili, and R. Kimwaga, "Characterization of wastewater from an abattoir in Rwanda and the impact on downstream water quality," *International Journal of Ecology, Development*, vol. 16, no. 10, pp. 30–46, 2010.

[6] A. O. Aniebo, S. N. Wekhe, and I. C. Okoli, "Abattoir blood waste generation in rivers state and its environmental implications in the Niger Delta," *Toxicological and Environmental Chemistry*, vol. 91, no. 4, pp. 619–625, 2009.

[7] O. Chukwu, "Analysis of groundwater pollution from abattoir Waste in Minna, Nigeria," *Research Journal of Diary Science*, vol. 2, pp. 74–77, 2008.

[8] J. Grady, G. Daigger, and H. Lim, *Biological Wastewater Treatment*, Marcel Dekker, New York, NY, USA, 1999.

[9] I. Ruiz, M. C. Veiga, P. de Santiago, and R. Blfizquez, "Treatment of slaughterhouse wastewater in a UASB reactor and an anaerobic filter," *Bioresource Technology*, vol. 60, no. 3, pp. 251–258, 1997.

[10] D. I. Massé and L. Masse, "Treatment of slaughterhouse wastewater in anaerobic sequencing batch reactors," *Canadian Agricultural Engineering*, vol. 42, no. 3, pp. 131–137, 2000.

[11] K. Sombatsompop, A. Songpim, S. Reabroi, and P. Inkongngam, "A comparative study of sequencing batch reactor and movingbed sequencing batch reactor for piggery wastewater treatment," *Maejo International Journal of Science and Technology*, vol. 5, no. 2, pp. 191–203, 2011.

[12] Y. Rahimi, A. Torabian, N. Mehrdadi, and B. Shahmoradi, "Simultaneous nitrification-denitrification and phosphorus removal in a fixed bed sequencing batch reactor (FBSBR)," *Journal of Hazardous Materials*, vol. 185, no. 2-3, pp. 852–857, 2011.

[13] E. Bazrafshan, F. K. Mostafapour, M. Farzadkia, K. A. Ownagh, and A. H. Mahvi, "Slaughterhouse wastewater treatment by combined chemical coagulation and electrocoagulation process," *PLOS ONE*, vol. 7, no. 6, 2012.

[14] R. Rajakumar, T. Meenambal, P. M. Saravanan, and P. Ananthanarayanan, "Treatment of poultry slaughterhouse wastewater in hybrid upflow anaerobic sludge blanket reactor packed with pleated poly vinyl chloride rings," *Bioresource Technology*, vol. 103, no. 1, pp. 116–122, 2012.

[15] G. C. Sunder and S. Satyanarayan, "Efficient treatment of slaughter house wastewater by anaerobic hybrid reactor packed with special floating media," *International Journal of Chemical and Physical Sciences*, vol. 2, pp. 73–81, 2013.

[16] European Commission, *Integrated Pollution Prevention and Control: Reference Document on Best Available Techniques in the Slaughterhouses and Animal by-Products Industries*, 2005.

[17] A. H. Mahvi, "Sequencing batch reactor: a promising technology in wastewater treatment," *Iranian Journal of Environmental Health Science and Engineering*, vol. 5, no. 2, pp. 79–90, 2008.

[18] N. Z. Al-Mutairi, M. F. Hamoda, and I. A. Al-Ghusain, "Slaughterhouse wastewater treatment using date seeds as adsorbent," *Journal of Environment Science and Health*, vol. 55, pp. 678–710, 2007.

[19] R. Boopathy, C. Bonvillain, Q. Fontenot, and M. Kilgen, "Biological treatment of low-salinity shrimp aquaculture wastewater using sequencing batch reactor," *International Biodeterioration and Biodegradation*, vol. 59, no. 1, pp. 16–19, 2007.

[20] H. S. Kim, Y. K. Choung, S. J. Ahn, and H. S. Oh, "Enhancing nitrogen removal of piggery wastewater by membrane bioreactor combined with nitrification reactor," *Desalination*, vol. 223, no. 1–3, pp. 194–204, 2008.

[21] N. Z. Al-Mutairi, F. A. Al-Sharifi, and S. B. Al-Shammari, "Evaluation study of a slaughterhouse wastewater treatment plant including contact-assisted activated sludge and DAF," *Desalination*, vol. 225, no. 1–3, pp. 167–175, 2008.

[22] D. Roy, K. Hassan, and R. Boopathy, "Effect of carbon to nitrogen (C : N) ratio on nitrogen removal from shrimp production waste water using sequencing batch reactor," *Journal of Industrial Microbiology and Biotechnology*, vol. 37, no. 10, pp. 1105–1110, 2010.

[23] R. Rajagopal, N. Rousseau, N. Bernet, and F. Béline, "Combined anaerobic and activated sludge anoxic/oxic treatment for piggery wastewater," *Bioresource Technology*, vol. 102, no. 3, pp. 2185–2192, 2011.

[24] J. Palatsi, M. Vinas, M. Guivernau, B. Fernandez, and X. Flotats, "Anaerobic digestion of slaughterhouse waste: main process limitations and microbial community interactions," *Bioresource Technology*, vol. 102, no. 3, pp. 2219–2227, 2011.

[25] C. Kern and R. Boopathy, "Use of sequencing batch reactor in the treatment of shrimp aquaculture wastewater," *Journal of Water Sustainability*, vol. 2, no. 4, pp. 221–232, 2012.

[26] F. Wang, Y. Liu, J. Wang, Y. Zhang, and H. Yang, "Influence of growth manner on nitrifying bacterial communities and nitrification kinetics in three lab-scale bioreactors," *Journal of Industrial Microbiology and Biotechnology*, vol. 39, no. 4, pp. 595–604, 2012.

[27] D. Obaja, S. Mac, and J. Mata-Alvarez, "Biological nutrient removal by a sequencing batch reactor (SBR) using an internal organic carbon source in digested piggery wastewater," *Bioresource Technology*, vol. 96, no. 1, pp. 7–14, 2005.

[28] K. V. Lo and P. H. Liao, "A full-scale sequencing batch reactor system for swine wastewater treatment," *Journal of Environmental Science and Health*, vol. 42, no. 2, pp. 237–240, 2007.

[29] A. H. Mahvi, A. R. Mesdaghinia, and F. Karakani, "Nitrogen removal from wastewater in a continuous flow sequencing batch reactor," *Pakistan Journal of Biological Sciences*, vol. 7, no. 11, pp. 1880–1883, 2004.

[30] R. Lemaire, Z. Yuan, B. Nicolas, M. Marcelino, G. Yilmaz, and J. Keller, "A sequencing batch reactor system for high-level biological nitrogen and phosphorus removal from abattoir wastewater," *Biodegradation*, vol. 20, no. 3, pp. 339–350, 2009.

[31] S. Q. Aziz, H. A. Aziz, M. S. Yusoff, and M. J. K. Bashir, "Landfill leachate treatment using powdered activated carbon augmented sequencing batch reactor (SBR) process: optimization by response surface methodology," *Journal of Hazardous Materials*, vol. 189, no. 1-2, pp. 404–413, 2011.

[32] G. Durai, N. Rajamohan, C. Karthikeyan, and M. Rajasimman, "Kinetics studies on biological treatment of tannery wastewater using mixed culture," *International Journal of Chemical and Biological Engineering*, vol. 3, no. 2, pp. 105–109, 2010.

[33] M. Faouzi, M. Merzouki, and M. Benlemlih, "Contribution to optimize the biological treatment of synthetic tannery effluent by the sequencing batch reactor," *Journal of Materials and Environmental Science*, vol. 4, no. 4, pp. 532–541, 2013.

[34] S. Dey and S. Mukherjee, "Performance and kinetic evaluation of phenol biodegradation by mixed microbial culture in a batch reactor," *International Journal of Water Resources and Environmental Engineering*, vol. 2, no. 3, pp. 40–49, 2010.

[35] American Public Health Association, American Water Works Association, Water Pollution Control Federation, *Standard Methods for the Examination of Water and Wastewater*, American Water Works Association, Washington, DC, USA, 20th edition, 1998.

[36] H. Furumai, A. Kazmi, Y. Furuya, and K. Sasaki, "Modeling long term nutrient removal in a sequencing batch reactor," *Water Research*, vol. 33, no. 11, pp. 2708–2714, 1999.

[37] A. Tremblay, R. D. Tyagi, and R. Y. Surampalli, "Effect of SRT on nutrient removal in SBR system," *Practice Periodical of Hazardous, Toxic, and Radioactive Waste Management*, vol. 3, no. 4, pp. 183–190, 1999.

[38] A. W. Lawrence and P. L. McCarty, "Unified basis for biological treatment design and operation," *Journal of the Sanitary Engineering Division*, vol. 96, no. 3, pp. 757–778, 1970.

[39] J. P. Li, M. G. Healy, X. M. Zhan, and M. Rodgers, "Nutrient removal from slaughterhouse wastewater in an intermittently aerated sequencing batch reactor," *Bioresource Technology*, vol. 99, no. 16, pp. 7644–7650, 2008.

[40] P. Fongsatitkul, D. G. Wareham, P. Elefsiniotis, and P. Charoensuk, "Treatment of a slaughterhouse wastewater: effect of internal recycle rate on chemical oxygen demand, total Kjeldahl nitrogen and total phosphorus removal," *Environmental Technology*, vol. 32, no. 15, pp. 1755–1759, 2011.

[41] R. Kanimozhi and N. Vasudevan, "Effect of organic loading rate on the performance of aerobic SBR treating anaerobically digested distillery wastewater," *Clean Technologies and Environmental Policy*, vol. 15, pp. 511–528, 2013.

[42] D. Kulikowska and E. Klimiuk, "Removal of organics and nitrogen from municipal landfill leachate in two-stage SBR reactors," *Polish Journal of Environmental Studies*, vol. 13, no. 4, pp. 389–396, 2004.

[43] J. Doyle, S. Watts, D. Solley, and J. Keller, "Exceptionally high-rate nitrification in sequencing batch reactors treating high ammonia landfill leachate," *Water Science and Technology*, vol. 43, no. 3, pp. 315–322, 2001.

[44] Metcalf and Eddy Inc., *Wastewater Engineering Treatment Disposal Reuse*, Tata McGraw-Hill, 3rd edition, 1995.

[45] D. P. Barnes and P. J. Bliss, *Biological Control of Nitrogen in Wastewater Treatment*, E. & F.N. Spon, London, UK, 1983.

Hindawi Publishing Corporation
BioMed Research International
Volume 2013, Article ID 813519, 8 pages
http://dx.doi.org/10.1155/2013/813519

Research Article

Pesticide Residue Screening Using a Novel Artificial Neural Network Combined with a Bioelectric Cellular Biosensor

Konstantinos P. Ferentinos,[1] Costas P. Yialouris,[1] Petros Blouchos,[2] Georgia Moschopoulou,[2] and Spyridon Kintzios[2]

[1] *Laboratory of Informatics, School of Food Science, Biotechnology and Development, Agricultural University of Athens, Iera Odos 75, 11855 Athens, Greece*
[2] *Laboratory of Enzyme Technology, School of Food Science, Biotechnology and Development, Agricultural University of Athens, Iera Odos 75, 11855 Athens, Greece*

Correspondence should be addressed to Spyridon Kintzios; skin@aua.gr

Received 9 April 2013; Revised 12 June 2013; Accepted 3 July 2013

Academic Editor: Eldon R. Rene

We developed a novel artificial neural network (ANN) system able to detect and classify pesticide residues. The novel ANN is coupled, in a customized way, to a cellular biosensor operation based on the bioelectric recognition assay (BERA) and able to simultaneously assay eight samples in three minutes. The novel system was developed using the data (time series) of the electrophysiological responses of three different cultured cell lines against three different pesticide groups (carbamates, pyrethroids, and organophosphates). Using the novel system, we were able to classify correctly the presence of the investigated pesticide groups with an overall success rate of 83.6%. Considering that only 70,000–80,000 samples are annually tested in Europe with current conventional technologies (an extremely minor fraction of the actual screening needs), the system reported in the present study could contribute to a screening system milestone for the future landscape in food safety control.

1. Introduction

The contribution of quality tests of exported food and other agricultural commodities to the total food quality sector has a market value of 1.7 billion €. A major part of the initiative for reduced use of pesticides belongs to the food industry and retail trade. In particular, various business-to-business systems have been developed to certify the quality of Integrated Crop Management (ICM) products on a worldwide scale, some of them with considerable success (e.g., EUREPGAP in Europe) [1, 2]. Therefore, there is a vivid demand by the international food producers and industry for pesticide residue screening tools as proximal as possible to the production and processing sites. The issue of screening capacity, realized through rapid, cost-efficient, and high throughput pesticide residue testing, is an indispensable goal, especially considering the astonishingly low number of samples tested annually with conventional methods at certified laboratories all over Europe. The availability of a system providing growers, food companies, and distributors with the flexibility to routinely screen for a range of residues regularly in a cost effective way would allow the identification of remedial solutions quicker than is currently possible.

As one of currently major cellular biosensor technologies, the bioelectric recognition assay (BERA) utilizes live, functional cells in a gel matrix coupled with a sensor system able to measure changes in the cellular electric properties. Cells that are able to specifically interact with a target analyte produce a unique pattern of electrical potential as a result of their interaction with this analyte.

The BERA working principle has been already utilized for screening pesticide residues as target analytes (more specifically, carbamate and organophosphate pesticide residues in different food matrices [3, 4]). Although this system is sufficient for application by an expert user on a small, laboratory scale, it suffers from a drawback: the inevitable use of an empirical way (examining the biosensor's response data) to identify a pesticide in a sample. It would be highly desirable

Table 1: Composition of the different pesticide groups used for training the novel ANN (all pesticides were added at a concentration of 0.01 ppm).

Group	Target compounds	Concentration of active compound (%) in formulation	Commercial name	Manufacturer
Organophosphates	Acephate	75	Forten	VETERIN
	Azinphos methyl	25	Azin	AGROCHIMIKI
	Chlorpyrifos	48	Echo	MAKHTESHIM
	Chlorpyrifos methyl	22.5	Reldan	DOW
	Dimethoate	40	Perfekthion	BASF
	Malathion	50	Malathion	AVENTIS
	Methamidophos	50	Tabamor	AGROELLINIKI
	Pirimiphos methyl	50	Actellic	SYGENTA
	Profenofos	50	Selecron	SYGENTA
	Triazophos	42	Hostathion	AVENTIS
Carbamates	Carbendazim	25	Carbendazim	BAYER
	Carbofuran	10	Carbofuran	NITROFARM
	Phenmedipham + desmedipham	8 8	Record	ALFA
	Methiocarb	50	Mesurol	BAYER
	Methomyl	90	Dimethilin	K&N
	Oxamyl	10	Judo	FARMA-CHEM
	Iprodione	50	Rovral Aquaflo	BASF
	Propamocarb	53	Previcur Energy	BAYER
	Thiophanate methyl	70	Neotopsin	K&N
Pyrethroids	Abamectin	1.8	Rotam	ACARAMIC
	Cyfluthrin	5	Baythroid	DU PONT
	Cyhalothrin-lambda	10	Cyhalothrin	SYGENTA
	Cypermethrin	10	Assist	CERDE
	Deltamethrin	2.5	K-Othine	BAYER
	Fenpropathrin	10	Danitol	SUMITOMO
	Fenvalerate	30	Sumicidin	SUMITOMO
	Tau-fluvalinate	24	Mavrik	MAKHTESHIM

to avail over a pesticide classification software as a component of the biosensors, at the same time learning during use and therefore obtaining a better classification accuracy.

One option in this direction is the employment of computational models that try to approximate a function from sample data, such as artificial neural networks (ANNs) [5]. Having become popular with the development of the back-propagation training algorithm [6], their training includes a sufficient number of data to "learn" the process behind the production of these data. In the particular case of chemical and biological applications, characterized by highly nonlinear processes, the use of a variety of ANN methodologies has been proven to be very successful [7–10].

In the present study, we developed and trained a customized feedforward ANN [11] for the classification of three different pesticide groups (pyrethroids, carbamates, and organophosphates) detected by a cell-based biosensor operating on the BERA principle and combined with a high throughput measurement device. The novel system classified correctly the presence of the pesticide groups under detection with an overall success rate of 83.6%. The results of the application of the proposed ANN systems support the adoption of the novel classification methodology which can become a key component of an integrated high throughput, rapid, high capacity screening system for pesticide residues.

2. Experimental Setup

2.1. Materials. Mouse neuroblastoma (N2a), human neuroblastoma (SK-N-SH), and African green monkey kidney (Vero) cell cultures were originally provided from LGC promochem (UK). Standard pesticide solutions were prepared from commercial formulations purchased from various manufacturers (Table 1). Pesticide mixtures were prepared thereof daily in double distilled water. All other reagents were purchased from Fluka (Switzerland). Cells were cultured in Dulbecco's medium with 10% fetal bovine serum (FBS), 1 U μg^{-1} antibiotics (penicillin/streptomycin), and 2 mM L-glutamine. Cells were detached from the culture and concentrated by centrifugation (2 min, 1200 rpm, 25°C), at a density

of 2.5×10^6 mL^{-1}. During each assay (see below, Section 2.2) cells were used at a density of 1000 μL^{-1}.

2.2. Biosensor Principle. The biosensor was based on cellular biorecognition elements, which are natural targets of the pesticide groups under investigation. The first two cell lines (N2a, SK-N-SH), being neuronal, are natural targets of all three pesticide groups, due to the inhibition of either acetylcholine esterase (AChE) (organophosphates, carbamates) or ion channels (pyrethroids). Under control conditions (no pesticides present), when acetylcholine is added to the cells, it causes a temporary depolarization of the cell membrane (excitation), which is rapidly cancelled out by the specific cellular mechanisms. However, when pesticides are present, they inhibit these mechanisms (such as AChE), thus allowing for a continuous stimulation of the neural cells. This means that, when AChE/ion channels are inhibited by pesticide residues in the sample, addition of ACh will cause the excessive stimulation of N2a or SK-N-SH cells, which will further lead to membrane depolarization above a predetermined threshold [12].

As documented in previous studies [13, 14], the third cell line (Vero) also responds to the pesticides with a general toxicity response, which is acetylcholine-independent (i.e., no addition of acetylcholine is required).

Following an initial calibration of the biosensor system (analytical results are not shown here), the N2a, SK-N-SH, and Vero cell lines were identified as the optimal biorecognition elements for the pyrethroid, organophosphate, and carbamate pesticide groups, respectively.

2.3. Biosensor Device. A customized device was developed (Uniscan, Buxton, UK) in order to measure electric signals from the cellular biorecognition elements and allowing for high throughput screening and high speed of assay. The device is a portable potentiometer, having a replaceable guide bearing eight pairs of electrodes connecting on the underside. The system provides a connection interface to insert electrode strips directly into the instrument, utilizing one electrode strip per channel. Each electrode strip comprised a 0.5 mm thick ceramic substrate with three screen printed electrodes (working electrode—WE, reference electrode—RE, and counter electrode—CE). In order to facilitate high throughput screening, DRP-8X110 disposable sensor strips (WE: carbon, RE: Ag/AgCl) bearing eight electrode pairs (corresponding to eight measurement channels) were purchased from DropSens (Asturias, Spain) (Figure 1). Thus, the potentiometer, through its array of eight electrode pairs, received measurements from corresponding eight units of cellular biorecognition elements interacting with the assayed sample(s).

2.4. Creation of Pesticide Group Mixtures. The next step was to select the pesticides which composed the representative mixtures for each separate pesticide group. The basic criteria for the selection were the occurrence of residues of the respective pesticides as well as their commercial availability. After an extensive survey, we concluded the formulation

Figure 1: Details of biosensor device used for measuring cell-pesticide interactions. The eight-channel disposable sensor is connected to the potentiometer through a customized interface.

Table 2: Composition of control and positive sample sets.

MRL dilution	Control sample set	Positive sample set
0	60%	
MRL/20	20%	
MRL/10	20%	
MRL/2		50%
MRL		50%

presented in Table 1. This formulation is constructed in such way to include, within each group, pesticidal compounds which are representative (i) of actual compounds currently used in European agriculture and (ii) of different levels of solubility in water or polar solvents, since nonpolar solvents are not suitable for use with cellular biorecognition elements.

Within each pesticide group, and due to the fact that individual pesticides are associated with different maximum residue level (MRL) values, also depending on the food commodity under investigation, we decided to create the three different mixtures (corresponding to the three different pesticide groups) by adding pesticides at the concentration corresponding to the lowest MRL within each group. In this way, we secured that the biosensor would be developed on the principle of maximum sensitivity, in respect of the cumulative MRL of each group (actually 0.01 ppm for all groups).

Next, we created two types of sample sets (collections) for training the ANN. The first type of sample set was considered the control sample set, which contained pesticide-free samples as well as samples with pesticides at a cumulative concentration of MRL/20 and MRL/10 (i.e., too low). The second type of sample set was the positive sample set, which contained samples with pesticides at a cumulative concentration of MRL/2 and MRL. The relative composition of each MRL dilution in each sample set is presented in Table 2.

2.5. Assay Procedure. For screening the presence of a particular pesticide group, the corresponding cultured cells in suspension (see Section 2.2) were placed on the top of each of the eight carbon screen-printed electrodes contained in each disposable sensor strip (40 μL $\approx 40 \times 10^3$ cells) with the help of a multichannel automatic pipette (Figure 2). Next, the sample was added (pesticide mixture) (5 μL), followed by 5 μL Ach (10 mM).

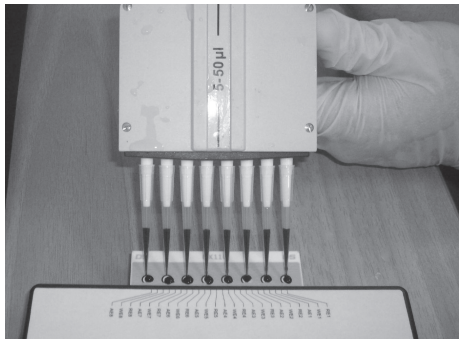

Figure 2: Pouring of cultured cells in suspension placed on the top of each of the eight carbon screen-printed electrodes contained in each disposable sensor strip.

The response of the cells to the different samples (control and positive sample sets from pesticide group) was recorded as a time series of potentiometric measurements (in Volts). The duration of each measurement was 180 sec, and 360 values/sample were recorded at a sampling rate of 2 Hz.

2.6. ANN Design and Training Process. Three main aspects of feedforward ANN modeling were considered for the development of the classification systems:

(i) network architecture (number of nodes in one or two hidden layers);

(ii) the type of backpropagation training algorithm:

(1) steepest-descent algorithm,
(2) quasi-Newton algorithm,
(3) Levenberg-Marquardt algorithm,
(4) Conjugate-gradient algorithm;

(iii) the type of activation function in the hidden nodes:

(1) logistic function,
(2) hyperbolic tangent (tanh) function.

Trial-and-error experimentations were conducted for the discovery of the best combinations of these parameters. Network weights were randomly initialized, thus several training trials were performed for each possible combination. The widely used methodology of cross-validation [11] was used for terminating the training process, so that overtraining was avoided, and good generalization capabilities were ensured. All training algorithms, ANN modeling and experimentations were implemented in MATLAB.

In addition to the trial-and-error approach for the design and parameterization of the ANN model, an evolutionary methodology that combines network design and parameterization with feature extraction from time series was also used (a detailed description of the system is presented in [15]). Its primary goal was to produce meta-data from the information contained in the original time-series, reduce the dimensionality of the input data space, and reduce the noise contained in the initial raw information. A genetic algorithm was used to normalize the initial information and discover the optimal design and parametrization of the ANN model. This evolutionary approach gave poorer results than the trial-and-error approach combined with the feature extraction technique presented.

2.6.1. Meta-Data Creation. Each time series of data consisted of 360 sequential measurements (see also Section 2.5). One way to feed time-series data into an ANN is to convert the information of the time-series data into more suitable meta-data. These meta-data must be much fewer than the number of data samples of each time-series and must capture, in the maximum possible degree, the characteristics of the time series data samples. After some experimentations with several statistical variables (e.g., minimum, maximum, mean, median, standard deviation, skewness) and ways of segmenting the time-series data, from each time series the following set of meta-data was extracted to be used as ANN inputs:

(i) mean and standard deviation of all 360 data samples;

(ii) mean and standard deviation of each quarter part of the data samples (data samples were divided into four equal-length segments);

(iii) minimum and maximum values of all data samples.

Thus, each time series of 360 measurements was converted into 12 single values.

2.6.2. Initial ANN System Development. As a first approach, we used only the 12 meta-data values as inputs of the ANN model. This approach was initially tested on the development of a classification model for the pesticides of the pyrethroid group. The available data were 450 time series (each containing 360 measurements), that is, 214 control time series (negative) and 236 MRL time series (positive). For each time series, the only available information was the existence or not of pesticide in the sample. These available time series were divided into training and testing sets. 30 random "control" time-series and 30 random "MRL" time series (i.e., 60 in total) constituted the testing set, leaving the rest 390 time-series to form the training set.

The ANN had one output, denoting the existence (value equal to 1) or not (value equal to 0) of the pesticides under question. The training was performed with the values 0 and 1, but the actual output of the network was a real value (normally, but necessarily, between the values of 0 and 1). During the testing of model, all values less than 0.5 were considered to be 0, and all values greater than or equal to 0.5 were considered to be 1.

Several trial-and-error experimentations were conducted, concerning the parameters mentioned before (network architecture, type of backpropagation algorithm, and type of activation functions). The best performance during these training experimentations was given by a 1-hidden-layer network with 10 hidden nodes and hyperbolic tangent activation functions, trained with the quasi-Newton minimization algorithm.

Table 3: Best ANN models for the pyrethroid group.

	Hidden layers/nodes	Activation functions (hidden nodes/output node)	Minimization algorithm in backpropagation algorithm
ANN-P1	1-HL/23	Logistic/linear summation	Levenberg-Marquardt
ANN-P2	2-HL/5, 15	Logistic/linear summation	Levenberg-Marquardt
ANN-P3	2-HL/10, 10	Logistic/linear summation	Levenberg-Marquardt

The ANN that gave the best results during the training and parameterization process described above was further trained for a larger number of training iterations. The performance of the final ANN system was evaluated on the testing data set. The correct classification rate was 70%.

2.6.3. Final ANN Systems Development. The correct classification rate of 70% was not considered satisfactory. Therefore, it was decided that additional information for each time series was necessary. For that reason, two additional parameters were recorded:

(i) the *age* of the cells (in days),

(ii) the *generation* number of the cells (four different generation values).

These two additional inputs were added to the 12 metadata inputs, so the final ANNs had in total 14 inputs.

3. Results

Following appropriate validation, the ANN architectures and minimization algorithms combinations that gave the best results during training were further trained and tuned, leading to the development of the final ANNs. These models were evaluated in specific testing data sets, that is, new data, different than those used during training. The analytical results for each pesticide group are presented.

3.1. ANN Models for the Pyrethroid Group. The available data were 809 time-series (each containing 360 measurements and the corresponding values of the two additional inputs). Specifically, they included 405 control time series (negative) and 404 positive time series. These available time series were divided into training and testing sets. Thirty random "control" time series and 30 random "positive" time series (i.e., 60 in total) constituted the testing set, leaving the rest 749 time series to form the training set.

Similarly to the initial models, the ANN had one output with values corresponding to the existence (1) or nonexistence (0) of pesticides of the pyrethroid group.

Again, several trial-and-error experimentations were conducted, concerning the usual parameters described before (network architecture, type of backpropagation algorithm, and type of activation functions). The parameters of the ANNs with the best performance during these training experimentations are presented in Table 3, while their corresponding performances on the testing data set are presented in Table 4. Their actual outputs on the testing set are shown in Figures 3, 4, and 5. The best ANN (*ANN-P3*) achieved an overall success rate equal to 86.7%. In comparison, the best ANN designed by the evolutionary approach described in Section 2.6 gave an overall success rate equal to 83%.

Table 4: Correct classifications for the pyrethroid group (number of samples and corresponding percentages) during the testing process of the ANNs.

	ANN-P1	*ANN-P2*	*ANN-P3*
Control (negative) sample set	28/30 (93.3%)	26/30 (86.7%)	27/30 (90.0%)
Positive sample set	23/30 (76.7%)	25/30 (83.3%)	25/30 (83.3%)
Overall	51/60 (85.0%)	51/60 (85.0%)	52/60 (86.7%)

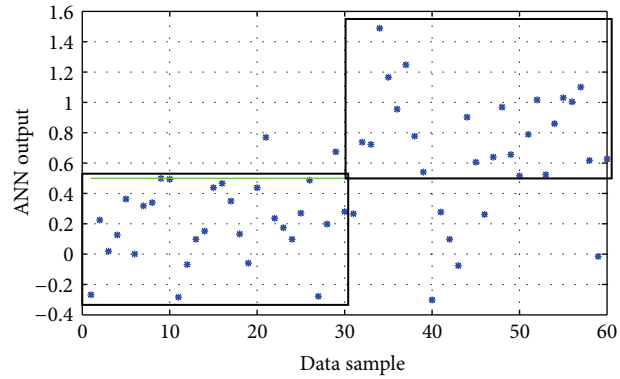

Figure 3: The actual output of *ANN-P1* model on the testing data of the pyrethroid group (the two black boxes represent the correct classification areas). Success rate: 85%.

3.2. ANN Models for the Organophosphate Group. The available data were 1206 time series (each containing 360 measurements and the corresponding values of the two additional inputs). Specifically, they included 506 control time series (negative) and 700 positive time series. These available time series were divided into training and testing sets. Fifty random "control" time series and 50 random "positive" time series (i.e., 100 in total) constituted the testing set, leaving the rest 1106 time-series to form the training set. The ANN had one output with values corresponding to the existence (1) or nonexistence (0) of pesticides of the organophosphates group.

The ANN with the best performance during these training experimentations was a 2-hidden-layer network with 4 and 19 nodes, respectively, and logistic activation functions (linear summation function in the output node), trained with the *Levenberg-Marquardt* backpropagation algorithm.

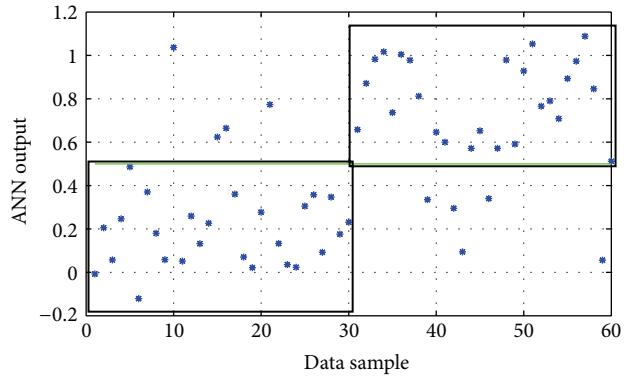

Figure 4: The actual output of *ANN-P2* model on the testing data of the pyrethroid group (the two black boxes represent the correct classification areas). Success rate: 85%.

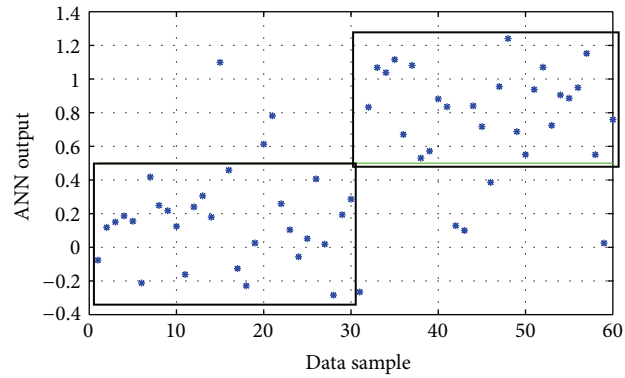

Figure 5: The actual output of *ANN-P3* model on the testing data of the pyrethroid group (the two black boxes represent the correct classification areas). Success rate: 86.7%.

Its evaluation on the testing data set gave a correct classification rate equal to 81% (Table 5). The actual output of the ANN on the testing set is shown in Figure 6. In comparison, the evolutionary-designed ANN gave a correct rate equal to 77%.

3.3. ANN Models for the Carbamate Group. The available data contained 1170 time series (each containing 360 measurements and the corresponding values of the two additional inputs). Specifically, they included 585 control time series (negative) and 585 positive time series. These available time series were divided into training and testing sets. Thirty random "control" time series and 30 random "positive" time series (i.e., 60 in total) constituted the testing set, leaving the rest 1110 time series to form the training set. Similarly to the other models, the ANN had one output with values corresponding to the existence (1) or nonexistence (0) of pesticides of the carbamates group.

The ANN with the best performance during these training experimentations was an *1-hidden-layer network* with 10 nodes and logistic activation functions (linear summation function in the output node), trained with the *Levenberg-Marquardt* backpropagation algorithm. Its evaluation on the testing data set gave a correct classification rate equal to 85% (Table 6). The actual output of the ANN on the testing set is shown in Figure 7. In comparison, the evolutionary-designed ANN gave a correct rate equal to 78%.

4. Discussion

Biosensors designed for performing food quality and toxicity analysis can have a significant social, economical and commercial impact. Such sensing units can be of invaluable use for both public authorities (such as custom offices) or private bodies (e.g., food production industry) for the "in situ" monitoring of food quality. Such units will provide reliable information on the food quality, eliminating dangers emerging from adulteration, chemical or biological contamination, improper storage conditions, and chemical residues.

Table 5: Correct classifications for the organophosphate group (number of samples and corresponding percentages) during the testing process of the ANNs.

	Correct classification
Control (negative) sample set	36/50 (72.0%)
Positive sample set	45/50 (90.0%)
Overall	81/100 (81.0%)

During the last years, several applications of multiclassifier systems have been developed. These have been particularly useful for the interpretation of data retrieved from biosensors, which are usually associated with difficult pattern recognition problems. For example, a multinet biosensor system for the detection of plant viruses was reported by Frossyniotis et al. [16]. Similar to the present study, the system was based on a BERA sensor. The results showed that the ANN approach performed better than empirical techniques. Another critical parameter in real-life applications, the corresponding time of the proposed classification system, was very competitive compared to the relatively long time required by an expert to make a decision by examining a data curve. Concerning the same end application, Glezakos et al. [17] used the evolutionary approach (see [15] for details) to produce meta-data from the information contained in the original time series, reduce the dimensionality of the input space and drastically decrease the noise contained in the initial raw information.

Over the last years, the use of ANN methodologies in combination with biosensor-based analytical methods is steadily increasing. Typical examples are ANNS used for the detection of glucose and sucrose [18], phenolic compounds [19–21], and neuroactive compounds [22]. In direct association with the present study, ANNs have been used in the biosensor-based determination of various insecticides, such as paraoxon (organophosphate) and carbofuran (carbamate) [23], as well as a series of organophosphate pesticides such as chlorpyrifos-oxon, chlorfenvinphos and azinphos-methyl oxon [24–26], dipterex, dichlorvos, and omethoate [27]. In this context, the novel system presented here allows, for

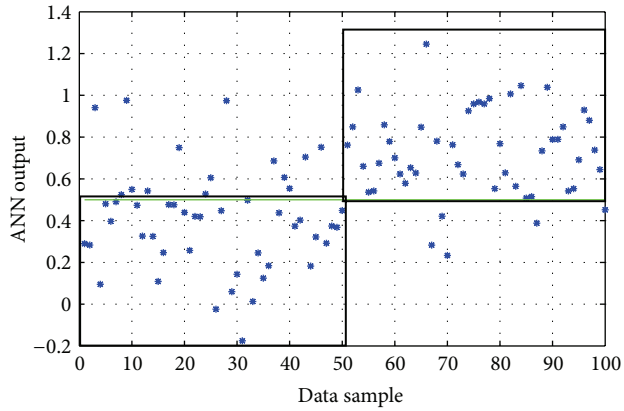

Figure 6: The actual output of the "2-HL/4, 19 nodes/logistic fun's" ANN model on the testing data of the organophosphates group (the two black boxes represent the correct classification areas). Success rate: 81%.

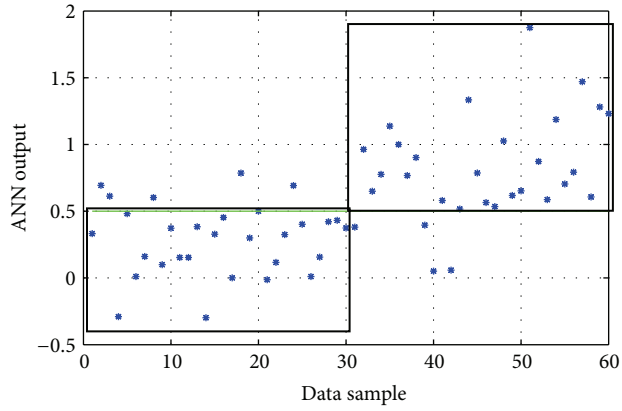

Figure 7: The actual output of the "1-HL/10 nodes/logistic fun's" ANN model on the testing data of the carbamates group (the two black boxes represent the correct classification areas). Success rate: 85%.

Table 6: Correct classifications for the carbamate group (number of samples and corresponding percentages) during the testing process of the ANNs.

	Correct classification
Control (negative) sample set	25/30 (83.3%)
Positive sample set	26/30 (86.7%)
Overall	51/60 (85.0%)

the first time, the successful discrimination among pesticides belonging to three different groups. In this way, it allows for a broader coverage of screened chemical residues than previously achieved. More importantly, perhaps, the novel ANN completes an advanced pesticide screening system in such way that it is fully operational and ready to use. The integrated biosensor platform described in this study has the additional advantage of rapid results (three minutes from sample input to classification report), which makes it attractive for routine use.

5. Conclusions

The present report is a demonstration of the classification properties of artificial neural networks, such that they can fully replace the traditional technique of empirical examination of biosensor's response data curve and therefore boosting the utilization potential of the coupled cellular bioelectric assay system. At this stage of development, the performance of the system is quite satisfactory, considering the noisy nature of the measurements and the biological factors involved in the entire process. It was shown that although the initial ANN system performed quite poorly it was radically improved by the inclusion of additional biological factors (age of the cells and their generation number). Obviously, the system can be further improved, but the improvement of the assay principle that would lead to better and more accurate measurements is necessary. The basic scope of the current work was to validate, with real measurements, the viability of the proposed system at different matrix environments.

The reliability of the novel system is safeguarded due to the use of different cell lines as biorecognition elements, all of which are targets of the screen pesticide groups, as well as the large number of time series used for training. The spectrum of detected substances can be increased by adding other cell lines with differential susceptibility to pesticides. In addition, we envisage that, either by enriching the composition of test (control and positive) sample sets with more pesticide compounds or by creating sample sets for other pesticide groups and then proceed with ANN training, end-users will be able to use the integrated biosensor system for screening essentially all types of residues in food commodities. This is particularly important considering that currently only 70,000–80,000 samples are annually tested in Europe, an extremely minor fraction of the actual screening needs. Therefore, we feel that the present report could contribute to a screening system milestone for the future landscape in food safety control. We currently conduct a series of tests with real samples in order to validate the performance of the system at different food matrix environments.

Abbreviations

ANN: Artificial neural network
BERA: Bioelectric recognition assay
MRL: Maximum residue level
PBS: Phosphate buffer saline.

Conflict of Interests

The authors certify that there is no conflict of interests with any financial organization regarding the material discussed in the paper.

Acknowledgment

The research was financially supported by the European Union FP7 Research for SMEs Project FOODSCAN

"Development of an automated, novel biosensor platform for pesticide residue detection" (no. 286442).

References

[1] Eurostat, *Agricultural Statistics: Main Results 2009-2010*, Luxemburg, 2011.

[2] FiBL/IFOAM, Data Tables on Organic Horticulture Worldwide 2006–2010: Development, crop categories, country data, Frick, 2012.

[3] S. Mavrikou, K. Flampouri, G. Moschopoulou, O. Mangana, A. Michaelides, and S. Kintzios, "Assessment of organophosphate and carbamate pesticide residues in cigarette tobacco with a novel cell biosensor," *Sensors*, vol. 8, no. 4, pp. 2818–2832, 2008.

[4] K. Flampouri, S. Mavrikou, S. Kintzios, G. Miliadis, and P. Aplada-Sarlis, "Development and validation of a cellular biosensor detecting pesticide residues in tomatoes," *Talanta*, vol. 80, no. 5, pp. 1799–1804, 2010.

[5] S. I. Gallant, *Neural Network Learning and Expert Systems*, The MIT Press, Cambridge, Mass, USA, 1993.

[6] D. E. Rumelhart, G. E. Hinton, and R. J. Williams, "Learning representations by back-propagating errors," *Nature*, vol. 323, no. 6088, pp. 533–536, 1986.

[7] I. Seginer, T. Boulard, and B. J. Bailey, "Neural network models of the greenhouse climate," *Journal of Agricultural Engineering Research*, vol. 59, no. 3, pp. 203–216, 1994.

[8] R. Lacroix, F. Salehi, X. Z. Yang, and K. M. Wade, "Effects of data preprocessing on the performance of artificial neural networks for dairy yield prediction and cow culling classification," *Transactions of the American Society of Agricultural Engineers*, vol. 40, no. 3, pp. 839–846, 1997.

[9] K. P. Ferentinos and L. D. Albright, "Predictive neural network modeling of pH and electrical conductivity in deep-trough hydroponics," *Transactions of the American Society of Agricultural Engineers*, vol. 45, no. 6, pp. 2007–2015, 2002.

[10] K. P. Ferentinos, "Biological engineering applications of feedforward neural networks designed and parameterized by genetic algorithms," *Neural Networks*, vol. 18, no. 7, pp. 934–950, 2005.

[11] T. L. Fine, *Feedforward Neural Network Methodology*, Springer, New York, NY, USA, 1999.

[12] M. Marinovich, B. Viviani, V. Capra et al., "Facilitation of acetylcholine signaling by the dithiocarbamate fungicide propineb," *Chemical Research in Toxicology*, vol. 15, no. 1, pp. 26–32, 2002.

[13] P. A. Davies, W. Wang, T. G. Hales, and E. F. Kirkness, "A novel class of ligand-gated ion channel is activated by Zn^{2+}," *The Journal of Biological Chemistry*, vol. 278, no. 2, pp. 712–717, 2003.

[14] T. Houtani, Y. Munemoto, M. Kase, S. Sakuma, T. Tsutsumi, and T. Sugimoto, "Cloning and expression of ligand-gated ion-channel receptor L2 in central nervous system," *Biochemical and Biophysical Research Communications*, vol. 335, no. 2, pp. 277–285, 2005.

[15] T. J. Glezakos, T. A. Tsiligiridis, and C. P. Yialouris, "Piecewise evolutionary segmentation for feature extraction in time series models," *Neural Computing and Applications*, 2012.

[16] D. Frossyniotis, Y. Anthopoulos, S. Kintzios, A. Perdikaris, and C. P. Yialouris, "A multisensor fusion system for the detection of plant viruses by combining artificial neural networks," in *Artificial Neural Networks*, vol. 4132 of *Lectures notes in Computer Science*, pp. 401–409, 2006.

[17] T. J. Glezakos, G. Moschopoulou, T. A. Tsiligiridis, S. Kintzios, and C. P. Yialouris, "Plant virus identification based on neural networks with evolutionary preprocessing," *Computers and Electronics in Agriculture*, vol. 70, no. 2, pp. 263–275, 2010.

[18] L. S. Ferreira, M. B. de Souza Jr., and R. O. M. Folly, "Development of an alcohol fermentation control system based on biosensor measurements interpreted by neural networks," *Sensors and Actuators B*, vol. 75, no. 3, pp. 166–171, 2001.

[19] A. Gutés, F. Céspedes, S. Alegret, and M. del Valle, "Determination of phenolic compounds by a polyphenol oxidase amperometric biosensor and artificial neural network analysis," *Biosensors and Bioelectronics*, vol. 20, no. 8, pp. 1668–1673, 2005.

[20] J. Abdullah, M. Ahmad, L. Yook Heng, N. Karuppiah, and H. Sidek, "Evaluation of an optical phenolic biosensor signal employing artificial neural networks," *Sensors and Actuators B*, vol. 134, no. 2, pp. 959–965, 2008.

[21] J. S. Torrecilla, M. L. Mena, P. Yáñez-Sedeño, and J. García, "Field determination of phenolic compounds in olive oil mill wastewater by artificial neural network," *Biochemical Engineering Journal*, vol. 38, no. 2, pp. 171–179, 2008.

[22] C. Ziegler, A. Harsch, and W. Göpel, "Natural neural networks for quantitative sensing of neurochemicals: an artificial neural network analysis," *Sensors and Actuators B*, vol. 65, no. 1, pp. 160–162, 2000.

[23] T. T. Bachmann and R. D. Schmid, "A disposable multielectrode biosensor for rapid simultaneous detection of the insecticides paraoxon and carbofuran at high resolution," *Analytica Chimica Acta*, vol. 401, no. 1-2, pp. 95–103, 1999.

[24] G. A. Alonso, G. Istamboulie, T. Noguer, J.-L. Marty, and R. Muñoz, "Rapid determination of pesticide mixtures using disposable biosensors based on genetically modified enzymes and artificial neural networks," *Sensors and Actuators B*, vol. 164, no. 1, pp. 22–28, 2012.

[25] G. A. Alonso, G. Istamboulie, A. Ramirez-Garcia, T. Noguer, J.-L. Marty, and R. Muñoz, "Artificial neural network implementation in single low-cost chip for the detection of insecticides by modeling of screen-printed enzymatic sensors response," *Computers and Electronics in Agriculture*, vol. 74, no. 2, pp. 223–229, 2010.

[26] G. Istamboulie, M. Cortina-Puig, J.-L. Marty, and T. Noguer, "The use of artificial neural networks for the selective detection of two organophosphate insecticides: chlorpyrifos and chlorfenvinfos," *Talanta*, vol. 79, no. 2, pp. 507–511, 2009.

[27] B. Li, Y. He, and C. Xu, "Simultaneous determination of three organophosphorus pesticides residues in vegetables using continuous-flow chemiluminescence with artificial neural network calibration," *Talanta*, vol. 72, no. 1, pp. 223–230, 2007.

Hindawi Publishing Corporation
BioMed Research International
Volume 2013, Article ID 165198, 9 pages
http://dx.doi.org/10.1155/2013/165198

Research Article

Rhizobium pongamiae sp. nov. from Root Nodules of *Pongamia pinnata*

Vigya Kesari, Aadi Moolam Ramesh, and Latha Rangan

Department of Biotechnology, Indian Institute of Technology Guwahati, Assam 781 039, India

Correspondence should be addressed to Latha Rangan; latha_rangan@yahoo.com

Received 27 April 2013; Accepted 6 June 2013

Academic Editor: Eldon R. Rene

Pongamia pinnata has an added advantage of N2-fixing ability and tolerance to stress conditions as compared with other biodiesel crops. It harbours "rhizobia" as an endophytic bacterial community on its root nodules. A gram-negative, nonmotile, fast-growing, rod-shaped, bacterial strain VKLR-01^T was isolated from root nodules of *Pongamia* that grew optimal at 28°C, pH 7.0 in presence of 2% NaCl. Isolate VKLR-01 exhibits higher tolerance to the prevailing adverse conditions, for example, salt stress, elevated temperatures and alkalinity. Strain VKLR-01^T has the major cellular fatty acid as $C_{18:1}$ ω7c (65.92%). Strain VKLR-01^T was found to be a nitrogen fixer using the acetylene reduction assay and PCR detection of a *nif*H gene. On the basis of phenotypic, phylogenetic distinctiveness and molecular data (16S rRNA, *rec*A, and *atp*D gene sequences, G + C content, DNA-DNA hybridization etc.), strain VKLR-01^T = (MTCC 10513^T = MSCL 1015^T) is considered to represent a novel species of the genus *Rhizobium* for which the name *Rhizobium pongamiae* sp. nov. is proposed. *Rhizobium pongamiae* may possess specific traits that can be transferred to other rhizobia through biotechnological tools and can be directly used as inoculants for reclamation of wasteland; hence, they are very important from both economic and environmental prospects.

1. Introduction

Pongamia pinnata (L.) Pierre is a nonedible "pioneer" biodiesel and medicinal tree species of the family Leguminosae that grows in multiple geoclimatic conditions, ranging from humid, tropical, subtropical regions to cooler and semiarid zones [1–3]. Nitrogen is an important nutrient for plant growth and yield; however, its availability in soils is limited. Modern agriculture depends on chemically synthesized N fertilizers which are expensive and require fossil fuels for production, adding to greenhouse gas emissions. Biological nitrogen fixation is a useful and important alternative [4], especially in biofuel production [2, 5]. *Pongamia* can grow on low-fertility land due to its nodulation properties and good N_2-fixing symbiotic associations with "rhizobia" (a polyphyletic assemblage of alphaproteobacteria family: *Rhizobiaceae*), thus minimizing competition with food crops or related fertilizer, water, and land resources needed for food and fodder production [6]. The sustainable production of plant oils for biodiesel production from a tree crop such as *P. pinnata*, which can be cultivated on marginal lands, has the potential to not only provide a renewable energy resource but in addition alleviate the competitive situation that exists with food crops as biofuels and associated arable land and water use. It is also used in agriculture and environmental management, due to its insecticidal and nematicidal properties [7]. Finally, *Pongamia* has been identified as a resource for agroforestry, urban landscaping to suspend the pollutants and the bioameloriation of degraded lands.

Isolation and identification of authentic and effective rhizobia isolates are required to support *P. pinnata* plantations in nitrogen-poor soils. *Pongamia* trees are purportedly able to grow in a wide range of environments: in the tropics, with temperatures from 13–45°C, saline soils, and in soils with a range of pH including sodic soils, and they are an ideal candidate for reforestation of marginal lands [3, 5]. The ability of rhizobia to grow in these diverse environmental conditions will be important for the establishment and success of *Pongamia* plantations on these unfertile lands. It, thus, satisfies all "sustainability criteria" expected from modern

second- and third-generation biofuel crops. However, little attention has been paid to the occurrence of nitrogen-fixing endophytic bacteria in the rhizospheres of this biodiesel tree which is important for their diverse applicabilities as well as agronomic and ecological significances. In preliminary studies, the effective nodulations of *P. pinnata* with three strains of rhizobia (*Bradyrhizobium japonicum* strain CB1809, *Bradyrhizobium sp.* strain CB564, and *Rhizobia sp.* strain NGR234) were demonstrated [1].

The importance of characterizing indigenous rhizobia of *Pongamia* cannot be overemphasized. Still there has not been any detailed study of phenotypic characteristics and symbiotic effectiveness of rhizobia isolates which naturally nodulate *Pongamia* considering its potential value in sustainable agriculture and role in agroforestry. Therefore, in this work, we attempt to isolate the nitrogen-fixing rhizobial symbiont strain from nodules of *P. pinnata* occurring in North Guwahati, Assam, India. The objectives were to determine the exact taxonomic position of isolated and identified strain by using a polyphasic characterization that included determination of phenotypic and biochemical properties, phylogenetic investigations based on 16S rRNA, *atp*D, and *rec*A gene sequences, and genetic analysis. Further investigations were also performed in order to verify the nodulation and nitrogen-fixing property of the isolated bacterium strain.

2. Materials and Methods

2.1. Soil Sampling and Isolation of Rhizobia. *P. pinnata* saplings approximately 2-3 months old found in North Guwahati (26°14′6″ N; 91°41′28″ E), Assam, India, were uprooted during April 2010 containing distinct nodules. Nodules excised from the roots were surface sterilized with 70% (v/v) ethanol for 1 min. Subsequently, nodules were treated with 10% (w/v) sodium hypochlorite for 15 min and washed with sterile distilled water (3x). Single surface-sterilized nodule (approximately 2 mm) was opened into two halves with a sterile blade, and the central parts of the nodule were scooped with blunt needle, macerated, and diluted in 500 μL of saline water (0.9%). Roughly 100 μL of the inoculum was spread on yeast extract-mannitol (YEM) and tryptone-yeast extract (TYE) agar plates and incubated at 28°C for 1–3 days. The purity of the culture was verified by repeated streaking of single colony onto YEM agar [8] with 25 mg Kg^{-1} (w/v) congo red. Single purified isolate was maintained in YEM broth containing 20% (v/v) glycerol at −80°C.

2.2. Growth and Phenotypic Characteristics. Cell size and morphology of the root nodule isolate were determined using scanning electron microscopy (LEO 1430 VP; Leo Electron Microscopy, Ltd., Cambridge, the UK) at 10 kV. For the micromorphology study, cells from the exponential growth phase (grown in YEM broth at 28°C) were harvested by centrifugation and fixed in 2.5% (w/v) glutaraldehyde for 45 min. The cells were washed with phosphate-buffered saline (PBS) and applied to ethanol dehydration series (at 50%, 70%, 90%, and 100% for 10 min each) (v/v) followed by critical-point drying with CO_2 and sputter-coating with gold as described by Boyde and Wood [15]. A growth characteristic of isolate was recorded at different temperatures (4, 25, 28, 30, 37, 42, and 50°C) in YEM broth and agar until 48 h of culture. The ability to grow in acid and alkaline media was also tested by inoculating the isolate onto YEM broth and YEM agar plates adjusted to various pH values (pH 4.0–11.0 at intervals of 1 pH units) using 1 N HCl/1 N NaOH. The NaCl tolerance of the isolate was tested by growing in YEM broth and YEM agar plates containing 0%, 1%, 2%, 3%, 4%, and 5% (w/v) NaCl.

2.3. Gram Staining: Biochemical and Physiological Characteristic. Gram reaction was determined with the bioMérieux Gram-stain kit according to the manufacturer instructions. Acid production from different carbohydrates was determined by employing the API 50 CH system (bioMérieux) according to the manufacturers instructions. The ability of the isolate to utilize various carbon and amino acids compounds as sole carbon and nitrogen source was investigated using the method described by Lindström and Lehtomäki [16]. Def 9 (carbon source) and Def 8 (nitrogen source) agar mediums were used, and appropriate controls were maintained. Results were noted after 3 days of incubation at 28°C. A set of physiological characteristics including catalase and oxidase tests and nitrate reduction were assessed using protocols described by Shieh et al. [17]. Gelatin hydrolysis and methyl red test were also performed using the methods of Smibert and Krieg [18]. The intrinsic antibiotic resistance tests for the isolate were performed by disc-diffusion assay in YEM agar against 16 different antibiotics (Discs, HiMedia) of concentrations ranging from 2 to 100 μg. Cell biomass for the analysis of isoprenoid quinones was obtained from the isolate grown on yeast extract-mannitol broth (YEM) (12 h, 28°C, 180 rpm).

2.4. FAME Analysis. Fatty acid methyl esters (FAMEs) of the isolate were extracted and prepared according to the standard protocol of the MIDI Sherlock/Hewlett Packard Microbial Identification System as described by Sasser [19]. For cellular FAME analysis, isolate was grown on trypticase soy broth agar (TSBA), which consists of 30 g trypticase soy broth and 15 g of agar (BBL) for 12 h at 28°C under aerobic conditions (180 rpm). The fatty acid methyl esters extracts were analyzed by Gas Chromatography MODEL 6850 (Agilent Gas Chromatography) equipped with an Agilent ultra 2 capillary column.

2.5. DNA Extraction, PCR Amplification, and Sequencing. Cell biomass for DNA extraction was obtained from the isolate grown on yeast extract-mannitol (YEM) broth (12 h, 28°C, 180 rpm). Chromosomal DNA was isolated and purified using Sigma's GenElute Bacterial Genomic Kit. The 16S rRNA gene was amplified by PCR using two consensus primer fD1 and rD1 [20]. Polymerase chain reaction (PCR) of 16S rRNA gene was performed in 25 μL volume mixing the template DNA (10 ng) with 1x PCR buffer (Bioline), 2.5 mM $MgCl_2$ (Bioline), 0.5 U *Taq* DNA polymerase (Bioline), 2.5 mM dNTPs each, 0.4 μM (each) primers fDl and rDl using a DNA thermal cycler (Applied Biosystems, USA). The following temperature profile was

used for DNA amplification: an initial denaturation at 95°C for 5 min followed by 35 cycles of 94°C for 1 min, 55°C for 1 min, and 72°C for 2 min and a final extension step of 72°C for 10 min. Reaction products were electrophoresed on a 1.3% (w/v) agarose gel and were purified using a Qiaquick PCR purification kit (Qiagen) before sequencing. Sequencing reactions were performed using the ABI PRISM Dye Terminator Cycle Sequencing Kit (Applied Biosystems, USA) with the primers IRF1, 1050R, 800F, and 800R [21], and they were analyzed in an automatic sequencer ABI PRISM 3730 sequencer (Applied Biosystems). PCR amplifications of other housekeeping genes *rec*A and *atp*D were performed under the conditions described by Yoon et al. [9]. The primer sequences that were used for amplification and sequencing of 16S rRNA, *rec*A, and *atp*D genes are listed in (Supplementary Table 1; see Supplementary Material available online at http://dx.doi.org/10.1155/2013/165198.) The sequences of these genes were compared with the sequences available from GenBank using BLASTN program [22] and were aligned using ClustalW2 multiple sequence alignment [23]. Phylogenetic trees were inferred using the neighbor-joining method [24], and distances were determined according to the Kimura-2 model [25]. Bootstrap analysis was based on 1000 resamplings. The MEGA 4.0 version [26] was used for all analyses.

2.6. Nitrogen Fixation and Nodulation Assessment Test. The acetylene reduction assay (ARA) was used to test the isolate for potential nitrogen fixations. The amount of ethylene produced was measured using 10% (v/v) acetylene according to the method of Li and MacRae [27] using a Hewlett Packard 4890 GC equipped with a Porapak N column. Isolate was subjected to *nif* H-specific PCR amplification using the primers (Supplementary Table 1) of Poly et al. [28]. Nodulation test for isolate was performed by PCR amplification of *nod*D gene (Supplementary Table 1) as described by Yoon et al. [9].

2.7. DNA Hybridization and G + C Content. The DNA G + C content was determined as described by Tamaoka and Komagata [29]. Isolate was disrupted using a French pressure cell (ThermoSpectronic), and the DNA in the crude lysate was purified by chromatography on hydroxyapatite as described by Cashion et al. [30]. DNA was hydrolyzed, dephosphorylated, and analyzed for its G + C content by HPLC [31]. Nonmethylated Lambda DNA (Sigma) was used as a reference. DNA-DNA hybridization was assessed for isolate against reference strain *Rhizobium radiobacter* DSM 30147^T (= AB247615) that showed 97% sequence similarity. DNA-DNA hybridization was carried out as described by De Ley et al. [32] under consideration of the modifications described by Huss et al. [33] using a model Cary 100 Bio UV/VIS spectrophotometer equipped with Peltier-thermostatted 6 × 6 multicell changer and a temperature controller with *in situ* temperature probe (Varian). The highest and lowest values obtained were excluded, and the means of the duplicates were quoted as DNA-DNA relatedness values. Analysis of respiratory quinones was carried out by the Identification Service and Dr. Brian Tindall, DSMZ, Braunschweig, Germany, according to the method of Komagata and Suzuki [34].

3. Results and Discussion

Since *P. pinnata* is introduced as the most important multipurpose tree for biodiesel production, it has become the most widespread legume in India and other parts of the world. This predominance has resulted from the massive implantation of the species for multipurpose use in a broad edaphic range including urban and social forestries to alleviate the environmental imbalance. The community structure of *Pongamia* root-nodule bacteria has been addressed by a few studies that assessed nodulation ability by endogenous rhizobia and also few strains commonly associated with *Glycine max* and their stimulatory effect on nodule number and plant growth [1, 35]. In this present study, we extend the work on *Pongamia* root-nodulating bacteria to isolate and characterize the novel *Rhizobium* species with traits that make it competitive in stress environments from the root nodules of biodiesel crop *P. pinnata* from North Guwahati, Assam, India.

3.1. Trapping and Isolating Root-Nodulating Bacteria. Root nodules were observed in all of the *Pongamia* saplings uprooted from the sampling site, indicating that root nodules occur widely in this legume crop growing naturally in North Guwahati, Assam, India. The plants, however, varied in the extent to which they were nodulated as nodules varied in shapes and sizes formed on primary as well as secondary roots (Supplementary Figure 1). Different shapes of root nodules of *P. pinnata* observed in the present study may be related to different developmental phases of the nodule ontogeny, and it is, therefore, not surprising that the nodule morphology has been used as a taxonomic marker [36]. Phenotypic traits of *Pongamia* saplings, namely, mean shoot length, mean root length, and the number of nodules observed in *P. pinnata,* were 28.25 ± 3.24, 12.17 ± 2.19, and 9.90 ± 2.31, respectively. Transverse section of single nodule (approximately 20 μm thick) in SEM image revealed the absence of any visible bacteria in the outer wall portion of the nodule. But when the middle portion was focused, each cell was fully filled with rod-shaped bacteria (Supplementary Figures 2A and 2B). Therefore, the middle portion of the root nodule was further used for isolation of single pure bacterial colony specific to *P. pinnata* and named as VKLR-01.

3.2. Growth, Phenotypic, Biochemical and Physiological Characteristics of Isolate. The first visible growth of the bacterium was observed as a small white shiny dot-like structure which increased in size from 1.5–3.5 mm (24 h) to 4.0–5.5 mm (48 h) in both YEM and TYE plates at 28°C (Supplementary Figure 3A). The generation time noted was 0.67 h in YEM medium. Pure culture was obtained from individual colony designated as VKLR-01. Isolate VKLR-01 showed creamy or white opaque, round or convex, and gummy colonies, with little or moderate extracellular polysaccharide production (EPS) having a diameter of 1.5–3.5 mm after growth for 24 h at 28°C. Metabolism is strictly aerobic. Isolate VKLR-01 appears to be a fast-growing rhizobial strain, forming colonies of 4–5.5 mm in diameter in 2-day time. Existing reports show that trees are as often nodulated by fast-growing as by slow-growing rhizobia [37].

Table 1: Phenotypic characteristics of *Rhizobium pongamiae* VKLR-01^T and type strains of phylogenetically related *Rhizobium* species.

Characteristic	1	2	3	4
Origin	Root nodule of *P. pinnata* (North Guwahati, Assam)	*Galega orientalis* (Finland)	ND	*Ficus benjamina* (Florida)
Cell morphology (μm)	Rods (0.4–0.5 × 1.4–1.6)	Rods (0.9–1.0 × 1.5–1.8)[a]	Rods (0.6–1 × 1.5–3.0)	Rods
Flagella	ND	1-2	Several, peritrichous	Several, peritrichous
Nodulation	+	+	−	−
pH range	6–11	5.0–9.5[a]	ND	ND
Growth at/in				
40°C	+	−	ND	−
1% NaCl	+	+	+	+
2% NaCl	+	−	+	+
4% NaCl	+	−	−	−
Utilization as carbon source				
Sucrose	+	+	ND	ND
Arabinose	−	+	+	ND
Mannitol	+	+	+	ND
Lactose	+	−	ND	ND
Glucose	−	+	ND	ND
Maltose	+	ND	+	+
Melibiose	+	+	+	ND

Strains: 1, *R. pongamiae* VKLR-01^T (present study); 2, *R. galegae* LMG 6214^T 3; 3, *A. tumefaciens* (biovar 1); 4, *R. larrymoorei* AF3-10^T [9–12]. [a]Unpublished data of Wang et al. (personal communication) [13]. +: positive; −: negative; ND: data not available. All strains are Gram negative, aerobic, rod shaped, and nonspore forming. All 7 strains are positive for oxidase, catalase, and nitrate reductase tests.

The SEM image of the purified isolate VKLR-01 from an exponential phase revealed the bacterium to be rod shaped, nonmotile having a cell dimension of 0.4-0.5 μm width and 1.4–1.6 μm length, respectively (Supplementary Figure 3B). Isolate VKLR-01 occurs at temperature range of 25–30°C (optimal at 28°C) and can tolerate up to 42°C, but no growth at 4 and 50°C. Isolate VKLR-01 can tolerate the salt concentration varied in the range of 1%–4% NaCl, but no visible growth was observed at 5% NaCl concentration in the YEM medium. The isolate also grew at pH 6.0 to pH 11.0, but no visible growth was observed at and below pH 5.0. Optimum growth conditions for the isolate VKLR-01 were temperature of 28–30°C, pH of 7.0–8.0, and 2% (w/v) NaCl. Temperature is known to influence survival, growth, and nitrogen fixation of *Rhizobium* [38]. Isolate VKLR-01 can tolerate extreme environmental conditions such as temperature up to 42°C and 4% NaCl, which differentiates this strain from other species. Similar results were found with rhizobia that nodulate *Lotus corniculatus* [39]. Generally, rhizobia collected from high temperature areas are resistant to high temperatures, and their tolerance is probably due to their adaptation to the extreme air temperatures inherent of tropical climate [40]. Salinity tolerance of the host is often the limiting factor in determining effective symbiosis of compatible rhizobia under saline conditions [41]. As the isolate VKLR-01 is able to adapt even in the presence of such unfavorable environmental conditions, this strain may be used for generation of genetically modified rhizobia by using genetic engineering tools. There is a report available that showed transferring of a 10 kb DNA fragment constructed from a wild-type strain of *Sinorhizobium* to *Rhizobium etli* (a sensitive strain) having resistance to several antibiotics, 4% NaCl, low and high pHs, heavy metals, and a temperature as high as 43°C [42]. Another application of this strain would be as an inoculum for a number of crop legumes that will significantly improve nodulation and nitrogen fixation and may lead to increase in plant dry matter under a low-level N fertilizer in low-fertility land.

Isolate VKLR-01 is Gram negative and nonspore forming. Gas is not produced from raffinose, sucrose, arabinose, mannitol, lactose, and glucose. Acid was produced from fermentation of sucrose, mannitol, and lactose but not from raffinose, arabinose, and glucose. Report showed that slow growth of rhizobia associated with woody tree species is related to alkali production, and fast growth is related to acid producers [43]. In the absence of specific taxonomic information, very fast-, fast-, and intermediate-growing (all acid-producing) will be referred to here as *Rhizobium*. In this study, mean generation times of the acid-producing isolate VKLR-01 were within the ranges reported in the literature for *Rhizobium* [38].

Isolate VKLR-01 did not grow in media without a carbon source (control). Isolate VKLR-01 utilizes lactose, sucrose, mannitol, D-ribose, maltose, D-galactose, glycerol, sorbitol, sodium citrate, inositol, D-fructose, D-mannose, N-acetyl glucosamine, pyruvate, dextran, α-ketoglutarate, and melibiose as the sole carbon sources and L-histidine, L-arginine, and L-proline as the sole nitrogen sources. Isolate VKLR-01

was positive for oxidase, catalase, and nitrate reduction test; however, it showed negative result for gelatin hydrolysis and methyl red tests. The intrinsic antibiotic resistance test for different antibiotics revealed that the isolate VKLR-01 is highly sensitive to antibiotics such as gentamicin, streptomycin, and tetracycline and is resistant to antibiotics like penicillin G, whereas for antibiotics like ampicillin and chloramphenicol it either mildly sensitive or moderately sensitive. Phenotypic characteristics of the isolate is VKLR-01 are shown in Table 1. Isolate VKLR-01 contained ubiquinone-10 (Q-10), at a peak ratio of approximately 100% as the predominant isoprenoid quinone.

3.3. FAME Analysis. The most abundant fatty acids are summed feature 8 (65.92%; comprising $C_{18:1}$ ω7c and/or $C_{18:1}$ ω6c) followed by $C_{16:0}$ iso (10.43%), summed feature 2 (7.42%, comprising $C_{14:0}$ 3OH/$C_{16:1}$ iso I and an unidentified fatty acid with an equivalent chain length of 10.9525) followed by $C_{16:0}$ 3OH (4.19%), $C_{13:1}$ at 12-13 (2.80%), and $C_{19:0}$ cyclo ω8c (2.76%), and summed feature 3 (2.42%; comprising $C_{16:1}$ ω7c/$C_{16:1}$ ω6c). Studies also showed that CFA profile of 5 *Rhizobium* species (*R. soli* DS-42^T, *R. huautlense* LMG 18254^T, *R. galegae* LMG 6214^T, *R. loessense* CIP 108030^T, and *R. cellulosilyticum* DSM 18291^T) contains $C_{18:1}$ ω7c as the major fatty acid, although there were differences in the proportions of some other fatty acids [9]. The cellular fatty acid profile for isolate VKLR-01 is shown in Table 2.

3.4. Genotyping by 16S rRNA, recA, and atpD Gene Sequences. Ribosomal RNA is consider the most useful of the highly conserved sequences available for the measurement of phylogenetic relationships [10]. The almost complete 16S rRNA gene sequence of isolate VKLR-01 determined in this study comprised 1428 nucleotides (approximately 95% of the *Escherichia coli* 16S rRNA sequences). In the neighbor-joining tree based on 16S rRNA gene sequences, isolate VKLR-01 fell within the clade comprising *Rhizobium* species (Figure 1). The gene sequence similarities between isolate VKLR-01 and *Rhizobium radiobacter* LMG 383^T were 97% and were 94% with *Rhizobium rubi* LMG 156^T, *Rhizobium alkalisoli* CCBAU 01393^T, and *Rhizobium vignae* CCBAU 05176^T, respectively. Gene sequence similarity values of not more than 93% were found when isolate VKLR-01 was compared with other species in the genus *Rhizobium*. The node to which isolate VKLR-01 belonged was also supported in phylogenetic trees generated with the maximum-likelihood and maximum parsimony algorithms (data not shown). In the neighbor-joining tree based on *rec*A gene and *atp*D gene sequences, isolate VKLR-01 formed distinct phylogenetic lineages within the clade comprising *Rhizobium* species (Supplementary Figures 4A and 4B). Isolate VKLR-01 exhibited 81 to 92% *rec*A gene sequence similarity and 80% to 94% *atp*D gene sequence similarity to *Rhizobium* species used in this study, respectively. In the present study, phylogenetic analysis of 16S rRNA housekeeping gene, other housekeeping genes like *atp*D and *rec*A, and other methods of genomic investigations revealed that the isolate VKLR-01 from the root nodules of *P. pinnata* occurring in North Guwahati, Assam, India,

Table 2: Cellular fatty acid composition (%) of *Rhizobium pongamiae* VKLR-01^T and type strains of phylogenetically related *Rhizobium* species.

Fatty acid	1	2	3
Straight-chain fatty acid			
12:0	00.55	—	—
14:0	00.75	—	0.11
15:0	—	—	0.29
16:0	10.43	7.7	9.03
17:0			0.13
18:0	00.66	0.9	0.17
Unsaturated fatty acid			
13:1 at 12-13	02.80	—	0.49
16:1 ω5c	—	—	—
17:1 ω8c	00.52	—	—
15:1 ω8c	—	0.8	—
17:1 ω6c	—	—	—
17:1 ω8c	—	—	0.22
18:1 ω5c	—	—	—
18:1 ω7c	—	76.2	—
Hydroxy fatty acid	—	—	—
12:0 3-OH	—	—	—
13:0 2-OH	—	—	—
15:0 3-OH	—	—	0.03
15:1 3-OH iso	—	—	—
16:0 3-OH	04.19	2.0	4.76
17:0 3-OH	—	—	0.18
18:0 2-OH	—	—	—
18:0 3-OH	00.58	0.7	—
15:1 G iso	—	—	—
16:0 iso	00.67	—	—
10-Methyl 18:0 TBSA	00.34	—	—
10-Methyl 19:0	—	2.1	1.09
11-Methyl 18:1 ω7c	—	—	0.23
17:0 cyclo	—	—	1.60
19:0 cyclo ω8c	02.76	3.9	18.78
20:2 ω6, 9c	—	—	0.01
20:3 ω6, 9, 12c	—	—	0.33
Unknown (ECL 18.794)	—	—	—
Summed features*	—	—	—
2	7.41	4.6	8.18
3	02.42	0.52	—
4	—	—	1.62
7	—	—	52.41
8	65.92	—	—

Strains: 1, *R. pongamiae* sp. nov.; 2, *R. galegae* LMG 6214^T 12 [9]; 3, *A. tumefaciens* [14]. Values are percentages of the total amount of fatty acid compounds present for those 14 species. ECL: equivalent chain length.
—: not detected.
*Summed features 2 (12:0 aldehyde? and/or 16:1 iso I and/or 14:0 3-OH and/or unknown ECL 10.928 and/or unknown ECL 10.9525 and/or 15:1 iso H/I, 13:0 3-OH).
*Summed features 3 (16:1 ω7c and/or 16:1 ω6c and/or 15:0 iso 2-OH).
*Summed features 4 (iso-17:1 I and/or anteiso-17:1 B and/or 15:0 iso 2-OH, 16:1 ω7c).
*Summed features 7 (18:1 ω7c and/or ω9 trans and/or ω12 trans and/or 18:1 ω7c and/or ω9c and/or ω12trans).
*Summed features 8 (18:1 ω7c and/or 18:1 ω6c).

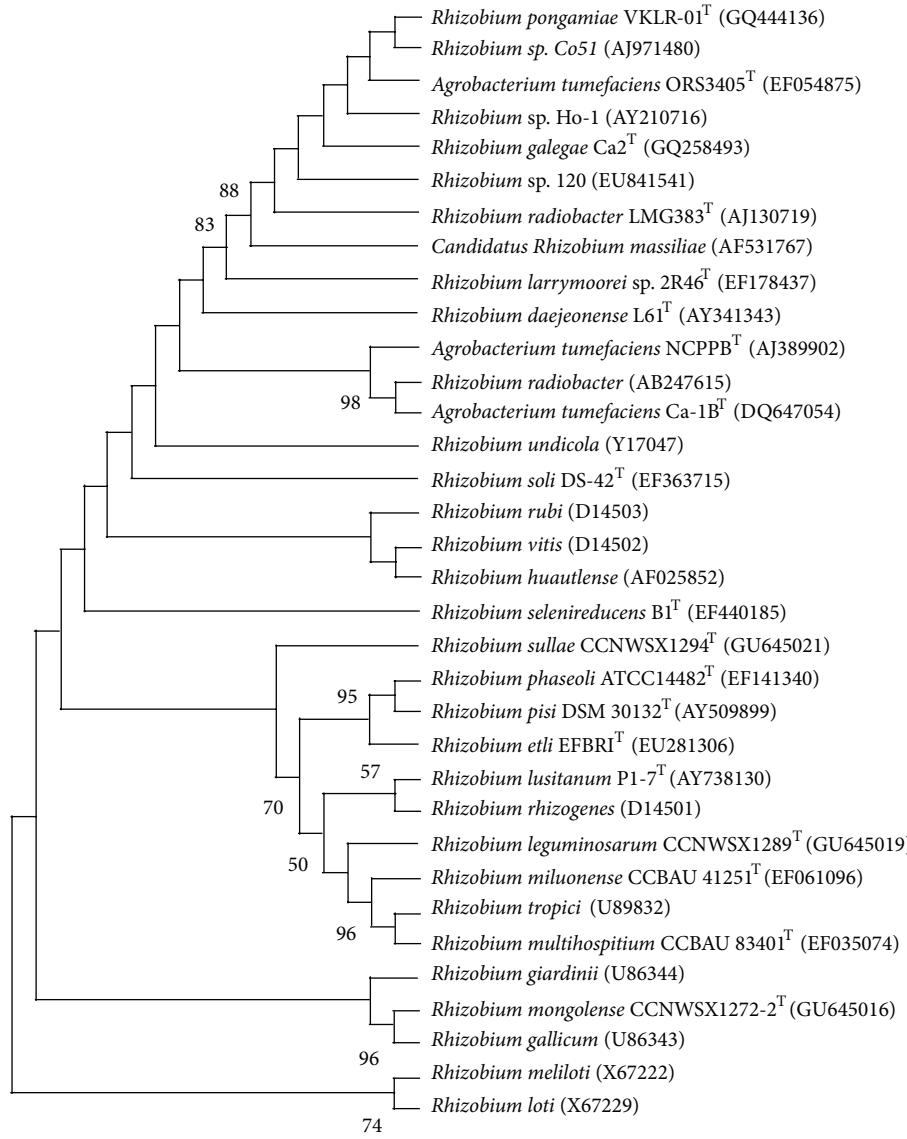

Figure 1: Dendrogram depicting the phylogenetic relationships of *Rhizobium pongamiae* VKLR-01^T within the family *Rhizobiaceae* determined using 16S rRNA gene sequence analysis and generated with the MEGA 4.0 software as described in text. Bootstrap values based on 1000 replications are listed as percentages at branching points. Bootstrap values below 50 were omitted from the dendrogram. Bar, 0.002 substitutions per nucleotide position.

represented distinct genotype. These gene sequence similarity values are below the cut-off value of 97%, the level normally judged sufficient to justify the proposal of a novel bacterial species [44].

3.5. Nitrogen Fixation and Nodulation Assessment Test. In addition to 16S, multilocus sequence analysis (MLSA) is recommended for better resolution of phylogenetic relationships and species identification of novel bacterial strains [45]. In this study, we choose the *nod*D and *nif*H genes and corresponding primers from *R. leguminosarum biovar trifolii, R. leguminosarum biovar viciae,* and *S. meliloti*, which works well with fast-growing rhizobia. Isolate VKLR-01 was able to reduce acetylene to ethylene, and when subjected to *nif*H-specific amplification, it amplified an expected product of 620 bp (Supplementary Figure 5A). The amplified 620 bp fragments of isolate VKLR-01 were sequenced and were found to show 83.0% to 90.0% sequence similarity with other *nif*H sequences from the NCBI database. Nodulation test was performed by PCR amplification of *nod*D gene. Isolate VKLR-01 amplified an expected product of 540 bp (Supplementary Figure 5B). The *nif*H and *nod*D genes amplification results confirm that the isolate VKLR-01 is a nitrogen fixer and plays a role in nodule formation. This will have important implications for biofuel production where reducing inputs (urea-based fertilizers) is highly desirable for production on nutrient-exhausted land [5].

3.6. G + C and DNA Hybridization Tests. The DNA G + C content of the isolate VKLR-01 is 59.1 mol% well within the

range of values for the genus *Rhizobium* [46]. However, DNA G + C content of the isolate VKLR-01 was lower than that of the type strains *R. soli* DS-42^T (60.8 mol%), *R. galegae* LMG 6214^T (63.0 mol%), *R. loessense* CIP 108030^T (59.5 mol%), *R. tianshanense* 6 (63 mol%), and *R. tianshanense* A-1BS^T (61 mol%), but higher than that of *R. huautlense* LMG 18254^T (57 mol%) and *R. cellulosilyticum* DSM 18291^T (57 mol%), respectively [9, 47], and it exhibited mean DNA-DNA relatedness values of 51.9% to the type strain of phylogenetically related *Rhizobium* species (*Rhizobium radiobacter* DSM 30147^T).

DNA-DNA hybridization provides a useful strategy to establish the taxonomic place and identity of novel strain [48]. Isolate VKLR-01 exhibited mean DNA-DNA relatedness values of 51.9% to the type strain of phylogenetically related *Rhizobium* species (*Rhizobium radiobacter* DSM 30147^T). Since isolate VKLR-01 shares DNA-DNA hybridization value of less than 70% with reference strain DSM 30147^T, the isolate is regarded as a distinct *Rhizobium* species [47]. The phylogenetic distinctiveness, together with the DNA-DNA relatedness data and differential phenotypic properties, is sufficient to allocate isolate VKLR-01 to a species that is separate from the recognized *Rhizobium* species and named as *Rhizobium pongamiae* [44].

3.7. Rhizobium pongamiae sp. nov. On the basis of characterization of phenotypic features, cellular fatty acid profile, cluster analysis, PCR amplification of *nif*H and *nod*D genes, and DNA base composition, DNA-DNA hybridization, the isolate VKLR-01 (= MTCC 10513^T = MSCL 1015^T) from root nodules of *P. pinnata* is considered to represent a novel species within the genus *Rhizobium*. The name for isolate VKLR-01^T proposed is *Rhizobium pongamiae* sp. nov. (pon.ga'mi.ae. N.L. gen. n. pongamiae of Pongamia).

4. Conclusion

In conclusion, the results based on diverse phenotypic, physiological, biochemical, and molecular studies confirmed the novelty as well as abiotic stress-tolerance potential of the isolated bacterium *Rhizobium pongamiae* (strain VKLR-01^T) obtained from root nodules of *P. pinnata*, a legume biodiesel crop growing in North Guwahati, Assam, India. Metabolism of the isolate is strictly aerobic and able to fix atmospheric nitrogen and could be defined as a novel species according to the current standards for definition of bacterial (rhizobial) species. The ecological success of the *R. pongamiae* (strain VKLR-01^T) is that it has specific traits for abiotic stresses, for example, salt, drought, and alkaline tolerance as revealed from the results discussed above which may reflect its advantages for wasteland reclamation, reforestation, and native ecosystem restoration of low-fertility soil. These specific traits of *R. pongamiae* may also be transferred to other rhizobia through biotechnological tools to generate genetic engineered rhizobia beneficial for agricultural point of view. *R. pongamiae* may also be used in several other biotechnological applications such as the production of polysaccharides, enzymes, and antibiotics, which will be the focus of research in future investigations for biotechnological purposes.

Disclosure

The GenBank/EMBL/DDBJ accession numbers for the 16S rRNA, *rec*A, and *atp*D gene sequences of strain VKLR-01^T are GQ444136, HM626171, and HM626172, respectively. The isolated novel bacterium *R. pongamiae* VKLR-01^T has assigned culture collection numbers (= MTCC 10513^T = MSCL 1015^T).

Conflict of Interests

There is no conflict of interests.

Authors' Contribution

All of the authors contributed to a similar extent overall, and all authors have seen and agreed to the submitted paper.

Funding

Vigya Kesari and Aadi Moolam Ramesh acknowledge the Council of Scientific and the Industrial Research (CSIR) and the Ministry of Human Resources Development (MHRD), Government of India, for the award of the Senior Research Fellowship (SRF). Latha Rangan acknowledges support from the Department of Biotechnology (DBT), the Government of India, for funding the research.

Acknowledgments

The authors would like to thank Professor H. G. Truper for his suggestions on Latin nomenclature for the novel isolate. Thanks are expressed to the Royal Life Sciences Pvt., Ltd., Secunderabad and DSMZ GmbH, Germany, for their excellent technical assistance related to FAME and molecular analyses. The support extended by the Central Instrument Facility (CIF), the Indian Institute of Technology Guwahati (IITG), related to scanning electron microscopy studies is greatly acknowledged. Authors are thankful to the Forest Department Officials of Sila Forest, North Guwahati, India, for the kind supply of study material.

References

[1] P. T. Scott, L. Pregelj, N. Chen, J. S. Hadler, M. A. Djordjevic, and P. M. Gresshoff, "*Pongamia pinnata*: an untapped resource for the biofuels: industry of the future," *Bioenergy Research*, vol. 1, pp. 2–11, 2008.

[2] V. Kesari, A. Das, and L. Rangan, "Physico-chemical characterization and antimicrobial activity from seed oil of *Pongamia pinnata*, a potential biofuel crop," *Biomass and Bioenergy*, vol. 34, no. 1, pp. 108–115, 2010.

[3] N. Mukta and Y. Sreevalli, "Propagation techniques, evaluation and improvement of the biodiesel plant, *Pongamia pinnata* (L.)

Pierre-A review," *Industrial Crops and Products*, vol. 31, no. 1, pp. 1–12, 2010.

[4] M. Sahgal and B. N. Johri, "The changing face of rhizobial systematics," *Current Science*, vol. 84, no. 1, pp. 43–48, 2003.

[5] H. T. Murphy, D. A. O'Connell, G. Seaton et al., "A common view of the opportunities, challenges and research actions for *Pongamia* in Australia," *Bioenergy Research*, vol. 5, no. 3, pp. 773–800, 2012.

[6] I. O. A. Odeh, D. K. Y. Tan, and T. Ancev, "Potential suitability and viability of selected biodiesel crops in Australian marginal agricultural lands under current and future climates," *Bioenergy Research*, vol. 4, no. 3, pp. 165–179, 2011.

[7] K. E. Kabir, F. Islam, and A. R. Khan, "Insecticidal effect of the petroleum ether fraction obtained from the leaf extract of *Pongamia glabra* Vent. on the American cockroach, *Periplaneta americana* (L.) (Dictyoptera: Blattidae)," *International Pest Control*, vol. 43, pp. 152–154, 2001.

[8] J. M. Vincent, *A Manual for the Practical Study of the Root-Nodule Bacteria: IBP Handbook no. 15*, Blackwell Scientific, Oxford, UK, 1970.

[9] J.-H. Yoon, S.-J. Kang, H.-S. Yi, T.-K. Oh, and C.-M. Ryu, "*Rhizobium soli* sp. nov., isolated from soil," *International Journal of Systematic and Evolutionary Microbiology*, vol. 60, no. 6, pp. 1387–1393, 2010.

[10] C. R. Woese, "Bacterial evolution," *Microbiological Reviews*, vol. 51, no. 2, pp. 221–271, 1987.

[11] H. Bouzar and J. B. Jones, "Agrobacterium larrymoorei sp. nov., a pathogen isolated from aerial tumours of Ficus benjamina," *International Journal of Systematic and Evolutionary Microbiology*, vol. 51, no. 3, pp. 1023–1026, 2001.

[12] B. De Las Rivas, Á. Marcobal, and R. Muñoz, "Allelic diversity and population structure in Oenococcus oeni as determined from sequence analysis of housekeeping genes," *Applied and Environmental Microbiology*, vol. 70, no. 12, pp. 7210–7219, 2004.

[13] E. T. Wang, P. Van Berkum, D. Beyene et al., "*Rhizobium huautlense* sp. nov., a symbiont of *Sesbania herbacea* that has a close phylogenetic relationship with *Rhizobium galegae*," *International Journal of Systematic Bacteriology*, vol. 48, no. 3, pp. 687–699, 1998.

[14] S. W. Tighe, P. De Lajudie, K. Dipietro, K. Lindström, G. Nick, and B. D. W. Jarvis, "Analysis of cellular fatty acids and phenotypic relationships of *Agrobacterium, Bradyrhizobium, Mesorhizobium, Rhizobium and Sinorhizobium* species using the Sherlock Microbial Identification System," *International Journal of Systematic and Evolutionary Microbiology*, vol. 50, no. 2, pp. 787–801, 2000.

[15] A. Boyde and C. Wood, "Preparation of animal tissues for surface-scanning electron microscopy," *Journal of Microscopy*, vol. 90, no. 3, pp. 221–249, 1969.

[16] K. Lindström and S. Lehtomäki, "Metabolic properties, maximum growth temperature and phage sensitivity of *Rhizobium* sp. (Galega) compared with other fast-growing rhizobia," *FEMS Microbiology Letters*, vol. 50, no. 2-3, pp. 277–287, 1988.

[17] W. Y. Shieh, A.-L. Chen, and H.-H. Chiu, "*Vibrio aerogenes* sp. nov., a facultatively anaerobic marine bacterium that ferments glucose with gas production," *International Journal of Systematic and Evolutionary Microbiology*, vol. 50, no. 1, pp. 321–329, 2000.

[18] R. M. Smibert and N. R. Krieg, "Phenotypic characterization," in *Methods for General and Molecular Bacteriology*, P. Gerhardt, R. G. E. Murray, W. A. Wood, and N. R. Krieg, Eds., pp. 607–654, American Society for Microbiology, Washington, DC, USA, 1994.

[19] M. Sasser, "Identification of bacteria through fatty acid analysis," in *Methods in Phytobacteriology*, Z. Klement, K. Rudoolph, and D. C. Sands, Eds., pp. 199–204, Akademiai Kiado, Budapest, Hungary, 1990.

[20] G. Laguerre, M.-R. Allard, F. Revoy, and N. Amarger, "Rapid identification of rhizobia by restriction fragment length polymorphism analysis of PCR-amplified 16S rRNA genes," *Applied and Environmental Microbiology*, vol. 60, no. 1, pp. 56–63, 1994.

[21] D. J. Lane, "16S/23S rRNA sequencing," in *Nucleic Acid Techniques in Bacterial Systematic*, E. Strackebrandt and M. Goodfellow, Eds., pp. 115–175, Wiley, Chischester, UK, 1991.

[22] S. F. Altschul, W. Gish, W. Miller, E. W. Myers, and D. J. Lipman, "Basic local alignment search tool," *Journal of Molecular Biology*, vol. 215, no. 3, pp. 403–410, 1990.

[23] R. Chenna, H. Sugawara, T. Koike et al., "Multiple sequence alignment with the Clustal series of programs," *Nucleic Acids Research*, vol. 31, no. 13, pp. 3497–3500, 2003.

[24] N. Saitou and M. Nei, "The neighbor-joining method: a new method for reconstructing phylogenetic trees," *Molecular biology and evolution*, vol. 4, no. 4, pp. 406–425, 1987.

[25] M. Kimura, "A simple method for estimating evolutionary rates of base substitutions through comparative studies of nucleotide sequences," *Journal of Molecular Evolution*, vol. 16, no. 2, pp. 111–120, 1980.

[26] K. Tamura, J. Dudley, M. Nei, and S. Kumar, "MEGA4: Molecular Evolutionary Genetics Analysis (MEGA) software version 4.0," *Molecular Biology and Evolution*, vol. 24, no. 8, pp. 1596–1599, 2007.

[27] R. Li and I. C. MacRae, "Specific identification and enumeration of *Acetobacter diazotrophicus* in sugarcane," *Soil Biology and Biochemistry*, vol. 24, no. 5, pp. 413–419, 1992.

[28] F. Poly, L. J. Monrozier, and R. Bally, "Improvement in the RFLP procedure for studying the diversity of nifH genes in communities of nitrogen fixers in soil," *Research in Microbiology*, vol. 152, no. 1, pp. 95–103, 2001.

[29] J. Tamaoka and K. Komagata, "Determination of DNA base composition by reversed-phase high-performance liquid chromatography," *FEMS Microbiology Letters*, vol. 25, no. 1, pp. 125–128, 1984.

[30] P. Cashion, M. A. Holder Franklin, J. McCully, and M. Franklin, "A rapid method for the base ratio determination of bacterial DNA," *Analytical Biochemistry*, vol. 81, no. 2, pp. 461–466, 1977.

[31] M. Mesbah, U. Premachandran, and W. B. Whitman, "Precise measurement of the G+C content of deoxyribonucleic acid by High-Performance Liquid Chromatography," *International Journal of Systematic Bacteriology*, vol. 39, no. 2, pp. 159–167, 1989.

[32] J. De Ley, H. Cattoir, and A. Reynaerts, "The quantitative measurement of DNA hybridization from renaturation rates," *European Journal of Biochemistry*, vol. 12, no. 1, pp. 133–142, 1970.

[33] V. A. R. Huss, H. Festl, and K. H. Schleifer, "Studies on the spectrophotometric determination of DNA hybridization from renaturation rates," *Systematic and Applied Microbiology*, vol. 4, no. 2, pp. 184–192, 1983.

[34] K. Komagata and K. Suzuki, "Lipid and cell wall analysis in bacterial systematic," *Methods in Microbiology*, vol. 19, pp. 161–206, 1987.

[35] M. H. Siddiqui, "Nodulation study of a few legume tree species during seedling stage," *Nitrogen Fixing Tree Research Reports*, vol. 7, p. 6, 1989.

[36] P. Felker and P. R. Clark, "Nitrogen fixation (acetylene reduction) and cross inoculation in 12 *Prosopis* (mesquite) species," *Plant and Soil*, vol. 57, no. 2-3, pp. 177–186, 1980.

[37] F. M. S. Moreira, K. Haukka, and J. P. W. Young, "Biodiversity of rhizobia isolated from a wide range of forest legumes in Brazil," *Molecular Ecology*, vol. 7, no. 7, pp. 889–895, 1998.

[38] P. H. Graham, M. J. Sadowsky, H. H. Keyser et al., "Proposed minimal standards for the description of new genera and species of root- and stem-nodulating bacteria," *International Journal of Systematic Bacteriology*, vol. 41, no. 4, pp. 582–587, 1991.

[39] A. Baraibar, L. Frioni, M. E. Guedes, and H. Ljunggren, "Symbiotic effectiveness and ecological characterization of indigenous *Rhizobium loti* populations in Uruguay," *Pesquisa Agropecuaria Brasileira*, vol. 34, no. 6, pp. 1011–1017, 1999.

[40] A. Fterich, M. Mahdhi, and M. Mars, "TThe effects of Acacia tortilis sub. raddiana, soil texture and soil depth on soil microbial and biochemical characteristics in arid zones of Tunisia," *Land Degradation and Development*, 2011.

[41] G. F. Craig, C. A. Atkins, and D. T. Bell, "Effect of salinity on growth of four strains of *Rhizobium* and their infectivity and effectiveness on two species of Acacia," *Plant and Soil*, vol. 133, no. 2, pp. 253–262, 1991.

[42] R. Defez, B. Senatore, and D. Camerini, "Genetically modified rhizobia as a tool to improve legume growth in semi-arid conditions," in *Mediterranean Conference of Rhizobiology Workshop on Symbiotic Nitrogen Fixation for Mediterranean Area*, Montpellier, France, July 2000.

[43] D. W. Odee, J. M. Sutherland, E. T. Makatiani, S. G. McInroy, and J. I. Sprent, "Phenotypic characteristics and composition of rhizobia associated with woody legumes growing in diverse Kenyan conditions," *Plant and Soil*, vol. 188, no. 1, pp. 65–75, 1997.

[44] E. Stackebrandt and B. M. Goebel, "Taxonomic note: a place for DNA-DNA reassociation and 16S rRNA sequence analysis in the present species definition in bacteriology," *International Journal of Systematic Bacteriology*, vol. 44, no. 4, pp. 846–849, 1994.

[45] R. Rivas, M. Martens, P. de Lajudie, and A. Willems, "Multilocus sequence analysis of the genus *Bradyrhizobium*," *Systematic and Applied Microbiology*, vol. 32, no. 2, pp. 101–110, 2009.

[46] W. Chen, E. Wang, S. Wang, Y. Li, X. Chen, and Y. Li, "Characteristics of *Rhizobium tianshanense* sp. nov., a moderately and slowly growing root nodule bacterium isolated from an arid saline environment in Xinjiang, People's Republic of China," *International Journal of Systematic Bacteriology*, vol. 45, no. 1, pp. 153–159, 1995.

[47] L. G. Wayne, D. J. Brenner, R. R. Colwell et al., "Report of the ad hoc committee on reconciliation of approaches to bacterial systematic," *International Journal of Systematic Bacteriology*, vol. 37, pp. 463–464, 1987.

[48] A. Willems, F. Doignon-Bourcier, J. Goris et al., "DNA-DNA hybridization study of *Bradyrhizobium* strains," *International Journal of Systematic and Evolutionary Microbiology*, vol. 51, no. 4, pp. 1315–1322, 2001.

Hindawi Publishing Corporation
BioMed Research International
Volume 2013, Article ID 796373, 19 pages
http://dx.doi.org/10.1155/2013/796373

Review Article

Natural Treatment Systems as Sustainable Ecotechnologies for the Developing Countries

Qaisar Mahmood,[1,2] Arshid Pervez,[2] Bibi Saima Zeb,[2] Habiba Zaffar,[2] Hajra Yaqoob,[2] Muhammad Waseem,[3] Zahidullah,[3] and Sumera Afsheen[4]

[1] *Department of Plant and Soil Sciences, University of Kentucky, Lexington, KY 40546-0091, USA*
[2] *Department of Environmental Sciences, COMSATS Institute of Information Technology, Abbottabad 22060, Pakistan*
[3] *Department of Biology, Allama Iqbal Open University, H-8, Islamabad 44000, Pakistan*
[4] *Department of Zoology, University of Gujrat, Gujrat 50700, Pakistan*

Correspondence should be addressed to Qaisar Mahmood; mahmoodzju@gmail.com

Received 5 April 2013; Revised 4 June 2013; Accepted 6 June 2013

Academic Editor: Eldon R. Rene

The purpose of natural treatment systems is the re-establishment of disturbed ecosystems and their sustainability for benefits to human and nature. The working of natural treatment systems on ecological principles and their sustainability in terms of low cost, low energy consumption, and low mechanical technology is highly desirable. The current review presents pros and cons of the natural treatment systems, their performance, and recent developments to use them in the treatment of various types of wastewaters. Fast population growth and economic pressure in some developing countries compel the implementation of principles of natural treatment to protect natural environment. The employment of these principles for waste treatment not only helps in environmental cleanup but also conserves biological communities. The systems particularly suit developing countries of the world. We reviewed information on constructed wetlands, vermicomposting, role of mangroves, land treatment systems, soil-aquifer treatment, and finally aquatic systems for waste treatment. Economic cost and energy requirements to operate various kinds of natural treatment systems were also reviewed.

1. Introduction

Rightly defined by Mitsch and Jørgensen [1], "the ecological engineering is the design of sustainable ecosystems that integrate human society with its natural environment for the benefit of both." It involves the restoration of ecosystems that have been substantially disturbed by human activities such as environmental pollution or land disturbance and the development of new sustainable ecosystems that have both human and ecological values. The development of ecological engineering was spawned by several factors, including loss of confidence in the view that all pollution problems can be merely solved through technological means and the realization that with technological means, pollutants are just being moved from one form to another. Conventional approaches require massive amounts of resources to solve these problems, and that in turn perpetuates carbon and nitrogen cycle problems, for example [1].

Currently, economic growth in developed nations, human population explosion in certain areas of Asia and Africa, deforestation, and destruction of natural habitats for the conservation of biodiversity are the biggest challenges for implementing the principles of ecological engineering in most of the developing nations. Currently, economic crunch in many developed as well as developing nations is forcing to implement low-cost natural treatment systems for the domestic and industrial wastewater treatment. In case the technological treatment facilities are installed in many developing countries, the energy input is difficult to be supplied in view of the global energy crisis, and very high operational cost is a bottleneck to their affordability. These all factors are compelling the employment of low cost natural

treatment systems for not only waste treatment but also for conserving biological communities in poor nations of the world. The conventional systems that may be appropriate in industrialized regions and densely populated areas with guaranteed power supplies, easily replaceable parts, and a skilled labor force to ensure operation and maintenance requirements might not be suitable for those regions with limited resources [2]. Hence, natural treatment systems particularly suit to developing countries of the world.

Sustainable sanitation systems require low cost, with low energy consumption and low mechanical technology. Better choices of low cost treatment systems for rural areas are decentralized processes [3]. Treatment systems with a very small energy input, low operational cost, and low surplus sludge generation are anaerobic digesters and constructed wetlands [3–6]. Other examples of low cost natural treatment systems include oxidation ponds, anaerobic ponds, facultative ponds, terrestrial treatment systems, and vermicomposting constructed wetlands. The objective of the current review was to describe some recent advancements in the design and efficiency of various natural treatment systems and the comparison of their efficiencies. Following sections will highlight the recent developments regarding various types of natural treatment systems.

2. Constructed Wetlands

Seidel [7] presented the ideas of improving inland waters suffering from high nutrients originating from sewage and sanitation through native plant species. However, at that time, experts only considered physicochemical and bacterial wastewater treatment only, and no attention was paid to controlled use of macrophytes for water purification [8]. Figure 1 shows various components of a constructed wetland [9]. Classification of constructed wetlands is based on two parameters, that is, type of macrophytic growth and water flow regime (surface and subsurface) [9]. CW can be used for the treatment of different types of wastewaters, that is, municipal, industrial, leachate, acid mine drainage, surface runoff, and so forth [10]. The emerging technology for the treatment of a variety of wastewaters is constructed wetlands (CWs) [11]. The natural wetland system uses mostly natural energy, requires low construction and operational costs, and so is energetically sustainable [12–14]. However, this assumption is not true for constructed wetlands where some energy input from human source is also required. The constructed wetlands are classified into two type, that is, free water surface (FWS) and subsurface flow (SSF) systems. In case of FWS systems, plants are rooted in the sediment layer, and water flow is above ground (surface flow). In SSF systems, plants are rooted in a porous media such as gravels or aggregates through which water flows and treatment are accomplished. SSF systems are further divided into two types: horizontal flow SSF (HSSF) and vertical flow SSF (VSSF). Compared to HSSF, the subsurface vertical flow constructed wetland (SVFCW) system is more effective for the mineralization of biodegradable organic matter and has greater oxygen transport ability [15]. For the removal of suspended solids, carbon and nitrification process vertical flow CW is more efficient, because of aerobic conditions and denitrification is poor. In VSSF CWs, feeding is intermittent (discontinuous), and the flow of wastewater is vertically administered through a substrate layer which mainly consists of sand, gravel, or a mixture of all these components [16].

Constructed wetlands can be used as an accepted ecotechnology, in small towns or industries that cannot afford conventional treatment systems [17–19]. In the free water surface (FWS) type of wetland, the water is filtered through a dense stand of aquatic plants as it flows over the bed surface [20–22]. Another constructed wetland system, known as the subsurface flow wetland consists of a lined shallow basin with a gravel media and emergent aquatic plants [23–28]. Worldwide, now thousands of constructed wetlands are in use which are receiving and treating a variety of municipal, industrial, and other wastewaters [29–31]. Due to operational simplicity and cost efficiency, the utilization of constructed wetlands in Taiwan is gaining greater popularity [12, 22, 29, 32, 33]. The constructed wetland technology is now well established, but its use for treating specific industrial effluents has not been well documented [34–36]. Various kinds of constructed wetlands have been shown in Figure 1.

The technology which uses plants for the removal of contaminants from a specified area is known as green technology [37], and the process is known as phytoremediation. Phytoextraction, phytovolatilization, rhizospheric degradation, phytodegradation, and hydraulic control are the five mechanisms involved in the phytoremediation for the removal of pollutants. Different types of pollutants can be removed by phytoremediation such as heavy metals, pesticides, petroleum hydrocarbons, explosives, radionuclides, and CVOCs [38]. Heavy metals are the chemical substances whose densities are greater than $5\,g\,cm^3$ [39]; metals cleanup requires their immobilization and toxicity reduction or removal, and they cannot be degraded like organic compounds [40]. Sedimentation/coagulation, filtration, plant uptake/removal efficiency, adsorption (binding to sand particles and root), formation of solid compounds, cation exchange, and microbial-mediated reactions, especially oxidation, are the different processes through which different types of metals can be removed in the constructed wet lands [41].

2.1. The Components of CW. The basic components employed in the construction of CW are containers, plant species, and sand and gravel media in certain ratios. Other invertebrates and microbes develop naturally [42]. Combination of anaerobic reactors, vegetated reactors (CW), and natural wetlands forms ecological treatment systems. In ecologically engineered systems, different functions are performed by different communities of flora, fauna, minerals, and microbes [43]. Another important component of ecological treatment systems is microbes which carry out the different important processes like hydrolysis, mineralization, nitrification, and denitrification. Plants are critical as an attachment surface for microbes [43]. For the construction of constructed wetland, three forms of macrophytes are basically used:

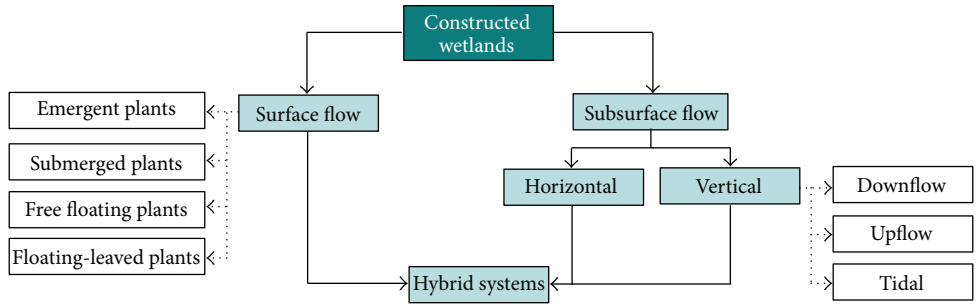

Figure 1: Various types of constructed wetlands [9].

Table 1: Typical characteristics of plant species used in constructed wetlands (modified after Crites and Tchobanoglous [170], Reed [171]).

Characteristic	Bulrush	Cattail	Reeds
Distribution	Worldwide	Worldwide	Worldwide
Preferred temperature (°C)	16–27	10–30	12–23
Preferred pH range	4–9	4–10	2–8
Salinity tolerance (ppt*)	20	30	45
Root penetration (m)	≈0.6	≈0.3	≈0.4
Drought resistant	moderate	Possible	high
Growth	Moderate to rapid	Rapid	Very rapid

*ppt: parts per thousand.

(1) floating macrophytes (i.e., *Lemna* spp. or *Eichornia crassipes*),

(2) submerged macrophytes (i.e., *Elodea canadiensis*),

(3) rooted emergent macrophytes (i.e., *Phragmites australis*, *Typha* spp.).

The plant used for phytoremediation should have high biomass, high growth rate, and ability to accumulate the target metal in the above-ground parts. They should be able to tolerate high metal concentration and have tolerance for several metals simultaneously [44]. Table 1 describes desirable features of plant species to be used in constructed wetlands.

2.2. Removal of Organic Matter in CW. In case of removing organic compounds by wetland plants, the focus is generally on three types of compounds, that is, chlorinated solvents, petroleum hydrocarbons, and explosives. But researchers also addressed the potential of plant species to treat other organic contaminants, such as polycyclic aromatic hydrocarbons (PAHs) and polychlorinated biphenyls (PCB) [45–47]. For wastewater purification, different natural systems involving plants, such as facultative ponds [48–50], terrestrial systems [51–55], and wetlands [8, 56–58], have been used. Floating aquatic plant systems usually contain floating macrophytes. The extensive root systems of floating leaved plants have large surface area, and rhizoplane provides an excellent site for the adhesion of rhizobacteria. In such treatment processes, rhizobacteria play an important role in the pollutant degradation and uptake [8]. A wealth of the literature has been published on the use of emergent plants [59, 60] and floating plants such as *Elodea canadensis* [61]. Although, water hyacinth is very efficient in nutrient uptake, the removal of naphthalene at toxic concentrations by *Eichhornia crassipes* has not yet been determined. *E. crassipes* is highly effective for the remediation of municipal sewage for a retention time of 2 to 5 days [62–64].

The natural systems containing various plant species were regarded as very effective and inexpensive technology for the cleanup of hazardous waste sites polluted with hydrocarbons, metals, pesticides, and chlorinated solvents [65–67]. The treatment of organic pollutants by plants may involve four mechanisms:

(1) direct uptake, accumulation, and metabolism of contaminants, in plant tissues (detoxification),

(2) transpiration of volatile organic hydrocarbons from leaves (avoidance),

(3) release of exudates from the roots that will stimulate microbial activity and biochemical transformations (chelation), and finally,

(4) the presence of mycorrhizal fungi and microbial consortia associated with the root surfaces can enhance the mineralization of pollutants in rhizosphere [68].

Photosynthetic activity and growth rate of plants are the two factors which render economic success of the treatment process by plants. Due to fast growth and large biomass production, water hyacinth (*Eichhornia crassipes* (Mart.) Solms) is largely used for the wastewater treatment [69]. Water hyacinth through uptake and accumulation can effectively remove inorganic contaminants such as nitrate, ammonium and soluble phosphorus [70, 71], and heavy metals [72, 73]. Different organic pollutants such as phenols can also be

absorbed [74], but their removal mechanisms were rarely studied to confirm that the removal of these pollutants involved uptake or the enhancement of mineralization by microbial consortia associated with the root surface.

A system comprising two parallel horizontal subsurface-flow constructed wetlands following an upflow anaerobic sludge blanket (UASB) reactor, treating municipal wastewater from the city of Belo Horizonte, Brazil, served as the basis for the evaluation of simple first-order kinetic performance models [75]. One unit was planted (*Typha latifolia*), and the other was unplanted. Tracer (Br^-) studies were undertaken, and samples of filtered COD were collected from the inlet, outlet, and three intermediate points along the longitudinal length of the units. The following kinetic models were used, and the related reaction coefficients were calculated: (i) plug-flow model; (ii) dispersed-flow model; and (iii) tanks-in-series model. For the three models, the following variants were analysed: without and with residual COD and without and with taking into account water losses due to evapotranspiration. In general, the dispersed-flow model and the tanks-in-series model, both adjusted for residual COD and incorporating water losses, were able to give the best predictions and led to the same reaction coefficients, which were also likely to best represent the actual first-order kinetic coefficients [75].

2.3. Removal of Inorganics and Metals by CW. Since 1990s, CWs have been used for the treatment of wastewater to remove solids, N, P, heavy metals, and organic pollutants [76–79]. CW have also been used for the removal of coliforms from storm water, municipal sewage, and agricultural runoff [80–83]. The presence of angiospermic plants in a wetland ecosystem improves treatment efficiencies [84–86]. The unique wetlands along the coastline of tropical and subtropical regions are mangroves. Mangroves could be used in CWs for wastewater treatment as shown by different studies [81, 87, 88].

The rapid increase of shortages in resources of chemical elements (and ores) used for an increasing industrial production raises the question of alternative strategies for their acquisition [89]. Simultaneously, the elemental load in aquatic ecosystems increases by anthropogenic activities. Polluted waters are purged actively by technical treatment plants or passively by wetlands. Wetlands are known to eliminate/fix pollutants with a potentially high efficiency. Regarding this elimination/fixation potential less is known about different types of wetlands for elemental recovery. This paucity of information prompted to us to assess the impact of main processes in different types of wetlands on the recovery potential of chemical elements showing advantages and disadvantages of autochthonous and allochthonous wetlands and possible solutions. We show that autochthonous as well as allochthonous wetlands are able to accumulate high amounts of elements, but it is suggested that combining autochthonous/allochthonous processes should result in a higher efficiency [90].

The recent applications and trend of CWs in China were reviewed by Hench et al. [81] and presented the status quo, prospect, and influencing factors in CWs construction, technology application, and operation management in China based on the available data. The results of the systematic survey showed that CWs technology achieved gradual perfection under the pushes of national policies, market demand, and technical feasibility, with the capacity of wastewater treatment increasing year by year. However, there were still some problems concerning engineering operation and management. Moreover, the results demonstrated that limited by the economic level, the degree of industrialization and urbanization, climatic conditions, and land availability, CWs were distributing predominately in the region of 20°13′N–35°20′N in China, which covered the central areas with a subtropical monsoon climate and southern or central areas at province level. In these areas, there were more than 40 plant species, which accounted for 57.14% of the total number of common wetland plants. Most of the CWs composted series or parallel combination forms of the vertical flow and free water surface flow CWs units, and they were suitable to treat more than 20 different types of wastewaters. For these CWs, the effluent COD, biological oxygen demand BOD, TN, and total phosphorous (TP) reached in the ranges of 20–60 mg/L, 4–20 mg/L, 1–20 mg/L, and 0.2–1 mg/L, respectively. The effluents from CWs were reused in more than eight ways, such as for agricultural irrigation, supplying surface water, and green belt sprinkling [81].

Galvão and Matos [91] evaluated the buffering capacity of constructed wetlands by analyzing the response to sudden organic load changes. Nine horizontal flow experimental beds were divided into three equal groups and monitored in a three-phase experiment. Influent COD mass loads during Phase I were 11.4, 5.3, and 0 g/m^2/day for Groups A–C, respectively. During Phase II there was a rise in COD mass load, and Phase III restored initial conditions. Group A showed a reduction in COD removal efficiencies with mass load increase despite more intense microbiological activity. In Group B planted beds there was a reduction of the mass load removal, which could have been due to a biofilm disturbance caused by an invasive millipede species. When mass load was lowered, removal efficiencies improved. Group C showed residual effluent COD during Phase I but provided adequate removal efficiencies (75–84%) when supplied with 1.7 g/m^2/day during Phase II. The results of this study suggest that the buffering capacity of constructed wetlands may not be enough to maintain COD removal efficiencies during a sudden organic load increase [91].

Three free water surface constructed wetlands (FWSCWs) were built in the border of the Lake *L'Albufera de Valencia* (Valencia, Spain) [92]. The lake is the emblematic element of one of the most important wetlands in Spain, *L'Albufera de Valencia Natural Park*, and it is highly eutrophicated. The function of the set of CWs (9 ha) is treating the eutrophic water from the lake with the objective of reducing the phytoplankton population and nutrients. The treatment wetlands named as *FG* and *fp* are comprised of three basins in a series, while the last, *F4*, consists of a single cell. During the first 2 years of operation, the inflow from lake was gradually increased from 0.01 m^3/s (April 2009)

to 0.13 m^3/s (December 2010) with the goal of establishing the maximum hydraulic loading rate (HLR) and finding the highest removal efficiency. Input concentrations of different water quality variables studied showed a high variability. The inflow contained 8.80–94 mg/L TSS, 0.16–1.13 mg/L TP, 1–17.30 mg/L TN, 0.13–13.10 mg N/L DIN, 0.10–11.50 mg NO_3-N/L, and 3.34–257.03 μg/L Chl *a*. The best removal results for these parameters were obtained in the *FG* wetland, where the average mass removal efficiencies were 75% TSS, 65% TP, 52% TN, 61% DIN, 58% NO_3-N, and 46% Chl *a*. In the set of constructed wetlands the removal rates increased with the hydraulic load rate for TSS and TP but neither for nitrogen species nor Chl *a*; for these variables the input concentrations are a key factor in removal. For instance, mean removal rate for nitrate is 101 mg N m^{-2} d^{-1}, but values higher than 400 mg N/m^2 d were obtained when input concentrations were about 7 mg NO_3-N/L. Values of first-order constant aerial rate (k_A) have been obtained for all variables. The corresponding values for nitrogen species and total phosphorus are higher than obtained in previous studies, but the k_A value for TSS is low (94.9 m/year) owing to the eutrophic characteristics of water, and a k_A value for phytoplankton-Chl *a* of 65.1 m/year is introduced. The management of CWs implies the harvest of vegetation, not for removing nitrogen because nitrification-denitrification processes reduce the 83.3% of TN that enters, but for the phosphorus, limiting nutrient in the *Lake L'Albufera*, that now is accumulated in plants and soils but could be sent back in several years [92].

In 2008, concentrations of iron and manganese in the sediments of seven constructed wetlands (CWs) with horizontal subsurface flow in the Czech Republic were evaluated [93]. The surveyed constructed wetlands varied in the length of operation between 2 and 16 years at the time of sampling. In each constructed wetland three samples of sediment were taken in the inflow, middle, and outflow zones to the depth of 0.6 m. The sample was divided into top (0–20 cm) and bottom (20–60 cm) sections, resulting in a total number of 18 samples in each system. In each sample the amount of sediment on dry mass basis was evaluated and concentrations of Fe and Mn in the sediment were determined using ICP-MS. The survey revealed that the amount of sediments in the filtration bed increases with the length of operation. In general, greater sediments were located at the bottom layers due to the wastewater distribution near the bottom. Concentrations of manganese in the sediment were highest in the new systems and decreased with length of operation. With the exception of one CW, in all other constructed wetlands Mn concentration in the sediment was significantly higher within the top layer. Mn concentrations in sediments found in that study were found within the concentration range commonly occurring in natural unpolluted wetlands. Iron concentration in the sediment also decreased with the increasing length of operation, but the dependence on the operation time was not as clear as for manganese. The concentration of iron was comparable with other studies from constructed wetlands treating sewage but higher as compared to polluted sediments which are usually highly anaerobic. The results clearly demonstrated that in order to evaluate the amount of iron and manganese in the filtration beds it is necessary to take into consideration both concentration of the elements and the amount of sediment accumulated in the filtration bed. Despite the lowest concentrations in the sediment the highest accumulated amount of both iron and manganese was found in the oldest CW Spálené Poříčí because of the highest concentration of sediment in the filtration bed [94].

In another investigation by Paulo et al. [93], the blackwater fraction was treated in an evapotranspiration tank (TEvap) system, whereas the greywater fraction was treated by a compact setup including a grease trap, sedimentation tank, and two constructed wetlands. Results of both systems, obtained during a 400-day trial in a 9-person household in Campo Grande-MS, Brazil, showed that ecological system could be an economical alternative to conventional septic tank solutions. The treatment system managed both greywater and blackwater at household level, enabling the development of green areas, improving microclimate and allowing for the reuse of grey water and the nutrients present in black water. The TEvap system was essentially maintenance free, but the constructed wetlands did require attention, to prevent clogging of subsystems [93].

2.4. Role of Rhizosphere in Pollutant Uptake. The term "rhizosphere" was introduced by the German scientist Hiltner [95]. Rhizosphere is a border line between soil and plants, which plays an important role in the agroenvironmental structure [96], where physiochemical and biological characteristics of soil, biomass activity, and community structure of microorganisms are significantly affecting each other [97]. The rhizosphere is an environment around plants where pathogenic and beneficial microorganisms create a potential strength on plant growth and health [98]. The rhizosphere is usually occupied by microbial groups like bacteria, fungi, nematodes, protozoa, algae, and microarthropods [98, 99]. Proper understanding of the ecosystem is necessary for the waste treatment through beneficial integration of microorganisms and suitable selection of microbes [100].

It has been proved that plant roots attract soil microorganisms through their exudates which ultimately results in variations of the rates of metabolic activity of the rhizosphere microbial communities and those of the nonrhizosphere soil [101]. Generally, the plants associated bacteria migrate from the soil to the rhizosphere of living plant and ultimately colonize the rhizosphere and roots of plants [102]. These rhizobacteria are symbiotic partners of plants and are considered as plants growth promoting microbes [103]. Due to natural activities of colonizing, bacterial species along the surface of the roots of the inoculated plants enhance the growth rate of plants [104].

The exudates released by plant roots and associated microbes may significantly mobilize heavy metals and ultimately increase their bioavailability [105]. Bacteria are the most common type of soil microorganisms due to their rapid growth and utilization of wide range of substances like carbon or nitrogen sources. Rhizospheric microbes may play a dual

role in soil ecological potential both constructively as well as destructively. The number and variety of harmful and useful microorganisms are related to the quality and quantity of rhizodeposits and the effect of the microbial relations that occurs in the rhizosphere [106].

An alternate way for the remediation of heavy metals toxicity is the use of rhizospheric microorganisms [107]. A variety of useful free-living soil bacteria are usually referred to as plant growth-promoting rhizobacteria and are found in association with the roots of diverse plants species [108]. Plants and microbes possess a strong and valuable relationship but may have strong competition for resources, including nutrients and water [109]. In both natural and manmade ecosystems, plant associated bacteria play a key role in host adaptation to a changing environment. These microorganisms can modify plant metabolism, so that upon exposure to heavy metal stress, the plants are able to tolerate their high concentrations [110]. Several authors have pointed out bacterial biosorption or bioaccumulation mechanism and other plant growth promoting factors; the production of ACC deaminase and phytohormones were regarded as key for better plant growth in heavy metals contaminated soils [111–113]. *Sedum alfredii*, a terrestrial Zn/Cd hyperaccumuluator, of Zn, Cd, Cu, and Pb from contaminated water evidently improved the phytoremediation in the presence of naturally occurring rhizospheric bacteria, also by using antibiotic ampicillin [114].

2.5. Vermicomposting and Constructed Wetlands. Vermicomposting principally employs earthworms to ingest organic matter and consequently egests a nutrient-rich cast that can be used as a soil conditioner. After fragmentation and ingestion, the microbial activity for the decomposition process is enhanced [115]. The process was also studied in relation to the changes in the composition properties of the wastes [116]. The advantages of this technology include speeding up and assisting the composting process as well as the quality of the end products. In addition, vermicomposting is considered to be odor-free because earthworms release coelomic fluids in the decaying waste biomass which have antibacterial properties [117]. Pathogens are also killed according to this effect. Many workers have highlighted the great reduction of pathogenic microorganisms by vermicomposting [118–120]. Among vermicomposters, earthworms are the most important invertebrates which play a significant role in the degradation of organic matters to humus. Earthworms can be classified as detritivores and geophages according to their feeding habit [121]. Detritivores feed on plant litter or dead roots and other plant debris as well as on mammalian dung. These earthworms are called humus formers, and they include the epigeic and anecic earthworms like *Perionyx excavatus*, *Eisenia fetida*, *Eudrilus euginae*, and *Polypheretima elongate* [122]. Geophagous worms mostly influence the aeration and mixing of subsoil; that is why they are called endogeic earthworms. Both types have their role, either as composters of detritivores or fieldworkers for geophages [123].

For using earthworms in constructed wetlands, it is imperative to understand their growth conditions. Species such as *Perionyx excavatus* and *Eudrilus eugeniae* are more common in warmer climates. They would be more suitable for the vermicomposting process in those regions. For instance, in Africa it is recommended to use *Eudrilus eugeniae*, which can reach sexual maturity in as little as five weeks compared with *E. fetida* which requires 6–8 weeks [124] and *Perionyx excavatus* in Asia as they are widely distributed. Both of these species are most productive at 25°C, which is higher than the optimal temperature quoted for other species in temperate regions [125]. In Thailand, the species commonly used is *Pheretima peguana*. The tolerance under different temperatures varies considerably for each species, whereas their optimum moisture requirements, C : N ratio, and ammonia content do not vary greatly [119]. The temperature tolerance for some species as well as their distribution is described and compared in Table 2.

In principle, earthworms prefer an aerobic condition [119]. Therefore, this should be applicable for the VSFCWs due to intermittent feeding rather than the anaerobically-operated HSFCWs. VSFCWs could offer a viable habitat for earthworm populations because of their ability to transfer oxygen to the root zone. This ability creates the aerobic micro-sites within the largely anoxic environment [126]. Under anoxic conditions, the earthworms will die. Edwards [119] has described some optimal conditions for breeding earthworms (*E. fetida*) in animal and vegetable wastes. However, future researches should be focused on the performance of earthworm based vermicomposting CW which are fed by various kinds of wastewaters like domestic, municipal, and some selected industrial wastewaters containing inorganic toxic pollutants like ammonia, heavy metals, and low DO. Nuengjamnong et al. [127] treated swine wastewater by integrating earthworms into constructed wetlands. They investigated the application of integrating earthworms (*Pheretima peguana*) into two-stage pilot-scale subsurface-flow constructed wetlands (SFCWs) receiving swine wastewater in terms of their treatment performance, namely, organic content, total Kjeldahl nitrogen (TKN), and solid reduction as well as the quantity of sludge production. There was a minor difference in terms of removal efficiency according to each parameter when comparing the unit with earthworms to the one without earthworms. Both achieved the TKN, BOD, COD, total volatile suspended solids (TVSS), suspended solids (SS), and total solids (TS) removal by more than 90%. The earthworms helped in reducing the sludge production on the surface of constructed wetlands 40% by volume, which resulted in lowering operational costs required to empty and treat the sludge. The plant biomass production was higher in the wetlands without earthworms. Further research could be undertaken in order to effectively apply earthworms inside the wetlands [127].

Enhancement of rural domestic sewage treatment performance and assessment of microbial community diversity and structure using tower vermifiltration was investigated by Wang et al. [128]. The performance of a novel three-stage vermifiltration (VF) system using the earthworm, *Eisenia fetida*, for rural domestic wastewater treatment was studied

Table 2: Comparison of some vermicomposting earthworm species in terms of the optimal and tolerable temperature ranges [119, 124, 172].

Species	Temperature ranges (°C)		Distribution
	Tolerated	Optimum	
Eisenia fetida	0–35	20–25	Temperate regions
Eudrilus eugeniae	9–30	20–28	Africa, India, North, and South America
Perionyx excavatus	9–30	15–30	Asia and Australia
Eisenia veneta	3–33	15–25	Europe

during a 131-day period. The average removal efficiencies of the tower VF planted with *Penstemon campanulatus* were as follows: COD, 81.3%; ammonium, 98%; total nitrogen, 60.2%; total phosphorus, 98.4%; total nitrogen, mainly in the form of nitrate. Soils played an important role in removing the organic matter. The three-sectional design with increasing oxygen demand concentration in the effluents and the distribution of certain oxides in the padding were likely beneficial for ammonium and phosphorus removal, respectively. The microbial community profiles revealed that band patterns varied more or less in various matrices of each stage at different sampling times, while the presence of earthworms intensified the bacterial diversity in soils. Retrieved sequences recovered from the media in VF primarily belonged to unknown bacterium and *Bacilli of Firmicutes* [128]. Wang et al. [129] investigated the impact of fly ash and phosphatic rock on metal stabilization and bioavailability during sewage sludge vermicomposting. Sewage sludge (SS) was mixed with different proportions of fly ash (FA) and phosphoric rock (PR), as passivators, and earthworms, *Eisenia fetida*, were introduced to allow vermicomposting. The earthworm growth rates, reproduction rates, and metal (except Zn and Cd) concentrations were significantly higher in the vermireactors containing FA and PR than in the treatments without passivators. The total organic carbon (TOC) and total metal concentrations in the mixtures decreased, and the mixtures were brought to approximately pH 7 during vermicomposting. There were significant differences in the decreases in the metal bioavailability factors (BFs) between the passivator and control treatments, and adding 20% FA (for Cu and Zn) or 20% PR (for Pb, Cd, and As) to the vermicompost were the most effective treatments for mitigating metal toxicity. The BF appeared to be dependent on TOC in the all treatments but was not closely dependent on pH in the different vermibeds [129].

2.6. Role of Mangroves. Mangroves are sole wetlands along the coastline of tropical and subtropical areas. They have unique adaptations to stressed environments and a massive requirement for nutrients because of fast growth, high primary productivity, metabolism, and yield. Studies suggested that mangroves could be used in CWs for wastewater treatment [81, 88, 130]. Studies were focused on the treatment efficiency of the mangrove species *Kandelia candel*. Little work has been done on the assessment of nutrient removal efficiency of different mangrove species [131]. They have special adaptations to stressful saline environments and a huge demand for nutrients because of rapid growth, high primary productivity, metabolism, and turnover. Many studies have demonstrated that mangroves could be used in CWs for wastewater treatment [81, 88, 130]. Plants can affect their growth medium by excreting exogenous enzymes and can also affect microbial species composition and diversity by releasing oxygen into the rhizosphere that in turn indirectly influences enzyme activity [132, 133]. Nevertheless, the relationship between plant species composition and enzyme activities in CW systems is poorly understood. The subsurface vertical flow constructed wetland (SVFCW) system with unsaturated flow possesses greater oxygen transport ability than the horizontal subsurface flow beds and is more effective for the mineralization of biodegradable organic matter.

The use of a mangrove plantation as a constructed wetland for municipal wastewater treatment was studied by Boonsong et al. [89]. The study evaluated the possibility of using mangrove plantation to treat municipal wastewater. Two types of pilot scale ($100 \times 150\,m^2$) free water surface constructed wetlands were set up at the Royal Laem Phak Bia Environmental Research and Development Project in central Thailand. One system is a natural *Avicennia marina* dominated forest system. The other system is a new mangrove plantation system in which seedlings of *Rhizophora* spp., *A. marina*, *Bruguiera cylindrical,* and *Ceriops tagal* were planted at 1.5×1.5 mintervals, making up 4 strips of $37.5 \times 100\,m^2$ each. Wastewater from municipal and nearby areas was collected and pumped into the systems then retained within the systems for 7 and 3 days, respectively, before discharging. The results indicated that the average removal percentage of TSS, BOD, NO_3-N, NH_4-N, TN, PO_4-P, and TP in the new-plantation systems were 27.6–77.1, 43.9–53.9, 37.6–47.5, 81.1–85.9, 44.8–54.4, 24.7–76.8, and 22.6–65.3, respectively, whereas the removal percentage of those parameters in the natural forest system were 17.1–65.9, 49.5–51.1, 44.0–60.9, 51.1–83.5, 43.4–50.4, 28.7–58.9, and 28.3–48.0, respectively. Generally, the removal percentage within the new-plantation system and the natural forest system was not significantly different. However, when the removal percentages with detention time were compared, TSS, PO_4-P, and TP removed percentages were significantly higher in the 7-day detention time treatment. Even with the highly varied and temporally dependent percentage removal of TSS, BOD, and nutrients, the overall results showed that a mangrove plantation could be used as a constructed wetland for municipal wastewater treatment in a similar way to the natural mangrove system. Therefore, the use of mangrove plantations for municipal wastewater treatment is applicable [89].

A pilot-scale mangrove wetland was constructed in Futian (China) for municipal sewage treatment by Yang et al. [134]. Three identical belts (length: 33 m, width: 3 m,

and depth: 0.5 m) were filled with stone (bottom), gravel, and mangrove sand (surface). Seedlings of two native mangrove species (*Kandelia candel, Aegiceras corniculatum*) and one exotic species (*Sonneratia caseolaris*) were transplanted to the belts with one species for each belt. The hydraulic loading was 5 $m^3 d^{-1}$ and hydraulic retention time 3 d. High levels of removal of COD, BOD(5), TN, TP, and NH_3-N were obtained. The treatment efficiency of *S. caseolaris* and *A. corniculatum* was higher than that of *K. candel*. Faster plant growth was obtained for *S. caseolaris*. The substrate in the *S. caseolaris* belt also showed higher enzyme activities including dehydrogenase, cellulase, phosphatase, urease, and beta-glucosidase. The removal rates of organic matter and nutrients were positively correlated with plant growth. The results indicated that mangroves could be used in a constructed wetland for municipal sewage treatment, providing that posttreatment to remove coliforms was also included [134]. Saline municipal wastewater treatment was investigated in constructed mangrove wetland by Li et al. [135]. The feasibility of using constructed mangrove wetlands to treat saline municipal wastewater was evaluated in the study. Constructed wetland, acting as an ecological engineering alternative, is capable of reducing NH_4^+-N TN TP and COD from saline wastewater. During the 10 months' operating period, the constructed wetland was operated with salinity increasing from 10 to 50 parts per thousands (ppt). When the salinity of wastewater was below 30 ppt, the removal rates of NH_4^+-N>, TN>, TP, and COD were 71.6 79.8%, 75.5–89.6%, 82.7–97.4, and 66.6–85.3%, respectively. The removal rate of COD decreased to about 40% when the salinity increased to 50 ppt. A good performance of COD removal was obtained when the constructed mangrove wetland was operated at loading rate between 12.6–18.9 g m^{-2} d^{-1}. The preliminary result showed that constructed mangrove wetland for saline municipal wastewater treatment had a broad future [135].

3. Land Treatment Systems

Terrestrial or land treatment systems utilize land to treat wastewater. The land is generally allowed to flood with wastewater to be treated; the extent and treatment conditions usually depend on many factors like soil characteristics, the characteristics of wastewater, topography, the presence of additional media in soil, and so forth. When these systems are used, large buffer areas and fencing may be required to ensure minimal human exposure [136]. Also, given the nature of these systems, all requirements include disinfection and significant pretreatment before application. In wet and cold areas, an additional basin for storage or a larger dosing tank is necessary to eliminate possible runoff from the application area. The most used variation of these systems is the spray irrigation system. Spray irrigation systems distribute wastewater evenly on a vegetated plot for final treatment and discharge. Spray irrigation can be useful in areas where conventional onsite wastewater systems are unsuitable due to low soil permeability, shallow water depth table or impermeable layer, or complex site topography. Spray irrigation is not often used for residential onsite systems because of its large areal demands, the need to discontinue spraying during extended periods of cold weather, and the high potential for human contact with the wastewater during spraying. Spray irrigation systems are among the most land-intensive disposal systems. Buffer zones for residential systems must often be as large as, or even larger than, the spray field itself to minimize problems [137].

In spray irrigation system, pretreatment of the wastewater is normally provided by a septic tank (primary clarifier) and aerobic unit, as well as a sand (media) filter and disinfection unit. The pretreated wastewater in spray irrigation systems is applied at low rates to grassy or wooded areas. Vegetation and soil microorganisms metabolize most nutrients and organic compounds in the wastewater during percolation through the first several inches of soil. The cleaned water is then absorbed by deep-rooted vegetation, or it passes through the soil to the ground water [136].

Rapid infiltration (RI) is a soil-based treatment method in which pretreated (clarified) wastewater is applied intermittently to a shallow earthen basin with exposed soil surfaces. It is only used where permeable soils are available. Because loading rates are high, most wastewater infiltrates the subsoil with minimal losses to evaporation. Treatment occurs within the soil before the wastewater reaches the ground water. The RI alternative is rarely used for onsite wastewater management. It is more widely used as a small-community wastewater treatment system in the United States and around the world [136].

The third and last type of land surface treatment is the overland flow (OF) process. In this system, pretreated wastewater is spread along a contour at the top of a gently sloping site that has minimum permeability. The wastewater then flows down the slope and is treated by microorganisms attached to vegetation as it travels by sheet flow over very impermeable soils until it is collected at the bottom of the slope for discharge. This system requires land areas similar to the spray irrigation system. However, surface water discharge requirements (e.g., disinfection) from the OF system must still be met. Overland flow, like rapid infiltration, is rarely used for onsite wastewater management [136].

Land treatment systems comprise a possible alternative solution for wastewater management in cases where the construction of conventional (mechanical) wastewater treatment plants (WWTPs) are not afforded or other disposal option are not accessible. They have established to be an ideal technology for small rural communities, homes, and small industrial units due to low energy, low operational, and maintenance costs [137]. They depend upon physical, chemical, and biological reactions on and within the soil. Slow rate OF systems require vegetation, both to take up nutrients and other contaminants and to slow the passage of the effluent across the land surface to ensure the maximum contact times between the effluents and the plants/soils. Slow rate subsurface infiltration systems and RI systems are "zero discharge" systems that rarely discharge effluents directly to streams or other surface waters. Each system has different constraints regarding soil permeability. Slow rate OF systems are the most expensive among all the natural systems to put into practice.

The OF systems are a land application treatment technique in which treated effluents are ultimately discharged to surface water. The major profits of these systems are their low maintenance and technical manpower requirements. Subsurface infiltration systems are designed for municipalities of less than 2,500 people. They are usually designed for individual homes (septic tanks), but they can be designed for clusters of homes. Although they do require specific site conditions, they can be low-cost methods of wastewater disposal.

The use of subsurface infiltration systems has been expanded to treat various types of wastewater, including landfill leachates [138], dairy effluents [139], meat processing wastewater [140], olive oil mill wastewater [141], agricultural drainage [142], and contaminated groundwater [143]. Recognizing the importance of wastewater management in meeting future water demands, preventing environmental degradation, and ensuring sustainable growth, the use of subsurface infiltration systems in wastewater management is expected to increase.

3.1. Fundamental Processes. Slow rate systems purify the applied wastewater through physical, chemical, and biological mechanisms that occur concurrently in the soil, water, and atmosphere environment. These mechanisms include filtration, transformation, degradation, predation, natural die off, soil adsorption, chemical precipitation, denitrification, volatilization, and plant uptake. Detailed knowledge of the factors regulating these fundamental processes, as well as the complex interactions among them, is prerequisite for achieving a reliable treatment, particularly in terms of organic matter degradation, pathogen elimination, and nutrient removal. Moreover, the long-term treatment performance and the sustainability of the land remain equally important issues. Plant selection is among the most critical components mediating the successful performance of SRS [144]. Vegetation may dramatically affect the performance of land treatment systems through its effects on hydraulic loading, nutrient uptake, biomass production, microbial community (structure and activity), and other particular functions such as trace elements uptake/inactivation and toxic organics degradation/inactivation.

3.2. Vegetation of Terrestrial Systems. The primary criteria for vegetation selection are (a) water requirements, (b) the potential for nutrient uptake, (c) salt tolerance, (d) trace elements uptake and/or tolerance, and (e) biomass production.

Table 3 shows some examples of popular plant species for wastewater treatment. Further features that should be taken into consideration include climate (frosts, temperature, photoperiod, and length of growing season), soil properties (pH, salt, and nutrient concentration), plant availability, length of vegetation cycle, and production direction (e.g., pulp, wood, biofuels, and other products). Currently, a variety of annual crops, perennial grasses, and forest trees are used in slow rate systems (SRS) worldwide. Comparative accounts of various design features of all terrestrial treatment systems have been demonstrated in Table 4.

3.3. Soil-Aquifer Treatment (SAT). The soil layers in an SAT system allow the recycled water to undergo further physical, biological, and chemical purification as it passes through the soil. Physical treatment takes place by the soil acting as a filter, removing particles that may still be in the water. The biological treatment takes place as the microorganisms that naturally live in the soil consume or break down the organic matter that may still be in the recycled water. Chemical treatment occurs in the soil through such natural processes as neutralization, reduction, and oxidation during which one substance or compound in the recycled water is removed, broken down, or transformed into another. Changes also take place as the recycled water reaches the groundwater aquifer and mixes with the water already there and moves through the aquifer to extraction wells [145]. There are two zones where physical, chemical, and biological purification processes take place underground. The first is in what is called the unsaturated zone. The second is the saturated zone.

The unsaturated zone consists of the upper layers of the soil, unconsolidated sediments, and bedrock where spaces between soil particles are not completely filled with water like a kitchen sponge that is damp (i.e., not saturated). Scientists may also call this area the vadose zone or soil percolation zone. The top few inches of the soil are called the infiltration interface where the recycled water is in contact with the soils for only a few minutes. It is a very active zone of treatment. The rest of the unsaturated or soil percolation zone is typically 10 to 100 ft. deep where the recycled water is in contact with the soils ranging from several hours to days where additional purification occurs [145].

The saturated zone consists of lower layers of the soil and sediment and rock formations where all the spaces are filled with water like a kitchen sponge that is completely wet (e.g., saturated). The thickness of the saturated zone is the vertical depth or extent of an aquifer. The upper surface of the saturated zone is called the water table. After the SAT water reaches the saturated zone or aquifer, it mixes together with the underground water and then moves slowly to extraction wells. During this contact time with the aquifer material and mixing with the native groundwater, further purification of the recycled water occurs [145].

A pilot study was carried out in Sabarmati River bed at Ahmedabad, India for renovation of primary treated municipal wastewater through soil aquifer treatment (SAT) system [146]. The infrastructure for the pilot SAT system comprised of two primary settling basins, two infiltration basins, and two production wells located in the centre of infiltration basins for pumping out renovated wastewater. The performance data indicated that SAT has a very good potential for removal of organic pollutants and nutrients as well as bacteria and viruses. The SAT system was found to be more efficient and economical than the conventional wastewater treatment systems and hence recommended for adoption. A salient feature of the study was the introduction of biomat concept and its contribution in the overall treatment process [146]. SAT proved to be efficient, economical, and feasible method for wastewater treatment [147]. SAT system achieved an excellent reduction of BOD, suspended solids, and fecal coliform. About 90% of water applied to SAT site was returned to

Table 3: Various plants species involved in wastewater treatment.

Plant species	Nature of waste	References
Arundo donax (reeds) *Eucalyptus botryoides* (Southern mahogany)	Primary effluents* Meat processing effluent	[173, 174]
Eucalyptus camaldulensis (red gum)*Eucalyptus ovata* (swamp gum) *Eucalyptus grandis* (rose gum)	Primary effluents*, storm water pond Meat processing effluent	[173–175]
Eucalyptus globulus (Tasmanian bluegum) *Eucalyptus cyanophylla* (blue leaved mallee)	Secondary effluent**, storm water pond	[175–177]
Chloris gayana (Rhodes grass)	Secondary effluent** enriched with nitrogen	[178]
Eucalyptus robusta (swamp mahogany)	Secondary effluent** enriched with nitrogen	[178]

*The liquid portion of wastewater leaving primary treatment like sedimentation but not biological oxidation.
**The liquid portion of wastewater leaving secondary treatment facility involving biological processes.

Table 4: Design features of terrestrial treatment system.

Feature	Slow rate	Rapid infiltration	Infiltration	Overland flow
Soil texture	Sandy loam	Sand and sandy	Sand to clayey, silty, loam, and clay loam	Clayey loam
Depth to	3 ft	3 ft	3 ft Not critical	Groundwater
Vegetation	Required	Optional	Not applicable	Required
Climatic restrictions	Growing season	None	None	Growing season
Slope	<20%, Not critical	Not applicable	2%–8% slopes cultivated land	<40%, uncultivated land

[179].

watershed. A case study was made to increase the efficiency of the system [148]. A water quality model for water reuse was made by mathematics induction [148]. The relationship among the reuse rate of treated wastewater (R), pollutant concentration of reused water (C_s), pollutant concentration of influent (C_0), removal efficiency of pollutant in wastewater (E), and the standard of reuse water were discussed in this study. According to the experiment result of a toilet wastewater treatment and reuse with membrane bioreactors, R would be set at less than 40%, on which all the concerned parameters could meet with the reuse water standards. To raise R of reuse water in the toilet, an important way was to improve color removal of the wastewater [148].

Through the use of innovative analytical tools, the removal/transformation of wastewater effluent organic matter (EfOM) has been tracked through soil aquifer treatment (SAT) [149]. While the total amount of EfOM is significantly reduced by SAT, there are trends of shorter term versus longer term removals of specific EfOM fractions. The preferential removal of nonhumic components (e.g., proteins, polysaccharides) of EfOM occurs over shorter travel times/distances, while humic components (i.e., humic substances) are removed over longer travel times/distances, with the removal of both by sustainable biodegradation. Dissolved organic nitrogen (DON), a surrogate for protein-like EfOM, is also effectively removed over shorter term SAT. There is some background humic-like natural organic matter (NOM), associated with the drinking water source within the watershed that persists through SAT. While most effluent-derived trace organic compounds are removed to varying degrees as a function of travel time and redox conditions, a few persist even through longer term SAT [149].

The design of a proper soil-aquifer treatment (SAT) groundwater recharge system is proposed after studying the geological and hydrogeological regime of the coastal aquifer system at Nea Peramos, NE Greece [150]. The investigation of the qualitative problem of the study area included groundwater level measurements and groundwater sampling and chemical analyses, respectively. The paper also includes the design of necessary maps, such as geological, piezometric, and distribution of specific qualitative parameters. The investigation concluded to further research and managerial useful proposals [150].

4. Aquatic Systems

Any watery environment, from small to large, from pond to ocean, in which plants and animals interact with the chemical and physical features of the environment is called an aquatic system. Since ages, the usual practice of wastewater disposal was its release into natural aquatic water bodies. Groundwater and surface water systems should be protected from organic matter, pathogens, and nutrients, coming from natural and anthropogenic resources. Both grey and black water coming from any residential units should be treated prior to its discharge to surface waters for reclamation and secondary uses so that it may not make hazards to human beings and to the environment [151]. Natural aquatic systems work on the natural ecological principals where aquatic plants, algae, and other microbes absorb pollutants found in

the wastewater to accomplish treatment. Wastewater ponds are one of the convenient options for the effective pollutant removal [152]. The proceeding section has been reserved for recent advancements on the use of various ponds to treat wastewaters.

4.1. Design of Wastewater Pond Systems. Wastewater ponds are natural systems whose biochemical and hydrodynamic processes are influenced by meteorological factors such as sunshine, wind, temperature, rainfall, and evaporation [153]. Sun is the driving force in the purification process of pond systems as is in any natural water body. Wastewater ponds, however, differ greatly from natural water bodies, for example, lakes and oceans in nutrient loading, oxygen demand, depth, size, water residence time, material residence time, and flow pattern [154]. Variations in meteorological factors often trigger fluctuations in water quality parameters, such as, temperature, pH, and dissolved oxygen (DO) both seasonally and diurnally. Photosynthetic oxygenation, which is essential for aerobic oxidation of the waste organics, varies diurnally with light intensities with peaks occurring between 1300 and 1500 h in the tropics [155]. It is not uncommon to find dissolved oxygen supersaturation between 300% and 400% on the top water layers of algal ponds on warm sunny afternoons in the tropics [50, 155–157]. The pH of algal ponds increases with photosynthesis as algae continue consuming carbon dioxide faster than it can be produced by bacterial respiration. As CO_2 diffusion from the atmosphere is minimal, primarily due to elevated surface water temperatures, the CO_2 deficit during peak photosynthesis is met from the dissociation of bicarbonate ions. This bicarbonate dissociation with concomitant consumption of CO_2 by algae increases the concentration of hydroxyl ions in the water column causing the pH to rise to well over 10 [158–160].

Temperature has a pronounced effect on both biochemical and hydrodynamic processes of pond systems. During the daylight hours, solar radiation heats up the top water layer thus causing thermal stratification with a consequence of the warmer and lighter water overlaying the cooler and denser deeper water. Such density stratification reduces the performances of pond systems by increasing short-circuiting and disrupting the internal diffusive and advective mass transfer mechanisms. Thermal stratification also localizes algae into bands of 10–15 cm width that move up and down through the water column in response to changes in light intensity [161]. Seasonal and diurnal variations of temperature, pH, and dissolved oxygen in advanced integrated wastewater pond system treating tannery effluent were studied by Tadesse et al. [161]. Seasonal and diurnal fluctuations of pH, dissolved oxygen (DO), and temperature were investigated in a pilot-scale advanced integrated wastewater pond system (AIWPS) treating tannery effluent. The AIWPS was comprised of advanced facultative pond (AFP), secondary facultative pond (SFP), and maturation pond (MP) all arranged in series. The variations of pH, DO, and temperature in the SFP and MP followed the diurnal cycle of sunlight intensity. Algal photosynthesis being dependent on sunlight radiation, its activity reached climax at early afternoons with DO saturation in the SFP and MP in excess of over 300% and pH in the range of 8.6–9.4. The SFP and MP were thermally stratified with gradients of 3–5°C/m, especially, during the time of peak photosynthesis. The thermal gradient in the AFP was moderated by convective internal currents set in motion as a result of water temperature differences between the influent wastewater and contents of the reactor. In conclusion, the AFP possessed remarkable ability to attenuate process variability with better removal efficiencies than SFP and MP. Hence its use as a lead treatment unit, in a train of ponds treating tannery wastewaters, should always be considered [161].

To improve the hydraulic characteristics of the pond system, various innovations and modifications have been made in basic designs of the pond systems in the last two decades along with the advances of efficient aeration tools. There is a wide range of the pond systems depending upon the processes, characteristics, design methods, and operating procedures, that is, complete mix ponds, complete retention pond, facultative ponds, partial-mix ponds, anaerobic ponds, high-performance aerated pond systems (complex designs), controlled discharge pond, hydrograph controlled release, proprietary in pond systems for nitrogen removal, for nitrification, and denitrification, high-performance modified aerated pond systems, phosphorus removal ponds, ponds coupled with wetlands and gravel beds system for nitrogen removal, nitrification filters and settling basins for control of algae, and hydraulic control of ponds.

4.2. Overview of Pond Systems for Wastewater Treatment. If inexpensive ground is available then stabilization pond is one of the frequent wastewater treatment methodologies. Usually, waste stabilization ponds (WSPs) are huge, man-made water ponds [151]. The waste stabilization pond involves the construction of an artificial pond or the setting aside of a suitable natural pond or lagoon. The liquid sewage, released into the pond either before or after preliminary treatment, is held there to permit desired microbiological transformations to take place [162]. These ponds are firstly overflowed with wastewater and then treated by means of natural processes. Separately or connected in a series for improved wastewater treatment ponds can be used. There are three types of stabilization ponds, that is, (1) anaerobic ponds, (2) facultative ponds, and (3) aerobic (maturation) ponds. All of these have different action and design distinctiveness [152]. For effective performance, WSPs should be connected in a sequence of three or more with waste matter to be transferred from the anaerobic to the facultative pond and finally to the aerobic pond. As a pretreatment phase, the anaerobic pond minimizes the suspended solids (SS) and biological oxygen demand (BOD) [163]. Where the entire deepness of the pond is anaerobic, the pond is a man-made deep lake. Anaerobic ponds are built for a depth of 2 to 5 m for little detention time of 1 to 7 days. A complete design manual must be consulted for all kinds of WSPs, and the actual design will depend on the wastewater characterization and the loading rates [152]. Organic carbon is converted into methane through anaerobic bacteria, and it also removes about 60 to 65% of the BOD.

To offer a high level of pathogen removal numerous aerobic ponds can be built in series. Away from residential areas and public spaces, they are particularly suitable for rural community that has open unused lands. They are not suitable for very dense or urban areas. WSPs are mainly competent in warm, sunny climate and work in most climates. For efficient treatment, the retention times and loading rates can be adjusted in case of cold climates [151].

The primary costs associated with constructing an anaerobic pond are the cost of the land, building earthwork appurtenances, constructing the required service facilities, and excavation. Costs for forming the embankment, compacting, lining, service road and fencing, and piping and pumps must also be considered. Operating costs and energy requirements are minimal [164].

To examine and assess the possible alternatives in modern societies, environmental management programs use models of systems [151]. Waste stabilization ponds are commonly well thought-out as being efficient for intestinal parasites removal [165]. Rectangular and cross baffle shapes are popularly capable to improve water quality. To maintain the ponds formation of scum, surplus solids and compost and garbage should be avoided to enter in the ponds. To make sure that animals and people stay away from the area, a fence should be installed, and surplus trash should not enter in the ponds [166].

Aerated pond is a huge, outside, diverse aerobic reactor. Mechanical aerators are installed to give oxygen (O_2) and to sustain the aerobic microorganisms mixed and suspended in the water body for high rate nutrient removal and organic degradation [151]. To reduce the interference with the aerators influent must be subjected to screening and pretreatment to remove trash fine and coarse particles [152]. Increased mixing along aeration through mechanical components in aerated ponds ensures high organic loading in the ponds. This results the increased organic matter degradation and pathogen removal. In colder climates, aerated ponds can sustain because of the continuous supply of oxygen by the mechanical units besides the light-induced photosynthesis [163]. A settling tank is necessary to separate the effluent from the solids, since the exposure to air causes turbulence. They are mainly suitable for the areas of reasonably priced lands that are away from residences settlements and businesses communities [151].

The advantages include reliable BOD_5 removal; significant nitrification of NH_3 possible with sufficient mean cell resident time; treatment of influent with higher BOD_5 in less space; and reduced potential for unpleasant odors. Aerated ponds are more complicated to design and construct, which increases capital and O&M costs. A larger staff is needed for whom training must be provided on a regular basis. Finally, sludge removal is more frequent and requires secondary treatment for disposal off-site [164].

Construction costs associated with partially mixed aerobic ponds include cost of the land, excavation, and inlet and outlet structures. If the soil where the system is constructed is permeable, there will be an additional cost for lining. Excavation costs vary, depending on whether soil must be added or removed. Operating costs of partial mix ponds include operation and maintenance of surface or diffused aeration equipment [164].

Facultative ponds have been in use for more than 100 years in USA [164]. These ponds are usually 1.2–2.4 m in depth and are not mechanically mixed or aerated. The layer of water near the surface contains sufficient DO from atmospheric reaeration and photosynthetic oxygenation by microalgae growing in the photic zone to support the growth of aerobic and facultative bacteria that oxidize and stabilize wastewater organics. The bottom layer of a conventional facultative pond includes sludge deposits that are decomposed by anaerobic bacteria. These shallow ponds tend to integrate carbon and primary solids undergoing acetogenic fermentation but only intermittent methane fermentation. The intermediate anoxic layer, called the facultative zone, ranges from aerobic near the top to anaerobic at the bottom. These three strata or layers may remain stable for months due to temperature-induced water density differentials, but normally twice a year during the spring and fall seasons, conventional facultative ponds will overturn, and the three strata will mix bottom to top, top to bottom. This dimictic overturn inhibits CH_4 fermentation by O_2 intrusion into the bottom anaerobic stratum, and, as a result, C is integrated rather than being converted into biogas [167]. The presence of algae, which release O_2 as they disassociate water molecules photochemically to assimilate hydrogen during photosynthesis, is essential to the successful performance of conventional, as well as advanced, facultative ponds [164].

The advantages of facultative ponds include infrequent need for sludge removal, effective removal of settle-able solids, BOD_5, pathogens, fecal coliform, and, to a limited extent, NH_3. They are easy to operate and require little energy, particularly if designed to operate with gravity flow. The disadvantages include higher sludge accumulation in shallow ponds or in cold climates and variable seasonal NH_3 levels in the effluent. Emergent vegetation must be controlled to avoid creating breeding areas for mosquitoes and other vectors. Shallow ponds require relatively large areas. During spring and fall dimictic turnover, odors can be an intermittent problem [164].

4.3. Energy Requirements for Various Natural Treatment Systems. The available cost data for different types of natural treatments systems are difficult to interpret given the number of design constraints placed on the various systems. The size required and resulting costs will vary depending upon whether the systems are designed to remove BOD_5, TSS, NH_3, or total N. Various reports by different authors have highlighted the costs involved in the construction and operation of these systems which include EPA [164], Crites and Fehrmann [168] and Shilton [169]. Energy consumption is a major factor in the operation of wastewater treatment facilities. As wastewater treatment facilities are built to incorporate current treatment technology and to meet regulatory performance standards, the cost of the energy to run the processes must be considered more carefully in the designing and planning of the facilities. Planners and designers should seek out the most recent information on energy requirements

Table 5: Total annual energy for typical 1 mgd system including electrical plus fuel, expressed as 1000 kwh/yr [180].

Treatment system	Energy (1000 KwH/yr)
Rapid infiltration (facultative pond)	150
Slow rate, ridge, and furrow (facultative pond)	181
Overland flow (facultative pond)	226
Facultative pond + intermittent sand filter	241
Facultative pond + microscreens	281
Aerated pond + intermittent sand filter	506
Extended aeration + sludge drying	683
Extended aeration + intermittent sand filter	708
Trickling filter + anaerobic digestion	783
RBC + anaerobic digestion	794
Trickling filter + gravity filtration	805
Trickling filter + N removal + filter	838
Activated sludge + anaerobic digestion	889
Activated sludge + anaerobic digestion + filter	911
Activated sludge + nitrification + filter	1051
Activated sludge + sludge incineration	1440
Activated sludge + AWT	3809
Physical chemical advanced secondary	4464

These energy requirements were reported for meeting the four effluent quality standards, that is, BOD_5, TSS, P, and N.

so as to develop a system that incorporates the most efficient and affordable type and use of energy to treat wastewater to meet regulatory requirements consistently and reliably [164]. Expected energy requirements for various wastewater treatment processes are shown in Table 5. Facultative ponds and land application processes can produce excellent quality effluent with smaller energy budgets.

5. Conclusions

Currently, economic crunch in many developed as well as developing nations is forcing to implement low-cost natural treatment systems for the domestic and industrial wastewater treatment. In case the technological treatment facilities are installed in many developing countries, the energy input is difficult to be supplied in view of the global energy crisis and its affordability due to very high operational cost. These all factors are compelling the employment of principles of ecological engineering for not only waste treatment but also for conserving biological communities in poor nations of the world.

The performance of various wetlands, land, and aquatic treatment were reviewed. Constructed wetlands are designed based on principles of natural wetlands, employing different aquatic plants like floating, submerged, and rooted macrophytes. The prominent feature of these treatment systems is extensive root system which helps to absorb various pollutants from their growth medium. The presence of various planktonic forms also aids in treatability of constructed wetlands. The constructed wetlands have been found useful in metals absorption, nutrients uptake (especially nitrogen and phosphorus), and reduction of BOD. Vermicomposting constructed wetlands have been found as useful in organic matter removal and it is a recent trend to include earthworms in wetlands for assisting the composting process as well as the quality of the end products. In addition, vermicomposting produces to be odor-free end products.

The unique adaptations of mangroves to stressed environments and a massive requirement for nutrients due to fast growth and high primary productivity, metabolism and yield which can be exploited for environmental remediation. The mangrove plants can modify their growth medium by excreting exogenous enzymes and can also affect microbial species composition and diversity by releasing oxygen into the rhizosphere that in turn indirectly influences enzyme activity and thus treatment process.

Land treatment systems comprise a possible alternative solution for wastewater management in cases where the constructions of conventional wastewater treatment plants are not afforded or other disposal option are not accessible. The terrestrial treatment systems present many variations in their treatability and composition. These systems rely on soil characteristics, the characteristics of wastewater, topography, the presence of additional media in soil, and so forth. This system comprises spray irrigation system, rapid infiltration, and overland flows. Soil aquifer treatment system uses soil as a filter, removing particles found in the applied water. Biological processes also take place during soil aquifer treatment by microorganisms in the soil, while chemical treatment is accomplished by natural processes as neutralization, reduction, and oxidation during which one substance or compound in the recycled water is removed, broken down, or transformed into another.

Natural aquatic systems work on the natural ecological principals where aquatic plants, algae, and other microbes absorb pollutants found in the wastewater to accomplish treatment. Aerobic, anaerobic, and facultative wastewater

treatment ponds along their design characteristics were reviewed in current review. Stabilization pond is one of the frequent wastewater treatment methodologies where inexpensive land is available. Facultative ponds and land application processes can produce excellent quality effluent with smaller energy budgets.

Conflict of Interests

It is declared that the authors neither have any conflict of interests nor financial gain for this paper.

Acknowledgment

Qaisar Mohmood is highly grateful to Fulbright Scholarship Program of USA for providing financial support for staying in USA to accomplish this piece of work.

References

[1] W. J. Mitsch and S. E. Jørgensen, "Ecological engineering: a field whose time has come," *Ecological Engineering*, vol. 20, no. 5, pp. 363–377, 2003.

[2] P. Denny, "Implementation of constructed wetlands in developing countries," *Water Science and Technology*, vol. 35, no. 5, pp. 27–34, 1997.

[3] P. Lens, G. Zeeman, and G. Lettinga, *Decentralised Sanitation and Reuse: Concepts, Systems and Implementation*, IWA, London, UK, 2001.

[4] M. Von Sperling, "Comparison among the most frequently used systems for wastewater treatment in developing countries," *Water Science and Technology*, vol. 33, no. 3, pp. 59–62, 1996.

[5] R. H. Kadlec, R. L. Knight, J. Vymazal, H. Brix, P. Cooper, and R. Haberl, "Constructed wetlands for pollution control: processes, performance, design and operation, IWA specialist group on ise of macrophytes in water pollution control," Scientific and Technical Report 8, IWA, London, UK, 2000.

[6] H. Hoffmann, C. Platzer, D. Heppeler, M. Barjenbrunch, J. Tränckner, and P. Belli, "Combination of anaerobic treatment and nutrient removal of wastewater in Brazil," in *Proceedings of the 3rd Water World Congress*, Melbourne, Australia, April 2002.

[7] K. Seidel, "Pflanzungen zwischen gewassern und land," *Mitteilungen Max-Planck Gesselschaft*, pp. 17–20, 1953.

[8] J. Vymazal, "Constructed wetlands for wastewater treatment," *Ecological Engineering*, vol. 25, no. 5, pp. 475–477, 2005.

[9] V. Nikolić, D. Milićević, S. Milenković, and A. Milivojević, "Constructed wetland application in waste water treatment processes in Serbia, BALWOIS, 2010—Ohrid," Republic of Macedonia, pp. 3, May 2010.

[10] T. Zhang, D. Xu, F. He, Y. Zhang, and Z. Wu, "Application of constructed wetland for water pollution control in China during 1990–2010," *Ecological Engineering*, vol. 47, pp. 189–197, 2012.

[11] J. L. Faulwetter, V. Gagnon, C. Sundberg et al., "Microbial processes influencing performance of treatment wetlands: a review," *Ecological Engineering*, vol. 35, no. 6, pp. 987–1004, 2009.

[12] Y.-F. Lin, S.-R. Jing, D.-Y. Lee, and T.-W. Wang, "Nutrient removal from aquaculture wastewater using a constructed wetlands system," *Aquaculture*, vol. 209, no. 1-4, pp. 169–184, 2002.

[13] J. R. Lloyd, D. A. Klessa, D. L. Parry, P. Buck, and N. L. Brown, "Stimulation of microbial sulphate reduction in a constructed wetland: microbiological and geochemical analysis," *Water Research*, vol. 38, no. 7, pp. 1822–1830, 2004.

[14] N. Ran, M. Agami, and G. Oron, "A pilot study of constructed wetlands using duckweed (*Lemna gibba* L.) for treatment of domestic primary effluent in Israel," *Water Research*, vol. 38, no. 9, pp. 2240–2247, 2004.

[15] S. Kantawanichkul, S. Kladprasert, and H. Brix, "Treatment of high-strength wastewater in tropical vertical flow constructed wetlands planted with *Typha angustifolia* and *Cyperus involucratus*," *Ecological Engineering*, vol. 35, no. 2, pp. 238–247, 2009.

[16] N. Chiarawatchai, *Implementation of earthworm-assisted constructed wetlands to treat wastewater and possibility of using alternative plants in constructed wetlands [Ph.D. thesis]*, Technical University of Hamburg-Harburg, Hamburg, Germany, 2010.

[17] S.-R. Jing, Y.-F. Lin, D.-Y. Lee, and T.-W. Wang, "Nutrient removal from polluted river water by using constructed wetlands," *Bioresource Technology*, vol. 76, no. 2, pp. 131–135, 2001.

[18] A. D. Karathanasis, C. L. Potter, and M. S. Coyne, "Vegetation effects on fecal bacteria, BOD, and suspended solid removal in constructed wetlands treating domestic wastewater," *Ecological Engineering*, vol. 20, no. 2, pp. 157–169, 2003.

[19] M. R. Karim, F. D. Manshadi, M. M. Karpiscak, and C. P. Gerba, "The persistence and removal of enteric pathogens in constructed wetlands," *Water Research*, vol. 38, no. 7, pp. 1831–1837, 2004.

[20] L. Xianfa and J. Chuncai, "Constructed wetland systems for water pollution control in North China," *Water Science and Technology*, vol. 32, no. 3, pp. 349–356, 1995.

[21] P. Cooper, P. Griffin, S. Humphries, and A. Pound, "Design of a hybrid reed bed system to achieve complete nitrification and denitrification of domestic sewage," *Water Science and Technology*, vol. 40, no. 3, pp. 283–289, 1999.

[22] S. R. Jing, Y. F. Lin, T. W. Wang, and D. Y. Lee, "Microcosm wetlands for wastewater treatment with different hydraulic loading rates and macrophytes," *Journal of Environmental Quality*, vol. 31, no. 2, pp. 690–696, 2002.

[23] B. Gopal, "Natural and constructed wetlands for wastewater treatment: potentials and problems," *Water Science and Technology*, vol. 40, no. 3, pp. 27–35, 1999.

[24] P. A. M. Bachand and A. J. Horne, "Denitrification in constructed free-water surface wetlands: II. Effects of vegetation and temperature," *Ecological Engineering*, vol. 14, no. 1-2, pp. 17–32, 1999.

[25] D. A. Mashauri, D. M. M. Mulungu, and B. S. Abdulhussein, "Constructed wetland at the University of Dar es Salaam," *Water Research*, vol. 34, no. 4, pp. 1135–1144, 2000.

[26] C. M. Kao, J. Y. Wang, K. F. Chen, H. Y. Lee, and M. J. Wu, "Non-point source pesticide removal by a mountainous wetland," *Water Science and Technology*, vol. 46, no. 6-7, pp. 199–206, 2002.

[27] J. García, E. Ojeda, E. Sales et al., "Spatial variations of temperature, redox potential, and contaminants in horizontal flow reed beds," *Ecological Engineering*, vol. 21, no. 2-3, pp. 129–142, 2003.

[28] M. E. Kaseva, "Performance of a sub-surface flow constructed wetland in polishing pre-treated wastewater—a tropical case study," *Water Research*, vol. 38, no. 3, pp. 681–687, 2004.

[29] M. B. Green, P. Griffin, J. K. Seabridge, and D. Dhobie, "Removal of bacteria in subsurface flow wetlands," *Water Science and Technology*, vol. 35, no. 5, pp. 109–116, 1997.

[30] K. Cameron, C. Madramootoo, A. Crolla, and C. Kinsley, "Pollutant removal from municipal sewage lagoon effluents with a free-surface wetland," *Water Research*, vol. 37, no. 12, pp. 2803–2812, 2003.

[31] M. L. Solano, P. Soriano, and M. P. Ciria, "Constructed wetlands as a sustainable solution for wastewater treatment in small villages," *Biosystems Engineering*, vol. 87, no. 1, pp. 109–118, 2004.

[32] C. M. Kao and M. J. Wu, "Control of non-point source pollution by a natural wetland," *Water Science and Technology*, vol. 43, no. 5, pp. 169–174, 2001.

[33] C. Y. Lee, C. C. Lee, F. Y. Lee, S. K. Tseng, and C. J. Liao, "Performance of subsurface flow constructed wetland taking pretreated swine effluent under heavy loads," *Bioresource Technology*, vol. 92, no. 2, pp. 173–179, 2004.

[34] P. Worrall, K. J. Peberdy, and M. C. Millett, "Constructed wetlands and nature conservation," *Water Science and Technology*, vol. 35, no. 5, pp. 205–213, 1997.

[35] C. M. Kao and M. J. Wu, "Control of non-point source pollution by a natural wetland," *Water Science and Technology*, vol. 43, no. 5, pp. 169–174, 2001.

[36] J. García, P. Aguirre, R. Mujeriego, Y. Huang, L. Ortiz, and J. M. Bayona, "Initial contaminant removal performance factors in horizontal flow reed beds used for treating urban wastewater," *Water Research*, vol. 38, no. 7, pp. 1669–1678, 2004.

[37] V. Mudgal, N. Madaan, and A. Mudgal, "Heavy metals in plants: phytoremediation: plants used to remediate heavy metal pollution," *Agriculture and Biology Journal of North America*, vol. 1, pp. 40–46, 2010.

[38] S. McCutcheon and J. Schnoor, Eds., *Phytoremediation Transformation and Control of Contaminants*, John Wiley & Sons, Hoboken, NJ, USA, 2003.

[39] D. C. Adriano, *Trace Elements in Terrestrial Environments, Biochemistry, Bioavailability and Risks of Metals*, Springer, New York, NY, USA, 2001.

[40] C. D. Jadia and M. H. Fulekar, "Phytoremediation: the application of vermicompost to remove zinc, cadmium, copper, nickel and lead by sunflower plant," *Environmental Engineering and Management Journal*, vol. 7, no. 5, pp. 547–558, 2008.

[41] D. G. A. Ganjo and A. I. Khwakaram, "Phytoremediation of wastewater using some of aquatic macrophytes as biological purifiers for irrigation purposes: removal efficiency and heavy metals Fe, Mn, Zn and Cu," *World Academy of Science, Engineering and Technology*, vol. 66, pp. 565–572, 2010.

[42] APHA (American Public Health Association), AWWA (American Water Works Association), and WPFC (Water Pollution Control Federation), *Standard Methods for the Examination of Water and Waste Water*, American Public Health Association, Wash, USA, 19th edition, 1998.

[43] J. Todd and B. Josephson, "The design of living technologies for waste treatment," *Ecological Engineering*, vol. 6, no. 1–3, pp. 109–136, 1996.

[44] E. Pilon-Smits and M. Pilon, "Phytoremediation of metals using transgenic plants," *Critical Reviews in Plant Sciences*, vol. 21, no. 5, pp. 439–456, 2002.

[45] J. Fismes, C. Perrin-Ganier, P. Empereur-Bissonnet, and J. L. Morel, "Soil-to-root transfer and translocation of polycyclic aromatic hydrocarbons by vegetables grown on industrial contaminated soils," *Journal of Environmental Quality*, vol. 31, no. 5, pp. 1649–1656, 2002.

[46] T. Spriggs, M. K. Banks, and P. Schwab, "Phytoremediation of polycyclic aromatic hydrocarbons in manufactured gas plant-impacted soil," *Journal of Environmental Quality*, vol. 34, no. 5, pp. 1755–1762, 2005.

[47] C. Collins, M. Fryer, and A. Grosso, "Plant uptake of non-ionic organic chemicals," *Environmental Science and Technology*, vol. 40, no. 1, pp. 45–52, 2006.

[48] A. Pano and E. J. Middlebrooks, "Ammonia nitrogen removal in facultative wastewater stabilization ponds," *Journal of the Water Pollution Control Federation*, vol. 54, no. 4, pp. 344–351, 1982.

[49] S. C. Reed, R. W. Crites, and E. J. Middlebrooks, *Natural Systems for Waste Management and Treatment*, McGraw-Hill, New York, NY, USA, 2nd edition, 1995.

[50] B. Picot, A. Bahlaoui, S. Moersidik, B. Baleux, and J. Bontoux, "Comparison of the purifying efficiency of high rate algal pond with stabilization pond," *Water Science and Technology*, vol. 25, no. 12, pp. 197–206, 1992.

[51] H. Bouwer and R. L. Chaney, "Land Treatment of Wastewater," *Advances in Agronomy*, vol. 26, no. C, pp. 133–176, 1974.

[52] H. Bouwer, "Renovation of wastewater with rapid infiltration land treatment systems," in *Artificial Recharge of Groundwater*, T. Aslano, Ed., pp. 249–282, Butterworth, Boston, Mass, USA, 1985.

[53] W. H. Fuller and A. W. Warrick, *Soils in Waste Treatment and Utilization: Land Treatment*, CRC Press, Boca Raton, Fla, USA, 1985.

[54] A. Yediler, P. Grill, T. Sun, and A. Kettrup, "Fate of heavy metals in a land treatment system irrigated with municipal wastewater," *Chemosphere*, vol. 28, no. 2, pp. 375–381, 1994.

[55] Q.-X. Zhou, Q.-R. Zhang, and T.-H. Sun, "Technical innovation of land treatment systems for municipal wastewater in Northeast China," *Pedosphere*, vol. 16, no. 3, pp. 297–303, 2006.

[56] R. H. Kadlec and R. L. Knight, *Treatment Wetlands*, CRC Press, Boca Raton, Fla, USA, 1995.

[57] C. R. Gómez, M. L. Suárez, and M. R. Vidal-Abarca, "The performance of a multi-stage system of constructed wetlands for urban wastewater treatment in a semiarid region of SE Spain," *Ecological Engineering*, vol. 16, no. 4, pp. 501–517, 2001.

[58] J. Vymazal, "The use of sub-surface constructed wetlands for wastewater treatment in the Czech Republic: 10 years experience," *Ecological Engineering*, vol. 18, no. 5, pp. 633–646, 2002.

[59] K. Maillacheruvu and S. Safaai, "Naphthalene removal from aqueous systems by *Sagittarius* sp.," *Journal of Environmental Science and Health A*, vol. 37, no. 5, pp. 845–861, 2002.

[60] Z. Wang, X.-Q. Shan, and S. Zhang, "Comparison between fractionation and bioavailability of trace elements in rhizosphere and bulk soils," *Chemosphere*, vol. 46, no. 8, pp. 1163–1171, 2002.

[61] I. A. Tumaikina, O. V. Turkovskaya, and V. V. Ignatov, "Degradation of hydrocarbons and their derivatives by a microbial association on the base of Canadian pondweed," *Applied Biochemistry and Microbiology*, vol. 44, no. 4, pp. 382–388, 2008.

[62] Y. Zimmels, F. Kirzhner, and A. Malkovskaja, "Application of *Eichhornia crassipes* and *Pistia stratiotes* for treatment of urban sewage in Israel," *Journal of Environmental Management*, vol. 81, no. 4, pp. 420–428, 2006.

[63] Y. Zimmels, F. Kirzhner, and A. Malkovskaja, "Advanced extraction and lower bounds for removal of pollutants from wastewater by water plants," *Water Environment Research*, vol. 79, no. 3, pp. 287–296, 2007.

[64] Y. Zimmels, F. Kirzhner, and A. Malkovskaja, "Application and features of cascade aquatic plants system for sewage treatment," *Ecological Engineering*, vol. 34, no. 2, pp. 147–161, 2008.

[65] T. Macek, M. Macková, and J. Káš, "Exploitation of plants for the removal of organics in environmental remediation," *Biotechnology Advances*, vol. 18, no. 1, pp. 23–34, 2000.

[66] S. Susarla, V. F. Medina, and S. C. McCutcheon, "Phytoremediation: an ecological solution to organic chemical contamination," *Ecological Engineering*, vol. 18, no. 5, pp. 647–658, 2002.

[67] H. Xia, L. Wu, and Q. Tao, "A review on phytoremediation of organic contaminants," *Chinese Journal of Applied Ecology*, vol. 14, no. 3, pp. 457–460, 2003.

[68] J. L. Schnoor, L. A. Licht, S. C. McCutcheon, N. L. Wolfe, and L. H. Carreira, "Phytoremediation of organic and nutrient contaminants," *Environmental Science and Technology*, vol. 29, no. 7, pp. 318–323, 1995.

[69] V. Singhal and J. P. N. Rai, "Biogas production from water hyacinth and channel grass used for phytoremediation of industrial effluents," *Bioresource Technology*, vol. 86, no. 3, pp. 221–225, 2003.

[70] K. R. Reddy, "Fate of nitrogen and phosphorus in a waste-water retention reservoirant containing aquatic macrophytes," *Journal of Environmental Quality*, vol. 12, no. 1, pp. 137–141, 1983.

[71] K. R. Reddy, K. L. Campbell, D. A. Graetz, and K. M. Portier, "Use of biological filters for treating agricultural drainage effluents," *Journal of Environmental Quality*, vol. 11, no. 4, pp. 591–595, 1982.

[72] S. Muramoto and Y. Oki, "Removal of some heavy metals from polluted water by water hyacinth (*Eichhornia crassipes*)," *Bulletin of Environmental Contamination and Toxicology*, vol. 30, no. 2, pp. 170–177, 1983.

[73] Y. L. Zhu, A. M. Zayed, J.-H. Qian, M. De Souza, and N. Terry, "Phytoaccumulation of trace elements by wetland plants: II. Water hyacinth," *Journal of Environmental Quality*, vol. 28, no. 1, pp. 339–344, 1999.

[74] M. Q. Nora and R. O. Jesus, "Water hyacinth [*Eichhornia crassipes*(Mart.) Solms-Laub], an alternative for the removal of phenol in wastewater," *Acta Biologica Venezuelica*, vol. 17, pp. 57–64, 1997.

[75] M. von Sperling and A. C. de Paoli, "First-order COD decay coefficients associated with different hydraulic models applied to planted and unplanted horizontal subsurface-flow constructed wetlands," *Ecological Engineering*, vol. 57, pp. 205–209, 2013.

[76] W. H. Zachritz, L. L. Lundie, and H. Wang, "Benzoic acid degradation by small, pilot-scale artificial wetlands filter (AWF) systems," *Ecological Engineering*, vol. 7, no. 2, pp. 105–116, 1996.

[77] S. Wallace, "Advanced designs for constructed wetlands," *BioCycle*, vol. 42, no. 6, pp. 40–43, 2001.

[78] Q. Yang, Z.-H. Chen, J.-G. Zhao, and B.-H. Gu, "Contaminant removal of domestic wastewater by constructed wetlands: effects of plant species," *Journal of Integrative Plant Biology*, vol. 49, no. 4, pp. 437–446, 2007.

[79] C.-B. Zhang, W.-L. Liu, J. Wang et al., "Plant functional group richness-affected microbial community structure and function in a full-scale constructed wetland," *Ecological Engineering*, vol. 37, no. 9, pp. 1360–1368, 2011.

[80] G. Lakatos, M. K. Kiss, M. Kiss, and P. Juhász, "Application of constructed wetlands for wastewater treatment in Hungary," *Water Science and Technology*, vol. 35, no. 5, pp. 331–336, 1997.

[81] K. R. Hench, G. K. Bissonnette, A. J. Sexstone, J. G. Coleman, K. Garbutt, and J. G. Skousen, "Fate of physical, chemical, and microbial contaminants in domestic wastewater following treatment by small constructed wetlands," *Water Research*, vol. 37, no. 4, pp. 921–927, 2003.

[82] A. D. Karathanasis, C. L. Potter, and M. S. Coyne, "Vegetation effects on fecal bacteria, BOD, and suspended solid removal in constructed wetlands treating domestic wastewater," *Ecological Engineering*, vol. 20, no. 2, pp. 157–169, 2003.

[83] K. Sleytr, A. Tietz, G. Langergraber, and R. Haberl, "Investigation of bacterial removal during the filtration process in constructed wetlands," *Science of the Total Environment*, vol. 380, no. 1–3, pp. 173–180, 2007.

[84] R. A. Orson, R. L. Simpson, and R. E. Good, "A mechanism for the accumulation and retention of heavy metals in tidal freshwater marshes of the upper Delaware River estuary," *Estuarine, Coastal and Shelf Science*, vol. 34, no. 2, pp. 171–186, 1992.

[85] U. N. Rai, S. Sinha, R. D. Tripathi, and P. Chandra, "Wastewater treatability potential of some aquatic macrophytes: removal of heavy metals," *Ecological Engineering*, vol. 5, no. 1, pp. 5–12, 1995.

[86] D. O. Huett, S. G. Morris, G. Smith, and N. Hunt, "Nitrogen and phosphorus removal from plant nursery runoff in vegetated and unvegetated subsurface flow wetlands," *Water Research*, vol. 39, no. 14, pp. 3259–3272, 2005.

[87] Y. S. Wong, N. F. Y. Tam, and C. Y. Lan, "Mangrove wetlands as wastewater treatment facility: a field trial," *Hydrobiologia*, vol. 352, no. 1–3, pp. 49–59, 1997.

[88] Y. Ye, N. F. Tam, and Y. S. Wong, "Livestock wastewater treatment by a mangrove pot-cultivation system and the effect of salinity on the nutrient removal efficiency," *Marine Pollution Bulletin*, vol. 42, no. 6, pp. 513–521, 2001.

[89] K. Boonsong, S. Piyatiratitivorakul, and P. Patanaponpaiboon, "Potential use of mangrove plantation as constructed wetland for municipal wastewater treatment," *Water Science and Technology*, vol. 48, no. 5, pp. 257–266, 2003.

[90] J. Schaller, J. Vymazal, and C. Brackhage, "Retention of resources (metals, metalloids and rare earth elements) by autochthonously/allochthonously dominated wetlands: a review," *Ecological Engineering*, vol. 53, pp. 106–114.

[91] A. Galvão and J. Matos, "Response of horizontal sub-surface flow constructed wetlands to sudden organic load changes," *Ecological Engineering*, vol. 49, pp. 123–129, 2012.

[92] M. Martín, N. Oliver, C. Hernández-Crespo, S. Gargallo, and M. C. Regidor, "The use of free water surface constructed wetland to treat the eutrophicated waters of lake L'Albufera de Valencia (Spain)," *Ecological Engineering*, vol. 50, pp. 52–61, 2013.

[93] P. L. Paulo, C. Azevedo, L. Begosso, A. F. Galbiati, and M. A. Boncz, "Natural systems treating greywater and blackwater on-site: integrating treatment, reuse and landscaping," *Ecological Engineering*, vol. 50, pp. 95–100, 2013.

[94] J. Vymazal and J. Švehla, "Iron and manganese in sediments of constructed wetlands with horizontal subsurface flow treating municipal sewage," *Ecological Engineering*, vol. 50, pp. 69–75, 2013.

[95] L. Hiltner, "Über neuere erfahrungen und probleme auf dem gebiet der berücksichtigung der gründüngung und brache," *Arbeiten der Deutschen Landwirtschaftlichen Gesellschaft*, vol. 98, pp. 59–78, 1904.

[96] H. Wand, P. Kuschk, U. Soltmann, and U. Stottmeister, "Enhanced removal of xenobiotics by halophytes," *Acta Biotechnologica*, vol. 22, pp. 175–181, 2002.

[97] J. Sorensen, "The rhizosphere as a habitat for soil microorganisms," in *Modern Soil Microbiology*, J. D. van Elsas, J. T. Trevors, and E. M. H. Wellington, Eds., pp. 21–45, Marcel Dekker, New York, NY, USA, 1997.

[98] J. Lynch, *The Rhizosphere*, Wiley, London, UK, 1990.

[99] J. M. Raaijmakers, "Rhizosphere and rhizosphere competence," in *Encyclopedia of Plant Pathology*, O. C. Maloy and T. D. Murray, Eds., pp. 859–860, Wiley, New York, NY, USA, 2001.

[100] G. Díaz, C. Azcón-Aguilar, and M. Honrubia, "Influence of arbuscular mycorrhizae on heavy metal (Zn and Pb) uptake and growth of *Lygeum spartum* and *Anthyllis cytisoides*," *Plant and Soil*, vol. 180, no. 2, pp. 241–249, 1996.

[101] M. J. Brimecombe, F. A. De Lelj, and J. M. Lynch, "The rhizosphere: the effect of root exudates on rhizosphere microbial populations," in *The Rhizosphere: Biochemistry and Organic Substances at the Soil-Plant Interface*, R. Pinton, Z. Varanini, and P. Nannipieri, Eds., pp. 95–140, Marcel Dekker, New York, NY, USA, 2001.

[102] J. W. Kloepper and M. N. Schroth, "Plant growth promoting rhizobacteria on radishes," in *Proceedings of the 4th International Conference on Plant Pathogenic Bacteria*, vol. 2, pp. 879–882, Angers, France, 1978.

[103] Y. Kapulnik, "Plant growth promotion by rhizosphere bacteria," in *Plant Roots—The Hidden Half*, Y. Waisel, A. Eshel, and U. Kafkafi, Eds., pp. 769–781, Dekker, New York, NY, USA, 1996.

[104] P. K. Mishra, S. Mishra, G. Selvakumar et al., "Characterisation of a psychrotolerant plant growth promoting *Pseudomonas* sp. strain PGERs17 (MTCC 9000) isolated from North Western Indian Himalayas," *Annals of Microbiology*, vol. 58, no. 4, pp. 561–568, 2008.

[105] W. W. Wenzel, D. C. Adriano, D. Salt, and R. Smith, "Phytoremediation: a plant-microbe-based remediation system," in *Agronomy Monograph*, D. C. Adriano, J.-M. Bollag, W. T. Frankenberger, and R. C. Sims, Eds., vol. 37, pp. 457–508, Madison, Wis, USA, 1999.

[106] E. Somers, J. Vanderleyden, and M. Srinivasan, "Rhizosphere bacterial signalling: a love parade beneath our feet," *Critical Reviews in Microbiology*, vol. 30, no. 4, pp. 205–240, 2004.

[107] G. I. Burd, D. G. Dixon, and B. R. Glick, "Plant growth-promoting bacteria that decrease heavy metal toxicity in plants," *Canadian Journal of Microbiology*, vol. 46, no. 3, pp. 237–245, 2000.

[108] B. R. Glick, C. L. Patten, G. Holguin, and D. M. Penrose, *Biochemical and Genetic Mechanisms Used by Plant Growthpromoting Bacteria*, Imperial College Press, London, UK, 1999.

[109] J. P. Kaye and S. C. Hart, "Competition for nitrogen between plants and soil microorganisms," *Trends in Ecology and Evolution*, vol. 12, no. 4, pp. 139–143, 1997.

[110] G. E. Welbaum, A. V. Sturz, Z. Dong, and J. Nowak, "Managing soil microorganisms to improve productivity of agroecosystems," *Critical Reviews in Plant Sciences*, vol. 23, no. 2, pp. 175–193, 2004.

[111] S. Zaidi, S. Usmani, B. R. Singh, and J. Musarrat, "Significance of Bacillus subtilis strain SJ-101 as a bioinoculant for concurrent plant growth promotion and nickel accumulation in *Brassica juncea*," *Chemosphere*, vol. 64, no. 6, pp. 991–997, 2006.

[112] M. Madhaiyan, S. Poonguzhali, and T. Sa, "Metal tolerating methylotrophic bacteria reduces nickel and cadmium toxicity and promotes plant growth of tomato (*Lycopersicon esculentum* L.)," *Chemosphere*, vol. 69, no. 2, pp. 220–228, 2007.

[113] K. V. Kumar, S. Srivastava, N. Singh, and H. M. Behl, "Role of metal resistant plant growth promoting bacteria in ameliorating fly ash to the growth of *Brassica juncea*," *Journal of Hazardous Materials*, vol. 170, no. 1, pp. 51–57, 2009.

[114] J. Xiong, Z. He, D. Liu, Q. Mahmood, and X. Yang, "The role of bacteria in the heavy metals removal and growth of *Sedum alfredii* Hance in an aqueous medium," *Chemosphere*, vol. 70, no. 3, pp. 489–494, 2008.

[115] R. M. Atiyeh, S. Subler, C. A. Edwards, G. Bachman, J. D. Metzger, and W. Shuster, "Effects of vermicomposts and composts on plant growth in horticultural container media and soil," *Pedobiologia*, vol. 44, no. 5, pp. 579–590, 2000.

[116] O. Y. Kalinina, O. G. Chertov, and A. I. Popova, "Changes in the composition and agroecological properties of livestock waste during vermicomposting with *Eisenia foetida*," *Eurasian Soil Science*, vol. 35, no. 9, pp. 951–958, 2002.

[117] R. K. Sinha, S. Herat, S. Agarwal, R. Asadi, and E. Carretero, "Vermiculture and waste management: study of action of earthworms *Elsinia foetida*, *Eudrilus euginae* and *Perionyx excavatus* on biodegradation of some community wastes in India and Australia," *Environmentalist*, vol. 22, no. 3, pp. 261–268, 2002.

[118] J. Domínguez and C. A. Edwards, "Effects of stocking rate and moisture content on the growth and maturation of *Eisenia andrei* (Oligochaeta) in pig manure," *Soil Biology and Biochemistry*, vol. 29, no. 3-4, pp. 743–746, 1997.

[119] C. A. Edwards, *Earthworm Ecology*, CRC Press, Boca Raton, Fla, USA, 2nd edition, 2004.

[120] L. C. Vigueros and E. R. Camperos, "Vermicomposting of sewage sludge: a new technology for Mexico," *Water Science and Technology*, vol. 46, no. 10, pp. 153–158, 2002.

[121] K. E. Lee, *Earthworms Their Ecology and Relationships with Soil and Land Use*, Academic Press, Sydney, Australia, 1985.

[122] S. A. Ismail, *Vermicology: the Biology of Earthworms*, Orient Longman, Chennai, India, 1997.

[123] J. C. Buckerfield, "Appropriate earthworms for agriculture and vermiculture," Tech. Rep. 2/1994, Division of Soils, CSIRO Australia, Adelaide, Australia, 1994.

[124] C. A. Edwards and I. Burrows, "The potential of earthworm composts as plant growth media," in *Earthworms in Waste and Environmental Management*, C. A. Edwards and E. Neuhauser, Eds., pp. 21–32, SPB Academic Press, The Hague, The Netherlands, 1988.

[125] J. Dominguez, C. A. Edwards, and J. Dominguez, "The biology and population dynamics of *Eudrilus eugeniae* (Kinberg) (Oligochaeta) in cattle waste solids," *Pedobiologia*, vol. 45, no. 4, pp. 341–353, 2001.

[126] H. Brix, "Do macrophytes play a role in constructed treatment wetlands?" *Water Science and Technology*, vol. 35, no. 5, pp. 11–17, 1997.

[127] C. Nuengjamnong, N. Chiarawatchai, C. Polprasert, and R. Otterpohl, "Treating swine wastewater by integrating earthworms into constructed wetlands," *Journal of Environmental Science and Health A*, vol. 46, no. 7, pp. 800–804, 2011.

[128] L. Wang, F. Guo, Z. Zheng, X. Luo, and J. Zhang, "Enhancement of rural domestic sewage treatment performance, and assessment of microbial community diversity and structure using tower vermifiltration," *Bioresource Technology*, vol. 102, no. 20, pp. 9462–9470, 2011.

[129] Y. J. Wang, S. P. Liu, and X. R. Chen, "A survey on winter birds in Shenzhen Futian Mangrove," *Ecological Science*, vol. 12, pp. 74–84, 1993.

[130] P. E. Lim, T. F. Wong, and D. V. Lim, "Oxygen demand, nitrogen and copper removal by free-water-surface and subsurface-flow constructed wetlands under tropical conditions," *Environment International*, vol. 26, no. 5-6, pp. 425–431, 2001.

[131] V. J. Shackle, C. Freeman, and B. Reynolds, "Carbon supply and the regulation of enzyme activity in constructed wetlands," *Soil Biology and Biochemistry*, vol. 32, no. 13, pp. 1935–1940, 2000.

[132] F. Caravaca, M. M. Alguacil, P. Torres, and A. Roldán, "Plant type mediates rhizospheric microbial activities and soil aggregation in a semiarid Mediterranean salt marsh," *Geoderma*, vol. 124, no. 3-4, pp. 375–382, 2005.

[133] D. K. Singh and S. Kumar, "Nitrate reductase, arginine deaminase, urease and dehydrogenase activities in natural soil (ridges with forest) and in cotton soil after acetamiprid treatments," *Chemosphere*, vol. 71, no. 3, pp. 412–418, 2008.

[134] Q. Yang, N. F. Y. Tam, Y. S. Wong et al., "Potential use of mangroves as constructed wetland for municipal sewage treatment in Futian, Shenzhen, China," *Marine Pollution Bulletin*, vol. 57, no. 6-12, pp. 735–743, 2008.

[135] C. Li, F. Gao, W.-H. Jin, and Z.-S. Chen, "Saline municipal wastewater treatment by constructed mangrove wetland," in *Proceedings of the 2011 International Conference on Electronics, Communications and Control (ICECC '11)*, pp. 2825–2828, Zhejiang, China, September 2011.

[136] EPA, "Onsite wastewater treatment systems technology," Fact Sheet 12, Land Treatment Systems, http://www.adwwa.org/tech_fs_12.pdf.

[137] N. V. Paranychianakis, A. N. Angelakis, H. Leverenz, and G. Tchobanoglous, "Treatment of wastewater with slow rate systems: a review of treatment processes and plant functions," *Critical Reviews in Environmental Science and Technology*, vol. 36, no. 3, pp. 187–259, 2006.

[138] K. Hasselgren, "Use of municipal waste products in energy forestry: highlights from 15 years of experience," *Biomass and Bioenergy*, vol. 15, no. 1, pp. 71–74, 1998.

[139] G. P. Sparling, L. A. Schipper, and J. M. Russell, "Changes in soil properties after application of dairy factory effluent to New Zealand volcanic ash and pumice soils," *Australian Journal of Soil Research*, vol. 39, no. 3, pp. 505–518, 2001.

[140] L. B. Guo and R. E. H. Sims, "Soil response to eucalypt tree planting and meatworks effluent irrigation in a short rotation forest regime in New Zealand," *Bioresource Technology*, vol. 87, no. 3, pp. 341–347, 2003.

[141] F. Cabrera, R. López, A. Martinez-Bordiú, E. De Dupuy Lome, and J. M. Murillo, "Treatment of olive oil mill wastewater," *International Biodeterioration and Biodegradation*, vol. 38, no. 3-4, pp. 215–225, 1996.

[142] J. D. Rhoades, "Intercepting, isolating and reusing drainage waters for irrigation to conserve water and protect water quality," *Agricultural Water Management*, vol. 16, no. 1-2, pp. 37–52, 1989.

[143] M. C. Negri, E. G. Gatliff, J. J. Quinn, and R. R. Hinchman, "Root development and rooting at depths," in *Phytoremediation: Transformation and Control of Contaminants*, S. C. McCutcheon and J. L. Schnoor, Eds., pp. 233–262, Wiley, New York, NY, USA, 2003.

[144] R. W. Crites and E. J. Middlebrooks, *Natural Wastewater Treatment Systems*, CRC, Taylor and Francis Group, Boca Raton, Fla, USA, 2006.

[145] "Soil aquifer treatment," 2013, http://www.watersmartproject.org/watersmart/sat/sat_sat.asp.

[146] P. Nema, C. S. P. Ojha, A. Kumar, and P. Khanna, "Techno-economic evaluation of soil-aquifer treatment using primary effluent at Ahmedabad, India," *Water Research*, vol. 35, no. 9, pp. 2179–2190, 2001.

[147] S. Kaur and M. Singh, "Soil Aquifer Treatment (SAT) System: a case study," *Indian Journal of Environmental Health*, vol. 44, no. 3, pp. 244–246, 2002.

[148] Y. B. Fan, W. B. Yang, G. Li, L. L. Wu, and Y. S. Wei, "Reuse rate of treated wastewater in water reuse system," *Journal of Environmental Sciences*, vol. 17, no. 5, pp. 842–845, 2005.

[149] G. Amy and J. Drewes, "Soil aquifer treatment (SAT) as a natural and sustainable wastewater reclamation/reuse technology: fate of wastewater effluent organic Matter (EfoM) and trace organic compounds," *Environmental Monitoring and Assessment*, vol. 129, no. 1–3, pp. 19–26, 2007.

[150] F. Pliakas, A. Kallioras, I. Diamantis, and M. Stergiou, "Groundwater recharge using a Soil Aquifer Treatment (SAT) system in NE Greece," in *Advances in the Research of Aquatic Environment, Environmental Earth Sciences*, L. N. Nicolaos, G. Stournaras, and K. Katsanou, Eds., pp. 291–298, 2011.

[151] H. Abbas, R. Nasr, and H. Seif, "Study of waste stabilization pond geometry for the wastewater treatment efficiency," *Ecological Engineering*, vol. 28, no. 1, pp. 25–34, 2006.

[152] A. Jail, F. Boukhoubza, A. Nejmeddine, S. Sayadi, and L. Hassani, "Co-treatment of olive-mill and urban wastewaters by experimental stabilization ponds," *Journal of Hazardous Materials*, vol. 176, no. 1–3, pp. 893–900, 2010.

[153] WHO, "Wastewater stabilization ponds: principles of planning and practice," WHO-EMRO Technical Publication no. 10, WHO-EMRO, Alexandria, Egypt, 1987.

[154] R. Gu and H. G. Stefan, "Stratification dynamics in wastewater stabilization ponds," *Water Research*, vol. 29, no. 8, pp. 1909–1923, 1995.

[155] M. B. Pescod and D. D. Mara, "Design, operation and maintenance of wastewater stabilization ponds," in *Treatment and Use of Sewage Effluent For Irrigation*, M. B. Pescod and A. Arar, Eds., pp. 93–115, Butterworths, UK, 1988.

[156] A. Vonshak, A. Abeliovich, S. Boussiba, S. Arad, and A. Richmond, "Production of spirulina biomass: effects of environmental factors and population density," *Biomass*, vol. 2, no. 3, pp. 175–185, 1982.

[157] A. Richmond, "Outdoor mass cultures of microalgae," in *Handbook of Microalgal Mass Culture*, A. Richmond, Ed., pp. 285–330, CRC Press, Boca Raton, Fla, USA, 1986.

[158] Y. Azov, "Effect of pH on inorganic carbon uptake in algal cultures," *Applied and Environmental Microbiology*, vol. 43, no. 6, pp. 1300–1306, 1982.

[159] H. O. Buhr and S. B. Miller, "A dynamic model of the high-rate algal-bacterial wastewater treatment pond," *Water Research*, vol. 17, no. 1, pp. 29–37, 1983.

[160] D. D. Mara and H. W. Pearson, in *Design Manual for Waste Stabilization Ponds in Mediterranean Countries*, Lagoon Technology, Leeds, UK, 1998.

[161] I. Tadesse, F. B. Green, and J. A. Puhakka, "Seasonal and diurnal variations of temperature, pH and dissolved oxygen in advanced integrated wastewater pond system treating tannery effluent," *Water Research*, vol. 38, no. 3, pp. 645–654, 2004.

[162] R. Porges and K. M. Mackenthun, "Waste stabilization ponds: use, function, and biota," *Biotechnology and Bioengineering*, vol. 5, pp. 255–273, 1963.

[163] D. D. Mara and H. Pearson, "Artificial freshwater environment: waste stabilisation ponds," in *Biotechnology*, H. J. Rehm and G. Reeds, Eds., VCH Verlagsgesellschaft, Weinheim, Germany, 1986.

[164] EPA, *Principles of Design and Operations of Wastewater Treatment Pond Systems For Plant Operators, Engineers and Managers*, U.S. Environmental Protection Agency, Cincinnati, Ohio, USA, 2011.

[165] O. Amahmid, S. Asmama, and K. Bouhoum, "Urban wastewater treatment in stabilization ponds: Occurrence and removal of pathogens," *Urban Water*, vol. 4, no. 3, pp. 255–262, 2002.

[166] E. Tilley, C. Lüthi, A. Morel, C. Zurbrügg, and R. Schertenleib, *Compendium of Sanitation Systems and Technologies*, The Water Supply and Sanitation Collaborative Council (WSSCC), Geneva, Switzerland, 2008.

[167] W. J. Oswald, F. Bailey Green, and T. J. Lundquist, "Performance of methane fermentation pits in advanced integrated wastewater pond systems," *Water Science and Technology*, vol. 30, no. 12, pp. 287–295, 1994.

[168] R. W. Crites and R. C. Fehrmann, "Land application of winery stillage wastes," in *Proceedings of the 3rd Annual Madison Conference on Applied Research in Municipal Industrial Waste*, p. 12, 1980.

[169] A. Shilton, Ed., *Pond Treatment Technology*, IWA, London, UK, 2005.

[170] R. Crites and G. Tchobanoglous, *Small and Decentralized Wastewater Management Systems*, McGraw-Hill Press, Singapore, 1998.

[171] S. C. Reed, "Nitrogen removal in wastewater stabilization ponds," *Journal of the Water Pollution Control Federation*, vol. 57, no. 1, pp. 39–45, 1985.

[172] R. J. Blakemore, "Vermicology I—ecological considerations of the earthworm species used in vermiculture," in *Proceedings of the International Conference on Vermiculture and Vermicomposting*, Kalamazoo, Mich, USA, September 2000.

[173] V. A. Tzanakakis, N. V. Paranychianakis, S. Kyritsis, and A. N. Angelakis, "Wastewater treatment and biomass production by slow rate systems using different plant species," *Water Science and Technology: Water Supply*, vol. 3, no. 4, pp. 185–192, 2003.

[174] T. Manios, E. Gaki, S. Banou, A. Klimathianou, N. Abramakis, and N. Sakkas, "Closed wastewater cycle in a meat producing and processing industry," *Resources, Conservation and Recycling*, vol. 38, no. 4, pp. 335–345, 2003.

[175] D. L. Rockwood, S. M. Pisano, R. R. Sprinkle, and A. Leavell, "Stormwater remediation by tree crops in Florida," in *Proceedings of the 4th Biennial Stormwater Research Conference*, Southwest Florida Water Management District, Clearwater, Fla, USA, October 1995.

[176] R. A. Falkiner and C. J. Smith, "Changes in soil chemistry in effluent-irrigated *Pinus radiata* and *Eucalyptus grandis* plantations," *Australian Journal of Soil Research*, vol. 35, no. 1, pp. 131–147, 1997.

[177] M. J. Duncan, G. Baker, and G. C. Wall, "Wastewater irrigated tree plantations: productivity and sustainability," in *Proceedings of the 61st Annual Water Industry Engineers and Operators' Conference*, Shepparton, Australia, 1998.

[178] M. Edraki, H. B. So, and E. A. Gardner, "Water balance of swamp mahogany and Rhodes grass irrigated with treated sewage effluent," *Agricultural Water Management*, vol. 67, no. 3, pp. 157–171, 2004.

[179] USEPA, "Wastewater treatment/disposal for small communities," (EPA-625/R-92-005), Cincinnati, Ohio, USA, 1992.

[180] E. J. Middlebrooks, C. H. Middlebrooks, and S. C. Reed, "Energy requirement for small wastewater treatment systems," *Journal of the Water Pollution Control Federation*, vol. 53, no. 7, pp. 1172–1198, 1981.

Hindawi Publishing Corporation
BioMed Research International
Volume 2013, Article ID 714232, 9 pages
http://dx.doi.org/10.1155/2013/714232

Research Article

Persistent Organic Pollutants Induced Protein Expression and Immunocrossreactivity by *Stenotrophomonas maltophilia* PM102: A Prospective Bioremediating Candidate

Piyali Mukherjee[1] and Pranab Roy[2]

[1] *Department of Biotechnology, University of Burdwan, Golapbag More, Burdwan, West Bengal 713104, India*
[2] *Department of Biotechnology, Haldia Institute of Technology, Haldia, West Bengal 721657, India*

Correspondence should be addressed to Pranab Roy; pranabroy@rediffmail.com

Received 9 April 2013; Revised 26 May 2013; Accepted 5 June 2013

Academic Editor: Aiyagari Ramesh

A novel bacterium capable of growth on trichloroethylene as the sole carbon source was identified as *Stenotrophomonas maltophilia* PM102 by 16S rDNA sequencing (accession number of NCBI GenBank: JQ797560). In this paper, we report the growth pattern, TCE degradation, and total proteome of this bacterium in presence of various other carbon sources: toluene, phenol, glucose, chloroform, and benzene. TCE degradation was comparatively enhanced in presence of benzene. Densitometric analysis of the intracellular protein profile revealed four proteins of 78.6, 35.14, 26.2, and 20.47 kDa while the extracellular protein profile revealed two distinct bands at 14 kDa and 11 kDa that were induced by TCE, benzene, toluene, and chloroform but absent in the glucose lane. A rabbit was immunised with the total protein extracted from the bacteria grown in 0.2% TCE + 0.2% peptone. Antibody preadsorbed on proteins from peptone grown PM102 cells reacted with a single protein of 35.14 kDa (analysed by MALDI-TOF-mass-spectrometry) from TCE, benzene, toluene, or chloroform grown cells. No reaction was seen for proteins of PM102 grown with glucose. The PM102 strain was immobilised in calcium alginate beads, and TCE degradation by immobilised cells was almost double of that by free cells. The beads could be reused 8 times.

1. Introduction

Many substances with toxic properties have been brought into the environment through human activity. These substances vary in level of toxicity and danger to human health [1]. Trichloroethylene, mainly used as a metal degreasing solvent, a suspected carcinogen [2], and a USEPA priority pollutant, is the most commonly reported contaminant of groundwater at hazardous waste sites [3]. Toluene is a common solvent, able to dissolve paints, paint thinners, and silicone sealants [4]. Toluene is, however, much less toxic than benzene and has, as a consequence, largely replaced it as an aromatic solvent in chemical preparation. Benzene is a known carcinogen, whereas toluene has very little carcinogenic potential [5]. The major use of phenol involves its conversion to plastics or related materials. Phenol, is a strong neurotoxin and if injected into the blood stream it can lead to instant death [6]. The major use of chloroform today is in the production of the chlorodifluoromethane, a major precursor to tetrafluoroethylene, that is used in the production of teflon. The US National Toxicology Program's twelfth report on carcinogen implicates it as reasonably anticipated to be a human carcinogen [7].

Conventional methods to remove or reduce toxic substances introduced into soil or ground water via human activities include pump and treat systems, soil vapour extraction, incineration, and containment, which suffer from recognizable drawbacks and may involve some level of risk. Bioremediation is an option that offers the possibility to destroy or render harmless various contaminants using natural biological activity. The cometabolic degradation of TCE and other chlorinated and aromatic solvents such as benzene,

toluene, phenol, and chloroform by different bacteria has been extensively studied [8–11]. This research paper highlights how the soil bacterium: *Stenotrophomonas maltophilia* PM102 expresses a single 35.14 kDa protein induced in the presence of not only trichloroethylene but also toluene, benzene, and chloroform. This may be a major defence protein employed by the bacterium to degrade such toxic contaminants.

Immobilised bacterial cells and enzymes have been used in a variety of scientific, environmental, and industrial applications. Encapsulated cells have numerous advantages over free cells as seen for increased metabolic activity [12], protection from toxic substances [13], and increased plasmid stability [14]. In the present work, the study of the encapsulation of *S. maltophilia* PM102 in calcium alginate beads was implemented.

2. Materials and Methods

2.1. Bacterial Isolate. The bacterium *Stenotrophomonas maltophilia* PM102, capable of growing on TCE as the sole carbon source, was isolated from the waste disposal site of the industrial belt lining Asansol and Dhanbad, India, by serial dilution and plating technique. 10 g soil sample was suspended in 100 mL sterile distilled water. The soil particles were allowed to settle down, and 1 mL of the supernatant was transferred to 9 mL sterile distilled water containing 0.9% NaCl. Serial dilutions up to 10^{-6} were performed. 0.1 mL from all tubes was spread on plates containing King's B (KB) medium with TCE (2 μL/mL). The molecular identification of the isolated bacterium was done by 16S rDNA sequencing (universal primers 27F: 5′ AGA GTT TGA TCC TGG CTC AG 3′ and 1492R: 5′ TAC GGY TAC CTT GTT ACG ACT T 3′ were used) that was compared with reported sequences in the Genbank database. Phylogenetic tree was constructed by aligning PM102 sequence with reference sequences obtained from NCBI GenBank (Figure 1).

TCE degradation by the isolate PM102 was studied using Fujiwara test and the release of chloride ions by mineralization [15].

2.2. Growth Conditions. The PM102 strain was grown in 100 mL minimal King's B medium (Na_2HPO_4—1 g/L, K_2HPO_4—3 g/L, NH_4Cl—1 g/L, and $MgSO_4 \cdot 7H_2O$—0.4 g/L), pH 7 with 0.2% of different carbon sources, that is, toluene, phenol, glucose, chloroform, and benzene, each with 0.1% peptone by shaking at 90 rpm at 34°C for 48 hours. Growth of the bacteria was determined by measuring the absorbance at 620 nm.

2.3. Fujiwara Test to Determine TCE Degradation in Presence of Other Organic Pollutants. In the Fujiwara test, polychlorinated hydrocarbons in presence of pyridine and alkali give a red colour [16]. PM102 cells harvested from 100 mL culture in minimal medium with 0.2% TCE were suspended in 20 mL phosphate buffer with 0.3% TCE in acetone and 0.2% other carbon sources (toluene, benzene, chloroform, and phenol resp.) and incubated at 34°C at rpm 100. After every 60-minute interval, 2 mL of the cell suspension was taken and treated with 2 mL pyridine and 2 mL 5 N NaOH followed by heating at 80°C for 2 minutes. The experiment was carried out from 0 hours (just after inoculation) to 3 hours. Absorbance of the red aqueous phase was noted at 470 nm.

2.4. Protein Extraction

2.4.1. Intracellular Proteins. The cells from 100 mL culture was harvested by centrifugation at 4°C, rpm 10,000 for 10 minutes. Cell pellet thus obtained was suspended in 1 mL solution 1 (10 mM EDTA pH 8, 50 mM glucose, and 25 mM Tris-HCl pH 8) with 200 μL of 10 mg/mL lysozyme, vortexed, and incubated at 37°C for 1 hr followed by 30 minutes incubation at 4°C. Lysozyme extraction gave better cell lysis when followed by temperature shock. The suspension was centrifuged at 10,000 rpm for 10 minutes at 4°C, and the pellet containing cell debris was discarded. Supernatant thus obtained containing the intracellular proteins was stored at −20°C. Concentration of proteins was determined by Bradford's method [17].

2.4.2. Extracellular Proteins. The supernatant obtained from 100 mL culture of PM102 cells in KB medium with 0.2% carbon sources plus 0.1% peptone was treated with 30% TCA and kept at 4°C overnight. The suspension was centrifuged at 12,000 rpm for 10 minutes. The protein precipitate thus obtained was washed thrice with chilled acetone and finally dissolved in 100 μL stacking gel buffer (0.5 M Tris-HCl). Protein concentration was determined by Bradford's method.

2.5. Total Protein Profile of PM102. The extracted protein samples were boiled with Laemmli buffer (1% SDS, 5% Mercaptoethanol, 0.05% Bromophenol Blue in 25 mM Tris-HCl, and 10% glycerol, pH 6.8) for 10 minutes and electrophoresed on a 12% gel at 200 volts. Equal amount of protein was loaded in each well, that is, 40 μg intracellular proteins and 30 μg extracellular proteins, in two separate gels. The gel was stained with Coomassie Blue R250 (0.2%) and destained with 30% destainer (30 mL methanol, 7 mL acetic acid, and the rest distilled water to make a total volume of 100 mL). The gel was analysed by image analysis tool of Quantum Capt software in the gel documentation system (Vilber Lourmat, France).

2.6. Immunisation of Rabbit. A rabbit was immunised with the total protein of the bacteria grown in 0.2% TCE + 0.2% peptone. The rabbit was injected subcutaneously at 4 to 5 different sites with this protein homogenate mixed 1 : 1 with Freund's complete adjuvant twice (once per month) followed by two more injections of the same protein homogenate mixed 1 : 1 with Freund's incomplete adjuvant.

2.7. Western Blot. The SDS PAGE gel of the intracellular proteins obtained from cells grown in TCE, toluene, benzene, chloroform, glucose, and peptone, after electrophoresis (unstained), was electroblotted onto nitrocellulose membrane BA85 (Sigma Aldrich, USA) at 45 volts for 3 hours. The nitrocellulose membrane was blocked with 3% milk powder

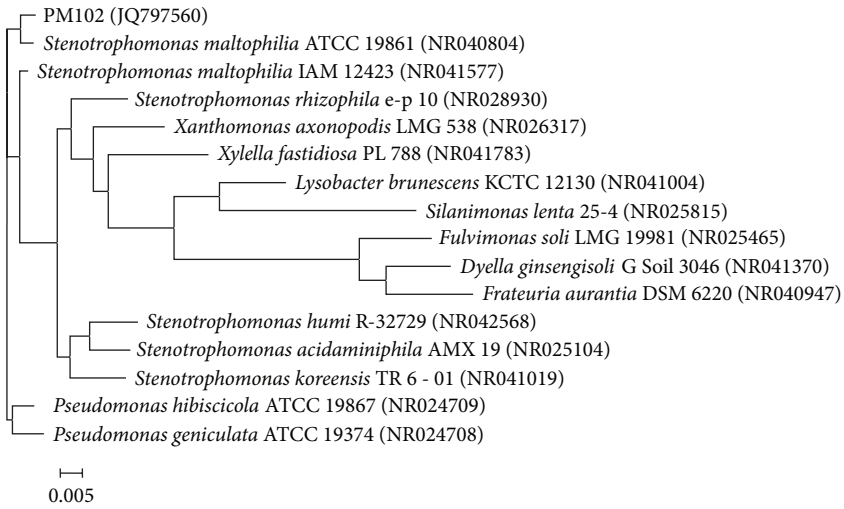

Figure 1: Neighbour joining tree based on PM102 16S rRNA gene sequence comparison with 16S rRNA gene sequences retrieved from the NCBI GenBank, constructed using MEGA 5 software. The numbers in parentheses are GenBank accession numbers (see [15]).

for 1 hour at room temperature and washed thrice with buffer A (10 mM tris HCl pH 8, 1 mM EDTA pH 8, 0.05% tween 20 and 0.9% NaCl), followed by incubation in 1 : 100 dilution of the rabbit antiserum in the same buffer, at 4°C overnight. Then the membrane was washed with buffer A thrice, five minutes each, and incubated in 1 : 15,000 dilution of goat anti-rabbit IgG coupled to alkaline phosphatase (Sigma Aldrich, USA) in buffer A for 2 hours at room temperature. The membrane was again washed in buffer A, 5 minutes each, for three times and equilibrated for 20 minutes in alkaline phosphatase buffer (100 mM tris HCl pH 9.5, 100 mM NaCl, and 5 mM $MgCl_2$). The membrane was stained with BCIP/NBT (5-bromo,4-chloro,3-indolyl phosphate/nitroblue tetrazolium) in alkaline phosphatase buffer for colour development within 15 minutes.

2.8. Preadsorption of the Serum Antibody. Small strips of nitrocellulose membrane were soaked in peptone grown cellular proteins and air dried. These strips were immersed in 1 : 100 dilution of the antiserum in buffer A and incubated by gentle shaking for 1 hour. This process was repeated until all the antibodies against the common peptone antigens were removed.

2.9. MALDI-TOF/MS Analysis. The 35.14 kDa band was excised from the Coomassie blue stained gel, destained with 250 μL 100 mM ammonium bicarbonate/acetonitrile (1 : 1 v/v) for 30 minutes with occasional vortexing. This step was repeated till all of the blue stain got removed. 500 μL 100% acetonitrile was added for 15 minutes till the gel pieces shrunk and became white in colour. Acetonitrile was discarded, and gel pieces were air dried for 10 minutes in room temperature and reswollen in 25 ng/μL Trypsin (Sigma Aldrich, USA). Trypsin digestion was performed in ice for 1 hour followed by overnight incubation at 37°C with mild shaking. The trypsinised peptide solution was taken in a fresh Eppendorf tube and lyophilised for 1 hour. The lyophilised product was dissolved in 5 μL 30% acetonitrile with 0.1% TFA solution. 4.5 μL of the peptide solution was spotted on target plate along with 4.5 μL of CHCA matrix solution and analysed with MALDI TOF Proteomics Analyzer (Applied Biosystems, Darmstadt, Germany). This was carried out at the Indian Institute of Chemical Biology, Kolkata.

2.10. Cell Immobilisation. PM102 cells were grown in 200 mL minimal KB medium with 0.2% TCE, for 48 hrs. Cells were harvested by centrifugation at 10,000 rpm, 4°C for 10 minutes. The cells thus obtained were suspended in 3.5 mL 0.05 M Tris-HCl pH 8.5 and mixed with 3.5 mL of 4% sodium alginate solution. This suspension was added dropwise to a magnetically stirred cold solution of 100 mM calcium chloride with a micropipette. All solutions were autoclaved and the entire work was performed under the laminar airflow hood. Cells immobilised in beads of calcium alginate were stirred in the calcium chloride solution for another hour at 20°C. Then the beads were washed thrice in sterile water to remove any traces of chloride and finally suspended in 50 mL solution of 0.05 mM Tris and stored at 4°C. Alginate beads without cells were used as control.

2.11. Cell Viability Test. One bead was suspended in 1 mL sterile water in an Eppendorf tube and crushed with a sterile glass rod. This 1 mL suspension was added to 9 mL sterile distilled water and serially diluted to 10^{-3} dilutions. 0.1 mL from each of the dilution tubes was spread on plates containing minimal KB medium with 0.2% TCE and incubated for 72 hrs. The number of colonies formed was counted and total number of PM102 cells present in each bead was calculated by the formula: (The number of colonies in plate × amount of inoculum added)/stage of serial dilution. Cell viability in the immobilised beads was checked after each treatment cycle.

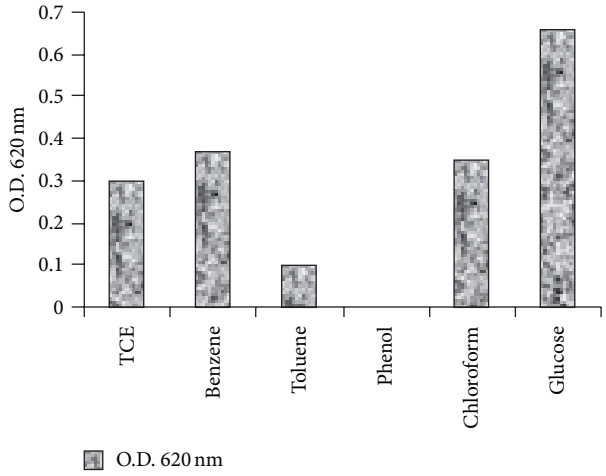

Figure 2: Growth of *S. maltophilia* PM102 in presence of different carbon sources after 48 hrs.

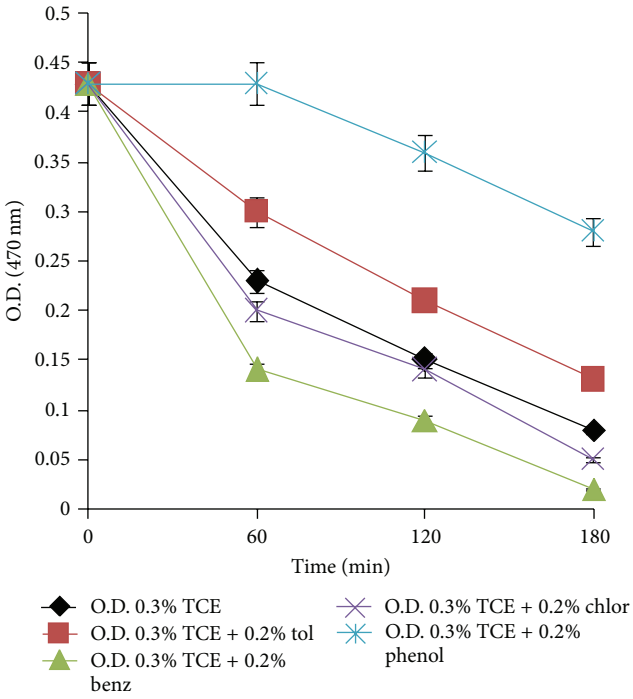

Figure 3: Degradation of 0.3% TCE by PM102 in presence of 0.2% of different carbon sources (toluene, benzene, chloroform, and phenol) as observed by Fujiwara test. Error bars with 5% SEM are displayed.

2.12. Monitoring TCE Degradation by Free and Immobilised Cells. PM102 cells, grown in 200 mL minimal KB medium with 0.2% TCE, were immobilised in calcium alginate. PM102 cells were grown in 200 mL of the same medium and harvested by centrifugation. Free cells thus obtained were used as control in the TCE degradation experiment to determine if cell immobilisation affected the rate of TCE degradation. Mineralisation of TCE to release free chloride by PM102 cells was tested by titration with silver nitrate in the presence of K_2CrO_4 as indicator. Initially, a white precipitate of AgCl,

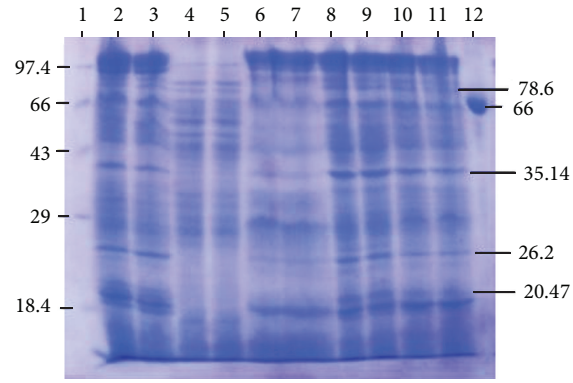

Figure 4: 12% SDS PAGE of intracellular proteins of *S. maltophilia* PM102 with different carbon sources. Lane 1 has medium molecular weight marker (kDa). Lanes 2, 3—0.2% TCE + 0.1% pep; lanes 4, 5—0.2% glucose + 0.1% pep; lanes 6, 7—0.2% toluene + 0.1% pep; lanes 8, 9—0.2% chloroform + 0.1% pep; lanes 10, 11—0.2% benzene + 0.1% pep; lane 12—BSA.

is formed when free chloride is present in the suspension but when free chloride is no longer left in the medium, the solution turns reddish brown due to the formation of Ag_2CrO_4.

The free and immobilised PM102 cells were suspended separately in 50 mL 0.05 mM Tris with 0.2% TCE and incubated at 37°C by gentle shaking for 48 hrs. 10 mL of this suspension was centrifuged and the cell pellet was discarded. The supernatant was taken in a flask, and 10 drops of 0.3 M K_2CrO_4 was added and titrated against 10 mM $AgNO_3$ at 0 hrs (just after suspension) and after 48 hrs. A standard curve was plotted by varying the concentration of NaCl from 3 mM to 15 mM, (Figure 10(a)), from which the concentration of free chloride released after the respective time intervals was calculated. The experiment was done in triplicate and mean values of the readings are given.

3. Results and Discussion

3.1. Growth in Presence of Different Carbon Sources. When the PM102 strain was grown in 0.2% of the various carbon sources, TCE, toluene, phenol, glucose, chloroform, and benzene with 0.1% peptone, an interesting growth pattern was observed (Figure 2). No growth was detected in presence of phenol even when 0.1% peptone was present in the medium, indicating that phenol has an inhibitory effect on the bacterium. Growth in presence of TCE, benzene, and chloroform was almost the same, whereas comparatively less growth was seen in presence of toluene. Glucose gave maximum growth and was used as control for the protein profile studies.

3.2. TCE Degradation in Presence of Other Organic Pollutants. In Fujiwara test, the intensity of red colour (absorbance at 470 nm) indicates the amount of polychlorinated compound still present in the medium. In the Fujiwara test for TCE

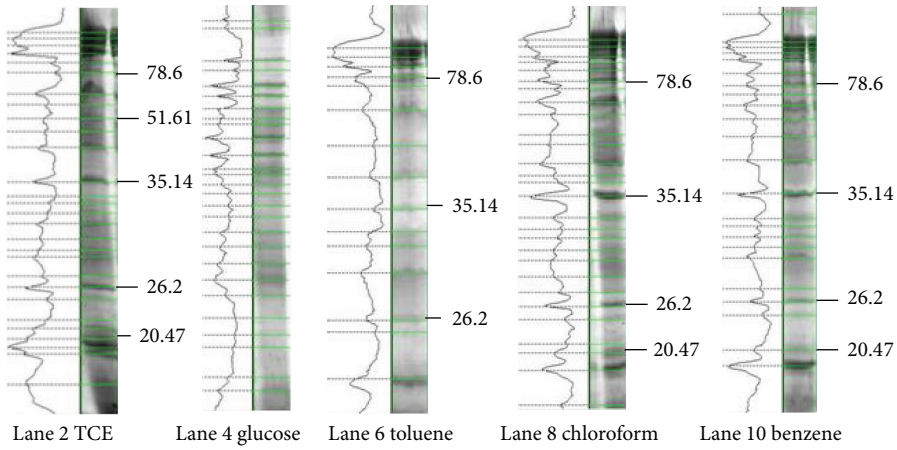

Figure 5: Densitometric analysis of the 12% gel by Quantum Capt software showing the differential expression of proteins under varying culture conditions—0.1% peptone and 0.2% of TCE, glucose, toluene, chloroform, and benzene, respectively.

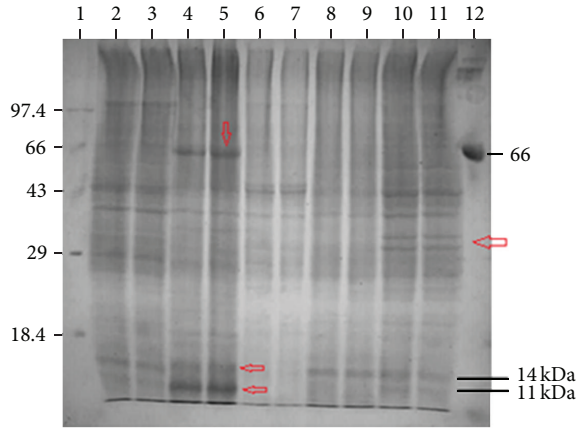

Figure 6: 12% SDS PAGE of extracellular proteins of *S. maltophilia* PM102 with different carbon sources. Lane 1 has medium molecular weight marker (kDa). Lanes 2, 3—0.2% TCE + 0.1% pep; lanes 4, 5—0.2% toluene + 0.1% pep; lanes 6, 7—0.2% glucose + 0.1% pep; lanes 8, 9—0.2% chloroform + 0.1% pep; lanes 10, 11—0.2% benzene + 0.1% pep; lane 12—BSA.

degradation by PM102, a decrease in absorbance corresponding to decrease in colour intensity of the aqueous phase with time was noted, thus confirming TCE degradation. This TCE disappearance was more rapid in presence of 0.2% benzene and 0.2% chloroform as compared to that of 0.2% toluene. A marked decrease in TCE degradation rate was noted in presence of 0.2% phenol (Figure 3).

3.3. Intracellular Protein Profile of PM102 Grown in Different Carbon Sources. Figure 4 shows the 12% SDS PAGE of lysozyme extracted intracellular proteins. Densitogram analysis of the above gel (Figure 5) clearly revealed 3 major bands of molecular weights 78.6, 35.14, and 26.2 kDa induced in the presence of TCE, toluene, chloroform, and benzene, separately. These proteins were not present when the PM102 strain was grown in the same medium with glucose as the carbon source. These carbon sources were not given in combination. PM102 cells were grown in KB medium with these carbon sources separately and intracellular proteins were extracted. A 20.47 kDa band was seen for TCE, benzene, and chloroform that was absent in toluene and glucose lanes. Thus, these induced proteins might have a possible role in the degradation of toxic pollutants like TCE, toluene, benzene, and chloroform, although further experiments are required to document the exact mechanism of degradation.

3.4. Extracellular Protein Profile of PM102 Grown in Different Carbon Sources. From the extracellular protein profile of the bacteria grown with different carbon sources, a major expressed band of 67 kDa and two prominent low molecular weight bands of 14 kDa and 11 kDa were seen in presence of toluene, which were not there in presence of glucose. These bands could be induced in presence of toluene. The low molecular weight bands were also seen in presence of the other carbon sources but were absent in the glucose lane (Figure 6).

3.5. Western Blot. Western blot analysis was carried out with intracellular proteins obtained by lysozyme extraction from PM102 strain grown with different carbon sources. In the western blot analysis with the total antiserum, bands were observed in response to TCE, toluene, benzene, and chloroform grown proteins as well as glucose grown proteins of PM102 (Figure 7(a)). Although several proteins of molecular weights 78.6, 26.2, and 20.47 kDa were induced in presence of the different carbon sources, the 35.14 kDa band was of interest because after the antiserum was preadsorbed on proteins of the PM102 isolate grown in peptone, strong response was obtained only against this single band of 35.14 kDa for TCE, benzene, toluene, or chloroform grown proteins of PM102 while no response for glucose grown proteins from PM102 was seen (Figure 7(b)).

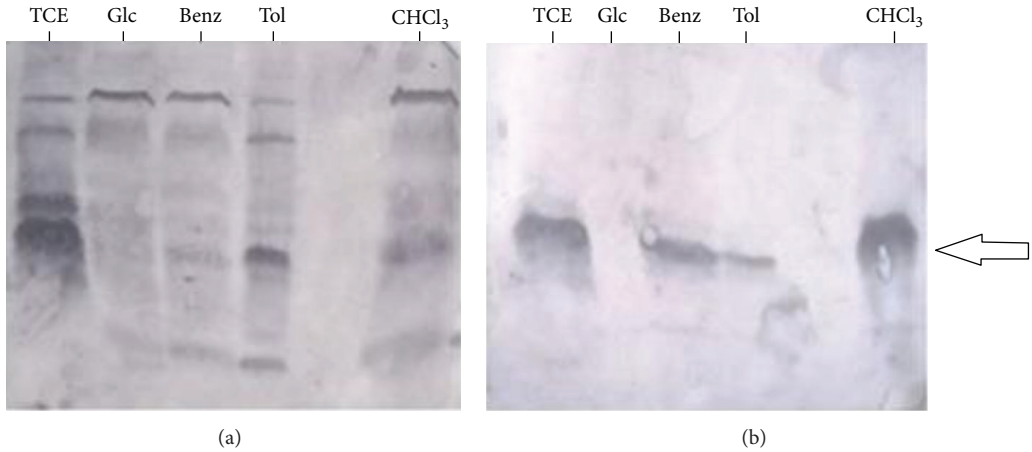

Figure 7: (a) Western blot with total antibody against intracellular proteins of PM102. First lane shows reaction against proteins from PM102 grown in 0.2% TCE + 0.1% peptone; second lane shows total antibody response against proteins extracted from PM102 isolate grown in 0.2% glucose with 0.1% peptone; third lane shows reaction against proteins from PM102 grown in 0.2% benzene and 0.1% peptone; fourth lane shows reaction of total antibody against proteins from PM102 grown with 0.2% toluene + 0.1% peptone; the last lane shows antibody response against proteins of PM102 grown in 0.2% chloroform with 0.1% peptone. (b) Western blot with antibody preadsorbed in proteins from PM102 grown in peptone. The preadsorbed antibody reacted against a single 35.14 kDa protein from PM102 grown with TCE, benzene, toluene, or chloroform. No reaction was seen against proteins from PM102 grown in glucose.

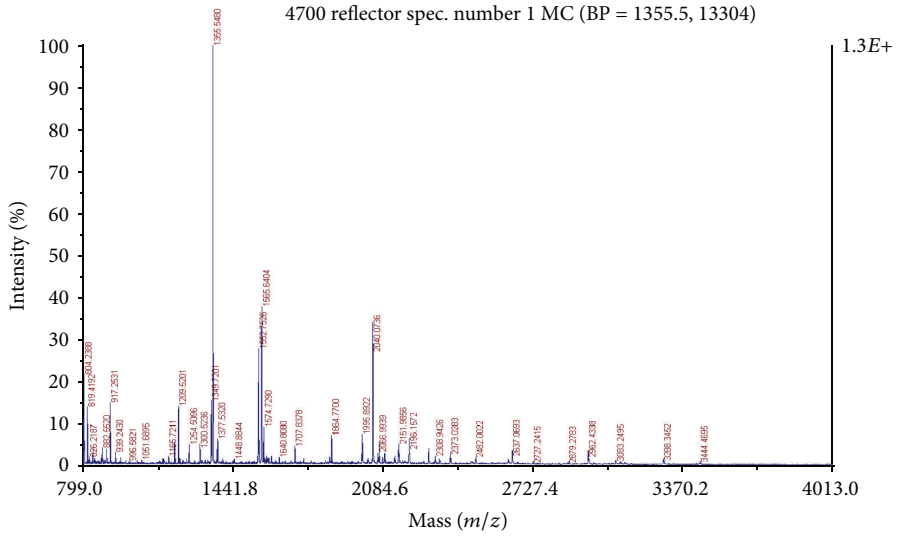

Figure 8: MS/MS spectrum of the 35.14 kDa protein following in gel digestion with 25 ng/μL trypsin.

3.6. MALDI-TOF/MS Analysis. Unless the genome of the species of interest is completely sequenced, the possible way of identifying a protein is through peptide mass fingerprinting (PMF) [18]. There is no guarantee that the true sequence of the analyte protein is actually present in the database. If it is missing, then high scoring matches from other species are of interest because they are likely to be homologous to the unknown as seen with our protein of interest. Mass spectra of the 35.14 kDa TCE inducible protein are shown in Figure 8. This data was analysed with peptide mass fingerprinting (PMF) platform: The Global Proteome Machine (Global Proteome Machine Organization) and Protein Pilot (Applied Biosystems, Foster City, CA). The PMF data was aligned to 15 proteins with existing PMF data of the group "other proteobacteria" as the PM102 isolate belonged to the class of γ proteobacteria. The highest score (60) obtained was with a hypothetical uncharacterised protein of unknown function from *Bacteroides thetaiotaomicron* (UniProtKB/TrEMBL Acc no: Q8A696) (Table 1).

The proteome of *Bacteroides thetaiotaomicron* includes an elaborate apparatus for acquiring and hydrolyzing otherwise indigestible dietary polysaccharides and an associated environment-sensing system consisting of a large repertoire of extracytoplasmic function, sigma factors, and one- and two-component signal transduction systems [19]. The PM102 strain also has extreme metabolic capabilities as it can grow

Table 1: Detailed PMF data of the 35.14 kDa protein as matched with the hypothetical protein from *Bacteroides thetaiotaomicron* (UniProtKB/TrEMBL accession number: Q8A696).

Cal mass	Obs mass	±da	±ppm	Start seq.	End seq.	Sequence	Modification
1209.5933	1209.5203	−0.073	−60	305	314	DQIMAEYALR	
1547.7498	1547.6216	−0.1282	−83	136	146	ARYWYMIQCLK	Oxidation (M) [6]
1550.752	1550.745	−0.007	−5	64	76	LANDLKNDYPEMK	
1564.7286	1564.6475	−0.0811	−52	220	233	FLVEMGAGFAFMGR	Oxidation (M) [5, 12]
1855.8795	1855.8904	0.0109	6	1	15	MENQNHAFNYAYLLK	
2040.0193	2040.0731	0.0538	26	216	233	HIEKFLVEMGAGFAFMGR	
2134.9824	2134.9143	−0.0681	−32	28	45	AIYTANEEMLSMYWDIGK	
2150.9773	2150.9834	0.0061	3	28	45	AIYTANEEMLSMYWDIGK	Oxidation (M) [9]
2279.0723	2278.8794	−0.1929	−85	27	45	KAIYTANEEMLSMYWDIGK	Oxidation (M) [10]
3081.4648	3081.2236	−0.2412	−78	191	215	DPYIFDMLTFTEEYDERDIELGLIK	Oxidation (M) [7]

on trichloroethylene as the sole carbon source and on other persistent organic pollutants in presence of peptone. The complete genome of *Stenotrophomonas maltophilia* K279a has been sequenced and found to contain organic solvent resistant gene (ostA) that encodes for organic solvent tolerance protein besides heavy metal resistance genes [20]. It is a well-known fact that trichloroethylene is used as an organic solvent for oils and resins and metal degreasing purpose [21]. As the PM102 isolate is different from the K279a strain, it may not possess the same protein (PMF data of the 35.14 kDa protein from the PM102 isolate did not match to any of the proteins from K279a in the database records as seen by MASCOT search). Thus, the 35.14 kDa protein seems to be novel without prior record in the database.

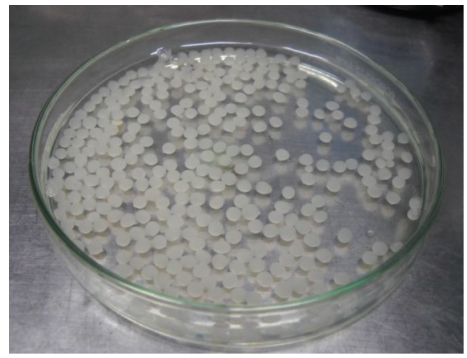

Figure 9: Calcium alginate beads containing immobilised cells of *S. maltophilia* PM102.

3.7. Monitoring TCE Degradation by Free versus Immobilised Cells. The encapsulation of the bacterial cell offers space for the cell growth and good diffusion properties and reusability which provide an extra edge to the encapsulated cells as far as bioremediation is concerned. Initial attempts of cell immobilisation failed causing disruption of the beads within 24 hrs. Initially, PM102 cells were suspended in chloride-free minimal medium: K_2HPO_4—3 g/L, Na_2HPO_4—1 g/L, $(NH_4)_2SO_4$—1 g/L, and $MgSO_4{\cdot}7H_2O$—0.4 g/L. It was assumed that phosphates present in the minimal medium weakened the cross links in the calcium alginate beads, causing bead disruption. Then, immobilisation experiment was entirely carried out by suspending the cells and beads in 0.05 mM Tris, and stability and integrity of the beads were restored (Figure 9).

The initial number of viable cells present in each bead was 1×10^6. After 5 treatment cycles, cell viability in each bead was 5×10^5. Cell leakage from the beads was measured spectrophotometrically at 620 nm. O.D. value for cell leakage was 0.1 for five cycles, but cell leakage increased to 0.5 from the 6th cycle onwards. Each treatment cycle was repeated by washing the spent medium and resuspending the beads in fresh buffer with freshly added 0.2% TCE.

The beads could be reused 8 times. After cell immobilisation, significant increase in TCE degradation was obtained (Figure 10(b)). Chloride released at 0 hours, that is, just after cell inoculation, minimal chloride (0.02 mM), was detected in the solution of 0.05 mM Tris with 0.2% TCE. After 48 hours, chloride released by free cells was 8.6 mM while by immobilised cells was 13.4 mM, as calculated from the standard curve (Figure 10(a)). Reusability was measured in terms of TCE degradation capacity. The beads retained TCE degradation capacity for 8 treatment cycles but the free cells lost TCE degradation ability from the 2nd cycle onwards. Although some amount of cell leakage was found, persistence of viable cells in the beads was detected till the 8th treatment cycle. TCE is known to be degraded to TCE epoxide or chloral hydrates that are toxic for the cell. The calcium alginate layer protects the bacterial cells from the cytotoxic attack. This is a useful characteristic of the immobilised cell that can be exploited for bioremediation of TCE.

4. Conclusion

The *Stenotrophomonas maltophilia* PM102 isolate was found to utilise trichloroethylene as the sole carbon source. The bacterium does not have the capability to grow when toluene, benzene, and chloroform are present in the medium as the only carbon source, but 0.1% peptone is needed for growth. When phenol is present, even 0.1% peptone cannot help the bacterium to survive. The PM102 isolate could degrade TCE efficiently when it was present as the sole carbon source, but TCE degradation was enhanced in presence of benzene

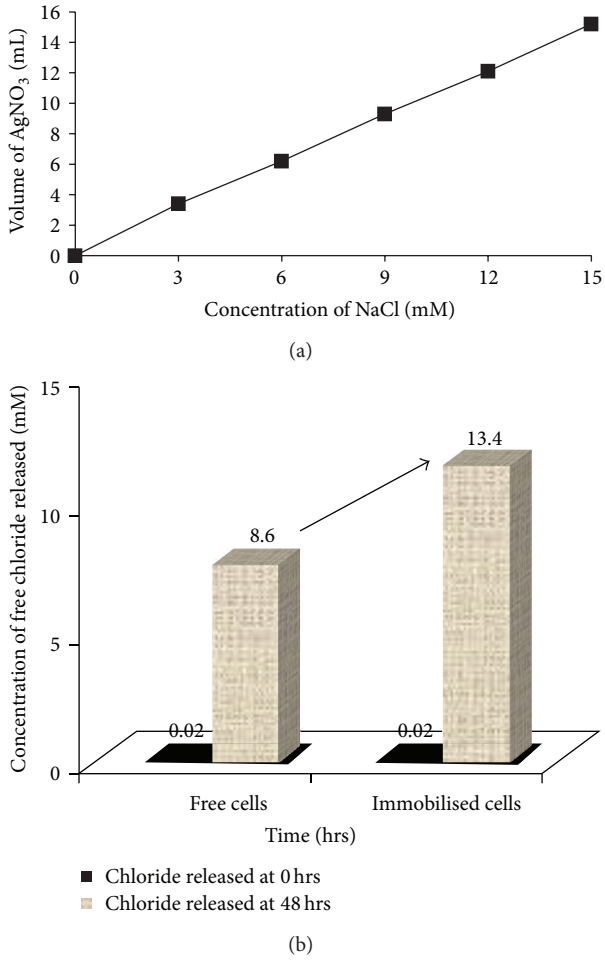

Figure 10: (a) Standard curve of chloride estimation by titration with 10 mM silver nitrate. (b) Concentration of free chloride released by mineralisation of TCE by the PM102 isolate before and after immobilisation, as plotted from the standard curve. Data shown for the first treatment cycle.

and chloroform. This indicates that some enzymes involved in the TCE degradation pathway may be common to the catabolic mechanism employed by this bacterium for the degradation of other chlorinated or aromatic contaminants. Further evidence confirming this hypothesis was obtained from the western blot where the antibody raised against TCE inducible proteins of PM102 strain also cross-reacted to toluene-, benzene- and chloroform, induced proteins obtained from the same strain. MALDI-TOF/MS identification of the common 35.14 kDa protein revealed that there is no prior record of this protein in the database. Further work involving purification and structural evaluation of this novel protein needs to be done.

The theoretical amount of chloride released from 0.2% TCE is 15.22 mM, considering that all the TCE added remains in solution. In the titration experiment, chloride released by PM102 free cells was found to be 8.6 mM, after 48 hours, that increased considerably to 13.4 mM when PM102 cells were immobilised in calcium alginate. Thus, this bacterium could mineralise 0.2% TCE added initially to free chloride by 57% while after immobilisation TCE mineralisation by the same bacterium was enhanced to 88%.

Conflict of Interests

This is to declare that there is no conflict of interest among the authors of this paper or with any other person regarding the processes/software used for this research work.

Acknowledgments

The authors would like to acknowledge the Department of Science and Technology (DST), New Delhi, India, for the grant of INSPIRE fellowship (Innovation in Science Pursuit for Inspired Research) and supporting this research work. The authors also acknowledge Mrigendranath Mondal endowment to the Department of Biotechnology, Burdwan University.

References

[1] M. Van den Berg, L. S. Birnbaum, M. Denison et al., "The 2005 World Health Organization reevaluation of human and mammalian toxic equivalency factors for dioxins and dioxin-like compounds," *Toxicological Sciences*, vol. 93, no. 2, pp. 223–241, 2006.

[2] T. Brüning, G. Weirich, M. A. Hornauer, H. Höfler, and H. Brauch, "Renal cell carcinomas in trichloroethene (TRI) exposed persons are associated with somatic mutations in the von Hippel-Lindau (VHL) tumour suppressor gene," *Archives of Toxicology*, vol. 71, no. 5, pp. 332–335, 1997.

[3] http://ntp.niehs.nih.gov/index.cfm?objectid=72016262-BDB7-CEBA-FA60E922B18C2540.

[4] Dual cure, "Low-solvent silicone pressure sensitive adhesives," Patent 6387487.

[5] C. Dees, M. Askari, and D. Henley, "Carcinogenic potential of benzene and toluene when evaluated using cyclin-dependent kinase activation and p53-DNA binding," *Environmental Health Perspectives*, vol. 104, no. 6, pp. 1289–1292, 1996.

[6] S. Budavari, Ed., *The Merck Index: An Encyclopedia of Chemical, Drugs, and Biologicals*, Merck, Whitehouse Station, NJ, USA, 1996.

[7] International Agency for Research on Cancer (IARC), "- Summaries & evaluations: chloroform," http://www.inchem.org/documents/iarc/vol73/73-05.html.

[8] M.-K. Chang, T. C. Voice, and C. S. Criddle, "Kinetics of competitive inhibition and cometabolism in the biodegradation of benzene, toluene, and *p*-xylene by two *Pseudomonas* isolates," *Biotechnology and Bioengineering*, vol. 41, no. 11, pp. 1057–1065, 1993.

[9] M. R. Fries, L. J. Forney, and J. M. Tiedje, "Phenol- and toluene-degrading microbial populations from an aquifer in which successful trichloroethene cometabolism occurred," *Applied and Environmental Microbiology*, vol. 63, no. 4, pp. 1523–1530, 1997.

[10] P. Juteau, V. Côté, M.-F. Duckett et al., "*Cryptanaerobacter phenolicus* gen. nov., sp. nov., an anaerobe that transforms phenol into benzoate via 4-hydroxybenzoate," *IJSEM*, vol. 55, no. 1, pp. 245–250, 2005.

[11] M. Rehfuss and J. Urban, "Rhodococcus phenolicus sp. nov., a novel bioprocessor isolated actinomycete with the ability to degrade chlorobenzene, dichlorobenzene and phenol as sole carbon sources," *Systematic and Applied Microbiology*, no. 8, pp. 695–701, 2005, Erratum in *Systematic and Applied Microbiology*, vol. 29, no. 2, pp. 182, 2006.

[12] B. Hilge-Rotmann and H.-J. Rehm, "Comparison of fermentation properties and specific enzyme activities of free and calcium-alginate-entrapped *Saccharomyces cerevisiae*," *Applied Microbiology and Biotechnology*, vol. 33, no. 1, pp. 54–58, 1990.

[13] M. K. Kim, I. Singleton, C.-R. Yin, Z.-X. Quan, M. Lee, and S.-T. Lee, "Influence of phenol on the biodegradation of pyridine by freely suspended and immobilized *Pseudomonas putida* MK1," *Letters in Applied Microbiology*, vol. 42, no. 5, pp. 495–500, 2006.

[14] X.-A. Chen, Z.-N. Xu, P.-L. Cen, and W. K. R. Wong, "Enhanced plasmid stability and production of hEGF by immobilized recombinant *E. coli* JM101," *Biochemical Engineering Journal*, vol. 28, no. 3, pp. 215–219, 2006.

[15] P. Mukherjee and P. Roy, "Identification and characterisation of a bacterial isolate capable of growth on trichloroethylene as the sole carbon source," *Advances in Microbiology*, vol. 2, no. 3, pp. 184–194, 2012.

[16] M. S. Moss and H. J. Rylance, "The Fujiwara reaction: some observations on the mechanism," *Nature*, vol. 210, no. 5039, pp. 945–946, 1966.

[17] M. M. Bradford, "A rapid and sensitive method for the quantitation of microgram quantities of protein utilizing the principle of protein dye binding," *Analytical Biochemistry*, vol. 72, no. 1-2, pp. 248–254, 1976.

[18] B. Thiede, W. Höhenwarter, A. Krah et al., "Peptide mass fingerprinting," *Methods*, vol. 35, pp. 237–247, 2005.

[19] J. Xu, M. K. Bjursell, J. Himrod et al., "A genomic view of the human-*Bacteroides thetaiotaomicron* symbiosis," *Science*, vol. 299, no. 5615, pp. 2074–2076, 2003.

[20] L. C. Crossman, V. C. Gould, J. M. Dow et al., "The complete genome, comparative and functional analysis of *Stenotrophomonas maltophilia* reveals an organism heavily shielded by drug resistance determinants," *Genome Biology*, vol. 9, no. 4, article no. R74, 2008.

[21] United States National Institute for Occupational Safety and Health, Centres for Disease Control and Prevention, "Workplace safety and health topics," http://www.cdc.gov/niosh/topics/organsolv/.

Hindawi Publishing Corporation
BioMed Research International
Volume 2013, Article ID 392573, 9 pages
http://dx.doi.org/10.1155/2013/392573

Research Article

Enhanced Removal of a Pesticides Mixture by Single Cultures and Consortia of Free and Immobilized *Streptomyces* Strains

María S. Fuentes,[1] Gabriela E. Briceño,[2,3] Juliana M. Saez,[1] Claudia S. Benimeli,[1,4,5] María C. Diez,[2] and María J. Amoroso[1,4,6]

[1] *Planta Piloto de Procesos Industriales Microbiológicos (PROIMI-CONICET), Avenida Belgrano y Pasaje Caseros, 4000 Tucumán, Argentina*
[2] *Núcleo de Desarrollo Científico Tecnológico, Universidad de La Frontera, Avenida Francisco Salazar 01145, 4780000 Temuco, Chile*
[3] *Departamento de Ingeniería Química, Universidad de La Frontera, Avenida Francisco Salazar 01145, 4780000 Temuco, Chile*
[4] *Universidad del Norte Santo Tomás de Aquino, 9 de Julio 165, 4000 Tucumán, Argentina*
[5] *Unidad de Administración Territorial, Centro Científico Tecnológico, CONICET-Tucumán, Crisóstomo Álvarez 722, 4000 Tucumán, Argentina*
[6] *Facultad de Bioquímica, Química y Farmacia, Universidad Nacional de Tucumán, Ayacucho 491, 4000 Tucumán, Argentina*

Correspondence should be addressed to María J. Amoroso; mjamoroso@ciudad.com.ar

Received 24 April 2013; Revised 7 June 2013; Accepted 13 June 2013

Academic Editor: Kannan Pakshirajan

Pesticides are normally used to control specific pests and to increase the productivity in crops; as a result, soils are contaminated with mixtures of pesticides. In this work, the ability of *Streptomyces* strains (either as pure or mixed cultures) to remove pentachlorophenol and chlorpyrifos was studied. The antagonism among the strains and their tolerance to the toxic mixture was evaluated. Results revealed that the strains did not have any antagonistic effects and showed tolerance against the pesticides mixture. In fact, the growth of mixed cultures was significantly higher than in pure cultures. Moreover, a pure culture (*Streptomyces* sp. A5) and a quadruple culture had the highest pentachlorophenol removal percentages (10.6% and 10.1%, resp.), while *Streptomyces* sp. M7 presented the best chlorpyrifos removal (99.2%). Mixed culture of all *Streptomyces* spp. when assayed either as free or immobilized cells showed chlorpyrifos removal percentages of 40.17% and 71.05%, respectively, and for pentachlorophenol 5.24% and 14.72%, respectively, suggesting better removal of both pesticides by using immobilized cells. These results reveal that environments contaminated with mixtures of xenobiotics could be successfully cleaned up by using either free or immobilized cultures of *Streptomyces*, through *in situ* or *ex situ* remediation techniques.

1. Introduction

The agriculture sector is a very important part of the economy and provides foods and raw materials needed for a sustainable development. For this reason, this sector uses different resources as pesticides, chemical fertilizers, equipment, and machines [1]. Pesticides are usually applied simultaneously or one after another for crop protection, and this type of pesticide application often leads to a combined contamination of these compound residues in the soil environment [2]. Among the pesticides, compounds such as organochlorines, organophosphates, carbamates, and pyrethroids are commonly used in vegetables and other crops, in order to increase the productivity [3]. As a result, an increase in the pesticide application translates into an increase in their residues in all spheres of environment [4], especially in agricultural soils.

Because of the restriction imposed on toxic organophosphate compounds, chlorpyrifos (CP), a broad-spectrum and moderately toxic organophosphate insecticide, has gained the status of one of the most widely used commercial compounds [5]. The widespread use of this pesticide and its resulting residues, which accumulates on agricultural crops, produces an increase of not only environmental contamination but

also health hazards to consumers [6]. Moreover, it has been determined that CP resistance to biodegradation is increased due to the accumulation of one of its main byproducts known as 3,5,6-trichloro-2-pyridinol (TCP). TCP is listed as a persistent and mobile pollutant by the US Environmental Protection Agency [7] and shows relatively high antimicrobial effects on microorganisms, which prevents its own degradation [8]. The contamination of soil by CP can be caused by the handling of the pesticide in the farmyard and by the rinsing of containers [6]. CP, among others pesticides, has been detected in groundwater in Greece: 0.005–0.01 $\mu g\,L^{-1}$, and in Brazil in superficial water, rivers, and lakes: 0.001–0.174 $\mu g\,L^{-1}$ [9].

Other substances widely used in both agricultural and industrial sector are chlorophenolic compounds, which are applied as broad spectrum biocides [10]. Among them, pentachlorophenol (PCP) and its sodium salt have been used as wood and leather preservatives [11]. PCP is toxic to all life forms since it inhibits oxidative phosphorylation [12]. Furthermore, it can accumulate in living organisms and thus produce adverse effect as carcinogenicity and acute toxicity [13]. In addition, this compound is highly recalcitrant due to the stability of the aromatic ring and its high degree of chlorination [14], whereby it can be considered as a hazardous pollutant for the environment. In surface waters from different countries, PCP was detected at concentrations ranging from trace levels to 10,500 $\mu g\,L^{-1}$ [13]. In Chile, it was found in water samples of the Limari river basin [9].

Thus, remediation of CP and PCP-contaminated sites is urgently required. A number of methods, including chemical treatment, volatilization, photodecomposition, incineration, and stockpiling, can be applied for the detoxification of these xenobiotic compounds [15–17]. However, most of them are not applicable for diffused contamination at low concentration making it expensive, slow, inefficient, and not always environmental friendly. Thus, biotic degradation is one of the most viable options for the remediation of CP and PCP in soil and water.

In some early studies, CP was reported to be resistant to biodegradation due to accumulation of the antimicrobial degradation products in soil [18]. However, subsequent studies have revealed that many microorganisms are capable of degrading CP efficiently [19–22]. Moreover, different researchers have reported PCP degrading microorganisms from the natural environment. Several bacterial strains such as *Arthrobacter, Pseudomonas, Sphingobium chlorophenolicum,* and *Serratia marcescens* capable of PCP degradation have been reported [23–26]. Among Gram-positive microorganisms, actinobacteria have a great potential for biodegradation of organic and inorganic toxic compounds, and previous studies demonstrated the ability of different genera of actinobacteria to degrade pesticides such as lindane, chlordane, methoxychlor, CP, diuron, and PCP [6, 27, 28].

Complete mineralization of pesticides or their transformation to nontoxic products is desirable in bioremediation process, which is more reasonable with the use of microbial consortia rather than single cultures [29]. Microbial consortia have been shown to be more suitable for bioremediation of recalcitrant compounds as their biodiversity supports environmental survival and increase the number of catabolic pathways available for contaminant biodegradation [30]. However, there are no reports about simultaneous bioremediation of CP and PCP, particularly by actinobacteria consortia. Thus, the aim of this work was to evaluate the ability of pure as well as mixed actinobacteria cultures isolated from different contaminated environments, to degrade a pentachlorophenol and chlorpyrifos mixture, using free and immobilized microbial cells.

2. Materials and Methods

2.1. Chemicals. Chlorpyrifos (CP) (99% pure) and pentachlorophenol (PCP) (98% pure) were purchased from Sigma-Aldrich Co. (St. Louis, MO, USA). All other chemicals used throughout the study were of analytical grade and were purchased from standard manufacturers.

2.2. Microorganisms and Culture Media. Four *Streptomyces* spp. (A2, A5, A11, and M7) isolated from organochlorine pesticides contaminated Argentinian soils and sediments [27, 31], and other two strains (*Streptomyces* spp. AC5 and AC7) isolated from a Chilean soil contaminated with organophosphorus pesticides [6], were used in this study. These actinobacteria were grown as single cultures and combined as different microbial consortia. The first mixed culture was an Argentinian microbial consortium (*Streptomyces* spp. A2-A5-A11-M7), known for its lindane biodegradation potential [32]; the second one was a combination of the two Chilean strains (*Streptomyces* spp. AC5 and AC7), and the third consortium consisted of the six actinobacteria strains together.

Starch-casein medium (SC) was used for antagonism assays, consisting of ($g\,L^{-1}$): starch, 10.0; casein, 1.0; K_2HPO_4, 0.5; agar, 15.0. The pH was adjusted to 7.0 prior to sterilization.

Minimal medium (MM) was used for growth of the microorganisms and pollutants removal assays. It consisted of ($g\,L^{-1}$): L-asparagine, 0.5; K_2HPO_4, 0.5; $MgSO_4{\cdot}7H_2O$, 0.2; $FeSO_4{\cdot}7H_2O$, 0.01 [33]. The same medium was added with agar, 15.0 $g\,L^{-1}$, for tolerance to toxicity of CP and PCP assay. The pH was adjusted to 7.0 prior to sterilization.

Tryptic Soy Broth (TSB), containing ($g\,L^{-1}$): trypticase, 15.0; soy peptone, 3.0; NaCl, 5.0; K_2HPO_4, 2.5; glucose, 2.5, was used for the inocula preparation for the immobilization technique. The pH was adjusted to 7.3 ± 0.2 prior to sterilization.

All media were sterilized by autoclaving at 121°C for 15 min.

2.3. Antagonism and Tolerance Assays. In order to determine the potential presence of antagonistic effects among the *Streptomyces* spp. strains studied, a modification of Bell et al. [34] technique was used. One *Streptomyces* strain was spread in the center of a Petri dish containing SC medium and faced transversely with the other *Streptomyces* spp. strains. One strain was considered to be antagonistic to the other when a growth inhibition was observed. Thereby, the presence of antagonism among the six studied

strains was assessed by considering all possible combinations [32].

To evaluate the tolerance of *Streptomyces* spp. strains to the pesticide mixture (CP and PCP), a qualitative assay was performed using MM agar plates. Rectangular troughs were cut in the centre of the plate and then filled with a filter-sterilized solution of the mixed pesticides (CP and PCP, each at a concentration of 1.66 mg L^{-1}). The actinobacteria strains were inoculated by streaking perpendicularly to the troughs. Microbial growth was used as a qualitative parameter of the tolerance to the pesticides mixture. The Petri dishes were incubated at 30°C for seven days. Growth controls were performed using plates without pesticides [35].

2.4. Study of the Ability of Pure and Mixed Actinobacteria Cultures to Grow and Remove the Pesticide Mixture. 2 g L^{-1} of biomass (wet weight) of the microbial consortia *Streptomyces* spp. A2-A5-A11-M7 and *Streptomyces* spp. AC5 and AC7 and the six pure actinobacteria strains were inoculated in different Erlenmeyer flasks containing 30 mL MM spiked with the pesticides mixture (1.66 mg L^{-1} of each one). Cultures were incubated at 30°C for 72 h on a rotary shaker at 200 rpm and then centrifuged (8,500 ×g, 10 min and 4°C). Ten milliliters of the supernatant were aseptically taken out in each case for residual pesticides determination. Microbial growth was measured as dry weight at 105°C. All experiments were carried out in triplicate, and the results are given as the means.

2.5. Removal of Pesticides Mixture by a Free and Immobilized Consortium of Six Streptomyces spp. Strains. All *Streptomyces* spp. strains were individually cultured in TSB for 72 h at 30°C and 200 rpm. The cultures were centrifuged at 8,500 ×g for 10 min, and the pellets obtained were then washed with sterile distilled water for the immobilization. For this, the actinobacteria consortium (*Streptomyces* spp. A2-A5-A11-M7-AC5-AC7, each strain at equal proportion), was mixed with a sodium alginate solution, obtaining a final concentration of 7.5% of biomass in the support (w/v, wet weight) of the mixed culture [36]. This mixture was poured into 2% $CaCl_2 \cdot 2H_2O$ solution and incubated at room temperature for 1 h. Then, the beads (3–5 mm diameter) were washed three times with sterile distilled water [37]. All the materials used for the preparation of the entrapped cells were sterilized, and the operations were carried out under sterile conditions.

The immobilized consortium was inoculated into MM containing mixed pesticides (CP and PCP, 1.66 mg L^{-1} of each one) and subsequently incubated for 72 h at 30°C. Samples collected every 24 h were analyzed for residual pesticides concentrations.

For free cell culture assays with all the *Streptomyces* spp. strains together, the methodology used was the same described above (see Section 2.4).

2.6. Analysis of Pentachlorophenol and Chlorpyrifos. Supernatant samples of the centrifuged cultures were used to determine residual CP and PCP concentrations. For residual CP concentration determination, 1 mL of each sample was diluted to a volume of 10 mL with distilled water, and then it was extracted twice with 10 mL of hexane. The organic extracts were combined and dehydrated with Na_2SO_4. The samples were stored at −20°C before chromatographic analysis. A Shimadzu gas chromatograph GC-2014 equipped with an RTX-5 capillary column (crossbond 5% diphenyl/95% dimethyl polysiloxane, 30 m, 0.32 mm i.d., film thickness 0.25 μm), and NPD detector was used. The injection and detector temperatures were set at 280°C and 300°C, respectively. The oven temperature program began at 90°C for 1 min, increased to 180°C at 15°C/min, then increased to 240°C at 5°C/min, and finally increased to 280°C at 15°C/min. The obtained data were analyzed with the program GC Solution Version 2.30.00 (GC Solution Analysis Copyright 2000–2004 Shimadzu) [6]. The retention time for CP was 12.5 min. The recovery of CP in the liquid medium was 90%.

Residual PCP concentration was determined with an HPLC equipped with a Merck-Hitachi L-7100 pump, a Rheodyne 7725 injector with a 20-μL loop, a Merck-Hitachi L-7455 diode array detector operating at 215 nm and a Hitachi D-7000 data processor. A LiCHrospher 60 RP select B 250 × 4 mm column of 5 μm particle size with a LichroCART 4-4 guard column (Merck) was used. The mobile phase consisted of acetonitrile and phosphoric acid (1% aqueous solution) 1 : 1 (v/v) with a flow rate of 1 mL min^{-1}. In these operative conditions, PCP retention time was 12 min [38]. Method calibration and quantification was performed by the pure reference standard (0.05–5 mg L^{-1}). The recovery of PCP ranged from 97% to 100%.

2.7. Statistical Analysis. All the results are the average of three replicates per sample. One-way analysis of variance (ANOVA) and Tukey test were performed to test the significant differences among treatments. When significant differences were found, Tukey post-test was used to separate the effects among treatments. Tests were considered significantly different at $P < 0.05$. Professional versions of Infostat and Statistic 6.0 software were used.

3. Results and Discussion

3.1. Antagonism and Tolerance Assays. In order to formulate mixed cultures, all the studied actinobacteria were assayed to determine the presence of antagonistic effects among them. The antagonistic phenomenon is a common event showed in a mixed microbial population [39]. In case of *Streptomyces* spp. strains isolated from Argentinean and Chilean environments, no antagonistic effect on their individual growth was observed (Figure 1), which suggests that all the strains could be cultured together as a consortium. In contrast, Thouand et al. [40] observed the presence of antagonistic relations in a mixed microbial population, which exerted a negative impact on the ability of oil degradation in liquid systems. In fact, van Hamme et al. [41] showed the presence of antagonistic relations in bacterial populations within a mixed community, due to the metabolites production capable of killing or inhibiting the growth of other populations.

Although it have been described actinobacteria capable of tolerating and/or degrading CP or PCP [6, 28, 42, 43],

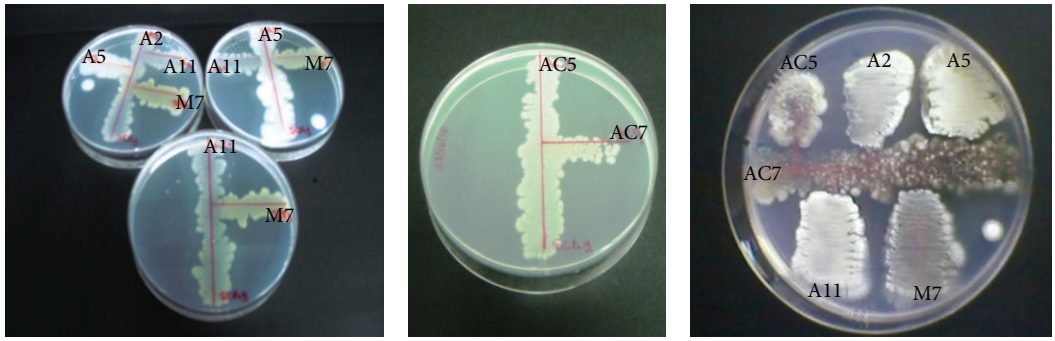

(a) (b) (c)

Figure 1: Antagonism assays among: (a) *Streptomyces* spp. A2, A5, A11, and M7; (b) *Streptomyces* spp. AC5 and AC7; and (c) the six *Streptomyces* spp. strains.

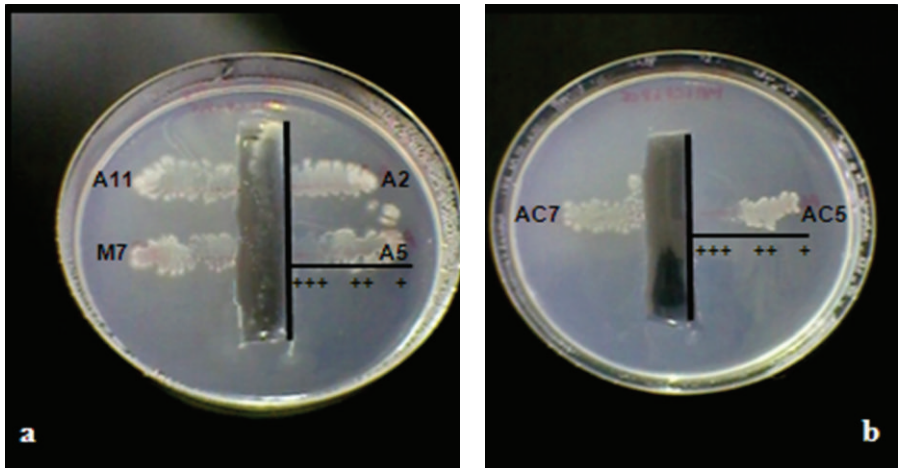

(a) (b)

Figure 2: Tolerance assays of the studied actinobacteria to the mixture of CP and PCP (1.66 mg L^{-1} of each one). (a) *Streptomyces* spp. A2, A5, A11, and M7. (b) *Streptomyces* spp. AC5 and AC7. (+++) Abundant growth: highly tolerant, (++) moderate growth: tolerant, (+) scarce growth: lowly tolerant, and (−) no growth: not tolerant.

it was necessary to evaluate the ability of the actinobacteria to tolerate the pesticides mixture. Thereby, when the actinobacteria tolerance to the mixed pesticides was tested, it was observed that four of them (*Streptomyces* spp. A2, A11, M7 and AC7) showed a high degree of tolerance to the toxic mixture, while the other two strains (*Streptomyces* spp. A5 and AC5) presented moderate tolerance, based on qualitative analyses taking into account the degree of growth of each strain in the surroundings of the mixture of pesticides (Figure 2). This experimental technique was used previously for systematic screening on heavy metals resistance and organochlorine pesticides tolerance by actinobacteria [31, 44]. The results presented here would indicate that the pesticides mixture concentration used were not toxic for these actinobacteria strains under the evaluated experimental conditions.

3.2. Microbial Growth and Removal of Pesticides Mixture by Pure and Mixed Actinobacteria Cultures. Based on obtained results (Section 3.1) and previous studies, which describe the actinobacteria abilities to use compounds with chlorine atoms in their molecules as carbon source [6, 27, 28, 43, 45], the growth of the strains as pure and mixed cultures in liquid MM supplemented with the pesticides mix (CP + PCP) was evaluated. Microbial biomass (dry weight) of the pure cultures ranged between 5 and 21.7 mg L^{-1}, whereas the growth of the mixed cultures was significantly higher ($P < 0.05$), reaching a biomass of 98.3 mg L^{-1} for the mixed culture of *Streptomyces* spp. AC5-AC7 and 101.67 mg L^{-1} for *Streptomyces* spp. A2-A5-A11-M7 (Figure 3). In absence of the pesticides mixture in the culture medium, no growth was detected. The highest biomass production of mixed cultures could be explained due to a metabolic action complementary among actinobacteria in the consortia, which make them capable of allowing the most efficient use of these pesticides as carbon source. In previous studies, Yang et al. [46] observed a high atrazine mineralizing efficiency when a mixed culture *of Klebsiella* sp. A1 and *Comamonas* sp. A2 was used. However, when these authors used pure cultures, they obtained no or poor growth and no or less atrazine degrading ability. In the present study, the results showed an increase of the biomass

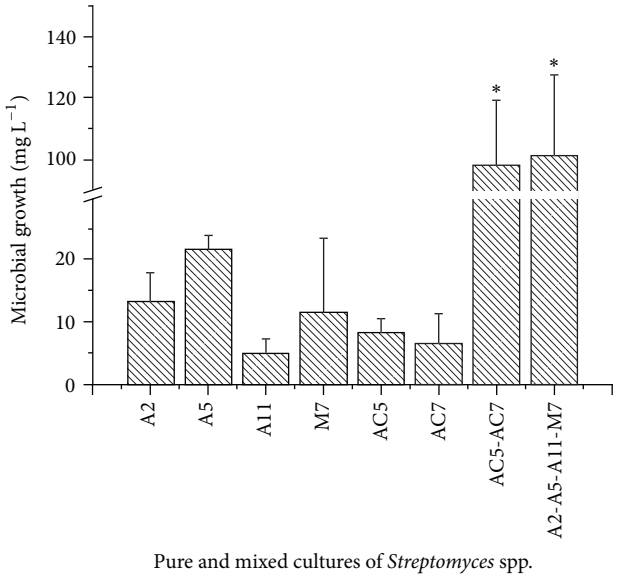

Figure 3: Microbial growth of pure and mixed cultures of *Streptomyces* spp. in MM contaminated with a mixture of chlorpyrifos (CP) and pentachlorophenol (PCP). Bars showing asterisk indicate they were significantly different to all others ($P < 0.05$, Tukey post-test).

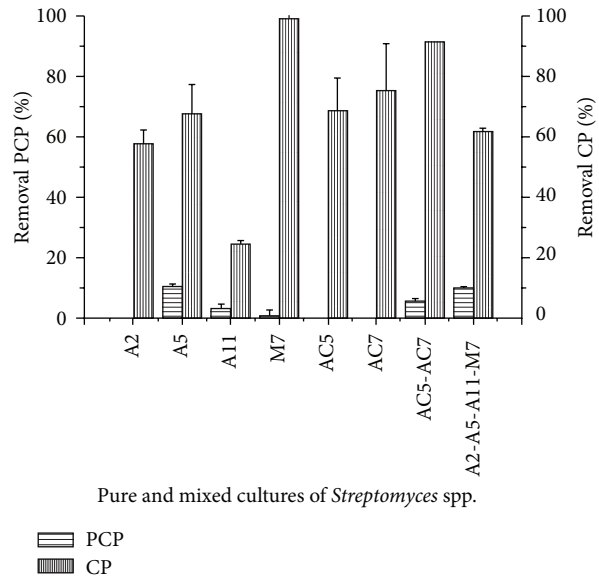

Figure 4: Removal percentages of pentachlorophenol (PCP) and chlorpyrifos (CP) in pure and mixed cultures of *Streptomyces* spp. in minimal medium contaminated with the pesticides mixture.

when increasing the number of strains in the culture medium, demonstrating that there is no inhibition of growth by the presence of pesticides or antagonism among strains.

The pesticide removal abilities of the pure and mixed cultures were determined by analyzing CP and PCP residual concentrations. It was observed that *Streptomyces* sp. A5 and the mixed culture *Streptomyces* spp. A2-A5-A11-M7 presented similar PCP removal percentages (10.6 and 10.1%, resp.); the mixed culture *Streptomyces* spp. AC5-AC7 only removed 6% of PCP; instead *Streptomyces* spp. A2, AC5, and AC7 in pure cultures did not show the ability to remove PCP (Figure 4). Compared to most of the pure cultures, removal of PCP was significantly enhanced ($P < 0.05$) when these strains were grown in a coculture. Similar enhanced degradation has been observed in many studies of different pesticide-degrading consortia. For instance, Sørensen et al. [47] reported an enhancement of 59% in the mineralization of isoproturon when *Sphingomonas* sp. SRS2 was grown in coculture with SRS1 strain, rather than pure. Other coculture was able to mineralize a 62% of the added diuron (10 mg L^{-1}) in a mineral medium due to the cooperative degradative capacities of *Arthrobacter globiformis* strain D47 and *Variovorax* sp. strain SRS16, since neither strain D47 nor strain SRS16 was capable of performing extensive mineralization of the herbicide in pure culture [48]. In natural environments, microorganisms are heterogeneously distributed and possibly occur in multispecies rather than single-species communities [47]. Close proximity within the community may synergistically improve the metabolism of organic pollutants introduced into the environment [47]. In these studies, neither strain *Streptomyces* sp. AC5 nor strain *Streptomyces* sp AC7 conclusively removed PCP in MM but combined the constructed two-member consortium removed approximately 6% of PCP, demonstrating that synergistic interactions between both strains may be involved in the degradation of PCP.

All the pure and mixed actinobacteria cultures were able to remove CP, reaching removal percentages greater than PCP removal. The strain *Streptomyces* sp. M7 in pure culture showed the best CP removal capability (99.2%) but the mixed culture *Streptomyces* spp. AC5-AC7 also showed high ability for CP removal (91.52%) (Figure 4). In previous studies, Krishna and Philip [3] observed great differences in the removal efficiency of three toxic compounds in a submerged soil system contaminated with a mixture of pesticides (carbofuran, lindane, and methyl parathion at a final concentration of 2 mg g^{-1} of soil), where carbofuran degradation was maximum whereas minimum degradation was observed for lindane, both in the soil phase and in the liquid phase. They also found that in the mixture of these pesticides, the degradation efficiency was minor than the efficiency detected in systems contaminated with one pesticide at a time. This phenomenon was attributed to the lower number of microorganisms available to degrade specific individual pesticides. In the present work, this phenomenon could also explain the low PCP removal obtained in comparison to CP removal, although further studies are required to prove it. On the other hand, Buono et al. [49], who studied the toxic effects of pesticides of current use (PCP, azinphos-methyl (AZM) and CP) on the development of *Paracentrotus lividus* embryos, demonstrated that the most toxic pesticides were PCP and AZM at EC50 (median toxic effect concentration 50%) level. They also observed that PCP toxic effects were not significant at concentrations below 0.03 mg L^{-1}, but at higher concentrations, such as 0.3 mg L^{-1}; the effects were significant. In this work, the PCP concentration was approximately 5.5 times higher than 0.3 mg L^{-1}, which could be

another reason for the minor removal of this compound. On the contrary, Matamoros et al. [50], in a study pertaining to behavior of organic pollutants in constructed wetlands, found that PCP removal efficiency was higher (>90%) than CP removal (80%–90%), starting with an initial concentration of 2.5 mg L^{-1} of each pollutant. Although in the present study, the CP was the pesticide with the highest removal percentages from the mixture.

All *Streptomyces* strains studied at the present work have been previously exposed to different chlorinated pesticides. Thus, these microorganisms could have the enzymatic ability to release chloride ions, favoring its degradation. The cross-adaptation phenomenon suggests that one pesticide may be rapidly degraded in soil in which it has never been applied; provided that the same soil had been previously exposed to a pesticide belonging to the same chemical group [51]. This could explain removal percentages obtained for both pesticides, PCP and CP, for strains as *Streptomyces* sp. A5 or *Streptomyces* sp. M7.

Another actinobacteria strain, *Kocuria* sp. CL2 isolated from secondary sludge of pulp and paper mill, able to use PCP as the sole source of carbon and degrade this pesticide, had been reported [28].

3.3. Removal of Pesticides Mixture by a Consortium of Six Streptomyces spp. Strains Free and Immobilized. Different researchers have demonstrated that cell immobilization techniques can significantly increase the removal efficiency of different pesticides compared with free cells [36, 52]. Thus, removal of a pesticides mixture (CP and PCP) by a six actinobacteria consortium, either free or immobilized in alginate beads, was compared.

The results revealed that CP removal was higher than PCP removal, following the same trend observed in previous assays (see Section 3.2), both in free and immobilized mixed cultures. CP removal percentages were 40.17 and 71.05 for free and immobilized cells, respectively. For PCP removal, the obtained values were 5.24% and 14.74% for the free and immobilized systems, respectively (Table 1). Thus, it is evident the increase of the removal of both pesticides by using the microbial immobilization technique. A possible reason for this could be that the alginate beads allow the optimal diffusion of contaminants [53–55] and besides; the support could be also acting as a protection for the cells against the detrimental effects of the surrounding medium such as pH and toxic substances, also enhancing the degrading ability of the cells [56, 57]. In fact, several researchers have demonstrated that calcium alginate immobilization improved the removal of toxic compounds. For instance, a *Pseudomonas* strain immobilized in calcium alginate mineralized a 50% more of phenol than free cells under the same conditions [58]. Also, Yañez-Ocampo et al. [52] studied the removal of two organophosphate pesticides by a bacterial consortium, and they obtained a percentage of methyl parathion removed 31% higher when the consortium was immobilized in alginate beads, compared with a suspension culture.

On the other hand, the pesticide sorption phenomenon to the alginate support was registered for both compounds.

Table 1: Pesticides removal percentages of the six actinobacteria strains culture in free and immobilized cells systems.

Sixfold culture	PCP removal (%)	CP removal (%)
Free cells	5.24 ± 0.56	40.17 ± 1.79
Immobilized cells	14.74 ± 4.73	71.05 ± 0.88

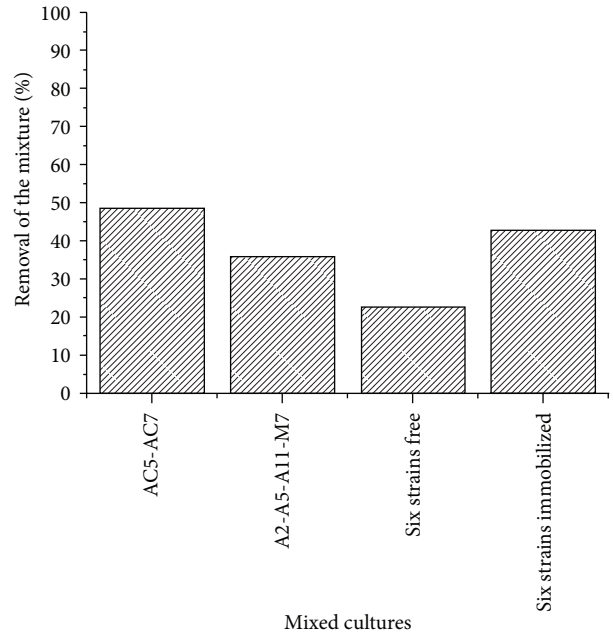

Figure 5: Removal percentages of the mixture (CP + PCP) for mixed cultures of *Streptomyces* spp. strains (A2, A5, A11, M7, AC5, AC7) as free and immobilized cells.

However, analysis of CP removal showed that the phenomenon of sorption was gradual, increasing up to 72 h, whereas for PCP it remained almost stable from 24 h until the end of the assay (data not shown). The sorption percentage was higher for CP (60.34% ± 0.42%) than for PCP (5.97% ± 2.41%) (data not shown), although the pesticides removal percentages observed by using alginate beads with or without microorganisms were significantly different ($P < 0.05$), evidencing the microbial activity. The sorption of different compounds, such as dyes and pesticides, on different immobilization supports was also reported by other researchers [36, 59].

Furthermore, when comparing the ability of removing the pesticides among all the free cell cultures, it might be concluded that the use of the six *Streptomyces* strains together did not present the best percentages of removal of the pesticides. These results are similar to those obtained by Fuentes et al. [32] in which mixed cultures consisting in two, three, and four strains improved the lindane removal compared with pure cultures, whereas combinations of five and six strains were not efficient for the removal of the pesticide from the culture medium.

Moreover, the analysis of the removal percentage of the pesticides mixture, calculated as the average between the removal percentages of CP and PCP for the mixed cultures,

showed that the double consortium (*Streptomyces* spp. AC5-AC7) and the mixed culture of the six strains immobilized (*Streptomyces* spp. A2-A5-A11-M7-AC5-AC7) were the consortia with higher ability to removal the toxic mixture (48.64% and 42.90%, resp.) (Figure 5).

4. Conclusions

Six *Streptomyces* spp. strains were able to tolerate a mixture of PCP and CP and did not show antagonistic effects among them. These strains were also able to grow and remove mixed pesticides, in pure as well as in mixed cultures. The immobilization of the cells allowed an increase of the removal of both pesticides. Our results reveal that *Streptomyces* strains could be used in mixed cultures and in immobilized systems as a potential tool for remediation of environments contaminated with multiple xenobiotics.

Conflict of Interests

This research was not influenced by any conflict of interests.

Acknowledgments

This work was financially supported by Consejo de Investigaciones de la Universidad Nacional de Tucumán (CIUNT), Agencia Nacional de Promoción Científica y Tecnológica (ANPCyT), Consejo Nacional de Investigaciones Científicas y Técnicas (CONICET), FONDECYT Postdoctoral Project no. 3100118, and Program of Scientific International Cooperation CONYCYT/MINCYT 2009-111. The authors gratefully acknowledge Mr. G. Borchia for his technical assistance.

References

[1] B. Kumari, V. K. Madan, and T. S. Kathpal, "Status of insecticide contamination of soil and water in Haryana, India," *Environmental Monitoring and Assessment*, vol. 136, no. 1–3, pp. 239–244, 2008.

[2] X. Chu, H. Fang, X. Pan et al., "Degradation of chlorpyrifos alone and in combination with chlorothalonil and their effects on soil microbial populations," *Journal of Environmental Sciences*, vol. 20, no. 4, pp. 464–469, 2008.

[3] K. R. Krishna and L. Philip, "Bioremediation of single and mixture of pesticide-contaminated soils by mixed pesticide-enriched cultures," *Applied Biochemistry and Biotechnology*, vol. 164, no. 8, pp. 1257–1277, 2011.

[4] J. Stocka, M. Tankiewicz, M. Biziuk, and J. Namieśnik, "Green aspects of techniques for the determination of currently used pesticides in environmental samples," *International Journal of Molecular Sciences*, vol. 12, no. 11, pp. 7785–7805, 2011.

[5] J. M. Kuperberg, K. F. A. Soliman, F. K. R. Stino, and M. G. Kolta, "Effects of time of day on chlorpyrifos-induced alterations in body temperature," *Life Sciences*, vol. 67, no. 16, pp. 2001–2009, 2000.

[6] G. Briceño, M. S. Fuentes, G. Palma, M. A. Jorquera, M. J. Amoroso, and M. C. Diez, "Chlorpyrifos biodegradation and 3,5,6-trichloro-2-pyridinol production by actinobacteria isolated from soil," *International Biodeterioration & Biodegradation*, vol. 73, pp. 1–7, 2012.

[7] K. L. Armbrust, "Chlorothalonil and chlorpyrifos degradation products in golf course leachate," *Pest Management Science*, vol. 57, no. 9, pp. 797–802, 2001.

[8] T. Cáceres, W. He, R. Naidu, and M. Megharaj, "Toxicity of chlorpyrifos and TCP alone and in combination to *Daphnia carinata*: the influence of microbial degradation in natural water," *Water Research*, vol. 41, no. 19, pp. 4497–4503, 2007.

[9] M. C. Diez, "Biological aspects involves in the degradation of organic pollutants," *Journal of Soil Science and Plant Nutrition*, vol. 10, pp. 244–267, 2010.

[10] A. Vallecillo, P. A. Garcia-Encina, and M. Peña, "Anaerobic biodegradability and toxicity of chlorophenols," *Water Science and Technology*, vol. 40, no. 8, pp. 161–168, 1999.

[11] C. M. Kaoa, C. T. Chaib, J. K. Liub, T. Y. Yehc, K. F. Chena, and S. C. Chend, "Evaluation of natural and enhanced PCP biodegradation at a former pesticide manufacturing plant," *Water Research*, vol. 38, pp. 663–672, 2004.

[12] C.-F. Yang, C.-M. Lee, and C.-C. Wang, "Isolation and physiological characterization of the pentachlorophenol degrading bacterium *Sphingomonas chlorophenolica*," *Chemosphere*, vol. 62, no. 5, pp. 709–714, 2006.

[13] A. Remes, A. Pop, F. Manea, A. Baciu, S. J. Picken, and J. Schoonman, "Electrochemical determination of pentachlorophenol in water on a multi-wall carbon nanotubes-epoxy composite electrode," *Sensors*, vol. 12, pp. 7033–7046, 2012.

[14] S. D. Copley, "Evolution of a metabolic pathway for degradation of a toxic xenobiotic: the patchwork approach," *Trends in Biochemical Sciences*, vol. 25, no. 6, pp. 261–265, 2000.

[15] S. G. Muhamad, "Kinetic studies of catalytic photodegradation of chlorpyrifos insecticide in various natural waters," *Arabian Journal of Chemistry*, vol. 3, no. 2, pp. 127–133, 2010.

[16] M. B. Carvalho, S. Tavares, J. Medeiros et al., "Degradation pathway of pentachlorophenol by *Mucor plumbeus* involves phase II conjugation and oxidation-reduction reactions," *Journal of Hazardous Materials*, vol. 198, pp. 133–142, 2011.

[17] Y. Gao, S. Chen, M. Hu, Q. Hu, J. Luo, and Y. Li, "Purification and characterization of a novel chlorpyrifos hydrolase from *Cladosporium cladosporioides* Hu-01," *PLoS One*, vol. 7, no. 6, Article ID e38137, 2012.

[18] K. D. Racke, D. A. Laskowski, and M. R. Schultz, "Resistance of chlorpyrifos to enhanced biodegradation in soil," *Journal of Agricultural and Food Chemistry*, vol. 38, no. 6, pp. 1430–1436, 1990.

[19] B. K. Singh and A. Walker, "Microbial degradation of organophosphorus compounds," *FEMS Microbiology Reviews*, vol. 30, no. 3, pp. 428–471, 2006.

[20] J. Zhu, Y. Zhao, and J. Qiu, "Isolation and application of a chlorpyrifos-degrading *Bacillus licheniformis* ZHU-1," *African Journal of Microbiology Research*, vol. 4, no. 22, pp. 2410–2413, 2010.

[21] G. Kulshrestha and A. Kumari, "Fungal degradation of chlorpyrifos by *Acremonium* sp. strain (GFRC-1) isolated from a laboratory-enriched red agricultural soil," *Biology and Fertility of Soils*, vol. 47, no. 2, pp. 219–225, 2011.

[22] Z. Liu, X. Chen, Y. Shi, and Z. C. Su, "Bacterial degradation of chlorpyrifos by *Bacillus cereus*," *Advanced Materials Research*, vol. 356–360, pp. 676–680, 2012.

[23] R. U. Edgehill, "Pentachlorophenol removal from slightly acidic mineral salts, commercial sand, and clay soil by recovered *Arthrobacter* strain ATCC 33790," *Applied Microbiology and Biotechnology*, vol. 41, no. 1, pp. 142–148, 1994.

[24] I. S. Thakur, P. Verma, and K. Upadhayaya, "Molecular cloning and characterization of pentachlorophenol-degrading monooxygenase genes of *Pseudomonas* sp. from the chemostat," *Biochemical and Biophysical Research Communications*, vol. 290, no. 2, pp. 770–774, 2002.

[25] R. I. Dams, G. I. Paton, and K. Killham, "Rhizoremediation of pentachlorophenol by *Sphingobium chlorophenolicum* ATCC 39723," *Chemosphere*, vol. 68, no. 5, pp. 864–870, 2007.

[26] S. Singh, R. Chandra, D. K. Patel, and V. Rai, "Isolation and characterization of novel *Serratia marcescens* (AY927692) for pentachlorophenol degradation from pulp and paper mill waste," *World Journal of Microbiology and Biotechnology*, vol. 23, no. 12, pp. 1747–1754, 2007.

[27] M. S. Fuentes, C. S. Benimeli, S. A. Cuozzo, and M. J. Amoroso, "Isolation of pesticide-degrading actinomycetes from a contaminated site: bacterial growth, removal and dechlorination of organochlorine pesticides," *International Biodeterioration and Biodegradation*, vol. 64, no. 6, pp. 434–441, 2010.

[28] S. K. Karn, S. K. Chakrabarti, and M. S. Reddy, "Degradation of pentachlorophenol by *Kocuria* sp. CL2 isolated from secondary sludge of pulp and paper mill," *Biodegradation*, vol. 22, no. 1, pp. 63–69, 2011.

[29] M. A. Castillo, N. Felis, P. Aragón, G. Cuesta, and C. Sabater, "Biodegradation of the herbicide diuron by streptomycetes isolated from soil," *International Biodeterioration and Biodegradation*, vol. 58, no. 3-4, pp. 196–202, 2006.

[30] D. Smith, S. Alvey, and D. E. Crowley, "Cooperative catabolic pathways within an atrazine-degrading enrichment culture isolated from soil," *FEMS Microbiology Ecology*, vol. 53, no. 2, pp. 265–273, 2005.

[31] C. S. Benimeli, M. J. Amoroso, A. P. Chaile, and G. R. Castro, "Isolation of four aquatic streptomycetes strains capable of growth on organochlorine pesticides," *Bioresource Technology*, vol. 89, no. 2, pp. 133–138, 2003.

[32] M. S. Fuentes, J. M. Sáez, C. S. Benimeli, and M. J. Amoroso, "Lindane biodegradation by defined consortia of indigenous *Streptomyces* strains," *Water, Air, and Soil Pollution*, vol. 222, no. 1–4, pp. 217–231, 2011.

[33] D. A. Hopwood, "Genetic analysis and genome structure in *Streptomyces coelicolor*," *Bacteriological reviews*, vol. 31, no. 4, pp. 373–403, 1967.

[34] D. K. Bell, H. D. Wells, and C. R. Markham, "*In vitro* antagonism of *Trichoderma* species against six fungal plant pathogens," *Phytopathology*, vol. 72, pp. 379–382, 1980.

[35] M. J. Amoroso, G. R. Castro, F. J. Carlino, N. C. Romero, R. T. Hill, and G. Oliver, "Screening of heavy metal-tolerant actinomycetes isolated from the Sali River," *Journal of General and Applied Microbiology*, vol. 44, no. 2, pp. 129–132, 1998.

[36] J. M. Saez, C. S. Benimeli, and M. J. Amoroso, "Lindane removal by pure and mixed cultures of immobilized actinobacteria," *Chemosphere*, vol. 89, pp. 982–987, 2012.

[37] P. Pattanapipitpaisal, N. L. Brown, and L. E. Macaskie, "Chromate reduction by *Microbacterium liquefaciens* immobilised in polyvinyl alcohol," *Biotechnology Letters*, vol. 23, no. 1, pp. 61–65, 2001.

[38] O. Rubilar, G. R. Tortella, R. Cuevas, M. Cea, S. Rodríguez-Couto, and M. C. Diez, "Adsorptive removal of pentachlorophenol by *anthracophyllum discolor* in a fixed-bed column reactor," *Water, Air and Soil Pollution*, vol. 223, no. 5, pp. 2463–2472, 2012.

[39] E. E. O. Odjadjare, S. O. Ajisebutu, E. O. Igbinosa, O. A. Aiyegoro, M. R. Trejo-Hernandez, and A. I. Okoh, "Escravos light crude oil degrading potentials of axenic and mixed bacterial cultures," *Journal of General and Applied Microbiology*, vol. 54, no. 5, pp. 277–284, 2008.

[40] G. Thouand, P. Bauda, J. Oudot, G. Kirsch, C. Sutton, and J. F. Vidalie, "Laboratory evaluation of crude oil biodegradation with commercial or natural microbial inocula," *Canadian Journal of Microbiology*, vol. 45, no. 2, pp. 106–115, 1999.

[41] J. D. van Hamme, A. Singh, and O. P. Ward, "Recent advances in petroleum microbiology," *Microbiology and Molecular Biology Reviews B*, vol. 67, no. 4, pp. 503–549, 2003.

[42] O. Zaborina, B. Baskunov, L. Baryshnikova, and L. Golovleva, "Degradation of pentachlorophenol in soil by *Streptomyces rochei* 303," *Journal of Environmental Science and Health*, vol. 32, no. 1, pp. 55–70, 1997.

[43] C. H. Sasikala, S. Jiwal, P. Rout, and M. Ramya, "Biodegradation of chlorpyrifos by bacterial consortium isolated from agriculture soil," *World Journal of Microbiology and Biotechnology*, vol. 28, no. 3, pp. 1301–1308, 2012.

[44] M. A. Polti, M. J. Amoroso, and C. M. Abate, "Chromium(VI) resistance and removal by actinomycete strains isolated from sediments," *Chemosphere*, vol. 67, no. 4, pp. 660–667, 2007.

[45] M. S. Fuentes, A. Alvarez, J. M. Saez, C. S. Benimeli, and M. J. Amoroso, "Methoxychlor bioremediation by defined consortium of environmental *Streptomyces* strains," *International Journal of Environmental Science and Technology*, 2013.

[46] C. Yang, Y. Li, K. Zhang et al., "Atrazine degradation by a simple consortium of *Klebsiella* sp. A1 and *Comamonas* sp. A2 in nitrogen enriched medium," *Biodegradation*, vol. 21, no. 1, pp. 97–105, 2010.

[47] S. R. Sørensen, Z. Ronen, and J. Aamand, "Growth in coculture stimulates metabolism of the phenylurea herbicide isoproturon by *Sphingomonas* sp. strain SRS2," *Applied and Environmental Microbiology*, vol. 68, no. 7, pp. 3478–3485, 2002.

[48] S. R. Sørensen, C. N. Albers, and J. Aamand, "Rapid mineralization of the phenylurea herbicide diuron by *Variovorax* sp. strain SRS16 in pure culture and within a two-member consortium," *Applied and Environmental Microbiology*, vol. 74, no. 8, pp. 2332–2340, 2008.

[49] S. Buono, S. Manzo, G. Maria, and G. Sansone, "Toxic effects of pentachlorophenol, azinphos-methyl and chlorpyrifos on the development of *Paracentrotus lividus* embryos," *Ecotoxicology*, vol. 21, no. 3, pp. 688–697, 2012.

[50] V. Matamoros, J. Puigagut, J. García, and J. M. Bayona, "Behavior of selected priority organic pollutants in horizontal subsurface flow constructed wetlands: a preliminary screening," *Chemosphere*, vol. 69, no. 9, pp. 1374–1380, 2007.

[51] D. Prakash, A. Chauhan, and R. K. Jain, "Plasmid-encoded degradation of p-nitrophenol by *Pseudomonas cepacia*," *Biochemical and Biophysical Research Communications*, vol. 224, no. 2, pp. 375–381, 1996.

[52] G. Yañez-Ocampo, E. Sanchez-Salinas, G. A. Jimenez-Tobon, M. Penninckx, and M. L. Ortiz-Hernández, "Removal of two organophosphate pesticides by a bacterial consortium immobilized in alginate or tezontle," *Journal of Hazardous Materials*, vol. 168, no. 2-3, pp. 1554–1561, 2009.

[53] J.-Y. Wu, K.-C. Chen, C.-T. Chen, and S.-C. J. Hwang, "Hydrodynamic characteristics of immobilized cell beads in a liquid-solid fluidized-bed bioreactor," *Biotechnology and Bioengineering*, vol. 83, no. 5, pp. 583–594, 2003.

[54] I. Banerjee, J. M. Modak, K. Bandopadhyay, D. Das, and B. R. Maiti, "Mathematical model for evaluation of mass transfer limitations in phenol biodegradation by immobilized *Pseudomonas putida*," *Journal of Biotechnology*, vol. 87, no. 3, pp. 211–223, 2001.

[55] J. H. Niazi and T. B. Karegoudar, "Degradation of dimethylphthalate by cells of Bacillus sp. immobilized in calcium alginate and polyurethane foam," *Journal of Environmental Science and Health A*, vol. 36, no. 6, pp. 1135–1144, 2001.

[56] L. Zhou, G. Li, T. An, J. Fu, and G. Sheng, "Recent patents on immobilized microoganism technology and its engineering application in wastewater treatment," *Recent Patents on Engineering*, vol. 2, no. 1, pp. 28–35, 2008.

[57] A. Pannier, M. Mkandawire, U. Soltmann, W. Pompe, and H. Böttcher, "Biological activity and mechanical stability of sol-gel-based biofilters using the freeze-gelation technique for immobilization of *Rhodococcus* ruber," *Applied Microbiology and Biotechnology*, vol. 93, no. 4, pp. 1755–1767, 2012.

[58] P. Y. A. Ahamad and A. A. M. Kunhi, "Enhanced degradation of phenol by *Pseudomonas* sp. CP4 entrapped in agar and calcium alginate beads in batch and continuous processes," *Biodegradation*, vol. 22, no. 2, pp. 253–265, 2011.

[59] B.-E. Wang and Y.-Y. Hu, "Comparison of four supports for adsorption of reactive dyes by immobilized *Aspergillus fumigatus* beads," *Journal of Environmental Sciences*, vol. 19, no. 4, pp. 451–457, 2007.